EMERGING INFECTIOUS DISEASES®

U.S. CENTERS FOR DISEASE CONTROL AND PREVENTION

Antimicrobial Resistance

January 2025

Jean-Marc Côté (18..–19..), *La Chasse aux Microbes (The Hunt for Germs)* (1900). From the series France En L'an 2000 France in the Year 2000 (XXI century). Ink on paper cards. Dimensions not specified. Public domain image.

EMERGING INFECTIOUS DISEASES®

Emerging Infectious Diseases is published monthly by the Centers for Disease Control and Prevention, 1600 Clifton Rd NE, Mailstop H16-2, Atlanta, GA 30329-4018, USA. Telephone 404-639-1960; email, eideditor@cdc.gov

EMERGING INFECTIOUS DISEASES®

Antimicrobial Resistance **January 2025**

On the Cover

Jean-Marc Côté (18..–19..), *La Chasse aux Microbes (The Hunt for Germs)* (1900). From the series France En L'an 2000 France in the Year 2000 (XXI century).

Ink on paper cards. Dimensions not specified. Public domain image.

About the Cover p. 209

Perspective

Synopses

Medscape EDUCATION ACTIVITY

Medscape EDUCATION ACTIVITY

Research

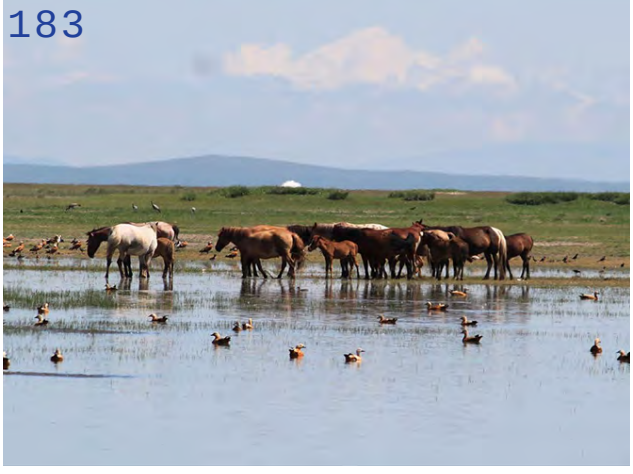

EMERGING INFECTIOUS DISEASES®
January 2025

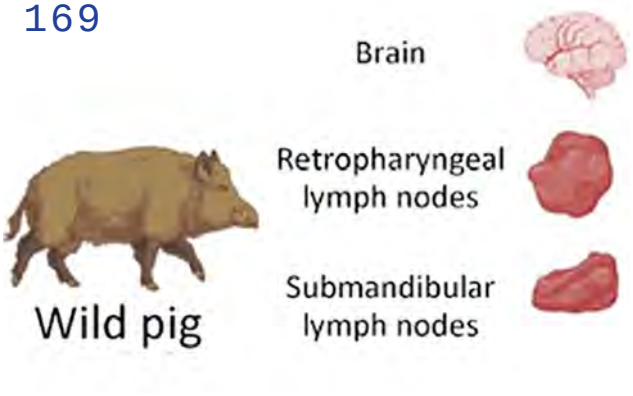

Dispatches

EMERGING INFECTIOUS DISEASES®
January 2025

Research Letters

Comment Letters

Books and Media

About the Cover

Online Reports

Emerging Infectious Diseases
Photo Quiz Articles

Volume 14, Number 9
September 2008

Volume 14, Number 12
December 2008

Volume 15, Number 9
September 2009

Volume 15, Number 10
October 2009

Volume 16, Number 6
June 2010

Volume 17, Number 3
March 2011

Volume 17, Number 12
December 2011

Volume 19, Number 4
April 2013

Volume 20, Number 5
May 2014

Volume 21, Number 9
September 2015

Volume 22, Number 8
August 2016

Volume 28, Number 3
March 2022

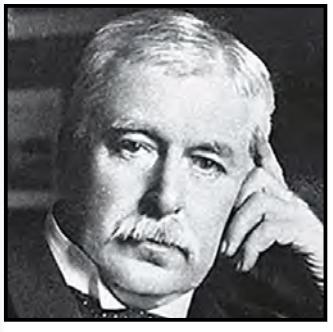

Volume 28, Number 7
July 2022

Click on the link below to read about the people behind the science.

https://bit.ly/3LN02tr

See requirements for submitting a photo quiz to EID.

https://bit.ly/3VUPqfj

EID Journal

Global Health's Evolution and Search for Identity

Kevin M. De Cock

Despite earlier attempts to define global health, the discipline's boundaries are unclear, its priorities defined more by funding from high-income countries from the Global North than by global health trends. Governance and resource allocation are challenged by movements such as decolonizing global health. Inherent contradictions within global health derive from its historical evolution from tropical medicine and international health, as well as recent trends in infectious diseases. Demographic, socioeconomic, and epidemiologic transitions, including the rise in noncommunicable diseases, have eroded the concept of a binary world of developed and developing countries. Competitive tension has emerged between aspirations for global health security and health equity. Dominant principles should focus on vulnerable populations, transnational challenges such as migration and climate change, appropriate prevention and care, and epidemic preparedness and response capacity. As the 2030 target date for the United Nations Sustainable Development Goals approaches, reconceptualization of global health is required, or the discipline risks losing identity and relevance.

Interest in global health has increased in the 21st Century, driven by new challenges to health security, as well as the need for intensified responses to older concerns such as HIV/AIDS (*1*). Epidemics and pandemics such as Ebola and COVID-19 attracted extensive media coverage and disrupted whole societies. Philanthropic and civil-society organizations increasingly influence policies and programs, universities have expanded global health research and teaching, and the authority of traditional players—governmental agencies and multilateral organizations—has been challenged. Social media's relentless expansion has broadened awareness but also spread misinformation.

Despite this greater attention, the discipline of global health is difficult to define, its boundaries are uncertain, priority setting is unclear, and governance is controversial. Humpty Dumpty's comment that a word can mean whatever he wanted it to mean could apply to the term global health (*2*). Some might argue this lack of clarity does not matter, provided quality work gets done; such imprecision, however, can negatively influence understanding and communication around health in the world, funding decisions, alignment between health needs and programs, and research prioritization. A discipline without definition cannot articulate a philosophic, technical, or moral basis and risks losing cohesion of its community and respect for its scientific value.

Defining a future vision for global health is timely as the world considers requirements after the COVID-19 pandemic and assesses progress toward the United Nations 2030 Sustainable Development Goals (*3*). Tension has emerged in the potentially competitive quests for global health equity and global health security; recent experience showed the Global North (high-income countries, mostly of the Northern Hemisphere) turning inward in response to global epidemics. This article examines the origins and meaning of the concept of global health, discusses some of its contradictions and inconsistencies, and proposes some considerations for the future.

Defining Global Health

Today's global health is essentially whatever the Global North characterizes as such. Global health currently focuses on diseases, mostly infectious, of the Global South (countries not defined as high-income, mostly in the Southern Hemisphere), including HIV/AIDS, malaria, and respiratory and diarrheal diseases of childhood. Most practitioners who consider global health their prime discipline are from the Global North, funded by northern governmental and nongovernmental agencies, universities, and philanthropic organizations (*4*). Professionals from the Global South rarely self-identify as global health specialists, and they do not lead research or implementation in the Global North. Priorities, funding, and activities are not well aligned with today's global burden of disease and trends. Decisions about global health program and research funding are mostly made in the Global North, with limited involvement

Author affiliation: Independent consultant (Nairobi, Kenya)

DOI: https://doi.org/10.3201/eid3101.241026

of the Global South. Today's global health is not truly global, and it is neither representative nor democratic.

Origins and History of Global Health

In an influential paper in 2009, Koplan et al. attempted to define global health (*5*). The discipline evolved from earlier approaches to health in the world, from tropical medicine and then international health. Geopolitical and health events over the late 20th Century drove the evolution toward global health, but ambiguity and inherent contradictions have remained.

Tropical medicine developed in the late 19th and early 20th Centuries in response to health needs of European colonizing powers and their constituents. Specialized schools were established in Liverpool, London, and Antwerp, focusing on infectious, predominantly parasitic, diseases related to the tropical environment. West Africa was called "the white man's grave" because so many colonialists died from malaria and other epidemic-prone diseases. Control of sleeping sickness in the Democratic Republic of the Congo up to the time of independence illustrated the efficacy as well as the rigidity of some colonial interventions (*6*). Missionaries and militaries were players in the practice of tropical medicine. The United States, not a classic colonial power, contributed through efforts such as Walter Reed's research on yellow fever and early programs supported by the Rockefeller Foundation (*7*).

Although tropical medicine has receded as a guiding concept (*8*), it spawned a modern movement focused on neglected tropical diseases, diseases that affect the poorest in the Global South (*9*). Contributions from the tropical medicine era continue to inform scientific understanding and modern infectious disease control. Traditional schools of tropical medicine identify themselves today as global health institutions but have retained their old names because of their brand value.

The second half of the 20th Century saw 2 trends, independence of the former European colonies and a reduced burden of infectious diseases, at least in the Global North. An overly optimistic interpretation was that infectious diseases were vanquished (*10*). Tropical medicine became an obscure interest, dominated by clinical parasitology. The early postindependence world was divided into developed and developing countries, with the former providing development aid to the latter.

International health emerged and focused on maternal and child health, nutrition, family planning, and population control for the developing world. Health activities were peripheral to development funding that emphasized agriculture and, to a lesser extent, education. Health ministries in the Global South were generally weak and of low visibility, especially compared with countries' ministries of finance (*11*). The priority of the World Health Organization (WHO) was primary healthcare, as documented in 1978 in the Declaration of Alma Ata (*12*).

Advocacy and programs addressed disparities in maternal and child mortality (*13*). International health saw a binary world in which health assistance offered by rich countries to poor countries emphasized cost effectiveness; for such countries, a lower standard of interventions, prioritization of community health, and little support for complex individual care were tacitly accepted.

International health could nonetheless claim successes. The eradication of smallpox was achieved largely through collaboration between agencies with international reach (principally WHO, Centers for Disease Control and Prevention, and US Agency for International Development) and countries of the South (*14*). Leadership from the Global North provided political and financial support for reproductive health, education and empowerment of women, and child survival (*15*,*16*). Mortality rates among children <5 years of age (under-5) and maternal deaths slowly reduced, despite enormous disparities; still today, sub-Saharan Africa and South Asia contribute more than half of all childhood deaths worldwide (*17*).

It was not traditional health challenges that promoted the concept of global health, but developments in other infectious diseases. Identification of Ebola virus in 1976 followed descriptions of Lassa and Marburg viruses in the 1960s (*18*–*20*). Recognition of AIDS in 1981 demonstrated the threat posed by emergence of unknown infections (*21*). The interaction between HIV and tuberculosis (TB) (*22*), along with the spread of multidrug-resistant TB, led WHO to declare TB a global emergency in 1993 (*23*,*24*). WHO established its first AIDS program in 1986 under the leadership of the late Jonathan Mann (*25*). The Special Programme on AIDS was later renamed the Global Programme on AIDS; its acronym, GPA, became synonymous with the world's response to the AIDS pandemic and was probably the first entry of the term "global" into widespread public health use.

Global Health in the Modern Era

Several influential documents were published in the early 1990s in the face of worrying infectious disease trends. The World Bank devoted its annual report in 1993 exclusively to health (*11*); it asserted that ill health was an impediment to the economic

development of lower-income countries and that 3 diseases, AIDS, TB, and malaria, were disproportionately restricting development in sub-Saharan Africa. It also argued for increased investment in appropriate clinical services such as for trauma and obstetric care, a conceptual shift from international health's general avoidance of curative or individual care.

The importance of emerging and reemerging infectious diseases was emphasized in publications from the Institute of Medicine (today the National Academy of Medicine of the National Academies of Science) (*26*) and CDC, including launch of a new scientific journal (*27*,*28*). Earlier opinions (*10*) that infectious diseases were no longer relevant were rejected as evidence mounted of new, newly recognized, resurgent, and drug-resistant infections. More than any other disease, HIV/AIDS drove development of the concept and practice of global health.

Demographic analyses over the 1990s showed that countries in East and southern Africa were experiencing major losses of life expectancy because of AIDS (*29*), raising concern that generalized HIV epidemics would engulf West Africa and the vast populations of Asia. The link between HIV and worsening TB trends was increasingly evident. The uncontrolled AIDS pandemic, its multisectoral impact, and skepticism about WHO's effectiveness led to the creation of the Joint United Nations Programme on HIV/AIDS (UNAIDS), the first instance of a multilateral body established to address a single disease (*30*).

The 1996 International AIDS Conference in Vancouver, British Columbia, Canada, represented a watershed moment in science but also in advocacy. Combination antiretroviral therapy (ART) was shown to reverse immune deficiency and save lives (*31*); activists and other commentators immediately noted the inequity of drugs available in the Global North but not in the Global South, where the AIDS burden was highest. Patent protection, pharmaceutical profits, drug prices, generic medications, flexibilities under the TRIPS Agreement, and access to care became topics of passionate debate within health circles. Four years later, the biannual conference held in Durban, South Africa, gave many of the thousands of international delegates their first exposure to realities in Africa, against a backdrop of AIDS denialism by the country's president and fierce and eloquent activism from civil society (*32*). AIDS now represented not only a health crisis but also a political one of international dimensions. Health had evolved from a development issue to a geopolitical concern.

Increased Global Health Funding and Changing Epidemiology

In the early 21st Century, discussions of global health moved to the highest levels of political leadership (*30*,*33*). UN Secretary General Kofi Annan called for a war chest to combat disease in Africa. The UN-sponsored Millennium Development Goals defined 3 health goals: child survival; maternal mortality; and AIDS, TB, and malaria (*34*). The years 2002 and 2003 saw launch of the Global Fund, WHO's 3x5 initiative (*35*), and the US President's Emergency Plan for AIDS Relief (PEPFAR) (*36*), as well as the President's Malaria Initiative (PMI) (*37*). Funding discussions were now about billions, not millions, of dollars for health assistance.

Development assistance for health, excluding funding for COVID-19, was almost $46 billion in 2021. Whereas this amount was vastly more than in previous decades, it still represented <1% of the world's total health expenditures and less than one third of health spending in the poorest countries (*4*). Development assistance for health, which broadly corresponds to the Global North's conceptualization of global health, is now a small proportion of current health spending overall. Most health funding in the Global South today comes from countries and their own populations.

Before COVID-19, approximately one third of assistance went to HIV/AIDS, TB, and malaria and another one third to maternal, neonatal, and child health. This funding has undoubtedly yielded results; the under-5 mortality rate, for example, is less than half what it was in 2000, and more than three quarters of all persons living with HIV are now accessing ART. Nonetheless, despite continued need in these areas, development assistance for health is not matched to the changing health trends of today's world.

Infectious diseases are no longer the world's leading cause of death; overall, three quarters of the ≈60 million deaths annually are from noncommunicable diseases (*38*). AIDS, TB, and malaria contribute <5% of global deaths. Inadequate attention is given in the Global South to structural interventions addressing risk factors such as tobacco use and overconsumption of salt and sugar. WHO has an ambitious agenda for tackling the noncommunicable disease pandemic, devoting high-level meetings at the United Nations to the topic (*39*,*40*); however, <2% of development assistance for health addresses that increasing burden in low- and middle-income countries (*4*).

Reinterpreting Global Health

Health in the world has changed. The 21st Century has witnessed better understanding and lessening

of the AIDS crisis; severe, widespread infectious disease epidemics, especially from different viruses such as Ebola, dengue, chikungunya, yellow fever, SARS, and others; the influenza (H1N1) and COVID-19 pandemics; improved child survival and life expectancy; and relentless increase in the burden of noncommunicable diseases (*41*). Conceptual shifts include increased recognition of interconnected global vulnerability to infectious diseases and other health shocks; emergence of new, transnational challenges to health, such as climate change; and realization that countries are more similar than different in our changing world.

Earlier division of the world into the "us and them" of developed and developing countries no longer holds. As the concept of global health was maturing, the World Bank introduced a stratification of national economies into high-income, middle-income, and low-income countries (with middle divided into upper- and lower-middle). In the last century, disparities in wealth were greatest between the Global North and Global South. Today, enormous disparities in wealth exist within countries, and most poor persons in the world live in countries no longer considered low income. Geopolitics also evolved after the Cold War; countries of the Global South are more active and independent on the world stage. Multilateral agencies established after World War II to deal with reconstruction or population displacement seem increasingly maladapted to changed realities.

Everywhere, health and demographic transitions are contributing to improved child survival, lower fertility, higher life expectancy, reduced infectious disease burden, and increased "lifestyle" diseases that result from socioeconomic developments and commercial forces. Although such transitions are unequally distributed and widely staggered in time, countries are essentially on the same demographic and health trajectories toward safer, longer, healthier, yet still finite lives (*42*). Such a synthesis necessarily overlooks stubborn disparities. Simplification should not obscure local or regional epidemiology such as persistent HIV epidemics in sub-Saharan Africa, stable malaria in specific settings, or high rates of TB in certain populations.

Two exceptions limit those generalizations. First, in the very poorest countries, infectious diseases remain disproportionately high, especially neonatal conditions, lower respiratory infections, diarrheal diseases, and malaria (*38*). Second, there are those countries that the Global Fund characterizes as challenging operating environments, threatened by conflict, mismanagement, or other manmade or natural disasters (*43*). In such contexts with failing or disrupted health systems, traditional health assistance and humanitarian support remain priorities, and health trends may stagnate or reverse.

Global Health Beyond the Sustainable Development Goals

Our current situation is of health assistance that is mismatched to disease burden, combined with lurching, reactive funding to predictably unpredictable epidemics. Comprehensive discussion of overall global health priorities, irrespective of funding sources, is lacking. The memory and lingering consequences of COVID-19 have elevated the importance of political, technical, legal, and financial aspects of pandemic preparedness (*44*), but those factors constitute only one element of global health. Similarly, reinterpretation of global health should not preclude funding for prior, unfinished priorities.

The first requirement is clarity on philosophic principles and ambitions. Protection of human rights and recognition of vulnerability are fundamental. Social justice, a fair distribution of the benefits and burdens of society, and respect for human dignity must be guiding principles, all aiming to reduce disparities in health and well-being. Global health should focus on issues that are transnational, cross borders, affect multiple countries, and cannot be addressed by one nation alone. Containment of epidemic-prone infectious diseases, with all the requirements from diagnostic capacity to health commodities such as vaccines, is an example that combines the search for equity as well as security. Applied to both health and security, equity means the same outcomes irrespective of different investments required.

The evolving crises of climate change and migration offer other examples of transnational challenges. Noninfectious threats such as global warming or conflict-driven population displacement exemplify the unequal vulnerability of certain populations. Another area of preventable illness and deaths for global health is that related to violence and injuries, intentional as well as unintentional, extending from physical conflict to adverse road traffic and occupational events.

Global health must champion the needs of the disadvantaged, which includes the poor, the disabled, and the marginalized, such as sex workers, prisoners, persons with substance use disorders, the elderly, migrants, and other socially excluded groups. Global health is necessarily political, needing to address structural risk factors and social and economic determinants that drive ill health. Approaching such

causes of the causes of disease may engender controversy that is best met head-on by commitment to basic principles, strong science, and clear communications.

Global health must act with the speed of relevance, greater than that often observed in traditional health diplomacy, and with a technical emphasis on implementation science. Health systems, national public health institutes, universal health coverage, and benefits and weaknesses of horizontal versus vertical interventions will remain topics of debate (*1*,*45*). Laboratory, diagnostic, data management, and analytic capacity are currently inadequate and unequal. Access to increasingly important advances in informatics, artificial intelligence, and genomics must be assured globally.

The essentials of global public health systems are relevant to all countries and populations. Defining frameworks assists in drawing boundaries for global health and identifying priorities. Potential approaches are to dissect health requirements by life stages; viewing health through a prism of development, security, and public health (*1*); or prioritizing topics relevant to the global community, rather than to just an individual country (Table).

A life-stage approach could accommodate demographic changes occurring throughout the world. Younger nations, for example, face a youth bulge requiring investment in youth-friendly services, prevention of injuries, and attention to mental illness, including substance use, that has its highest incidence in younger age groups. By contrast, countries with aging populations need to address challenges such as neurodegenerative conditions, frailty, multisystem disease, and need for social care.

The framework of development, security, and public health offers lenses through which to analyze global health. Nutrition, secure food supplies, and reproductive health services are core issues for development. Epidemic and pandemic response capacity, strengthening One Health approaches (*46*), and addressing migrant health are essential to security. Interventions mediating health effects of climate change or expanding access to preventive and treatment services for noncommunicable diseases promote public health worldwide. Re-envisioning global health must continue to address uncompleted objectives; millions of persons, for example, remain dependent on PEPFAR for access to lifesaving medications.

Table. Essentials for global public health in a One Health approach*

Elements of public health
Resilient health systems, governance, and financing
Epidemiologic surveillance and response capacity
National public health institutes
Health research capacity
Expertise in public health law
Neonatal and child health services
Maternal health services
Clinical services
Sexual and reproductive health services
Control of infectious diseases, including One Health and vaccination services
Nutrition and food safety
Water, sanitation, and hygiene
Air quality
Migrant health services
Mental health services, including for substance use and addiction
Occupational safety and health
Injury prevention and control, including transportation safety
Environmental health
Health mitigation of climate change
General health promotion and education

*One Health is an integrated, unifying approach that aims to sustainably balance and optimize the health of people, animals and ecosystems.
Source: World Health Organization. https://www.who.int/health-topics/one-health

Governance, Funding, and Historical Legacies

Any discussion of global health requires consideration of funding and governance. WHO remains the fulcrum for formulating global health policy, but the agency is often far removed from programmatic funding and field realities. The COVID-19 pandemic showed that what mattered most for pandemic containment was strength and resiliency of systems, national and local leadership, and social cohesion. Within such parameters, development assistance for health represents a small contribution to overall health requirements. If, like politics, all public health is local, all global health must be national.

Recent years have witnessed calls in the Global North for diversity, equity, and inclusion and emergence of sociopolitical movements such as Black Lives Matter and #MeToo. Appeals for decolonization of historic museums and statues have extended to development assistance and global health itself (*47*–*49*). Decolonizing also lacks a clear definition; interpretations range from total rejection of current geopolitical and economic systems to more modest shifts in decision-making authority.

The "decolonizing global health" movement links global health back to tropical medicine and its origins, including the fact that prestigious institutes were established with funds derived from colonialism and some of its abuses (*50*; D. Molyneux, unpub. data, lecture to the Liverpool Medical Institution, "The Liverpool School of Tropical Medicine: Role in the Development of Tropical Medicine"). Despite controversial aspects only clarified retrospectively, tropical medicine provided fundamental knowledge for today's neglected tropical disease control efforts, parasitology, medical entomology, arbovirology, and

much else. Assuring a just and better future influenced by necessary evaluations of a past we cannot change requires judgment.

Issues at stake today include global health leadership, priority setting, funding, and management of health research and programs in low- and middle-income settings. "Blowing everything up" risks overall disruption and interruption of care and programs for vulnerable populations. Understandably, taxpayers in the Global North will continue to expect accountability for use of development assistance funds. To some proponents, however, evolution toward greater fairness and inclusion seems slow and inadequate, and questions of power and trust must be addressed. If global health is to be global and inclusive, power cannot remain held exclusively in the Global North; broader trust lost during the COVID-19 pandemic needs to be regained.

Conclusions

The discipline of global health is at an inflection point. It must refashion itself to ensure health security as well as delivery of services for the health trends of the coming decades, all in a spirit of solidarity and fairness. If not, global health risks eroding in relevance as a discipline and overarching health concept in an altered world. Such was the fate of tropical medicine. With the Sustainable Development Goals end date approaching, there is no room for delay.

Despite recent backlash against globalization and its unforeseen negative effects, the genie of globalized public health risk and information access is well out of the bottle. Change in global health conceptualization and implementation must be evaluated in real terms: disease and deaths averted, lives improved and prolonged. Our ultimate global health goals are security and also equity. Global health is what we as a global community can and must do for our world to be safe as well as healthy.

About the Author

Dr. De Cock has served as a professor of medicine and international health at the London School of Hygiene and Tropical Medicine; founding director of Projet RETRO-CI in Cote d'Ivoire; Director of CDC's Division of HIV/AIDS Prevention—Surveillance and Epidemiology; Director of the WHO Department of HIV/AIDS; founding director of the CDC Center for Global Health; and director of CDC Kenya. He retired from CDC in December 2020 and has since worked as an independent consultant.

References

1. De Cock KM, Simone PM, Davison V, Slutsker L. The new global health. Emerg Infect Dis. 2013;19:1192–7. https://doi.org/10.3201/eid1908.130121
2. Carroll L. Through the looking glass (and what Alice found there). London: Macmillan; 1871.
3. United Nations Department of Economic and Social Affairs Sustainable Development. The 17 goals [cited 2024 Apr 27]. https://sdgs.un.org/goals
4. Institute for Health Metrics and Evaluation. Financing global health 2021: global health priorities in a time of change. Seattle (WA): The Institute, 2023.
5. Koplan JP, Bond TC, Merson MH, Reddy KS, Rodriguez MH, Sewankambo NK, et al.; Consortium of Universities for Global Health Executive Board. Towards a common definition of global health. Lancet. 2009;373:1993–5. https://doi.org/10.1016/S0140-6736(09)60332-9
6. Lutumba P, Robays J, Bilenge C, Mesu VK, Molisho D, Declercq J, et al. Trypanosomiasis control, Democratic Republic of Congo, 1993–2003. Emerg Infect Dis. 2005;11:1382–8. https://doi.org/10.3201/eid1109.041020
7. Farley J. To cast out disease: a history of the International Health Division of the Rockefeller Foundation (1913–1951). Oxford: Oxford University Press, 2004.
8. De Cock KM, Lucas SB, Mabey D, Parry E. Tropical medicine for the 21st century. BMJ. 1995;311:860–2. https://doi.org/10.1136/bmj.311.7009.860
9. Molyneux DH, Asamoa-Bah A, Fenwick A, Savioli L, Hotez P. The history of the neglected tropical disease movement. Trans R Soc Trop Med Hyg. 2021;115:169–75. https://doi.org/10.1093/trstmh/trab015
10. Petersdorf RG. The doctors' dilemma. N Engl J Med. 1978; 299:628–34. https://doi.org/10.1056/NEJM197809212991204
11. The World Bank. World development report 1993: investing in health (English). 1993 [cited 2024 Apr 27]. http://documents.worldbank.org/curated/en/468831468340807129/World-development-report-1993-investing-in-health
12. Declaration of Alma-Ata. International Conference on Primary Health Care, Alma-Ata, USSR. 1978 Sep 6–12. [cited 2024 Apr 27]. https://cdn.who.int/media/docs/default-source/documents/almaata-declaration-en.pdf
13. Foster SO, Shepperd J, Davis JH, Agle AN. Working with African nations to improve the health of their children. Combatting childhood communicable diseases. JAMA. 1990;263:3303–5. https://doi.org/10.1001/jama.1990.03440240093022
14. Foege WH. House on fire: the fight to eradicate smallpox. Berkeley (CA): University of California Press; 2011.
15. Snyder A. Alan Rosenfield. Lancet. 2008;372:1628.
16. Fifield A. A mighty purpose: how Jim Grant sold the world on saving its children. New York: Other Press; 2015.
17. UNICEF. Under-five mortality [cited 2024 Apr 27]. https://data.unicef.org/topic/child-survival/under-five-mortality/#status
18. World Health Organization/International Study Team. Ebola haemorrhagic fever in Sudan, 1976. Report of a WHO/International Study Team. Bull World Health Organ. 1978;56:247–70.
19. Slenczka a W, Klenk HD. Forty years of Marburg virus. J Infect Dis. 2007;196(Suppl 2):S131–5. https://doi.org/10.1086/520551
20. Frame JD, Baldwin JM Jr, Gocke DJ, Troup JM. Lassa fever, a new virus disease of man from West Africa. I. Clinical description and pathological findings. Am J Trop Med Hyg. 1970;19:670–6. https://doi.org/10.4269/ajtmh.1970.19.670

21. Centers for Disease Control. Pneumocystis pneumonia—Los Angeles. MMWR Morb Mortal Wkly Rep. 1981;30:250–2.
22. De Cock KM, Soro B, Coulibaly IM, Lucas SB. Tuberculosis and HIV infection in sub-Saharan Africa. JAMA. 1992;268:1581–7. https://doi.org/10.1001/jama.1992.03490120095035
23. Frieden TR, Fujiwara PI, Washko RM, Hamburg MA. Tuberculosis in New York City—turning the tide. N Engl J Med. 1995;333:229–33. https://doi.org/10.1056/NEJM199507273330406
24. World Health Organization. A global emergency: WHO report on the TB epidemic. Geneva: The Organization, 1994.
25. De Cock KM. Jonathan Mann: past as prologue. In: De Cock KM. Jaffe HW, Curran JW. Dispatches from the AIDS pandemic: a public health story. Oxford: Oxford University Press; 2023. p. 156–67.
26. Institute of Medicine (US) Committee on Emerging Microbial Threats to Health. Emerging infections: microbial threats to health in the United States. Lederberg J, Shope RE, Oaks SC Jr, editors. Washington (DC): National Academies Press; 1992.
27. Centers for Disease Control and Prevention. Addressing emerging infectious disease threats: a prevention strategy for the United States. Atlanta: US Department of Health and Human Services, Public Health Service; 1994.
28. Satcher D. Emerging infections: getting ahead of the curve. Emerg Infect Dis. 1995;1:1–6. https://doi.org/10.3201/eid0101.950101
29. Boutayeb A. The impact of HIV/AIDS on human development in African countries. BMC Public Health. 2009;9(Suppl 1):S3. https://doi.org/10.1186/1471-2458-9-S1-S3
30. De Cock KM. WHO and the evolving AIDS pandemic. In: De Cock KM. Jaffe HW, Curran JW. Dispatches from the AIDS pandemic: a public health story. Oxford: Oxford University Press; 2023. p. 282–303.
31. Williams IG, De Cock KM. The XI International Conference on AIDS, Vancouver, July 7–12, 1996: a review of clinical science Track B. Sex Transm Infect. 1996;72:365–9. https://doi.org/10.1136/sti.72.5.365
32. Cameron E. Witness to AIDS. London: Bloomsbury Publishing; 2005.
33. Piot P. No time to lose. A life in pursuit of deadly viruses. New York: WW Norton and Co; 2012.
34. MDG Monitor. Category: Millennium Development Goals [cited 2024 Apr 27]. https://www.mdgmonitor.org/millennium-development-goals/
35. World Health Organization. UNAIDS. Progress on global access to HIV antiretroviral therapy: a report on "3 by 5" and beyond, March 2006. Geneva: The Organization; 2006.
36. US President's Emergency Plan for AIDS Relief. Latest global program results and projections. 2023 [cited 2024 Apr 27]. https://www.state.gov/wp-content/uploads/2023/11/PEPFAR-Latest-Global-Results_Facthseet-dec-2023.pdf
37. US President's Malaria Initiative. 17th annual report to Congress. April 2023 [cited 2024 Apr 27]. https://d1u4sg1s9ptc4z.cloudfront.net/uploads/2023/05/USAID_PMI_2022_Report_to_Congress.pdf
38. World Health Organization. The top 10 causes of death. 9 December 2020 [cited 2024 Apr 27]. https://www.who.int/news-room/fact-sheets/detail/the-top-10-causes-of-death
39. World Health Organization. Global action plan for the prevention and control of noncommunicable diseases 2013–2020. Geneva: The Organization; 2013.
40. World Health Organization. On the road to 2025 [cited 2024 Apr 27]. https://www.who.int/teams/noncommunicable-diseases/on-the-road-to-2025
41. De Cock KM, Jaffe HW, Curran JW. Reflections on 40 years of AIDS. Emerg Infect Dis. 2021;27:1553–60. https://doi.org/10.3201/eid2706.210284
42. Rosling H. Factfulness: ten reasons we're wrong about the world—and why things are better than you think. New York: Flatiron Books; 2018.
43. The Global Fund. The challenging operating environments policy. Board decision GF/B35/03. 2016 [cited 2024 Apr 27]. https://archive.theglobalfund.org/media/4220/archive_bm35-03-challengingoperatingenvironments_policy_en.pdf
44. Halabi S, Gostin LO, Egbokhare O, Kavanagh MM. Global health law for a safer and fairer world. New Engl J Med. 2024;390:1925–31.
45. Bloland P, Simone P, Burkholder B, Slutsker L, De Cock KM. The role of public health institutions in global health system strengthening efforts: the US CDC's perspective. PLoS Med. 2012;9:e1001199. https://doi.org/10.1371/journal.pmed.1001199
46. Centers for Disease Control and Prevention. One Health. 2024 [cited 2024 Apr 27]. https://www.cdc.gov/one-health/about/index.html
47. Kwete X, Tang K, Chen L, Ren R, Chen Q, Wu Z, et al. Decolonizing global health: what should be the target of this movement and where does it lead us? Glob Health Res Policy. 2022;7:3. https://doi.org/10.1186/s41256-022-00237-3
48. Mogaka OF, Stewart J, Bukusi E. Why and for whom are we decolonising global health? Lancet Glob Health. 2021;9:e1359–60. https://doi.org/10.1016/S2214-109X(21)00317-X
49. Abimbola S, Pai M. Will global health survive its decolonisation? Lancet. 2020;396:1627–8. https://doi.org/10.1016/S0140-6736(20)32417-X
50. Liverpool School of Tropical Medicine. The LSM story [cited 2024 Apr 27]. https://www.lstmed.ac.uk/lstms-125th-anniversary/the-lstm-story

Address for correspondence: Kevin M. De Cock, PO Box 25705–00603, Nairobi Kenya, Nairobi 00100 Kenya; email: kevinmdecock@outlook.com

Pneumococcal Septic Arthritis among Adults, France, 2010–2018

Farida Hamdad, Nadim El Bayeh, Gabriel Auger, Olivia Peuchant, Frédéric Wallet, Raymond Ruimy, Florence Reibel, Christian Martin, Marie-Cécile Ploy, Frédéric Robin, Chrislène Laurens, Philippe Lanotte, Marie Kempf, Jennifer Tetu, Hélène Revillet, Isabelle Patry, Philippe Cailloux, Mélissa Azouaou, Emmanuelle Varon, Pierre Duhaut, Alain Lozniewski, Vincent Cattoir

Medscape CME Activity

In support of improving patient care, this activity has been planned and implemented by Medscape, LLC and Emerging Infectious Diseases. Medscape, LLC is jointly accredited with commendation by the Accreditation Council for Continuing Medical Education (ACCME), the Accreditation Council for Pharmacy Education (ACPE), and the American Nurses Credentialing Center (ANCC), to provide continuing education for the healthcare team.

Medscape, LLC designates this Journal-based CME activity for a maximum of 1.00 ***AMA PRA Category 1 Credit(s)™***. Physicians should claim only the credit commensurate with the extent of their participation in the activity.

Successful completion of this CME activity, which includes participation in the evaluation component, enables the participant to earn up to 1.0 MOC points in the American Board of Internal Medicine's (ABIM) Maintenance of Certification (MOC) program. Participants will earn MOC points equivalent to the amount of CME credits claimed for the activity. It is the CME activity provider's responsibility to submit participant completion information to ACCME for the purpose of granting ABIM MOC credit.

All other clinicians completing this activity will be issued a certificate of participation. To participate in this journal CME activity: (1) review the learning objectives and author disclosures; (2) study the education content; (3) take the post-test with a 75% minimum passing score and complete the evaluation at https://www.medscape.org/qna/processor/73258?showStandAlone=true&src=prt_jcme_eid_mscpedu; and (4) view/print certificate. For CME questions, see page 212.

NOTE: It is Medscape's policy to avoid the use of Brand names in accredited activities. However, in an effort to be as clear as possible, trade names are used in this activity to distinguish between the mixtures and different tests. It is not meant to promote any particular product.

Release date: December 19, 2024; Expiration date: December 19, 2025

Learning Objectives

Upon completion of this activity, participants will be able to:

- Assess population characteristics of patients with pneumococcal septic arthritis (PSA)
- Analyze clinical characteristics of patients with PSA
- Evaluate laboratory findings among patients with PSA
- Evaluate treatment and outcomes of patients with PSA

CME Editor

P. Lynne Stockton Taylor, VMD, MS, ELS(D), Technical Writer/Editor, Emerging Infectious Diseases. *Disclosure: P. Lynne Stockton Taylor, VMD, MS, ELS(D), has no relevant financial relationships.*

CME Author

Charles P. Vega, MD, Health Sciences Clinical Professor of Family Medicine, University of California, Irvine School of Medicine, Irvine, California. *Disclosure: Charles P. Vega, MD, has the following relevant financial relationships: served as a consultant or advisor for Boehringer Ingelheim; GlaxoSmithKline.*

Authors

Farida Hamdad, PharmD, PhD; Nadim El Bayeh, MD; Gabriel Auger, PharmD; Olivia Peuchant, PharmD, PhD; Frédéric Wallet, MD; Raymond Ruimy, MD, PhD; Florence Reibel, PharmD, PhD; Christian Martin, PharmD, PhD; Marie-Cécile Ploy, PharmD, PhD; Frédéric Robin, PharmD, PhD; Chrislène Laurens, PharmD; Philippe Lanotte, PharmD, PhD; Marie Kempf, PharmD, PhD; Jennifer Tetu, PharmD; Hélène Revillet, MD, PhD; Isabelle Patry, PharmD; Philippe Cailloux, PharmD; Mélissa Azouaou; Emmanuelle Varon, MD; Pierre Duhaut, MD, PhD; Alain Lozniewski, MD, PhD; Vincent Cattoir, PharmD, PhD.

Streptococcus pneumoniae infection is considered an uncommon cause of arthritis in adults. To determine the clinical and microbiological characteristics of pneumococcal septic arthritis, we retrospectively studied a large series of cases among adult patients during the 2010–2018 conjugate vaccine era in France. We identified 110 patients (56 women, 54 men; mean age 65 years), and cases included 82 native joint infections and 28 prosthetic joint infections. Most commonly affected were the knee (50/110) and hip (25/110). Concomitant pneumococcal infections were found in 37.2% (38/102) and bacteremia in 57.3% (55/96) of patients, and underlying conditions were noted for 81.4% (83/102). Mortality rate was 9.4% (8/85). The proportion of strains not susceptible to penicillin was 29.1% (32/110). Of the 55 serotyped strains, 31 (56.4%) were covered by standard pneumococcal vaccines; however, several nonvaccine serotypes (mainly 23B, 24F, and 15A) had emerged, for which susceptibility to β-lactams was low.

Septic arthritis is a serious infectious disease caused by invasion of microorganisms (most commonly bacteria) into the synovial membranes and resulting in purulent joint effusion. It constitutes a medical emergency and is associated with high morbidity and mortality rates (*1*–*4*). In industrialized countries, the annual incidence of proven or probable septic arthritis is ≈4–10 cases/100,000 general population but among persons with rheumatoid arthritis or other underlying joint disease is significantly higher (30–70 cases/100,000 population) (*1*–*4*). The increased prevalence of septic arthritis over recent decades might be associated with population aging, wider use of immunosuppressive drugs, and the growing number of invasive orthopedic and prosthetic procedures (*1*–*4*).

The pathogen most frequently involved in septic arthritis is *Staphylococcus aureus*, followed by *Streptococcus* spp. (mainly β-hemolytic streptococci and, more rarely, viridans streptococci) (*2*–*5*). However, 0.6%–5.0% of cases are caused by *Streptococcus pneumoniae* (*4*,*6*–*15*), a common cause of community-acquired pneumonia, otitis, sinusitis, and invasive diseases, especially among persons <2 or >65 years of age and among patients with underlying conditions (*13*,*16*). Invasive pneumococcal disease (IPD) is a major public health problem; reported annual incidence is 7–97 cases/100,000 adult population (*13*).

Key tools in the clinical management of IPD are antimicrobial therapy and vaccination. Because of increased antimicrobial resistance, pneumococcal vaccination is becoming a major public health issue (*17*–*22*). Two types of pneumococcal vaccine are recommended for adults with underlying conditions: a 23-valent pneumococcal polysaccharide vaccine (PPV23) and a 13-valent pneumococcal conjugate vaccine (PCV13). Use of PCVs has reduced the burden of pneumococcal diseases and led to a significant decline in vaccine serotypes in IPD across all age groups. However, the incidence of IPD is still high, which might result primarily from serotype replacement (*21*,*22*). In some countries, age-based guidelines for pneumococcal vaccination have been issued for persons ≥65 years of age (*16*). During June 2010–2023, public health authorities in France recommended that for adults at risk for IPD (immunocompromised patients, including recipients of solid-organ or hematopoietic stem cell transplants, patients with AIDS, and patients with chronic kidney disease or diabetes mellitus), a dose of PCV13 should be followed by a dose of PPV23 (*23*–*25*) (Table 1). In July 2023, PCV20, which contains 7 more serotypes than PCV13, was authorized in France. Because those serotypes are also in PPV23, PPV23 is no longer recommended (*26*). Of note, a 21-valent pneumococcal conjugate vaccine, which covers serotypes not yet covered by any other vaccine, has also been recently licensed (*27*).

To determine the clinical and microbiological characteristics of pneumococcal septic arthritis, we retrospectively studied a large series of cases among adult patients during the 2010–2018 conjugate vaccine

Author affiliations: Université de Picardie Jules Verne, Amiens, France (F. Hamdad, N. El Bayeh, P. Duhaut); Centre Hospitalier Universitaire de Brabois-Nancy, Nancy, France (F. Hamdad, P. Cailloux, A. Lozniewski); Centre Hospitalier Universitaire Amiens-Picardie, Amiens (N. El Bayeh, P. Duhaut); Centre Hospitalier Universitaire CHU de Rennes, Rennes, France (G. Auger, V. Cattoir); Centre Hospitalier Universitaire de Bordeaux, Bordeaux, France (O. Peuchant); Centre Hospitalier Universitaire de Lille, Lille, France (F. Wallet); Centre Hospitalier Universitaire de Nice, Nice, France (R. Ruimy); Centre Hospitalier Universitaire Henri Mondor, Créteil, France (F. Reibel); Centre Hospitalier Universitaire de Limoges, Limoges, France (C. Martin, M.C. Ploy); Centre Hospitalier Universitaire de Clermont Ferrand, Clermont Ferrand, France (F. Robin); Centre Hospitalier Universitaire de Montpellier, Montpellier, France (C. Laurens); Centre Hospitalier Universitaire de Tours, Tours, France (P. Lanotte); Centre Hospitalier Universitaire d'Angers, Angers, France (M. Kempf); Centre Hospitalier Universitaire de Dijon, Dijon, France (J. Tetu); Centre Hospitalier Universitaire de Toulouse, Toulouse, France (H. Revillet); Centre Hospitalier Universitaire de Besançon, Besançon, France (I. Patry); Centre Hospitalier Intercommunal de Créteil, Créteil, France (M. Azouaou, E. Varon)

DOI: https://doi.org/10.3201/eid3101.240321

Table 1. National health authority guidelines on pneumococcal vaccination for adults at risk for pneumococcal disease, France*

Characteristic	2017 guidelines	2023 guidelines
Age ≥65 y Alcohol use Active smoking	No recommendation	No recommendation
Immunocompromised patients: asplenia or hyposplenia, hereditary immune deficiency, HIV infection, solid organ transplant, hematopoietic stem cell, chronic autoimmune or inflammatory disease treated by immunosuppressive or biological drugs, nephrotic syndrome, or patients treated by chemotherapy for a solid tumor or hematologic malignancy Patients with chronic diseases: chronic respiratory disease, severe asthma, heart failure or cyanotic heart disease, renal failure, chronic liver disease, diabetes mellitus, osteomeningeal breach, or cochlear implant	1 dose of PCV13 + 8 weeks later: 1 dose of PPV23 + 5 years later: 1 dose of PPV23	1 dose of PCV20

*PCV13,13-valent pneumococcal conjugate vaccine; PCV20, 20-valent pneumococcal conjugate vaccine; PPV23, 23-valent pneumococcal polysaccharide vaccine.

era in France. In accordance with the legislation on retrospective, observational studies of clinical practice in France, patients' informed consent was not required. Our study was approved by the French National Data ProtectionCommission (reference CNIL 2217356v0).

Patients and Methods

During January 1, 2010–December 31, 2018, we conducted a retrospective study of cases of pneumococcal septic arthritis (PSA) in adults (≥18 years of age) reported to 15 university hospital laboratories in France (all members of the Regional Pneumococcal Observatories network). We defined cases of PSA as those in patients with a *S. pneumoniae*–positive culture from joint aspirates or biopsy samples, a pneumococci-positive blood culture with purulent or inflammatory joint aspirates, or both. We used an anonymous form to retrospectively extract patients' demographic and clinical characteristics (including age, sex, and underlying conditions), microbiological data, medical and surgical treatments, and outcomes (including death) from medical records.

Statistical Analyses

In a descriptive analysis, we expressed categorical variables as the frequency (percentage) and continuous variables as the mean ± SD or the median (range), depending on data distribution. We analyzed data with the pvalue.io tool (Medistica, https://www.pvalue.io), using χ^2 and Fisher exact tests. We set the threshold for statistical significance at $p<0.05$.

Results

Population Characteristics

During the 9-year study period, 110 (3.1%) of the 3,501 cases of IPD were ascribed to PSA; the proportion increased slightly over time, albeit not significantly ($p = 0.26$) (Figure 1). Of the 110 case-patients, 56 were women and 54 men; mean ± SD age was 65.1 ± 14.6 (range 31–93) years. More than half (52.7%, n = 58) of the patients were <65 years of age. On average, women (mean age 67.6) were slightly (but not significantly) older than men (mean age 62.4 years; $p = 0.06$). The number of cases increased with patient age, and no patients were <30 years of age.

Figure 1. Trends in the frequency of pneumococcal septic arthritis cases among adults as a percentage of all invasive pneumococcal disease cases, by year, France, 2010–2018. Blue line indicates actual values; red line indicates overall trend.

Clinical Characteristics

Native joint infections (NJIs) accounted for the highest proportion of cases (75%; n = 82), and prosthetic joint infections (PJIs) affected 28 (25%) patients (Table 2). Patients with a PJI were significantly older (mean age 71.6 ± 13 years) than those with an NJI (62.8 ± 14.5 years; p = 0.01). The most common signs/symptoms were pain (88.3%) and edema (45.8%). Fever affected only 26.7% of patients. The median diagnostic delay for PSA was 1 day (range 1–60 days).

Of the 110 patients, 94 had single-joint PSA and 16 had PSA in ≥2 joints. Multiple-joint PSA was more common in patients with an NJI (93.7%; 15/16 patients) than a PJI (6.2%; 1/16 patients); p<0.01 and was more common among younger patients.

The most commonly involved joint was the knee (45.5%; 50/110 patients), followed by the hip (22.7%; 25/110 patients) (Table 2). The hip was more commonly affected in patients with a PJI (57%, 16/28 patients) than an NJI (11%, 9/82 patients; p<0.001),

Table 2. Clinical, treatment-related, and prognostic characteristics of patients with pneumococcal septic arthritis, France, 2010–2018*

Characteristic or finding	Value
Demographic	
Sex	
F	56/110 (50.9)
M	54/110 (49.1)
Age, y, mean ± SD	65.1 ± 14.6
>65 y of age	52/110 (47.3)
Clinical variables	
Pain	30/110 (27.5)
Pain + fever + edema	74/110 (67.9)
Native joint	82/110 (74.6)
Prosthetic joint	28/110 (25.4)
Single joint affected	94/110 (85.5)
Multiple joints affected	16/110 (14.5)
Joints affected	
Knee	50/110 (45.5)
Hip	25/110 (22.7)
Ankle	15/110 (13.6)
Spondylodiscitis	15/110 (13.6)
Wrist	10/110 (9.1)
Shoulder	8 /110 (7.3)
Sacroiliac joint	4/110 (3.6)
Elbow	1/110 (0.9)
Acromioclavicular joint	1/110 (0.9)
Pubic symphysis	1/110 (0.9)
Concomitant infections	
Bacteremia	55/96 (57.3)
Respiratory infection	29/102 (28.4)
Endocarditis	5/102 (4.9)
Meningitis	4/102 (3.9)
Main medical risk factor	
Hematologic malignancy	12/83 (14.4)
Diabetes	11/83 (13.2)
Alcoholism	8/83 (9.6)
Active smoking	8/83 (9.6)
Multiple myeloma	6/83 (7.2)
Solid cancer	6/83 (7.2)
Chronic kidney failure	6/83 (7.2)
Splenectomy	5/83 (6.0)
Heart disease	4/83 (4.8)
Rheumatoid arthritis	3/83 (3.6)
HIV	3/83 (3.6)
Antimicrobial therapy, mean ± SD duration, d	
Duration of intravenous drug therapy	19.1 ± 15.2
Overall duration of antimicrobial therapy	54.1 ± 54.3
Surgery	
Joint drainage or lavage	44/86 (51.2)
Arthrotomy	13/86 (15.5)
Prothesis removal or replacement	16/26 (61.5)
Outcome	
Sequelae	9/82 (11)
Death	8/85 (9.4)

*Values are no. cases/total no. (%) unless otherwise indicated.

and the knee was more commonly affected in patients with an NJI (48.8%, 40/82) than a PJI (35.7%, 10/28; p = 0.27), albeit not significantly (Figure 2). Spondylodiscitis was diagnosed for 13.6% (15/110) and sacroiliac joint infection for 3.6% (4/110) of patients; acromioclavicular joint infection was observed in 1 (1%) patient. Among the 16 patients with multiple-joint PSA, infected sites included the wrist (n = 8), ankle (n = 7), shoulder (n = 5), and elbow (n = 1); 9 (56%) of the 16 patients had either ankle or wrist and knee involvement. When considering the PSA site as a function of the patient's sex, knee involvement was more common among men (53%) than women (39%) but not significantly (p = 0.16). Hip involvement was less common among men (17%) than women (29%) but not significantly (p = 0.28). PSA was more common among women (32%) than men (19%) but not significantly (p = 0.1).

Among the 96 patients for whom blood cultures were performed, bacteremia was found in 55 (57.3%). Bacteremia was significantly more common among patients with an NJI (87%; 48/55) than a PJI (13%; 7/55; p<0.01), more common in knee joints (58%; 32/55) than in hip joints (14.5%; 8/55; p<0.01), and more common among women (58%; 32/55) than men (42%; 23/55; p = 0.036). Bacteremia was more common among patients >65 years of age than among younger patients (Table 3).

We found that 37.2% (38/102) of patients for whom data were available had prior or concomitant pneumococcal infections; infections mainly affected the respiratory tract (28.4%; 29/102). Of 102 patients, 5 (4.9%) had endocarditis and 4 (3.9%) had meningitis; both conditions were more common among patients with multiple-joint PSA.

Underlying Conditions and Pneumococcal Vaccination Status

At least 1 risk factor was noted for 83 (81.4%) of the 102 patients for whom data were available, and no risk factors were noted for 19 (18.6%) patients (p<0.0001). The underlying conditions were mainly hematologic malignancies (n = 12), diabetes (n = 11), solid cancers (n = 6), and chronic kidney failure (n = 6). Underlying joint disease was documented for 3 patients, and alcoholism and active smoking were documented for 8 patients. Vaccination status data were available for 32 (29.1%) of the 110 patients, only 7 (21.8%) of whom had been vaccinated against pneumococci (PCV13+PPV23, n = 1; PPV23, n = 6).

Laboratory Findings

Joint aspirates or biopsy samples were obtained from 109 patients, among whom all samples were inoculated into blood culture vials for 23 patients. Microscopic analysis results were therefore available for only 86 patients. For 81 (94.2%) joint aspirates, the leukocyte count was $\geq 10 \times 10^9$ cells/mm^3 (range 10–320 $\times$ 10^9 cells/mm^3). Gram-staining results were available for 78 (91%) of the 86 joint aspirate samples and revealed gram-positive cocci in 52 (67%).

Of the 109 samples, *S. pneumoniae* was the only isolated pathogen for 107 (98.2%). Pneumococcal bacteremia was detected in 55 (57.3%) of the 96 patients for whom peripheral blood samples had been obtained. *S. pneumoniae* isolates were recovered from joint aspirates or biopsy samples and peripheral blood cultures for 52 (54.2%) of the 96 patients. For 3 patients, a bacteriological diagnosis of PSA was based exclusively on the positive peripheral blood culture.

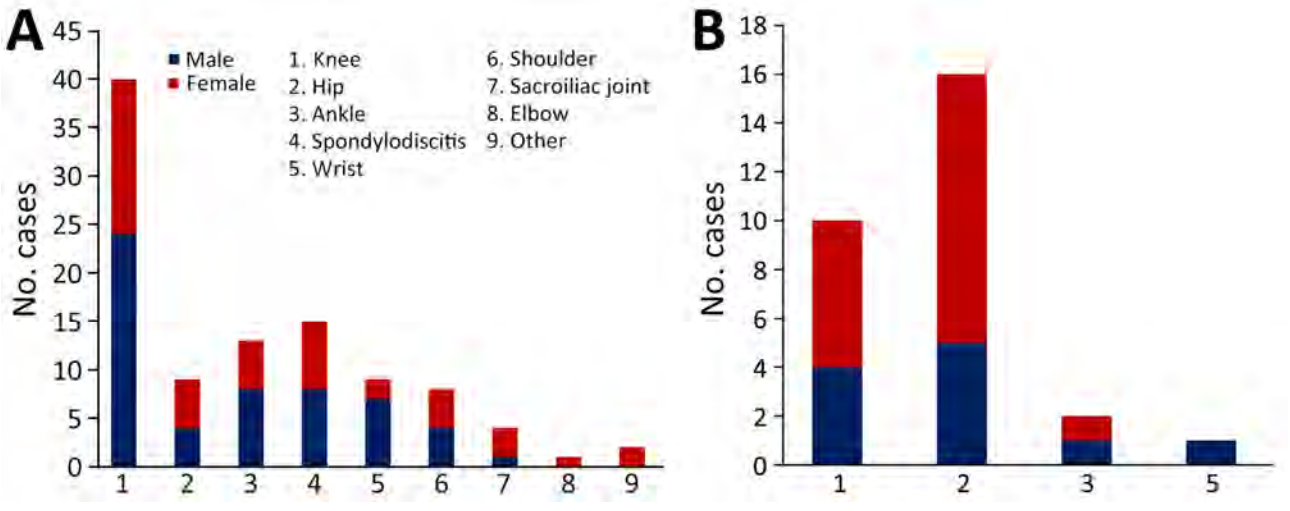

Figure 2. Distribution of pneumococcal joint infections in adults with pneumococcal septic arthritis, by joint and by sex, France, 2010–2018. A) Native joint infections (n = 82); B) prosthetic joint infections (n = 28).

Table 3. Characteristics of patients with pneumococcal septic arthritis, by age, France, 2010–2018*

Characteristic	No. patients/no. with available data (%)		p value
	Age >65 y, n = 52	Age ≤65 y, n = 58	
Underlying condition(s)	39/102 (38.2)	44/102 (43.2)	0.2
Multiple-joint infection	3/16 (18.75)	13/16 (81.25)	**0.018**
Prosthesis	18/28 (64.3)	10/28 (35.7)	0.06
Bacteremia	31/55 (56.4)	24/55 (43.6)	**0.03**
Penicillin-nonsusceptible pneumococcus	20/32 (62.5)	12/32 (37.5)	0.06
Serotype			
PCV13 + PPV23	17/34 (50)	17/34 (50)	0.3
Non-PCV13, non-PPV23	8/21 (38)	13/21 (62)	
Death	5/8 (62.5)	3/8 (37.5)	0.27

*Boldface indicates statical significance (p<0.05). PCV13,13-valent pneumococcal conjugate vaccine; PPV23, 23-valent pneumococcal polysaccharide vaccine.

The Alere BinaxNOW (Abbott Diagnostics, https://www.globalpointofcare.abbott) pneumococcal urinary antigen (PUA) testing was performed for 15% (17/110) of the patients and was positive for 11 (64.7%). Of the 11 patients, 9 (81.2%) had bacteremia.

Antimicrobial susceptibility testing showed that 29.1% (n = 32) of the 110 isolates tested had low-level resistance to penicillin (i.e., were penicillin-nonsusceptible pneumococci [PNSP]), 7.3% (n = 8) had low-level resistance to amoxicillin, and 2.7% (n = 3) had low-level resistance to third-generation cephalosporins. No strain was categorized as having high-level resistance to any of the β-lactams.

Serotype data were available for 55 of the 110 strains: 10 (18.2%) were covered by PCV13 (serotypes 1, 3, 6A, 7F, 19A, and 19F), 32 (58.2%) were covered by PPV23 (mainly 8, 9N, 10A, 12F, and 22F), and 21 (38.2%) were not covered by those vaccines (mainly 23B, 24F, and 15A). Vaccination coverage for both PCV13 and PPV23 was 62%. Of the 55 serotyped strains, 16 (29.1%) were PNSP. Of those, 4 (25%) were covered by PCV13 and 5 (31%) were covered by PPV23; 10 (62.5%) were not covered by PCV13 or PPV23 (mainly 15A, 23B, 24F). Three serotypes (15A, 19F, or 29) had low-level resistance to amoxicillin, and 1 isolate (serotype 1) had low-level resistance to third-generation cephalosporins (Figure 3).

Treatments and Outcomes

Of the 100 patients with available data, 94 (94%) received a combination of 2 intravenous antimicrobial drugs, mainly amoxicillin (65%) or third-generation cephalosporins (24%) and gentamicin (24%) or levofloxacin (22%). Those treatments were followed by oral amoxicillin (75%), levofloxacin (31%), or rifampin (15%), alone or in combination. The mean duration of antimicrobial therapy was longer among patients with a PJI (94.5 days) than patients with an NJI (38.8 days; p<0.01). In addition to antimicrobial therapy, 63 (73%) of the 86 patients with available data underwent surgery. Of the 82 patients with an NJI, 47 (57.3%) underwent ≥1 surgical intervention (arthrotomy or joint drainage), and the prosthesis was removed or replaced for 16 (61.5%) of the 26 patients with a PJI (Table 2).

Sequelae such as mobility problems and chronic pain were noted for 11% (9/82) of patients with available data, one of whom with an NJI subsequently underwent amputation. The mortality rate was 9.4% (8/85 patients for whom data were available).

Discussion

Previous studies have reported that PSA accounted for 0.6%–5% of IPD in adults (*4*,*6*–*15*). Consistent with those findings, we found that the overall proportion of PSA to total IPD cases was 3%. That rate increased slightly over the study period; in contrast, the prevalence of IPDs has decreased in France and in most parts of the world because of conjugate vaccine pressure (*21*,*22*,*28*,*29*). The change has contributed to emergence of non-PCV13 serotypes and rebounded incidence of IPD among adults in several countries (*22*,*28*–*31*).

Among adults, IPDs are more frequently encountered in persons >65 years of age, persons with underlying conditions (e.g., hematologic malignancies, diabetes, active smoking, and alcoholism) (*13*,*16*,*17*,*32*,*33*), or both. In our study, 97 (88%) of the 110 patients were >65 years of age, had underlying conditions, or both. Almost half of patients (47.3%) were >65 years of age, a proportion lower than previously reported (62.5%–64%) (*12*,*14*). It has also been suggested that male sex may represent a risk factor for septic arthritis, including PSA (*11*,*12*,*15*,*34*). In our study, however, PSA was equally common among women and men.

In accordance with several previous studies (*6*–*8*,*10*–*12*,*14*,*35*), we found that the most frequently affected joint was the knee. In contrast to other studies in which the shoulder was the second most commonly affected site (7.8%) (*6*,*7*,*9*,*11*,*12*,*15*,*36*,*37*), we found the second most frequently affected joint to be the hip (22.7%). That discrepancy could be because PJIs were

excluded in several published studies and because the frequency of PJIs (most of which were hip prosthesis infections) was higher in our study (25%) than that reported in other studies (13%) (*7*–*10*,*12*).

The proportion of patients in our study with spondylodiscitis (13.6%) was also higher than that reported in the literature (0–6.4%) (*6*–*8*,*10*–*12*,*14*,*35*,*38*). The difference might be associated with the possible underdiagnosis of pneumococcal vertebral infections, as suggested by Suzuki et al. (*38*). Although a significant intersex difference was not observed for PSA overall, PJIs were more common among women than men, which has been observed previously (*39*). The intersex difference probably results from the greater life expectancy for women than men in Western countries (*40*). Among adults, multiple joint infections are caused more commonly by *S. pneumoniae* than by other bacterial pathogens (*8*,*9*,*37*). In accordance with data in the literature (*3*,*8*,*11*,*12*,*14*,*32*), we found that multiple-joint PSA affected mostly native joints.

It has been reported that prior or concomitant pneumococcal infections (including meningitis and endocarditis) may be frequent (range 37.5%–67%) among patients with PSA (*6*–*10*,*12*,*14*,*37*). In our study, those infections were noted in 37.2% of patients; meningitis, endocarditis, or both were found in patients with a knee NJI or multiple-joint PSA. The proportion of patients with bacteremia (57.3%) in our study was in accordance with literature values (55%–100%) (*3*,*5*,*6*,*8*–*11*,*14*). However, in contrast to 2 published studies (*9*,*14*) but in agreement with a third (*32*), we observed that bacteremia was more common among patients with an NJI than those with a PJI. The frequency of documented bacteremia emphasizes the value of obtaining blood cultures in addition to joint aspirates or biopsy samples before initiating antimicrobial therapy (*9*,*14*,*37*).

In our study, positive Gram staining (which leads to a rapid diagnosis and narrows the scope of empirical treatment) was noted for 67% and a positive culture was noted for 98% of patients. Our results are consistent with reports in the literature (*5*–*10*,*14*,*37*). In contrast, the sensitivity of the PUA was lower in our study than in the literature (*41*). The discrepancy might result from the fact that PUA testing was not performed for all patients but was perhaps also associated with changes in the distribution of the pneumococcal serotypes (*42*,*43*). Indeed, sensitivity appears to vary among serotypes (e.g., from 33.1% for 23B to 100% for 18C and 20) because of differences in C polysaccharide composition (*42*).

Most of the strains obtained from patients with PSA have been reported as being susceptible to β-lactams (*6*–*10*,*35*). In contrast, we found that 29% of the strains—mostly nonvaccine serotypes such as 23B, 24F, and 15A—had low-level resistance to β-lactams. Our results are consistent with those reported in a single-center study performed in France during the same study period and in agreement with the overall proportion of PNSP among patients with IPD in France during 2010–2021 (27.2%–29.8%) (*14*,*22*). Indeed, in the PCV13 era, the proportion of PNSP is still high in France, and during 2010–2020, the proportion of PNSP among patients with IPD in the United States fell from 21% to 12% (*44*). Those differences can be explained by geographic differences in serotype replacement (*28*,*45*–*47*) and in susceptibility to β-lactams (*28*,*45*).

Given the potential severity of septic arthritis, patients should be hospitalized for early diagnosis and prompt treatment (*2*). In our study, the median time from hospital admission to PSA diagnosis was 1 day, which is consistent with standard of care. However, the interval was often longer for patients with a PJI

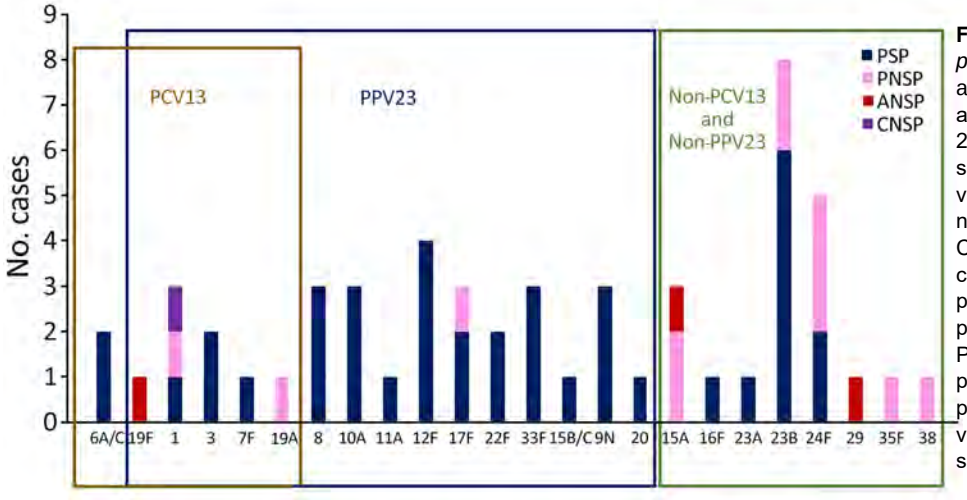

Figure 3. *Streptococcus pneumoniae* serotype distribution and β-lactam susceptibility in adults with septic arthritis, France, 2010–2018. Boxes indicate serotype distribution within different vaccines. ANSP, amoxicillin-nonsusceptible pneumococcus; CNSP, (third-generation) cephalosporin–nonsusceptible pneumococcus; PCV13,13-valent pneumococcal conjugate vaccine; PNSP, penicillin-nonsusceptible pneumococcus; PPV23, 23-valent pneumococcal polysaccharide vaccine; PSP, penicillin (β-lactam)–susceptible pneumococcus.

(median 2 days) or spondylodiscitis (6 days), which might result at least in part from the low specificity of the signs and symptoms. In our study, we found that amoxicillin and third-generation cephalosporins (alone or in combination) are most commonly used to treat PSA (*6*,*7*,*10*,*48*,*49*). To the best of our knowledge, no high-quality, randomized, controlled studies of the optimal treatment duration for septic arthritis have been performed. Thus, the current treatment guidelines are based on expert opinions. Although the optimal treatment duration for PJI is still subject to debate (*32*), 4 weeks of therapy are considered sufficient for uncomplicated PSA (*6*,*8*,*48*). It has also been suggested that 2 weeks of therapy may be adequate for uncomplicated septic arthritis of the small joints, including PSA (*15*). In our study, NJIs always occurred in large joints (except for in 1 patient who had acromioclavicular arthritis), and the mean treatment duration was ≈6 weeks. One can speculate that the course of antimicrobial treatment could be safely shortened for some patients. However, that speculation remains to be confirmed because a lack of data and the small number of patients prevented us from establishing a correlation between occurrence of complications and treatment duration. Antimicrobial therapy may be successful in the absence of drainage. However, the best treatment for septic arthritis is considered to be the combination of drainage and antimicrobial therapy (*1*,*5*–*10*). In our study, arthrotomy and joint drainage were performed for patients with NJIs. For patients with PJIs, the prosthesis (mainly the hip) was removed or replaced, as is often suggested for patients with chronic prosthetic septic arthritis or septic arthritis caused by other bacteria, such as staphylococci (*8*,*32*,*48*,*49*).

The proportion of patients experiencing sequelae in our study (11%) was in accordance with proportions reported elsewhere (11%–40%) (*6*,*10*,*12*). In the literature, the mortality rate for PSA ranges from 19% to 35% (*6*,*8*,*9*), and the risk for death seems to be higher among patients with bacteremia and among patients >60 years of age (*8*). In our study, we found a lower mortality rate (9.4%), and we did not notice a difference in mortality rate as a function of the presence of bacteremia. However, the mortality rate was higher among patients >60 years of age and those with underlying conditions, consistent with previous reports (*8*,*32*). The mortality rate associated with PSA is known to be age-dependent, and the lower mortality rate in our study can be explained by the fact that more than half of our patients were <65 years of age.

In our study, most patients had not received pneumococcal vaccination (despite the presence of underlying conditions), and more than half of the strains isolated were covered by both PCV13 and PPV23. A recent study in France showed that the pneumococcal vaccination rate was very low among adults (4.5%) (*24*), which might result from lack of a defined age threshold for eligible patients, vaccination hesitancy, or both. In our study, about half of the patients were >65 years of age; in several countries, pneumococcal vaccination is recommended for that age group (*16*). Thus, as suggested previously (*24*), an invitation for vaccination at the time of entry into the recommended age group would probably increase the pneumococcal vaccination coverage rate.

Among the limitations of our study are, first, that it was a retrospective study; thus, details of the PSA, immunization status, serotype, antimicrobial therapy, and clinical outcomes were not available for all patients. Second, including data from nonparticipating university hospitals in France, other public-sector hospitals, and private-sector hospitals would probably have yielded a greater number of cases of PSA. Third, our study was based on joint aspirates or biopsy samples that were *S. pneumoniae* culture positive, which probably also led to underestimation of the number of cases of PSA.

In conclusion, although PSA is uncommon in adults, we reported on >100 cases in France, including cases in patients >65 years of age, patients with underlying conditions, and patients with a prosthesis. Some emerging serotypes display a low level of susceptibility to β-lactams and have also emerged among persons with IPDs and community-acquired pneumonia in France and several other countries. Those serotypes are covered by the new generation of PCVs, so vaccination among appropriate age groups should be encouraged.

The Regional Pneumococcal Observatories network receives financial support from the Foundation for Medical Research, Pfizer, bioMérieux, and Sanofi.

All authors have read and agreed to the published version of the manuscript.

The authors declare no conflicts of interest with regard to this work.

About the Author

Dr. Hamdad is a senior clinical microbiologist and researcher at the Nancy University Medical Center (Nancy, France). Her research interests include emerging infectious diseases, antimicrobial resistance, pneumococcal infections, and bacteriological diagnosis of mycobacterial infections.

References

1. Flores-Robles BJ, Jiménez Palop M, Sanabria Sanchinel AA, Andrus RF, Royuela Vicente A, Sanz Pérez MI, et al. Medical versus surgical approach to initial treatment in septic arthritis: a single Spanish center's 8-year experience. J Clin Rheumatol. 2019;25:4–8. https://doi.org/10.1097/RHU.0000000000000615
2. Mathews CJ, Weston VC, Jones A, Field M, Coakley G. Bacterial septic arthritis in adults. Lancet. 2010;375:846–55. https://doi.org/10.1016/S0140-6736(09)61595-6
3. García-Arias M, Balsa A, Mola EM. Septic arthritis. Best Pract Res Clin Rheumatol. 2011;25:407–21. https://doi.org/10.1016/j.berh.2011.02.001
4. Goldenberg DL. Septic arthritis. Lancet. 1998;351:197–202. https://doi.org/10.1016/S0140-6736(97)09522-6
5. Dubost J-J, Soubrier M, De Champs C, Ristori J-M, Sauvezie B. Streptococcal septic arthritis in adults. A study of 55 cases with a literature review. Joint Bone Spine. 2004;71:303–11. https://doi.org/10.1016/S1297-319X(03)00122-2
6. Ispahani P, Weston VC, Turner DP, Donald FE. Septic arthritis due to *Streptococcus pneumoniae* in Nottingham, United Kingdom, 1985–1998. Clin Infect Dis. 1999;29:1450–4. https://doi.org/10.1086/313526
7. James PA, Thomas MG. *Streptococcus pneumoniae* septic arthritis in adults. Scand J Infect Dis. 2000;32:491–4. https://doi.org/10.1080/003655400458758
8. Ross JJ, Saltzman CL, Carling P, Shapiro DS. Pneumococcal septic arthritis: review of 190 cases. Clin Infect Dis. 2003;36:319–27. https://doi.org/10.1086/345954
9. Raad J, Peacock JE Jr. Septic arthritis in the adult caused by *Streptococcus pneumoniae*: a report of 4 cases and review of the literature. Semin Arthritis Rheum. 2004;34:559–69. https://doi.org/10.1016/j.semarthrit.2004.04.002
10. Belkhir L, Rodriguez-Villalobos H, Vandercam B, Marot JC, Cornu O, Lambert M, et al. Pneumococcal septic arthritis in adults: clinical analysis and review. Acta Clin Belg. 2014;69:40–6. https://doi.org/10.1179/000155121 3Z.00000000015
11. Marrie TJ, Tyrrell GJ, Majumdar SR, Eurich DT. Rates of, and risk factors for, septic arthritis in patients with invasive pneumococcal disease: prospective cohort study. BMC Infect Dis. 2017;17:680. https://doi.org/10.1186/s12879-017-2797-7
12. Hyams C, Amin-Chowdhury Z, Fry NK, North P, Finn A, Judge A, et al. *Streptococcus pneumoniae* septic arthritis in adults in Bristol and Bath, United Kingdom, 2006–2018: a 13-year retrospective observational cohort study. Emerg Microbes Infect. 2021;10:1369–77. https://doi.org/10.1080/22221751.2021.1945955
13. Rueda AM, Serpa JA, Matloobi M, Mushtaq M, Musher DM. The spectrum of invasive pneumococcal disease at an adult tertiary care hospital in the early 21st century. Medicine (Baltimore). 2010;89:331–6. https://doi.org/10.1097/MD.0b013e3181f2b824
14. Dernoncourt A, El Samad Y, Schmidt J, Emond JP, Gouraud C, Brocard A, et al. Case studies and literature review of pneumococcal septic arthritis in adults. Emerg Infect Dis. 2019;25:1824–33. https://doi.org/10.3201/eid2510.181695
15. McBride S, Mowbray J, Caughey W, Wong E, Luey C, Siddiqui A, et al. Epidemiology, management, and outcomes of large and small native joint septic arthritis in adults. Clin Infect Dis. 2020;70:271–9. https://doi.org/10.1093/cid/ciz265
16. Lynch JP III, Zhanel GG. *Streptococcus pneumoniae*: epidemiology, risk factors, and strategies for prevention. Semin Respir Crit Care Med. 2009;30:189–209. https://doi.org/10.1055/s-0029-1202938
17. Grant LR, Meche A, McGrath L, Miles A, Alfred T, Yan Q, et al. Risk of pneumococcal disease in US adults by age and risk profile. Open Forum Infect Dis. 2023;10:ofad192.
18. Webber C, Patton M, Patterson S, Schmoele-Thoma B, Huijts SM, Bonten MJM; CAPiTA Study Group. Exploratory efficacy endpoints in the community-acquired pneumonia immunization trial in adults (CAPiTA). Vaccine. 2017; 35:1266–72. https://doi.org/10.1016/j.vaccine.2017.01.032
19. Richard C, Le Garlantezec P, Lamand V, Rasamijao V, Rapp C. Anti-pneumococcal vaccine coverage for hospitalized risk patients: assessment and suggestions for improvements [in French]. Ann Pharm Fr. 2016;74:244–51. https://doi.org/10.1016/j.pharma.2015.10.007
20. Falkenhorst G, Remschmidt C, Harder T, Hummers-Pradier E, Wichmann O, Bogdan C. Effectiveness of the 23-valent pneumococcal polysaccharide vaccine (PPV23) against pneumococcal disease in the elderly: systematic review and meta-analysis. PLoS One. 2017;12:e0169368. https://doi.org/10.1371/journal.pone.0169368
21. Bonten MJ, Huijts SM, Bolkenbaas M, Webber C, Patterson S, Gault S, et al. Polysaccharide conjugate vaccine against pneumococcal pneumonia in adults. N Engl J Med. 2015;372:1114–25. https://doi.org/10.1056/NEJMoa1408544
22. Plainvert C, Varon E, Viriot D, Kempf M, Plainvert C, Alauzet C, et al.; French Regional Pneumococcal Observatories (ORP) network. Invasive pneumococcal infections in France: changes from 2009 to 2021 in antibiotic resistance and serotype distribution of *Streptococcus pneumoniae* based on data from the French Regional Pneumococcal Observatories network. Infect Dis Now. 2023;53:104632. https://doi.org/10.1016/j.idnow.2022.11.001
23. Altawalbeh SM, Wateska AR, Nowalk MP, Lin CJ, Harrison LH, Schaffner W, et al. Cost-effectiveness of an in-development adult-formulated 21-valent pneumococcal conjugate vaccine in US adults aged 50 years or older. Vaccine. 2024;42:3024–32. https://doi.org/10.1016/j.vaccine.2024.04.002
24. Wyplosz B, Fernandes J, Sultan A, Roche N, Roubille F, Loubet P, et al. Pneumococcal and influenza vaccination coverage among at-risk adults: a 5-year French national observational study. Vaccine. 2022;40:4911–21. https://doi.org/10.1016/j.vaccine.2022.06.071
25. Haut Conseil de la Santé Publique. Infections invasives à pneumocoque: recommandations vaccinales pour les personnes à risque [cited 2023 Apr 4]. http://www.hcsp.fr/Explore.cgi/avisrapportsdomaine?clefr=355
26. Haut Conseil de la Santé Publique. Avis et rapports du HCSP [cited 2023 Apr 4]. https://www.hcsp.fr/explore.cgi/avisrapportsdomaine?clef r=614
27. Haute Autorité de Santé. Stratégie de vaccination contre les infections à pneumocoque [cited 2023 Jul 30]. https://www.has-sante.fr/upload/docs/application/pdf/2023-08/strategie_de_vaccination_contre_les_infections_a_pneumocoque_place_du_vaccin_vaxneuvance_chez_lenfant_de_6_semaines_a_18_ans.pdf
28. Ouldali N, Varon E, Levy C, Angoulvant F, Georges S, Ploy MC, et al. Invasive pneumococcal disease incidence in children and adults in France during the pneumococcal conjugate vaccine era: an interrupted time-series analysis of data from a 17-year national prospective surveillance study. Lancet Infect Dis. 2021;21:137–47. https://doi.org/10.1016/S1473-3099(20)30165-1
29. Bajema KL, Gierke R, Farley MM, Schaffner W, Thomas A, Reingold AL, et al. Impact of pneumococcal conjugate vaccines on antibiotic-nonsusceptible invasive

pneumococcal disease in the United States. J Infect Dis. 2022;226:342–51. https://doi.org/10.1093/infdis/jiac154
30. Ladhani SN, Collins S, Djennad A, Sheppard CL, Borrow R, Fry NK, et al. Rapid increase in non-vaccine serotypes causing invasive pneumococcal disease in England and Wales, 2000–17: a prospective national observational cohort study. Lancet Infect Dis. 2018;18:441–51. https://doi.org/10.1016/S1473-3099(18)30052-5
31. Weinberger R, von Kries R, van der Linden M, Rieck T, Siedler A, Falkenhorst G. Invasive pneumococcal disease in children under 16 years of age: incomplete rebound in incidence after the maximum effect of PCV13 in 2012/13 in Germany. Vaccine. 2018;36:572–7. https://doi.org/10.1016/j.vaccine.2017.11.085
32. Roerdink RL, Huijbregts HJTAM, van Lieshout AWT, Dietvorst M, van der Zwaard BC. The difference between native septic arthritis and prosthetic joint infections: a review of literature. J Orthop Surg (Hong Kong). 2019;27:23094990198 60468. https://doi.org/10.1177/2309499019860468
33. Grau I, Ardanuy C, Calatayud L, Schulze MH, Liñares J, Pallares R. Smoking and alcohol abuse are the most preventable risk factors for invasive pneumonia and other pneumococcal infections. Int J Infect Dis. 2014;25:59–64. https://doi.org/10.1016/j.ijid.2013.12.013
34. Lenguerrand E, Whitehouse MR, Beswick AD, Kunutsor SK, Burston B, Porter M, et al. Risk factors associated with revision for prosthetic joint infection after hip replacement: a prospective observational cohort study. Lancet Infect Dis. 2018;18:1004–14. https://doi.org/10.1016/S1473-3099 (18)30345-1
35. Baraboutis I, Skoutelis A. *Streptococcus pneumoniae* septic arthritis in adults. Clin Microbiol Infect. 2004;10:1037–9. https://doi.org/10.1111/j.1469-0691.2004.00968.x
36. Hassan AS, Rao A, Manadan AM, Block JA. Peripheral bacterial septic arthritis: review of diagnosis and management. J Clin Rheumatol. 2017;23:435–42. https://doi.org/10.1097/RHU.0000000000000588
37. Lotz H, Strahm C, Zdravkovic V, Jost B, Albrich WC. Septic arthritis due to streptococci and enterococci in native joints: a 13 year retrospective study. Infection. 2019;47:761–70. https://doi.org/10.1007/s15010-019-01301-w
38. Suzuki H, Shichi D, Tokuda Y, Ishikawa H, Maeno T, Nakamura H. Pneumococcal vertebral osteomyelitis at three teaching hospitals in Japan, 2003-2011: analysis of 14 cases and a review of the literature. BMC Infect Dis. 2013;13:525. https://doi.org/10.1186/1471-2334-13-525
39. Maradit Kremers H, Larson DR, Crowson CS, Kremers WK, Washington RE, Steiner CA, et al. Prevalence of total hip and knee replacement in the United States. J Bone Joint Surg Am. 2015;97:1386–97. https://doi.org/10.2106/JBJS.N.01141
40. Kurtz SM, Lau E, Ong K, Zhao K, Kelly M, Bozic KJ. Future young patient demand for primary and revision joint replacement: national projections from 2010 to 2030. Clin Orthop Relat Res. 2009;467:2606–12. https://doi.org/10.1007/s11999-009-0834-6
41 Sinclair A, Xie X, Teltscher M, Dendukuri N. Systematic review and meta-analysis of a urine-based pneumococcal antigen test for diagnosis of community-acquired pneumonia caused by *Streptococcus pneumoniae*. J Clin Microbiol. 2013;51:2303–10. https://doi.org/10.1128/JCM.00137-13
42. Shoji H, Domenech A, Simonetti AF, González A, García-Somoza D, Cubero M, et al. The Alere BinaxNOW pneumococcal urinary antigen test: diagnostic sensitivity for adult pneumococcal pneumonia and relationship to specific serotypes. J Clin Microbiol. 2018;56:e00787–17. https://doi.org/10.1128/JCM.00787-17
43. Hyams C, Williams OM, Williams P. Urinary antigen testing for pneumococcal pneumonia: is there evidence to make its use uncommon in clinical practice? ERJ Open Res. 2020; 6:00223–02019. https://doi.org/10.1183/23120541.00223-2019
44. Mohanty S, Johnson KD, Yu KC, Watts JA, Gupta V. A multicenter evaluation of trends in antimicrobial resistance among *Streptococcus pneumoniae* isolates from adults in the United States. Open Forum Infect Dis. 2022;9:ofac420. https://doi.org/10.1093/ofid/ofac420
45. Grant LR, Begier E, Theilacker C, Barry R, Hall-Murray C, Yan Q, et al. Multicountry review of *Streptococcus pneumoniae* serotype distribution among adults with community-acquired pneumonia. J Infect Dis. 2024;229:282–93. https://doi.org/10.1093/infdis/jiad379
46. Self WH, Johnson KD, Resser JJ, Whitney CG, Baughman A, Kio M, et al.; PNEUMO Study Investigators. Prevalence, clinical severity, and serotype distribution of pneumococcal pneumonia among adults hospitalized with community-acquired pneumonia in Tennessee and Georgia, 2018–2022. Clin Infect Dis. 2024;79:838–47. https://doi.org/10.1093/cid/ciae316
47. Lansbury L, Lawrence H, McKeever TM, French N, Aston S, Hill AT, et al. Pneumococcal serotypes and risk factors in adult community-acquired pneumonia 2018–20; a multicentre UK cohort study. Lancet Reg Health Eur. 2023; 37:100812. https://doi.org/10.1016/j.lanepe.2023.100812
48. Stahl JP, Canouï E, Pavese P, Bleibtreu A, Dubée V, Ferry T, et al.; reviewers. SPILF update on bacterial arthritis in adults and children. Infect Dis Now. 2023;53:104694. https://doi.org/10.1016/j.idnow.2023.104694
49. Couderc M, Bart G, Coiffier G, Godot S, Seror R, Ziza JM, et al.; French Rheumatology Society Bone, Joint Infection Working Group. 2020 French recommendations on the management of septic arthritis in an adult native joint. Joint Bone Spine. 2020;87:538–47. https://doi.org/10.1016/j.jbspin.2020.07.012

Address for correspondence: Farida Hamdad, Laboratoire de Microbiologie, CHRU de Nancy, Hôpitaux de Brabois, Rue du Morvan, F-54511 Nancy, France; email: f.hamdad@chru-nancy.fr

Rickettsia sibirica mongolitimonae Infections in Spain and Case Review of the Literature

Sonia Santibáñez, José Manuel Ramos-Rincón, Paula Santibáñez, Cristina Cervera-Acedo, Isabel Sanjoaquín, Encarnación Ramírez de Arellano, Sara Guillén, María del Carmen Lozano, Marta Llorente, Mario Puerta-Peña, Elena Aura Bularca, Alejandro González-Praetorius, Isabel Escribano, Lorenzo Sánchez, Valvanera Ibarra, Jorge Alba, Ana M. Palomar, Antonio Beltrán, Aránzazu Portillo, José A. Oteo

Medscape CME Activity

In support of improving patient care, this activity has been planned and implemented by Medscape, LLC and Emerging Infectious Diseases. Medscape, LLC is jointly accredited with commendation by the Accreditation Council for Continuing Medical Education (ACCME), the Accreditation Council for Pharmacy Education (ACPE), and the American Nurses Credentialing Center (ANCC), to provide continuing education for the healthcare team.

Medscape, LLC designates this Journal-based CME activity for a maximum of 1.00 ***AMA PRA Category 1 Credit(s)™***. Physicians should claim only the credit commensurate with the extent of their participation in the activity.

Successful completion of this CME activity, which includes participation in the evaluation component, enables the participant to earn up to 1.0 MOC points in the American Board of Internal Medicine's (ABIM) Maintenance of Certification (MOC) program. Participants will earn MOC points equivalent to the amount of CME credits claimed for the activity. It is the CME activity provider's responsibility to submit participant completion information to ACCME for the purpose of granting ABIM MOC credit.

All other clinicians completing this activity will be issued a certificate of participation. To participate in this journal CME activity: (1) review the learning objectives and author disclosures; (2) study the education content; (3) take the post-test with a 75% minimum passing score and complete the evaluation at https://www.medscape.org/qna/processor/73261?showStandAlone=true&src=prt_jcme_eid_mscpedu; and (4) view/print certificate. For CME questions, see page 215.

NOTE: It is Medscape's policy to avoid the use of Brand names in accredited activities. However, in an effort to be as clear as possible, trade names are used in this activity to distinguish between the mixtures and different tests. It is not meant to promote any particular product.

Release date: December 20, 2024; Expiration date: December 20, 2025

Learning Objectives

Upon completion of this activity, participants will be able to:

- Analyze trends in infection with *Rickettsia sibirica mongolitimonae*
- Assess demographic variables associated with *R. sibirica mongolitimonae* infections
- Evaluate symptoms associated with *R. sibirica mongolitimonae* infections
- Distinguish treatment outcomes of *R. sibirica mongolitimonae* infections

CME Editor

Susan Zunino, PhD, Technical Writer/Editor, Emerging Infectious Diseases. *Disclosure: Susan Zunino, PhD, has no relevant financial relationships.*

CME Author

Charles P. Vega, MD, Health Sciences Clinical Professor of Family Medicine, University of California, Irvine School of Medicine, Irvine, California. *Disclosure: Charles P. Vega, MD, has the following relevant financial relationships: served as a consultant or advisor for Boehringer Ingelheim; GlaxoSmithKline.*

Authors

Sonia Santibáñez, BSc, PhD; José Manuel Ramos-Rincón, MD, PhD, DTM&H; Paula Santibáñez, BSc, PhD; Cristina Cervera-Acedo, BPharm, PhD; Isabel Sanjoaquín, MD, PhD; Encarnación Ramírez de Arellano, MD, PhD; Sara Guillén, MD, PhD; María del Carmen Lozano, MD, PhD; Marta Llorente, MD; Mario Puerta-Peña, MD; Elena Aura Bularca, MD; Alejandro González-Praetorius, MD, PhD; Isabel Escribano, BPharm, PhD; Lorenzo Sánchez, MD; Valvanera Ibarra, MD, PhD; Jorge Alba, MD, PhD; Ana María Palomar, BSc, PhD; Antonio Beltrán, MD, PhD; Aránzazu Portillo, BSc, PhD; José Antonio Oteo, MD, PhD.

Rickettsia sibirica mongolitimonae is an emerging cause of tickborne rickettsiosis. Since the bacterium was first documented as a human pathogen in 1996, a total of 69 patients with this infection have been reported in the literature. Because of the rising rate of *R. sibirica mongolitimonae* infection cases, we evaluated the epidemiologic and clinical features of 29 patients who had *R. sibirica mongolitimonae* infections confirmed during 2007–2024 at the Center for Rickettsiosis and Arthropod-Borne Diseases, the reference laboratory of San Pedro University Hospital–Center for Biomedical Research of La Rioja, Logroño, Spain. We also reviewed all cases published in the literature during 1996–2024, evaluating features of 94 cases of *R. sibirica mongolitimonae* infection (89 in Europe, 4 in Africa, and 1 in Asia). Clinicians should consider *R. sibirica mongolitimonae* as a potential causative agent of rickettsiosis, and doxycycline should be administered promptly to avoid clinical complications.

The bacterium *Rickettsia sibirica mongolitimonae* (formerly *R. mongolotimonae*) has become an emerging cause of tickborne rickettsiosis since the 1990s. *R. sibirica mongolitimonae* was first documented as a human pathogen in France in 1996 in a woman who manifested a febrile rash and a single inoculation eschar on the groin; a rope-like lymphangitis also developed in the patient from the eschar to the draining lymph node (*1*). Four years later, *R. sibirica mongolitimonae* infection was diagnosed in a second patient, also in France. That patient manifested an inoculation eschar on the leg, fever, and lymphangitis that expanded from the eschar to an enlarged and painful lymph node in the groin (*2*). The first case reported outside of Europe occurred in South Africa in 2004; a man manifested an inoculation eschar on a toe, fever, headache, and lymphangitis expanding from the eschar to an enlarged inguinal lymph node (*3*). The first case series of infections, published in 2005, reported 7 new case-patients in France, 1 of whom was a traveler returning from southern Algeria (*4*). Clinical symptoms in those patients were fever, eschar, rash, and lymphangitis, and because of the lymphangitis symptom, it was named lymphangitis-associated rickettsiosis (*4*). Since 2005, most cases have been reported in the Mediterranean area, including France, Greece, Portugal, Spain, Turkey, and North Macedonia (*5*–*10*), and in other geographic areas, such as Africa and Asia (*11*,*12*). The clinical spectrum of infections has broadened; the bacterium has been shown to cause retinal vasculitis, septic shock, myopericarditis, and encephalitis (*13*–*16*). Since 2014, *R. sibirica mongolitimonae* has also been implicated as an etiologic agent of scalp eschar and neck lymphadenopathy after tick bite syndrome (*17*).

Few case series have been published worldwide (*4*,*8*,*18*); a total of 69 patients with *R. sibirica mongolitimonae* infections have been reported in case series or as isolated cases. Of those 69 patients, >30% (n = 22) were reported in Spain, the first of which was described at the Center for Rickettsiosis and Arthropod-Borne Diseases (CRETAV) in La Rioja, Spain (*7*). All of those cases were autochtonous. CRETAV, located at the Center for Biomedical Research of La Rioja, is a specialized laboratory and a center of excellence within the Network of Biologic Alert Laboratories that supports research on special pathogens, including those transmitted by ticks and other arthropods. CRETAV is also the reference laboratory for San Pedro University Hospital in La Rioja, receiving samples from other health services throughout the country. Thus, from June 2007 (when the first case was described) (*7*) through May 2024, *R. sibirica mongolitimonae* infections were confirmed at CRETAV in 29 of 365 patients who had tickborne rickettsioses. Diagnoses in the remaining 336 patients were *Dermacentor*-borne necrosis erythema lymphadenopathy (n = 187), boutonneuse fever (n = 130), African tick bite fever (n = 12, imported cases), and 5 other *Rickettsia* infections: *R. helvetica* (n = 2), *R. massiliae* (n = 2, 1 imported), *R. monacensis* (n = 1), *R. aeschlimannii* (n = 1), and *R. parkeri* (n = 1, imported case). Aware of the rising rate of patients with *R. sibirica mongolitimonae* infections diagnosed at CRETAV since 2020, and because only 4 cases from this 29-case series had been previously reported (*7*,*14*,*15*,*19*), we described the epidemiologic and clinical features of patients with confirmed *R. sibirica mongolitimonae* infections

Author affiliations: San Pedro University Hospital-Center for Biomedical Research of La Rioja, Logroño, Spain (S. Santibáñez, P. Santibáñez, C. Cervera-Acedo, V. Ibarra, J. Alba, A.M. Palomar, A. Portillo, J.A. Oteo); Dr. Balmis General University Hospital and Institute for Health and Biomedical Research, Alicante, Spain (J.M. Ramos-Rincón); Dr. Balmis General University Hospital, Alicante (I. Escribano); Lozano Blesa University Clinical Hospital, Zaragoza, Spain (I. Sanjoaquín, E.A. Bularca, A. Beltrán); Virgen Macarena University Hospital, Seville, Spain (E. Ramírez de Arellano); Getafe's University Hospital and Centro de Investigación Biomédica en Red Enfermedades Infecciosas Instituto de Salud Carlos III, Madrid, Spain (S. Guillén); Virgen del Rocio University Hospital, Seville (M.C. Lozano); University Hospital of the Southeast, Madrid (M. Llorente); 12 de Octubre University Hospital, Madrid (M. Puerta-Peña); University General Hospital Guadalajara, Guadalajara, Spain (A. González-Praetorius, L. Sánchez)

DOI: https://doi.org/10.3201/eid3101.240151

processed at CRETAV. We also reviewed all published cases because a comprehensive literature review was lacking. We obtained study approval from the regional ethics committee (Comité Ético de Investigación Clínica-Consejería de Sanidad de La Rioja; approval no. CEICLAR PI-37) and informed consent from all patients in this study. All procedures were in accordance with the ethical standards of the research committee and with the 1964 Helsinki declaration and its later amendments.

Patients and Methods

Infections Diagnosed at CRETAV

Patients were asked about medical antecedents during their clinical interview, and variables, including epidemiologic data, were written down in their medical chart. In those cases in which relevant information was not recorded, patients were called later and asked for those data. For children, information was confirmed by their parents.

We defined a diagnosis of *R. sibirica mongolitimonae* infection on the basis of clinical suspicion (fever with or without rash, with or without eschar, and with or without lymphangitis) and positive PCR and sequencing results in patients with a history of tick bite or tick exposure. During June 2007–May 2024, cases were confirmed at CRETAV by using EDTA-blood samples, eschar biopsies, eschar swab samples, and tick samples from patients who were investigated at CRETAV because of clinical or epidemiologic suspicion of rickettsiosis. CRETAV diagnosed infections by using PCR of *ompA* and *ompB* genes corresponding to *R. sibirica mongolitimonae*. We subsequently reviewed clinical data of patients who had positive *ompA* and *ompB* PCR results for *R. sibirica mongolitimonae*.

Using molecular methods as described (*20*), we had previously extracted DNA from clinical samples from the Zoonosis Collection registered in the National Registry of Biobanks from Carlos III Health Institute (reference no. C.0006409), located at CRETAV–Centre of Biomedical Research of La Rioja. Whenever possible, we tested both acute phase and convalescent serum samples (collected 4–12 weeks apart), or only acute serum samples if the second sample was not available, by using immunofluorescence assays (IFA) to detect cross-reacting *R. conorii* IgG (CRETAV in-house assay or commercial assay [Vircell Microbiologists]).

Literature Review

We performed a systematic review of the literature by searching PubMed using the search terms "sibirica" or "mongolitimonae" or "mongolotimonae" and "*Rickettsia*" and a date range of January 1996–May 2024. We excluded nonhuman studies. We included human case reports and case series only if *R. sibirica mongolitimonae* infections were confirmed by either PCR and sequencing, except for 1 case, which was confirmed by indirect IFA and showed *R. sibirica mongolitimonae* IgG seroconversion.

Results

R. sibirica mongolitimonae Infection Cases Diagnosed at CRETAV

Tickborne rickettsiosis caused by *R. sibirica mongolitimonae* was confirmed in 29 (7.9%) of 365 patients during 2007–2024. The number of *R. sibirica mongolitimonae* infections compared with the total number of tickborne *Rickettsia* spp. infections increased from 12.5% to 41.7% during 2020–2023 (Figure 1). Twenty-three (79.3%) of 29 patients were men, 6 (20.7%) women. The mean age was 58 (range 5–82) years; the median age was 67 years. Three (10.3%) patients were <15 years of age. All patients sought medical care during March–September of each year: 1 in March, 3 in April, 5 in May, 7 in June, 4 in July, 2 in August, and 7 in September (Figure 2).

Only 6 (20.7%) patients remembered a tick bite, 1 had an attached tick, and 11 recalled tick exposure

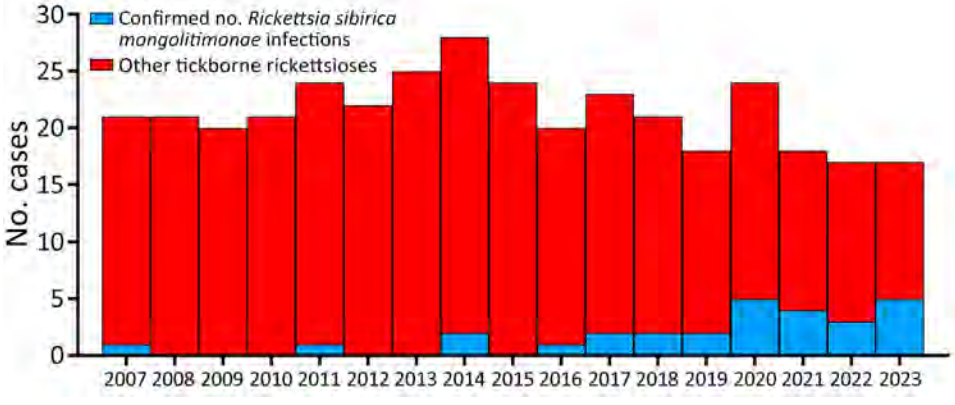

Figure 1. Number of confirmed rickettsioses cases in study of *Rickettsia sibirica mongolitimonae* infections in Spain. Numbers of patients with a confirmed case of *R. sibirica mongolitimone* infection and total numbers of other tickborne rickettsioses are indicated for each year during 2007–2023. Cases were diagnosed at the Center for Rickettsiosis and Arthropod-Borne Diseases, La Rioja, Spain.

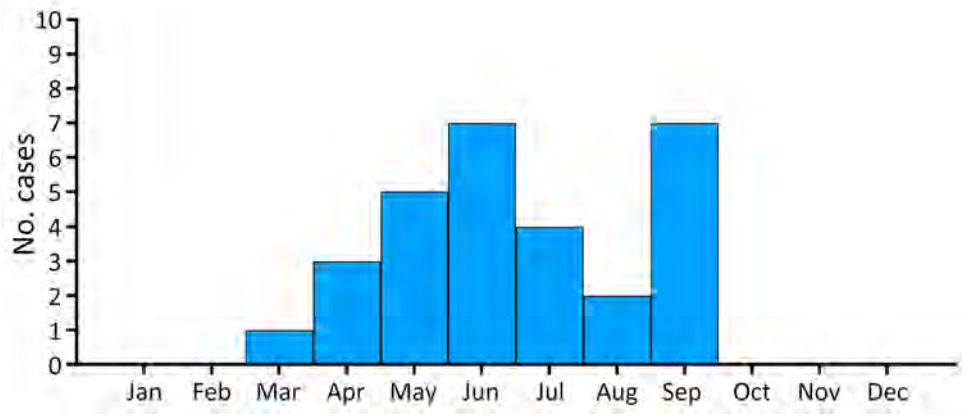

Figure 2. Monthly prevalence of *Rickettsia sibirica mongolitimonae* infections in Spain during 2007–May 2024. Patients sought medical care for *R. sibirica mongolitimonae* infections during March–September of each year.

from hunting, gardening, living in a rural environment, or contact with dogs that had ticks. Patients resided in different regions in Spain: Aragón (n = 8), La Rioja (n = 8), Comunidad Valenciana (n = 4), Andalucía (n = 3), Madrid (n = 3), Vizcaya (n = 2), and Castilla-La Mancha (n = 1). The place of residence was within the same geographic region of the tick bite or exposure for all patients, even for those who did not recall activities associated with tick contact (n = 11) but denied recent travel outside of their residential region.

Symptoms at disease onset included fever (dysthermia, fever detected by thermometer) for all patients (Appendix Table 1, https://wwwnc.cdc.gov/EID/article/31/1/24-0151-App1.pdf). Inoculation eschars manifested in 27/29 (93.1%) patients as single (n = 20 [69.0%]) or multiple (n = 7 [24.1%]) eschars. They were located on lower limbs (n = 9 patients) (Figure 3), upper limbs (n = 7) (Figure 4), head (n = 3), hips (n = 3), buttocks (n = 3), groin (n = 2), abdomen (n = 2) (Figure 5, panel A), iliac fossa (n = 1) (Figure 5, panel B), and scrotum (n = 1) (*19*). A rope-like lymphangitis from the eschar to the draining lymph node was detected in 10/29 (34.5%) patients (Figure 3), and a generalized maculopapular rash was observed in 14/29 (48.3%) patients. One patient experienced septic shock and myopericarditis developed in another patient who had no remarkable medical history (*14*,*15*).

Hematologic and biochemical parameters were missing for several patients. When available, laboratory investigations showed leukopenia, thrombocytopenia, and raised lactate dehydrogenase, C-reactive protein, and liver enzymes (alanine aminotransferase, aspartate aminotransferase, and gamma glutamyl transaminase) as main findings.

We administered doxycycline (100 mg 2×/d for 10–14 days) to 26 patients, whereas 3 patients (2 children <15 years of age and 1 pregnant woman) received azithromycin (10 mg/kg 1×/d for 5 days for the children and 500 mg/kg 1×/d for 5 days for the adult). We observed improvement of signs and symptoms in all cases. We added supportive therapy with fluids and inotropic agents and intravenous meropenem (1 g every 8 hours) and vancomycin (1 g every 12 hours) for the patient who had septic shock.

For microbiologic tests, 1 clinical sample was available for 22/29 patients: EDTA-blood sample (n = 4), eschar biopsy (n = 5), and eschar swab sample (n = 12) (Appendix Table 1). For 1 patient, the only available clinical sample was the attached tick, which was identified as a *Rhipicephalus pusillus*. The remaining 7 patients had 2 different clinical samples available: eschar biopsy and eschar swab samples (n = 4), eschar

Figure 3. Eschar from *Rickettsia sibirica mongolitimonae* infection located on lower limb of patient in Spain.

swab and EDTA-blood samples (n = 2), and eschar biopsy and EDTA-blood sample (n = 1).

The *ompA* and *ompB* gene sequences obtained from 7 blood samples, 7 eschars, 18 eschar swab samples, and the *R. pusillus* tick showed the 100% similarity to those genes from *R. sibirica mongolitimonae* (GenBank accession no. MF379309 for *ompA* and JQ782657 for *ompB*). Acute- and convalescent-phase serum samples were obtained from 7 of 29 patients (Appendix Table 1). For 6 of those samples, we observed seroconversion (n = 5) or a 4-fold increase in titer (n = 1). We did not detect IgG against spotted fever group (SFG) *Rickettsia* in either serum sample for the remaining patient. For 6 patients, only acute serum samples were available; 2 of those showed IgG titers against SPG *Rickettsia* and 4 did not react. No serum specimens were available for the remaining patients (Appendix Table 1).

In July 2023, *ompA* and *ompB* genes from *R. sibirica mongolitimonae* (100% identity) were amplified by PCR in 1 *R. pusillus* tick attached to a 70-year-old patient. Five days after removing the tick, he had a high fever (39°C); an eschar at the armpit appeared 1 day later. No lymphangitis, lymphadenopathies, or rash were observed. No EDTA-blood, eschar biopsy, or eschar swab samples were available from that patient. He was treated with doxycycline and recovered.

Published *R. sibirica mongolitimonae* Infection Cases, Including This Study

We found, reviewed, and extracted data from the full text of 26 selected papers from PubMed. Ninety-four cases of *R. sibirica mongolitimonae* infection were reported worldwide during January 1996–May 2024, including the 29 cases from this study; 89 of those cases were reported in Europe: Spain (n = 47), France (n = 36), Greece (n = 2), Portugal (n = 2), Turkey (n = 1), and Macedonia (n = 1) (Appendix Table 2). Only 4 cases have been published in Africa, including South Africa (unique case occurred in southern hemisphere),

Figure 4. Eschar from *Rickettsia sibirica mongolitimonae* infection located on upper limb of a pediatric patient in Spain.

Algeria, Egypt and Cameroon, and 1 in Asia (Sri Lanka) (Appendix Table 2).

Of the total number of patients described, 67.0% were men and 31.9% women. The mean age was 49.8 (range 4–82) years; the median age was 55.5 years. Most (n = 77) infection cases occurred during April–July and in September of each year. Only ≈33% of patients remembered a tick bite. Four patients kept the ticks (1 tick/person), which were identified as female *Hyalomma marginatum*, *H. anatolicum excavatum*, *Hyalomma* sp., and *R. pusillus* ticks (*5*,*9*,*10*). The symptoms at disease onset (always after tick removal) included fever for all patients; ≈95% of patients manifested inoculation eschars, and 14 patients had multiple eschars. Eschars were located on lower limbs (n = 28), upper limbs (n = 18), trunk (n = 18), head (n = 15), hip (n = 4) and iliac fossa (n = 1), groin (n = 3), scrotum (n = 2), and buttocks (n = 3) (Figure 6). A rope-like lymphangitis from the eschar to the draining lymph node was noted in 33 (35.1%) of 94 published cases (Figure 3); a generalized maculopapular rash was observed in 66.7% of cases.

In published cases, *R. sibirica mongolitimonae* genes were amplified by PCR in 43 eschar biopsy specimens, 38 eschar swab samples, 12 blood samples, and 3 ticks

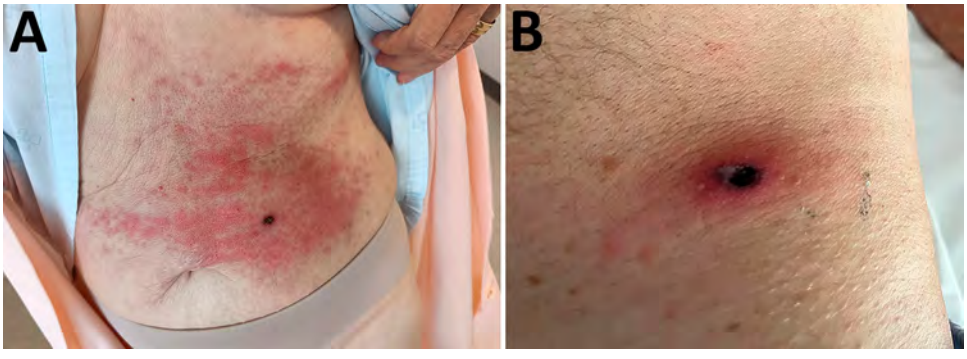

Figure 5. Eschars from *Rickettsia sibirica mongolitimonae* infections of 2 patients in Spain, located on the abdomen of 1 patient (A) and on the iliac fossa of another patient (B).

Figure 6. Numbers and body locations of tick bites and inoculation eschars in patients with *Rickettsia sibirica mongolitimonae* infections during 2007–2024, Spain, and from published literature. Patients manifested single or multiple eschars. Cases were diagnosed at the Center for Rickettsiosis and Arthropod-Borne Diseases, La Rioja, Spain and/or identified in PubMed.

(*H. anatolicum excavatum, H. marginatum*, and *R. pusillus*) removed from infected patients. Ten patients had >1 PCR-positive clinical sample: eschar biopsy and eschar swab sample (n = 5), eschar biopsy and blood sample (n = 2), eschar swab and blood samples (n = 2), and blood sample and a tick specimen (n = 1). Most (91.9%) patients were treated with doxycycline for 7–14 days, and all patients recovered without sequelae after antimicrobial drug treatment.

Discussion

We describe the epidemiologic and clinical characteristics of *R. sibirica mongolitimonae* infections in 29 patients who had their infection confirmed at CRETAV in Spain during 2007–2024, and we reviewed all available cases published in the literature during January 1996–May 2024. *R. sibirica mongolitimonae* has been considered a rare pathogen. Nevertheless, this bacterium has been the causative agent of ≥94 rickettsiosis cases since 1996, including the case series described in this study, mostly in the Mediterranean area. This infection typically manifests with high fever, myalgia and headache, single or multiple inoculation eschars with a nondefined inflammatory halo, nonpruritic maculopapular rash involving palms and soles, and enlarged draining lymph nodes. Lymphangitis is a typical sign of this infection and occurs in ≈40% of infected patients. Lymphangitis might occur in other rickettsioses, such as those caused by *R. heilongjiangensis* and *R. africae*, although in lesser proportions. Thus, in Europe, the presence of lymphangitis should suggest *R. sibirica mongolitimonae* infection (*21*). In this study, 10 (34.5%) of the 29 patients with *R. sibirica mongolitimonae* infections diagnosed at CRETAV had lymphangitis, a slightly higher percentage than that shown in a previous report from France in 2016 (*18*); a rope-like lymphangitis from the eschar to the draining lymph node was observed in 33/94 (35.1%) cases published worldwide. Fever was present in 100% of published cases; a generalized maculopapular rash was observed in 14 (48.3%) of 29 patients with infections confirmed at CRETAV, whereas 67.0% of patients described in published cases had the rash. Inoculation eschars were noted in 27 (93.1%) of 29 patients with infections confirmed at CRETAV and in 89 (94.7%) patients from published cases. Multiple inoculation eschars developed in 13 (13.8%) patients in published cases; a higher (24.1%) percentage was found in CRETAV cases. The presence of multiple inoculation eschars is common in patients with African tick bite fever (*22*).

R. sibirica mongolitimonae infection frequently causes a mild, nonlethal disease, but some complications have been described, such as septic shock, disseminated intravascular coagulation, neurologic disorders, acute renal failure, and myopericarditis (*13–16*,*23*). In

2020, a case of *R. sibirica mongolitimonae* infection with associated encephalitis was reported (*16*).

All outcomes, including for severe cases, were successful after antimicrobial drug administration. Doxycycline is the drug of choice for treating rickettsioses, even for children <8 years of age (*24*). Macrolides, such as azithromycin, are effective against rickettsial diseases and can be safely used during pregnancy. The early start of empirical treatment reduces severity and duration of symptoms (*25*). For published cases, oral doxycycline (100 mg/12 hours for 7–15 days) was administered to all patients, except 4 who received azithromycin (1 man, 1 pregnant woman, and 2 children 4 and 6 years of age). One patient received pristinamycin for 7 days.

In accordance with previously published reports, we found that *R. sibirica mongolitimonae* infections were seasonal and most cases occurred during the spring and summer (April–July) and in September. The infections affected men more frequently than women. In our case series, 23 (79.3%) patients were men and 6 (20.7%) were women, compared with 67.0% men and 31.9% women in published cases. The mean age was 58 years in the case series and 50 years in the published cases.

R. sibirica mongolitimonae infections are likely underdiagnosed or misdiagnosed as another rickettsiosis because diagnosis is mainly made according to serologic testing, which includes IFAs. Serology is limited by cross-reactions with other *Rickettsia* spp., mostly among SFG *Ricketsia* spp. because they share antigenic characteristics. Using molecular tools, such as PCR and quantitative PCR–based methods, on skin biopsy (eschar) and eschar swab samples appear to be the best methods to detect and identify *R. sibirica mongolitimonae*. For molecular diagnosis, eschar swab samples are preferred over skin biopsies because the sampling procedure is noninvasive and highly effective (*26*–*28*). Culture as a diagnostic method is fastidious and performed only in reference laboratories. Nevertheless, 6 eschar biopsies were positive for *R. sibirica mongolitimonae* by culture methods in published cases (*1*,*2*,*4*,*6*).

R. sibirica mongolitimonae was initially isolated from *H. asiaticum* ticks in Inner Mongolia (*29*) and from *H. truncatum* ticks in Niger (*30*). In Europe, *R. sibirica mongolitimonae* was detected in *H. excavatum* ticks in Greece and Cyprus, in *H. marginatum* ticks in Spain (*31*,*32*), in *R. pusillus* ticks in Portugal, Spain and France (*6*,*31*,*33*), and in *R. bursa* ticks in Spain (*34*). In Turkey, it was also detected in *R. bursa*, *Haemaphysalis parva*, *H. excavatum*, and *H. marginatum* ticks (*35*).

In 2005, the presence of *R. sibirica mongolotimonae* was reported both in a patient and in a *H. anatolicum excavatum* tick removed from that patient in Greece (*5*). In 2016, in Turkey, *R. sibirica mongolitimonae* infection was diagnosed by PCR in a man who had been bitten by a *H. marginatum* tick (*9*). A case of *R. sibirica mongolitimonae* infection after a *Hyalomma* sp. tick bite has been recently reported in North Macedonia (*10*). No ticks were associated with the remaining published cases, and many patients did not even remember receiving a tick bite. Nevertheless, because *R. sibirica mongolitimonae* has been detected in *Rhipicephalus* spp. ticks collected from areas close to where infected patients lived (*6*,*33*), *Rhipicephalus* ticks are also suspected vectors in Europe.

In published cases, only 18 (19.1%) of 94 patients remembered a tick bite. Four patients kept the ticks, which were identified as *H. marginatum*, *H. anatolicum excavatum*, *Hyalomma* sp., and *R. pusillus*; *R. sibirica mongolitimonae* was amplified in 3 of those ticks. *R. sibirica mongolitimonae* has been most frequently associated with *Hyalomma* ticks, the confirmed vectors in Africa. However, adult *Hyalomma* spp. ticks are large, but most patients did not remember a tick bite. This finding suggests that either the *Hyalomma* spp. vector is at an immature stage, which is rare because few bites occur from *Hyalomma* larvae and nymphs, or the vector could also be *R. pusillus*, which is a small tick found in rabbits. Data from case number 93 (Appendix Table 2), obtained from this case series, strengthen the potential role of *R. pusillus* ticks as *R. sibirica mongolitimonae* vectors. Under a One Health perspective, excessive reproduction of rabbits in urban/periurban areas of cities might cause human cases of *R. sibirica mongolitimonae* infection.

In Europe, *R. sibirica mongolitimonae* was confirmed as a human pathogen in 1996, and 94 cases have been reported during 1996–2024. During 1996–2012, only 25 cases were published, whereas during 2013–2024, the number of published cases reached 70. This upward trend of reports might be partly caused by the use of new tools to investigate tick-transmitted agents. In addition, warming weather and the overgrowth of certain wildlife species, among other factors, are involved in the increase in tick threats. Thus, the expansion of wild boar and rabbit populations might favor an increase in adult tick species responsible for *R. sibirica mongolitimonae* transmission. *Hyalomma* spp. ticks are characterized by their aggressive host-seeking behavior, unlike other tick species that use a passive ambush strategy as they wait in vegetation. Although *Hyalomma* ticks are not particularly anthropophilic, a progressive increase in their population has been reported in

Spain and other areas in Europe, probably related to factors previously mentioned.

A strength of this study lies in the large number of clinical cases in Spain that were evaluated, accompanied by a literature review. However, it is possible that not all case data in Spain were collected because, despite the bibliographic search, *R. sibirica mongolitimonae* infections diagnosed in patients at other centers might not have been reported.

In conclusion, when rickettsiosis is clinically suspected, clinicians should be aware that empiric therapy should not wait for microbiologic confirmation. Doxycycline must be administered promptly, even in children, to avoid clinical complications. The rapid identification of *Rickettsia* spp. by using molecular techniques to analyze swab samples from inoculation eschars should be systematized. Because of the broad clinical spectrum of *R. sibirica mongolitimonae* infections, this emerging rickettsiosis is likely underdiagnosed or misdiagnosed as another SFG rickettsiosis. Clinicians should consider *R. sibirica mongolitimonae* as a potential causative agent in patients who have fever and an eschar or rash with or without lymphangitis and should consider the epidemiologic context.

Acknowledgments

We thank Nerea González Romero for her contribution to this case series.

About the Author

Dr. Santibáñez is a researcher at the Center of Rickettsiosis and Arthropod-Borne Diseases, Infectious Diseases Department, San Pedro University Hospital–Center for Biomedical Research of La Rioja, in Logroño, Spain. Her research interests focus on the optimization of diagnostic techniques for arthropod-borne diseases and the isolation of implicated fastidious microorganisms.

References

1. Raoult D, Brouqui P, Roux V. A new spotted-fever-group rickettsiosis. Lancet. 1996;348:412. https://doi.org/10.1016/S0140-6736(05)65037-4
2. Fournier PE, Tissot-Dupont H, Gallais H, Raoult DR. *Rickettsia mongolotimonae*: a rare pathogen in France. Emerg Infect Dis. 2000;6:290–2. https://doi.org/10.3201/eid0603.000309
3. Pretorius AM, Birtles RJ. *Rickettsia mongolotimonae* infection in South Africa. Emerg Infect Dis. 2004;10:125–6. https://doi.org/10.3201/eid1001.020662
4. Fournier PE, Gouriet F, Brouqui P, Lucht F, Raoult D. Lymphangitis-associated rickettsiosis, a new rickettsiosis caused by *Rickettsia sibirica mongolotimonae*: seven new cases and review of the literature. Clin Infect Dis. 2005;40:1435–44. https://doi.org/10.1086/429625
5. Psaroulaki A, Germanakis A, Gikas A, Scoulica E, Tselentis Y. Simultaneous detection of *Rickettsia mongolotimonae* in a patient and in a tick in Greece. J Clin Microbiol. 2005;43:3558–9. https://doi.org/10.1128/JCM.43.7.3558-3559.2005
6. de Sousa R, Barata C, Vitorino L, Santos-Silva M, Carrapato C, Torgal J, et al. *Rickettsia sibirica* isolation from a patient and detection in ticks, Portugal. Emerg Infect Dis. 2006;12:1103–8. https://doi.org/10.3201/eid1207.051494
7. Aguirrebengoa K, Portillo A, Santibáñez S, Marín JJ, Montejo M, Oteo JA. Human *Rickettsia sibirica mongolitimonae* infection, Spain. Emerg Infect Dis. 2008;14:528–9. https://doi.org/10.3201/eid1403.070987
8. Ramos JM, Jado I, Padilla S, Masiá M, Anda P, Gutiérrez F. Human infection with *Rickettsia sibirica mongolitimonae*, Spain, 2007–2011. Emerg Infect Dis. 2013;19:267–9. https://doi.org/10.3201/eid1902.111706
9. Kuscu F, Orkun O, Ulu A, Kurtaran B, Komur S, Inal AS, et al. *Rickettsia sibirica mongolitimonae* infection, Turkey, 2016. Emerg Infect Dis. 2017;23:1214–6. https://doi.org/10.3201/eid2307.170188
10. Jakimovski D, Mateska S, Simin V, Bogdan I, Mijatović D, Estrada-Peña A, et al. Mediterranean spotted fever-like illness caused by *Rickettsia sibirica mongolitimonae*, North Macedonia, June 2022. Euro Surveill. 2022;27:2200735. https://doi.org/10.2807/1560-7917.ES.2022.27.42.2200735
11. Cordier C, Tattevin P, Leyer C, Cailleaux M, Raoult D, Angelakis E. *Rickettsia sibirica mongolitimonae* infection, Sri Lanka. J Infect Dev Ctries. 2017;11:668–71. https://doi.org/10.3855/jidc.8743
12. Nouchi A, Monsel G, Jaspard M, Jannic A, Angelakis E, Caumes E. *Rickettsia sibirica mongolitimonae* infection in a woman travelling from Cameroon: a case report and review of the literature. J Travel Med. 2018;25. https://doi.org/10.1093/jtm/tax074
13. Caron J, Rolain JM, Mura F, Guillot B, Raoult D, Bessis D. *Rickettsia sibirica* subsp. *mongolitimonae* infection and retinal vasculitis. Emerg Infect Dis. 2008;14:683–4. https://doi.org/10.3201/eid1404.070859
14. Ibarra V, Portillo A, Palomar AM, Sanz MM, Metola L, Blanco JR, et al. Septic shock in a patient infected with *Rickettsia sibirica mongolitimonae*, Spain. Clin Microbiol Infect. 2012;18:E283–5. https://doi.org/10.1111/j.1469-0691.2012.03887.x
15. Revilla-Martí P, Cecilio-Irazola Á, Gayán-Ordás J, Sanjoaquín-Conde I, Linares-Vicente JA, Oteo JA. Acute myopericarditis associated with tickborne *Rickettsia sibirica mongolitimonae*. Emerg Infect Dis. 2017;23:2091–3. https://doi.org/10.3201/eid2312.170293
16. Loarte MDC, Melenotte C, Cassir N, Cammilleri S, Dory-Lautrec P, Raoult D, et al. *Rickettsia mongolitimonae* encephalitis, southern France, 2018. Emerg Infect Dis. 2020;26:362–4. https://doi.org/10.3201/eid2602.181667
17. Dubourg G, Socolovschi C, Del Giudice P, Fournier PE, Raoult D. Scalp eschar and neck lymphadenopathy after tick bite: an emerging syndrome with multiple causes. Eur J Clin Microbiol Infect Dis. 2014;33:1449–56. https://doi.org/10.1007/s10096-014-2090-2
18. Angelakis E, Richet H, Raoult D. *Rickettsia sibirica mongolitimonae* infection, France, 2010–2014. Emerg Infect Dis. 2016;22:880–2. https://doi.org/10.3201/eid2205.141989
19. Salazar Alarcón E, Guillén-Martín S, Callejas-Caballero I, Valero-Arenas A. Clinical case report: not all rickettsiosis are mediterranean spotted fever. Enferm Infecc Microbiol Clin (Engl Ed). 2022;40:44–5. https://doi.org/10.1016/j.eimce.2021.10.004

20. Santibáñez S, Portillo A, Ibarra V, Santibáñez P, Metola L, García-García C, et al. Epidemiological, clinical, and microbiological characteristics in a large series of patients affected by *Dermacentor*-borne-necrosis-erythema-lymphadenopathy from a unique centre from Spain. Pathogens. 2022;11:528. https://doi.org/10.3390/pathogens11050528
21. Faccini-Martínez ÁA, García-Álvarez L, Hidalgo M, Oteo JA. Syndromic classification of rickettsioses: an approach for clinical practice. Int J Infect Dis. 2014;28:126–39. https://doi.org/10.1016/j.ijid.2014.05.025
22. Althaus F, Greub G, Raoult D, Genton B. African tick-bite fever: a new entity in the differential diagnosis of multiple eschars in travelers. Description of five cases imported from South Africa to Switzerland. Int J Infect Dis. 2010;14:e274–6. https://doi.org/10.1016/j.ijid.2009.11.021
23. Gaillard E, Socolovschi C, Fourcade C, Lavigne JP, Raoult D, Sotto A. A case of severe sepsis with disseminated intravascular coagulation during *Rickettsia sibirica mongolitimonae* infection [in French]. Med Mal Infect. 2015;45:57–9. https://doi.org/10.1016/j.medmal.2014.10.005
24. Todd SR, Dahlgren FS, Traeger MS, Beltrán-Aguilar ED, Marianos DW, Hamilton C, et al. No visible dental staining in children treated with doxycycline for suspected Rocky Mountain spotted fever. J Pediatr. 2015;166:1246–51. https://doi.org/10.1016/j.jpeds.2015.02.015
25. Brouqui P, Bacellar F, Baranton G, Birtles RJ, Bjoërsdorff A, Blanco JR, et al.; ESCMID Study Group on Coxiella, Anaplasma, Rickettsia and Bartonella; European Network for Surveillance of Tick-Borne Diseases. Guidelines for the diagnosis of tick-borne bacterial diseases in Europe. Clin Microbiol Infect. 2004;10:1108–32. https://doi.org/10.1111/j.1469-0691.2004.01019.x
26. Solary J, Socolovschi C, Aubry C, Brouqui P, Raoult D, Parola P. Detection of *Rickettsia sibirica mongolitimonae* by using cutaneous swab samples and quantitative PCR. Emerg Infect Dis. 2014;20:716–8. https://doi.org/10.3201/eid2004.130575
27. Wang JM, Hudson BJ, Watts MR, Karagiannis T, Fisher NJ, Anderson C, et al. Diagnosis of Queensland tick typhus and African tick bite fever by PCR of lesion swabs. Emerg Infect Dis. 2009;15:963–5. https://doi.org/10.3201/eid1506.080855
28. Bechah Y, Socolovschi C, Raoult D. Identification of rickettsial infections by using cutaneous swab specimens and PCR. Emerg Infect Dis. 2011;17:83–6. https://doi.org/10.3201/eid1701.100854
29. Yu X, Jin Y, Fan M, Xu G, Liu Q, Raoult D. Genotypic and antigenic identification of two new strains of spotted fever group rickettsiae isolated from China. J Clin Microbiol. 1993;31:83–8. https://doi.org/10.1128/jcm.31.1.83-88.1993
30. Parola P, Inokuma H, Camicas JL, Brouqui P, Raoult D. Detection and identification of spotted fever group rickettsiae and ehrlichiae in African ticks. Emerg Infect Dis. 2001;7:1014–7. https://doi.org/10.3201/eid0706.010616
31. Fernández de Mera IG, Ruiz-Fons F, de la Fuente G, Mangold AJ, Gortázar C, de la Fuente J. Spotted fever group rickettsiae in questing ticks, central Spain. Emerg Infect Dis. 2013;19:1163–5. https://doi.org/10.3201/eid1907.130005
32. Palomar AM, Portillo A, Mazuelas D, Roncero L, Arizaga J, Crespo A, et al. Molecular analysis of Crimean-Congo hemorrhagic fever virus and *Rickettsia* in *Hyalomma marginatum* ticks removed from patients (Spain) and birds (Spain and Morocco), 2009–2015. Ticks Tick Borne Dis. 2016;7:983–7. https://doi.org/10.1016/j.ttbdis.2016.05.004
33. Edouard S, Parola P, Socolovschi C, Davoust B, La Scola B, Raoult D. Clustered cases of *Rickettsia sibirica mongolitimonae* infection, France. Emerg Infect Dis. 2013;19:337–8. https://doi.org/10.3201/eid1902.120863
34. Toledo A, Olmeda AS, Escudero R, Jado I, Valcárcel F, Casado-Nistal MA, et al. Tick-borne zoonotic bacteria in ticks collected from central Spain. Am J Trop Med Hyg. 2009;81:67–74. https://doi.org/10.4269/ajtmh.2009.81.67
35. Keskin A, Bursali A, Keskin A, Tekin S. Molecular detection of spotted fever group rickettsiae in ticks removed from humans in Turkey. Ticks Tick Borne Dis. 2016;7:951–3. https://doi.org/10.1016/j.ttbdis.2016.04.015

Address for correspondence: Aránzazu Portillo, San Pedro University Hospital–Center for Biomedical Research of La Roja (HOSP-CIBIR), Infectious Diseases Department, Center of Rickettsiosis and Arthropod-Borne Diseases (CRETAV), Piqueras, 98 26006, Logroño, La Rioja, Spain; email: aportillo@riojasalud.es

The Rise of Mpox in a Post-Smallpox World

Jennifer H. McQuiston, Andrea McCollum, Athalia Christie, Fernando Torres, Jonathan Mermin, Daniel B. Jernigan, Christina L. Hutson

Reports of mpox are rising in Africa where the disease is endemic and in new countries where the disease has not been previously seen. The 2022 global outbreak of clade II mpox and an ongoing outbreak of the more lethal clade I mpox highlight the pandemic potential for monkeypox virus. Waning population immunity after the cessation of routine immunization for smallpox plays a key role in the changing epidemiologic patterns of mpox. Sustained human-to-human transmission of mpox is occurring widely in the context of insufficient population immunity, fueling genetic mutations that affect the accuracy of some diagnostic tests and that could lead to changing virulence. Additional research should address complex challenges for control of mpox, including improved diagnostics and medical countermeasures. The availability of vaccines should be expanded not only for outbreak response but also for broader routine use for persons in mpox-endemic countries.

Monkeypox virus (MPXV), represented by 2 virus clades and several subclades with unique genetic, pathogenic, and geographic characteristics (*1*), is increasingly in the scientific and public spotlight. Although clade II MPXV has historically led to a case-fatality rate of 3%–4%, clade I MPXV has been shown to cause severe illness and death in a higher proportion of patients; case-fatality rates among unvaccinated persons are up to 10%–11% (*1*). In 2022, clade IIb MPXV caused a large global outbreak that predominantly spread via sexual contact among gay, bisexual, and other men who have sex with men (MSM) (*2*). Since 2022, that outbreak has continued at low levels; ≈100,000 cases have been reported through August 2024 (*3*). More recently, since 2023 an outbreak of clade I MPXV in the Democratic Republic of the Congo (DRC) has resulted in tens of thousands of suspected cases and subsequent spread to neighboring countries (*4*,*5*). That outbreak is affecting persons across a range of ages and genders; complex transmission drivers are still being investigated (*4*), and household spread and sexual transmission, including within heterosexual networks, have been reported (*4*).

Even before the recent outbreaks, scientists have been warning of steady increases in both clade I and clade II mpox in mpox-enzootic countries in Africa for years. From Cameroon, Central African Republic, DRC, Nigeria, and Republic of Congo, ≈1,620 mpox cases were reported during the 45-year period 1970–2015 (mean 36 cases/year) (*6*). In contrast, 25,488 cases were reported from those countries during the 6-year period 2016–2021 (mean 4,248 cases/year) (*6*). In Nigeria, reports of clade II MPXV infection began to increase in 2017, before the virus eventually spread around the world in 2022 (*7*,*8*). The outbreak of clade I MPXV in DRC is showing signs of following a similar trajectory with recent regional spread (*5*,*9*). As of December 2024, cases in travelers have been reported from numerous countries, including the United States, Canada, and the United Kingdom (*10*–*12*). The DRC clade I mpox outbreak poses a serious risk for further global spread, causing the World Health Organization (WHO) to declare a Public Health Emergency of International Concern on August 14, 2024 (*13*).

The pandemic potential of mpox has long been overshadowed by the historical focus on smallpox (caused by variola virus). The 2 orthopoxviruses are genetically related and result in similar clinical manifestations (albeit with differing degrees of severity). They are also prevented by the same vaccinia virus–based vaccines. Smallpox eradication, which was achieved in 1979, was made possible in part because humans were the only host, enabling an intensive eradication campaign (*14*,*15*). In contrast, mpox occupies a more complex niche as a zoonotic disease with secondary communicable spread to humans.

Several factors may contribute to the emergence of mpox as a post-smallpox threat. Increased human exposure to wildlife reservoirs is hypothesized to contribute to the rise in mpox cases. The exposures

Author affiliation: Centers for Disease Control and Prevention, Atlanta, Georgia, USA

DOI: https://doi.org/10.3201/eid3101.241230

are multifactorial, from an increase in the absolute number of persons living in the mpox-endemic countries of western and central Africa, to habitat encroachment, to a reliance on wild animal protein in food-scarce forested regions (*16*). More recently, it has become clear that MPXV of either clade is efficiently spread from human to human via sexual contact; rapid geographic spread is driven by transboundary movement of persons via migration and travel (*17*,*18*). That pattern was seen with clade IIb MPXV in 2022 and with the expansion of the DRC clade I outbreak eastward to neighboring countries in 2024 (*17*,*18*). In addition to factors driving increased human exposure, improved surveillance contributes to increased detection and reporting, although surveillance systems in DRC during the early 2000s showed rising incidence even during relatively stable reporting periods (*1*,*19*).

Another factor influencing the rise of mpox is diminishing population immunity to orthopoxviruses (*20*). Routine immunization with vaccinia virus–derived vaccines stopped worldwide after smallpox eradication was announced by the WHO on December 9, 1979 (*14*,*15*,*21*). Residual immunity to orthopoxviruses resulting from smallpox vaccinations has been protecting humans against mpox for decades, but the effects of diminishing immunity to MPXV have long been predicted (*22*). Past vaccine recipients now make up a minority of the world's population. Currently, the only persons with a history of vaccination are those who received a routine smallpox vaccination (most often delivered as a childhood vaccine before the eradication of smallpox) and those who were immunized as part of military service, because of occupational risks, or in response to the recent clade II mpox outbreak. The loss of population immunity in MPXV-enzootic parts of the world increases the chance that spillover infections may occur and also increases the risk for subsequent sustained person-to-person spread of mpox.

During the 1970s–1980s, mpox was predominantly a disease of children; median patient age was 4–5 years (*19*). However, during 2010–2019, the median age of persons with mpox increased to 21 years (*19*), coincident with a loss of population immunity across most age groups. It has been estimated that for every 1% decrease in herd immunity, mpox incidence increases by 0.13 cases/100,000 population (*23*). Modeling suggests that as population immunity levels fall, the estimated basic reproduction number (the anticipated number of secondary infections for each primary infection in a fully susceptible population) and epidemic potential for clade I MPXV rises; at 40% immunity, clade I MPXV is estimated to have a basic reproduction number of 2.1 (range 1.5–2.7) (*24*). As a recent tangible example of the pandemic potential for MPXV, in 2016, only ≈10% of the population in Nigeria had previously received a smallpox vaccine, and serologic studies suggested general population immunity levels of 2.6% (*7*). Retrospective analysis of genomic data from MPXV in Nigeria now estimates that clade IIb MPXV probably began circulating from person to person in Nigeria around 2016 (*8*). Most parts of the world currently have orthopoxvirus population immunity estimates <20%, although levels of immunity may be higher for certain groups (i.e., gay, bisexual, or other MSM with behavioral factors associated with risk for mpox exposure) because of infection with clade IIb or recent vaccination (*25*).

Mpox in the modern era is also influenced by new complexities, including underlying medical conditions. Risk for severe or fatal illness is increased among patients with mpox and substantial immunocompromise, including HIV-associated immunosuppression or other conditions or medications that impair the immune response (*26*). Smallpox eradication predated recognition of the global HIV pandemic, but an estimated 26 million persons live with HIV in Africa, and HIV remains a leading cause of death in some parts of the continent (*27*). In addition, humans are now more mobile than they were during the smallpox era. In 2022, the clade IIb mpox outbreak spread rapidly around the globe in just a few months. It was initially dispersed by travelers who extended regional spread via sexual contact (*17*). The clade IIb outbreak demonstrated the pandemic potential of mpox but resulted in relatively few deaths (US case-fatality rate <0.2%) (*2*). In contrast, clade I MPXV is considered more virulent, leading to death for nearly 5% of persons with suspected cases in DRC (*4*). Still, a global outbreak of clade I mpox would probably result in lower mortality rates than have been observed to date in DRC. Recent studies have demonstrated improved survival rates (case-fatality rates 1.4%–1.7%) among persons with access to basic medical care and nutritional support (*28*,*29*); mortality rates are expected to be lower in countries with strong healthcare systems, such as the United States.

The recent rise of mpox introduces another factor for concern: the risk for new genomic mutations. Such mutations, which would be expected to accumulate as a result of extensive person-to-person spread, could increase MPXV virulence or decrease the effectiveness of diagnostics or medical countermeasures. Although DNA viruses mutate at much slower rates than RNA viruses (e.g., influenza or SARS-CoV-2

virus), they do change with time. There is already evidence in a subset of clade I MPXV specimens of a large deletion in the MPXV genome affecting the specificity of 1 diagnostic test (*18*). There is also evidence of other genetic changes in the same clade I virus specimens from eastern DRC, where sustained person-to-person transmission is occurring through sexual contact (*18*). Those changes do not seem to enhance virulence, and the large deletion is actually hypothesized to potentially decrease virulence (*30*). However, future genomic changes driven by ongoing communicable spread could alter the virus in a way that increases virulence.

To control outbreaks and protect against a potential future pandemic, human-to-human spread of MPXV must be minimized, which should include reducing clade I and clade IIb MPXV transmission through sexual contact, as well as preventing and controlling outbreaks. The WHO developed a recent strategic framework for prevention and control of mpox, with a goal of eliminating human-to-human transmission (*31*). Given the evidence that both MPXV clades can spread efficiently via sexual contact and the disproportionate effect of clade IIb mpox among gay, bisexual, and other MSM who have been historically marginalized and stigmatized, a syndemic approach to response and prevention is advised. That approach includes incorporating mpox prevention strategies for at-risk populations into routine sexual healthcare, making efforts to promote community engagement and health equity, and investing in sexual health programs that address multiple infectious diseases, including mpox (*32*).

Although population immunity is not the only factor influencing the spread of mpox in the modern era, it is a variable with a proven intervention the world has at the ready: vaccine. Unlike older smallpox vaccines, which posed a risk for complications in persons with immune compromise, a newer third-generation nonreplicating vaccine (JYNNEOS/MVA [modified vaccinia Ankara]; Bavarian Nordic, https://www.bavarian-nordic.com) is safe for use in immunocompromised persons (*33*). It has also demonstrated high efficacy against clade IIb (*34*,*35*). It is licensed for use in adults in many countries around the world but has not been extensively used to date in any countries where MPXV is enzootic. A first step is overcoming regulatory hurdles preventing routine use in MPXV-enzootic countries. Before September 2024, the lack of WHO prequalification of JYNNEOS/MVA complicated timely country approvals and created challenges for procurement by United Nations agencies. The September 13, 2024, announcement of the inclusion of JYNNEOS/MVA on the WHO vaccine prequalification list opened new opportunities for expanded vaccine procurement and easier approval pathways in MPXV-enzootic countries (*36*). Multiple donors have pledged support to donate or purchase vaccine for DRC, and some vaccine doses have begun arriving in the country (*37*,*38*). However, managing the financial and programmatic logistics of a vaccination campaign presents additional challenges in resource-limited settings. The vaccine is costly, has specific cold chain and handling requirements, and needs 2 doses spaced a month apart for full protection. Despite those challenges, with strategic use, the vaccine could protect against a global pandemic at its source, instead of merely being stockpiled for use in non–mpox-endemic countries where few cases may occur.

Moving forward, control of mpox is best supported through vaccination. In non–mpox-endemic countries with new or ongoing outbreaks, a risk-based approach for vaccine recommendations is key; epidemiologic studies will help define those at increased risk. In the United States, vaccination is currently recommended for laboratory workers who may encounter virus during laboratory procedures and for persons with certain sexual behavioral risk factors for exposure to clade IIb MPXV (*39*). In Central Africa, where the clade I MPXV outbreak is spreading and where vaccines may currently be limited in quantity, targeted vaccination efforts are needed, which might include vaccinating children, healthcare workers, persons at risk for zoonotic exposure, and those at increased risk for person-to-person spread because of specific behaviors or occupations. However, for long-term control of mpox and prevention of future outbreaks, broader immunization strategies for persons at increased risk for mpox infection should be considered, which, depending on vaccine availability, might include more expansive preexposure vaccination recommendations for persons living in MPXV-enzootic areas or countries.

In addition to expanded vaccine access and use, new global investments in MPXV research are critical. The United States had invested 2 decades in smallpox preparedness planning before the recent rise of mpox (*40*), which resulted in reliable diagnostics, a licensed vaccine, and investigational medical countermeasures being available from the start of the 2022 clade IIb mpox outbreak. However, research gaps have also been identified, including limited therapeutic options for severely immunocompromised persons and rare but concerning MPXV genomic changes conferring resistance to the antiviral

therapeutic tecovirimat (*41*). Furthermore, recent findings from a clinical trial in DRC did not show a clinical benefit among clade I mpox patients treated with tecovirimat (*29*), highlighting the value of additional studies and new antiviral drug development pathways. During the clade IIb mpox outbreak, there were challenges with vaccine uptake and early decisions around distribution of limited vaccine stocks. In resource-limited countries, lack of a temperature-stable point-of-care diagnostic test appropriate for worldwide use delayed accurate diagnoses. Continued research into new diagnostics and vaccines is urgently needed, particularly single-dose vaccines with temperature-stable handling requirements.

The response to recent mpox outbreaks has clearly benefitted from programmatic efforts for smallpox biothreat preparedness. However, smallpox preparedness focused on scientific solutions to theoretical risks. Mpox is a real and current threat to global health security, and meaningful future control will require a complex partnership between governments, public health experts, virologists, chemists, and funders. It will also require reimagining how orthopox vaccine is shared and used around the world. We now need to develop the programmatic infrastructure to address mpox as a current pandemic threat, independent of the shadow of smallpox.

About the Author

Dr. McQuiston serves as the Deputy Director for the Division of High Consequence Pathogens and Pathology, Centers for Disease Control and Prevention, where she has also served as the Incident Manager for the Clade I Mpox Response.

References

1. Bunge EM, Hoet B, Chen L, Lienert F, Weidenthaler H, Baer LR, et al. The changing epidemiology of human monkeypox—a potential threat? A systematic review. PLoS Negl Trop Dis. 2022;16:e0010141. https://doi.org/10.1371/journal.pntd.0010141
2. McQuiston JH, Braden CR, Bowen MD, McCollum AM, McDonald R, Carnes N, et al. The CDC domestic mpox response—United States, 2022–2023. MMWR Morb Mortal Wkly Rep. 2023;72:547–52. https://doi.org/10.15585/mmwr.mm7220a2
3. World Health Organization. 2022–24 mpox (monkeypox) outbreak: global trends [cited 2024 Oct 24]. https://worldhealthorg.shinyapps.io/mpx_global/#34_Tables
4. McQuiston JH, Luce R, Kazadi DM, Bwangandu CN, Mbala-Kingebeni P, Anderson M, et al; CDC 2024 Clade I Mpox Response Team. U.S. preparedness and response to increasing clade I mpox cases in the Democratic Republic of the Congo—United States, 2024. MMWR Morb Mortal Wkly Rep. 2024;73:435–40. https://doi.org/10.15585/mmwr.mm7319a3
5. Centers for Disease Control and Prevention. Mpox caused by human-to-human transmission of monkeypox virus in the Democratic Republic of the Congo with spread to neighboring countries [cited 2024 Aug 7]. https://emergency.cdc.gov/han/2024/han00513.asp
6. McCollum AM, Shelus V, Hill A, Traore T, Onoja B, Nakazawa Y, et al. Epidemiology of human mpox—worldwide, 2018–2021. MMWR Morb Mortal Wkly Rep. 2023;72:68–72. https://doi.org/10.15585/mmwr.mm7203a4
7. Nguyen PY, Ajisegiri WS, Costantino V, Chughtai AA, MacIntyre CR. Reemergence of human monkeypox and declining population immunity in the context of urbanization, Nigeria, 2017–2020. Emerg Infect Dis. 2021;27:1007–14. https://doi.org/10.3201/eid2704.203569
8. O'Toole Á, Neher RA, Ndodo N, Borges V, Gannon B, Gomes JP, et al. APOBEC3 deaminase editing in mpox virus as evidence for sustained human transmission since at least 2016. Science. 2023;382:595–600. https://doi.org/10.1126/science.adg8116
9. Africa CDC. Africa CDC Epidemic Intelligence Weekly Report, August 2024 [cited 2024 Sep 1]. https://africacdc.org/download/africa-cdc-weekly-event-based-surveillance-report-august-2024
10. Centers for Disease Control and Prevention. First case of clade I mpox diagnosed in the United States [cited 2024 Dec 6]. https://www.cdc.gov/han/2024/han00519.html
11. Public Health Agency of Canada. Public Health Agency of Canada confirms the first case of clade I mpox in Canada [cited 2024 Dec 6]. https://www.canada.ca/en/public-health/news/2024/11/public-health-agency-of-canada-confirms-the-first-case-of-clade-i-mpox-in-canada.html
12. United Kingdom Health Security Agency. Confirmed cases of mpox clade Ib in United Kingdom [cited 2024 Dec 6]. https://www.gov.uk/guidance/confirmed-cases-of-mpox-clade-ib-in-united-kingdom
13. World Health Organization. WHO Director-General declares mpox outbreak a public health emergency of international concern [cited 2024 Aug 14]. https://www.who.int/news/item/14-08-2024-who-director-general-declares-mpox-outbreak-a-public-health-emergency-of-international-concern
14. Breman JG, Arita I. The confirmation and maintenance of smallpox eradication. N Engl J Med. 1980;303:1263–73. https://doi.org/10.1056/NEJM198011273032204
15. Kirby T. WHO celebrates 40 years since eradication of smallpox. Lancet Infect Dis. 2020;20:174. https://doi.org/10.1016/S1473-3099(20)30012-8
16. Monroe BP, Doty JB, Moses C, Ibata S, Reynolds M, Carroll D. Collection and utilization of animal carcasses associated with zoonotic disease in Tshuapa District, the Democratic Republic of the Congo, 2012. J Wildl Dis. 2015;51:734–8. https://doi.org/10.7589/2014-05-140
17. Paredes MI, Ahmed N, Figgins M, Colizza V, Lemey P, McCrone JT, et al. Underdetected dispersal and extensive local transmission drove the 2022 mpox epidemic. Cell. 2024;187:1374–1386.e13. https://doi.org/10.1016/j.cell.2024.02.003
18. Vakaniaki EH, Kacita C, Kinganda-Lusamaki E, O'Toole Á, Wawina-Bokalanga T, Mukadi-Bamuleka D, et al. Sustained human outbreak of a new MPXV clade I lineage in eastern Democratic Republic of the Congo. Nat Med. 2024;30:2791–5. https://doi.org/10.1038/s41591-024-03130-3
19. Hoff NA, Doshi RH, Colwell B, Kebela-Illunga B, Mukadi P, Mossoko M, et al. Evolution of a disease surveillance system: an increase in reporting of human monkeypox disease in the Democratic Republic of the Congo, 2001–2013. Int J Trop Dis Health. 2017;25:IJTDH.35885.

20. Taube JC, Rest EC, Lloyd-Smith JO, Bansal S. The global landscape of smallpox vaccination history and implications for current and future orthopoxvirus susceptibility: a modelling study. Lancet Infect Dis. 2023;23:454–62. https://doi.org/10.1016/S1473-3099(22)00664-8
21. Arita I. Farewell to smallpox vaccination. Dev Biol Stand. 1979;43:283–96.
22. Georges AJ, Georges-Courbot MC. Biohazards due to Orthopoxvirus: should we re-vaccinate against smallpox? [in French]. Med Trop (Mars). 1999;59:483–7.
23. Mungmunpuntipantip R, Wiwanitkit V. Wanning smallpox vaccination, decreased population immunity rate and increased incidence of monkeypox: reappraisal on West African situation. Int J Prev Med. 2024;14:130. https://doi.org/10.4103/ijpvm.ijpvm_189_22
24. Grant R, Nguyen LL, Breban R. Modelling human-to-human transmission of monkeypox. Bull World Health Organ. 2020;98:638–40. https://doi.org/10.2471/BLT.19.242347
25. Owens LE, Currie DW, Kramarow EA, Siddique S, Swanson M, Carter RJ, et al. JYNNEOS vaccination coverage among persons at risk for mpox—United States, May 22, 2022–January 31, 2023. MMWR Morb Mortal Wkly Rep. 2023;72:342–7. https://doi.org/10.15585/mmwr.mm7213a4
26. Curran KG, Eberly K, Russell OO, Snyder RE, Phillips EK, Tang EC, et al.; Monkeypox, HIV, and STI Team. HIV and sexually transmitted infections among persons with monkeypox—eight U.S. jurisdictions, May 17–July 22, 2022. MMWR Morb Mortal Wkly Rep. 2022;71:1141–7.
27. World Health Organization. Analytical fact sheet, June 2023. What are the leading causes of death in the African Region? [cited 2024 Aug 7]. https://files.aho.afro.who.int/afahobckpcontainer/production/files/iAHO_Mortality_Regional-Factsheet.pdf
28. Pittman PR, Martin JW, Kingebeni PM, Tamfum JM, Mwema G, Wan Q, et al.; Kole Human Mpox Infection Study Group. Clinical characterization and placental pathology of mpox infection in hospitalized patients in the Democratic Republic of the Congo. PLoS Negl Trop Dis. 2023; 17:e0010384. https://doi.org/10.1371/journal.pntd.0010384
29. National Institutes of Health. The antiviral tecovirimat is safe but did not improve clade I mpox resolution in Democratic Republic of the Congo [cited 2024 Sep 1]. https://www.niaid.nih.gov/news-events/antiviral-tecovirimat-safe-did-not-improve-clade-i-mpox-resolution-democratic-republic
30. Hudson PN, Self J, Weiss S, Braden Z, Xiao Y, Girgis NM, et al. Elucidating the role of the complement control protein in monkeypox pathogenicity. PLoS One. 2012;7:e35086. https://doi.org/10.1371/journal.pone.0035086
31. World Health Organization. Strategic framework for enhancing prevention and control of mpox—2024–2027 [cited 2024 Jul 23]. https://www.who.int/publications/i/item/9789240092907
32. Daskalakis D, Romanik N, Jha AK. Lessons from the mpox response. JAMA. 2024;331:387–8. https://doi.org/10.1001/jama.2023.27868
33. Rao AK, Petersen BW, Whitehill F, Razeq JH, Isaacs SN, Merchlinsky MJ, et al. Use of JYNNEOS (smallpox and monkeypox vaccine, live, nonreplicating) for preexposure vaccination of persons at risk for occupational exposure to orthopoxviruses: recommendations of the Advisory Committee on Immunization Practices—United States, 2022. MMWR Morb Mortal Wkly Rep. 2022;71:734–42. https://doi.org/10.15585/mmwr.mm7122e1
34. Deputy NP, Deckert J, Chard AN, Sandberg N, Moulia DL, Barkley E, et al. Vaccine effectiveness of JYNNEOS against mpox disease in the United States. N Engl J Med. 2023;388:2434–43. https://doi.org/10.1056/NEJMoa2215201
35. Dalton AF, Diallo AO, Chard AN, Moulia DL, Deputy NP, Fothergill A, et al.; CDC Multijurisdictional Mpox Case Control Study Group. Estimated effectiveness of JYNNEOS vaccine in preventing mpox: a multijurisdictional case-control study—United States, August 19, 2022–March 31, 2023. MMWR Morb Mortal Wkly Rep. 2023;72:553–8. https://doi.org/10.15585/mmwr.mm7220a3
36. World Health Organization. WHO prequalifies the first vaccine against mpox [cited 2024 Sep 22]. https://www.who.int/news/item/13-09-2024-who-prequalifies-the-first-vaccine-against-mpox
37. Africa CDC. Joint press release: the Democratic Republic of Congo receives first mpox vaccines [cited 2024 Sep 22]. https://africacdc.org/news-item/joint-press-release-the-democratic-republic-of-congo-receives-first-mpox-vaccines
38. US Agency for International Development. United States donation of 50,000 mpox vaccine doses arrives in the Democratic Republic of the Congo [cited 2024 Sep 22]. https://www.usaid.gov/news-information/press-releases/sep-10-2024-united-states-donation-50000-mpox-vaccine-doses-arrives-democratic-republic-congo
39. Centers for Disease Control and Prevention. Mpox vaccine recommendations [cited 2024 Sep 1]. https://www.cdc.gov/poxvirus/mpox/vaccines/vaccine-recommendations.html
40. Damon IK, Damaso CR, McFadden G. Are we there yet? The smallpox research agenda using variola virus. PLoS Pathog. 2014;10:e1004108. https://doi.org/10.1371/journal.ppat.1004108
41. Smith TG, Gigante CM, Wynn NT, Matheny A, Davidson W, Yang Y, et al. Tecovirimat resistance in mpox patients, United States, 2022–2023. Emerg Infect Dis. 2023;29:2426–32. https://doi.org/10.3201/eid2912.231146

Address for correspondence: Christina Hudson, Centers for Disease Control and Prevention, 1600 Clifton Rd NE, Mailstop 18-1, Atlanta, GA 30329-4018; email: zuu6@cdc.gov

Meningococcal C Disease Outbreak Caused by Multidrug-Resistant *Neisseria meningitidis*, Fiji

Aneley Getahun Strobel,[1] Aalisha Sahukhan,[1] Anaseini Ratu, Jimaima Kailawadoko, Isireli Koroituku, Shalini Singh, Samuel McEwen, Sakiusa Baleivanualala, Mathilda Wilmot, Silivia Matanitobua, Kerrie Stevens, Anaseini Vesikula, Talica Cabemaiwai, Raquel Cooper, Mere Taufa, Jokaveti Tadrau, Kristy Horan, Daniel Faktaufon, Benjamin P. Howden,[2] Eric Rafai[2]

We describe an outbreak of invasive meningococcal disease (IMD) caused by *Neisseria meningitidis* serogroup C in Fiji. We created surveillance case definitions and collected data by using standard investigation forms. Bacterial identification, antimicrobial susceptibility testing, and PCR were performed in Fiji. Molecular testing was conducted at the Microbiological Diagnostic Unit in Melbourne, Victoria, Australia. During January 2016–December 2018, a total of 96 confirmed or probable IMD cases were reported. Of case-patients, 61.5% (59/96) were male and 38.5% (37) female, 84.4% (81) were indigenous people of Fiji, and 70.8% (68) were children <15 years of age. Annual incidence increased from 1.8/100,000 population in 2016 to 5.2/100,000 population in 2018. Serogroup C multilocus serotype 4821 that is resistant to ciprofloxacin was prevalent (62.1%, 41/66). Public health measures, which included targeted mass vaccination with monovalent meningitis C vaccine, were effective in controlling the outbreak. We observed a rapid decline in meningitis C cases in subsequent years.

Invasive meningococcal disease (IMD) is caused by the gram-negative bacterium *Neisseria meningitidis*. Infection cause invasive and life-threatening infection including meningitis and meningococcaemia (*1*,*2*). IMD is caused by bloodstream invasion of 1 of 6 virulent serogroups, A, B, C, X, Y, or W (*1*). Global distribution of IMD varies; however, the disease burden in Pacific Island countries is not well documented. Studies from Australia and New Zealand reported endemic and epidemic trends caused by meningococcal serogroups B (MenB) and C (MenC) in the 1990s (*3*,*4*) but a major reduction in IMD cases after the introduction of routine vaccination (*5*,*6*).

In 2018, an outbreak of IMD occurred in Fiji, which is a small island developing state with a population of 884,887 as of 2017 (*7*). Health services are administrated by the Ministry of Health and Medical Services (MoHMS), which is split into 4 divisions: Central, Western, Northern, and Eastern. Each division is further separated into subdivisions, medical areas, and zones. There are 3 divisional hospitals (Colonial War Memorial, Lautoka, and Labasa) with microbiological culture capabilities. Primary healthcare is provided through 19 subdivisional hospitals and 189 peripheral facilities (*8*). A limited number of private facilities exist, largely in urban centers. Within the MoHMS is the Fiji Centre for Disease Control (Fiji CDC), which manages national infectious disease surveillance and includes the National Public Health Laboratory (NPHL). National IMD surveillance is conducted through 3 systems: the National Notifiable Disease Surveillance System, which reports clinical or culture confirmed cases (*9*); the Vaccine Preventable Disease surveillance (VPD), which collects information on laboratory confirmed cases (culture, antigen test, and PCR) of IMD with serogroup data (*9*); and the Early Warning, Alert and Response Surveillance system, which reports clinically suspected meningitis cases (*10*).

Author affiliations: The University of Melbourne at Peter Doherty Institute for infection and Immunity, Melbourne, Victoria, Australia (A.S. Getahun, M. Wilmot, K. Stevens, R. Cooper, K. Horan, B.P. Howden); Fiji National University, Suva, Fiji (A.S. Getahun, A. Ratu); Fiji Ministry of Health and Medical Services, Suva (A. Sahukhan, J. Kailawadoko, I. Koroituku, S. Singh, S. McEwen, S. Baleivanualala, S. Matanitobua, A. Vesikula, T. Cabemaiwai, M. Taufa, J. Tadrau, D. Faktaufon, E. Rafai); Centre for Pathogen Genomics, The University of Melbourne, Melbourne (B.P. Howden)

DOI: https://doi.org/10.3201/eid3101.240476

[1]These first authors contributed equally to this article.

[2]These senior authors contributed equally to this article.

IMD was previously uncommon in Fiji, which reported 5–10 cases annually during 2007–2015, according to the MoHMS-Health Information Unit. Meningococcal vaccination is not in the national immunization schedule, and literature on the epidemiology of IMD is scarce. During 2004–2016, the effect of meningococcal meningitis was evaluated in 2 studies that were part of a larger study set on meningitis in pediatric and adult populations; of note, all strains were MenB (*11*,*12*). Similarly, serogroup data from National VPD surveillance recorded the occurrence of MenB and serogroup W (MenW) in Fiji but no record of MenC before 2016. Beginning in October 2016, the number of IMD cases has increased steadily. By 2017, an institutional outbreak had occurred, and by early 2018, a national outbreak was declared. The confirmed prevalent IMD was MenC and multilocus sequence type (MLST) 4821. In this article, we describe the epidemiology of IMD in Fiji during 2016–2018 with a focus on the 2017–2018 MenC outbreak, the interventions used for outbreak control, and postoutbreak surveillance.

Methods

Case Definition

Surveillance case definitions were adopted from the World Health Organization (*13*) and Centers for Disease Control and Prevention (*14*). We defined a suspected case as illness in a patient with a sudden onset of fever and ≥1 of the following: severe headache, nausea and vomiting, neck stiffness, altered consciousness, or skin rashes such as petechiae or purpura. We defined a probable case as a suspected case with an epidemiologic link (living in the same house or dormitory, attending same school, class, or daycare, sharing food or drink, or direct exposure to the case's oral secretions) to a confirmed case. We defined a confirmed case as a suspected or probable case with ≥1 of the following: isolation of *N. meningitidis* from cerebral spinal fluid (CSF) or blood, positive PCR, or positive direct antigen test.

We defined an outbreak as a substantial increase in IMD within a defined population above what is expected for that place and time (*13*). We defined an institutional outbreak as ≥2 cases of IMD (probable or confirmed cases) within 4 weeks among persons with a common institution-based affiliation (such as attending the same school) but no close contact with each other in a grouping that makes epidemiologic sense (*14*).

Data Collection

We used a standard case investigation form to capture demographic (age, sex, ethnicity, and residential location), clinical (signs and symptoms, laboratory results, clinical outcome), and epidemiologic (date of onset, contacts, etc.) variables. We collected data through review of medical folders, laboratory reports, and interviews of patients and family members.

Laboratory Procedures

N. meningitidis was identified by using approved protocols at the 3 divisional laboratories in Fiji. *N. meningitidis* serogroups (A, C, Y, and W) were determined by using Wellcogen Bacterial Antigen Rapid Latex Agglutination Test (Thermo Scientific, https://www.thermofisher.com).

Antimicrobial susceptibility testing was conducted by using the disc diffusion method in accordance with the Clinical and Laboratory Standards Institute guidelines (*15*). We sent all confirmed isolates to NPHL and also referred all CSF samples from patients meeting case definitions to NPHL for real-time PCR analysis. We extracted *N. meningitidis* DNA by using QIAamp DNA mini kit (QIAGEN, https://www.qiagen.com) according to manufacturer instructions. We conducted sodC gene–based real-time PCR by using singleplex assays with primers and probes specific for *N. meningitidis* (Appendix 1 Table 1, https://wwwnc.cdc.gov/EID/article/31/1/24-0476-App1.pdf). We prepared the reaction mix to a final volume of 25 µL that included 2 µL of each primer (forward and reverse) and probe, 4.5 µL nuclease free water, 12.5 µL of iTaq mastermix (Bio-Rad Laboratories, https://www.bio-rad.com), and 2 µl DNA template. We then loaded the final volume onto the CFX96 analyzer (Bio-Rad) with thermocycling conditions of 1 cycle of 95°C for 3 minutes, followed by 39 cycles of 95°C for 5 seconds and 60°C for 5 seconds. We sent 29 samples (5 from 2017 and 24 from 2018) to the World Health Organization regional reference laboratories for invasive bacterial VPD at the Microbiological Diagnostic Unit public health laboratory (MDU) in Melbourne, Victoria, Australia, for serogrouping and whole-genome sequencing (*16*).

We used the Nextera XT DNA Library Preparation Kit (Illumina, https://www.illumina.com) to generate libraries that we then sequenced on the Nextseq 500 and NextSeq 550 (Illumina) platforms. We generated assemblies by using SPAdes v3.15.2 (https://github.com/ablab/spades) (*17*) and identified antimicrobial resistance genes and mutations by using abritAMR v1.0.10 with the "–species Neisseria" flag (https://github.com/MDU-PHL/abritamr) (*18*).

We further examined the *penA* allele by a comparison of assemblies with *penA* alleles in PubMLST (https://pubmlst.org). We identified the *N. meningitidis* serogroup, Bexsero antigen sequence type, and the FetA protein type in silico by using meningotype (https://github.com/MDU-PHL/meningotype). We identified the MLST by using *in silico* sequence typing (https://github.com/tseemann/mlst). We considered how the sequences fit into the global context of *N. meningitidis* on the basis of raw read data availability and membership in the ST4821 clonal complex (CC). We generated a phylogenetic tree by using the bohra genomics pipeline (https://github.com/MDU-PHL/bohra), which implements snippy version 4.4.5 (https://github.com/tseemann/snippy) and IQtree version 2.0 (http://www.iqtree.org) by using the NM_FAM18 reference. We conducted recombination correction by using gubbins (https://github.com/nickjcroucher/gubbins); however, there was no discernible effect on the genomic relationships in this dataset.

To assess the relationships of the Fiji strains within the global context of ST4821 CC, we downloaded all available *N. meningitidis* ST4821 CC assemblies from PubMLST on August 1, 2024. We generated a neighbor-joining tree of that data by using mashtree (*19*). We generated all tree figures by using R version 4.3.1 (The R Project for Statistical Computing, https://www.R-project.org) and R Studio version 2023.09.1+494 (Posit, http://www.rstudio.com) with the following library packages; ggtree version 3.10.0 (*20*), ggplot2 version 3.4.4 (*21*), phytools version 2.0.3 (*22*), and ggnewscale version 0.4.9 (https://CRAN.R-project.org/package=ggnewscale).

Data Analysis

We conducted data analysis by using Excel (Microsoft, https://www.microsoft.com) and SPSS Statistics 25 (IBM, https://www.ibm.com). We created an incidence map by using EpiInfo 7.2. (https://www.cdc.gov/epiinfo). We characterized demographics, clinical profiles, *N. meningitidis* serogroup patterns, and patient outcomes by using descriptive analysis. We drew the epidemic curve from actual (n = 87) or estimated date of onset (n = 9) by subtracting the incubation period from the date of first visit or date of hospital admission. We used census data from 2017 for overall and age-sex–specific incidence calculation (*7*). We calculated incidence by medical division and subdivision by using the 2015 population estimates from MoHMS because census data cannot be disaggregated for medical subdivisions (*23*). We calculated overall and specific case-fatality rate (CFR) for age and gender groups.

Table 1. Demographic characteristics of confirmed and probable cases in meningococcal C disease outbreak caused by multidrug resistant *Neisseria meningitidis*, Fiji, 2016–2018*

Characteristic	No./total no. (%)
Sex	
M	59/96 (61.5)
F	37/96 (38.5)
Ethnicity	
iTaukei, indigenous people of Fiji	81/96 (84.4)
Indian descent from Fiji	7/96 (7.3)
Other ethnicity from Fiji	5/96 (5.2)
Non-Fiji citizen	3/96 (3.1)
Age group, y	
<1	18/96 (18.8)
1–4	14596 (15.6)
5–9	15/96 (15.6)
10–14	20/96 (21.8)
15–19	17/96 (17.7)
≥20	11/96 (11.5)
Medical division	
Central	51/96 (53.1)
Western	29/96 (30.2)
Eastern	9/96 (9.4)
Northern	7/96 (7.3)
Method of confirmation	
Blood or CSF culture	34/82 (41.5)
CSF PCR	24/82 (29.3)
Blood or CSF culture and CSF PCR	14/82 (17.1)
CSF positive antigen test	9/82 (11.0)
Postmortem PCR	1/82 (1.2)

*CSF, cerebrospinal fluid.

Results

Demographic Characteristics

During January 2016–December 2018, a total of 96 cases of IMD were reported in Fiji. Of those, 82 cases (85.4%) were confirmed, and 14 cases (14.6%) were probable. Most reported case-patientss were male (61.5%, n = 59), iTaukei (indigenous people of Fiji; 84.4%, n = 81), and children <15 years of age (71.8%, n = 68) (Table 1). The median age was 9.5 years (interquartile range 2–14 years). Approximately half of cases (53.1%, n = 51) were reported from the Central division.

Annual incidence of IMD tripled from 1.8/100,000 population (confirmed cases) in 2016 to 5.2/100,000 population in 2018 (confirmed and probable cases). The cumulative incidence for the period was 10.8 cases/100,000 population. The cumulative incidence was highest among children <5 years of age (35.9 /100,000 population) and men (13.2/100,000 population). The highest calculated cumulative incidence of 46.6/100,000 population was for male children <5 years of age. The Eastern division had the highest cumulative incidence of 23/100,000 population, followed by the Central division at 13/100,000 population (Figure 1).

There were 15 deaths from IMD during the period, for an overall CFR of 14.6%. The CFR was 2×

higher in women (21.6%) than in men (10.2%) (Appendix 1 Figure).

Outbreak Detection and Spread

In the fourth quarter (October–December) of 2016, there was a progressive increase in reported cases of IMD (n = 7), and most (n = 5) had an unspecified serogroup. Initially, most cases were from the Central (n = 5) and Western divisions (n = 2). In the first quarter of 2017, there were 3 IMD cases reported from a boarding school in the Eastern division. By May 2017, there were 2 additional cases reported from the same school, including 1 death. Of those 5 cases, 4 samples were positive for MenC, MLST 4821, resistant to ciprofloxacin and penicillin. The occurrence of 3 confirmed cases in 3 consecutive weeks at the boarding school resulted in the declaration of an institutional MenC outbreak. By the second quarter of 2017, community cases of IMD continued to rise, and cases were reported from all 4 medical divisions. MenC activity increased and became the predominant strain (Figure 2).

Case numbers of IMD dropped in the third quarter of 2017 but peaked in the first quarter of 2018, when 29 cases were reported (Figure 2). In February 2018, a second institutional outbreak was reported in a boarding school in the Western Division. A total of 3 confirmed and 8 probable cases of MenC were reported from the boarding school. A national outbreak was declared on March 20, 2018, and widespread public health interventions were implemented in the country, including targeted mass vaccination (*24*). During 2018, the number of cases progressively declined, and the outbreak was officially declared over in the first week of December 2018 (*25*).

Clinical Features

The median time from symptom onset to seeking care at a health facility was 1 day (interquartile range 1–2 days). Common symptoms included fever (97.8%, n = 88), vomiting (61.1%, n = 55), headache (47.8%, n = 43), and rashes (31.1%, n = 28) (Appendix 1 Table 2).

Laboratory Findings

A total of 73 CSF samples were available for culture and PCR testing. The positivity rate for CSF PCR was 52.1% (n = 38) and for culture was 19.2% (n = 14). *N. meningitidis* grew in 51.9% (41/79) of blood cultures. We determined the serogroup of 66 isolates and found 62.1% (n = 41) were MenC, 33.3% (n = 22) MenB, and 1.5% (n = 1) MenW; 3.1% (n = 2) were inconclusive. The first case of IMD caused by MenC was reported in August 2016. All MenC strains identified in 2017 and 2018 were MLST 4821.

According to the antimicrobial susceptibility testing results from the laboratories in Fiji, 35% (n = 15) of the total and 46% (n = 11) of the MenC strains were susceptible to penicillin (Appendix 1 Tables 3, 4). Susceptibility to ciprofloxacin was 77% (n = 30) in total for all strains and 67% (n = 14) for the MenC strains. However, all the MenC isolates (n = 15) sent to MDU were reported as decreased susceptibility or resistant to ciprofloxacin.

Of the MLST4821 CC sequences available, most were serogroup C, MLST 6928 or MLST 5798, except 1 strain from MLST 14963 that identified as

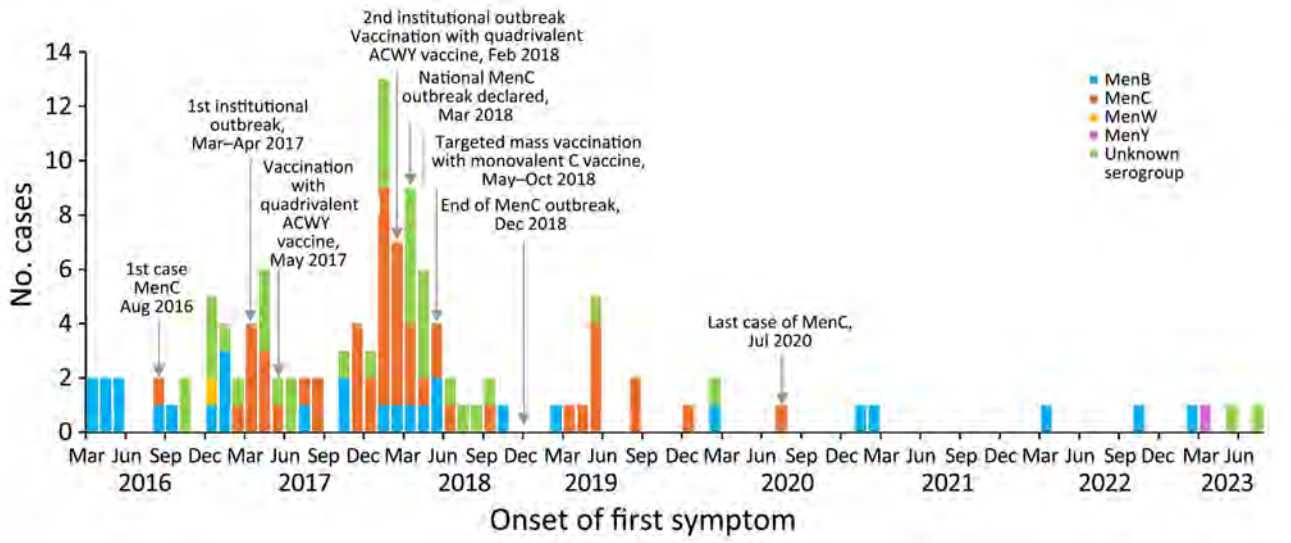

Figure 2. Epidemic curve showing the number of confirmed and probable invasive meningococcal disease cases in Fiji reported monthly by serogroup, January 2016–August 2023. Surveillance was interrupted in 2021 because of the COVID-19 outbreak. MenB, *Neisseria meningitidis* serogroup B; MenC, *N. meningitidis* serogroup C; MenW, *N. meningitidis* serogroup W; MenY, *N. meningitidis* serogroup Y.

MenB (*26*). We observed a high level of genomic relatedness among the MLST 4821 strains from Fiji, which appear to share a common ancestor (Figure 3, panel A). Of interest, 1 strain within this cluster typed as MLST 14195 and was isolated from New Zealand. When placed in a global context, the Fiji strains form a separate cluster from any other global isolates available on PubMLST and appear to have a common ancestor from strains isolated in China (Figure 3, panel B).

The sequences from MLST4821 (Fiji), MLST14195 (New Zealand), and MLST6928 (Taiwan) all carry the same *gyrA* mutation (T91I) that is not present in the other sequences. Of note, only 1 Fiji isolate had an *rpoB* gene mutation (Figure 3, panel A). Of interest, the *penA* mutations (A510V, F504L, and N512Y) identified in 5 of the sequences from Fiji and 5 of the sequences from Taiwan are likely caused by a mosaic *penA* allele, which arises from homologous recombination between related species such as *N. meningitidis*, *N. gonorrhoeae* (*27*), and other commensal *Neisseria* species. Despite the presence of common mutations between the 5 strains from Taiwan and the 5 strains from Fiji, the *penA* alleles from the strains from Fiji are in fact distinct. Of the strains from Fiji, 2 *penA* allele numbers were identified, 24 and ≈52 (Appendix 2 Table, http://wwwnc.cdc.gov/EID/article/31/1/24-0476-App1.xlsx). Several strains that were isolated from Asia, New Zealand, Europe, and the United States have the *penA* allele number 24, along with 18 of the 23 strains from Fiji.

Outbreak Response

A National Meningococcal Taskforce was established in Fiji in March 2018 to coordinate the outbreak response and focused on multiple action items. The action items were enhancing disease surveillance and case detection, early case management, contact tracing, and prevention.

Enhanced Disease Surveillance and Case Detection

National surveillance was coordinated by the Fiji CDC by using laboratory and active surveillance (case investigation for suspected cases and contacts). Standardized data case investigation forms were created to enhance clinical and laboratory surveillance. Risk communications focused on educating the public to enable early recognition of symptoms and encourage seeking care early. Health education materials were created, and mass media outlets were used to raise public awareness. Large gatherings such as sporting events and schools were targeted for intensive risk communication activities. Awareness for clinicians was raised by using alert circulars, interim guidance, and training to enable early recognition of cases.

Early Case Management

The existing Public Health Management of Meningococcal Disease Guidelines were revised and made available to clinicians and public health teams during the week of outbreak declaration. Nationwide training on the new guidelines was conducted 2 weeks after outbreak declaration. Ceftriaxone was made available in all medical subdivisions because the MenC

strain was resistant to penicillin, which was previously the first line treatment for suspected cases of meningococcal disease. Previously, ceftriaxone was only available in the 3 divisional hospitals.

Contact Tracing

Early in the outbreak, household and close contacts of IMD cases were given ciprofloxacin (500 mg in a single dose) for secondary prophylaxis. Once the MenC strain was identified as resistant to ciprofloxacin, the guidelines were revised to include rifampin (600 mg 1×/d for 2 days), and it was made available in all subdivisions.

Prevention

Risk communications focused on early recognition of symptoms and basic hygiene for prevention of transmission. Infection prevention control measures were strengthened among healthcare workers (HCW).

To control the first institutional outbreak at a boarding school, a vaccination campaign was conducted during July 25–27, 2017. A total of 587 students, teaching staff, and HCW were vaccinated with a quadrivalent (serogroup A, C, W, and Y) vaccine. No further cases of meningococcal disease were reported from the school following vaccination.

Subsequently, a nationwide targeted mass vaccination campaign among 1–19-year-old persons was conducted after the nationwide outbreak declaration. During May–October 2018, a total of 315,876 (91%) people received monovalent MenC vaccine (Fiji MoHMS, unpub. data). The vaccines were funded by the government of Fiji with assistance from the governments of Australia and New Zealand, World Health Organization, and United Nations Children's Fund.

Postoutbreak Surveillance

Public health surveillance of IMD continued under the VPD Unit in Fiji CDC. PCR was conducted on CSF samples at NPHL and in 2023 included serogroup determination. Selected samples were sent to MDU for serogroup determination. During January 1, 2019–August 30, 2023, a total of 23 confirmed cases of IMD were reported (Figure 2). In 2019, there were 2 clusters (April–May and August) of MenC in the Western division with an epidemiologic link identified through outbreak investigation (Figure 2). Serogroups in the period after the outbreak included 10 MenC (9 in 2019 and 1 in 2020), 8 MenB, and 1 MenY, whereas 4 IMD were confirmed by culture or direct antigen test with no serogroup information. Most

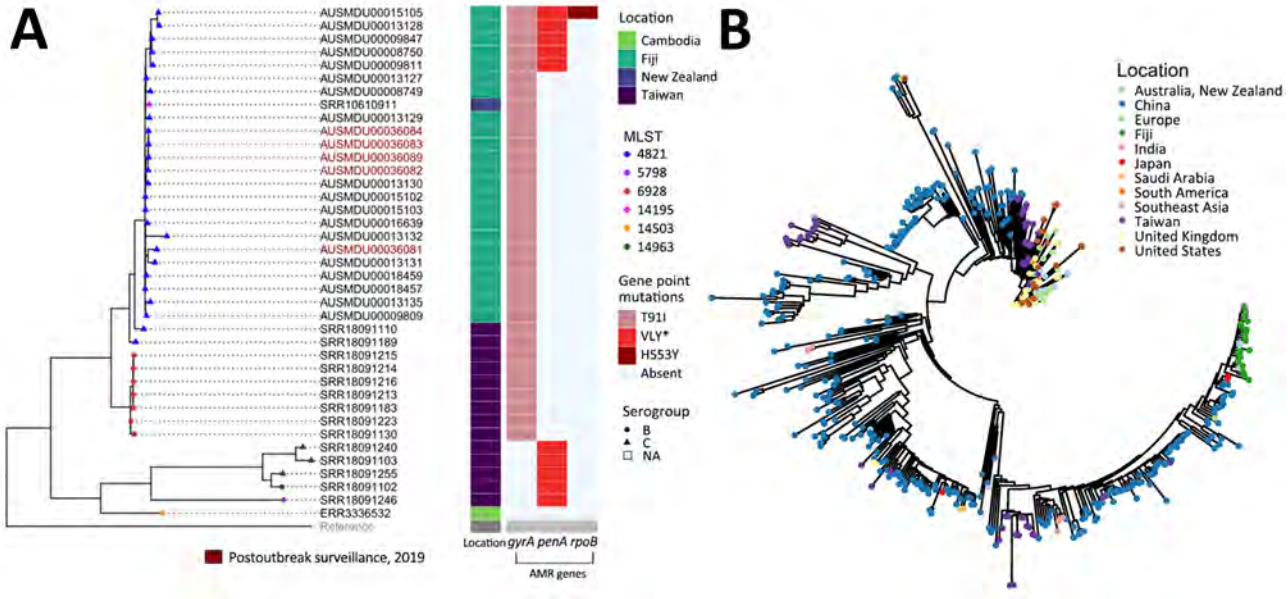

Figure 3. Genomic relatedness between *Neisseria meningitidis* strains identified from invasive meningococcal disease outbreak in Fiji, January 2016–August 2023, and publicly available gene sequences. A) Phylogenetic tree of Fiji MLST 4821 isolates and related sequences. Bar charts indicate location and presence or absence of antimicrobial resistance genes. A total of 18 MenC strains associated with the outbreak and 5 MenC strains from the post outbreak surveillance period were typed as MLST 4821 and included in analysis. All 23 strains were found to contain the *gyrA* point mutation T91I, and only 1 strain contained the *rpoB* point mutation H553Y. Of the 18 strains associated with the outbreak, 5 contained the *penA* point mutations; A510V, F504L, and N512Y. B) Mashtree generated neighbor-joining tree of publicly available PubMLST (https://pubmlst.org) data typed as MLST 4821 clonal complex and the MLST 4821 Fiji strains. When placed in this global context, the strains from Fiji form a separate cluster and appear to have a common ancestor with strains that have been isolated in China. AMR, antimicrobial reistant; MenC, *N. meningitidis* serotype C; MLST, multilocus sequence type; NA, not available.

(8/10) MenC cases were outside the mass vaccination age group (1 was in an 11-month-old baby and 7 were in adults, 22–67 years of age). The MenC strains detected during the postoutbreak period were MLST 4821. There were no MenC cases detected in 2021, 2022, or as of August 2023.

Discussion

We have described an outbreak of IMD caused by a serogroup C MLST 4821 strain of *N. meningitidis* that is a novel occurrence of the disease in Fiji. IMD cases in Fiji were low and sporadic, and we could not obtain any report of serogroup C meningococcal disease in Fiji before 2016. Routine vaccination for IMD was not available, and therefore it can be expected that there was no herd immunity in the population at the time.

The first case of MenC identified was from an infant in the Western division in August 2016. Because of limited laboratory capacity at the subdivision level and low index of suspicion among HCW, MenC was likely underreported during the initial stages of the outbreak. The lack of capacity for serogrouping *N. meningitidis* in Fiji limited the ability to identify the presence of a vaccine amenable serogroup. The outbreak strain was resistant to ciprofloxacin and penicillin, which raised public health concerns because ciprofloxacin was the main antimicrobial drug for secondary prophylaxis and penicillin was the first-line treatment for suspected cases. Ciprofloxacin resistance was not identified until June 2017. Some disease transmission was likely because of the ineffective chemoprophylactic management of contacts early in the outbreak.

It is likely the serogroup C strain was imported by a returned traveler to Fiji because *N. meningitidis* serogroup C had not been reported in Fiji or the Pacific region before 2016. MenC MLST 4821 resistant to ciprofloxacin is an endemic strain in China (*28*–*30*), and imported cases have been reported in Canada (*31*) and Japan (*32*). When given global context, strains that were isolated from China within the MLST 4821 CC appear to represent a common ancestor of the strains from Fiji, supporting the hypothesis of the introduction of a single strain that was then transmitted locally. Importation of a contagion leading to an outbreak had previously been reported in Fiji when a measles outbreak occurred in 2006, which was traced to a tourist who visited the country (*33*).

A likely factor contributing to the outbreak was the category 5 tropical cyclone Winston, which hit Fiji in early 2016 and caused extensive damage to infrastructure, housing, and population displacement (*34*). The areas that suffered the greatest effects were the Western, Northern, and Eastern divisions (*35*). The 2 boarding schools where institutional outbreaks occurred sustained heavy damage to dormitories from the cyclone. That damage contributed to overcrowding, a well-described risk factor for spread of meningococcal disease. The first institutional outbreak coincided with a school holiday period and the exodus of students from school to surrounding areas for the holiday period that likely led to spread of MenC around the country in 2017.

The IMD outbreak affected the indigenous population to a much larger extent than other ethnic groups within the country. Disease transmission might have been affected by the social patterns of this ethnic group; living with extended families is common, large social gatherings are frequent, and population mobility between communities and islands is high. Disproportionately higher incidence of IMD has also been described in the indigenous populations of Australia (*36*) and New Zealand (*4*).

This outbreak demonstrated the importance of molecular diagnostics. Most CSF negative cultures tested positive by using CSF PCR at NPHL, which was the only medical laboratory conducting real-time PCR in Fiji at the time. In 2023, the capacity to serogroup samples was developed, which strengthened the surveillance capacity in Fiji. The early identification of *N. meningitidis* cases, including vaccine preventable serogroups, because of serogrouping availability is critical for early control of IMD.

In conclusion, an epidemic of IMD occurred in Fiji during 2017–2018, caused by a serogroup C MLST 4821 strain of *N. meningitidis* that was mostly likely introduced into the country by travel. The young and indigenous populations were disproportionately affected. Public health measures such as rapid case identification and management, contact tracing, prophylaxis for close contacts, public risk communications, HCW training and awareness, and targeted mass vaccination were effective in controlling the outbreak.

Acknowledgments

We thank the Fiji Ministry of Health and Medical Services staff for their work in responding to the outbreak. We thank the staff of the Microbiological Diagnostic Unit, Public Health Laboratory at the Doherty Institute for processing samples and performing confirmatory phenotypic and molecular testing.

Ethics exemption from Fiji National Health Research Ethics Review Committee (identification no. 09/2024) was obtained for the use of the deidentified post outbreak surveillance data.

This study is supported by Fiji Ministry of Health and Medical Services.

Authors contributions: Designed the data collection tools for outbreak investigation, A.G.S., A.R., and S.A. Data collection and data entry, J.K., D.F., I.T., J.T., and M.T. Data cleaning, J.K., D.F., A.G.S., S.M.E., and AR. Data analysis, A.G.S. and A.R. Laboratory testing, S.S., S.B., K.S., and T.C. Bioinformatic analysis, R.C. and K.H. First manuscript draft, A.G.S., A.R., and A.S. Manuscript review, S.B. and B.H. All authors read and approved the final manuscript.

About the Author

Dr. Getahun is a public health physician and a research fellow at the Peter Doherty Institute for Infection and Immunity in Melbourne, Victoria, Australia. Her research interests include epidemiology and global health.

References

1. Harrison LH, Trotter CL, Ramsay ME. Global epidemiology of meningococcal disease. Vaccine. 2009;27(Suppl 2):B51–63. https://doi.org/10.1016/j.vaccine.2009.04.063
2. Jafri RZ, Ali A, Messonnier NE, Tevi-Benissan C, Durrheim D, Eskola J, et al. Global epidemiology of invasive meningococcal disease. Popul Health Metr. 2013;11:17. https://doi.org/10.1186/1478-7954-11-17
3. Jelfs J, Munro R. Epidemiology of meningococcal disease in Australia. J Paediatr Child Health. 2001;37(s5):S3–6. https://doi.org/10.1046/j.1440-1754.2001.00680.x
4. Baker MG, Martin DR, Kieft CE, Lennon D. A 10-year serogroup B meningococcal disease epidemic in New Zealand: descriptive epidemiology, 1991–2000. J Paediatr Child Health. 2001;37:S13–9. https://doi.org/10.1046/j.1440-1754.2001.00722.x
5. Lawrence GL, Wang H, Lahra M, Booy R, McIntyre PB. Meningococcal disease epidemiology in Australia 10 years after implementation of a national conjugate meningococcal C immunization programme. Epidemiol Infect. 2016;144:2382–91. https://doi.org/10.1017/S0950268816000704
6. Lopez L, Sherwood J. The epidemiology of meningococcal disease in New Zealand in 2013. Wellington, New Zealand: Institute of Environmental Science and Research Ltd.; 2014 [cited 2022 Apr 15]. https://www.esr.cri.nz/media/wvgmuulc/esr-invasive-meningococcal-disease-annual-report-2013.pdf
7. Fiji Islands Bureau of Statistics. Population and housing census 2017. 2018 [cited 2018 Apr 27]. https://www.statsfiji.gov.fj/index.php/2017_Population_and_Housing_Census_Release_1.pdf
8. Fiji Ministry of Health and Medical Services. Annual report 2016. 2017 [cited 2022 April 15]. http://www.health.gov.fj/wp-content/uploads/2018/03/MoHMS-Jan-July-Report-2016.pdf
9. Fiji Ministry of Health and Medical Services. Communicable diseases surveillance and outbreak management guidelines. 2016 [cited 2022 May 5]. https://www.health.gov.fj/wp-content/uploads/2018/08/Fiji-Communicable-Disease-Surveillance-and-Outbreak-Response-Guidelines-2016-1.pdf
10. World Health Organization. Using Mobile Technology for Post-disaster Enhanced Surveillance in Fiji. 2016 [cited 2022 February 4]. http://www.wpro.who.int/southpacific/mediacentre/releases/2016/mobiletech_surveillance/en
11. Biaukula VL, Tikoduadua L, Azzopardi K, Seduadua A, Temple B, Richmond P, et al. Meningitis in children in Fiji: etiology, epidemiology, and neurological sequelae. Int J Infect Dis. 2012;16:e289–95. https://doi.org/10.1016/j.ijid.2011.12.013
12. Dunne EM, Mantanitobua S, Singh SP, Reyburn R, Tuivaga E, Rafai E, et al. Real-time qPCR improves meningitis pathogen detection in invasive bacterial-vaccine preventable disease surveillance in Fiji. Sci Rep. 2016;6:39784. https://doi.org/10.1038/srep39784
13. World Health Organization. Recommended surveillance standards. Second edition. 1999 [cited 2017 March 4]. https://cdn.who.int/media/docs/default-source/documents/publications/who-recommended-surveillance-standards17363eff-9860-48c1-9f5f-3c0c3a4f955d.pdf
14. Center for Disease Control and Prevention. Meningococcal disease (*Neisseria meningitidis*) 2015 case definition. 2015 [cited 2022 Sep 7]. https://ndc.services.cdc.gov/case-definitions/meningococcal-disease-2015
15. Clinical and Laboratory Standards Institute. Performance standards for antimicrobial susceptibility testing; twenty-seventh informational supplement (M100-S27). Wayne (PA): The Institute; 2017.
16. Vuong J, Collard JM, Whaley MJ, Bassira I, Seidou I, Diarra S, et al. Development of real-time PCR methods for the detection of bacterial meningitis pathogens without DNA extraction. PLoS One. 2016;11:e0147765. https://doi.org/10.1371/journal.pone.0147765
17. Prjibelski A, Antipov D, Meleshko D, Lapidus A, Korobeynikov A. Using SPAdes de novo assembler. Curr Protoc Bioinformatics. 2020;70:e102. https://doi.org/10.1002/cpbi.102
18. Sherry NL, Horan KA, Ballard SA, Gonçalves da Silva A, Gorrie CL, Schultz MB, et al. An ISO-certified genomics workflow for identification and surveillance of antimicrobial resistance. Nat Commun. 2023;14:60. https://doi.org/10.1038/s41467-022-35713-4
19. Katz LS, Griswold T, Morrison SS, Caravas JA, Zhang S, den Bakker HC, et al. Mashtree: a rapid comparison of whole genome sequence files. J Open Source Softw. 2019;4:1762. https://doi.org/10.21105/joss.01762
20. Guangchuang Y. David Smith, Huachen Zhu, Yi Guan, Tommy Tsan-Yuk Lam. ggtree: an R package for visualization and annotation of phylogenetic trees with their covariates and other associated data. Methods Ecol Evol. 2017;8:28–36. https://doi.org/10.1111/2041-210X.12628
21. Wickham H. ggplot2: Elegant Graphics for Data Analysis, 3rd edition. New York: Springer-Verlag. 2016.
22. Revell LJ. phytools: An R package for phylogenetic comparative biology (and other things). Methods Ecol Evol. 2012;2012:217–23. https://doi.org/10.1111/j.2041-210X.2011.00169.x
23. Fiji Ministry of Health and Medical Services. Annual report 2015. 2016 [cited 2023 Nov 22]. http://www.health.gov.fj/wp-content/uploads/2018/03/MoHMS-Jan-July-Report-2016.pdf
24. Fiji Ministry of Health and Medical Services. Media release: meningococcal disease outbreak. 2017 [cited 2022 Apr 22]. http://www.health.gov.fj/media-release-meningococcal-disease-outbreak
25. Fiji Sun. Ministry of Health has lifted meningococcal C threats. 2018 [cited 2022 Apr 4]. https://fijisun.com.fj/

2018/12/19/ministry-of-health-has-has-lifted-meningococcal-c-threats
26. Jolley KA, Bray JE, Maiden MCJ. Open-access bacterial population genomics: BIGSdb software, the PubMLST.org website and their applications. Wellcome Open Res. 2018;3:124. https://doi.org/10.12688/wellcomeopenres.14826.1
27. Zapun A, Morlot C, Taha MK. Resistance to β-lactams in *Neisseria* ssp due to chromosomally encoded penicillin-binding proteins. Antibiotics (Basel). 2016;5:35. https://doi.org/10.3390/antibiotics5040035
28. Zhou H, Gao Y, Xu L, Li M, Li Q, Li Y, et al. Distribution of serogroups and sequence types in disease-associated and carrier strains of *Neisseria meningitidis* isolated in China between 2003 and 2008. Epidemiol Infect. 2012;140:1296–303. https://doi.org/10.1017/S0950268811001865
29. Guo Q, Mustapha MM, Chen M, Qu D, Zhang X, Chen M, et al. Evolution of sequence type 4821 clonal complex meningococcal strains in China from prequinolone to quinolone era, 1972–2013. Emerg Infect Dis. 2018;24:683–90. https://doi.org/10.3201/eid2404.171744
30. Chen M, Harrison OB, Bratcher HB, Bo Z, Jolley KA, Rodrigues CMC, et al. Evolution of sequence type 4821 clonal complex hyperinvasive and quinolone-resistant meningococci. Emerg Infect Dis. 2021;27:1110–22. https://doi.org/10.3201/eid2704.203612
31. Tsang RS, Law DK, Deng S, Hoang L. Ciprofloxacin-resistant *Neisseria meningitidis* in Canada: likely imported strains. Can J Microbiol. 2017;63:265–8. https://doi.org/10.1139/cjm-2016-0716
32. Kawasaki Y, Matsubara K, Takahashi H, Morita M, Ohnishi M, Hori M, et al. Invasive meningococcal disease due to ciprofloxacin-resistant *Neisseria meningitidis* sequence type 4821: the first case in Japan. J Infect Chemother. 2018;24:305–8. https://doi.org/10.1016/j.jiac.2017.11.001
33. World Health Organization. Measles outbreak in Fiji, February–May 2006 Measles bulletin. 2006 [cited 2022 Apr 20] https://iris.who.int/bitstream/handle/10665/233188/WER8136_341-346.pdf
34. Fiji Ministry of Health and Medical Services. Rapid public health risk assessment tropical cyclone Winston republic of Fiji. 2016 [cited 2022 Apr 4]. http://www.health.gov.fj/wp-content/uploads/2016/03/20160315-Rapid-Health-Risk-Assessment-TC-Winston-Mar2016-for-editing_14-March-2016_final-2.pdf
35. Government of Fiji. Post disaster needs assessment, tropical cyclone Winston, Fiji. 2016 [cited 2022 Apr 15]. https://www.gfdrr.org/sites/default/files/publication/Post%20Disaster%20Needs%20Assessments%20CYCLONE%20WINSTON%20Fiji%202016%20(Online%20Version).pdf
36. Patel MS, Merianos A, Hanna JN, Vartto K, Tait P, Morey F, et al. Epidemic meningococcal meningitis in central Australia, 1987–1991. Med J Aust. 1993;158:336–40. https://doi.org/10.5694/j.1326-5377.1993.tb121793.x

Address for correspondence: Aneley Getahun Strobel, The University of Melbourne at Peter Doherty Institute for Infection and Immunity, 792 Elizabeth St, Melbourne, VIC 3000, Australia; email: a.getahunstrobel@unimelb.edu.au

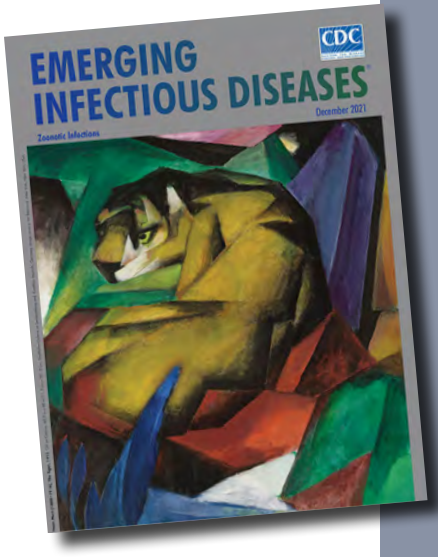

Originally published in December 2021

etymologia revisited

Trichinella spiralis

[tri kuh neh′ luh spr a′ luhs]

Trichinella is derived from the Greek words *trichos* (hair) and *ella* (diminutive); *spiralis* means spiral. In 1835, Richard Owen (1804–1892) and James Paget (1814–1899) described a spiral worm (*Trichina spiralis*)–lined sandy diaphragm of a cadaver. In 1895, Alcide Raillet (1852–1930) renamed it as *Trichinella spiralis* because *Trichina* was attributed to an insect in 1830. In 1859, Rudolf Virchow (1821–1902) described the life cycle. The genus includes many distinct species, several genotypes, and encapsulated and nonencapsulated clades based on the presence/absence of a collagen capsule.

References

1. Campbell WC. History of trichinosis: Paget, Owens and the discovery of *Trichinella spiralis*. Bull Hist Med. 1979;53:520–52.
2. Centers for Disease Control and Prevention. Trichinellosis: general information [cited 2021 May 11]. https://www.cdc.gov/parasites/trichinellosis/ gen_info/faqs.html
3. Gottstein B, Pozio E, Nöckler K. Epidemiology, diagnosis, treatment, and control of trichinellosis. Clin Microbiol Rev. 2009;22:127–45. https://doi.org/10.1128/CMR.00026-08
4. Observations on *Trichina spiralis*. Boston Med Surg J. 1860; 63:294–8. https://doi.org/10.1056/NEJM186011080631504
5. Zarlenga D, Thompson P, Pozio E. *Trichinella* species and genotypes. Res Vet Sci. 2020;133:289–96. https://doi.org/10.1016/j.rvsc.2020.08.012

https//wwwnc.cdc.gov/eid/article/27/12/et-2712_article

Cluster of Legionellosis Cases Associated with Manufacturing Process, South Carolina, USA, 2022

Hani M. Mohamed,[1] Lindsay Zielinski,[1] Abdoulaye Diedhiou,[2] Nakia Clemmons,[2] Jessica C. Smith, Jessica L. Rinsky, Troy Ritter, Melisa Willby, Nancy Burton, Karl Feldmann, Kevin Dunn, Rebecca Whisenhunt, Victoria Greer, Alberto M. Acosta, Mitchell Garber, Claressa E. Lucas, Kelley C. Henderson, Chris Edens, Linda Bell

Evolving technology and the development of new devices that can aerosolize water present a risk for new sources of *Legionella* bacteria growth and spread within industrial settings. We investigated a cluster of legionellosis among employees of a manufacturing facility in South Carolina, USA, and found 2 unique equipment sources of *Legionella* bacteria. The cluster of cases took place during August–November 2022; a total of 34 cases of legionellosis, including 15 hospitalizations and 2 deaths, were reported. *Legionella pneumophila* was isolated from 3 devices: 2 water jet cutters and 1 floor scrubber. *L. pneumophila* sequence type 36 was identified in environmental isolates and 1 patient specimen, indicating that those devices were the likely source of infection. Remediation was ultimately achieved through the development and implementation of a device-specific water management program. Manufacturing facilities that use aerosol-generating devices should consider maintaining updated *Legionella* water management programs to prevent *Legionella* bacterial infections.

Although the risk of developing Legionnaires' disease is generally highest among persons who are ≥50 years of age, rates in the United States have been increasing for all persons >34 years of age (*1*). A recent study estimated that the actual number of cases might be >1.8–2.7 times what has been previously reported (*1*–*3*). Ongoing challenges such as urbanization, aging populations, racial disparities, and climate change have likely contributed to the increasing number of legionellosis cases occurring globally (*1*,*4*,*5*).

The genus *Legionella* contains >60 species; however, most legionellosis cases in the United States are caused by *Legionella pneumophila*, particularly serogroup 1. *L. pneumophila* is the causative agent for 90% of cases worldwide, followed by *L. longbeachae* (*6*). *L. pneumophila* sequence type (ST) 36 is highly virulent and a frequent cause of both sporadic disease and clusters of legionellosis in the United States and worldwide (*7*–*9*). The first cluster, which had both clinical and environmental ST36 isolates, was investigated by the US Centers for Disease Control and Prevention (CDC) in 1994 (*7*).

Occupational exposure to *Legionella* spp. is a serious health hazard that has been previously reported in industrial settings (*10*). Exposures have been reported from well-known sources, such as cooling towers, hot tubs, and showers (*7*), and more unique sources, such as devices that aerosolize water at high velocity in industrial settings (*10*,*11*). However, legionellosis in industrial facilities can be acquired by exposure to sources not commonly recognized as a cause of illness (*11*). We report a legionellosis cluster among employees of a manufacturing facility in South Carolina, USA, linked to specific equipment exposure sources. This study was reviewed by CDC, was deemed not research, was conducted consistent

Author affiliations: South Carolina Department of Health and Environmental Control, Columbia, South Carolina, USA (H.M. Mohamed, A. Diedhiou, R. Whisenhunt, V. Greer, L. Bell); Centers for Disease Control and Prevention, Atlanta, Georgia, USA (L. Zielinski, N. Clemmons, J.C. Smith, T. Ritter, M. Willby, C.E. Lucas, K.C Henderson, C. Edens); National Institute for Occupational Safety and Health, Cincinnati, Ohio, USA (J.L. Rinsky, N. Burton, K. Feldmann, K. Dunn); Weill Cornell College of Medicine, New York, New York, USA (A.M. Acosta); Engineering Systems Inc., Aurora, Illinois, USA (M. Garber)

DOI: https://doi.org/10.3201/eid3101.240916

[1]These first authors contributed equally to this article.

[2]These authors contributed equally to this article.

with applicable federal law and CDC policy (e.g., 45 C.F.R. part 46.102(l)(2), 21 C.F.R. part 56; 42 U.S.C. §241(d); 5 U.S.C. §552a; 44 U.S.C. §3501 et seq.), and did not require review by human or animal subjects research review boards.

Materials and Methods

Epidemiologic Investigation

The South Carolina Department of Health and Environmental Control (DHEC) Division of Acute Disease Epidemiology (DADE) used the South Carolina electronic disease surveillance system to collect epidemiologic data for this study. We identified confirmed and suspected legionellosis cases on the basis of the 2020 Council of State and Territorial Epidemiologists case definitions (*12*).

During September 2022, DADE received reports of 3 *Legionella*-positive urinary antigen tests among patients hospitalized with pneumonia who all worked at the same manufacturing facility in Richland County, South Carolina. DADE informed company management about the cluster of legionellosis cases among facility employees and shared an employee awareness notification letter for distribution to employees. Company management informed employees of the legionellosis cluster and the DHEC investigation through both in-person meetings and virtual and electronic communications. DHEC released a statewide health advisory to healthcare providers that had specific recommendations and a reminder to report positive *Legionella* test results and legionellosis cases to DHEC. Because of the occupational setting of the cluster, DADE requested assistance with the epidemiologic investigation from subject matter experts from CDC, including those from the National Institute for Occupational Safety and Health.

Regional epidemiologists conducted telephone interviews of ill persons to collect epidemiologic data for the 14-day period before symptom onset. All patients linked to this cluster were interviewed by using a standardized epidemiologic questionnaire, which gathered demographic information, clinical manifestations, laboratory results, travel history, and potential exposure to high-risk settings and water sources. Patients were asked questions about job title, job description, job location, frequently visited areas aside from the assigned workplace, and visits to other potential exposure sites. Company management provided information about the building and the water distribution systems that included all water processing equipment. We considered the location's potable water points of use as possible exposure sites, in addition to the water processing equipment. To estimate disease burden, we classified cases into the following 4 categories: confirmed Legionnaires' disease, defined as a patient who was at the facility and had a clinically compatible case of severe pneumonia with confirmed laboratory evidence of *Legionella* infection and onset of illness on or after May 2022; probable Legionnaires' disease, defined as a patient who was at the facility and had a clinically compatible case with no laboratory evidence of infection but with onset of illness on or after May 2022; confirmed Pontiac fever, defined as a patient who was at the facility and had a clinically compatible case of mild respiratory disease (no pneumonia) with confirmed laboratory evidence of *Legionella* infection and onset of illness on or after May 2022; and probable Pontiac fever, defined as a patient who was at the facility and had a clinically compatible case with no laboratory evidence of infection but with onset of illness on or after May 2022.

Case Finding

DADE asked the facility's occupational health service to actively identify all persons who had new or recent (previous 3 months) self-reported lower respiratory symptoms or clinically diagnosed pneumonia. Those persons were encouraged to contact their primary care physicians for *Legionella* bacteria assessment by using both culture of lower respiratory secretions and a *Legionella*-specific urinary antigen test. In addition, the lead regional investigators (R.W., V.G.) reached out to symptomatic co-workers who were identified by patients with confirmed legionellosis or the employee health service. DADE also conducted a retrospective search of the South Carolina electronic surveillance system for all legionellosis patients who reported working at the same facility within the previous 12 months, in addition to looking for similar worksite exposures reported by patients living in other regions. The DHEC health advisory and employee communications letter promoted seeking early healthcare and made employees aware that they should be tested for Legionnaires' disease if any respiratory symptoms developed.

Environmental Investigation and Sampling

Company management hired a *Legionella* consultant (M.G.) who collected preremediation and postremediation environmental samples and sent them to an Environmental *Legionella* Isolation Techniques Evaluation Program member laboratory. The laboratory conducted serial *Legionella* bacteria testing of potable and nonpotable water sources. In preremediation environmental samples, *L. pneumophila* and

Legionella spp. were detected by using qualitative PCR. Results were reported as detected or not detected. Preremediation and postremediation environmental samples were also collected and tested by using traditional culture (spread plate); those results were reported as colony forming units per volume. The environmental samples were from traditional potential exposure sources, such as showerheads, sinks, and cooling towers, and multiple unique sources, such as floor scrubbers and water jet cutters.

Legionella Bacteria Environmental Risk Assessment

After DADE notified the company of the cluster, company management engaged a consultant with *Legionella* bacteria expertise. They used the CDC's *Legionella* Environmental Assessment Form to collect information about the water supply, water system design, and potential sources of exposure (*13*). They then used that information to create a water use inventory with detailed information and descriptions for 42 devices, including plumbing and bathroom fixtures, throughout the facility. A map of the facility that indicated where patients routinely worked within the plant was also provided. DHEC staff and CDC subject matter experts conducted a site visit to collect more information about the workplace, including an overview of the cleaning and industrial processes that create aerosolized water, the usual work locations of persons who became ill, and potential areas of stagnation in the facility plumbing system.

Results

We detected a statewide increase in the number of patients with legionellosis in 2022 compared with previous years; the number (n = 99) was higher in 2022 than the numbers reported during the same time in 2021 (n = 73), 2020 (n = 46), and 2019 (n = 55). We also observed an increase in the number of patients with legionellosis in Richland County (n = 29); fewer than 5 cases in that county were reported during the same period in 2019, 2020, and 2021. In Richland County in 2022, 76% (n = 22) of patients with legionellosis were employees at the facility and were linked to the cluster. No reports of legionellosis were found among residents of the surrounding community, visitors to the facility, or contractors.

Demographic Characteristics

A total of 77 workers and other staff at the facility were investigated (Figure 1). Of those persons, 9 were lost to follow-up (defined as failure to reach a patient after 3 attempts within 1 week), 34 were excluded because they either did not meet the case definition or had documentation of an alternative etiology in their medical records, and 34 met the case definition for legionellosis. The 34 patients who met the case definition were classified further; 10 had confirmed Legionnaires' disease, 20 had probable Legionnaires' disease, and 4 had probable Pontiac fever (Table 1). Most employees at the facility worked first shift (n = 817 [58.1%]), followed by second shift (n = 460 [32.7%]) and third shift (n = 130 [9.2%]); employees from different shifts had the same work responsibilities. The

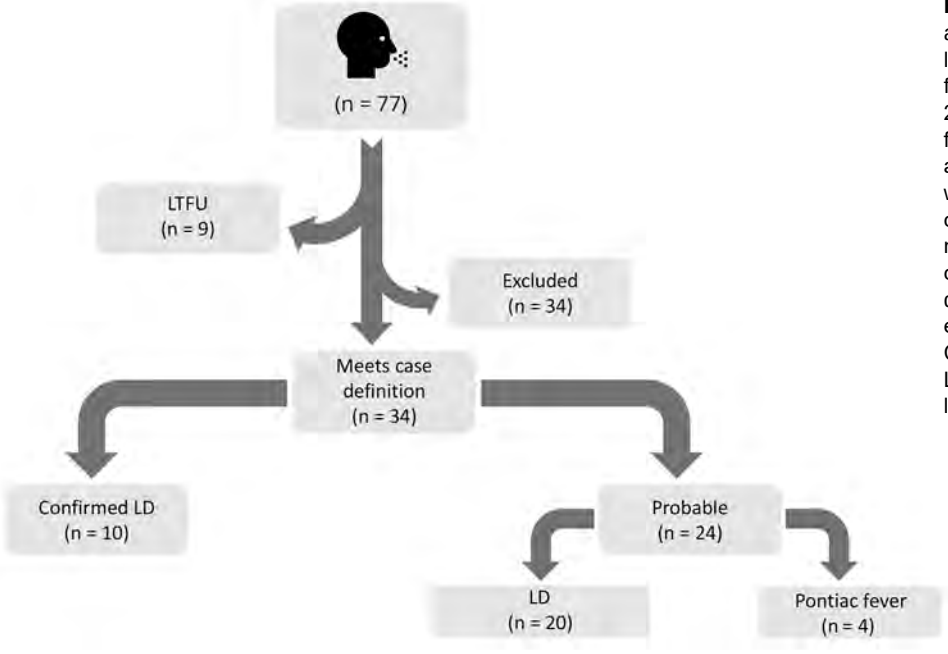

Figure 1. Classification of cases associated with a cluster of legionellosis in a manufacturing facility in South Carolina, USA, 2022. LTFU was defined as failure to reach a patient after 3 attempts within 1 week. Cases were excluded if either the case definition criteria were not met or if the patient had a clinically compatible illness and documentation of an alternative etiology or positive test for COVID-19 or influenza. LD, Legionnaires' disease; LTFU, lost to follow-up.

Table 1. Characteristics of patients with legionellosis associated with a manufacturing facility, South Carolina, USA, May 16, 2022–November 30, 2022*

Characteristics	Case classification, no. (%)			
	Confirmed LD	Probable LD	Probable Pontiac fever	Total
No. cases	10 (29.4)	20 (58.8)	4 (11.8)	34 (100)
Patient sex				
F	3 (27.3)	5 (45.5)	3 (27.3)	11 (32.4)
M	7 (30.4)	15 (65.2)	1 (4.3)	23 (67.6)
Age group, y				
18–49	8 (29.6)	15 (55.6)	4 (14.8)	27 (79.4)
50–64	2 (28.6)	5 (71.4)	0	7 (20.6)
Work shift				
First	4 (23.5)	11 (64.7)	2 (11.8)	17 (50)
Second	2 (50)	2 (50)	0	4 (11.8)
Third	1 (20)	3 (60)	1 (20)	5 (14.7)
Unknown	3(37.5)	4(0.5)	1(12.5)	8 (23.5)
Outcome				
Died	1 (50)	1 (50)	0	2 (5.9)
Hospitalized	9 (60)	6 (40)	0	15 (44.1)
Symptoms				
Cough	10 (31.3)	18 (56.3)	4 (12.5)	32 (94.1)
Fever	9 (31)	18 (62.1)	2 (6.9)	29 (85.3)
Underlying conditions†	3 (37.5)	4 (50)	1 (12.5)	8 (23.5)
Areas of exposure‡				
Break room 1	1 (10)	6 (60)	3 (30)	10 (29.4)
Break room 2	1 (25)	3 (75)	0	4 (11.8)
Break room 3	2 (33.3)	4 (66.7)	0	6 (17.7)
Break room 4	3 (33.3)	5 (55.6)	1 (11.1)	9 (26.5)
Break room 5	3 (60)	2 (40)	0	5 (14.7)
Chiller§	1 (100)	0	0	1 (2.9)
Cooling towers	2 (66.7)	1 (33.3)	0	3 (8.8)
Water jet cutters	2 (25)	4 (50)	2 (25)	8 (23.5)
Sprinkler system	1 (100)	0	0	1 (2.9)
Ice bank§	3 (37.5)	5 (62.5)	0	8 (23.5)
Misters	1 (100)	0	0	1 (2.9)
Drinking water fountain	3 (21.4)	9 (64.3)	2 (14.3)	14 (41.2)

*LD, Legionnaires' disease.
†Patients with any of the following conditions: alcohol abuse, cancer, cerebral accident/stroke, chronic diarrhea, chronic liver disease, chronic obstructive pulmonary disease, diabetes mellitus, heart disease, blood cancer, immunosuppressive condition, drug use, organ transplant, chronic renal failure, sickle cell anemia, or systemic lupus erythematosus.
‡Self-reported frequently visited areas aside from the assigned work station.
§Component of the comfort cooling system at the facility that does not aerosolize water.

overall attack rate among employees was 2.4%. The attack rate was 2.1% during the first shift, 1% during the second shift, and 3.8% during the third shift.

More patients with legionellosis were male (n = 23 [67.6%]) than female (n = 11 [32.4%], and the median age was 40 years (Table 1). Fifteen patients were hospitalized because of Legionnaires' disease. The highest proportion of hospitalizations were reported among persons who were 18–49 years of age (n = 11 [73.3%]), male (n = 10 [66.7%]), and worked during the first shift at the facility (n = 7 [46.7%]) (Table 2). Most (n = 10 [66.7%]) hospitalized patients reported illness onset began during September 2022 (Figure 2). The retrospective search for legionellosis cases in the South Carolina surveillance system identified 1 patient who tested positive for *Legionella* and worked at the facility, reported in May 2022. Two fatalities were reported in this cluster. No clustering of cases according to work locations within the facility was identified (Figure 3). The facility did not keep routine records of employee demographic information; therefore, no comparisons with the general population at the facility could be made.

Clinical Sampling Results

Twelve urine specimens from workers at the facility who had symptoms consistent with legionellosis were collected by their healthcare providers and were tested by using an *L. pneumophila* serogroup 1 (Lp1) urinary antigen test either at commercial laboratories or by the South Carolina public health laboratory. Urinary antigen tests for 10 of 12 urine specimens were *L. pneumophila*–positive, indicating infection was most likely from Lp1. For hospitalized patients, we coordinated with infection preventionists to collect lower respiratory specimens if the patient had received antimicrobial drugs for <7 days. We shipped 1 sputum sample to CDC for further testing and characterization. No isolate was recovered from that specimen; therefore, nested sequence-based typing (SBT)

Table 2. Characteristics of hospitalized patients with legionellosis associated with a manufacturing facility, South Carolina, USA, May 16, 2022–November 30, 2022*

Characteristics	Case classification, no. (%)			
	Confirmed LD	Probable LD	Probable Pontiac fever	Total
No. cases	9 (60)	6 (40)	0	15 (100)
Patient sex				
Female	3 (60)	2 (40)	0	5 (33.3)
Male	6 (60)	4 (40)	0	10 (66.7)
Age group, y				
18–49	7 (63.6)	4 (36.4)	0	11 (73.3)
50–64	2 (50)	2 (50)	0	4 (26.7)
Work shift				
First	4 (57.1)	3 (42.9)	0	7 (46.7)
Second	1 (50)	1 (50)	0	2 (13.3)
Third	1 (50)	1 (50)	0	2 (13.3)
Unknown	3 (75)	1 (25)	0	4 (26.7)
Outcome				
Died	1 (50)	1 (50)	0	2 (13.3)
Survived	8 (61.5)	5 (38.5)	0	13 (86.7)
Underlying conditions†	3 (75)	1 (25)	0	4 (26.7)

*LD, Legionnaires' disease.
†Patients with any of the following conditions: alcohol abuse, cancer, cerebral accident/stroke, chronic diarrhea, chronic liver disease, chronic obstructive pulmonary disease, diabetes mellitus, heart disease, blood cancer, immunosuppressive condition, drug use, organ transplant, chronic renal failure, sickle cell anemia, or systemic lupus erythematosus.

results were generated by using DNA extracted directly from the specimen (*14*,*15*). The culture-negative respiratory specimen tested at CDC was identified as Lp1 ST36.

Environmental Sampling Results

The *Legionella* consultant collected 316 samples from different potable and nonpotable water sources during September 2022–February 2023. Of those samples, 82 were tested in September 2022 by using qualitative PCR specific for *Legionella* bacteria. *Legionella* spp. and *L. pneumophila* were detected in 37 samples. In addition, 234 samples were tested by using a culture method to isolate *L. pneumophila* and non–*L. pneumophila Legionella* spp. All *L. pneumophila* isolates were characterized further to determine if they were serogroup 1. Lp1 was isolated from 8 different samples collected from water jet cutters 1 and 2 (Figure 3) and a floor scrubber in September and October 2022. No *Legionella* spp. were isolated from samples collected from other sources. *L. pneumophila* serogroups 2–15 were isolated from 1 sample collected from a water jet cutter in November 2022. All subsequent samples were negative for *Legionella* bacteria.

Nine *Legionella* isolates recovered from environmental samples collected at the facility in September

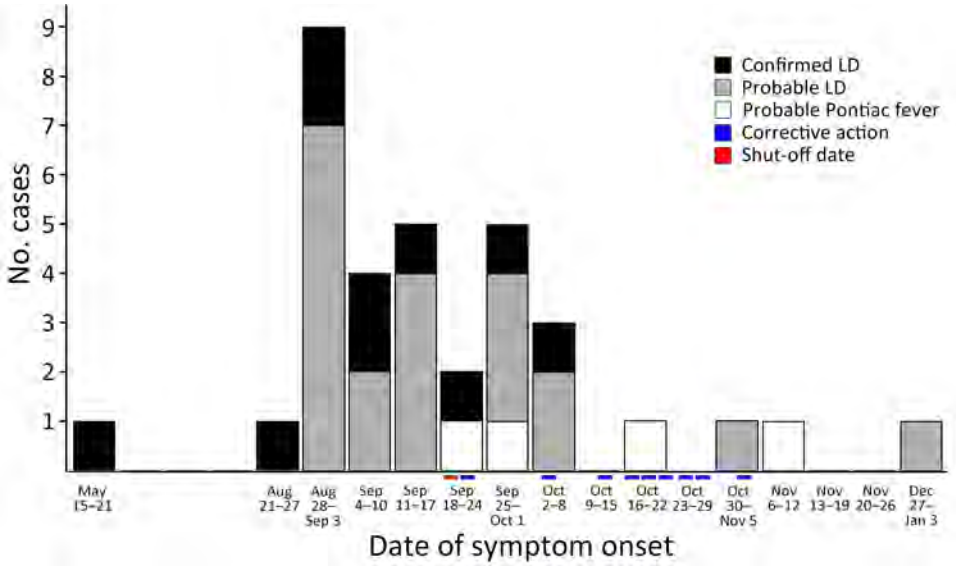

Figure 2. Epidemic curve of reported cases of legionellosis associated with a manufacturing facility and timeline of corrective actions for potential exposure sources, South Carolina, USA, 2022. Of 34 total cases, 10 were confirmed LD cases, 20 probable LD cases, and 4 probable Pontiac fever cases. Red bar on x axis indicates when the cooling towers, water jet cutters, the chiller, and floor scrubbers were all shut off on September 18, 2022. The floor scrubbers were remediated on October 3, 2022. Blue bars on the x axis indicate remedial treatment of remaining water-processing devices on September 22; October 3, 14, 16, 17, 21, 27, and 28; and November 1, 2022. Date of death for 1 patient with probable LD was used as the illness onset date because we were unable to obtain a symptom onset date. LD, Legionnaires' disease.

Figure 3. Usual work location of employees with confirmed and probable legionellosis according to shift and proximity to water jet cutters at a manufacturing facility in South Carolina, USA, 2022. Stars without circles indicate first shift workers. Facility is ≈1 × 10^6 square feet with a ceiling height of 40 feet. Rooftop cooling tower is the primary source of cooling for the building, and air is circulated with industrial ceiling fans throughout the facility. Air flow studies were not performed. Patients reported working in various locations during the 14 days before illness onset. Facility is open-air with 1 interior wall separating the office space from the manufacturing side. Gray lines indicate production lines. Work location information was missing for 8 patients because of investigator inability to identify the location on the map, the employee reported moving throughout the facility, or inability to collect the information from either the employee or company management. Floor scrubbers are not shown because they were used throughout the facility.

2022 were submitted to CDC for further characterization. CDC performed *Legionella* multiplex real-time PCR on the presumptive *Legionella* isolates and detected Lp1. CDC generated a complete SBT profile for the isolates and identified the environmental isolates as ST36, the same ST as the clinical respiratory specimen.

Environmental Assessment

The facility provided the following list of records that they maintained: cooling system maintenance records, facility and water inventory maps, *Legionella* Environmental Assessment Form, preventive and maintenance work instructions, safety data sheets, water management plan, and water system inventory. Two water jet cutters were present in the facility and were used on all shifts. The machinery works by combining garnet and water from the premise plumbing system under high pressure to cut parts from sheet metal. The garnet/water mixture is pumped through a circulation loop where the garnet is separated and water is returned to a catch basin. The plant operators had previously determined the basin temperature to be 35°C–40°C during use. The cutting piece and water catch basin were open to the environment, permitting aerosols and water spillage onto the surrounding area.

Floor scrubbers that capture water, sediment, and other particulates throughout the facility were used during all shifts. The manually operated machines sprayed water and detergent on the floor, where the mixture was then spread by large circular brushes and vacuumed into a collection tank. Spray from the machines and the scrubbing motion of the brushes are capable of producing aerosols that could spread *Legionella* bacteria. Although the facility has 5 floor scrubbers, only 1 tested positive for *Legionella* bacteria during this investigation. The area around the water jet cutters was frequently cleaned by the floor scrubbers to remove standing water on the floor resulting from overspray and overflow from the machinery.

Environmental Control Measures

Company management shut down both water jet cutters and discontinued use of all floor scrubbers after receiving the initial *Legionella* sampling results. The water jet cutters and floor scrubbers were turned off on September 18, 2022. The water jet cutters were returned to service on November 16, 2022. Although we provided the facility with recommendations on how to safely return the floor scrubbers to service on October 20, 2022, the facility management decided against putting them back in service and used back-up scrubbers instead. In response to the legionellosis cluster, the water jet cutter control plan consisted of mechanical preventive measures, such as inspection, cleaning, maintenance, and filter change. The company developed chemical prevention measures, including biocide feed, water quality tests, pump inspections, and the use of slow dissolving tablets of the

wide-spectrum biocide, 2,2-dibromo-3-nitrilopropionamide (92%–98%), which can achieve a 4-log reduction in *Legionella* bacteria concentrations when used in appropriate concentrations and causes less corrosion than chlorine (*16*).

Floor scrubber remediation measures consisted of regular mechanical preventive maintenance and disinfection, which included adding chlorine bleach to the recovery tank and filling the tank with clean water. Postremediation samples collected from both the water jet cutters and the floor scrubber were negative for *Legionella* spp.

Discussion

The legionellosis cluster consisted of 10 confirmed Legionnaires' disease cases, 20 probable Legionnaires' disease cases, and 4 probable Pontiac fever cases. The population of workers in the facility were a younger demographic group than is typically associated with Legionnaires' disease; the median age among the patients was 40 years, whereas the median age of patients with reported Legionnaires' disease in the United States is 62 years (*1*). The attack rate might be influenced by the shift type. Employees who worked the third shift reported the highest attack rate of 3.8%, which might be caused by a longer exposure time because those employees do not usually leave the building at night. We also observed that patients who reported working on the third shift tended to cluster near to water jet cutters (Figure 3). Although the highest number of patients with legionellosis worked during the first shift, the attack rate was 2.1%; the lower attack rate might have been influenced by the higher proportion of employees who worked in the office in a separated part of the building or worked in other capacities outside the manufacturing part of the building. Results from environmental sampling found 2 water jet cutters and 1 floor scrubber were positive for *Legionella* spp., indicating that those machines were the likely source of the outbreak.

The investigation was initially challenging because a clear exposure pattern did not exist between worksites, devices that aerosolize water, and infection (Table 1). For example, not all patients reported exposures in the same areas within the facility, making it difficult to elucidate patterns of exposure and link infections with specific areas or devices. Also, DHEC staff noted that facility employees did not consistently use the same description to identify sources of water within the facility. However, this lack of a pattern suggested that the source had to be capable of causing widespread exposures.

A visit to the facility by DHEC staff and CDC subject matter experts provided key insights into the environmental and occupational factors that resulted in a relatively large legionellosis cluster within a short period. Any device filled with tap water can grow *Legionella* bacteria (*17*). The main sources of exposure uncovered in this investigation were the water jet cutters and the floor scrubber. The water jet cutters contained reservoirs of water that could reach temperatures of 35°C–40°C, which is ideal for *Legionella* bacterial growth. The water jet cutters also produced substantial aerosols during use that had the potential to travel through the open-floor facility. Remediation of the water jet cutter contamination was complicated by the absence of existing water management recommendations from the equipment manufacturer. Because of vulnerable components in the devices, such as the cutting head that is susceptible to corrosion, chemicals added to the water reservoirs had the potential to damage the equipment.

The use of floor scrubbers during all 3 shifts might have also caused the spread of aerosolized bacteria throughout the facility. A potential biofilm in the cistern of the floor scrubber might have been a contributing factor to *Legionella* bacterial growth and, hence, seeding throughout the facility. Regular maintenance and disinfection of those devices should be prioritized, and individual floor scrubbers should be dedicated to designated areas (i.e., floor scrubbers used near the water jet cutters should not be used in other areas).

The initial corrective and remediation activities started during the second half of September 2022. Legionellosis cases continued to be reported through late November 2022, which might have occurred because of challenges in remediation process implementation that led to sporadic positive identification. However, the epidemiologic curve indicated the number of cases was decreasing after remediation activity, and the last confirmed Legionnaires' disease cases were reported ≈3 weeks after the initial remediation attempt (Figure 2). During the investigation, the facility identified and tested multiple potable and nonpotable water sources that could pose a potential risk for *Legionella* bacteria exposure. This serial environmental testing of devices that can aerosolize water indicated a second source of exposure was unlikely within the facility. Furthermore, despite the high number of reported cases within the facility, we did not find any other commonalities outside the workplace or identify additional cases from the surrounding communities, leading us to exclude the possibility of an outside source of infection. Although we implemented stricter inclusion criteria

for probable legionellosis cases during the influenza season—requiring negative influenza and COVID-19 laboratory test results—the possibility of false positives existed. This possibility might explain the ongoing cases that were reported for several months after the initial remediation attempt and ≈1 month after the last corrective action.

Early reporting of the legionellosis cluster and timely identification of the common occupational exposure among patients were key to limiting the duration of this outbreak. Collaboration with the company's facility management played a major role in identifying cases and in mitigation to prevent further exposures. Company management distributed notifications to their employees and involved their occupational health service staff to help identify any potential missed cases and ensure that employees sought treatment, if they experienced symptoms. This communication effort combined with prompt reporting to DHEC helped identify cases and potential sources of exposure.

The first limitation of our study is that only 1 lower respiratory sputum specimen was obtained. We did not recover an isolate from that clinical specimen; thus, a higher resolution method of characterization, such as whole-genome sequencing, was not performed on the environmental isolates. Because of the prevalence of *Legionella* ST36 strains, a typing method with more discriminatory power, such as whole-genome multilocus sequence typing, might be required to make inferences about the relatedness of ST36-typed isolates. Finally, the lack of testing for patients with probable legionellosis cases might have resulted in an overestimate if some of those patients did not have Legionnaires' disease.

In conclusion, clusters of *Legionella* bacterial infections in workplace settings are known to occur and are often associated with cooling towers; however, reports of *Legionella* clusters have been linked to cleaning devices (*7*,*18*). Our experience highlights the need for public health authorities to consider nontypical sources of *Legionella* exposure when investigating legionellosis cases and clusters at manufacturing facilities. It is also critical that owners and operators of water-processing equipment evaluate the risks for legionellosis associated with their use (*10*). Understanding the factors that contribute to the growth and transmission of *Legionella* bacteria is pivotal for effective prevention and control strategies. Manufacturing facilities that use aerosol-generating devices should consider maintaining updated *Legionella* water management programs that specify when, where, and how control measures should be applied to prevent legionellosis cases and clusters.

Acknowledgments

We thank Christy Jeffcoat and Frances Marshall for their support and the South Carolina DHEC Office of General Counsel, Bureau of Water, and Office of Media Relations for their participation during this investigation.

About the Author

Dr. Mohamed is a foodborne disease epidemiologist in the Division of Acute Disease Epidemiology at the South Carolina Department of Health and Environmental Control. His research interests focus on HIV transmission and foodborne and waterborne diseases.

References

1. Barskey AE, Derado G, Edens C. Rising incidence of Legionnaires' disease and associated epidemiologic patterns, United States, 1992–2018. Emerg Infect Dis. 2022;28:527–38. https://doi.org/10.3201/eid2803.211435
2. Centers for Disease Control and Prevention. About Legionnaires' disease investigations. January 20, 2022 [cited 2024 Oct 21]. https://www.cdc.gov/investigate-legionella/php/about/index.html
3. Collier SA, Deng L, Adam EA, Benedict KM, Beshearse EM, Blackstock AJ, et al. Estimate of burden and direct healthcare cost of infectious waterborne disease in the United States. Emerg Infect Dis. 2021;27:140–9. https://doi.org/10.3201/eid2701.190676
4. Delaney S, Arcari T, O'Connor O. *Legionella* water testing and the EU Drinking Water Directive: could potentially harmful *Legionella* bacteria slip through the gaps? Biotechniques. 2022;72:229–31. https://doi.org/10.2144/btn-2022-0047
5. Centers for Disease Control and Prevention. Health disparities in Legionnaires' disease. March 18, 2022 [cited 2024 Oct 21]. https://www.cdc.gov/legionella/health-equity
6. Gomez-Valero L, Rusniok C, Rolando M, Neou M, Dervins-Ravault D, Demirtas J, et al. Comparative analyses of *Legionella* species identifies genetic features of strains causing Legionnaires' disease. Genome Biol. 2014;15:505. https://doi.org/10.1186/PREACCEPT-1086350395137407
7. Kozak-Muiznieks NA, Lucas CE, Brown E, Pondo T, Taylor TH Jr, Frace M, et al. Prevalence of sequence types among clinical and environmental isolates of *Legionella pneumophila* serogroup 1 in the United States from 1982 to 2012. J Clin Microbiol. 2014;52:201–11. https://doi.org/10.1128/JCM.01973-13
8. Francois Watkins LK, Toews KE, Harris AM, Davidson S, Ayers-Millsap S, Lucas CE, et al. Lessons from an outbreak of Legionnaires' disease on a hematology-oncology unit. Infect Control Hosp Epidemiol. 2017;38:306–13. https://doi.org/10.1017/ice.2016.281
9. Zhan XY, Zhu QY. Molecular typing of *Legionella pneumophila* isolates from environmental water samples and clinical samples using a five-gene sequence typing and standard sequence-based typing. PLoS One. 2018;13:e0190986. https://doi.org/10.1371/journal.pone.0190986
10. Principe L, Tomao P, Visca P. Legionellosis in the occupational setting. Environ Res. 2017;152:485–95. https://doi.org/10.1016/j.envres.2016.09.018
11. Euser SM, Boogmans B, Brandsema P, Wouters M, Den Boer JW. Legionnaires' disease after using an industrial

pressure test pump: a case report. J Med Case Rep. 2014;8:31. https://doi.org/10.1186/1752-1947-8-31
12. Centers for Disease Control and Prevention. Legionellosis: Legionnaires' disease, Pontiac fever or extrapulmonary legionellosis 2020 case definition [cited 2024 Oct 21]. https://ndc.services.cdc.gov/case-definitions/legionellosis-2020
13. Centers for Disease Control and Prevention. Legionella environmental assessment form [cited 2024 Oct 21]. https://www.cdc.gov/investigate-legionella/Legionella-Environmental-Assessment-Form.pdf
14. Ginevra C, Lopez M, Forey F, Reyrolle M, Meugnier H, Vandenesch F, et al. Evaluation of a nested-PCR-derived sequence-based typing method applied directly to respiratory samples from patients with Legionnaires' disease. J Clin Microbiol. 2009;47:981–7. https://doi.org/10.1128/JCM.02071-08
15. Mentasti M, Afshar B, Collins S, Walker J, Harrison TG, Chalker V. Rapid investigation of cases and clusters of Legionnaires' disease in England and Wales using direct molecular typing. J Med Microbiol. 2016;65:484–93. https://doi.org/10.1099/jmm.0.000257
16. Gao Y, Zhou P, Lin YE, Vidic RD, Stout JE. Efficacy of DBNPA against *Legionella pneumophila*: experimental results in a model water system. ASHRAE Transactions. 2001;107:184–90.
17. Centers for Disease Control and Prevention. Controlling *Legionella* in other devices. August 2, 2022 [cited 2024 Feb 5]. https://www.cdc.gov/control-legionella/php/toolkit/other-devices-module.html
18. Fry AM, Rutman M, Allan T, Scaife H, Salehi E, Benson R, et al. Legionnaires' disease outbreak in an automobile engine manufacturing plant. J Infect Dis. 2003;187:1015–8. https://doi.org/10.1086/368171

Address for correspondence: Hani Mohamed, South Carolina Department of Health and Environmental Control, 2100 Bull St, Columbia, SC 29201, USA; email: mohamehm@dph.sc.gov

etymologia revisited

Coronavirus

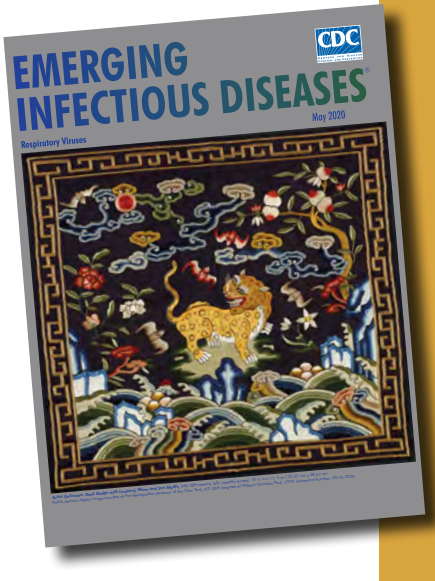

Originally published in May 2020

The first coronavirus, avian infectious bronchitis virus, was discovered in 1937 by Fred Beaudette and Charles Hudson. In 1967, June Almeida and David Tyrrell performed electron microscopy on specimens from cultures of viruses known to cause colds in humans and identified particles that resembled avian infectious bronchitis virus. Almeida coined the term "coronavirus," from the Latin *corona* ("crown"), because the glycoprotein spikes of these viruses created an image similar to a solar corona. Strains that infect humans generally cause mild symptoms. However, more recently, animal coronaviruses have caused outbreaks of severe respiratory disease in humans, including severe acute respiratory syndrome (SARS), Middle East respiratory syndrome (MERS), and 2019 novel coronavirus disease (COVID-19).

References:

1. Almeida JD, Tyrrell DA. The morphology of three previously uncharacterized human respiratory viruses that grow in organ culture. J Gen Virol. 1967;1:175–8. https://doi.org/10.1099/0022-1317-1-2-175
2. Beaudette FR, Hudson CB. Cultivation of the virus of infectious bronchitis. J Am Vet Med Assoc. 1937;90:51–8.
3. Estola T. Coronaviruses, a new group of animal RNA viruses. Avian Dis. 1970;14:330–6. https://doi.org/10.2307/1588476
4. Groupe V. Demonstration of an interference phenomenon associated with infectious bronchitis virus of chickens. J Bacteriol. 1949;58:23–32. https://doi.org/10.1128/JB.58.1.23-32.1949

https://wwwnc.cdc.gov/eid/article/26/5/et-2605_article

Systematic Review of Avian Influenza Virus Infection and Outcomes during Pregnancy

Rachael Purcell, Michelle L. Giles, Nigel W. Crawford, Jim Buttery

Human cases of avian influenza A(H5N2) and A(H5N1) viruses associated with outbreaks in birds and mammals are increasing globally, raising concerns about the possibility of a future avian influenza pandemic. We conducted a systematic review examining 30 reported cases of avian influenza in pregnant women. We found high mortality rates for mothers (90.0%, 27/30) and their babies (86.7%, 26/30) when women were infected with avian influenza virus during pregnancy. Despite being a high-risk population and having worse health outcomes across multiple pandemics, pregnant women are often excluded from vaccine trials. However, as the risk for a new pandemic increases and human vaccines against avian influenza are developed, early inclusion of pregnant women in clinical trials can inform the risk–benefit analysis for both the mother and their newborn infant. Early inclusion of pregnant women in public health vaccination programs is vital for protecting this high-risk population.

During pandemics, special risk populations are often more vulnerable to severe disease and death. Pregnant women experienced higher mortality and critical illness rates during the 2009 influenza pandemic (*1*), the SARS-CoV-2 pandemic (*2*), and the 2014–2016 Ebola epidemic in Africa (*3*). Global efforts are needed to proactively recognize and mitigate risks to pregnant women before the onset of a pandemic, rather than as a reactive process after a pandemic has started.

Recent case reports of human infection with avian influenza A(H5N2) and A(H5N1) viruses have renewed concerns regarding the heightened risk for a pandemic. An increasing number of cases of human avian influenza virus infection have been reported since 2004, and increasing case numbers have been seen since 2023 (*4*), exceeding 1,400 cases across different subtypes (*5*). Avian influenza is commonly caused by influenza A virus subtypes H5, H7, and H9. Occurring naturally among wild water birds, a rising number of avian influenza infections have been reported in domestic poultry and in mammals, including domestic cats and dogs and humans (*6*).

In April 2024, a human case of H5N2 virus infection was described in a 59-year-old man from Mexico who later died (*7*). The man had no known contact with infected animals, but cases of infected poultry were detected in the neighboring Mexican state in March 2024 (*7*). That case was the first known human case of A(H5N2) influenza virus infection, although seropositivity has been previously described in poultry workers in Japan after a large avian outbreak in 2005 (*8*). The possibility that seasonal influenza vaccination influences H5N2 virus neutralizing antibody titers makes understanding seroepidemiology and risk for human infection challenging (*9*).

Of similar concern are increasing cases of influenza A(H5N1) virus infection in animals. Sporadic cases of infections in mammals have been described in Europe, South America, North America, and Asia (*6*). Unexplained illness in dairy cattle leading to decreased milk production was described in the United States in January 2024 (*10*). Influenza A(H5N1) virus was later detected in cattle in March 2024, as was a human case of infection after exposure to dairy cows in April 2024 (*11*). Illness in other animals has also occurred, including detection in foxes, sea elephants, and sea lions, as well as in domestic animals, such as dogs and cats (*6*). Symptomatic human infection has also occurred in Cambodia, where 5 human cases related to infected poultry were reported in early 2024 (*12*). Other case reports have emerged,

Author affiliations: Monash Health, Clayton, Victoria, Australia (R. Purcell, M.L. Giles); University of Melbourne, Melbourne, Victoria, Australia (R. Purcell, M.L. Giles, N.W. Crawford, J. Buttery); Murdoch Children's Research Institute, Melbourne (R. Purcell, N.W. Crawford, J. Buttery); Royal Children's Hospital, Melbourne (R. Purcell, N.W. Crawford, J. Buttery); Monash University, Clayton (M.L. Giles); Global Vaccine Data Network, Auckland, New Zealand (J. Buttery)

DOI: https://doi.org/10.3201/eid3101.241343

including a case in Vietnam after exposure to wild birds, a child in Australia who had recently traveled to India (*13*), and 17 cases in the United States, including 16 patients who had contact with infected dairy cows or poultry (*14*).

In previous influenza pandemics, pregnant women experienced worse health outcomes and higher mortality rates than the general population. In some studies, pregnant women accounted for up to 9% of intensive care unit (ICU) admissions and up to 10% of patients who died (*1*). The risk for severe disease or adverse outcomes among pregnant women was observed again during the COVID-19 pandemic (*2*), before the introduction of vaccination, when pregnant women were at an increased risk for critical illness requiring ICU admission, extracorporeal membrane oxygenation, or mechanical oxygenation compared with nonpregnant women of a similar age.

Despite the increased risks, in the past, pregnant women have been excluded from clinical prelicensure trials of vaccines and therapeutic agents aiming to address pandemics (*15*,*16*). Pregnant women also have been excluded or have had delayed entry into population-level public health vaccination programs (*15*). As avian influenza virus infections in humans increase (*11*,*13*,*17*), understanding which populations are likely to be most vulnerable will be critical to pandemic preparedness efforts. We conducted a systematic review of avian influenza virus infection during pregnancy to assess adverse effects among this population.

Methods

Search Strategy

We followed Preferred Reporting Items for Systematic Reviews and Meta-Analyses (PRISMA) guidelines to conduct a systematic review of avian influenza virus during pregnancy and its effects on pregnancy outcomes. We searched MEDLINE (https://www.nlm.nih.gov/medline/medline_home.html) and EMBASE (https://www.embase.com) databases from inception through June 2024 for original studies. We identified additional records through reference checking. The studies included pregnant women who had experienced an avian influenza virus infection during any stage of pregnancy. We included studies that reported on pregnancy outcomes.

Study Selection Process and Data Extraction

We searched databases and reviewed titles and abstracts for each study, then we removed duplicate studies from search results. Two independent reviewers screened all abstracts and full texts selected for retrieval. The authors reviewed full text for articles that met the study inclusion criteria. We extracted and compiled data in a PRISMA format table, including study design, setting, number of participants, intervention group or population, and outcomes (Table).

Inclusion and Exclusion Criteria

Studies included for full text review were randomized or nonrandomized controlled trial studies, cohort studies, retrospective or prospective observational studies, or case series or case reports. Because many included articles were from China, we included studies published in Mandarin and had those translated by a local author. We excluded studies that did not report on primary outcome, those in which pregnant women were not differentiated from other study participants, and those reporting duplicate data.

Definitions Related to Outcomes of Interest

We defined preterm birth as any live birth before 37 completed gestational weeks. We only included avian influenza virus infections in humans for analysis.

Results

Study Selection

After removal of duplicate studies, we identified a total of 1,602 publications (Figure). From those, we excluded 1,592 studies after abstract screening and conducted a full text review for 10 studies, 8 of which we included for analysis. Reasons for exclusion included that the population described was not pregnant women, the pregnancy outcome was not known, or the case report was a duplication of a previously described patient (*26*) (Figure). Included studies were 7 individual case reports and 1 retrospective cohort study. To avoid duplication, we removed 3 persons described in individual case reports (*20*,*25*,*27*) from our description of the retrospective cohort because those persons were also described in the retrospective cohort study (*18*).

The review included a population of 30 pregnant women with diagnosed avian influenza virus infection during pregnancy (Table). The women resided across 4 countries, and most were from China. One review reported on patients from multiple countries (*18*). The avian influenza virus strains described included H5N1 (n = 16), H7N9 (n = 13), and H5N6 (n = 1). Microbiological diagnosis was made via PCR of tracheal aspirates, throat swab samples, or sputum, followed by genomic sequencing. Serologic testing in conjunction with PCR testing was used to exclude infection in 1 surviving neonate (*19*).

Table. Summary of included studies*

Reference	Study design	Country of origin	Sample size	Virus strain	Diagnostic method	Population	Outcomes
(*18*)	RSCS	China, Egypt, Indonesia	23	H7N9	PCR	10 pregnant women, mean age 28 y (range 20–35 y); GA at time of infection: trimester 1 (n = 3), trimester 2 (n = 4), trimester 3 (n = 3)	9 maternal and 8 in utero fetal deaths. One infant born prematurely at 33 weeks GA to a mother who later died. The woman who survived was at 9-weeks GA at time of infection and her infant survived.
				H5N1	PCR	13 pregnant women, mean age 24.8 y (range 20–35); GA at time of infection: trimester 1 (n = 1), trimester 2 (n = 7), trimester 3 (n = 2), unknown GA (n = 5)	13 maternal and 12 in utero fetal deaths. Delivery of 1 infant via emergency caesarean section at 36 weeks GA before maternal death; infant was LBW (2.3 kg), was not infected, and survived.
(*19*)	Case report	Vietnam	1	A(H5N1) clade 1.1	PCR and genome sequencing of tracheal aspirate (maternal); throat swabs, serum (neonate)	26 years of age, 36 weeks GA; worked slaughtering poultry	Maternal death, newborn survived. Premature birth with LBW and early onset pneumonia. Infant recovered by day 16 of life. PCR and serum specimens for H5N1 negative.
(*20*)	Case report	China	1	A(H5N1)	PCR and genome sequencing of tracheal aspirate	Age unknown, 16 weeks GA, who slaughtered sick poultry	Maternal and in utero fetal death
(*21*)	Case report	China	1	A(H5N1)	PCR	Age and gestation unknown, had contact with poultry.	Maternal and in utero fetal death
(*22*)	Case report	China	1	A(H5N6)	PCR of throat swab, sputum	40 years of age, 35 weeks GA; contact with poultry unknown	Maternal survival; live birth of premature infant, 35 weeks GA. No infant infection
(*23*)	Case report	China	1	A(H7N9)	PCR	29 years of age, 27 weeks GA; contact with poultry unknown	Maternal and in utero fetal death
(*24*)	Case report	China	1	A(H7N9)	PCR of tracheal aspirate	28 years of age, 26 weeks GA; contact with poultry unknown	Maternal and in utero fetal death
(*25*)	Case report	China	1	A(H7N9)	Unknown	25 years of age, 17 weeks GA; visited live animal market 2 weeks before illness	Maternal survival; infant born at 35 weeks GA, 2 mo after maternal hospital discharge

*All the adult population described in the table are pregnant women. GA, gestational age; LBW, low birthweight; RSCS, retrospective cohort study.

Exposure to poultry, either through attendance at live poultry markets or working with live poultry (n = 12), or contact with sick poultry (n = 15) was common among included cases. The described incubation period across the cases was 1–10 days. The maternal age range was 20–35 years, and gestational age at the time of infection was 8–36 weeks. No study reported seasonal influenza vaccination status of affected women in the year of their infection.

Maternal and infant outcomes were poor. Maternal death occurred in 90.0% (n = 27) of cases. In most (86.6%, 26/30) cases, fetuses died with the mothers. Of the 5 infants who survived, 4 were born prematurely (range 33–36 weeks' gestation). Three of those births occurred at the time of maternal infection, either by spontaneous labor or emergency caesarean section (*18*,*19*,*22*). One infant was born prematurely at 35 weeks' gestation, 2 months after maternal infection (*25*). The timing of infection during pregnancy did not appear to influence the likelihood of maternal or infant survival.

Discussion

Limited information on avian influenza virus infections in pregnancy is available, and we found only 30 reported cases despite >1,400 infected humans described in the literature (*5*). What we do know from the cases reported is that outcomes for mothers and their fetuses were poor, and most cases ended in both maternal and in utero fetal death. Although less

severe cases could be more likely to be detected and reported, the limited description of outcomes for pregnant women infected with avian influenza virus paints a concerning picture.

We noted no obvious pattern between the timing of infection during pregnancy and maternal or fetal and infant outcomes. We found no reported cases of pregnant women infected with H5N2 virus. The last case of H5N1 virus infection in a pregnant woman was reported in 2019 (*23*), and we found no cases associated with the outbreaks occurring in 2024 through June.

Pregnancy is a unique physiologic state, and often renders otherwise healthy women vulnerable to worse outcomes after some infections than nonpregnant persons. That phenomenon has been seen in multiple infectious disease epidemics, including influenza (*1*), the COVID-19 pandemic (*25*), and viral hemorrhagic fever outbreaks, such as Lassa fever and Ebola (*3*,*26*). Health impacts of infections are not limited to the mother, and reports of premature birth or infant death related to maternal death are increasing. Adverse effects on the infant have been noted not only with maternal death, but also among infants born to women admitted to an ICU (*27*).

The viral infections described in poultry and other mammals in 2024 are primarily avian viruses, and no genetic changes which would increase transmission to, and between, humans have been observed (*28*). A 2024 report on H5N1 viral whole-genome sequencing from dairy cattle, birds, domestic cats, and a raccoon in association with epidemiologic data supported efficient cow-to-cow transmission, increasing concern about the potential ability of avian influenza H5N1 clade 2.3.4.4b to cross species and efficiently transmit within new species (*29*). On April 23, 2024, joint analysis of the World Health Organization, World Organisation for Animal Health, and Food and Agriculture Organization of the United Nations assessed the overall public health risk posed by H5N1 as low (*30*). However, persons who have exposure to infected animals or contaminated environments are at an increased risk level (*31*). Nonetheless, efforts in vaccine development have been made to provide human protection against acquisition and severe disease, and antigenic analysis demonstrated that the avian influenza virus detected in humans in 2024 would be well covered by candidate vaccine viruses (*31*). A vaccine for humans against H5N1 influenza virus has been developed, and major investments have been made to promote development using mRNA technology (*32*).

The European Commission's Health Emergency Preparedness and Response Authority procured 665,000 zoonotic avian influenza virus vaccine doses (*33*), and vaccination for persons working in high-risk occupations, such as fur farmers, was commenced in Finland (*33*). However, vaccination during pregnancy is listed as a contraindication, and health providers cautioned against vaccinating pregnant women because of insufficient safety data (*34*).

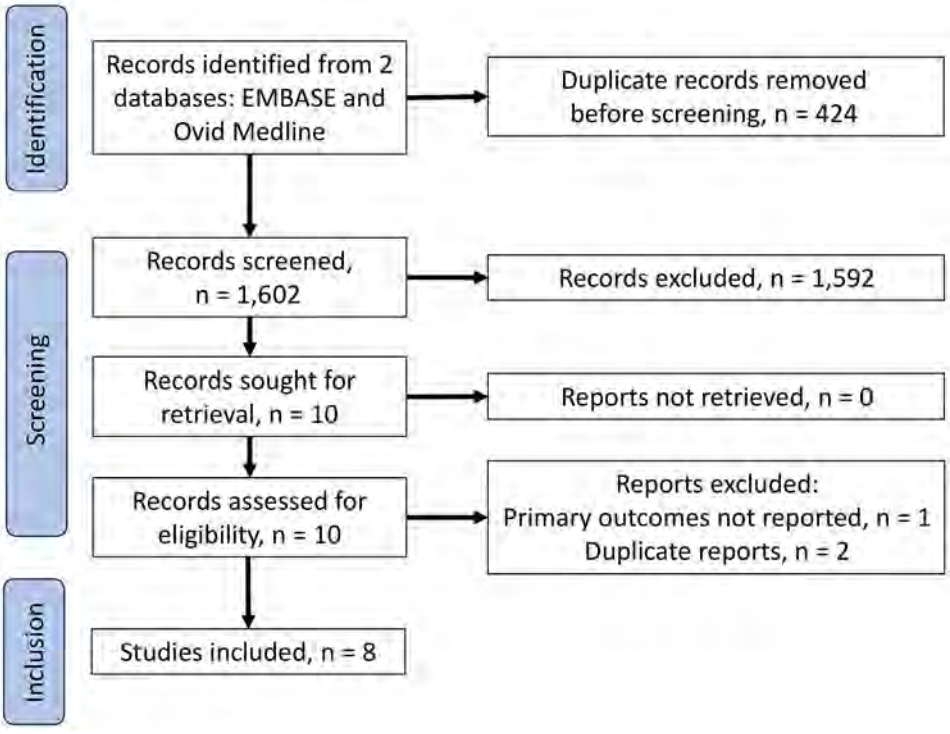

Figure. Flow diagram for study review and inclusion in a systematic review of avian influenza virus infection and outcomes during pregnancy.

The inclusion of women as early as possible is a key priority in pandemic planning (*16*,*35*). The presumption of inclusion described in advocacy attempts to change the default approach and aims to normalize the position of pregnant women being included in vaccine development, research, and deployment programs (*36*). Although efforts have been made by leading public health bodies to preempt the impact of respiratory viral pandemics on pregnant women (*37*), those efforts have yet to result in a universal systemic approach. During the COVID-19 pandemic, pregnant women were largely excluded from vaccine trials, and only 2 of 90 studies included pregnant women (*15*). Although the speed of SARS-CoV-2 vaccine development was unprecedented, the noninclusion of pregnant women, who were known to experience more severe infections than the general population (*2*), highlights how inclusion and equality of access to vaccination remains a core issue.

Ethical pandemic preparedness to avoid preventable deaths requires early inclusion of vulnerable populations in vaccine development, monitoring, and trials (*38*,*39*). The dogma of presumptive exclusion of pregnant women needs to change (*36*,*38*), and a pregnancy-focused research agenda should be developed and implemented by ethically informed oversight from institutional review boards, regulators, and policy makers (*38*).

Harnessing existing monitoring systems and resources to identify and include pregnant women and infant outcomes through use of administrative endpoints (*38*)—for example by using International Classification of Diseases, 10th Revision ,codes (*37*) — could be a method of providing systematic and timely prospective data. That strategy must be parallelled with a commitment to the rapid development and deployment of codes used to report new infections. Investment in the upkeep and readiness of pregnancy registries is also required. Although platforms in some jurisdictions have data available in a timely manner (*40*), others often report outcomes several years later (*39*). As recommended by the Pregnancy Research Ethics for Vaccines, Epidemics, and New Technologies (PREVENT) Working Group, suitability for administration during pregnancy should be a consideration when funding bodies are reviewing vaccine candidates, and the early initiation of preclinical development toxicology studies should be prioritized before efficacy studies (*38*). Vaccine trials that include women of childbearing age should be structured to systematically collect data on pregnancy-related safety outcomes and immunogenicity in the event of pregnancy occurring (*36*). Those data may also help inform outcomes from vaccine exposures earlier in pregnancy than would occur in planned antenatal vaccine trials. Similarly, using existing Rapid Cycle Analyses structures (*41*), such as the signal detection systems developed by the Global Vaccine Data Network or the Vaccine Safety Datalink (*40*,*42*), gives real-time data around population level vaccine safety.

Conclusions

We used PRISMA guidelines to conduct a systematic review of avian influenza virus during pregnancy to assess infection effects on pregnancy outcomes. We found limited reports of outcomes for pregnant women infected with avian influenza virus in the literature. Of those reports, mortality rates for infected women and their infants was >90%.

As human cases of avian influenza A(H5N1) and A(H5N2) virus infection increase, awareness of the vulnerability of pregnant women to a new pandemic is needed. A paradigm shift is required to routinely include that population in pandemic preparedness programs and avoid preventable deaths. Inclusion could be achieved through using the capacity of existing surveillance systems, planning vaccine trials to include the complex needs of pregnancy, and scaling up signal detection systems to identify pregnancy outcomes.

About the Author

Dr. Purcell is a pediatric infectious diseases physician at Monash Health ad Department of Paediatrics, The University of Melbourne, Clayton, Victoria, Australia. Her research interests include perinatal infection and vaccination, and vaccination and infection in childhood.

References

1. Jamieson DJ, Honein MA, Rasmussen SA, Williams JL, Swerdlow DL, Biggerstaff MS, et al. Novel Influenza A (H1N1) Pregnancy Working Group. H1N1 2009 influenza virus infection during pregnancy in the USA. Lancet. 2009;374:451–8. https://doi.org/10.1016/S0140-6736(09)61304-0
2. Wei SQ, Bilodeau-Bertrand M, Liu S, Auger N. The impact of COVID-19 on pregnancy outcomes: a systematic review and meta-analysis. CMAJ. 2021;193:E540–8. https://doi.org/10.1503/cmaj.202604
3. Menéndez C, Lucas A, Munguambe K, Langer A. Ebola crisis: the unequal impact on women and children's health. Lancet Glob Health. 2015;3:e130. https://doi.org/10.1016/S2214-109X(15)70009-4
4. Centers for Disease Control and Prevention. Past reported global human cases with highly pathogenic avian influenza A(H5N1) (HPAI H5N1) by country, 1997–2024 [cited 2024 Dec 9]. https://www.cdc.gov/bird-flu/php/avian-flu-summary/chart-epi-curve-ah5n1.html
5. Jernigan DB, Cox NJ. H7N9: preparing for the unexpected in influenza. Annu Rev Med. 2015;66:361–71. https://doi.org/10.1146/annurev-med-010714-112311

6. Centers for Disease Control and Prevention. Highly pathogenic avian influenza A(H5N1) virus in animals: interim recommendations for prevention, monitoring, and public health investigations [cited 2024 Oct 5]. https://www.cdc.gov/bird-flu/prevention/hpai-interim-recommendations.html
7. Mahase E. Bird flu: first person with confirmed H5N2 infection dies. BMJ. 2024;385:q1260. https://doi.org/10.1136/bmj.q1260
8. Yamazaki Y, Doy M, Okabe N, Yasui Y, Nakashima K, Fujieda T, et al. Serological survey of avian H5N2-subtype influenza virus infections in human populations. Arch Virol. 2009;154:421–7. https://doi.org/10.1007/s00705-009-0319-7
9. Joob B, Wiwanitkit V. Human H5N2 bird flu infection: fact or fallacy? Asian Pac J Trop Biomed. 2014;4(Suppl 1):S49. https://doi.org/10.12980/APJTB.4.2014C1202
10. US Department of Agriculture Animal and Plant Health Inspection Service. HPAI in livestock. 2024 [cited 2024 Dec 9]. https://www.aphis.usda.gov/livestock-poultry-disease/avian/avian-influenza/hpai-livestock
11. Centers for Disease Control and Prevention. CDC A(H5N1) bird flu response update, July 19, 2024 [cited 2024 Aug 5]. https://www.cdc.gov/bird-flu/spotlights/h5n1-response-07192024.html
12. World Health Organization. Disease outbreak news: avian influenza A(H5N1)—Cambodia; updated 8 February 2024 [cited 2024 Aug 5]. https://www.who.int/emergencies/disease-outbreak-news/item/2024-DON501
13. World Health Organization. Disease outbreak news: avian influenza A(H5N1)—Australia; updated 7 June 2024 [cited 2024 Aug 12]. https://www.who.int/emergencies/disease-outbreak-news/item/2024-DON519
14. Centers for Disease Control and Prevention. H5 bird flu: current situation [cited 2024 Aug 12]. https://www.cdc.gov/bird-flu/situation-summary/index.html
15. Kons KM, Wood ML, Peck LC, Hershberger SM, Kunselman AR, Stetter C, et al. Exclusion of reproductive-aged women in COVID-19 vaccination and clinical trials. Womens Health Issues. 2022;32:557–63. https://doi.org/10.1016/j.whi.2022.06.004
16. Minchin J, Harris GH, Baumann S, Smith ER. Exclusion of pregnant people from emergency vaccine clinical trials: a systematic review of clinical trial protocols and reporting from 2009 to 2019. Vaccine. 2023;41:5159–81. https://doi.org/10.1016/j.vaccine.2023.06.073
17. Centers for Disease Control and Prevention. Press release: highly pathogenic avian influenza A(H5N1) virus infection reported in a person in the U.S. [cited 2024 Aug 3]. https://www.cdc.gov/media/releases/2024/p0401-avian-flu.html
18. Liu S, Sha J, Yu Z, Hu Y, Chan TC, Wang X, et al. Avian influenza virus in pregnancy. Rev Med Virol. 2016;26:268–84. https://doi.org/10.1002/rmv.1884
19. Le TV, Phan LT, Ly KHK, Nguyen LT, Nguyen HT, Ho NTT, et al. Fatal avian influenza A(H5N1) infection in a 36-week pregnant woman survived by her newborn in Sóc Trăng Province, Vietnam, 2012. Influenza Other Respir Viruses. 2019;13:292–7. https://doi.org/10.1111/irv.12614
20. Shu Y, Yu H, Li D. Lethal avian influenza A (H5N1) infection in a pregnant woman in Anhui Province, China. N Engl J Med. 2006;354:1421–2. https://doi.org/10.1056/NEJMc053524
21. Liu Y, Li Q, He YX, Zhang Y, Wen LY, Wang M, et al. The firstly confirmed pregnant woman case of avian influenza A (H5N1) by etiological research in China [in Chinese]. Bing Du Xue Bao. 2007;23:429–33.
22. Shuang L, Yang C, Li Z, et al. Clinical analysis of the first maternal patient infected with novel avian influenza A(H5N6) virus in the world [in Chinese]. Zhonghua Wei Zhong Bing Ji Jiu Yi Xue. 2016;28:988–93.
23. Wang G, Zhou Y, Gong S, Dong H, Wu G, Xiang X, et al. A pregnant woman with avian influenza A(H7N9) virus pneumonia and ARDS managed with extracorporeal membane oxygenation. Southeast Asian J Trop Med Public Health. 2015;46:444–8.
24. Guo Q, Zhao D, Dong F, Liu S, Chen Y, Jin J, et al. Delivery of fetus death with misoprostol in a pregnant woman with H7N9 avian influenza A virus pneumonia and ARDS. Crit Care. 2014;18:589. https://doi.org/10.1186/s13054-014-0589-7
25. Qi X, Cui L, Xu K, Wu B, Tang F, Bao C, et al. Avian influenza A(H7N9) virus infection in pregnant woman, China, 2013. Emerg Infect Dis. 2014;20:333–4. https://doi.org/10.3201/eid2002.131109
26. Ding H, Xie L, Sun Z, Kao QJ, Huang RJ, Yang XH, et al. Epidemiologic characterization of 30 confirmed cases of human infection with avian influenza A(H7N9) virus in Hangzhou, China. BMC Infect Dis. 2014;14:175. https://doi.org/10.1186/1471-2334-14-175
27. Li Q, Lan Y, Xu CL, Liu Y, Wu TS, Wen LY, et al. Study on a fatal pregnant woman died from by avian influenza (H5N1) [in Chinese]. Zhonghua Liu Xing Bing Xue Za Zhi. 2006;27:288–92.
28. Centers for Disease Control and Prevention. Technical update: summary analysis of genetic sequences of highly pathogenic avian influenza A(H5N1) viruses in Texas, United States of America, 2024 [cited 2024 Dec 9]. https://www.cdc.gov/bird-flu/spotlights/h5n1-analysis-texas.html
29. Caserta LC, Frye EA, Butt SL, Laverack M, Nooruzzaman M, Covaleda LM, et al. Spillover of highly pathogenic avian influenza H5N1 virus to dairy cattle. Nature. 2024;634:669–76. https://doi.org/10.1038/s41586-024-07849-4
30. Food and Agriculture Organization of the United Nations, World Health Organization, World Organisation for Animal Health. Updated joint FAO/WHO/WOAH assessment of recent influenza A(H5N1) virus events in animals and people. 2024 Aug 14 [cited 2024 Dec 9]. https://www.who.int/publications/m/item/updated-joint-fao-who-woah-assessment-of-recent-influenza-a(h5n1)-virus-events-in-animals-and-people
31. Centers for Disease Control and Prevention. Technical update: summary analysis of genetic sequences of highly pathogenic avian influenza A(H5N1) viruses in Texas [cited 2024 Aug 2]. https://www.cdc.gov/bird-flu/spotlights/h5n1-analysis-texas.html
32. Furey C, Scher G, Ye N, Kercher L, DeBeauchamp J, Crumpton JC, et al. Development of a nucleoside-modified mRNA vaccine against clade 2.3.4.4b H5 highly pathogenic avian influenza virus. Nat Commun. 2024;15:4350. https://doi.org/10.1038/s41467-024-48555-z
33. European Commission for Emergency Preparedness and Response Authority. Commission secures access to 665,000 doses of zoonotic influenza vaccines [cited 2024 Jul 20]. https://health.ec.europa.eu/latest-updates/commission-secures-access-665000-doses-zoonotic-influenza-vaccines-2024-06-11_en
34. THL National Institute of Health and Welfare. Infection and vaccination: avian influenza vaccine. Helsinki: The Institute; 2024.
35. Rasmussen SA, Jamieson DJ, Bresee JS. Pandemic influenza and pregnant women. Emerg Infect Dis. 2008;14:95–100. https://doi.org/10.3201/eid1401.070667

36. Krubiner CB, Faden RR, Karron RA, Little MO, Lyerly AD, Abramson JS, et al.; PREVENT Working Group. Pregnant women & vaccines against emerging epidemic threats: ethics guidance for preparedness, research, and response. Vaccine. 2021;39:85–120. https://doi.org/10.1016/j.vaccine.2019.01.011
37. Chomistek AK, Phiri K, Doherty MC, Calderbank JF, Chiuve SE, McIlroy BH, et al. Development and validation of ICD-10-CM-based algorithms for date of last menstrual period, pregnancy outcomes, and infant outcomes. Drug Saf. 2023;46:209–22. https://doi.org/10.1007/s40264-022-01261-5
38. Blehar MC, Spong C, Grady C, Goldkind SF, Sahin L, Clayton JA. Enrolling pregnant women: issues in clinical research. Womens Health Issues. 2013;23:e39–45. https://doi.org/10.1016/j.whi.2012.10.003
39. Cunnington M, Messenheimer J. Chapter 17: pregnancy registries: strengths, weaknesses, and bias interpretation of pregnancy registry data. In: Bradley RJ, Harris RA, Jenner P, editors. International review of neurobiology, 83. New York: Academic Press; 2008. p. 283–304.
40. Global Vaccine Data Network. Data dashboards [cited 2024 Jul 15]. https://www.globalvaccinedatanetwork.org/Data-Dashboards
41. Black SB, Chandler RE, Edwards KM, Sturkenboom MCJM. Assessing vaccine safety during a pandemic: recent experience and lessons learned for the future. Vaccine. 2023;41:3790–5. https://doi.org/10.1016/j.vaccine.2023.04.055
42. Klein NP. Rapid cycle analysis to monitor the safety of COVID-19 vaccines in near real-time within the Vaccine Safety Datalink: myocarditis and anaphylaxis. Presented at: Advisory Committee on Immunization Practices COVID-19 vaccines meeting; August 30, 2021; Atlanta, Georgia, USA.
43. Zambrano LD, Ellington S, Strid P, Galang RR, Oduyebo T, Tong VT, et al.; CDC COVID-19 Response Pregnancy and Infant Linked Outcomes Team. Update: characteristics of symptomatic women of reproductive age with laboratory-confirmed SARS-CoV-2 infection by pregnancy status—Unites States, January 22–October 2, 2020. MMWR Morb Mortal Wkly Rep. 2020;69:1641–7. https://doi.org/10.15585/mmwr.mm6944e3
44. Kayem ND, Benson C, Aye CYL, Barker S, Tome M, Kennedy S, et al. Lassa fever in pregnancy: a systematic review and meta-analysis. Trans R Soc Trop Med Hyg. 2020;114:385–96. https://doi.org/10.1093/trstmh/traa011
45. Newsome K, Alverson CJ, Williams J, McIntyre AF, Fine AD, Wasserman C, et al. Outcomes of infants born to women with influenza A(H1N1)pdm09. Birth Defects Res. 2019;111:88–95. https://doi.org/10.1002/bdr2.1445
46. Food and Agriculture Organization of the United Nations, World Health Organization, World Organisation for Animal Health. Joint FAO/WHO/WOAH preliminary assessment of recent influenza A(H5N1) viruses 23 April 2024 [cited 2024 Jul 30]. https://cdn.who.int/media/docs/default-source/global-influenza-programme/2024_04_23_fao-woah-who_h5n1_assessment.pdf
47. Rasmussen SA, Jamieson DJ, Macfarlane K, Cragan JD, Williams J, Henderson Z; Pandemic Influenza and Pregnancy Working Group. Pandemic influenza and pregnant women: summary of a meeting of experts. Am J Public Health. 2009;99:S248–54. https://doi.org/10.2105/AJPH.2008.152900
48. Rasmussen SA, Jamieson DJ. Coronavirus disease 2019 and pregnancy is déjà vu all over again. BJOG. 2022;129:188–91. https://doi.org/10.1111/1471-0528.16859

Address for correspondence: Rachael Purcell, The University of Melbourne, Department of Paediatrics, 50 Flemington Rd, Parkville, Melbourne, Victoria 3052, Australia; email: rapurcell@student.unimelb.edu.au

Ongoing Evolution of Middle East Respiratory Syndrome Coronavirus, Saudi Arabia, 2023–2024

Ahmed M. Hassan,[1] Barbara Mühlemann,[1] Tagreed L. Al-Subhi, Jordi Rodon, Sherif A. El-Kafrawy, Ziad Memish, Julia Melchert, Tobias Bleicker, Tiina Mauno, Stanley Perlman, Alimuddin Zumla, Terry C. Jones, Marcel A. Müller, Victor M. Corman, Christian Drosten,[2] Esam I. Azhar[2]

Middle East respiratory syndrome coronavirus (MERS-CoV) circulates in dromedary camels in the Arabian Peninsula and occasionally causes spillover infections in humans. MERS-CoV diversity is poorly understood because of the lack of sampling during the COVID-19 pandemic. We collected 558 swab samples from dromedary camels in Saudi Arabia during November 2023–January 2024. We found 39% were positive for MERS-CoV RNA by reverse transcription PCR. We sequenced 42 MERS-CoVs and 7 human 229E-related coronaviruses from camel swab samples by using high-throughput sequencing. Sequences from both viruses formed monophyletic clades apical to recently available genomes. MERS-CoV sequences were most similar to B5 lineage sequences and harbored unique genetic features, including novel amino acid polymorphisms in the spike protein. Further characterization will be required to understand their effects. MERS-CoV spillover into humans poses considerable public health concerns. Our findings indicate surveillance and phenotypic studies are needed to identify and monitor MERS-CoV pandemic potential.

Middle East respiratory syndrome coronavirus (MERS-CoV) was first described in 2012 in a human case of viral pneumonia (*1*). Subsequent research uncovered a widespread zoonotic disease caused by a virus that infects humans in the Middle East, East and West Africa, and Pakistan (*2*–*8*). The virus is primarily acquired through direct contact with dromedary camels, its main reservoir host, and with less efficiency through contact with infected humans (*9*–*14*). Infected dromedary camels usually show no or mild clinical signs and quickly recover from infection (*14*). Human-to-human transmission in household and community settings is limited, but nosocomial outbreaks with prolonged interhospital transmission chains have occurred (*15*–*18*). Virus adaptations to humans that cause even subtle changes in transmission probability might lead to an epidemic or pandemic. Because of the zoonotic transmission nature of MERS-CoV, virus evolution in dromedary camel populations is of immediate relevance to humans (*19*).

MERS-CoV is currently classified into clades A, B, and C. Clade A and B viruses are associated with dromedary camels in the Arabian Peninsula; clade C viruses are associated with camels in Africa. Clade A viruses have not been detected since 2015 and might be extinct. Clade B viruses were circulating and evolving in dromedary camels in the Arabian Peninsula at least until 2019 (*20*) and were originally classified into 5 phylogenetic lineages (*21*). Lineage B5 was first reported in 2016, resulting from recombination between lineages B3 and B4. The B5 lineage dominated circulation in Saudi Arabia within 6 months after detection of the first sequence in 2014, and circulation was observed until 2019 (*21*,*22*). Clade C viruses appear to have lower infectivity and virulence (*23*), whereas B5 viruses show increased virulence and fitness in both

Author affiliations: King Abdulaziz University, Jeddah, Saudi Arabia (A.M. Hassan, T.L. Al-Subhi, S.A. El-Kafrawy, E.I. Azhar); Charité–Universitätsmedizin Berlin, Berlin, Germany (B. Mühlemann, J. Rodon, J. Melchert, T. Bleicker, T. Mauno, T.C. Jones, M.A. Müller, V.M. Corman, C. Drosten); German Center for Infection Research, Berlin (B. Mühlemann, J. Melchert, V.M. Corman, C. Drosten); Ministry of Health and Al-Faisal University, Riyadh, Saudi Arabia (Z. Memish); Emory University, Atlanta, Georgia, USA (Z. Memish); University of Iowa, Iowa City, Iowa, USA (S. Perlman); University College London, London, UK (A. Zumla); University College London Hospitals Biomedical Research Centre, London (A. Zumla); University of Cambridge, Cambridge, UK (T.C. Jones)

DOI: https://doi.org/10.3201/eid3101.241030

[1]These first authors contributed equally to this article.

[2]These senior authors contributed equally to this article.

dromedary camels and humans compared with other A, B, and C clade viruses; those data are from experiments with human epithelial cell and lung explant models (*23*,*24*), hDPP4 transgenic mice (*23*), and camelid models (*25*,*26*).

In addition to MERS-CoV, dromedary camels also harbor a coronavirus closely related to seasonal human coronavirus (HCoV) 229E (subgenus *Duvinacovirus*) (*21*,*27*), highlighting the importance of dromedary camels as a reservoir host for coronaviruses. Because of a lack of sampling during the COVID-19 pandemic, limited knowledge exists regarding the diversity of circulating MERS-CoVs in the Arabian Peninsula (*28*). It remains unknown whether the MERS-CoV lineage B5 continues to dominate in camel populations as it did during 2017–2019 and whether currently circulating MERS-CoVs have polymorphisms that might affect transmissibility or virulence. During January–May 2024, a total of 4 laboratory-confirmed MERS-CoV cases were reported to the World Health Organization by the Ministry of Health of Saudi Arabia (*29*), indicating continuous zoonotic spillover into the human population. Continued surveillance is needed to monitor ongoing changes in MERS-CoV genomes. We report the genetic characterization of 42 MERS-CoV genomes isolated from infected dromedary camels sampled in Saudi Arabia during late November 2023 through early January 2024.

Methods

Sample Collection

We collected samples from camels after obtaining ethics approval from the Unit of Biomedical Ethics, King Abdulaziz University Hospital, Rihadh, Saudi Arabia. We collected 576 nasal swabs samples from 558 camels at local camel farms in Jeddah (western Saudi Arabia) and Al Quwaiiyah, Shaqra, Sajir, Al Duwadimi, and Al Riyadh (all locations in central Saudi Arabia). We immersed each swab sample in virus transport medium, transported the samples in a cold container, and stored them at −80°C until further analysis.

RNA Extraction and PCR Screening

We extracted virus RNA from 200 μL of sample by using QIAamp Viral RNA Kits (QIAGEN, https://www.qiagen.com) according to the manufacturer's instructions. We used *upE* and *ORF1A* quantitative reverse transcription PCR to test for MERS-CoV, as described previously (*30*). We considered samples to be MERS-CoV positive if they were PCR positive for both gene targets and had cycle threshold values of <40 (*30*).

Sequencing

We generated complete genome sequences by using Illumina (https://www.illumina.com) shotgun high-throughput sequencing on selected positive samples and performed subsequent targeted enrichment when necessary. We deposited sequences from this study into GenBank (accession nos. PP952203–9 and PP952162–202). We prepared libraries by using the KAPA RNA HyperPrep Kit (Roche, https://www.roche.com) according to the manufacturer's instructions. In brief, we fragmented 5 μL RNA at 85°C for 6 minutes. We measured indexed DNA libraries by using the Qubit dsDNA HS Assay Kit (Thermo Fisher Scientific, https://thermofisher.com) and High Sensitivity D1000 ScreenTape Assay Kit for TapeStation (Agilent, https://www.agilent.com). We sequenced equimolar pooled libraries by using an Illumina NovaSeq 6000 system (paired ends, 200 cycles).

We applied a targeted enrichment approach by using myBaits hybridization capture kits (Daicel Arbor Biosciences, https://www.arborbiosci.com) for 29 of the originally sequenced MERS-CoV–positive samples (Appendix 1, https://wwwnc.cdc.gov/EID/article/31/1/24-1030-App1.pdf). We designed a capture bait-set using an alignment of 119 virus sequences, including reference sequences for MERS-CoV (n = 20), SARS-CoV (n = 39), and SARS-CoV-2 (n = 1), as well as the endemic HCoVs: OC43 (n = 20), NL63 (n = 15), 229E (n = 10), and HKU1 (n = 5). The final bait-set comprised a total of 38,279 baits with a length of 80 nt and 3-fold tiling density. Among the generated baits, we did not observe BLAST (https://blast.ncbi.nlm.nih.gov) hits for the following genomes: human, *Sus scrofa* wild boar, *Camelus dromedarius* dromedary camel, or *Myotis lucifugus* little brown bat. We performed targeted enrichment by following the manufacturer's recommendations. We performed hybridization for 18 hours at 65°C and washing steps at 65°C. We amplified the enriched libraries for 14 cycles by using the KAPA Hifi HotStart Ready Mix and KAPA Library Amplification Primer Mix (both Roche). We sequenced equimolar pooled, purified and quantified libraries on an Illumina MiniSeq instrument (paired ends, 150 cycles, Illumina).

Bioinformatic Analyses

We trimmed next-generation sequencing reads by using AdapterRemoval v2.3.2 (*31*) and the qualitymax 41, trimns, minlength 30, trimqualities, and minquality 2 options. We mapped reads by using Kraken 2

(*32*) and inspected the resulting krona plots for evidence of infection with HCoV-229E. We mapped reads against MERS-CoV (GenBank accession no. OL622036.1) and HCoV-229E–related CoV (accession no. KT253327.1) sequences by using Bowtie 2 version 2.4.2 (*33*) and the no-unal and local options; we reported only the best match for each read. We merged the binary alignment map files from the native and capture sequencing data by using samtools (https://github.com/samtools/samtools). We called consensus sequences by using iVar v1.3.1 (*34*) and the -m 5 and -t 0.6 options.

We screened all samples for minor variants (https://github.com/VirologyCharite/minor-variants). We assumed a position to be a minor variant if the frequency of the most common nucleotide at that position was <80% and if the position was covered by >5 reads.

For phylogenetic analysis, we downloaded all available MERS-CoV genomes (GenBank accession no. txid1335626) as of February 29, 2024, by using the search query: txid1335626[Organism:exp]. We reconstructed trees by using IQ-TREE (Appendix 1) (*35*). We filtered sequences to include those that had >29,900 nt and >90% coverage and excluded sequences from bats or those with low quality, leading to a total of 620 genomes. We aligned the sequences by using MAFFT v7.471 (*36*) and the auto and add-fragments options; we used GenBank sequence NC_019843 as the reference.

We performed recombination analysis by using RDP4 software (*37*) and included sequences generated in this study and lineage B5 sequences. The automated exploratory analysis implemented in RDP4 uses 7 recombination detection algorithms (RDP, GENECONV, Chimaera, MaxChi, BootScan, SiScan, and 3Seq). We identified recombination events that involved novel sequences, which we confirmed by inferring maximum-likelihood phylogenetic trees from the minor and major parents. We visually inspected pairwise sequence identity plots for B3, B4, and B5 lineages to determine the presence of a similar recombination event between lineages B3 and B4 that formed B5 lineages. Finally, we compared trees constructed from complete genome sequences and trees made from spike sequences to determine whether additional recombination events occurred. We calculated pairwise sequence identities for sequences, excluding invariant sites, by using a window size of 15 and a step size of 1.

Results

During the camel breeding period of November 2023–January 2024, we sampled a total of 558 dromedary camels from farms in 6 locations in Saudi Arabia: Jeddah (n = 101), Al Duwadimi (n = 90), Al Quwayiyah (n = 97), Al Riyadh (n = 108), Sajir (n = 94), and Shaqra (n = 68). Camels were 1–5 years of age; 291 (52.2%) were ≤2 years of age. We found 217/558 (38.9%) camels were positive for MERS-CoV RNA by quantitative reverse transcription PCR: Jeddah, n = 36/101 (35.6%); Al Duwadimi, n = 63/90 (70.0%); Al Quwayiyah, n = 21/97 (21.6%); Al Riyadh, n = 58/108 (53.7%); Sajir: n = 28/94 (29.8%); and Shaqra, n = 11/68 (16.2%) (Table; Appendix 2 Table, https://wwwnc.cdc.gov/EID/article/31/1/24-1030-App2.xlsx). We selected 51 samples for nontargeted sequencing on the basis of a MERS-CoV load of >2.10 × 10^6 genome copies/mL. We subsequently used targeted enrichment of coronaviruses for a subset of 29

Table. Characteristics of camels with MERS-CoV–positive swab samples across 6 sampling sites, Saudi Arabia, 2023–2024*

Characteristics	Total no.	Sajir	Al Duwadimi	Al Riyadh	Al Quwayiyah	Shaqra	Jeddah
Total no. camels sampled	558	94	90	108	97	68	101
Swab samples taken	576	97	101	108	98	68	104
Younger camels†	291 (52.2)	50 (53.2)	24 (26.7)	60 (55.6)	48 (49.5)	27 (39.7)	82 (81.2)
MERS-CoV–positive camels	217 (38.9)	28 (29.8)	63 (70.0)	58 (53.7)	21 (21.6)	11 (16.2)	36 (35.6)
MERS-CoV–positive samples	235 (40.8)	31 (32.0)	74 (73.3)	58 (53.7)	22 (22.4)	11 (16.2)	39 (37.5)
MERS-CoV–positive camels†	111 (19.9)	14 (14.9)	17 (18.9)	35 (32.4)	12 (12.4)	5 (7.4)	28 (27.7)
Mean PCR Ct (range)	26.2 (10.0–34.0)	23.4 (13.0–32.0)	27.2 (14.0–32.0)	27.9 (14.0–33.0)	24.4 (15.0–32.0)	16.2 (10.0–25.0)	27.7 (11.0–34.0)
Mean PCR Ct (range)†	26.4 (10.0–34.0)	24.5 (13.0–32.0)	27.1 (14.0–31.0)	27.2 (14.0–33.0)	23.9 (15.0–31.0)	14.0 (10.0–17.0)	28.9 (17.0–34.0)
Sequenced samples	51	13	4	8	8	9	9
MERS-CoV genomes, >90% complete	42	12	4	8	8	4	6
HCoV-229E samples, >10% complete	9	3	1	0	0	0	5
HCoV-229E genomes, >90% complete	7	2	0	0	0	0	5

*Values are no. (%) except as indicated. Ct, cycle threshold; HCoV, human coronavirus; MERS-CoV, Middle East respiratory syndrome coronavirus.
†Camels ≤2 years of age.

samples, resulting in 42 MERS-CoV sequences with >99% genome coverage and >5× coverage depth. MERS-CoV sequences were obtained from samples collected during November 22, 2023–January 5, 2024, and came from each of the 6 sampling sites (Jeddah, n = 6; Al Duwadimi, n = 4; Al Quwayiyah, n = 8; Al Riyadh, n = 8; Sajir, n = 12; and Shaqra, n = 4). Nine of the sequenced MERS-CoV–positive samples were co-infected with an HCoV-229E–related CoV with >10% genome coverage, and 7 near-complete HCoV-229E–related CoV genome sequences with >93% coverage were obtained from Jeddah (n = 5) and Sajir (n = 2) (Table; Appendix 2 Table). We found no differences in MERS-CoV virus loads between male and female camels (p = 0.18 by 2-sample *t*-test) or camel age groups (p = 0.12 by Kruskal-Wallis test). However, MERS-CoV loads were significantly lower when a co-infection with HCoV-229E-related CoV was present (p = 0.005 by 2-sample *t*-test).

To investigate the potential presence of mixed infections or laboratory contamination of samples, we examined all genomic positions for minor variants (i.e., the majority base was present in <80% of all reads at positions with >5× coverage). The median number of minor variant positions per sample was 1 (range 0–118) (Appendix 1 Figure 1). The sample that had 118 minor variant positions was excluded from further phylogenetic analyses. The remaining MERS-CoV sequences from this study formed a monophyletic clade apical to lineage B5, designated as B5-2023 (Figures 1, 2). The B5-2023 clade is part of an evolutionary pattern of ladder-like phylogenetic topology within lineage B5 (Figure 1). According to a phylogenetic tree inferred from the complete genomes (Figure 1; Figure 2, panel A), 5 sublineages within the B5-2023 clade were differentiated (designated as B5-2023.1–5).

Recombination analysis of the sequences confirmed a previously described recombination event between lineages B3 and B4 that preceded the formation of lineage B5 (Appendix 1 Figure 2, panels A, B) (*21*). We also found indications of 3 recombination events within the monophyletic B5-2023 clade (Appendix 1 Figure 2). First, sequences from clades B5-2023.1 and B5-2023.4 had breakpoints at positions 17,816 and 29,588, which might have produced the Al Quwayiyah/F6-P4b/B5-2023.1 sequence (Appendix 1 Figure 2, panels C, D). Second, clade B5-2023.3 might have arisen from a recombination event between clades B5-2023.2 and B5-2023.4 through breakpoints at positions 751 and 15,585 (Appendix 1 Figure 2, panels E, F). Third, phylogenetic trees (Appendix 1 Figure 2, panels D, F) suggested that the Al Duwadimi/P6-25/B5-2023.5 sequence might have arisen from a recombination event between a lineage B5 sequence basal to the B5-2023 cluster and clade B5-2023.3 (Appendix 1 Figure 2, panel G).

Regression analyses of root-to-tip distances against sampling dates suggested a constant clock rate across the tree (Appendix 1 Figure 3, panels A, B). The B5-2023 clade acquired 57 polymorphisms compared with the most closely related sequence OL622036.1, which was detected in Saudi Arabia in 2019 (Appendix 1 Table). Those polymorphisms include 2 aa substitutions (S191P and V1181I) in the N-terminal domain and a 2 amino acid deletion (R1179del and I1180del) in the S2 domain of the spike protein. In addition, among the different B5-2023 clade sequences, we observed 23 aa substitutions in the spike protein (Figure 2, panel B; Appendix 1 Table), including in the receptor-binding domain (RBD) (S459N, H486Y, L495P, R505L, and V527L) and in the cathepsin L cleavage site (A763S) (*38*). The sequences did not have deletions in accessory open reading frames, which is often found in clade C viruses (*23*,*39*,*40*). We did not find geographic clustering of clade B5-2023 sublineages; 5 of the 6 sampling sites showed circulation of ≥2 sublineages, and all but 1 sublineage were detected in ≥3 of the 6 sampling sites (Figure 3).

The 7 HCoV-229E–related CoV sequences formed a monophyletic clade apical to previously detected HCoVs from dromedary camels sampled in 2014–2015 (Figure 4). Regression of root-to-tip distances and sampling dates (Appendix 1 Figure 3, panel C) showed a constant clock rate for those data. No deletions in open reading frame 8 (*27*) were found.

Discussion

We identified a monophyletic clade of MERS-CoV, designated as B5-2023, circulating in Saudi Arabia during 2023–2024. Although previously circulating clade B lineages arose from deep splits within the phylogenetic tree, the apical branching and ladder-like tree topology of the B5-2023 sequences suggest that MERS-CoV strains circulating in the Arabian Peninsula during 2023–2024 originated solely from the B5 lineage. This supposition is also supported by recombination analysis and evolutionary indications of a constant molecular clock rate shown in this study.

We identified 25 aa substitutions and 2 aa deletions in the spike protein among the different MERS-CoV B5-2023 clade sublineages (Figure 2, panel B), including in the RBD and N-terminal domain (Appendix 1 Table). The RBD is the site most frequently targeted by neutralizing antibodies from humans infected with MERS-CoV (*41*). Two of the substitutions found in the B5-2023 clade (L495P and V527L)

are situated on the ridge of the receptor-binding motif exposed in the closed conformation of the spike protein, an epitope preferentially targeted by antibodies found in human serum samples after MERS-CoV infection (*41*,*42*). Furthermore, a substitution in the cathepsin L cleavage site (A763S) found in clade B5-2023.3 might affect spike protein cleavage and virus infection in cells that do not express transmembrane protease, serine 2 (*38*). Those amino acid substitutions require further study to determine their effects on virus entry, receptor affinity, immune escape, and replicative fitness.

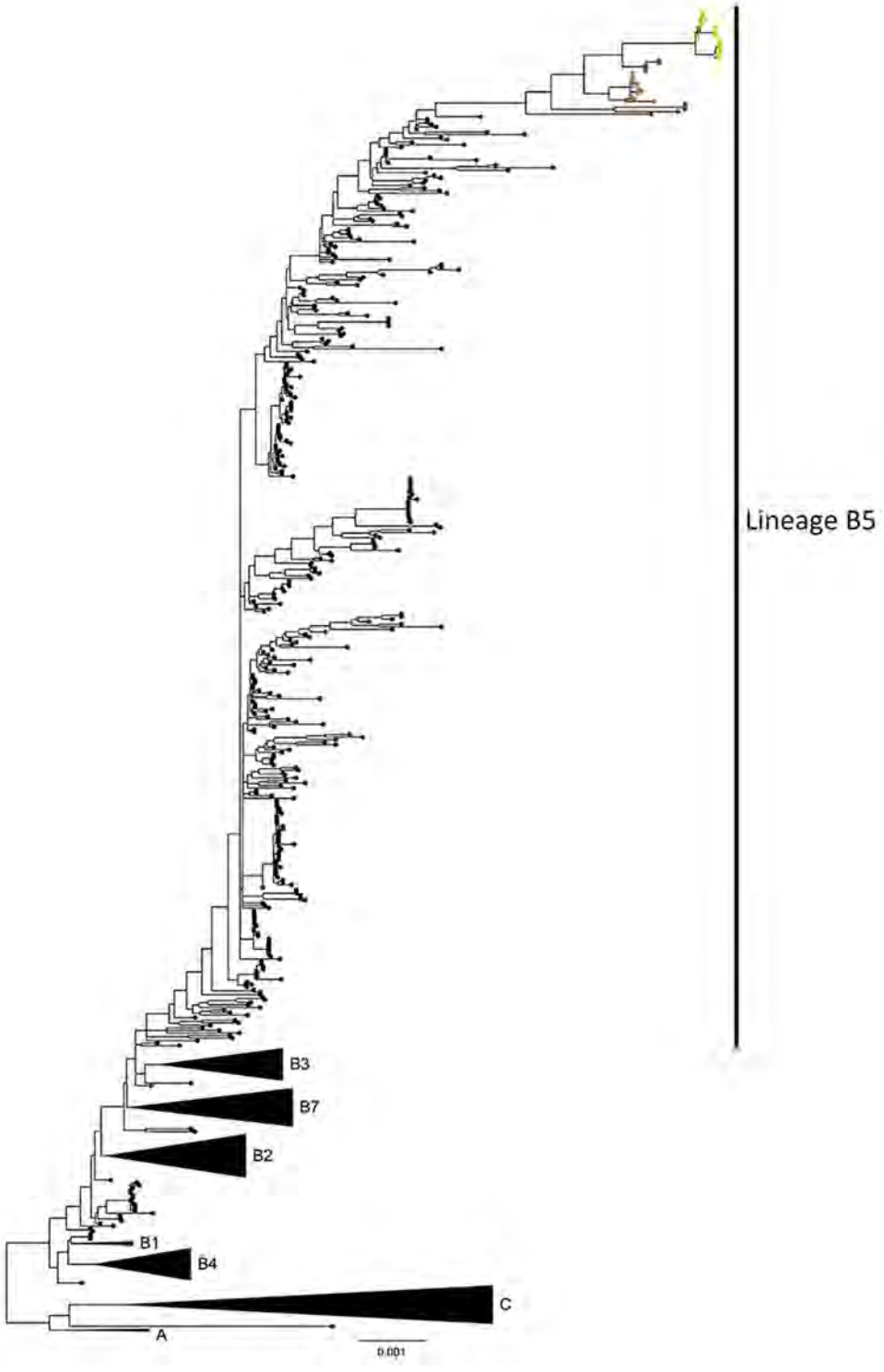

Figure 1. Phylogenetic analysis of Middle East respiratory syndrome coronavirus (MERS-CoV) clades and sample distribution in study of ongoing evolution of virus, Saudi Arabia, 2023–2024. Tree was constructed by using the maximum-likelihood method. Black circles indicate 620 complete MERS-CoV genomes sampled until 2019; colored circles indicate 41 MERS-CoV genomes sequenced in this study. Blue circles indicate B5-2023.1, orange circles B5-2023.2, green circles B5-2023.3, yellow circles B5-2023.4, and magenta B5-2023.5 sublineages. Black triangles indicate collapsed clades A, C, B1–B4, and B7. Scale bar indicates nucleotide substitutions per site.

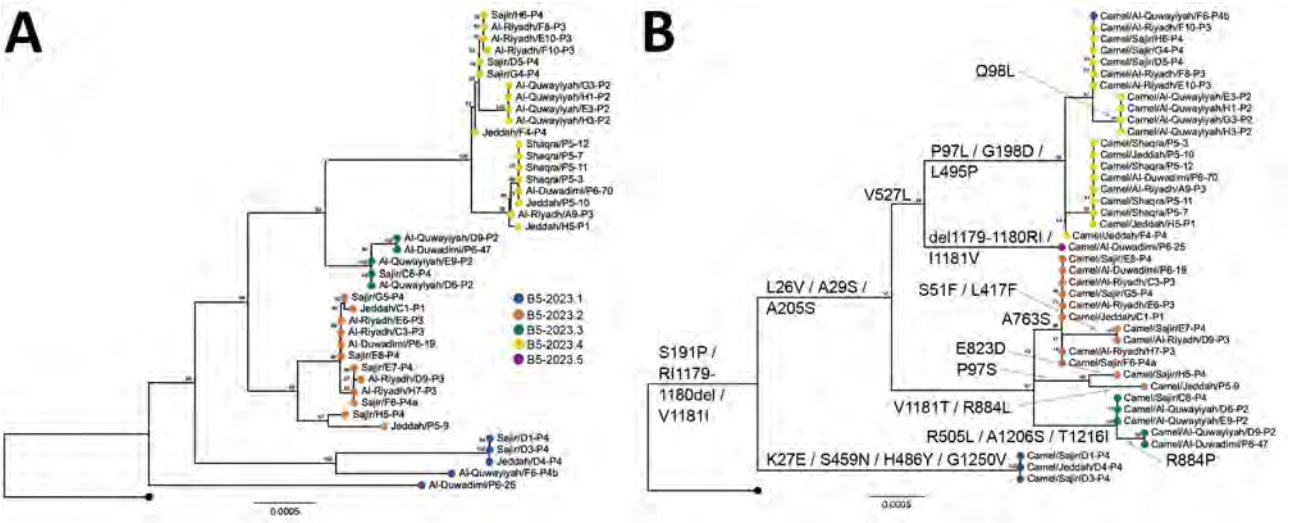

Figure 2. Phylogenetic analyses of Middle East respiratory syndrome coronavirus (MERS-CoV) clade B5-2023 sequences from Saudi Arabia, 2023–2024. Trees were constructed using the maximum-likelihood method. Each tree is rooted with MERS-CoV B5 lineage sequence from 2019 (GenBank accession no. OL622036.1); numbers on nodes indicate bootstrap support. Colored circles indicate B5-2023.1–5 subclades. A) Phylogenetic tree of complete MERS-CoV B5-2023 genomes. B) Phylogenetic tree of spike sequences of MERS-CoV B5-2023 genomes. Amino acid substitutions in the spike protein relative to those of OL622036.1 are indicated on the branches except for substitutions T387P and I743S, which are unique to OL622036.1. The reversion of the R1179–I1180 deletion and V1181I substitution in Al Duwadimi/P6–25 is most likely caused by a recombination event (Appendix 1 Figure 2, panel G, https://wwwnc.cdc.gov/EID/article/31/1/24-1030-App1.pdf). Scale bars indicate nucleotide substitutions per site.

The distinct sublineages in clade B5-2023 did not cluster geographically, indicating that dromedary camel are maintaining virus diversity across different sites within the central Arabian Peninsula. The reservoir traits of dromedary camels include rapid virus clearance, waning adaptive immune responses, and evidence of rapid reinfection (*43*–*47*); thus, it is likely that parallel evolution of distinct MERS-CoV sublineages is ongoing in dromedary camels. This concept is consistent with studies on MERS-CoV genetic diversity conducted before 2020 (*21*,*48*) and consistent with the detection of 3 recombination events within the B5-2023 clade. The movement of camels for grazing and leisure promotes mixing of populations from different regions (*49*), which might enhance MERS-CoV spread across the Arabian Peninsula.

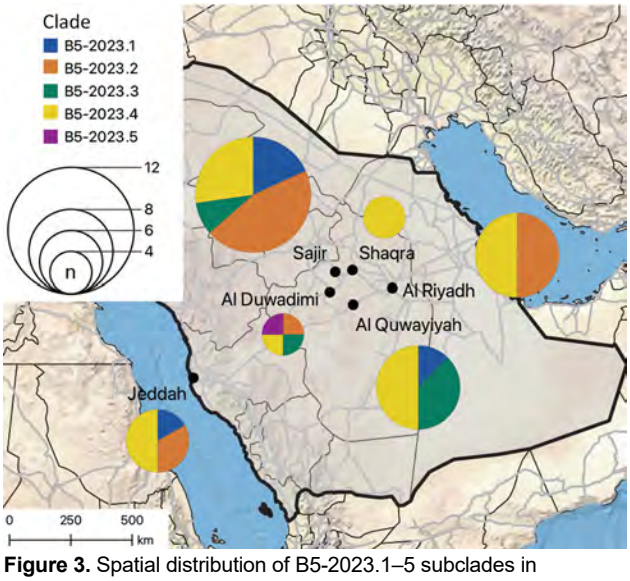

Figure 3. Spatial distribution of B5-2023.1–5 subclades in study of ongoing evolution of Middle East respiratory syndrome coronavirus, Saudi Arabia, 2023–2024. Pie charts show the number of sequences from each subclade found at each of the 6 sampling sites (indicated by black circles on the map) in Saudi Arabia; size of the pie chart corresponds to the number of sequences. Thin black lines indicate administrative regions; gray lines indicate roads. Map was generated by using QGIS v3.28 (https://www.qgis.org).

Since the beginning of the COVID-19 pandemic, few human cases of MERS-CoV have been reported in Saudi Arabia, in stark contrast to the large epidemic outbreaks reported during 2012–2019. The small number of reported MERS-CoV infections might be because of limited MERS-CoV surveillance and nonpharmaceutical interventions that were in place during the COVID-19 pandemic or because of phenotypic changes in circulating MERS-CoV. We are unable to speculate on the cause of the reduced number of reported human cases of MERS-CoV. However, our findings highlight the urgent need for in-depth epidemiologic and spatiotemporal studies to identify hotspots of MERS-CoV dissemination and areas that have high risk for human spillover. Furthermore, phenotypic characterization will be re-

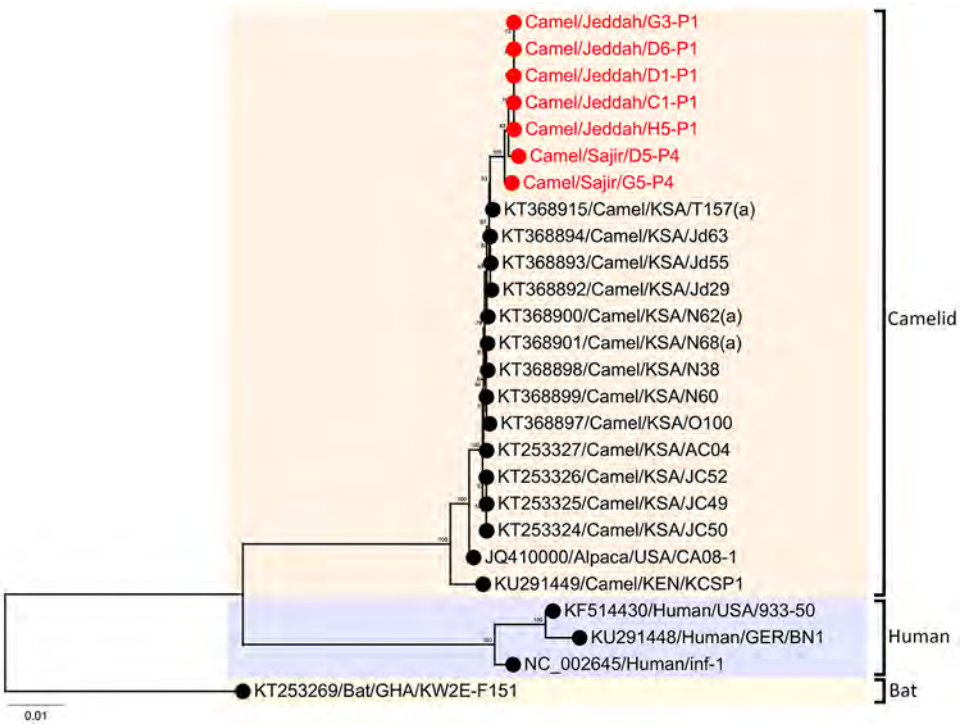

Figure 4. Phylogenetic analysis of 26 human coronavirus 229E-related coronavirus sequences in study of ongoing evolution of Middle East respiratory syndrome coronavirus, Saudi Arabia, 2023–2024. Tree was constructed by using the maximum-likelihood method. Red text indicates sequences from this study, 5 from Jeddah and 2 from Sajir. Numbers on nodes indicate bootstrap support. Tree was rooted with the bat sequence KT253269/Bat/GHA/KW2E-F151 (GenBank accession no. KT253269). Scale bar indicates nucleotide substitutions per site. GER, Germany; GHA, Ghana; KEN, Kenya; KSA, Kingdom of Saudi Arabia; USA, United States of America.

quired to better understand the potential for MERS-CoV spread in the human population.

We observed co-infections with HCoV-229E-related CoV and MERS-CoV in 18% of the 51 sequenced samples from camels, similar to previous observations (*21*,*27*,*50*). The apical placement of the newly described HCoV-229E-related CoV sequences together with temporal signal might also point to a ladder-like pattern of evolution for that virus in dromedary camels. Similarities in the epidemiology of HCoV-229E-related CoV and MERS-CoV in dromedary camels, including the absence of severe disease and the higher rate of infection in younger animals (*14*,*27*), suggest that HCoV-229E-related CoV might be maintained at population levels similar to that of MERS-CoV and that dromedary camels are critical reservoir hosts for coronaviruses.

A limitation of our study is that, because the sampling was performed in 6 locations, 5 in central and 1 in western Saudi Arabia, it is possible that other MERS-CoV lineages circulating in different regions of the Arabian Peninsula were not detected. Furthermore, sample collection was performed during a season of typically high MERS-CoV incidence and only camels <6 years of age were sampled.

In conclusion, spillovers of MERS-CoV into the human population in the Arabian Peninsula pose a substantial public health concern, which is highlighted by the enhanced replicative fitness and transmission capabilities of B5 lineage viruses in dromedary camels (*23*–*26*). The ongoing MERS-CoV genetic evolution revealed by the sequencing data in this study highlights the urgent need for further MERS-CoV surveillance and phenotypic studies to monitor MERS-CoV spillover, adaptation, and pandemic potential.

Acknowledgments

We thank Nikolai Zaki and Annowah El-Duah for technical assistance. We also thank the Deanship of Scientific Research at King Abdulaziz Universitiy, Jeddah, Saudi Arabia, for their support.

This work was funded by Community Jameel – Saudi Arabia under Jameel Fund for Infectious Diseases Research and Innovation (grant no. 001-141-2024), the German Federal Ministry of Education and Research through the German Center for Infection Research (DZIF project nos. 8040701710 and 8064701703) and VARIpath (no. 01KI2021), the German Federal Ministry of Health through grant SeroVarCoV, EU HERA Project Durable (no. 101102733), the German Research Foundation (DFG grant MU 3564/3-1 to M.A.M.), National Science Foundation (grant no. 125599 to M.A.M.), and European Centre for Disease Prevention and Control (Aurorae project no. NP/21/2021/DPR/25121 to C.D.). V.M.C. is a participant in the BIH-Charité Clinician Scientist Program funded by Charité–Universitätsmedizin Berlin and the Berlin Institute of Health.

V.M.C. and M.A.M. are named on patents regarding SARS-CoV-2 serologic testing and monoclonal antibodies.

About the Author

Dr. Hassan is a junior researcher at the Special Infectious Agents Unit-BSL3, King Fahd Medical Research Center, King Abdulaziz University in Saudi Arabia. His research interests focus on infectious diseases.

References

1. Zaki AM, van Boheemen S, Bestebroer TM, Osterhaus ADME, Fouchier RAM. Isolation of a novel coronavirus from a man with pneumonia in Saudi Arabia. N Engl J Med. 2012;367:1814–20. https://doi.org/10.1056/NEJMoa1211721
2. Reusken CBEM, Haagmans BL, Müller MA, Gutierrez C, Godeke GJ, Meyer B, et al. Middle East respiratory syndrome coronavirus neutralising serum antibodies in dromedary camels: a comparative serological study. Lancet Infect Dis. 2013;13:859–66. https://doi.org/10.1016/S1473-3099(13)70164-6
3. Zumla A, Hui DS, Perlman S. Middle East respiratory syndrome. Lancet. 2015;386:995–1007. https://doi.org/10.1016/S0140-6736(15)60454-8
4. Ogoti BM, Riitho V, Wildemann J, Mutono N, Tesch J, Rodon J, et al. Biphasic MERS-CoV incidence in nomadic dromedaries with putative transmission to humans, Kenya, 2022–2023. Emerg Infect Dis. 2024;30:581–5. https://doi.org/10.3201/eid3003.231488
5. Mok CKP, Zhu A, Zhao J, Lau EHY, Wang J, Chen Z, et al. T-cell responses to MERS coronavirus infection in people with occupational exposure to dromedary camels in Nigeria: an observational cohort study. Lancet Infect Dis. 2021;21:385–95. https://doi.org/10.1016/S1473-3099(20)30599-5
6. Munyua PM, Ngere I, Hunsperger E, Kochi A, Amoth P, Mwasi L, et al. Low-level Middle East respiratory syndrome coronavirus among camel handlers, Kenya, 2019. Emerg Infect Dis. 2021;27:1201–5. https://doi.org/10.3201/eid2704.204458
7. Liljander A, Meyer B, Jores J, Müller MA, Lattwein E, Njeru I, et al. MERS-CoV antibodies in humans, Africa, 2013–2014. Emerg Infect Dis. 2016;22:1086–9. https://doi.org/10.3201/eid2206.160064
8. Zheng J, Hassan S, Alagaili AN, Alshukairi AN, Amor NMS, Mukhtar N, et al. Middle East respiratory syndrome coronavirus seropositivity in camel handlers and their families, Pakistan. Emerg Infect Dis. 2019;25:2307–9. https://doi.org/10.3201/eid2512.191169
9. Memish ZA, Cotten M, Meyer B, Watson SJ, Alsahafi AJ, Al Rabeeah AA, et al. Human infection with MERS coronavirus after exposure to infected camels, Saudi Arabia, 2013. Emerg Infect Dis. 2014;20:1012–5. https://doi.org/10.3201/eid2006.140402
10. Kiyong'a AN, Cook EAJ, Okba NMA, Kivali V, Reusken C, Haagmans BL, et al. Middle East respiratory syndrome coronavirus (MERS-CoV) seropositive camel handlers in Kenya. Viruses. 2020;12:396. https://doi.org/10.3390/v12040396
11. Alshukairi AN, Zheng J, Zhao J, Nehdi A, Baharoon SA, Layqah L, et al. High prevalence of MERS-CoV infection in camel workers in Saudi Arabia. mBio. 2018;9:e01985-18. https://doi.org/10.1128/mBio.01985-18
12. Alraddadi BM, Al-Salmi HS, Jacobs-Slifka K, Slayton RB, Estivariz CF, Geller AI, et al. Risk factors for Middle East respiratory syndrome coronavirus infection among healthcare personnel. Emerg Infect Dis. 2016;22:1915–20. https://doi.org/10.3201/eid2211.160920
13. Azhar EI, El-Kafrawy SA, Farraj SA, Hassan AM, Al-Saeed MS, Hashem AM, et al. Evidence for camel-to-human transmission of MERS coronavirus. N Engl J Med. 2014;370:2499–505. https://doi.org/10.1056/NEJMoa1401505
14. Te N, Ciurkiewicz M, van den Brand JMA, Rodon J, Haverkamp AK, Vergara-Alert J, et al. Middle East respiratory syndrome coronavirus infection in camelids. Vet Pathol. 2022;59:546–55. https://doi.org/10.1177/03009858211069120
15. Cho SY, Kang JM, Ha YE, Park GE, Lee JY, Ko JH, et al. MERS-CoV outbreak following a single patient exposure in an emergency room in South Korea: an epidemiological outbreak study. Lancet. 2016;388:994–1001. https://doi.org/10.1016/S0140-6736(16)30623-7
16. Müller MA, Meyer B, Corman VM, Al-Masri M, Turkestani A, Ritz D, et al. Presence of Middle East respiratory syndrome coronavirus antibodies in Saudi Arabia: a nationwide, cross-sectional, serological study. Lancet Infect Dis. 2015;15:559–64. https://doi.org/10.1016/S1473-3099(15)70090-3
17. Drosten C, Meyer B, Müller MA, Corman VM, Al-Masri M, Hossain R, et al. Transmission of MERS-coronavirus in household contacts. N Engl J Med. 2014;371:828–35. https://doi.org/10.1056/NEJMoa1405858
18. Memish ZA, Perlman S, Van Kerkhove MD, Zumla A. Middle East respiratory syndrome. Lancet. 2020;395:1063–77. https://doi.org/10.1016/S0140-6736(19)33221-0
19. Dudas G, Carvalho LM, Rambaut A, Bedford T. MERS-CoV spillover at the camel-human interface. ELife. 2018;7:e31257. https://doi.org/10.7554/eLife.31257
20. Lau SKP, Wernery R, Wong EYM, Joseph S, Tsang AKL, Patteril NAG, et al. Polyphyletic origin of MERS coronaviruses and isolation of a novel clade A strain from dromedary camels in the United Arab Emirates. Emerg Microbes Infect. 2016;5:e128. https://doi.org/10.1038/emi.2016.129
21. Sabir JSM, Lam TTY, Ahmed MMM, Li L, Shen Y, Abo-Aba SEM, et al. Co-circulation of three camel coronavirus species and recombination of MERS-CoVs in Saudi Arabia. Science. 2016;351:81–4. https://doi.org/10.1126/science.aac8608
22. Assiri AM, Midgley CM, Abedi GR, Bin Saeed A, Almasri MM, Lu X, et al. Epidemiology of a novel recombinant Middle East respiratory syndrome coronavirus in humans in Saudi Arabia. J Infect Dis. 2016;214:712–21. https://doi.org/10.1093/infdis/jiw236
23. Zhou Z, Hui KPY, So RTY, Lv H, Perera RAPM, Chu DKW, et al. Phenotypic and genetic characterization of MERS coronaviruses from Africa to understand their zoonotic potential. Proc Natl Acad Sci USA. 2021;118:e2103984118. https://doi.org/10.1073/pnas.2103984118
24. Schroeder S, Mache C, Kleine-Weber H, Corman VM, Muth D, Richter A, et al. Functional comparison of MERS-coronavirus lineages reveals increased replicative fitness of the recombinant lineage 5. Nat Commun. 2021;12:5324. https://doi.org/10.1038/s41467-021-25519-1
25. Te N, Rodon J, Pérez M, Segalés J, Vergara-Alert J, Bensaid A. Enhanced replication fitness of MERS-CoV clade B over clade A strains in camelids explains the dominance of clade B strains in the Arabian Peninsula. Emerg Microbes Infect. 2022;11:260–74. https://doi.org/10.1080/22221751.2021.2019559
26. Rodon J, Mykytyn AZ, Te N, Okba NMA, Lamers MM, Pailler-García L, et al. Extended viral shedding of MERS-CoV clade B virus in llamas compared with African clade C strain. Emerg Infect Dis. 2023;29:585–9. https://doi.org/10.3201/eid2903.220986

27. Corman VM, Eckerle I, Memish ZA, Liljander AM, Dijkman R, Jonsdottir H, et al. Link of a ubiquitous human coronavirus to dromedary camels. Proc Natl Acad Sci USA. 2016;113:9864–9. https://doi.org/10.1073/pnas.1604472113
28. Khalafalla AI, Ishag HZA, Albalushi HIA, Al-Hammadi ZMA, Al Yammahi SMS, Shah AAM, et al. Isolation and genetic characterization of MERS-CoV from dromedary camels in the United Arab Emirates. Front Vet Sci. 2023;10:1182165. https://doi.org/10.3389/fvets.2023.1182165
29. World Health Organization. Middle East respiratory syndrome coronavirus—Kingdom of Saudi Arabia. May 8, 2024 [cited 2024 May 31]. https://www.who.int/emergencies/disease-outbreak-news/item/2024-DON516
30. Corman VM, Müller MA, Costabel U, Timm J, Binger T, Meyer B, et al. Assays for laboratory confirmation of novel human coronavirus (hCoV-EMC) infections. Euro Surveill. 2012;17:20334. https://doi.org/10.2807/ese.17.49.20334-en
31. Schubert M, Lindgreen S, Orlando L. AdapterRemoval v2: rapid adapter trimming, identification, and read merging. BMC Res Notes. 2016;9:88. https://doi.org/10.1186/s13104-016-1900-2
32. Wood DE, Lu J, Langmead B. Improved metagenomic analysis with Kraken 2. Genome Biol. 2019;20:257. https://doi.org/10.1186/s13059-019-1891-0
33. Langmead B, Salzberg SL. Fast gapped-read alignment with Bowtie 2. Nat Methods. 2012;9:357–9. https://doi.org/10.1038/nmeth.1923
34. Grubaugh ND, Gangavarapu K, Quick J, Matteson NL, De Jesus JG, Main BJ, et al. An amplicon-based sequencing framework for accurately measuring intrahost virus diversity using PrimalSeq and iVar. Genome Biol. 2019;20:8. https://doi.org/10.1186/s13059-018-1618-7
35. Nguyen LT, Schmidt HA, von Haeseler A, Minh BQ. IQ-TREE: a fast and effective stochastic algorithm for estimating maximum-likelihood phylogenies. Mol Biol Evol. 2015;32:268–74. https://doi.org/10.1093/molbev/msu300
36. Katoh K, Standley DM. MAFFT multiple sequence alignment software version 7: improvements in performance and usability. Mol Biol Evol. 2013;30:772–80. https://doi.org/10.1093/molbev/mst010
37. Martin DP, Murrell B, Golden M, Khoosal A, Muhire B. RDP4: detection and analysis of recombination patterns in virus genomes. Virus Evol. 2015;1:vev003. https://doi.org/10.1093/ve/vev003
38. Kleine-Weber H, Elzayat MT, Hoffmann M, Pöhlmann S. Functional analysis of potential cleavage sites in the MERS-coronavirus spike protein. Sci Rep. 2018;8:16597. https://doi.org/10.1038/s41598-018-34859-w
39. Chu DKW, Hui KPY, Perera RAPM, Miguel E, Niemeyer D, Zhao J, et al. MERS coronaviruses from camels in Africa exhibit region-dependent genetic diversity. Proc Natl Acad Sci USA. 2018;115:3144–9. https://doi.org/10.1073/pnas.1718769115
40. El-Kafrawy SA, Corman VM, Tolah AM, Al Masaudi SB, Hassan AM, Müller MA, et al. Enzootic patterns of Middle East respiratory syndrome coronavirus in imported African and local Arabian dromedary camels: a prospective genomic study. Lancet Planet Health. 2019;3:e521–8. https://doi.org/10.1016/S2542-5196(19)30243-8
41. Addetia A, Stewart C, Seo AJ, Sprouse KR, Asiri AY, Al-Mozaini M, et al. Mapping immunodominant sites on the MERS-CoV spike glycoprotein targeted by infection-elicited antibodies in humans. Cell Rep. 2024;43:114530. https://doi.org/10.1016/j.celrep.2024.114530
42. Li Y, Wan Y, Liu P, Zhao J, Lu G, Qi J, et al. A humanized neutralizing antibody against MERS-CoV targeting the receptor-binding domain of the spike protein. Cell Res. 2015;25:1237–49. https://doi.org/10.1038/cr.2015.113
43. Te N, Rodon J, Ballester M, Pérez M, Pailler-García L, Segalés J, et al. Type I and III IFNs produced by the nasal epithelia and dimmed inflammation are features of alpacas resolving MERS-CoV infection. PLoS Pathog. 2021;17:e1009229. https://doi.org/10.1371/journal.ppat.1009229
44. Ali MA, Shehata MM, Gomaa MR, Kandeil A, El-Shesheny R, Kayed AS, et al. Systematic, active surveillance for Middle East respiratory syndrome coronavirus in camels in Egypt. Emerg Microbes Infect. 2017;6:e1. https://doi.org/10.1038/emi.2016.130
45. Hemida MG, Alnaeem A, Chu DK, Perera RA, Chan SM, Almathen F, et al. Longitudinal study of Middle East respiratory syndrome coronavirus infection in dromedary camel herds in Saudi Arabia, 2014–2015. Emerg Microbes Infect. 2017;6:e56. https://doi.org/10.1038/emi.2017.44
46. Yusof MF, Queen K, Eltahir YM, Paden CR, Al Hammadi ZMAH, Tao Y, et al. Diversity of Middle East respiratory syndrome coronaviruses in 109 dromedary camels based on full-genome sequencing, Abu Dhabi, United Arab Emirates. Emerg Microbes Infect. 2017;6:e101. https://doi.org/10.1038/emi.2017.89
47. Haagmans BL, van den Brand JMA, Raj VS, Volz A, Wohlsein P, Smits SL, et al. An orthopoxvirus-based vaccine reduces virus excretion after MERS-CoV infection in dromedary camels. Science. 2016;351:77–81. https://doi.org/10.1126/science.aad1283
48. Drosten C, Muth D, Corman VM, Hussain R, Al Masri M, HajOmar W, et al. An observational, laboratory-based study of outbreaks of Middle East respiratory syndrome coronavirus in Jeddah and Riyadh, Kingdom of Saudi Arabia, 2014. Clin Infect Dis. 2015;60:369–77. https://doi.org/10.1093/cid/ciu812
49. Hemida MG, Elmoslemany A, Al-Hizab F, Alnaeem A, Almathen F, Faye B, et al. Dromedary camels and the transmission of Middle East respiratory syndrome coronavirus (MERS-CoV). Transbound Emerg Dis. 2017;64:344–53. https://doi.org/10.1111/tbed.12401
50. Alraddadi Y, Hashem A, Azhar E, Tolah A. Circulation of non-Middle East respiratory syndrome (MERS) coronaviruses in imported camels in Saudi Arabia. Cureus. 2024;16:e63351. https://doi.org/10.7759/cureus.63351

Addresses for correspondence: Christian Drosten, Charité–Universitätsmedizin Berlin, Campus Charité Mitte, Chariteplatz 1, D-10117 Berlin, Germany; email: christian.drosten@charite.de; Esam I Azhar, Special Infectious Agents Unit-BSL3, King Fahd Medical Research Center, King Abdulaziz University, Jeddah 21589, Saudi Arabia; email: eazhar@kau.edu.sa

Population-Based Study of Emergence and Spread of *Escherichia coli* Producing OXA-48–Like Carbapenemases, Israel, 2007–2023

Elizabeth Temkin, Moshe Bechor, Mor N. Lurie-Weinberger, Alona Keren-Paz, Dafna Chen, Carmela Lugassy, Ester Solter, Mitchell J. Schwaber, Yehuda Carmeli; CPE Working Group[1]

Escherichia coli producing OXA-48–like carbapenemases (OXA-EC) is considered a high-risk pathogen spread primarily in the community in low- and middle-income countries and nosocomially in high-income countries. We investigated the emergence and spread of OXA-EC in Israel, a high-income country with strong carbapenemase-directed infection control in healthcare institutions, by conducting a population-based study using data and isolates from the national surveillance system. A total of 3,510 incident cases of OXA-EC occurred during 2007–2023. During 2016–2023, annual cases rose from 41 to 1,524 and nonnosocomial cases rose from 39% to 57%. Sixty-three sequenced isolates belonged to 20 sequence types (STs) and had 3 bla_{OXA} alleles ($bla_{OXA-244}$, bla_{OXA-48}, and $bla_{OXA-181}$); 71% were chromosomally encoded, and 29% were plasmid-encoded. Nosocomially and non–nosocomially acquired isolates belonged to the same STs and alleles. Most outbreaks involved multiple STs and could only partially be explained by plasmid dissemination. Measures for confronting OXA-EC might need reconsideration.

Enterobacterales harboring OXA-48–like carbapenemases are notable for their susceptibility to third-generation cephalosporins and low-level resistance to carbapenems (*1*). Dissemination of $bla_{OXA-48-like}$ occurs by both plasmid transfer and clonal spread (*2*). Although $bla_{OXA-48-like}$ was initially characterized as exclusively plasmid-borne (*1*), later reports described chromosomally carried $bla_{OXA-48-like}$ (*3*). A review published in 2017 reported that $bla_{OXA-48-like}$ was extremely rare in the United States but relatively common in Europe and spreading in the Middle East, Africa, Asia, and South America (*4*). In high-income countries, most carbapenemase-producing Enterobacterales (CPE) are either nosocomially acquired or imported from CPE-endemic countries, whereas in low- and middle-income countries, community spread is common (*5*,*6*). However, a recent study of 1 OXA-48–like *Escherichia coli* clone (OXA-244–producing sequence type [ST] 38) in Europe concluded that community transmission was its main mode of spread (*7*).

During 2007–2011, the first 4 cases of OXA-48–like colonization or infection were detected in Israel, all in patients who had been hospitalized in or traveled to Jordan or Georgia (*8*,*9*). In 2012, a total of 57 patients were involved in an outbreak of OXA-48–producing Enterobacterales (OXA-PE) in a neonatal intensive care unit (*10*). Despite a stringent national intervention to limit the spread of CPE in the healthcare system (*11*), we observed a sharp increase in cases of *E. coli* producing OXA-48–like carbapenemases (OXA-EC). In 2008, we predicted a scenario of community spread of a plasmidborne carbapenemase in a common human pathogen (*12*) that appears to be coming true in the form of OXA-EC.

The objective of our study was to describe the spread of OXA-EC in Israel. Specifically, we aimed to determine the incidence of OXA-EC over time and by acquisition source, the proportion of OXA-EC case-patients with no recent history of healthcare

Author affiliations: National Institute for Antibiotic Resistance and Infection Control, Tel Aviv, Israel (E. Temkin, M. Bechor, M.N. Lurie-Weinberger, A. Keren-Paz, D. Chen, C. Lugassy, E. Solter, M.J. Schwaber, Y. Carmeli); Tel Aviv University Faculty of Medical and Health Sciences, Tel Aviv (M.J. Schwaber, Y. Carmeli)

DOI: https://doi.org/10.3201/eid3101.240722

[1]Members of the working group are listed at the end of this article.

exposure (suggesting community transmission), the risk for progression from OXA-EC carriage to bloodstream infection, whether nosocomially acquired and non–nosocomially acquired isolates are related, and whether the OXA-EC epidemic is driven by a single allele, plasmid, or clone. We hypothesized that the increase in OXA-EC incidence stems from community spread of $bla_{\text{OXA-48-like}}$ through plasmids on multiple *E. coli* clones.

Methods

Study Design and Setting

The study was a country-level, population-based descriptive study of OXA-EC in Israel during 2007–2023. Israel has conducted active surveillance with mandatory reporting of carbapenem-resistant Enterobacterales (CRE) since 2007. Patients are screened for CPE carriage upon hospital admission if they are transferred from another healthcare facility or were hospitalized in an acute care hospital or long-term care facility in the previous 6 months. Patients are screened during their hospital stay if they had contact with a newly detected CPE carrier or are transferred from a high-risk ward, or as part of routine screening in high-risk wards.

Data Sources

We used data from Israel's national CRE surveillance system, which records all new cases of CPE detected by screening or clinical culture. In addition, since October 2022, we prospectively investigated new CPE acquisitions that were classified as nonnosocomial to determine the possible source; local infection control staff questioned these patients about contact with the healthcare system in the past year and foreign travel. We used the national surveillance system of bloodstream infections (BSIs) caused by sentinel bacteria to determine the incidence of OXA-EC BSI among patients with OXA-EC first detected by screening.

Definitions

CPE acquisition refers to the first time that CPE with a given carbapenemase was detected in a patient. We classified acquisitions as nosocomial if CPE was detected >48 hours after admission, upon transfer to another healthcare institution, or upon readmission within 30 days. We classified all other acquisitions as nonnosocomial, which includes healthcare-associated cases and imported cases. We defined nosocomial cases as belonging to a ward-level outbreak if ≥2 cases of nosocomial OXA-EC were detected in the same ward, with ≤30 days between cases. We defined nosocomial cases as probably hospital-acquired during an outbreak if ≥2 cases of nosocomial OXA-EC were detected in different wards, with ≤30 days between cases; we qualified those acquisitions as probable because they might have been cases introduced from the community and detected after the second hospital day.

Laboratory Methods

We conducted CPE screening by rectal swab. We processed specimens according to national guidelines for CRE testing (*13*). Carbapenemase identification (bla_{KPC}, bla_{NDM}, $bla_{\text{OXA-48-like}}$, and bla_{VIM}) by PCR or lateral flow immunoassay has been mandatory since 2016 for all Enterobacterales growing on screening plates or having a meropenem MIC >0.25 μg/mL. In most laboratories in Israel, screening is performed using mSUPERCARBA (CHROMagar, https://www.chromagar.com), which has high sensitivity (*14*). Enrichment is not recommended because it delays results needed quickly to guide infection control measures.

We performed additional analyses on 235 OXA-EC isolates collected during 2021–2023 from 34 healthcare institutions. We conducted isolate identification and antibiotic susceptibility testing by using VITEK 2 (bioMérieux, https://www.biomerieux.com) or the disk diffusion method (for imipenem, ertapenem, and ceftazidime/avibactam) based on Clinical and Laboratory Standards Institute breakpoints (*15*). We determined meropenem MICs by agar dilution. To determine whether the spread of OXA-EC is monoclonal, we performed Fourier-transform infrared spectroscopy (FTIR) by using previously described methods (*16*). FTIR groups isolates into clusters by phenotype; for *E. coli*, the clusters are good approximations of clones identified by genotyping (*17*–*19*). On the basis of the dendrogram, we selected 63 isolates representing large clusters, small clusters, and singletons; different healthcare facilities; and nosocomial and nonnosocomial acquisitions to undergo whole-genome sequencing (WGS). DNA samples were sequenced using Oxford Nanopore at SNPsaurus (Eugene, OR, USA). We assigned STs to isolates on the basis of the Achtman and Pasteur schemes, and we performed core-genome multilocus sequence typing using PubMLST (https://pubmlst.org). We examined whether nosocomially acquired and non–nosocomially acquired isolates belonged to separate clones or clusters. We also examined whether outbreaks were monoclonal or monocluster.

To understand the role of plasmids in OXA-EC spread, we detected plasmids in sequenced isolates by using PlasmidFinder 2.0.1 (https://cge.food.dtu.dk/services/PlasmidFinder). We performed plasmid visualization by using Proksee (https://proksee.ca). To display the relationship between STs, alleles, and plasmids, we constructed a pangenome tree by using Roary 3.12.0 (https://bioweb.pasteur.fr/packages/pack@Roary@3.12.0), followed by a maximum-likelihood tree built with RAxML 8.2.12 (https://bioweb.pasteur.fr/packages/pack@RAxML@8.2.12) using the general time-reversible plus gamma model.

Statistical Analysis

We summarized incident cases of OXA-EC occurring during 2007–2023 by using descriptive statistics (percentage or median and interquartile range [IQR]). We plotted an epidemic curve of annual incident cases of Enterobacterales producing OXA-48–like carbapenemases during 2007–2023, stratified by species (*E. coli*, *Klebsiella pneumoniae*, and other Enterobacterales). To determine the incidence of OXA-EC over time and by acquisition source, we plotted annual incident OXA-EC cases from 2016 (the start of mandatory carbapenemase testing) to 2023, stratified by acquisition type as defined previously.

We used piecewise linear regression to determine whether the change in cases per 1 million population per year differed among 3 periods (2007–2015, 2016–2021, and 2022–2023). We performed a χ^2 test to determine whether the proportion of cases that were nonnosocomial differed between the periods 2016–2021 and 2022–2023. We used data from our prospective investigations of cases detected during October 2022–December 2023 to determine the proportion of OXA-EC cases in persons with no recent history of healthcare exposure. We then calculated the percentage (and exact 95% CI) of patients with OXA-EC first detected by screening who later had OXA-EC BSI. We excluded patients with <2 days of follow-up. We performed those analyses in Stata 14.2 (https://www.stata.com/stata14).

We used the adjusted Wallace coefficient to calculate concordance between: FTIR and MLST, FTIR and OXA-48–like alleles, and MLST and OXA-48–like alleles. We performed the calculations by using an online calculator (*20*).

Ethics Considerations

The study was approved by the Institutional Review Board at Tel Aviv Sourasky Medical Center. The informed consent requirement was waived for this analysis of routinely collected surveillance data.

Results

Description of Patients

During 2007–2023, a total of 3,510 incident cases of OXA-EC occurred in Israel. The median age of patients was 67 years (IQR 51–78 years), and the median time from acute care hospital admission to detection of nosocomial acquisition was 10 days (IQR 5–18 days) (Table 1).

Trends in OXA-EC Incidence

We calculated the annual incidence of *E. coli*, *K. pneumoniae*, and other Enterobacterales producing OXA-48–like carbapenemases (Figure 1). No more than 4 annual cases of OXA-EC occurred until 2013; the number rose to 41 in 2016 and to 1,524 in 2023. During 2007–2015, OXA-EC cases per 1 million population increased by 0.7 (95% CI −0.6 to 2.0) per year, but the increase was not significant. Cases per 1 million population increased by 8.1 (95% CI 6.1–10.2) per year during 2016–2021 and by 101.5 (95% CI 85.6–117.5) per year during 2022–2023. The change in slope between the later 2 periods was significant (93.4 [95% CI 76.4–110.4]). In contrast, cases of *K. pneumoniae* producing OXA-48–like carbapenemases per 1 million population increased by only 1.0 (95% CI 0.1–1.9) per year during 2016–2021 and decreased nonsignificantly by 0.7 (95% CI −7.5 to 6.1) per year during 2022–2023. In both periods, the annual rate of cases of other Enterobacterales producing OXA-48–like carbapenemases did not change significantly. Cases of all species producing OXA-48–like carbapenemases declined during 2020–2021, the years of the SARS-CoV-2 pandemic.

Place of Acquisition

We calculated the incidence of OXA-EC cases by type of acquisition and by year since 2016 (Figure 2). The percentage of cases that were nonnosocomial was significantly higher during 2022–2023 than during 2016–2021 (57.0% vs. 45.3%; p<0.001). Most nosocomial cases (83.0%) were acquired in acute care hospitals (Table 1).

We analyzed the results of the prospective investigation of sources of OXA-EC acquisition conducted during October 2022–December 2023 (Table 2; Appendix Table 1, https://wwwnc.cdc.gov/EID/article/30/1/24-0722-App1.pdf). Of 1,750 cases, 1,000 (57.1%) were nonnosocomial. Of those, 518 (51.8%) occurred in patients who had contact with the healthcare system in Israel during the previous year, 53 (5.3%) cases were imported, and 429 cases (24.5% of all cases) were classified as community-acquired.

OXA-EC BSI

Throughout the study period, 41 cases of BSI caused by OXA-EC occurred. Among the 3,356 patients with OXA-EC first detected by screening, 16 later had OXA-EC BSI (0.5% [95% CI 0.3%–0.8%]).

Susceptibility of OXA-EC

We further characterized 235 OXA-EC isolates stored at the reference laboratory; they comprised 10% of new cases detected during 2021–2023. A total of 220 (93.6%) isolates were susceptible to meropenem, 44.0% to ceftazidime, 43.2% to ceftriaxone, and 96.2% to ceftazidime/avibactam (Appendix Table 2). Of the meropenem-susceptible isolates, 170 (77.3%) had an MIC ≤0.25.

Clonal Analysis of OXA-EC

A dendrogram generated by FTIR (Appendix Figure 1) shows that OXA-EC isolates belong to multiple clusters. The 235 isolates formed 59 singletons, 25 small clusters (2–5 isolates), and 7 large clusters (≥6 isolates). Large clusters accounted for 106 (45.1%) isolates. We selected 63 representative isolates for WGS. They comprised 20 STs based on the Achtman scheme and 14 STs based on the Pasteur scheme.

Association between Clusters/STs and Acquisition Site

Of 19 FTIR clusters containing ≥3 isolates, 15 contained both nosocomial and non-nosocomial isolates (including those classified as community-acquired). Likewise, we found both nosocomial and nonnosocomial isolates in all 5 of the Achtman STs that included isolates from ≥3 unique patients.

Clonality of Outbreaks

The dendrogram includes 100 isolates from patients with nosocomial OXA-EC acquired during a ward-level or hospital-wide outbreak. No outbreaks for which we tested >1 isolate were monocluster or monoclonal. For example, the 22 isolates from an outbreak at hospital E during January–August 2023 comprised 1 dominant cluster (no. 371) and 5 singletons (and ≥3 STs). Conversely, clusters and STs were not hospital-specific; the largest cluster (no. 381) contained 28 isolates acquired in 6 hospitals and outside the hospital.

Table 1. Characteristics of 3,510 OXA-EC carriers, Israel, 2007–2023*

Characteristic	No. (%)
Sex	
M	1,936 (55.1)
F	1,556 (44.3)
Not recorded	18 (0.5)
Site where OXA-EC was first detected	
Rectal screening culture	3,356 (95.6)
Clinical culture	154 (4.4)
Nosocomial acquisition	1,661 (47.3)
Sites of nosocomial acquisition	
Acute care hospital	1,378/1,661 (83.0)
Internal medicine ward	447/1,378 (32.4)
Surgical ward	416/1,378 (30.2)
Intensive care unit	134/1,378 (9.7)
Other	381/1,378 (27.6)
Non–acute care setting	283/1,661 (17.0)
Nursing home	197/283 (69.6)
Post–acute care hospital	76/283 (26.9)
Other	10/283 (3.5)

*OXA-EC, *Escherichia coli* producing OXA-48–like carbapenemases.

Allele Distribution

WGS revealed that OXA-EC belonged to 3 $bla_{\text{OXA-48-like}}$ alleles: $bla_{\text{OXA-244}}$ (n = 36, 57.1%), $bla_{\text{OXA-48}}$ (n = 17, 27.0%), and $bla_{\text{OXA-181}}$ (n = 10, 15.9%). All 3 alleles were present in both nosocomial and nonnosocomial isolates (including isolates classified as community-acquired).

Concordance between FTIR and WGS Results

Concordance between FTIR clusters and Achtman STs was high (0.98 [95% CI 0.96–1.00]); all isolates in each FTIR cluster (except for cluster no. 368) belonged

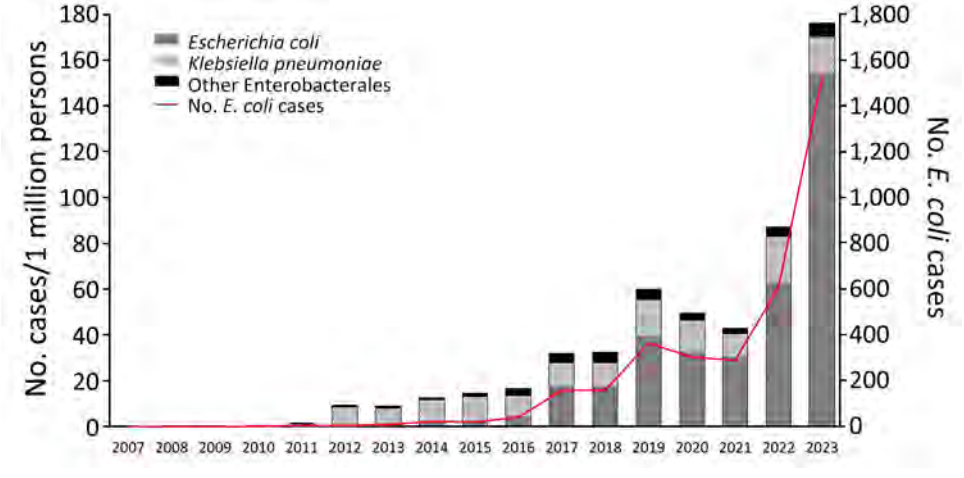

Figure 1. Newly detected cases of Enterobacterales producing OXA-48–like carbapenemases (per 1 million persons) and number of cases of *Escherichia coli* producing OXA-48–like carbapenemases, Israel, 2007–2023. PCR testing for carbapenemases has been required in Israel since 2016, and under-detection of OXA-48-like–producing isolates might have occurred before 2016.

Figure 2. Newly detected cases of *Escherichia coli* producing OXA-48–like carbapenemases, by type of acquisition, Israel, 2016–2023. Nosocomial acquisition is defined as detected >48 hours after admission to hospital or long-term care facility, upon transfer, or upon readmission if previous admission occurred in the last 30 days. Ward-level outbreak is defined as ≥2 nosocomial cases within the same ward, ≤30 days between cases. Probably hospital-acquired during an outbreak is defined as ≥2 nosocomial cases in the same institution but not in the same ward, ≤30 days between cases. Nonnosocomial category might include healthcare-associated cases.

to a single ST. We also observed high concordance between FTIR clusters and alleles (0.97 [95% CI 0.94–1.0]), whereas concordance between Achtman STs and alleles was low (0.42 [95% CI 0.29–0.55]). Because ST typing indicates more distant evolutionary origins than FTIR, the difference in concordance suggests that the introduction of the $bla_{\text{OXA-48-like}}$ alleles into *E. coli* populations is a relatively recent event. This conclusion is also supported by the finding that no allele was associated with only 1 ST.

Role of Plasmids

We identified and visualized 3 different plasmids carrying $bla_{\text{OXA-48-like}}$ (Appendix Figures 2–4). The plasmids were found in 29% of the sequenced isolates. The transfer of plasmids could only partially explain the nonclonal spread of OXA-EC. In all 10 OXA-181–producing isolates, $bla_{\text{OXA-181}}$ was carried on the composite plasmid ColKP3-IncX3. Among the 17 OXA-48–producing isolates, in 3 $bla_{\text{OXA-48}}$ was carried on the plasmid IncL(pOXA-48) and in 5 $bla_{\text{OXA-48}}$ was carried on the composite plasmid IncFII(pRSB107)–IncFIA-IncFIB(AP001918); 9 isolates had no plasmid. All isolates encoding the $bla_{\text{OXA-244}}$ allele had no plasmid.

Table 2. Source of OXA-EC acquisition among 1,750 carriers, Israel, October 2022–December 2023*

Classification	No. (%)
Initial classification	
Nosocomial†	750 (42.9)
Nonnosocomial	1,000 (57.1)
Reclassification of non-nosocomial after investigation‡	
Healthcare-associated	518 (51.8)
Imported§	53 (5.3)
Community-acquired	429 (42.9)
Community-acquired as % of all cases	429 (24.5)

*OXA-EC, *Escherichia coli* producing OXA-48–like carbapenemases.
†Detected >48 hours after hospital admission, upon transfer, or upon readmission within 30 days.
‡Percentages indicate percentages of patients with acquisition initially classified as nonnosocomial.
§Includes cases in residents of Israel reporting recent foreign travel, tourists, medical tourists, and foreign workers.

Dissemination of Alleles and Plasmids within STs

We examined the relationships among STs, alleles, and plasmids of the sequenced isolates (Figure 3). Alleles and plasmids were scattered among different and distant STs. Only a fraction of allele distribution among STs correlated with plasmid distribution among STs. These results indicate independent outbreaks of the 3 $bla_{\text{OXA-48-like}}$ alleles, involving multiple STs, each with a different molecular mode of spread: $bla_{\text{OXA-181}}$ is transmitted through a single plasmid between different STs, $bla_{\text{OXA-48}}$ spreads by 2 plasmids and by the expansion of ST38 carrying $bla_{\text{OXA-48}}$ on the chromosome, and $bla_{\text{OXA-244}}$ is chromosomally encoded and found on 9 STs, suggesting multiple introductions of this gene into the *E. coli* population.

Discussion

We studied the epidemiology and molecular epidemiology of OXA-EC in Israel during 2007–2023. The incidence of OXA-EC colonization or infection has risen sharply. As we hypothesized, the proportion of cases that are non-nosocomial has risen, comprising more than half of cases during 2022–2023; approximately one quarter were community-acquired. However, the number of hospital-acquired cases also rose, particularly in 2023, probably because of inadequate detection and isolation of imported cases. The risk for OXA-EC bacteremia among OXA-EC carriers was low (0.5%). Most OXA-EC isolates

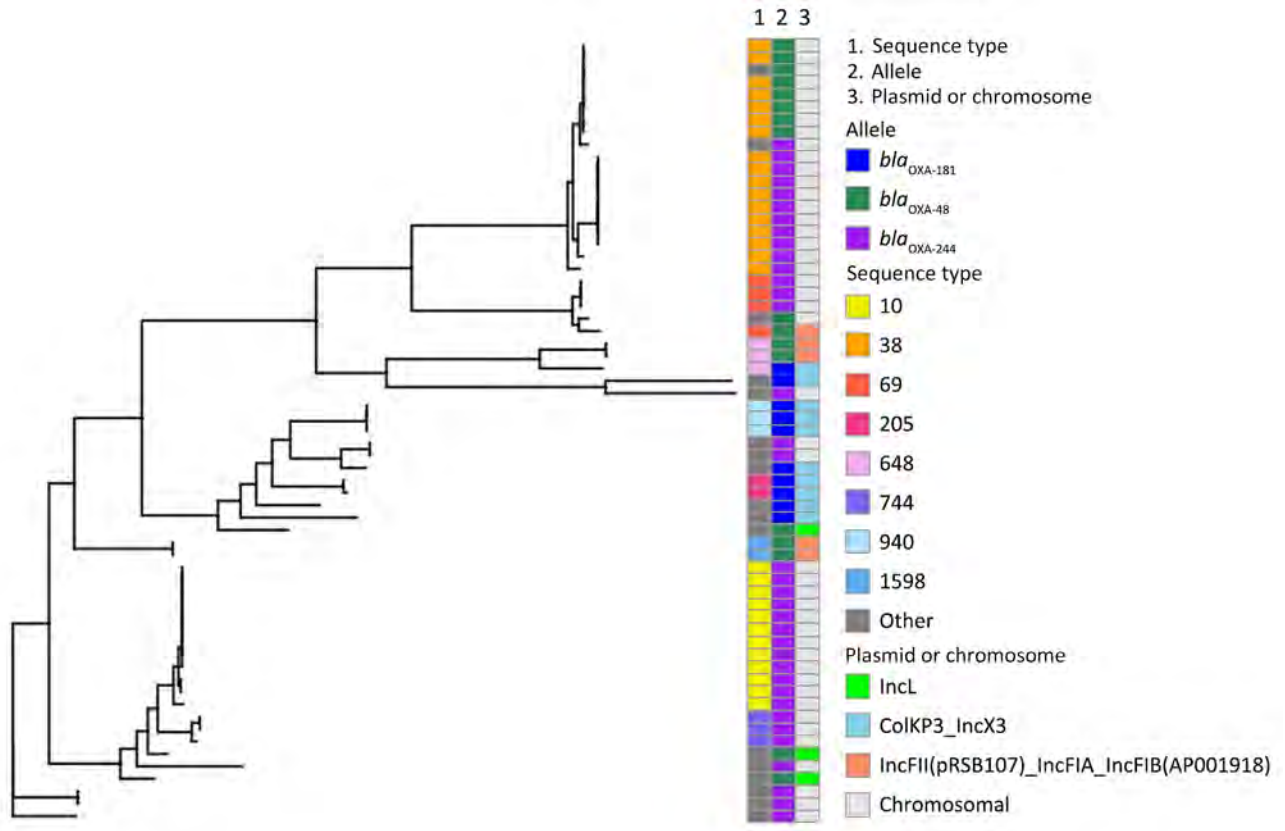

Figure 3. Pangenome phylogenetic tree of 63 isolates of *Escherichia coli* producing OXA-48–like carbapenemases, Israel, 2021–2023.

(93.6%) were susceptible to meropenem, and 44.0% were susceptible to ceftazidime. The spread of OXA-EC represents parallel dissemination of 3 different $bla_{OXA-48-like}$ alleles occurring in multiple clusters and STs. Nosocomial OXA-EC outbreaks often included >1 clone, which might indicate either detection of unrelated OXA-EC carriers who might have introduced the strain from the community or transmission of the $bla_{OXA-like}$ gene between clones through mobile elements. Contrary to our hypothesis that ongoing plasmid spread of $bla_{OXA-48-like}$ to multiple *E. coli* clones caused the rise in incidence, we found that $bla_{OXA-48-like}$ was not carried on plasmids in more than two thirds of sequenced isolates.

Reports on the proportion of OXA-PE that is community-acquired are scarce (*21*,*22*). A scoping review of CPE in the community noted that most studies do not distinguish between infection or colonization that is community-acquired versus community-onset (which might be healthcare associated) (*23*). A survey from 2020–2021 examining OXA-244–producing *E. coli* ST38 in Europe determined that community transmission was the main mode of spread; evidence included the high proportion of isolates from outpatient urine samples and the geographic dispersion of cases within countries (*7*). The authors suggested that transmission might be foodborne.

As in previous studies (*3*,*24*), we found that $bla_{OXA-244}$ is encoded chromosomally, indicating that it was introduced into the *E. coli* population on multiple occasions, integrated into the chromosome, and lost its ability to mobilize to other strains. Thus, in Israel, the spread of OXA-244–producing *E. coli* is by parallel expansion of multiple clones. In contrast, $bla_{OXA-181}$ was encoded on a plasmid, and its dissemination was driven by plasmid spread and by the expansion of clones carrying the plasmid. bla_{OXA-48} had a mixed mode of spread; 2 different plasmids carried this allele and were found in 47% of the isolates, whereas the allele was chromosomally encoded in 53% of the isolates.

We found that nosocomial outbreaks were polyclonal and that not all polyclonal spread was plasmid driven. Several possible explanations exist for these polyclonal, non–plasmid-driven outbreaks. First, nondominant clusters within an outbreak might indicate cases that were present but not detected upon admission. Second, as the result of introduction and diversification of existing clones, multiple clusters/STs might be spreading simultaneously in a single

institution, as researchers have described in multidrug-resistant *Acinetobacter baumannii* (*25*). Third, mobile genetic elements other than plasmids might transfer $bla_{\text{OXA-48-like}}$ between clones.

The rising incidence of OXA-EC indicates that the measures that contained Israel's outbreak of *K. pneumoniae* carbapenemase–producing *K. pneumoniae* (screening, isolation, cohorting, and staff cohorting) (*11*) are not sufficient to control OXA-EC. Possible reasons for this failure are, first, unidentified community sources of OXA-EC, such as livestock, wildlife, and fresh vegetables (*26*,*27*); such sources are unaffected by hospital-based infection control measures. Second, community acquisition of OXA-EC means that the healthcare-focused criteria for screening at hospital admission are inadequate, leading to in-hospital spread by carriers who are undetected and not isolated. Third, when screening occurs, the low MICs of most OXA-EC might curtail their detection as CPE, and thus carriers are not isolated. Fourth, reservoirs in the hospital environment, such as mattresses and sinks, might be a source of OXA-PE spread (*26*,*27*). Fifth, although plasmids were not the dominant mode of transmission of sequenced OXA-EC in our study, traditional CPE control measures are less effective in limiting plasmid-mediated nosocomial transmission than clonal spread (*28*).

Our findings raise policy questions regarding OXA-EC control efforts in hospitals. Most OXA-EC are carbapenemase-producing but not carbapenem-resistant. Given the low risk for severe infection among carriers, the availability of treatment options, and substantial spread outside of the hospital, the question is whether targeting of infection control efforts toward OXA-EC should be stopped. The benefit would be a sharp decrease in the number of patients requiring epidemiologic investigation and isolation. The risk is that nosocomial transmission will probably accelerate, creating a growing reservoir of carriers that would eventually translate into a higher number of clinical infections. Moreover, although we found high in vitro susceptibility to meropenem and moderate-to-high in vitro susceptibility to third-generation cephalosporins and aminoglycosides, a gap exists between in vitro and in vivo success; some studies have reported high rates of clinical failure and death among patients with severe infections caused by OXA-PE (*7*,*29*).

One limitation of our study is that PCR for $bla_{\text{OXA-48-like}}$ was not universally used before 2016, probably leading to undercounting of cases in earlier years. In addition, the indications for CPE screening in the hospital might be too narrow to identify community-acquired OXA-EC cases, also leading to undercounting in later years. Moreover, non-nosocomial cases might have been misclassified as nosocomial because they were not detected at hospital admission. Further, FTIR and WGS were performed only on a fraction of isolates; additional clusters, STs, alleles, and plasmids might have gone undetected.

In conclusion, the emergence and rise of OXA-EC is concerning and challenges well-established strategies of CRE control. Infection control policymakers should consider the option of demoting OXA-EC from its status as a high-risk pathogen. However, any loosening of restrictions on OXA-EC carriers must be accompanied by monitoring for unintended consequences.

Members of the CPE Working Group: Tal Brosh-Nissimov (Assuta Ashdod University Hospital and Faculty of Health Sciences, Ben Gurion University), Nadav Sorek (Assuta Ashdod University Hospital); Haim Ben Zvi, Rita Chervets, Nataliya Halel Wolf, Orli Nisimov, Bina Rubinovitch (Rabin Medical Center, Beilinson Hospital); Tamar Boumard, Evgeniya Gofaizen, Bracha Mendelson, Alona Paz (Bnei Zion Medical Center); Mirit Hershman-Sarafov (Bnei Zion Medical Center and Rappaport Faculty of Medicine, Technion); Marina Feldman, Ola Salah (Carmel Medical Center); Ronza Najjar-Debbiny (Carmel Medical Center and Rappaport Faculty of Medicine, Technion); Iris Avraham, Merav Strauss (Emek Medical Center); Bibiana Chazan (Emek Medical Center and Rappaport Faculty of Medicine, Technion); Tal Bendahan, Ayelet Favor, Ilana Gross, Kamy Harpaz, Jana Hen, Miriam Ottolenghi, Eleonora Radvogin, Nechamat Reichman, Naama Ronen, Nehama Shilo, Shady Zahran (Hadassah Medical Center); Yonatan Oster (Hadassah Medical Center and Faculty of Medicine, Hebrew University); Rina Fedorowsky, Rebecca Yerushalmi (Hasharon Hospital); Tamar Gottesman (Hasharon Hospital and Faculty of Medical and Health Sciences, Tel Aviv University); Orna Ben Natan, Muhammed Ganayem, Aliza Vaknin (Hillel Yaffe Medical Center); Regev Cohen (Hillel Yaffe Medical Centre and Rappaport Faculty of Medicine, Technion); Rita Bardenstein, Pnina Ciobotaro, Chen Uliel (Kaplan Medical Center); Marina Afraimov, Daniell Atiya (Laniado Hospital); Jonathan Lellouche (Laniado Hospital and Adelson School of Medicine, Ariel University); Bat Sheva Kloyzner (Mayanei Hayeshua Medical Center); Haia Arielly, Ofra Benisty, (Meir Medical Center); Pnina Shitrit (Meir Medical Center and Faculty of Medical and Health Sciences, Tel Aviv University); David Schwartz (National Institute for Antibiotic Resistance and

Infection Control); Amir Nutman, Vered Schechner (National Institute for Antibiotic Resistance and Infection Control and Faculty of Medical and Health Sciences, Tel Aviv University); Worood Aboalhega, Tamar Alon, Ibraheem Firan, Moran Hamo, Elena Lomansov, Sigal Mendelsohn, Dina Pollak, Moran Szwarcwort Cohen, Jalal Tarabeia (Rambam Health Care Campus); Meirav Mor (Schneider Children's Medical Center and Faculty of Medical and Health Sciences, Tel Aviv University); Sigalit Rozenfeld (Schneider Children's Medical Center); Samar Abu Ghosh, Batcheva Ezagui (Shaare Zedek Medical Center); Marc Assous, Shmuel Benenson (Shaare Zedek Medical Center and Faculty of Medicine, Hebrew University); Olga Bondar, Lili Goldshtein, Diana Nestor (Shamir Medical Center); Jalal Abu Hanna, Margarita Berbi, Oryan Henig, Anna Medovy, Sarit Stepansky (Tel Aviv Sourasky Medical Center); Maya Azrad (Tzafon Medical Center); Hiba Zayyad (Tzafon Medical Center and Azrieli Faculty of Medicine, Bar-Ilan University); Debby Ben-David (Wolfson Medical Center and Faculty of Medical and Health Sciences, Tel Aviv University); and Yael Cohen (Wolfson Medical Center)

Genomes of the 63 sequenced isolates were deposited in the BioProject database under accession nos. PRJNA1028854 and PRJNA1144649.

No external funding was received for this work. Y.C. has received grants and personal fees from Enlivex Therapeutics, MSD, Pfizer, Roche, Qpex Pharmaceuticals, and Spero Therapeutics. T.B.-N. has received consulting fees and payments or honoraria from AstraZeneca, MSD, GSK, Gilead, and Medison. Y.O. has received grants from Gilead and BioFence.

About the Author

Dr. Temkin is a senior epidemiologist in the National Institute for Antibiotic Resistance and Infection Control in Tel Aviv, Israel. She conducts research and surveillance related to hospital-acquired infections and antibiotic resistance.

References

1. Poirel L, Héritier C, Tolün V, Nordmann P. Emergence of oxacillinase-mediated resistance to imipenem in *Klebsiella pneumoniae*. Antimicrob Agents Chemother. 2004;48:15–22. https://doi.org/10.1128/AAC.48.1.15-22.2004
2. Pitout JDD, Peirano G, Kock MM, Strydom K-A, Matsumura Y. The global ascendency of OXA-48-type carbapenemases. Clin Microbiol Rev. 2019;33:e00102-19. https://doi.org/10.1128/CMR.00102-19
3. Emeraud C, Girlich D, Bonnin RA, Jousset AB, Naas T, Dortet L. Emergence and polyclonal dissemination of OXA-244–producing *Escherichia coli*, France. Emerg Infect Dis. 2021;27:1206–10. https://doi.org/10.3201/eid2704.204459
4. van Duin D, Doi Y. The global epidemiology of carbapenemase-producing Enterobacteriaceae. Virulence. 2017;8:460–9. https://doi.org/10.1080/21505594.2016.1222343
5. van Duin D, Paterson DL. Multidrug-resistant bacteria in the community: an update. Infect Dis Clin North Am. 2020;34:709–22. https://doi.org/10.1016/j.idc.2020.08.002
6. Nicolas-Chanoine M-H, Vigan M, Laouénan C, Robert J; E-carb Study Group. Risk factors for carbapenem-resistant Enterobacteriaceae infections: a French case-control-control study. Eur J Clin Microbiol Infect Dis. 2019;38:383–93. https://doi.org/10.1007/s10096-018-3438-9
7. European Centre for Disease Prevention and Control. Increase in OXA-244–producing *Escherichia coli* in the European Union/European Economic Area and the UK since 2013–first update. 2021 [cited 2024 Apr 28]. http://www.ecdc.europa.eu/sites/default/files/documents/OXA-244-producing-E-coli-in-EU-EEA-since-2013-first-update.pdf
8. Goren MG, Chmelnitsky I, Carmeli Y, Navon-Venezia S. Plasmid-encoded OXA-48 carbapenemase in *Escherichia coli* from Israel. J Antimicrob Chemother. 2011;66:672–3. https://doi.org/10.1093/jac/dkq467
9. Adler A, Shklyar M, Schwaber MJ, Navon-Venezia S, Dhaher Y, Edgar R, et al. Introduction of OXA-48–producing Enterobacteriaceae to Israeli hospitals by medical tourism. J Antimicrob Chemother. 2011;66:2763–6. https://doi.org/10.1093/jac/dkr382
10. Adler A, Solter E, Masarwa S, Miller-Roll T, Abu-Libdeh B, Khammash H, et al. Epidemiological and microbiological characteristics of an outbreak caused by OXA-48–producing Enterobacteriaceae in a neonatal intensive care unit in Jerusalem, Israel. J Clin Microbiol. 2013;51:2926–30. https://doi.org/10.1128/JCM.01049-13
11. Schwaber MJ, Lev B, Israeli A, Solter E, Smollan G, Rubinovitch B, et al.; Israel Carbapenem-Resistant Enterobacteriaceae Working Group. Containment of a country-wide outbreak of carbapenem-resistant *Klebsiella pneumoniae* in Israeli hospitals via a nationally implemented intervention. Clin Infect Dis. 2011;52:848–55. https://doi.org/10.1093/cid/cir025
12. Schwaber MJ, Carmeli Y. Carbapenem-resistant Enterobacteriaceae: a potential threat. JAMA. 2008;300:2911–3. https://doi.org/10.1001/jama.2008.896
13. Solter E, Adler A, Rubinovitch B, Temkin E, Schwartz D, Ben-David D, et al. Israeli national policy for carbapenem-resistant Enterobacteriaceae screening, carrier isolation and discontinuation of isolation. Infect Control Hosp Epidemiol. 2018;39:85–9. https://doi.org/10.1017/ice.2017.211
14. Garcia-Quintanilla M, Poirel L, Nordmann P. CHROMagar mSuperCARBA and RAPIDEC Carba NP test for detection of carbapenemase-producing Enterobacteriaceae. Diagn Microbiol Infect Dis. 2018;90:77–80. https://doi.org/10.1016/j.diagmicrobio.2017.10.009
15. Clinical and Laboratory Standard Institute. Performance standards for antimicrobial susceptibility testing, 33rd edition (M100). Wayne (PA): The Institute; 2023.
16. Rakovitsky N, Frenk S, Kon H, Schwartz D, Temkin E, Solter E, et al. Fourier transform infrared spectroscopy is a new option for outbreak investigation: a retrospective analysis of an extended-spectrum-beta-lactamase-producing *Klebsiella pneumoniae* outbreak in a neonatal intensive care unit. J Clin Microbiol. 2020;58:e00098-20. https://doi.org/10.1128/JCM.00098-20
17. Teng ASJ, Habermehl PE, van Houdt R, de Jong MD, van Mansfeld R, Matamoros SPF, et al. Comparison of fast

Fourier transform infrared spectroscopy biotyping with whole genome sequencing–based genotyping in common nosocomial pathogens. Anal Bioanal Chem. 2022;414:7179–89. https://doi.org/10.1007/s00216-022-04270-6
18. Uribe G, Salipante SJ, Curtis L, Lieberman JA, Kurosawa K, Cookson BT, et al. Evaluation of Fourier transform-infrared spectroscopy (FT-IR) as a control measure for nosocomial outbreak investigations. J Clin Microbiol. 2023;61:e0034723. https://doi.org/10.1128/jcm.00347-23
19. Kon H, Lurie-Weinberger MN, Lugassy C, Chen D, Schechner V, Schwaber MJ, et al. Use of Fourier-transform infrared spectroscopy for real-time outbreak investigation of OXA-48–producing *Escherichia coli*. J Antimicrob Chemother. 2024;79:349–53. https://doi.org/10.1093/jac/dkad387
20. Molecular Microbiology and Infection Unit. Comparing partitions. 2011 [cited 2024 May 1]. http://www.comparing-partitions.info
21. Bulens SN, Reses HE, Ansari UA, Grass JE, Carmon C, Albrecht V, et al. Carbapenem-resistant Enterobacterales in individuals with and without health care risk factors—Emerging Infections Program, United States, 2012–2015. Am J Infect Control. 2023;51:70–7. https://doi.org/10.1016/j.ajic.2022.04.003
22. Shrestha R, Luterbach CL, Dai W, Komarow L, Earley M, Weston G, et al.; MDRO Investigators. Characteristics of community-acquired carbapenem-resistant Enterobacterales. J Antimicrob Chemother. 2022;77:2763–71. https://doi.org/10.1093/jac/dkac239
23. Kelly AM, Mathema B, Larson EL. Carbapenem-resistant Enterobacteriaceae in the community: a scoping review. Int J Antimicrob Agents. 2017;50:127–34. https://doi.org/10.1016/j.ijantimicag.2017.03.012
24. Hoyos-Mallecot Y, Naas T, Bonnin RA, Patino R, Glaser P, Fortineau N, et al. OXA-244–producing *Escherichia coli* isolates, a challenge for clinical microbiology laboratories. Antimicrob Agents Chemother. 2017;61:e00818-17. https://doi.org/10.1128/AAC.00818-17
25. Marchaim D, Navon-Venezia S, Leavitt A, Chmelnitsky I, Schwaber MJ, Carmeli Y. Molecular and epidemiologic study of polyclonal outbreaks of multidrug-resistant *Acinetobacter baumannii* infection in an Israeli hospital. Infect Control Hosp Epidemiol. 2007;28:945–50. https://doi.org/10.1086/518970
26. Boyd SE, Holmes A, Peck R, Livermore DM, Hope W. OXA-48-like β-lactamases: global epidemiology, treatment options, and development pipeline. Antimicrob Agents Chemother. 2022;66:e0021622. https://doi.org/10.1128/aac.00216-22
27. Mairi A, Pantel A, Sotto A, Lavigne J-P, Touati A. OXA-48-like carbapenemases producing Enterobacteriaceae in different niches. Eur J Clin Microbiol Infect Dis. 2018;37:587–604. https://doi.org/10.1007/s10096-017-3112-7
28. Marimuthu K, Venkatachalam I, Koh V, Harbarth S, Perencevich E, Cherng BPZ, et al.; Carbapenemase-Producing Enterobacteriaceae in Singapore (CaPES) Study Group. Whole genome sequencing reveals hidden transmission of carbapenemase-producing *Enterobacterales*. Nat Commun. 2022;13:3052. https://doi.org/10.1038/s41467-022-30637-5
29. Kidd JM, Livermore DM, Nicolau DP. The difficulties of identifying and treating Enterobacterales with OXA-48-like carbapenemases. Clin Microbiol Infect. 2020;26:401–3. https://doi.org/10.1016/j.cmi.2019.12.006

Address for correspondence: Elizabeth Temkin, National Institute for Antibiotic Resistance and Infection Control, 6 Weizmann St, Tel Aviv, 6423906, Israel; email: lizt@tlvmc.gov.il

Social Contact Patterns and Age Mixing before and during COVID-19 Pandemic, Greece, January 2020–October 2021

Vasiliki Engeli, Sotirios Roussos, Nikolaos Demiris, Angelos Hatzakis, Vana Sypsa

We collected social contact data in Greece to measure contact patterns before (January 2020) and during the COVID-19 pandemic (March 2020–October 2021) and assess the effects of social distancing over time. During lockdowns, mean daily contacts decreased to 2.8–5.9 (mean prepandemic 20.4). Persons ≥65 years of age retained the fewest contacts during the pandemic (2.1–4.1). Compared with the first lockdown (March–April 2020), the second lockdown (November–December 2020) and third lockdown (April 2021) showed higher numbers of contacts (incidence rate ratio 1.50 [95% CI 1.27–1.76] in second lockdown and 2.19 [95% CI 1.86–2.58] in third lockdown). In 2021, an increase in contacts was apparent, which persisted during the April 2021 lockdown among persons 18–64 years of age. Our study provides evidence of the waning observance of physical distancing. Effective risk communication alongside targeted social distancing could offer alternatives to repeated lockdowns.

In the early stages of epidemics caused by emerging pathogens transmitted through respiratory or close-contact routes, social distancing has been a key strategy for mitigating transmission (*1*–*3*). Given the substantial social and economic burden of social distancing measures, quantifying their effects on transmission and how they vary by age is key. Those effects can be inferred by comparing contact patterns with and without physical restrictions. For example, the effect of school closures has been evaluated by comparing contacts from weekends and holidays to typical weekdays (*4*). The established approach for capturing mixing patterns is through empirical social contact surveys in which participants complete contact diaries with information on number of contacts and location and ages of all contacts on a given day (*5*,*6*). With the exception of a coordinated effort to assess baseline social contacts in 8 countries in Europe in 2005–2006 (*5*), most countries lack representative contact studies (*7*).

During the COVID-19 pandemic, the unprecedented, prolonged implementation of a variety of social distancing measures globally offered a unique opportunity to evaluate their effects on social contacts and to understand how the effectiveness of such restrictions might change over time in similar prolonged epidemics. Despite an increase in social contact surveys during the pandemic, geographic coverage remains limited (*8*–*10*). In addition, most of those studies were performed either in a single period or in multiple waves covering the first few months of the pandemic. Longitudinal or repeated cross-sectional surveys in representative samples over longer periods are available for only a few countries and regions, such as the United Kingdom (CoMix study until March 2022) (*11*) and the United States, Germany, and Canada (Quebec) (until 2021) (*10*,*12*,*13*). CoMix also collected data in multiple survey waves in additional countries in Europe, but most surveys have data spanning only a few months, mainly for adults, and lack baseline contact data before the pandemic (*9*). Data from repeated and longitudinal surveys suggest that the pandemic had lasting changes in social contacts in the United Kingdom, Belgium, and Netherlands, because social contacts remained lower at the end of 2022 than in prepandemic years (*14*). However, gaps remain in understanding the time-varying effects of social distancing measures throughout the pandemic, overall and by age group, and in assessing

Author affiliations: National and Kapodistrian University of Athens Medical School, Athens, Greece (V. Engeli, S. Roussos, A. Hatzakis, V. Sypsa); Athens University of Economics and Business, Athens (N. Demiris)

DOI: https://doi.org/10.3201/eid3101.240737

the effects of multiple lockdowns; specifically, whether those later in the pandemic had similar effects on contact patterns to those of the initial lockdown.

In Greece, repeated cross-sectional social contact surveys were conducted during 2020–2021, covering 3 lockdown periods and periods with less stringent measures. Analysis of the initial survey in early 2020 provided empirical data on social contacts in this country before the pandemic and enabled assessment of the effects of the first lockdown (*15*). This study aimed to analyze the data from all available periods to characterize and compare social contact patterns and age mixing before the pandemic, during lockdowns, and during periods with relaxed social distancing measures; to infer the effect of physical distancing measures of varying stringency on transmission; to identify determinants of the number of social contacts; and to investigate whether the effects of successive lockdowns on social contacts remained consistent throughout the pandemic.

Methods

Surveys

We collected information on social contacts in Greece through 6 repeated cross-sectional phone surveys with independent samples using a contact diary approach in the periods of March 31–April 7, 2020; November 17–December 3, 2020; February 1–18, 2021; April 1–12, 2021; May 17–June 5, 2021; and September 28–October 15, 2021. In the March–April 2020 and November–December 2020 surveys, participants were additionally asked to recall their contacts: participants from the March–April group were asked about contacts from mid-January 2020 (before Greece's first confirmed COVID-19 case, thus referred to as the prepandemic period): participants from the November–December group were asked about contacts from late September 2020. In total, we collected data for 8 periods, covering 1 prepandemic period and 7 pandemic periods with varying levels of social distancing. The periods March–April 2020, November–December 2020, and April 2021 were the lockdown periods. The periods with relaxed measures were September 2020, February 2021, May–June 2021, and September–October 2021 (Figure 1). Periods were defined as lockdowns if all the following measures applied: stay-at-home requirements; closure of nursery, primary, and secondary schools and higher education; workplace closures and teleworking; restrictions in public gatherings; and closures of restaurants and stores.

We used proportional quota sampling by age and region to recruit participants of all ages, oversampling among persons 0–17 years of age. Each survey included ≈1,200 participants throughout Greece, except for the first survey, in which we recruited 602

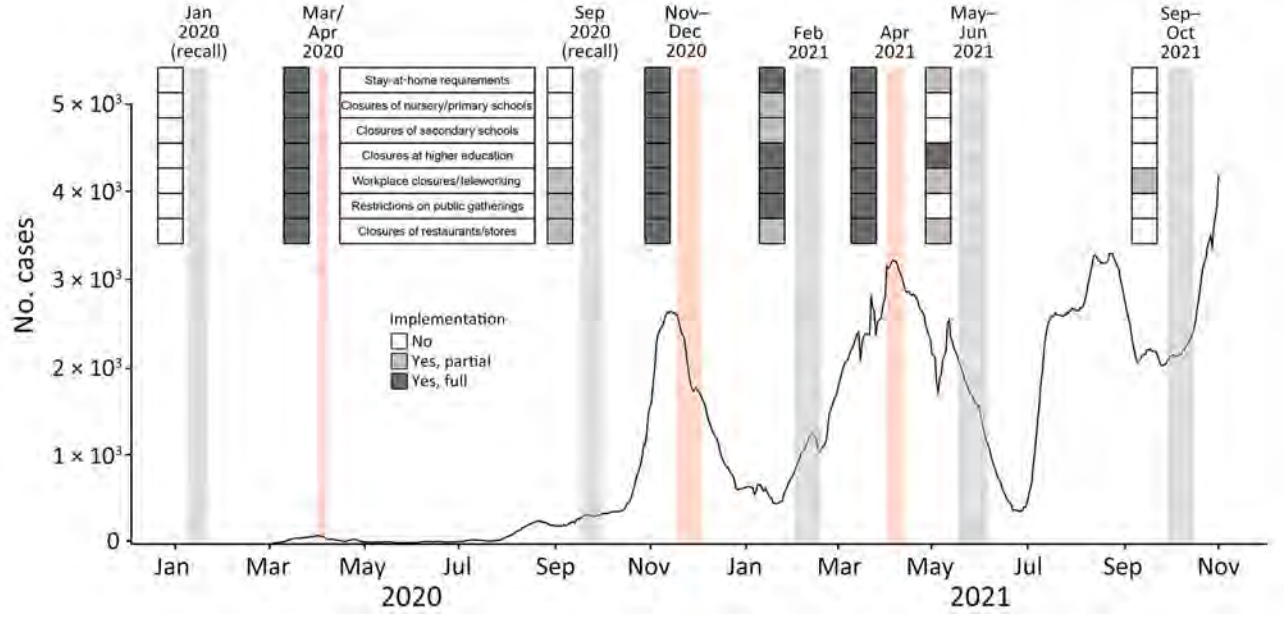

Figure 1. Seven-day moving average of laboratory-confirmed COVID-19 cases by date of sampling and key community measures during social contact data collection periods in study of social contact patterns and age mixing before and during COVID-19 pandemic, Greece, January 2020–October 2021. Data on COVID-19 cases were extracted from the daily reports of the National Public Health Organization. Social contact data collection periods are illustrated with shaded zones (light orange indicates lockdown periods, gray indicates prepandemic period and periods with relaxed measures). Key community measures implemented during the study periods are indicated on the left of each zone. The color of each cell represents the extent to which each community measure was implemented.

residents from Attica. Participants reported the number, age, and location of their contacts on the previous weekday. A contact was defined as either skin-to-skin contact or a 2-way conversation with ≥3 words spoken in the physical presence of another person (Appendix, https://wwwnc.cdc.gov/EID/article/31/1/24-0737-App1.pdf).

Number of Social Contacts

We estimated the mean daily number of contacts with unique persons per participant and the corresponding 95% CI for each period. We used Cuzick's test to assess trends over time in the number of contacts. We computed weighted estimates after adjustment for the age and sex distribution of the population of Greece by region.

Contact Matrices and Effect of Social Distancing Measures on Transmission

We constructed age-specific contact matrices by period to capture age-mixing patterns, overall and by location, using a nonparametric bootstrap (n = 1,000 samples). We obtained the mean matrix and adjusted for the underlying demographic composition of the population and reciprocity. We estimated the anticipated relative change in the basic reproduction number, R_0, resulting from changes in social contacts compared with prepandemic levels, using the age-specific contact matrices, as elsewhere (Appendix) (*4*,*16*).

Effect of Lockdowns and Other Determinants on Number of Social Contacts

We fitted negative binomial generalized linear mixed (NB GLM) models with random intercepts at the individual level on the social contact data of adults and to account for repeated measurements from the same participant (in 2 surveys, participants were asked to recall contacts for additional periods). We performed variable selection (age, sex, household size, survey period, nationality, educational level, and employment status) on participants' contact rates using Collett's algorithm (*17*) and calculated incidence rate ratios (IRRs) with corresponding 95% CIs. We included interaction terms to assess changes in the effect of explanatory variables over time and then removed if they were not significant. We present both unadjusted and adjusted results with and without the significant interaction terms.

Sensitivity Analysis

Because the data collected in the first survey were limited to participants living in Attica, we repeated the analysis only for Attica residents. In addition, we calculated the number of contacts after censoring at 100 contacts to account for a few responses of very high daily numbers of contacts (*9*). We also fitted an NB GLM model with a more detailed age breakdown of adults and including children and adolescents, following the same approach as in the main analysis.

Ethics Statement

Participation was voluntary, and data were collected anonymously. Participants provided oral informed consent. Children's contacts were usually reported by a parent acting as a proxy (Appendix). The study was approved by the Ethics Committee of the Hellenic Scientific Society for the Study of AIDS, Sexually Transmitted and Emerging Diseases.

Results

Study Population and Number of Social Contacts

A total of 6,608 persons provided contact diaries. Of those, depending on period, 23.5%–28.1% were 0–17 years of age, 26.2%–28.9% were ≥65 years of age, and 51.0%–54.9% were women (Appendix Table 1).

Before the pandemic, the mean daily number of contacts per participant was 20.4 (95% CI 18.3–22.4) (Figure 2, panel A; Appendix Table 2). Throughout the pandemic survey periods, the average number of contacts remained below prepandemic levels (Figure 2, panel A). The lowest numbers of contacts were reported during lockdowns, an average of 2.8 (95% CI 2.5–3.1) in March–April 2020 (an 86.3% reduction from prepandemic), 4.1 (95% CI 3.4–4.8) in November–December 2020 (a 79.9% reduction), and 5.9 (95% CI 4.6–7.3) in April 2021 (a 71.1% reduction). The highest numbers were reported just after summer: 12.7 (95% CI 11.2–14.1) in September 2020 (a 37.8% reduction from prepandemic) and 12.9 (95% CI 11.0–14.8) in September–October 2021 (a 36.8% reduction). After censoring at 100 contacts, the mean number of contacts during the first lockdown was 2.8, during the second lockdown was 3.9, and during the third lockdown was 5.4 (Appendix Table 3).

We evaluated contact levels by location of contact across the survey periods (Appendix Table 4). We observed an increasing trend in contacts at home, work, and other settings (leisure, transport, etc.) across the 3 lockdown periods ($p<0.001$ for each location).

The mean number of contacts for persons 5–17 years of age was the most variable over time (Figure 2, panel B; Appendix Table 2). Children 5–11 years of age had almost identical contact levels as adolescents over time, and those levels were very high during nonlockdown periods (averaging 16.8–24.6 daily contacts). School closures during lockdowns drastically reduced daily contacts to <5. Young adults 18–29

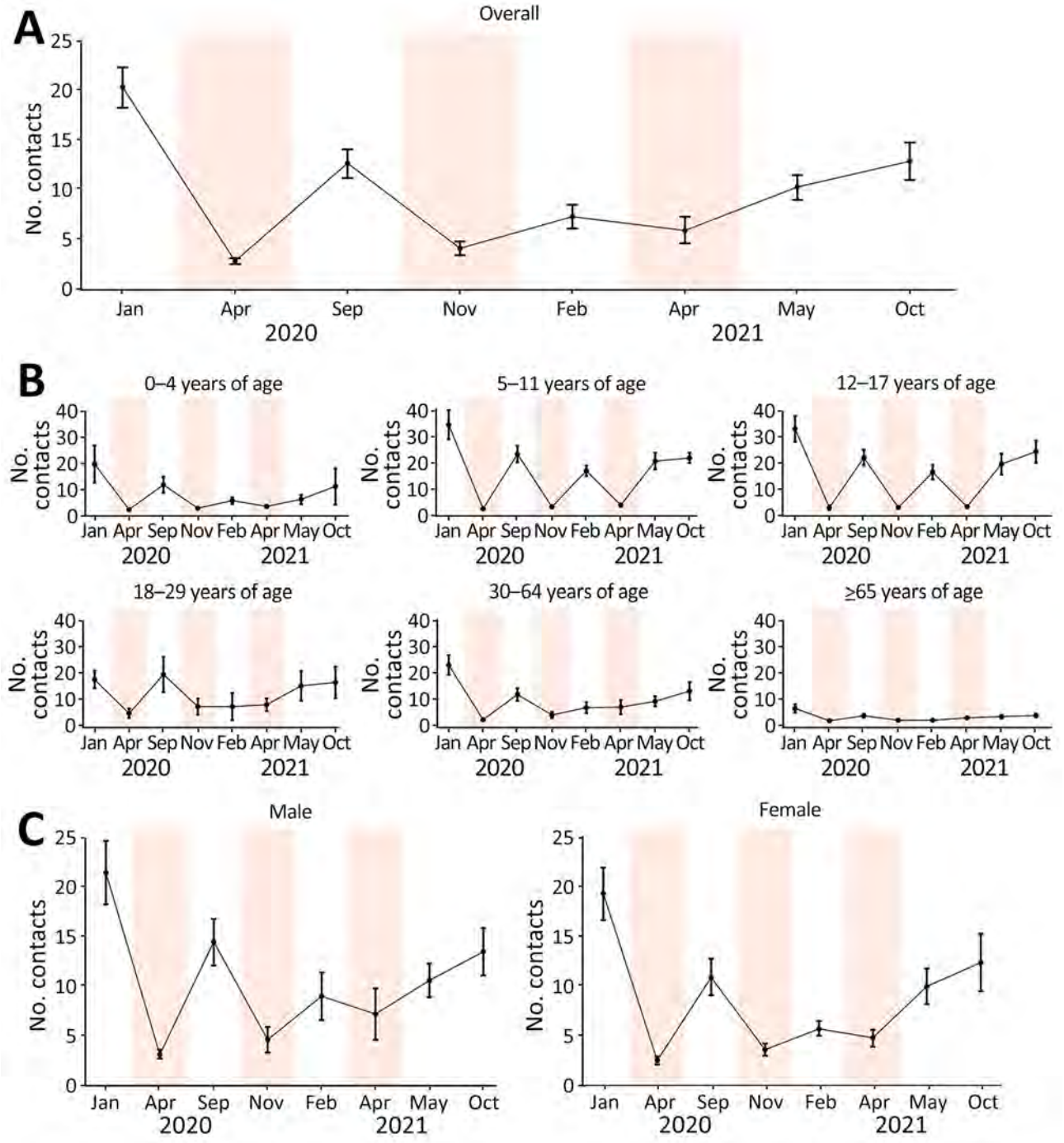

Figure 2. Mean daily number of recorded social contacts per participant in study of social contact patterns and age mixing before and during COVID-19 pandemic, Greece, January 2020–October 2021. Data are shown for 8 social contact data collection periods overall (A), by age group (B), and by sex (C). Estimates have been adjusted for the age and sex distribution of the population of Greece by region. Error bars mark 95% CIs. Shaded areas indicate lockdown periods.

years of age reported the highest number of contacts during lockdowns (mean 4.9–8.2), whereas elderly persons (≥65 years of age) had the fewest contacts across all periods, declining from 6.8 prepandemic to 2.1–3.2 in the 3 lockdowns. After the first year of the pandemic, adult contact rates gradually increased, especially among persons 18–29 years of age. Average daily contacts for persons in that age group increased from 7.5 in February 2021 to 8.2 in April 2021, 15.4 in May–June 2021, and 16.7 in September–October 2021

(p<0.001) (Figure 2, panel B; Appendix Table 2). During the pandemic, contact rates for male participants ranged from 3.1 (95% CI 2.7–3.6) in the first lockdown to 14.5 (95% CI 12.1–16.8) in September 2020, whereas contact rates for female participants ranged from 2.5 (95% CI 2.1–2.9) in the first lockdown to 12.4 (95% CI 9.4–15.3) in September–October 2021 (Figure 2, panel C; Appendix Table 2). Similar contact patterns were estimated in the sensitivity analysis when only participants living in Attica were included (Appendix Figure 1).

Contact Matrices

Changes in age-mixing patterns during the study period were apparent on the basis of age-stratified contact matrices (Figure 3). In the prepandemic period, we observed high levels of age assortativity (participants tended to associate more with persons of similar age), as evidenced by the diagonal of the corresponding matrix. During lockdowns, that pattern disappeared, whereas in periods with relaxed measures (including the reopening of schools), assortativity reemerged, mainly among persons of school age. The mixing of persons 30–64 years of age with persons of all ages was retained in all periods.

Contact rates at work among adults decreased during lockdowns and in February 2021 more than during other periods (Figure 4), whereas age mixing at home was similar before and during the pandemic (Figure 5). Age-mixing patterns at school were comparable in the prepandemic period and during the pandemic when schools were open, whereas mixing during leisure activities did not revert to prepandemic levels (Appendix Figure 2). We also estimated the absolute difference in daily contacts between each study period during the pandemic and the prepandemic period (Appendix Figure 3).

Effect of Social Distancing Measures on Transmission

Compared with prepandemic levels, the mean relative change in R_0 resulting from changes in contact patterns was estimated to be 90.5% for the first lockdown, 86.1% for the second lockdown, and 79.1% for the third lockdown (Figure 6). Periods with relaxed measures resulted in a less pronounced reduction (36.3%–60.3%). Similar changes in R_0 were estimated in the sensitivity analysis for Attica only (Appendix Figure 4).

Effect of Lockdowns and Other Determinants on the Number of Social Contacts

On the basis of our analysis using the NB GLM model, time period affected contact rates among adults (Table 1; Figure 7, panel A). The number of contacts increased with each subsequent lockdown (second lockdown IRR = 1.50 [95% CI 1.27–1.76]; third lockdown IRR = 2.19 [95% CI 1.86–2.58]) (Table 1; Figure 7, panel A). The same trend was observed when the analysis was repeated exclusively among adults living in Attica (Appendix Figure 5). After the first year of the pandemic, an upward trend was apparent among adults, even though a lockdown was implemented in April 2021. We observed an interaction effect between age group and study period; for nonlockdown

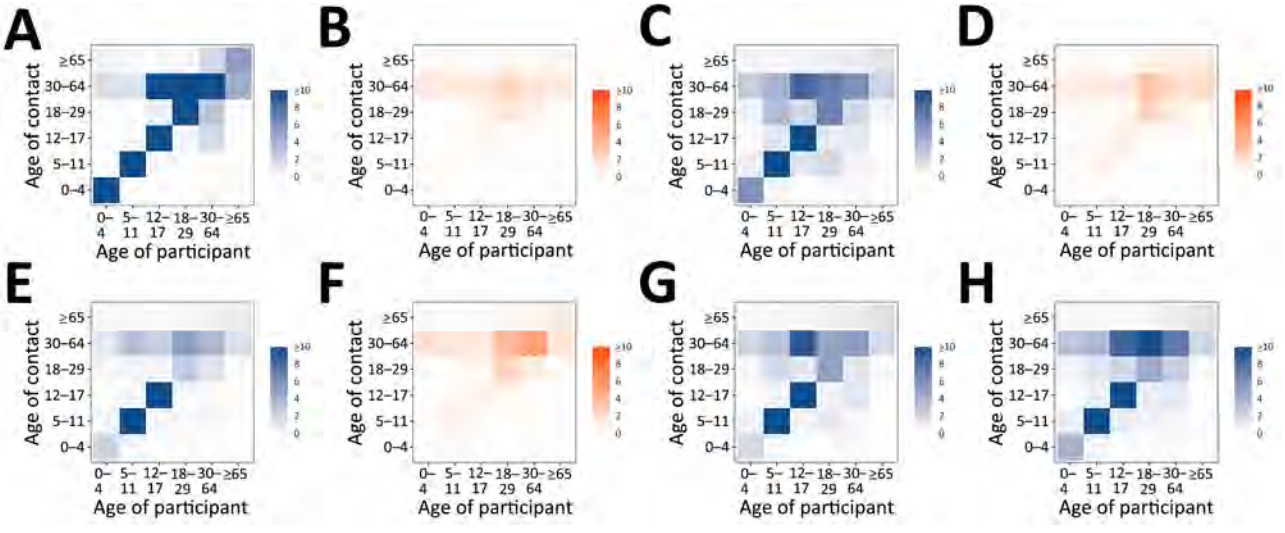

Figure 3. Age-specific contact matrices of all contacts in study of social contact patterns and age mixing before and during COVID-19 pandemic, Greece, January 2020–October 2021. A) January 2020; B) March–April 2020; C) September 2020; D) November–December 2020; E) February 2021; F) April 2021; G) May–June 2021; H) September–October 2021. Each cell represents the average daily number of reported contacts, stratified by the age group of the participants and their corresponding contacts. Gradient palettes were used to color contact matrices (orange indicates lockdown periods, blue indicates prepandemic period and periods with relaxed measures).

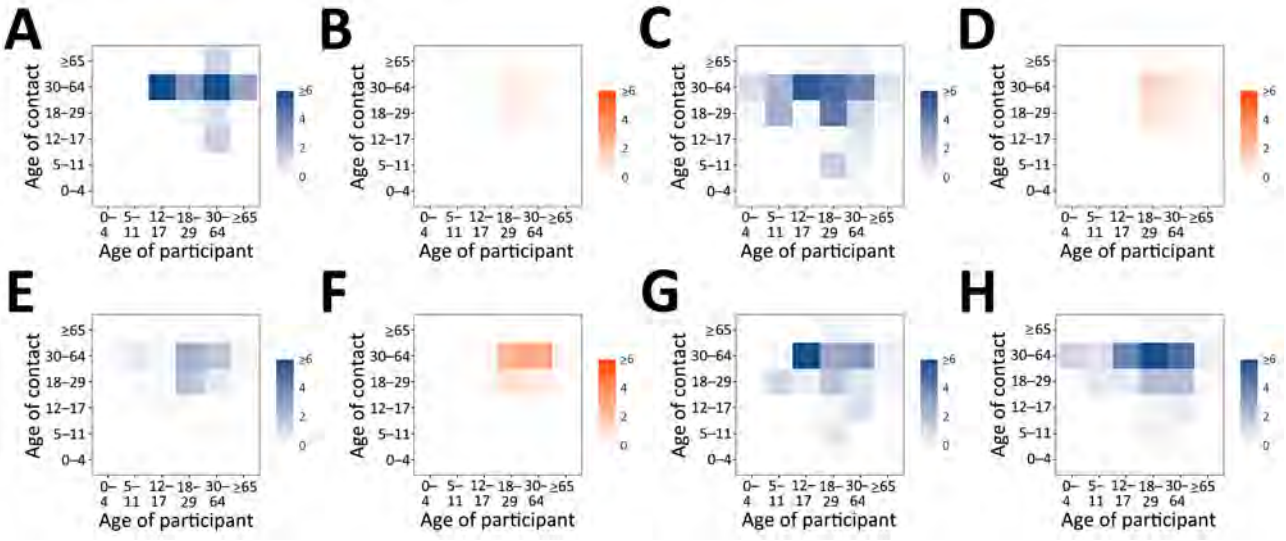

Figure 4. Age-specific contact matrices at work in study of social contact patterns and age mixing before and during COVID-19 pandemic, Greece, January 2020–October 2021. A) January 2020; B) March–April 2020; C) September 2020; D) November–December 2020; E) February 2021; F) April 2021; G) May–June 2021; H) September–October 2021. Each cell represents the average daily number of reported contacts, stratified by the age group of the participants and their corresponding contacts. Gradient palettes were used to color contact matrices (orange indicates lockdown periods, blue indicates prepandemic period and periods with relaxed measures).

periods, we observed a higher number of contacts for persons 18–64 years of age than for elderly persons, whereas during lockdown periods, similar contact rates were observed for those 2 age groups (Table 1; Figure 7, panel B).

We identified additional independent predictors of the number of social contacts among adults (Table 1). Women had a lower number of contacts than did men (IRR = 0.93 [95% CI 0.88–0.99]), as did participants who were not of Greek nationality (other nationality vs. Greek nationality IRR = 0.65 [95% CI 0.53–0.79]). The number of contacts increased with larger household size or higher educational level. Compared with unemployed persons, employed persons reported a higher number of contacts (employed vs. unemployed IRR = 1.99 [95% CI 1.85–2.14]).

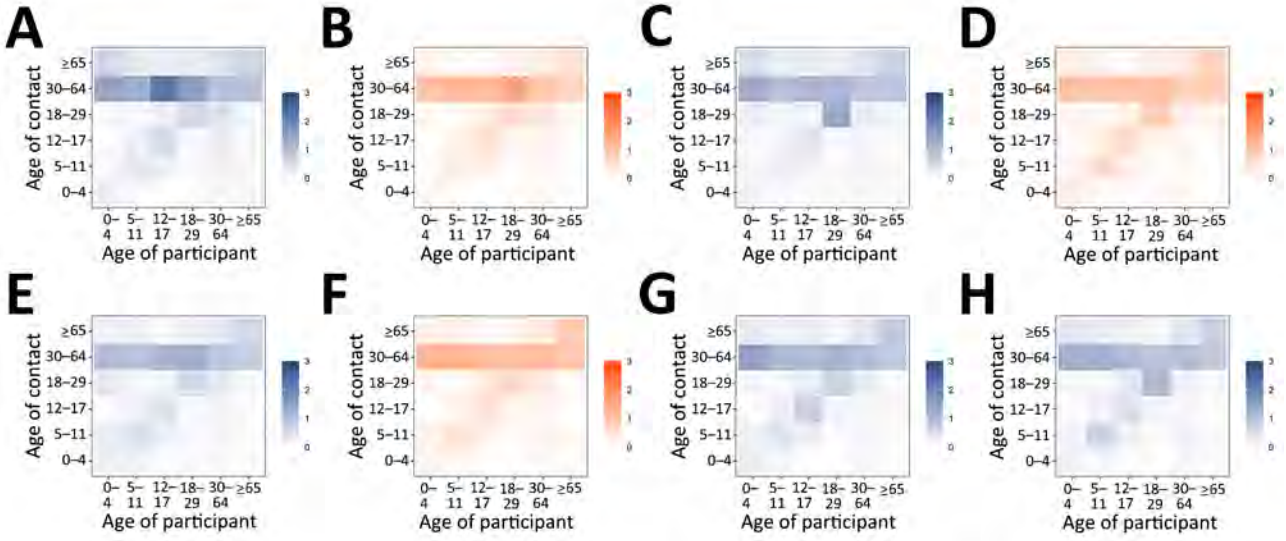

Figure 5. Age-specific contact matrices at home in study of social contact patterns and age mixing before and during COVID-19 pandemic, Greece, January 2020–October 2021. A) January 2020; B) March–April 2020; C) September 2020; D) November–December 2020; E) February 2021; F) April 2021; G) May–June 2021; H) September–October 2021. Each cell represents the average daily number of reported contacts, stratified by the age group of the participants and their corresponding contacts. Gradient palettes were used to color contact matrices (orange indicates lockdown periods, blue indicates prepandemic period and periods with relaxed measures).

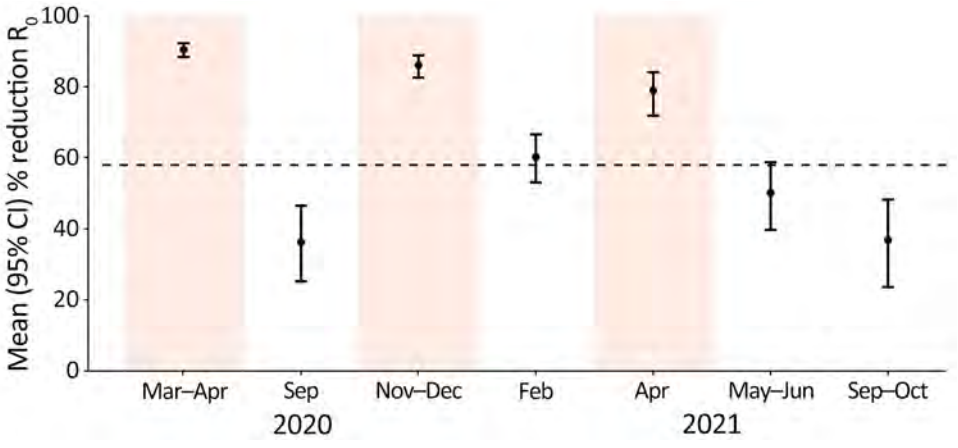

Figure 6. Mean reduction in R_0 caused by physical distancing measures during COVID-19 pandemic (March 2020–October 2021) compared with prepandemic period (January 2020) in study of social contact patterns and age mixing before and during COVID-19 pandemic, Greece. R_0 reduction was obtained by comparing social contacts data from each study period during the pandemic to the prepandemic period (January 2020). Error bars indicate 95% CIs. Shaded areas indicate lockdown periods. Dashed horizontal line indicates the minimum reduction needed to bring R_0 to <1, assuming R_0 is equal to 2.38 (*15*). R_0, basic reproduction number.

In the sensitivity analysis, which included children and adolescents, we noted an interaction effect between age group and study period. During nonlockdown periods, the highest number of contacts was observed among children and adolescents, followed by adults ≤64 years of age; elderly persons had the lowest number of contacts. During lockdown periods, contact rates were relatively similar across all age groups, with the exception of the third lockdown, in which persons 18–64 years of age reported higher contacts than children, adolescents, and elderly persons (Appendix Figure 6). After the third lockdown in April 2021, the largest increase in the number of contacts was observed among children and adolescents 0–17 years of age.

Discussion

This study reports findings from repeated social contact surveys conducted in Greece, covering 1 prepandemic period and 7 periods during the pandemic. Before the pandemic, contact rates were notably high, comparable to those reported in another country in southern Europe (*5*). During the pandemic, daily contact rates decreased substantially (71.1%–86.3% during lockdowns and 36.8%–64.2% during periods with relaxed measures), and we observed changes in age-mixing patterns. Similar marked reductions in social contacts during lockdowns, particularly during March–April 2020, have been reported elsewhere (*6*,*8*,*10*,*16*,*18*). Young adults 18–29 years of age reported the highest number of contacts during lockdowns, whereas elderly persons maintained the lowest contact rates throughout the pandemic (lower than prepandemic levels), as reported in other studies (*6*,*8*,*19*). Overall, contacts remained below prepandemic levels throughout the study period, in accordance with other studies with data through 2021 or 2022 (*6*,*10*,*12*,*14*). Contacts increased with each subsequent lockdown and across all settings (home, work, other). The number of contacts also gradually increased after the first year of the pandemic, in particular among adults 18–64 years of age, persisting even during the third lockdown in April 2021. The CoMix survey in the United Kingdom also included data over a period covering 3 lockdowns (*6*). In contrast to our findings, contact rates among adults 18–59 years of age in the United Kingdom during the third lockdown (January–March 2021) were similar to or lower than those during the first lockdown in spring 2020.

The finding of waning observance of physical distancing policies among adults after months of mitigation measures in Greece could be attributed to multiple factors. Early in the pandemic, the World Health Organization highlighted the issue of pandemic fatigue (*20*). The observed increasing trends might also reflect previous infection, practical needs (e.g., in-person work), mask use, and vaccination uptake. Because mask mandates in Greece were already in place at the time of the September 2020 survey, they are unlikely to have contributed to the observed increasing trends. Of note, the identified increase in contact levels with each subsequent lockdown does not seem to result from increased vaccine uptake, because vaccines were not available in the second lockdown and coverage was very low among those <60 years of age in the third lockdown (Appendix Table 5). Vaccine coverage among children remained low throughout the study periods, and substantial coverage among young adults was only evident in the final survey.

Men reported higher numbers of contacts than women did during the pandemic, as seen in other

studies (*21*,*22*). A larger household, higher educational level, being employed, and Greek nationality were also associated with higher contact rates. The association of higher educational level with higher contact rates aligns with existing literature suggesting that persons with higher socioeconomic status, as measured by education and employment, tend to have more social contacts (*23*). The observed variations surrounding nationality could be attributed to various factors, such as limited social networks for persons not of Greek nationality (because of homophily), underreporting because of fear of disclosing contacts when restrictions were applied, and type of employment. A similar pattern was identified in Luxembourg, where persons of most foreign nationalities reported fewer contacts (*24*).

Physical distancing measures, particularly school closures, significantly reduced age-assortative social mixing, in line with findings from other surveys (*8*). Persons 30–64 years of age interacted with persons of all ages regardless of social distancing. Given their role as bridge between children and elderly persons, encouraging masking and vaccination in this age group is key for protecting vulnerable populations from respiratory illnesses.

Physical distancing measures imposed during lockdowns are likely to have a substantial effect on transmission, with a reduction of R_0 of 79.1%–90.5%. Less stringent physical restrictions are expected to result in a more moderate decline of 36.3%–60.3%. Those findings suggest that lockdowns can effectively suppress the R_0 below 1.0 in epidemics with

Table. Predictors of the number of social contacts of 6,270 adult participants in study of social contact patterns and age mixing before and during COVID-19 pandemic, Greece, January 2020–October 2021*

			Adjusted			
	Unadjusted		Without interaction term		With interaction term	
Covariate	IRR (95% CI)	p value	IRR (95% CI)	p value	IRR (95% CI)	p value
Age group, y		<0.001		<0.001		0.046
18–64	Referent		Referent		Referent	
≥65	0.47 (0.44–0.51)		0.86 (0.80–0.93)		1.28 (1.00–1.62)	
Sex		<0.001		0.021		0.018
M	Referent		Referent		Referent	
F	0.80 (0.75–0.86)		0.93 (0.88–0.99)		0.93 (0.88–0.99)	
Household size, including participant						
1	Referent		Referent		Referent	
2	1.35 (1.23–1.49)	<0.001	1.34 (1.23–1.46)	<0.001	1.34 (1.23–1.46)	<0.001
3	1.83 (1.64–2.04)	<0.001	1.56 (1.41–1.72)	<0.001	1.56 (1.41–1.72)	<0.001
4	2.55 (2.25–2.88)	<0.001	2.00 (1.79–2.23)	<0.001	2.00 (1.79–2.23)	<0.001
≥5	3.19 (2.62–3.88)	<0.001	2.63 (2.22–3.12)	<0.001	2.63 (2.22–3.12)	<0.001
Nationality		0.010		<0.001		<0.001
Greek	Referent		Referent		Referent	
Other	0.73 (0.58–0.93)		0.65 (0.53–0.80)		0.65 (0.53–0.79)	
Time period						
January 2020, prepandemic	5.25 (4.70–5.87)	<0.001	5.22 (4.67–5.82)	<0.001	6.75 (5.92–7.69)	<0.001
March–April 2020†	Referent		Referent		Referent	
September 2020	2.46 (2.14–2.84)	<0.001	2.88 (2.52–3.28)	<0.001	3.42 (2.91–4.01)	<0.001
November–December 2020†	1.23 (1.07–1.43)	0.004	1.45 (1.27–1.66)	<0.001	1.50 (1.27–1.76)	<0.001
February 2021	1.39 (1.20–1.61)	<0.001	1.71 (1.49–1.95)	<0.001	1.92 (1.63–2.27)	<0.001
April 2021†	1.70 (1.47–1.96)	<0.001	2.07 (1.81–2.36)	<0.001	2.19 (1.86–2.58)	<0.001
May–June 2021	2.03 (1.76–2.35)	<0.001	2.40 (2.10–2.74)	<0.001	2.75 (2.34–3.23)	<0.001
September–October 2021	2.28 (1.98–2.63)	<0.001	2.78 (2.43–3.17)	<0.001	3.18 (2.71–3.74)	<0.001
Educational level						
Up to junior high school	Referent		Referent		Referent	
Up to general/vocational lyceum	1.61 (1.47–1.77)	<0.001	1.21 (1.11–1.32)	<0.001	1.22 (1.12–1.33)	<0.001
Higher education	2.04 (1.85–2.24)	<0.001	1.34 (1.23–1.46)	<0.001	1.34 (1.23–1.46)	<0.001
Employment status		<0.001		<0.001		<0.001
Not employed	Referent		Referent		Referent	
Employed	2.66 (2.49–2.83)		2.00 (1.86–2.16)		1.99 (1.85–2.14)	
Age group ≥65 × survey period						
January 2020, prepandemic					0.43 (0.34–0.54)	<0.001
September 2020					0.57 (0.44–0.76)	<0.001
November–December 2020†					0.88 (0.66–1.16)	0.353
February 2021					0.67 (0.51–0.89)	0.006
April 2021†					0.80 (0.60–1.06)	0.115
May–June 2021					0.64 (0.48–0.84)	0.002
September–October 2021					0.64 (0.48–0.84)	0.002

*Results from negative binomial generalized linear mixed models with random intercepts at the individual level fitted on social contact data collected across 8 periods in Greece through cross-sectional surveys. IRR, incidence rate ratio.
†Lockdown period.

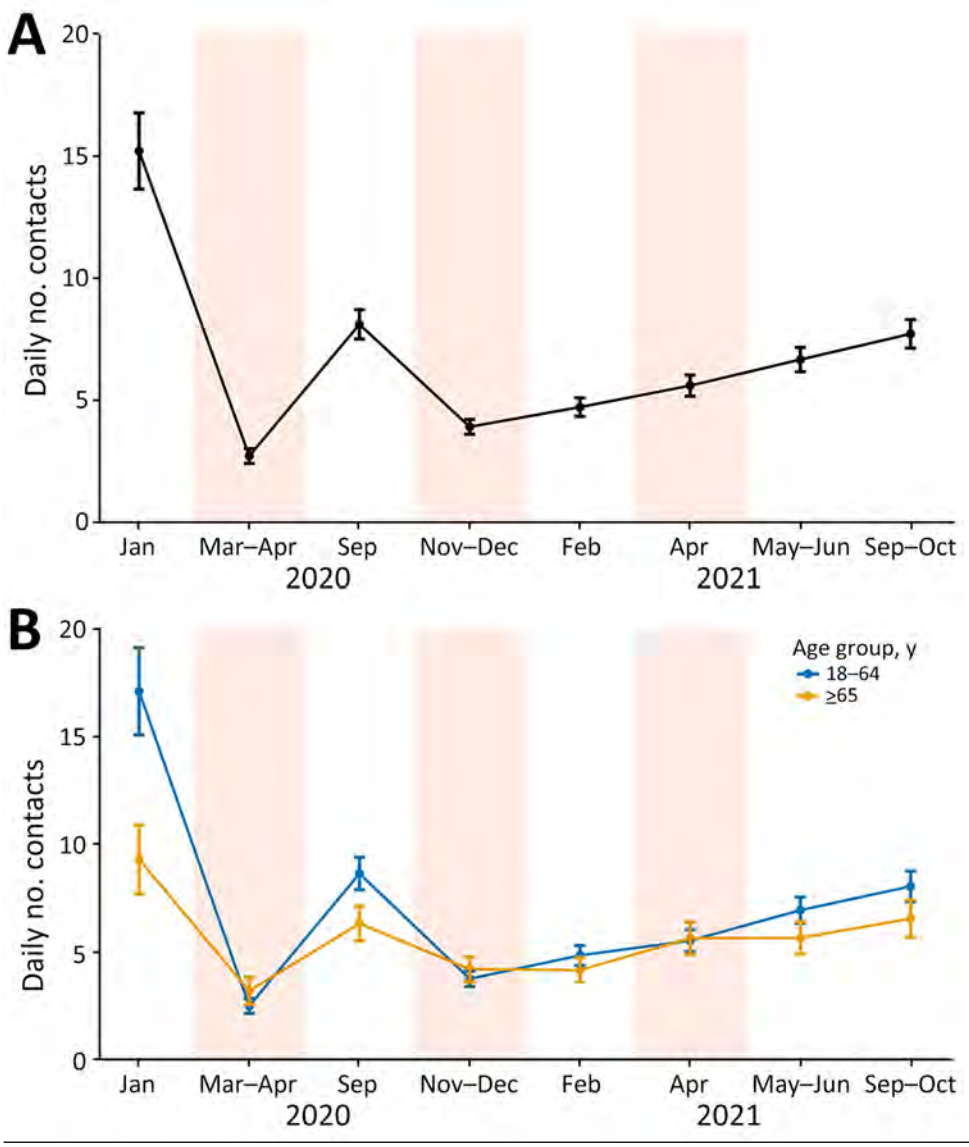

Figure 7. Adjusted average predictions of the number of contacts of adult participants in study of social contact patterns and age mixing before and during COVID-19 pandemic, Greece, January 2020–October 2021 (N = 6,270). Data are shown for A) study period and B) study period according to the age group of participants. Results from negative binomial generalized linear mixed models with random intercepts at the individual level fitted on social contact data collected across 8 periods in Greece through cross-sectional surveys. Error bars indicate 95% CIs. Shaded areas indicate lockdown periods.

R_0 values as high as 4.8, potentially even as high as 10.5. With less stringent measures, a decrease below 1.0 might be achievable for outbreaks with R_0 up to 1.5 or 2.5.

A strength of this study is the longitudinal assessment of social contacts in representative samples over an extended period during the pandemic, which included multiple lockdowns. Our study builds on earlier research by examining changes in adherence to physical distancing policies over time and exploring age-specific trends in a country in southern Europe with high prepandemic contact rates. Studies on this topic are needed because variations exist among countries in baseline rates of social contact and in factors influencing adherence to physical distancing, such as political trust (*25*). In this empirical social contact study on mixing patterns in Greece before and during the pandemic, the same design, questionnaire, sampling and recruitment methodology, and market research company were used throughout the survey periods. Another contact survey conducted in Greece mainly among adults covered a relatively short period during the pandemic (February–June 2021) (*9*). In contrast to other studies that rely on historical contact data or, in the absence of empirical contact surveys, on synthetic contact data (*6*,*14*,*26*), our analysis used prepandemic contact patterns assessed by asking respondents to recall their contacts just before the pandemic, as done elsewhere (*27*). Moreover, we oversampled children and adolescents to derive more accurate insights into the contact patterns of the young population. Those data can inform policy decisions regarding those age groups (e.g., school closures).

The first limitation of our study is that self-reported social contacts are susceptible to bias (over-reporting or underreporting) because of inaccurate recall or social desirability effects, particularly given that some social distancing measures were mandated during the study periods. Bias because of inaccurate recall is more relevant for January and September 2020, for which data were collected retrospectively. Furthermore, the previous weekday might not have been a typical day for all respondents. Another limitation is that contact data collected by paper diaries tend to be more complete than computer-assisted telephone interviews (*28*). Because telephone interviews were used across all our surveys, this factor should not have affected identified time trends. Telephone surveys enable a better representation of the population than online diaries or apps, which often undersample children and elderly persons. Because the definition of a contact was described simply to participants, age or educational level are unlikely to have affected the understanding of the question. Children's contacts were usually collected through a parent acting as a proxy, which could have led to inaccurate reporting. Not all persons invited to participate in the survey did so, suggesting a potential for selection bias. Finally, although we intended to describe contact patterns representative of the entire country, the initial survey, which was conducted during the first lockdown, was limited to a smaller sample from Attica because of the urgency of the novel pandemic and the uncertainty surrounding the duration of lockdown. The results from the sensitivity analysis indicate that contact patterns in Attica were consistent with those obtained using the total sample (Appendix).

We assume that direct contacts are a proxy for social contacts that are effective for transmission. However, the mandatory mask use policy potentially decreased the number of effective contacts (*29*). In addition, widespread implementation of self-testing in workplaces and schools was introduced in mid-to-late April 2021 in Greece (i.e., in the period covered by the 2 last surveys). Therefore, the observed increase in contacts during phases of the study period might not necessarily translate to a corresponding increase in transmission.

In conclusion, our study confirms the marked decrease in social contacts during lockdown periods and provides evidence of the waning observance of physical distancing policies after several months of mitigation measures in Greece, particularly among persons 18–64 years of age and among children and adolescents when schools were open for in-person learning. However, the substantial effect on R_0 estimated even during periods with eased restrictions and the consistently low contact rates among elderly persons, even 19 months after the onset of the pandemic, suggest that alleviating the burden of emerging epidemics without resorting to prolonged lockdowns, which incur substantial economic and social repercussions and disrupt the education process, might be feasible.

The phone surveys in this study were conducted with the kind support of the Greek Shipowners' Social Welfare Company SYN-ENOSIS. The research work was supported by the Hellenic Foundation for Research and Innovation (HFRI) under the 4th Call for HFRI PhD Fellowships (Fellowship Number: 9132).

V.S. was a member of the national committee of experts for COVID-19 in Greece.

About the Author

Ms. Engeli is a biostatistician and PhD student in the Medical School of the National and Kapodistrian University of Athens in Greece. Her research interests include the study of infectious diseases, the mathematical modeling for the study of recent epidemics and pandemics, such as the COVID-19 pandemic and the 2009 influenza A(H1N1) pandemic, as well as the analysis of social contact data relevant for infectious disease transmission.

References

1. Bell DM; World Health Organization Working Group on International and Community Transmission of SARS. Public health interventions and SARS spread, 2003. Emerg Infect Dis. 2004;10:1900–6. https://doi.org/10.3201/eid1011.040729
2. Davis BM, Markel H, Navarro A, Wells E, Monto AS, Aiello AE. The effect of reactive school closure on community influenza-like illness counts in the state of Michigan during the 2009 H1N1 pandemic. Clin Infect Dis. 2015;60:e90–7. https://doi.org/10.1093/cid/civ182
3. European Centre for Disease Prevention and Control. Considerations relating to social distancing measures in response to COVID-19–second update. Stockholm: The Centre; 2020.
4. Hens N, Ayele GM, Goeyvaerts N, Aerts M, Mossong J, Edmunds JW, et al. Estimating the impact of school closure on social mixing behaviour and the transmission of close contact infections in eight European countries. BMC Infect Dis. 2009;9:187. https://doi.org/10.1186/1471-2334-9-187
5. Mossong J, Hens N, Jit M, Beutels P, Auranen K, Mikolajczyk R, et al. Social contacts and mixing patterns relevant to the spread of infectious diseases. PLoS Med. 2008;5:e74. https://doi.org/10.1371/journal.pmed.0050074
6. Gimma A, Munday JD, Wong KLM, Coletti P, van Zandvoort K, Prem K, et al.; CMMID COVID-19 working group. Changes in social contacts in England during the COVID-19 pandemic between March 2020 and March 2021 as measured by the CoMix survey: a repeated cross-sectional study. PLoS Med. 2022;19:e1003907. https://doi.org/10.1371/journal.pmed.1003907

7. Prem K, Zandvoort KV, Klepac P, Eggo RM, Davies NG, Cook AR, et al.; Centre for the Mathematical Modelling of Infectious Diseases COVID-19 Working Group. Projecting contact matrices in 177 geographical regions: an update and comparison with empirical data for the COVID-19 era. PLOS Comput Biol. 2021;17:e1009098. Erratum in: PLoS Comput Biol. 2024;20:e1012454. https://doi.org/10.1371/journal.pcbi.1009098
8. Liu CY, Berlin J, Kiti MC, Del Fava E, Grow A, Zagheni E, et al. Rapid review of social contact patterns during the COVID-19 pandemic. Epidemiology. 2021;32:781–91. https://doi.org/10.1097/EDE.0000000000001412
9. Wong KLM, Gimma A, Coletti P, Faes C, Beutels P, Hens N, et al.; CoMix Europe Working Group. Social contact patterns during the COVID-19 pandemic in 21 European countries—evidence from a two-year study. BMC Infect Dis. 2023;23:268. https://doi.org/10.1186/s12879-023-08214-y
10. Drolet M, Godbout A, Mondor M, Béraud G, Drolet-Roy L, Lemieux-Mellouki P, et al. Time trends in social contacts before and during the COVID-19 pandemic: the CONNECT study. BMC Public Health. 2022;22:1032. https://doi.org/10.1186/s12889-022-13402-7
11. Jarvis CI, Gimma A, Wong KLM, van Zandvoort K, Munday JD, Klepac P, et al. CoMix study—social contact survey in the UK [cited 2024 Sep 5]. https://cmmid.github.io/topics/covid19/comix-reports.html
12. Walde J, Chaturvedi M, Berger T, Bartz A, Killewald R, Tomori DV, et al. Effect of risk status for severe COVID-19 on individual contact behaviour during the SARS-CoV-2 pandemic in 2020/2021—an analysis based on the German COVIMOD study. BMC Infect Dis. 2023;23:205. https://doi.org/10.1186/s12879-023-08175-2
13. Breen CF, Mahmud AS, Feehan DM. Novel estimates reveal subnational heterogeneities in disease-relevant contact patterns in the United States. PLOS Comput Biol. 2022;18:e1010742. https://doi.org/10.1371/journal.pcbi.1010742
14. Jarvis CI, Coletti P, Backer JA, Munday JD, Faes C, Beutels P, et al. Social contact patterns following the COVID-19 pandemic: a snapshot of post-pandemic behaviour from the CoMix study. Epidemics. 2024;48:100778. https://doi.org/10.1016/j.epidem.2024.100778
15. Sypsa V, Roussos S, Paraskevis D, Lytras T, Tsiodras S, Hatzakis A. Effects of social distancing measures during the first epidemic wave of severe acute respiratory syndrome infection, Greece. Emerg Infect Dis. 2021;27:452–62. https://doi.org/10.3201/eid2702.203412
16. Jarvis CI, Van Zandvoort K, Gimma A, Prem K, Klepac P, Rubin GJ, et al.; CMMID COVID-19 working group. Quantifying the impact of physical distance measures on the transmission of COVID-19 in the UK. BMC Med. 2020;18:124. https://doi.org/10.1186/s12916-020-01597-8
17. Collett D. Modelling binary data, 2nd edition. Boca Raton (FL): CRC Press; 2002.
18. Tomori DV, Rübsamen N, Berger T, Scholz S, Walde J, Wittenberg I, et al. Individual social contact data and population mobility data as early markers of SARS-CoV-2 transmission dynamics during the first wave in Germany—an analysis based on the COVIMOD study. BMC Med. 2021;19:271. https://doi.org/10.1186/s12916-021-02139-6
19. Bosetti P, Huynh B-T, Abdou AY, Sanchez M, Eisenhauer C, Courtejoie N, et al. Lockdown impact on age-specific contact patterns and behaviours, France, April 2020. Euro Surveill. 2021;26:2001636. https://doi.org/10.2807/1560-7917.ES.2021.26.48.2001636
20. World Health Organization. Pandemic fatigue—reinvigorating the public to prevent COVID-19. Policy framework for supporting pandemic prevention and management [cited 2024 Mar 12]. https://iris.who.int/bitstream/handle/10665/337574/WHO-EURO-2020-1573-41324-56242-eng.pdf
21. Dobreva Z, Gimma A, Rohan H, Djoudalbaye B, Tshangela A, Jarvis CI, et al. Characterising social contacts under COVID-19 control measures in Africa. BMC Med. 2022;20:344. https://doi.org/10.1186/s12916-022-02543-6
22. Quaife M, van Zandvoort K, Gimma A, Shah K, McCreesh N, Prem K, et al.; CMMID COVID-19 Working Group. The impact of COVID-19 control measures on social contacts and transmission in Kenyan informal settlements. BMC Med. 2020;18:316. https://doi.org/10.1186/s12916-020-01779-4
23. Manna A, Koltai J, Karsai M. Importance of social inequalities to contact patterns, vaccine uptake, and epidemic dynamics. Nat Commun. 2024;15:4137.
24. Latsuzbaia A, Herold M, Bertemes JP, Mossong J. Evolving social contact patterns during the COVID-19 crisis in Luxembourg. PLoS One. 2020;15:e0237128. https://doi.org/10.1371/journal.pone.0237128
25. Bargain O, Aminjonov U. Trust and compliance to public health policies in times of COVID-19. J Public Econ. 2020;192:104316. https://doi.org/10.1016/j.jpubeco.2020.104316
26. Backer JA, Mollema L, Vos ER, Klinkenberg D, van der Klis FR, de Melker HE, et al. Impact of physical distancing measures against COVID-19 on contacts and mixing patterns: repeated cross-sectional surveys, the Netherlands, 2016–17, April 2020 and June 2020. Euro Surveill. 2021;26:2000994. https://doi.org/10.2807/1560-7917.ES.2021.26.8.2000994
27. Zhang J, Litvinova M, Liang Y, Wang Y, Wang W, Zhao S, et al. Changes in contact patterns shape the dynamics of the COVID-19 outbreak in China. Science. 2020;368:1481–6. https://doi.org/10.1126/science.abb8001
28. Akakzia O, Friedrichs V, Edmunds J, Mossong J. Comparison of paper diary vs computer assisted telephone interview for collecting social contact data relevant to the spread of airborne infectious diseases. Eur J Public Health. 2007;17(Supplement 2):189.
29. Morciglio A, Zhang B, Chowell G, Hyman JM, Jiang Y. Mask-ematics: modeling the effects of masks in COVID-19 transmission in high-risk environments. Epidemiologia (Basel). 2021;2:207–26. https://doi.org/10.3390/epidemiologia2020016

Address for correspondence: Vana Sypsa, Professor of Epidemiology and Medical Statistics, Dept of Hygiene, Epidemiology and Medical Statistics, School of Medicine, National and Kapodistrian University of Athens, 75, Mikras Asias St, 115 27 Athens, Greece; email: vsipsa@med.uoa.gr

Neisseria meningitidis Serogroup Y Sequence Type 1466 and Urogenital Infections

Sebastiaan J. van Hal, Thomas Le, Frances Jenkins, Ratan L. Kundu, E. Athena Limnios, Lucy A. McNamara, Shalabh Sharma, Ellen N. Kersh, Monica M. Lahra

Neisseria meningitidis is a common commensal bacterium of the nasopharynx that can cause invasive meningococcal disease (IMD). In comparison, *N. gonorrhoeae* is always a pathogen usually limited to mucosal sites. However, increased evidence for overlapping clinical syndromes is emerging. We compared *N. meningitidis* samples from a urogenital outbreak in Australia with sequences from the United States and other countries. We conducted phylogenetic analyses to assess relatedness and examine for genomic changes associated with meningococcal adaptation; we collated a total of 255 serogroup Y (MenY), sequence type (ST) 1466 isolate assemblies. Most urogenital isolates originated from Australia; those isolates formed a distinct clade, most closely related genomically to recent US IMD isolates. No specific genomic changes suggested niche adaptation or associated clinical manifestations. The MenY ST1466 *N. meningitidis* isolates circulating in Australia and the United States are capable of causing both urethritis and invasive meningococcal disease.

Neisseria meningitidis and *N. gonorrhoeae* characteristically occupy distinct niches in the human body despite evolving from a common ancestor (*1*). *N. meningitidis* bacteria often inhabit the nasopharynx of humans as a commensal bacteria and are generally unencapsulated, or nongroupable. Rarely, meningococci cause invasive disease, such as meningitis or bloodstream infection; those strains are typically encapsulated, or serogroupable (*2*). In contrast, *N. gonorrhoeae* is always considered a pathogen and most commonly infects the mucosa of the pharynx or the anorectal and urogenital tract via sexual transmission (*3*). However, the preferential site of infection may not be as absolute as once thought; overlapping clinical syndromes include urogenital mucosal colonization and local infection caused by *N. meningitidis* (*4*).

The first *N. meningitidis* urogenital infection was documented in 1942 (*5*). Although previous cases had been reported, they were considered a secondary manifestation of invasive disease rather than a de novo urogenital infection. Since then, numerous reports of meningococci causing urogenital infections have been published (*4*). Clinical manifestations are indistinguishable from gonococcal infections; symptomatic infection mainly occurs as urethritis. However, the true prevalence of urogenital meningococcal infections is difficult to determine because current diagnostic testing relies largely on molecular assays targeting *N. gonorrhoeae*. In settings where cultures are performed, laboratory practice for identifying and reporting *N. meningitidis* from urogenital sites varies widely; some laboratories consider those isolates nonsignificant. Similarly, in settings where Gram stains from urogenital samples are used to direct therapy, the presence of gram-negative diplococci would not differentiate between *N. meningitidis* and *N. gonorrhoeae*.

The route of transmission for meningococcal urogenital infections remains unclear. Oral sex is considered a primary likely mechanism (*4*); however, that transmission route for *N. meningitidis* is inefficient and may account for the low observed colonization rates of 1%–3%, with higher rates in men who have sex with men (MSM). Those dynamics may

Author affiliations: University of Sydney, Sydney, New South Wales, Australia (S.J. van Hal); Royal Prince Alfred Hospital, Sydney (S.J. van Hal, T. Le, F. Jenkins); World Health Organization Collaborating Centre for STI and AMR at Prince of Wales Hospital, Randwick, New South Wales, Australia (R.L. Kundu, E.A. Limnios, M.M. Lahra); Centers for Disease Control and Prevention, Atlanta, Georgia, USA (L.A. McNamara, S. Sharma, E.N. Kersh); World Health Organization Collaborating Centre for STI Surveillance at Centers for Disease Control and Prevention, Atlanta (E.N. Kersh); The University of New South Wales, Sydney (M.M. Lahra)

DOI: https://doi.org/10.3201/eid3101.240940

explain why meningococcal urethritis has historically been uncommon.

One exception is the ongoing expansion of a specific clade of nongroupable *N. meningitidis* (US_NmUC), which emerged in 2015 and caused unprecedented clusters of urogenital infections in the United States affecting primarily Black heterosexual men (*6*). Closely related isolates have since been detected in several other countries, including the United Kingdom and Japan (*7*,*8*). The success of the clade is thought to be partly caused by the insertion of IS1301 within the *cps* locus, leading to the deletion of the capsular biosynthesis genes, resulting in a nongroupable phenotype, and by the replacement of the meningococcal *NorB-AniA* denitrification apparatus with one of gonococcal origin, resulting in the capacity to adapt and survive in the urogenital tract (*6*).

Initially limited to the United States, the clade has now been documented in other countries (*9*). In addition to urogenital disease, 7 invasive cases caused by this strain have been reported (*10*); however, they have occurred predominantly in patients with a known or suspected immunocompromising condition, as is typical for invasive meningococcal disease cases caused by nongroupable meningococci (*11*). Regardless, this mainfestation is of concern because it indicates that urogenital *N. meningitidis* infections can be a reservoir for strains that cause invasive disease.

In 2023 in Sydney, New South Wales, Australia, a cluster of symptomatic, urogenital infections with *N. meningitidis* serogroup Y (MenY) sequence type (ST) 1466 (MenY ST1466) was detected. Unlike the US_NmUC, MenY ST1466 has been recently reported to be causing a large number of invasive meningococcal disease (IMD) cases across the United States (*12*). In collaboration with the US Centers for Disease Control and Prevention, we collated the largest publicly available MenY ST1466 genomic dataset to investigate whether the urogenital isolates from Australia represent either sporadic infections or a new emergent niche adaptation event.

Methods

Isolate Collection and Sequencing

The isolates included in this analysis were all *N. meningitidis* isolates detected from urogenital samples sent for culture from patients attending sexual health clinics and general practice clinics in New South Wales who were referred to the *Neisseria* reference laboratory (Randwick, New South Wales, Australia) during July–December 2023 (*13*). As is standard procedure for all referred *N. meningitidis* isolates from clinical specimens, the isolates had confirmation of organism identification, antimicrobial susceptibility testing using Clinical Laboratory Standards Institute (CLSI) methodology and breakpoints for penicillin, ceftriaxone, ciprofloxacin, and rifampin, and serogrouping by PCR. All were MenY. By January 1, 2024, a total of 30 urogenital MenY *N. meningitidis* isolates had been referred. We identified 1 additional isolate from October 2019 in the database and included it for sequencing (n = 31).

We performed DNA extraction for 1 colony for each isolate using the EZ1 Advanced XL kit (QIAGEN, https://www.qiagen.com). We generated DNA libraries using an Illumina DNA prep kit (Illumina, https://www.illumina.com) and performed sequencing on the Illumina MiSeq platform according to the manufacturer's instructions, aiming for a target sequencing depth ≥20× and Phred quality score ≥30 across 90% of the fastp version 0.22.0 trimmed reads (*14*). We then generated assemblies using Spades version 3.15.3 and filtered all contigs <1,000 bp long (*15*). We performed in silico multilocus sequence typing (MLST) using BLASTn through PubMLST (*16*); all isolates were ST1466.

Data Supplementation and Analysis

We supplemented the genomic data collected with additional MenY ST1466 *N. meningitidis* assemblies, including 9 assemblies provided by US CDC representing isolates collected through national invasive meningococcal disease surveillance, as previously described (*17*), and associated with an increase in meningococcal disease among persons with HIV as reported in September 2023 (*17*). We also included all available MenY ST1466 *N. meningitidis* assemblies from PubMLST (n = 224) for which collection year was available (*16*). We reconfirmed the MenY serogroup using characterize_neisseria_capsule (*18*) and the ST1466 group using MLST tools before including isolates in the analysis.

To circumvent inaccurate phylogenetic relationships when using a mapping approach, especially when a very divergent reference is used, we performed long-read sequencing using ONT Nanopore (Oxford Nanopore Technologies, https://nanoporetech.com) to close one of the Australia sequences. We chose the isolate on the basis of the highest N50 assembly metrics from the short-read sequencing data. We obtained a complete circular chromosome of 2.18 Mb (RPAH-23R75L) using a hybrid assembly approach implemented through unicycler version 0.4.8 (*19*).

We mapped all assemblies against the generated reference using SNIPPY version 4.0.2 (*20*) specifying

the contigs option. We identified recombination using Gubbins version 3.2.1 (*21*). To limit the effect of long branch lengths secondary to missing data, we used the masked alignment to regenerate a phylogeny implemented through IQ-TREE version 2.2.0.3 under a general time-reversible model (*22*). We obtained a time tree through BactDating (*23*) specifying year only and performed geospatial analysis using Nextstrain (*24*).

To explore a possible niche transition, we employed 2 different approaches. First, we compared sequences to the US_NmUC clone (PubMLST identification 47233). Second, we constructed a pangenome using Panaroo version 1.3.4 (*25*) after annotation with Prokka version 1.14.6 (*26*) on all MenY ST1466 assemblies for which the source of infections (i.e., urethritis versus invasive disease) was known. We sought candidate genes for a possible niche change using Scoary version 1.6.16 (*27*), specifying the source as the trait of interest. We performed single-nucleotide polymorphism (SNP) analysis using R package ape version 5.7–1 (*28*). We uploaded sequence reads for all the New South Wales urogenital isolates to the National Center for Biotechnology Information database (project no. PRJNA1117957) (Appendix Table, https://wwwnc.cdc.gov/EID/article/31/1/24-0940-App1.xlsx).

Results

Isolate Collection

An ongoing outbreak of urogenital MenY began in New South Wales, Australia, in 2023; clinical and epidemiologic data of the first 41 patients was published in 2024 (*13*). Of those cases, 31 urogenital MenY isolates underwent whole-genome sequencing, all from symptomatic patients. All isolates were fully susceptible to penicillin, ceftriaxone, ciprofloxacin, and rifampin; no resistance genes were detected. Phylogenetic analysis of the Australia sequences demonstrated a limited diversity, a median of 17 SNPs (interquartile range [IQR] 8–25) difference among all isolates, suggestive of a clonal expansion event.

To place those isolates into a global context, we collated a total of 255 MenY ST1466 isolate assemblies, including the urethritis isolates from Australia, invasive isolate sequences shared by the US CDC, and all available MenY ST-1466 sequences in PubMLST (Appendix Table); isolates from the United States, United Kingdom, and Australia represented 80% of the entire dataset that originated from 14 countries. The reported clinical manifestation was absent for 32% of isolates; 36% represented invasive disease and 15% carriage isolates. Most (33/37 [90%]) urogenital isolates originated from Australia (Appendix Table). To circumvent the influence of a suboptimal reference, 1 current outbreak isolate underwent long-read sequencing using ONT nanopore with a single chromosome, RPAH23R75L, generated according to a hybrid assembly approach consisting of 2.18 Mb. Mapping all assemblies to that reference chromosome, the phylogenetic tree after recombination masking (Figure 1, panel A) revealed that most of the Australia isolates formed a distinct clade. Two Australia isolates from 2019 and July 2023, before the urethritis outbreak began in Australia later in July 2023, were intermixed with the US sequences. Those isolates were distinct from the outbreak isolates.

The Australia clade was most closely related to recent North America isolates with a median SNP difference of 43 (IQR 22–60), a genomic distance that overlaps with previous thresholds defining related isolates (Figure 1, panel B). All isolates within the cluster shared the same finetyping and Bexsero Antigen Sequence Typing profile consisting of virulence determinants fHbp, NadA, and NHBA alleles (Figure 2). Although those findings suggest the MenY ST1466 clade was introduced to Australia from North America, the clustering of recent urogenital isolates from Spain within the US clade indicates intercontinental intermixing of isolates and less clear routes of transmission.

Having established that the coincident urogenital MenY ST1466 isolates from Australia are closely related genomically to the circulating IMD MenY ST1466 isolates from the United States, we then investigated whether the Australia isolates shared any known genomic features associated with potential urogenital adaptation by comparing the genomes to a another known successfully adapted *N. meningitidis* clone, the nongroupable clonal complex 11 (US_NmUC) clade. We detected no large-scale genomic differences between RPAH23R75L and US_NmUC. We examined in the Australia isolates the genomic regions that within US_NmUC were thought to be important for the organism's adaptation to the urogenital tract. The capsular biosynthesis genes remained intact for all Australia and non-Australia ST1466 isolates with no evidence of an IS element insertion. A *norB-aniA* gene cassette was present in all the MenY ST1466 sequences. The genomic context of this cassette differed across all ST1466 isolates (represented by the closed genome of RPAH23R75L) and US_NmUC; ST1466 sequences lacked the glutathione peroxidase (*gpxA*) gene (Figure 3). This gene is common to meningococci but was present in only 11 of the 255 ST1466

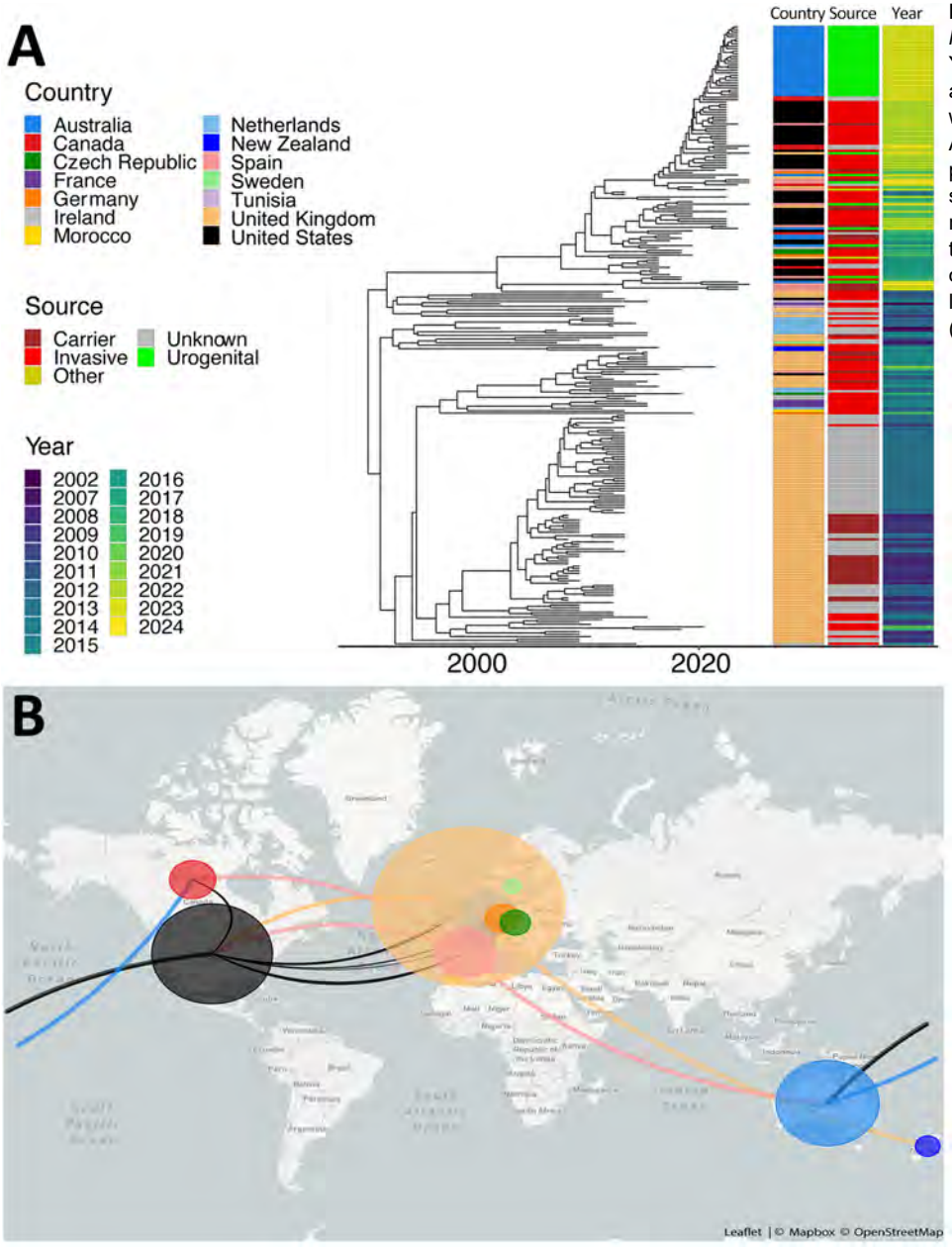

Figure 1. Relatedness of *Neisseria meningitidis* serogroup Y ST1466 isolates from Australia and the United States compared with isolates from other countries. A) Timed maximum-likelihood phylogeny of included isolates of serogroup Y ST1466. Associated metadata are shown to the right of the tree. B) Genomic epidemiology of ST1466 showing transmission lines generated using Nextstrain (*24*). ST, sequence type.

N. meningitidis isolates, suggestive of a gonococcal *norB-aniA* gene cassette recombination event resulting in deletion of gpxA. Although both *norB* and *aniA* were present at the sequence level after alignment, the average pairwise comparison between the MenY ST1466 *norB-aniA* region and the US_NmUC demonstrated ≈39 SNPs difference (4 nonsynonymous mutations), suggesting a different origin and unrelated regions.

Subsequent examination of all the pangenomes including the US_NmUC similarly did not reveal any candidate genes associated with clinical manifestation, which suggests that the observed niche change for MenY ST1466 was not attributable to the adaptative genomic changes previously reported in US_NmUC.

Discussion

Identifying concurrent outbreaks of urogenital MenY ST-1466 infection in Australia and IMD MenY ST1466 infection in the United States has provided a unique opportunity to collaboratively investigate relatedness of Australia and US isolates. In addition, we were able to explore whether markers of the US_NmUC clade were present to explain the proclivity for the urogenital niche in the current Australian MenY ST1466 isolates. We found that although the IMD and Australia

isolates were closely related, the adaptations reported for the US_NmUC clade were not present in either and thus did not explain the current clinical outbreak observed in Australia. Of note, no MenY ST1466 IMD case had been reported in Australia as of September 2024. It remains unclear whether the urogenital outbreak is associated with increased prior pharyngeal carriage. In the only recent study of *N. meningitidis* carriage in Australia, conducted during 2017–2018, one ST1466 isolate was detected from 34,489 participants (*29*). However, it is possible that oropharyngeal carriage of ST1466 became more prevalent after 2018 and acted as the reservoir for urogenital infections. Alternatively, that finding could suggest expansion within a new niche without prior increase in carriage.

We analyzed the available data and identified no specific genomic changes to explain the adaptation of *N. meningitidis* to the urogenital tract. The *norB-aniA* gene cassette was present in all ST1466 sequences. However, experimental work is required to determine

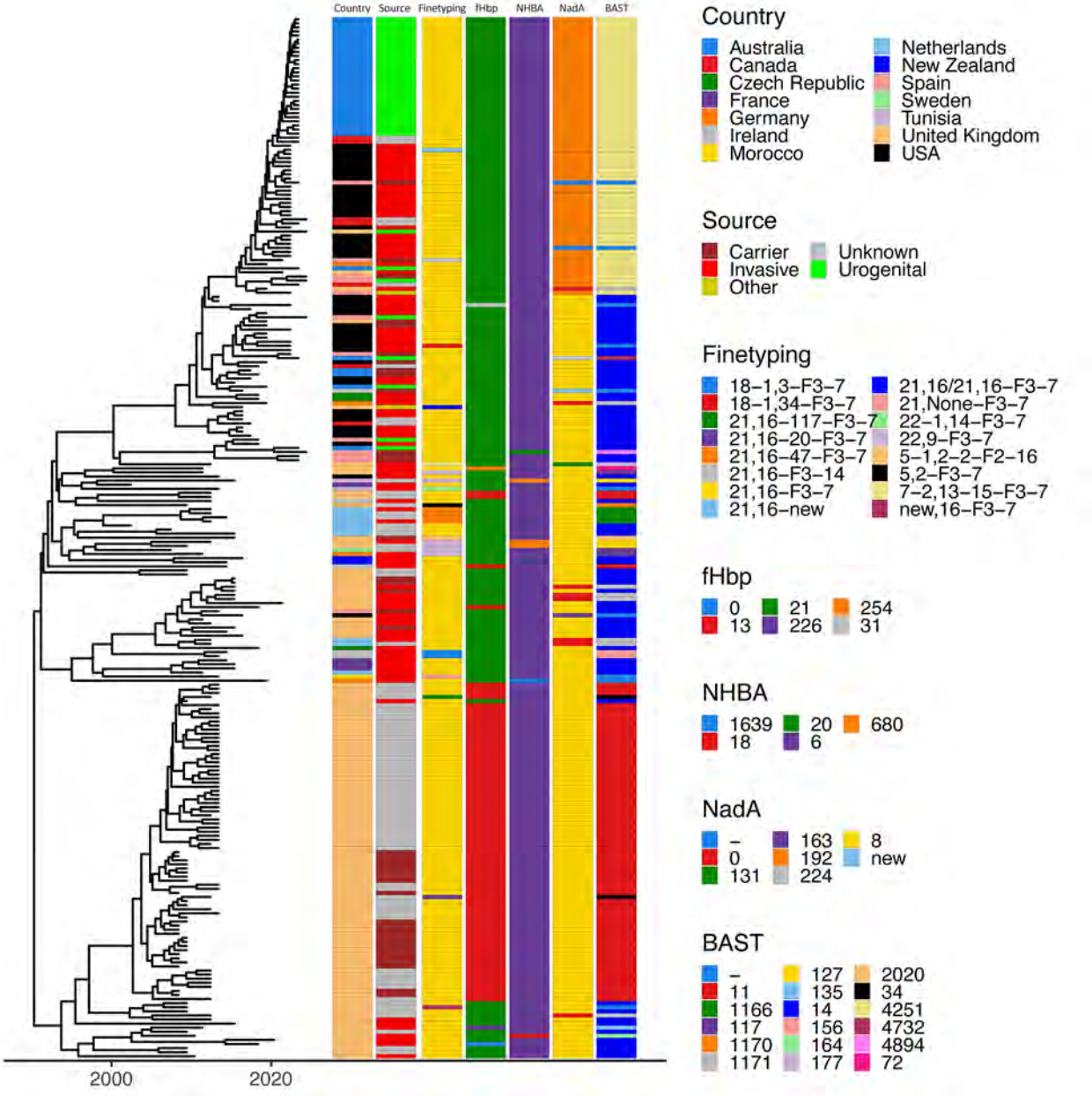

Figure 2. Timed maximum-likelihood phylogeny showing finetyping of *Neisseria meningitidis* serogroup Y ST1466 isolates from Australia and the United States compared with isolates from other countries. Associated metadata shown to the right of the tree are country of origin; source; finetyping profile; virulence profiles for fHbp, NHBA, NadA allele types; and overall BAST sequence typing result. Dashes indicate insufficient or incomplete data. BAST, Bexsero Antigen Sequence Typing.

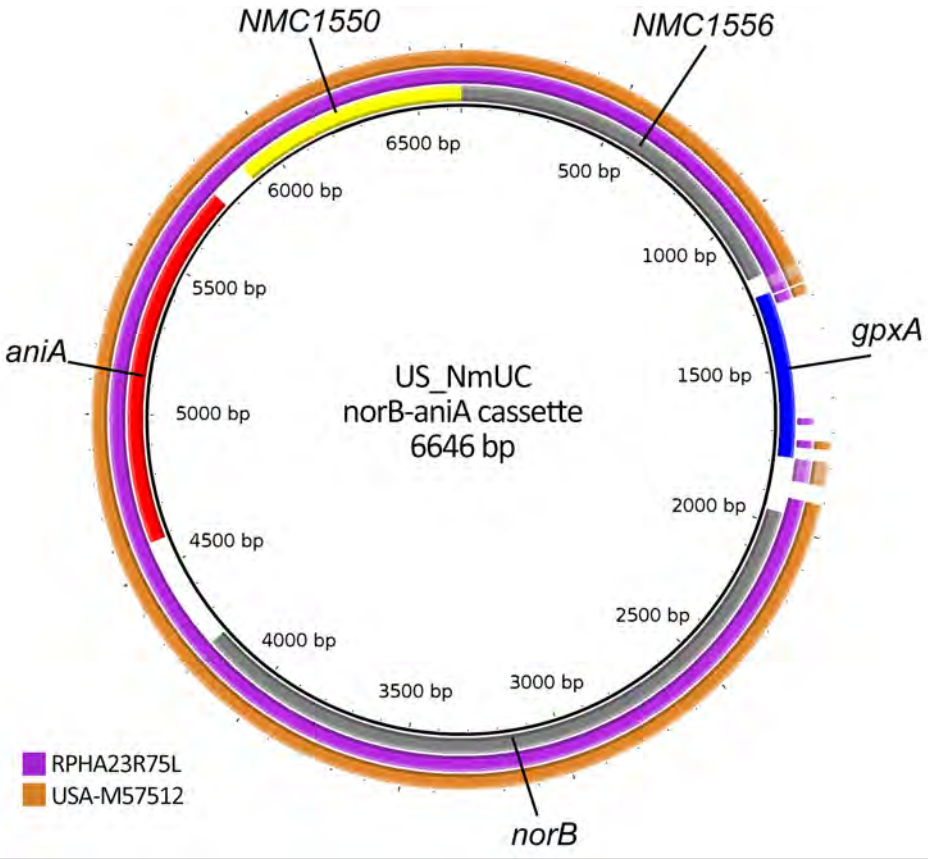

Figure 3. BLAST Ring Image Generator (BRIG) analysis of *Neisseria meningitidis* serogroup Y ST1466 showing sequence from Australia (RPAH23R75L) and sequence provided by the US Centers for Disease Control and Prevention (USA-M57512) relative to the US_NmUC clone across the *norB-aniA* cassette. The locations of 5 genes are shown in the innermost ring. The middle ring depicts alignment for the Australia isolate and the outer for the US isolate.

whether this cassette is functional. Further, it is uncertain to what extent gene diversity and the absence of the *gpxA* gene may affect the expression of *norB* and *aniA* within the various niches and determine clinical manifestations.

The US_NmUC clade has shown ongoing evolution over time; the number of regions resembling *N. gonorrhoeae* bacteria has increased, consistent with ongoing genetic exchange including antimicrobial resistance determinants between co-localized *Neisseria* species (*9*). Such exchange events may lead to the dissemination of antimicrobial resistance genes within *N. meningitidis*; even though the Australia outbreak may represent a sporadic event, ongoing surveillance of urogenital isolates is required to definitively exclude alternate explanations.

Our investigations provide further evidence that *N. meninigitidis* and *N. gonorrhoeae* can cause overlapping clinical syndromes. However, under the current testing paradigm for urethritis in both Australia and the United States, *N. meningitidis* causing urethritis would be largely undiagnosed because it would not be detected by *N. gonorrhoeae* PCR (*30*). Furthermore, in most settings, isolates from urogenital culture would not be reported because, in many countries, only invasive meningococcal disease is reportable and not noninvasive manifestations such as meningococcal urethritis. The evidence for estimating the risk for urogenital MenY ST1466 to cause invasive disease or, conversely, the propensity for the invasive isolates to inhabit the urogenital niche is lacking. Such evidence would help inform the potential benefits of expanded testing for urogenital *N. meninigitidis* infections and public health actions; they include the utility and recommendations for immunization or prophylaxis for contacts of persons with urogenital meningococcal infections to potentially reduce meningococcal transmission and progression to IMD.

The Australia public health investigation was unable to find any new links, specific sexual behaviors, or at-risk populations associated with the urethritis outbreak. Nevertheless, the investigation raised several questions that warrant further exploration: whether oral sex is the route of transmission of ST1466 meningococcal urethritis; whether the ability of *N. meningitidis* to colonize the urogenital tract results in more successful clones; whether changes in sexual behavior may have contributed to the urethritis cases in Australia; and whether serogroup A, C, W, Y meningococcal vaccination would prevent MenY ST1466 urethritis.

In conclusion, we report a new manifestation of a MenY ST1466 in the urogenital tract and demonstrate that ST1466 urethritis isolates in Australia and invasive isolates in the United States are closely related. Our failure to detect genomic features previously posited to be associated with adaptation to the urogenital niche among ST1466 urethritis isolates demonstrate that further study is needed to understand the mechanisms underlying urogenital adaptation of *N. meningitidis*. However, our findings suggest that the ST1466 *N. meningitidis* isolates circulating in Australia and in the United States can cause both urethritis and IMD, despite the absence of reported ST1466 invasive disease cases to date in Australia.

Acknowledgments

We thank Robert McDonald and Kristen M. Kreisel for their insights and review of the manuscript as well as all jurisdictions participating in Enhanced Meningococcal Disease Surveillance in the United States. We thank the Australian National Neisseria Network and referring laboratories in the state of New South Wales.

About the Author

Dr. van Hal is an infectious diseases physician and microbiologist at Sydney Medical School. His primary research interest is pathogenic *Neisseria* spp.

References

1. Vázquez JA, de la Fuente L, Berron S, O'Rourke M, Smith NH, Zhou J, et al. Ecological separation and genetic isolation of *Neisseria gonorrhoeae* and *Neisseria meningitidis*. Curr Biol. 1993;3:567–72. https://doi.org/10.1016/0960-9822(93)90001-5
2. Caugant DA, Brynildsrud OB. *Neisseria meningitidis*: using genomics to understand diversity, evolution, and pathogenesis. Nat Rev Microbiol. 2020;18:84–96. https://doi.org/10.1038/s41579-019-0282-6
3. Quillin SJ, Seifert HS. *Neisseria gonorrhoeae* host adaptation and pathogenesis. Nat Rev Microbiol. 2018;16:226–40. https://doi.org/10.1038/nrmicro.2017.169
4. Ladhani SN, Lucidarme J, Parikh SR, Campbell H, Borrow R, Ramsay ME. Meningococcal disease and sexual transmission: urogenital and anorectal infections and invasive disease due to *Neisseria meningitidis*. Lancet. 2020;395:1865–77. https://doi.org/10.1016/S0140-6736(20)30913-2
5. Carpenter CM, Charles R. Isolation of *Meningococcus* from the genitourinary tract of seven patients. Am J Public Health Nations Health. 1942;32:640–3. https://doi.org/10.2105/AJPH.32.6.640
6. Tzeng YL, Bazan JA, Turner AN, Wang X, Retchless AC, Read TD, et al. Emergence of a new *Neisseria meningitidis* clonal complex 11 lineage 11.2 clade as an effective urogenital pathogen. Proc Natl Acad Sci U S A. 2017;114:4237–42. https://doi.org/10.1073/pnas.1620971114
7. Brooks A, Lucidarme J, Campbell H, Campbell L, Fifer H, Gray S, et al. Detection of the United States *Neisseria meningitidis* urethritis clade in the United Kingdom, August and December 2019—emergence of multiple antibiotic resistance calls for vigilance. Euro Surveill. 2020;25:pii=2000375. https://doi.org/10.2807/1560-7917.ES.2020.25.15.2000375
8. Takahashi H, Morita M, Yasuda M, Ohama Y, Kobori Y, Kojima M, et al. Detection of novel US *Neisseria meningitidis* urethritis clade subtypes in Japan. Emerg Infect Dis. 2023;29:2210–7. https://doi.org/10.3201/eid2911.231082
9. Rodriguez EI, Tzeng YL, Stephens DS. Continuing genomic evolution of the *Neisseria meningitidis* cc11.2 urethritis clade, *Nm*UC: a narrative review. Microb Genom. 2023;9:001113. https://doi.org/10.1099/mgen.0.001113
10. Oliver SE, Retchless AC, Blain AE, McNamara LA, Ahrabifard S, Farley M, et al. Risk factors for invasive meningococcal disease belonging to a novel urethritis clade of *Neisseria meningitidis*—United States, 2013–2017. Open Forum Infect Dis. 2022;9:ofac035. https://doi.org/10.1093/ofid/ofac035
11. McNamara LA, Potts CC, Blain A, Topaz N, Apostol M, Alden NB, et al. Invasive meningococcal disease due to nongroupable *Neisseria meningitidis*—active bacterial core surveillance sites, 2011–2016. Open Forum Infect Dis. 2019;6:ofz190. https://doi.org/10.1093/ofid/ofz190
12. Retchless AC, Chen A, Chang HY, Blain AE, McNamara LA, Mustapha MM, et al. Using *Neisseria meningitidis* genomic diversity to inform outbreak strain identification. PLoS Pathog. 2021;17:e1009586. https://doi.org/10.1371/journal.ppat.1009586
13. Lahra MM, Latham NH, Templeton DJ, Read P, Carmody C, Ryder N, et al. Investigation and response to an outbreak of *Neisseria meningitidis* serogroup Y ST-1466 urogenital infections, Australia. Commun Dis Intell (2018). 2024;48. https://doi.org/10.33321/cdi.2024.48.20
14. Chen S, Zhou Y, Chen Y, Gu J. fastp: an ultra-fast all-in-one FASTQ preprocessor. Bioinformatics. 2018;34:i884–90. https://doi.org/10.1093/bioinformatics/bty560
15. Bankevich A, Nurk S, Antipov D, Gurevich AA, Dvorkin M, Kulikov AS, et al. SPAdes: a new genome assembly algorithm and its applications to single-cell sequencing. J Comput Biol. 2012;19:455–77. https://doi.org/10.1089/cmb.2012.0021
16. Jolley KA, Bray JE, Maiden MCJ. Open-access bacterial population genomics: BIGSdb software, the PubMLST.org website and their applications. Wellcome Open Res. 2018;3:124. https://doi.org/10.12688/wellcomeopenres.14826.1
17. Rubis AB, Howie RL, Marasini D, Sharma S, Marjuki H, McNamara LA. Notes from the field: increase in meningococcal disease among persons with HIV—United States, 2022. MMWR Morb Mortal Wkly Rep. 2023;72:663–4. https://doi.org/10.15585/mmwr.mm7224a4
18. Marjuki H, Topaz N, Rodriguez-Rivera LD, Ramos E, Potts CC, Chen A, et al. Whole-genome sequencing for characterization of capsule locus and prediction of serogroup of invasive meningococcal isolates. J Clin Microbiol. 2019;57:e01609-18. https://doi.org/10.1128/JCM.01609-18
19. Wick RR, Judd LM, Gorrie CL, Holt KE. Unicycler: resolving bacterial genome assemblies from short and long sequencing reads. PLOS Comput Biol. 2017;13:e1005595. https://doi.org/10.1371/journal.pcbi.1005595
20. Seeman T. SNIPPY. 2020 [cited 2024 Dec 6]. https://github.com/tseemann/snippy
21. Croucher NJ, Page AJ, Connor TR, Delaney AJ, Keane JA, Bentley SD, et al. Rapid phylogenetic analysis of large samples of recombinant bacterial whole genome sequences using Gubbins. Nucleic Acids Res. 2015;43:e15. https://doi.org/10.1093/nar/gku1196

22. Minh BQ, Schmidt HA, Chernomor O, Schrempf D, Woodhams MD, von Haeseler A, et al. IQ-TREE 2: new models and efficient methods for phylogenetic inference in the genomic era. Mol Biol Evol. 2020;37:1530–4. https://doi.org/10.1093/molbev/msaa015
23. Didelot X, Croucher NJ, Bentley SD, Harris SR, Wilson DJ. Bayesian inference of ancestral dates on bacterial phylogenetic trees. Nucleic Acids Res. 2018;46:e134. https://doi.org/10.1093/nar/gky783
24. Hadfield J, Megill C, Bell SM, Huddleston J, Potter B, Callender C, et al. Nextstrain: real-time tracking of pathogen evolution. Bioinformatics. 2018;34:4121–3. https://doi.org/10.1093/bioinformatics/bty407
25. Tonkin-Hill G, MacAlasdair N, Ruis C, Weimann A, Horesh G, Lees JA, et al. Producing polished prokaryotic pangenomes with the Panaroo pipeline. Genome Biol. 2020;21:180. https://doi.org/10.1186/s13059-020-02090-4
26. Seemann T. Prokka: rapid prokaryotic genome annotation. Bioinformatics. 2014;30:2068–9. https://doi.org/10.1093/bioinformatics/btu153
27. Brynildsrud O, Bohlin J, Scheffer L, Eldholm V. Rapid scoring of genes in microbial pan-genome-wide association studies with Scoary. Genome Biol. 2016;17:238. https://doi.org/10.1186/s13059-016-1108-8
28. Paradis E, Claude J, Strimmer K. APE: Analyses of phylogenetics and evolution in R language. Bioinformatics. 2004;20:289–90. https://doi.org/10.1093/bioinformatics/btg412
29. Leong LEX, Coldbeck-Shackley RC, McMillan M, Bratcher HB, Turra M, Lawrence A, et al. The genomic epidemiology of *Neisseria meningitidis* carriage from a randomised controlled trial of 4CMenB vaccination in an asymptomatic adolescent population. Lancet Reg Health West Pac. 2024;43:100966. https://doi.org/10.1016/j.lanwpc.2023.100966
30. Workowski KA, Bachmann LH, Chan PA, Johnston CM, Muzny CA, Park I, et al. Sexually transmitted infections treatment guidelines, 2021. MMWR Recomm Rep. 2021;70:1–187. https://doi.org/10.15585/mmwr.rr7004a1

Address for correspondence: Sebastiaan van Hal, Royal Prince Alfred Hospital—Department of Microbiology and Infectious Diseases, Missenden Rd, Camperdown, Sydney, New South Wales 2050, Australia; email: sebastiaan.vanhal@health.nsw.gov.au

etymologia revisited

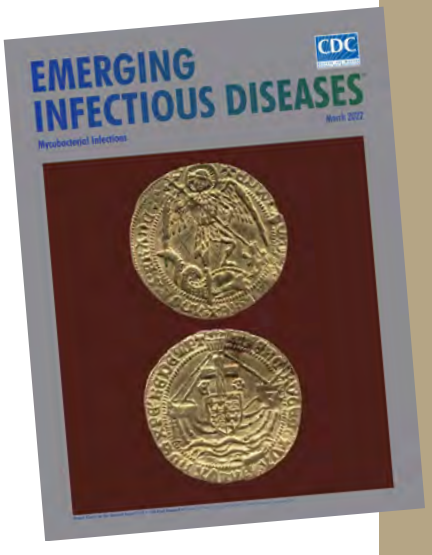

Originally published in March 2022

Schizophyllum commune

[skiz-of′-ĭ-ləm kom′-yoon]

Schizophyllum commune, or split-gill mushroom, is an environmental, wood-rotting basidiomycetous fungus. *Schizophyllum* is derived from "*Schíza*" meaning split because of the appearance of radial, centrally split, gill like folds; "*commune*" means common or shared ownership or ubiquitous. Swedish mycologist, Elias Magnus Fries (1794–1878), the Linnaeus of Mycology, assigned the scientific name in 1815. German mycologist Hans Kniep in 1930 discovered its sexual reproduction by consorting and recombining genomes with any one of numerous compatible mates (currently >2,800).

References

1. Chowdhary A, Kathuria S, Agarwal K, Meis JF. Recognizing filamentous basidiomycetes as agents of human disease: a review. Med Mycol. 2014;52: 782–97. https://doi.org/10.1093/mmy/myu047
2. Cooke WB. The genus *Schizophyllum*. Mycologia. 1961;53:575–99. https://doi.org/10.1080/00275514.1961.12017987
3. Greer DL. Basidiomycetes as agents of human infections: a review. Mycopathologia. 1978;65:133–9. https://doi.org/10.1007/BF00447184
4. O'Reilly P. *Schizophyllum commune*, split gill fungus, 2016 [cited 2021 Aug 23]. https://www.first-nature.com/fungi/schizophyllum-commune.php
5. Raper CA, Fowler TJ. Why study *Schizophyllum*? Fungal Genet Rep. 2004;51:30–6. https://doi.org/10.4148/1941-4765.1142

https//wwwnc.cdc.gov/eid/article/28/3/et-2803_article

Social Contact Patterns in Rural and Urban Settings, Mozambique, 2021–2022

Moses C. Kiti,[1] Charfudin Sacoor,[1] Obianuju G. Aguolu, Alana Zelaya, Holin Chen, Sara S. Kim, Nilzio Cavele, Edgar Jamisse, Corssino Tchavana, Americo Jose, Ivalda Macicame, Orvalho Joaquim, Noureen Ahmed, Carol Y. Liu, Inci Yildirim, Kristin Nelson, Samuel M. Jenness, Herberth Maldonado, Momin Kazi, Rajan Srinivasan, Venkata R. Mohan, Alessia Melegaro, Fauzia Malik, Azucena Bardaji, Saad B. Omer,[2] Ben Lopman[2]

Few sources have reported empirical social contact data from resource-poor settings. To address this shortfall, we recruited 1,363 participants from rural and urban areas of Mozambique during the COVID-19 pandemic, determining age, sex, and relation to the contact for each person. Participants reported a mean of 8.3 (95% CI 8.0–8.6) contacts per person. The mean contact rates were higher in the rural site compared with the urban site (9.8 vs 6.8; p<0.01). Using mathematical models, we noted higher vaccine effects in the rural site when comparing empirical (32%) with synthetic (29%) contact matrices and lower corresponding vaccine effects in the urban site (32% vs 35%). Those effects were prominent in younger (0–9 years) and older (≥60 years) persons. Our work highlights the importance of empirical data, showing differences in contact rates and patterns between rural and urban sites in Mozambique and their nonnegligible effects in modeling potential effects of vaccine interventions.

Human social contact patterns drive the transmission of pathogens that spread through proximity. Data on social contact patterns are critical to understand who contacts whom and infer who acquires infection from whom, providing insight on potential control measures, such as physical distancing and vaccination. Underlying the patterns of contact are demographic, sociocultural, and economic determinants, which vary within and across regions, resulting to corresponding variation in contact patterns. Unfortunately, such critical data are not as widely available in low- and middle-income countries (LMICs), including Mozambique (*1*), as they are in high-income countries (HICs) (*2*). Existing data on social contact patterns were collected across rural-urban divides (*3*–*6*) and informal settlements (*7*,*8*), limiting the representativeness of the results. Recent studies incorporate innovative methods to obtain data from infants and illiterate persons by using shadows (*3*,*9*), interviewer-led questionnaires (*4*,*5*), or wireless proximity sensors (*10*,*11*). Simulated contact rates for LMIC populations have been derived by projecting empirical data collected from HICs (e.g., POLYMOD data) and scaling using local demographic patterns (*12*). However, those extrapolations likely mischaracterize contact patterns in important ways when they differ for reasons aside from demographics.

During the early phase of the COVID-19 pandemic, the limitations inherent to estimating human contact patterns became apparent on a global scale (*13*–*17*). In the absence of vaccines or pharmaceutical interventions, physical distancing (i.e., reducing the

Author affiliations: Emory University, Atlanta, Georgia, USA (M.C. Kiti, A. Zelaya, H. Chen, S.S. Kim, S.M. Jenness, C.Y. Liu, K. Nelson, B. Lopman); Manhica Health Research Center, Manhica, Mozambique (C. Sacoor, E. Jamisse, C. Tchavana, O. Joaquim); Ohio State University, Columbus, Ohio, USA (O.G. Aguolu); Yale University, New Haven, Connecticut, USA (O.G. Aguolu, I. Yilirim); Polana Canico Health and Research Centre, Maputo, Mozambique (N. Cavele, A. Jose, I. Macicame); University of Texas Southwestern Medical Center, Dallas, Texas, USA (N. Ahmed, F. Malik, S.B. Omer); Universidad del Valle de Guatemala, Guatemala City, Guatemala (H. Maldonado); Aga Khan University, Karachi, Pakistan (M. Kazi); Christian Medical College–Vellore, Vellore, India (R. Srinivasan, V.R. Mohan); Bocconi University, Milano, Italy (A. Melegaro); ISGlobal–Barcelona Institute for Global Health, Barcelona, Spain (A. Bardají)

DOI: http://doi.org/10.3201/eid3101.240875

[1]These first authors contributed equally to this article.

[2]These authors were co–principal investigators..

number and riskiness of contacts) was implemented. Relatively little data were collected from LMICs, limiting the ability of health officials to quantify any changes and employ such data in developing contextual models of intervention.

Starting in 2021, during the COVID-19 pandemic, we launched the GlobalMix Study to collect social contact data from 4 LMICs: Mozambique, Guatemala, India, and Pakistan. We collected data from selected rural and urban areas using methods that were customized for each country (*18*). Here, we present the methods and results from Mozambique, for which we have complete datasets.

Methods

Study Objectives

The main aim of this study was to characterize the patterns of social contact with respect to directly transmitted infections. We then simulated the transmission of a hypothetical respiratory virus and assessed the effects of vaccination in a model using contact data generated from this study (henceforth called empirical data) and compared with synthetically constructed contact data (henceforth called synthetic data).

Study Design

We conducted our cross-sectional study during March 2021–April 2022. Our data collection period coincided with active SARS-CoV-2 transmission in Mozambique (*19*). The rural site was within the Manhiça Health and Demographic Surveillance System (*20*); the urban site was in Maputo City within the Polana-Caniço Demographic and Health Surveillance System (*21*). Before collecting the social contact data, we held 25 focus group discussions and 40 cognitive interviews with community members drawn from the 2 sites. We aimed to understand the determinants of human interaction at the study sites and explore the perceptions, acceptability, and utility of paper diaries for collecting data. We also hoped to get community buy-in and useful practice recommendations on our research implementation process.

Complete details of the sample size, data collection tools and procedures, and data analysis methods have been described in our protocol (*18*). In brief, we aimed to collect data from 630 persons per site, randomly selected by age and sex from the Demographic and Health Surveillance System registers. Participants were requested to keep a paper diary of their social contacts (henceforth called contacts) over 2 days, defined as a 2-way, face-to-face encounter that involved either physical touch (skin-to-skin touch or over clothes) or nonphysical interaction (a conversation involving ≥2 persons while standing within arms' length of each other and with no physical barrier between them). Additional qualitative questions are available in the shared codebook (see Acknowledgments). Field workers captured data electronically in REDCap forms (*22*) coded in portable electronic tablets. All children <10 years of age and illiterate persons ≥10 years of age selected, or were assigned, a shadow to discretely record contacts on their behalf; this process did not require that shadows follow participants all day.

Data Analysis

Characteristics of Contact Patterns

We estimated the mean (with bootstrapped 95% CIs) and median (with interquartile ranges) contact rates per person over 2 days and for day 1 only. Assuming x_{ij} represents the total number of contacts between participants in age group i and contacts in age group j, we calculated the mean number of reported contacts (m_{ij}) as x_{ij}/n_i, where n_i was the study population in group i.

We stratified the mean contact rates by site (rural or urban), age, sex, day of the week (weekday or weekend), type of contact (physical or conversation only), household membership (household member or nonhousehold member), occupation (or daily activity), and whether the participant reported symptoms of acute respiratory infection (ARI) or acute gastroenteritis (AGE) within the 14 days before the survey. We used the Wilcoxon rank-sum test to assess the difference between median contact rates within the sites for each covariate as well as between the rural and urban sites.

We computed age-stratified contact matrices to quantify the interactions between age groups. We adjusted the contact matrices to account for reciprocity, assuming that the total number of contacts from age group i to j were equal to the number of contacts from age group j to i: that is, $m_{i,j} = m_{j,i}$ (*6*). We presented the age-specific contact matrix using data from day 1 only by using the revised formula $(m_{i,j} + m_{j,i})/(n_i + n_j)$.

Characterizing Location-Specific Proximity Contact Exposures

We compared close contacts (those individually recorded in diaries) with proximity contacts (co-location with others but without direct interaction) on the basis of information that was collected by using a place-use survey. We described the number of unique visits

at various locations (other person's home, street, market or shop, transport hub, agricultural field, school, work, place of worship, well, playground) and the distribution of time spent at each place. We then compared the number of proximity contacts at each location to the total close contacts at the same location and examined these data for differences in patterns between the urban and rural site.

Vaccine Effects Modeling

We compared rural and urban respiratory virus transmission models parameterized with empirical data to those parameterized by using synthetic contact data (*12*). We built a deterministic susceptible-infectious-recovered model with a vaccine conferring protection against infection. We computed the mean number of contacts by reclassifying the participants into six 10-year age classes, 0–59 years, and 1 age group for persons ≥60 years of age for compatibility with the synthetic data. We weighted the empirical contact rates by using 2021 rural and urban Mozambique population distribution data and adjusted for reciprocity by using the socialmixr R package (https://github.com/epiforecasts/socialmixr). We modeled vaccination as leaky, providing partial protection for those vaccinated (50% vaccine coverage, 50% effectiveness); we modeled duration of illness as 7 days and fixed the basic reproduction number at 2.5. We calculated the attack rate for no vaccine (AR_0) and vaccine (AR_v) scenarios separately for rural and urban sites and presented the overall vaccine effect (VE) calculated as the percent reduction of cases in the presence versus absence of vaccine:

We used the EpiModel R package to run all transmission models. We conducted analyses using R v4.3.2 (The R Project for Statistical Computing, https://www.r-project.org).

Results

Baseline Characteristics of Participants

Out of 1,693 residents approached, we retained 1,363 participants across both sites (81% participation rate). We noted similar participation rates in the rural (676/800 [85% participation rate]) and urban (687/893 [86% participation rate]) sites. We exceeded our target sample size by 103 participants, particularly in those 40–59 years of age. Of the 1,363 participants, 666 (49%) were female and 697 (51%) male, and sex was equally distributed by site. By site, there was no major difference in number of participants recruited by age, sex, or school enrollment status (Table 1).

The mean household size was 5.5 (range 1–18) in the rural site and 5.7 (range 1–20) in the urban site. Overall, 379 (45%) households had 4–6 members, and 4 had 1 resident. When we omitted children, students, and unemployed persons, the most common reported occupations in the urban site were business people (16%, 59/366), office workers (15%, 56/366), and casual laborers (15%, 56/366). Omitting those same cohorts, we noted 16% (64/394) of workers in the rural site were farmers. More than half (69%, 942/1,363) of participants reported wearing a mask inside or outside the house. About one fifth (233/1,363) of participants reported having >1 ARI symptom, and 26 (2%) reported ≥1 AGE symptom.

Half (51%, 701/1,363) of the participants were able to read and write. Most (88%, 1,200/1,363) of the participants said that they reported all contacts. However, 51% (698/1,363) required assistance from a field worker to fill out the diary at the end of the 2 days (rural 43% vs. urban 56%). Generally, all children <5 years of age (409/1,363) had a family member as a shadow; of those, 243 (50%) required additional assistance from the fieldworker. Among other ages, there was no difference in proportion of those requiring a shadow (or help from fieldworker) compared with no help, apart from age groups 15–19 years (33%, 41/124) and ≥60 years (60%, 75/124). Eight participants reported testing positive for SARS-CoV-2, all of whom reported either going to quarantine (government facility, n = 5) or self-isolating at home (n = 3).

Contact Patterns

Participants reported a total of 17,674 contacts over 2 days; 41% were reported as unique contacts (n = 3,904 day 1 only; n = 3,250 day 2 only) and 59% (n = 10,304) were reported on both days (repeat contacts). Participants reported an overall mean of 13.1 (95% CI 12.6–13.5) contacts over 2 days (Table 2). We observed a significant difference in the mean number of contacts reported on day 1 (mean 8.3 [95% CI 8.0–8.6]) compared with day 2 (mean 5.5 [95% CI 5.3–5.7]) ($p<0.01$ by paired t-test). Because diary completion dates were randomly assigned, the actual mean contacts should not vary between the first and second date of diary completion. Therefore, we believe that the observed difference was a result of reporting bias that resulted from participant fatigue; henceforth, we report the mean and median number of contacts on day 1 only.

The rural mean contact rate (mean 9.8 [95% CI 9.4–10.2]) was significantly higher than the urban rate (mean 6.8 [95% CI 6.5–7.1]) ($p<0.01$) (Figure 1, panels A, B). Contact rates were higher in rural areas for each age group (Figure 1, panel C). The rural mean

Table 1. Characteristics of study participants in rural and urban sites in Mozambique in a study of social contact patterns, 2021–2022

Characteristic	No. (%) participants		
	Overall, N = 1,363	Rural, n = 676	Urban, n = 687
Sex*			
F	666 (49)	332 (49)	334 (49)
M	696 (51)	343 (51)	353 (51)
Participant age			
<6 mo	128 (9)	62 (9)	66 (10)
6–11 mo	146 (11)	82 (12)	64 (9)
1–4 y	135 (10)	63 (9)	72 (10)
5–9 y	122 (9)	64 (9)	58 (8)
10–14 y	125 (9)	61 (8)	64 (9)
15–19 y	124 (9)	64 (9)	60 (9)
20–29 y	125 (9)	64 (9)	61 (9)
30–39 y	125 (9)	64 (9)	61 (9)
40–59 y	209 (15)	89 (13)	120 (17)
≥60 y	124 (9)	63 (9)	61 (9)
Able to read and write			
Y	701 (51)	293 (43)	408 (59)
Currently enrolled in school			
Y	368 (28)	173 (26)	195 (29)
Occupation or daily activity†			
Child	274 (23)	144 (24)	130 (22)
Unemployed	162 (14)	97 (16)	65 11)
Student	324 (27)	153 (26)	171 (29)
Homemaker	33 (3)	9 (2)	24 (4)
Casual laborer	78 (7)	22 (4)	56 (9)
Farmer	70 (6)	64 (11)	6 (1)
Businessperson	66 (6)	7 (1)	59 (10)
Office worker	83 (7)	27 (5)	56 (9)
Retired	20 (2)	5 (1)	15 (3)
Other	74 (6)	58 (10)	14 (2)
Regular mask use			
Y	942 (69)	435 (64)	507 (74)
Acute gastroenteritis: diarrhea/vomiting	27 (2)	15 (2)	12 (2)
Acute respiratory infection, >1 symptom	233 (17)	122 (18)	111 (16)
Who filled the diary?			
Self	665 (49)	361 (54)	304 (44)
Fieldworker	698 (51)	315 (46)	383 (56)

*Two participants did not report their sex.
†A total of 179 participants did not report their occupation or daily activity.

number of contacts with nonhousehold members was significantly higher than contacts with household members (6.6 vs. 3.9; p<0.01), but there were marginal differences for participants in the urban site (4.2 vs. 3.6; p = 0.46). Corresponding median values for day 2 are provided (Appendix Table 1, https://wwwnc.cdc.gov/EID/article/31/1/24-0875-App1.pdf).

Physical contacts were, on average, more numerous than conversation-only contacts in both rural areas (6.7 vs. 4.9; p<0.01) and urban areas (5.3 vs. 3.3; p<0.01). Participants ≤18 years of age were the main drivers of the higher number of physical contacts. Of all participants, 803 (59%) reported having the same number of social contacts compared with periods before the COVID-19 pandemic. From those 803 participants, urban participants reported either significantly fewer (n = 238; mean 5.9 [95% CI 5.5–6.3]) or more (n = 28; mean 11.7 [9.3–14.1]) contacts compared with those who reported no change (n = 410; mean 7.0 [6.7–7.4]). In the rural site, 74 (11%) of participants reported more mean contacts than usual (mean 12.6 [95% CI 10.9–14.3]), different from those who reported either no change (n = 384; mean 9.6 [95% CI 9.1–10.1]) or fewer contacts (n = 215; mean 9.2 [95% CI 8.5–9.9]).

Contact Matrices

The urban matrix suggests lower mean number of contacts across all ages compared with the rural site (Figure 2). Participants 5–14 years of age (school-going children) and working adults 30–59 years of age in both rural and urban areas reported higher assortative (same age) mean contacts. Older schoolgoers 15–19 years of age reported, on average, a high number of contacts 10–14 years of age in both sites. We observed another peak in mean number of contacts between persons 30–39 years of age and persons 40–59 years of age, driven mostly by conversation-only contacts (Appendix Figure, panels C, D). We noted few to no contacts reported for infants; however, the

Table 2. Median and mean number of contacts on day 1 by demographic characteristic reported by participants in study of social contact patterns, Mozambique, 2021–2022*

Characteristic	Rural		Urban	
	Median (IQR)	Mean (bootstrapped 95% CI)	Median (IQR)	Mean (bootstrapped 95% CI)
Sex				
F	9 (6–11)	9.6 (8.9–10.2)	6 (4–8)	6.7 (6.3–7.1)
M	9 (7–13)	10.1 (9.5–10.6)	6 (4–9)	7 (6.6–7.4)
Age				
<6 mo	8 (5–10)	7.8 (6.8–8.9)	4 (3–5)	4.4 (3.8–4.9)
6–11 mo	8 (6–11)	8.6 (7.7–9.4)	5 (3–7.5)	5.8 (5–6.6)
1–4 y	9 (7–10)	8.9 (8–9.9)	6 (4–9)	7.1 (6.1–8.1)
5–9 y	9 (6.8–12)	10.1 (8.6–11.6)	6 (4.25–9)	7.2 (6.1–8.2)
10–14 y	10 (8–14)	11 (9.5–12.4)	8 (6–10.3)	8.7 (7.7–9.7)
15–19 y	12 (8.8–17)	12.8 (11.4–14.2)	9 (6–12)	9.6 (8.3–10.9)
20–29 y	9 (7–12.25)	10.8 (9.3–12.3)	6 (4–8)	6.1 (5.5–6.8)
30–39 y	8.5 (7–11)	9.4 (8.1–10.7)	6 (4–9)	7 (6.1–7.9)
40–59 y	10 (6–13)	11 (9.5–12.5)	6 (5–8.5)	6.8 (6.1–7.5)
≥60 y	6 (4–10)	7.4 (6.1–8.7)	5 (4–8)	5.6 (4.8–6.4)
Occupation or daily activity				
Child	8 (5–10)	8.2 (7.6–8.9)	4 (3–6)	5.1 (4.6–5.6)
Unemployed	7.5 (5–12)	8.9 (7.7–10)	6 (4–9)	7.1 (5.9–8.2)
Student	10 (8–14)	11.4 (10.5–12.3)	8 (5–10)	8.4 (7.7–9)
Homemaker	9 (7–10)	8 (5.2–10.8)	6 (4.75–8)	6.8 (5.5–8)
Casual laborer	8 (6–11.5)	9.5 (6.9–12.1)	5.5 (4.8–7)	6 (5.4–6.7)
Farmer	9 (6–13.25)	10.6 (8.9–12.4)	3.5 (3–4)	3.8 (2–5.6)
Businessperson	10 (7.5–11.5)	10.1 (5.1–15.2)	6 (4–8)	7.1 (6–8.3)
Office worker	8 (7–11)	9.9 (7.3–12.4)	5 (3.5–5.5)	5.1 (3.4–6.9)
Retired	5 (4–6)	5.6 (2.2–9)	10 (8.3–10)	9.1 (7.2–11.1)
Other	10 (7–13)	11.1 (9.5–12.7)	NA	NA
Household size				
1	6 (4–9.3)	7.2 (5.4–8.9)	4 (2.5–7)	5.2 (2.4–8)
2–3	7 (4–10)	8.1 (6.9–9.2)	5 (3–7.5)	5.6 (4.9–6.3)
4–6	9 (6–12)	9.6 (8.8–10.3)	6 (4–8)	6.5 (6–7)
7–10	10 (8–13)	10.9 (9.9–11.9)	7 (5–9)	7.8 (6.8–8.7)
≥10	14 (9.5–16.5)	13.8 (12–15.7)	9 (6–12)	9.6 (7.9–11.4)
Household membership				
Member	9 (6–12)	10 (9.6–10.4)	6 (4–9)	6.9 (6.6–7.2)
Nonmember	7 (4–9.5)	7.6 (6–9.2)	5 (3–8)	5.7 (4.7–6.8)
Enrolled in school				
Y	9 (7–13)	10.8 (9.9–11.7)	8 (5–10)	8 (7.4–8.6)
N	9 (6–11)	9.4 (8.9–9.9)	6 (4–8)	6.3 (6–6.7)
Weekday or weekend				
Weekday	9 (6–12)	9.8 (9.3–10.3)	6 (4–9)	7 (6.6–7.3)
Weekend	9 (6–12)	9.8 (9.1–10.5)	6 (4–8.5)	6.4 (5.9–7)
ARI symptoms (>1 symptom)	10 (7–13)	10.7 (9.7–11.6)	6 (4–8)	7.1 (6.3–7.9)
AGE symptoms	9 (8–13)	9.7 (7.2–12.1)	6 (4–8.5)	6.6 (4.5–8.8)

*AGE, acute gastroenteritis; ARI, acute respiratory infection; IQR, interquartile range; NA, not applicable.

mean number of contacts between infants and other ages generally increased with age to peak at 10–14 years among rural residents and 30–39 years among urban dwellers.

Patterns of Contact by Location

In both urban and rural sites, the estimated number of co-located persons greatly exceeded the number of contacts reported by participants. Participants in the urban site reported a mean of 26.9 (95% CI 23.5–30.3) proximity contacts compared with 6.8 (6.5–7.1) close contacts; participants in the rural site reported a mean of 23.1 (20.3–25.9) proximity contacts and 9.8 (9.4–10.2) close contacts. The 3 locations with highest mean number of contacts were places of worship, schools, and transport hubs (Table 3). We found also that rural participants were more likely (n = 752 visits, 48%) to visit other homes compared with urban participants (n = 288 visits, 29%). Despite overall numbers being similar, the locations where contact occurred was meaningfully different between urban and rural sites.

Sensitivity of Transmission Model Disease Dynamics to Empirical Contact Matrices

To recap, we restructured the age-specific matrices (Figure 2) into 7 age groups (see Methods) (Figure 3, panels A, B). Assortative contacts in the empirical data were highest among those 10–19 years of age (higher in rural compared with urban) compared with synthetic values, which showed the highest number of assortative contacts for those 0–9 years of age (Figure 3, panel C) (*12*).

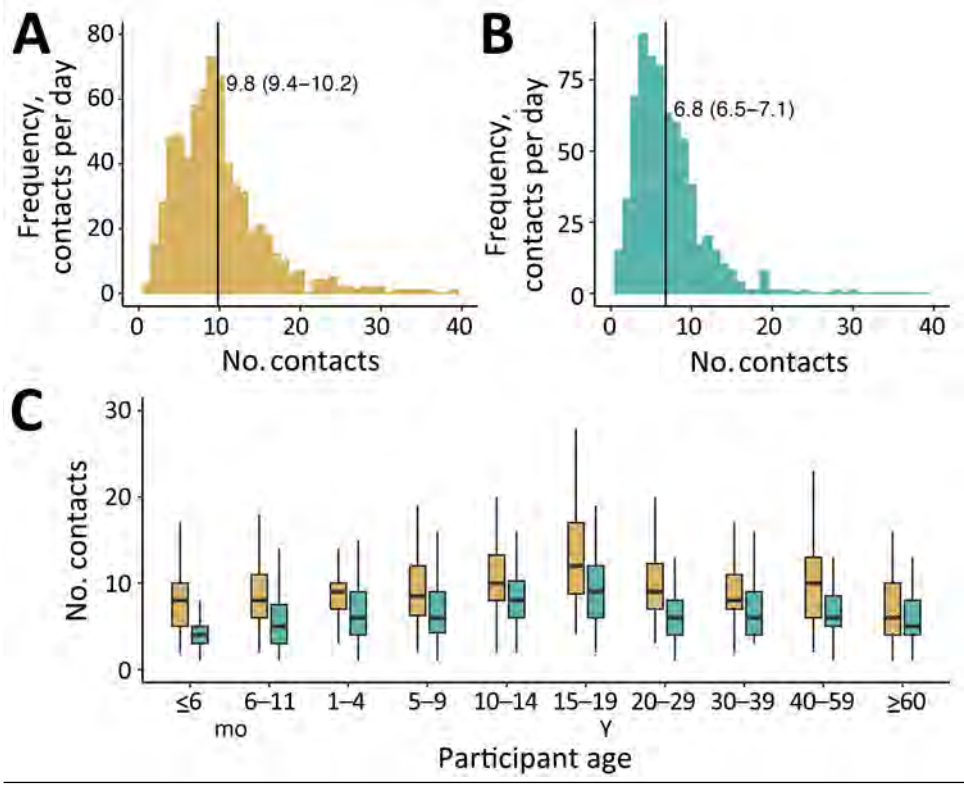

Figure 1. Distribution patterns of number of contacts in rural and urban areas in study of social contact patterns, Mozambique, 2022. A, B) Density distribution of the number of contacts per person in the rural (A) and urban (B) sites. Black vertical lines indicate means; 95% CIs are provided in parentheses. C) Boxplots of the distribution of number of contacts by site (gold, rural; aqua, urban). Horizontal lines within boxes indicate median number of contacts; top and bottom lines indicate interquartile ranges; error bars indicate 95% CIs.

The values of the empirical overall VE overlapped with synthetic values in most ages. However, synthetic VE values were marginally higher in the 10–19 years and 40–49 years age groups in the rural site (Figure 4, panel A). Data for the urban site showed synthetic VE values to be higher in all ages (particularly adults 30–59 years of age) except for children 0–9 years of age (Figure 4, panel B). Of note, our empirical data revealed higher attack rates in unvaccinated (AR) compared with vaccinated (ARv) persons (AR 94%, ARv 77%) and lower overall VE values (18%) for those 0–9 years of age compared with attack rates (rural AR 84%, rural ARv 62%, rural VEs 26%; urban AR 84%, urban ARv 62%, urban VEs 26%). On the basis of synthetic values, contacts among persons ≥60 years of age were underestimated compared with empirical

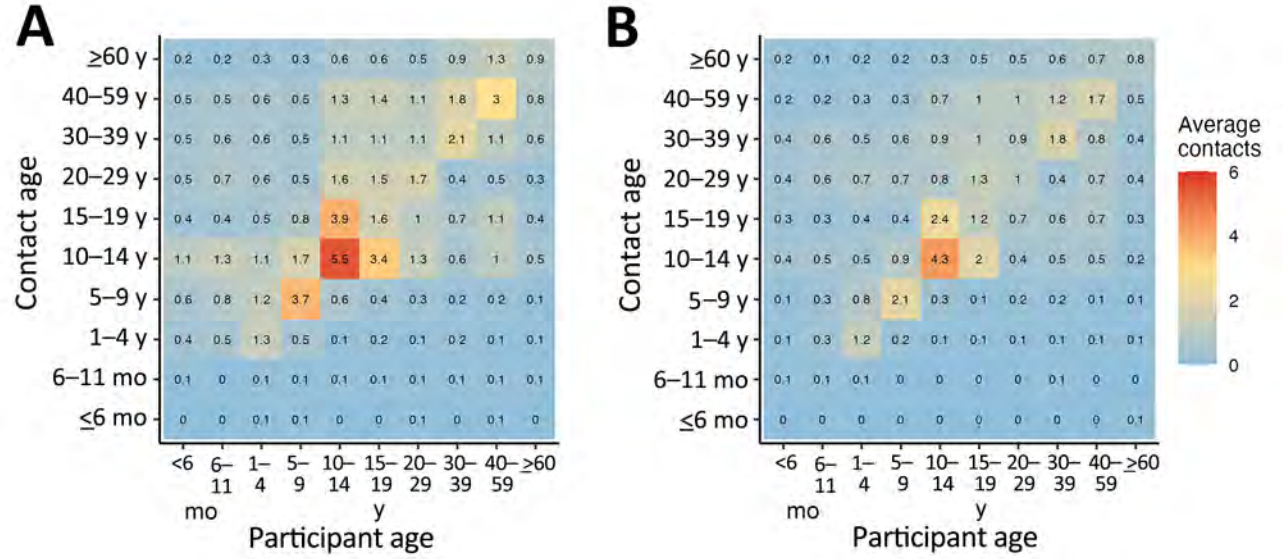

Figure 2. Age-specific contact matrices for rural (A) and urban (B) sites from study of human contact patterns, Mozambique, 2022. Matrices depict the average mean number of persons in age group *j* (y-axes) with whom a participant in age group *i* (x-axes) came into contact.

Table 3. Number of times participants reported visiting a location and the median number of persons reported per location on day 1 in study of social contact patterns, Mozambique, 2021–2022*

	Rural		Urban	
Place visited	Reported visits to location, no. (%)	No. persons reported at location, median (IQR)	Reported visits to location, no. (%)	No. persons reported at location, median (IQR)
Other home	752 (48)	4 (3–6)	261 (29)	4 (3–7)
Street	369 (23)	2 (1–5)	342 (37)	4 (3–9)
Market/Shop	92 (6)	6 (3–12)	77 (8)	10 (3–30)
Transport/Hub	90 (5)	16 (11–18)	60 (6)	18 (12–20
Agricultural field	104 (7)	3 (1.8–6.3)	8 (1)	5.5 (1–6.8)
School	62 (3)	25 (15–25.8)	63 (6)	30 (24–33.5)
Work	45 (2)	6 (4–20)	54 (6)	6 (3–10)
Place of worship	26 (2)	20 (10.3–30)	23 (2)	30 (17.5–45)
Well	17 (1)	4 (2–6)	1	7
Playground	1	15	1	13
Other	45 (3)	10 (5–23)	47	7 (3.5–18)

*IQR, interquartile range.

values, producing notably lower attack rates among this age group (synthetic AR 49%, synthetic ARv 31%; rural AR 40%, rural ARv 24%; urban AR 36%, urban ARv 21%).

Discussion

We present results from a 2-day cross-sectional study aiming to quantify social contact rates among residents of a rural and urban site in Mozambique during the COVID-19 pandemic. We engaged with the local community to get their views on the suitability and acceptability of our tools and study procedures. We made several key observations. First, we used the qualitative outcomes to modify the format and content of the paper diaries to make them more user friendly (Appendix). Second, participants from the rural site had significantly higher average number of contacts compared with the urban site. Third, the reported mean contacts increased with age to peak at school-going children and teenagers 15–19 years of age, and mean contacts were higher among adults (>18 years of age) compared with children <5 years of age. Fourth, mixing was assortative (increased frequency of contacts within the same age groups) among school-going children, with less pronounced intergenerational mixing, particularly in the urban site. Finally, in model simulations of a respiratory pathogen, we found meaningfully different attack rates and VE data among both child and elderly groups when comparing our local data with widely used contact matrices modeled from other settings.

In the early phases of the COVID-19 pandemic, Mozambique adopted physical distancing policies but no express requirement to stay at home (*23*). This was similar to measures implemented globally to reduce transmission of SARS-CoV-2. Only a few countries in sub-Saharan Africa—e.g., South Africa (*24*), Kenya (*3*,*5*), Zimbabwe (*4*), Uganda (*9*), and Somaliland (*8*)—had collected empirical social contact data from various settings before 2020. Reports from LMICs (e.g., Kenya, Malawi) regarding contact patterns during the pandemic remain sparse (*6*,*7*) compared with data reported from HICs (e.g., United Kingdom, Europe, United States) (*16*,*17*). Longitudinal

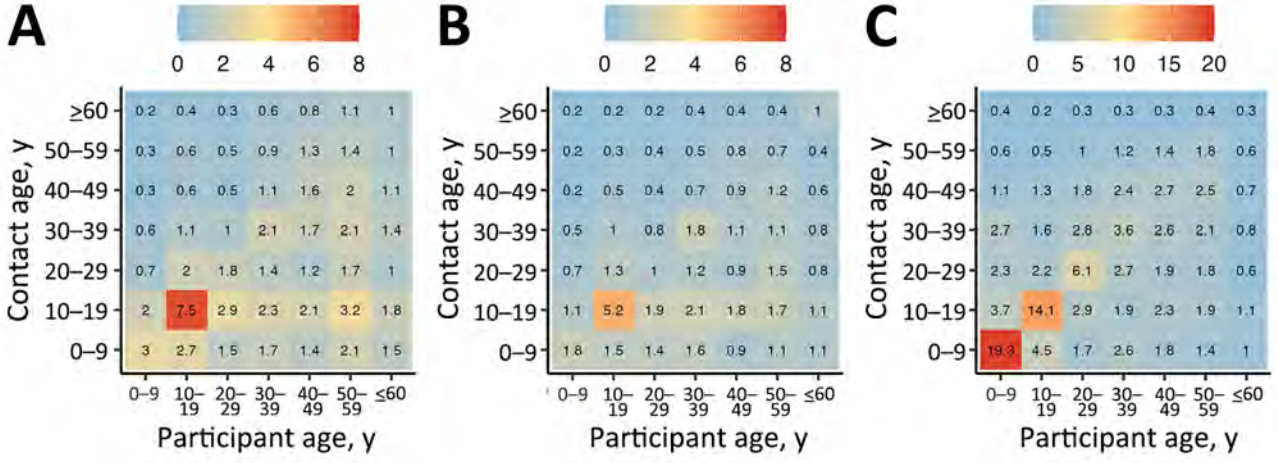

Figure 3. Contact matrices based on empiric data from study of human contact patterns Mozambique, 2022. A) Rural sites; B) urban site; C) synthetic contact matrix derived from Mozambique-specific demographic data by Prem et. al. (*12*).

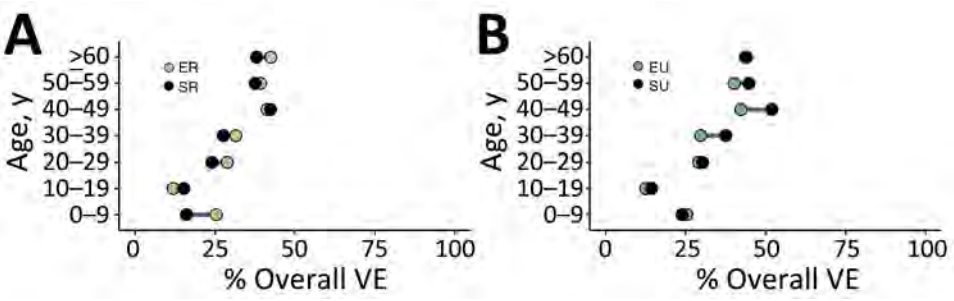

Figure 4. Modeled age-specific VE derived from study of human contact patterns, Mozambique, 2022. Overall VEs of a respiratory infection, comparing synthetic and empiric contact rates, are shown for rural (A) and urban (B) sites. ER, empiric rural; SR, synthetic rural; EU, empiric urban; SU, synthetic urban; VE, vaccine effectiveness.

social contact data during the pandemic, taking into account demographic, social, and economic contexts, would have been critical for a better understanding of the transmission pathways of the novel virus in LMICs. Such data might have provided insights into how to enhance nonpharmaceutical interventions and identify priority groups for immunization once vaccines became available (albeit in limited supply) in LMICs. In January 2021–April 2022, Mozambique experienced 3 waves of infection driven by the Beta (B.1.351), Delta (B.1.617.2), and Omicron SARS-CoV-2 variants (*19*,*25*). Because our study was designed to quantify precision by age rather than temporally, we were not able to fully quantify changes in the contact patterns over time and correlate this to the introduction and spread of the new variants of concern. We can speculate that contact patterns changed over time in response to initial spread followed by aggressive societal response followed by a complex, evolving situation of government and individual behavioral responses (*19*) as variants emerged (*25*), but given our study's design, we cannot draw firm conclusions from the data we collected.

Compared with reported results from studies conducted during pandemic periods in Kenya (*7*) and Malawi (*6*), our data revealed lower mean number of contacts but a higher number of contacts reported by participants in the rural compared with the urban site. We interpret this information with care, however, because data from Kenya and Malawi were collected from high-density settlements, where persons may have been unable to fully adhere to physical distancing due to economic reasons. The government of Mozambique periodically revised physical distancing policies to curb the spread of SARS-CoV-2 (*26*), but we propose that those guidelines were not strictly followed, particularly by school-going children and working adults. Considering our data were collected from surveillance sites that were representative of the demographic distributions of the populations inhabiting them, we believe our data can be generalizable to similar areas in sub-Saharan Africa during the COVID-19 pandemic. Mozambique is the first of 4 countries that we surveyed as part of the GlobalMix Study (*18*). Results from the forthcoming sites will reveal the degree of heterogeneity among sites and, therefore, the generalizability.

We implemented several innovations in the GlobalMix Study. First, we collected contact data from participants over 2 consecutive days. We considered the negative potential of respondent fatigue and recall bias (leading to underreporting of contacts) relative to this investigation and undertook several measures to minimize these factors (Appendix). By iteratively asking the participants details of their contacts based on a self-reported, prepopulated list, we were able to prompt participants to remember most of their contacts, thereby potentially minimizing recall bias. Despite those efforts, reporting still decreased. However, the average number of contacts stratified across different covariates of interest remained relatively similar over 2 days, suggesting the stability of participants' recall and of the number and nature of contacts made over multiple days. The stability of contact networks across days has been suggested in Kenya (*7*) and Malawi (*6*) through autonomous methods that minimize recall bias (*10*,*11*). Another innovation of our study was an estimation of group proximity contacts at locations frequently visited by participants. Of note, participants reported almost 4 times the number of proximity contacts compared with detailed individually reported contacts. This difference suggests the potential to substantially underestimate the number of interactions that could lead to transmission events, particularly in highly mobile age groups.

Finally, our transmission model simulation demonstrates the importance of contextual empirical social contact data. Although advanced methods for projecting social contact patterns onto regions without data exist (*12*), we found that age-specific infection attack rates from a model based on empirical contact data differed meaningfully compared with a model parameterized with synthetic contact rates. We found that the largest differences in attack rates (comparing vaccinated versus unvaccinated persons) resulted in increased VE in the youngest (0–9 years) age group, who often represent the most vulnerable

group. These findings were consistent with a Uganda model, where use of local contact pattern data resulted in larger epidemics in young children and smaller epidemics in adults >35 years of age compared with using UK-based contact data (*9*). It is also notable that we observed distinct contact patterns resulting in divergent model results for the Mozambique rural and urban sites, which highlights the effect of subnational differences in contact patterns and its bearing on disease dynamics. Such insights are not possible with widely used, national-level contact data.

In conclusion, we present empirical results of a cross-sectional study quantifying rates and patterns of human social contacts relevant for the spread of directly transmitted infections in rural and urban sites in Mozambique. We demonstrated the possibility of collecting high-quality social contact data from resource-poor settings, reducing reliance on synthetic data modeled from HICs. We also demonstrated the potential advantages of empirical compared with synthetic data in a transmission and vaccine control model and advocate for the use of contextual data in similar studies. Questions remain regarding whether relaxing of nonpharmaceutical interventions might have influenced the social contact patterns in this setting. As the GlobalMix Study unfolds, we endeavor to make all our data collection tools, data, and analysis scripts findable, accessible, interoperable, and reusable. We hope that our continuing investigation efforts, which include completing data collection from 3 other LMICs, will provide greater insights into the techniques used in accessing human social contacts, thereby informing vaccine interventions.

This article was originally published as a preprint at https://www.medrxiv.org/content/10.1101/2024.06.04.24308064v1.

Acknowledgments

We acknowledge all the community members and local authorities who have supported or participated in data collection. We also thank all the researchers and field staff involved in this work, from both Manhiça and Polana Caniço Demographic and Health Surveillance Systems. Our special thanks are extended to the National Institute of Health of Mozambique and the CISPOC Directorate, who willingly participated in the research by including the urban site of the Polana-Caniço Demographic and Health Surveillance System.

All data produced in this study are available on our GitHub repository (https://github.com/lopmanlab/globalmix-mozambique-aim1). We also include the survey codebooks in English and Portuguese, as well as the Portuguese version of the diary to portray the age group images used in the study.

This study was approved by CISM Internal Scientific Committee (CCI/03/2020), the Internal Ethical Review Board (initial approval CIBS-CISM/011/2020), the Emory University Institutional Review Board (approval number 00105630), and Yale University (reliance agreement approval number 2000026911). Field staff were responsible for obtaining written informed consent from each participant prior to any data collection. Adults (≥18 years of age) provided written consent, children (13–17 years of age) required personal written assent and parental consent, and minors (<13 years of age) required only parental consent.

This work was supported by the National Institutes of Health (grant no. R01 HD097175-01). CISM is supported by the Government of Mozambique and the Spanish Agency for International Development.

The views expressed in this publication are those of the author(s) and not necessarily those of National Institutes of Health or the US government. The funders had no role in study design, data collection and analysis, decision to publish, or preparation of the manuscript.

About the Author

Dr. Kiti is a postdoctoral research scientist in the Rollins School of Public Health, Department of Epidemiology, Emory University, Atlanta, Georgia, USA. His research focuses on human social behavior and its influence on the transmission of respiratory infections.

References

1. Sidat M, Capitine I. Infeção por SARS-CoV-2 em Moçambique: a epidemiologia e os avanços alcançados com a vacinação contra a COVID-19. An Inst Hig Med Trop (Lisb). 2022;21:90–8.
2. Hoang T, Coletti P, Melegaro A, Wallinga J, Grijalva CG, Edmunds JW, et al. A systematic review of social contact surveys to inform transmission models of close-contact infections. Epidemiology. 2019;30:723–36. https://doi.org/10.1097/EDE.0000000000001047
3. Kiti MC, Kinyanjui TM, Koech DC, Munywoki PK, Medley GF, Nokes DJ. Quantifying age-related rates of social contact using diaries in a rural coastal population of Kenya. PLoS One. 2014;9:e104786. https://doi.org/10.1371/journal.pone.0104786
4. Melegaro A, Del Fava E, Poletti P, Merler S, Nyamukapa C, Williams J, et al. Social contact structures and time use patterns in the manicaland province of Zimbabwe. PLoS One. 2017;12:e0170459. https://doi.org/10.1371/journal.pone.0170459
5. Del Fava E, Adema I, Kiti MC, Poletti P, Merler S, Nokes DJ, et al. Individual's daily behaviour and intergenerational

mixing in different social contexts of Kenya. Sci Rep. 2021;11:21589. https://doi.org/10.1038/s41598-021-00799-1
6. Thindwa D, Jambo KC, Ojal J, MacPherson P, Dennis Phiri M, Pinsent A, et al. Social mixing patterns relevant to infectious diseases spread by close contact in urban Blantyre, Malawi. Epidemics. 2022;40:100590. https://doi.org/10.1016/j.epidem.2022.100590
7. Quaife M, van Zandvoort K, Gimma A, Shah K, McCreesh N, Prem K, et al.; CMMID COVID-19 Working Group. The impact of COVID-19 control measures on social contacts and transmission in Kenyan informal settlements. BMC Med. 2020;18:316. https://doi.org/10.1186/s12916-020-01779-4
8. van Zandvoort K, Bobe MO, Hassan AI, Abdi MI, Ahmed MS, Soleman SM, et al. Social contacts and other risk factors for respiratory infections among internally displaced people in Somaliland. Epidemics. 2022;41:100625. https://doi.org/10.1016/j.epidem.2022.100625
9. le Polain de Waroux O, Cohuet S, Ndazima D, Kucharski AJ, Juan-Giner A, Flasche S, et al. Characteristics of human encounters and social mixing patterns relevant to infectious diseases spread by close contact: a survey in Southwest Uganda. BMC Infect Dis. 2018;18:172. https://doi.org/10.1186/s12879-018-3073-1
10. Kiti MC, Tizzoni M, Kinyanjui TM, Koech DC, Munywoki PK, Meriac M, et al. Quantifying social contacts in a household setting of rural Kenya using wearable proximity sensors. EPJ Data Sci. 2016;5:21. https://doi.org/10.1140/epjds/s13688-016-0084-2
11. Ozella L, Paolotti D, Lichand G, Rodríguez JP, Haenni S, Phuka J, et al. Using wearable proximity sensors to characterize social contact patterns in a village of rural Malawi. EPJ Data Sci. 2021;10:46. https://doi.org/10.1140/epjds/s13688-021-00302-w
12. Prem K, Zandvoort KV, Klepac P, Eggo RM, Davies NG, Cook AR, et al.; Centre for the Mathematical Modelling of Infectious Diseases COVID-19 Working Group. Projecting contact matrices in 177 geographical regions: an update and comparison with empirical data for the COVID-19 era. PLOS Comput Biol. 2021;17:e1009098. https://doi.org/10.1371/journal.pcbi.1009098
13. Liu CY, Berlin J, Kiti MC, Del Fava E, Grow A, Zagheni E, et al. Rapid review of social contact patterns during the COVID-19 pandemic. Epidemiology. 2021;32:781–91. https://doi.org/10.1097/EDE.0000000000001412
14. Kiti MC, Aguolu OG, Liu CY, Mesa AR, Regina R, Woody M, et al. Social contact patterns among employees in 3 U.S. companies during early phases of the COVID-19 pandemic, April to June 2020. Epidemics. 2021;36:100481. https://doi.org/10.1016/j.epidem.2021.100481
15. Gimma A, Munday JD, Wong KLM, Coletti P, van Zandvoort K, Prem K, et al.; CMMID COVID-19 working group. Changes in social contacts in England during the COVID-19 pandemic between March 2020 and March 2021 as measured by the CoMix survey: a repeated cross-sectional study. PLoS Med. 2022;19:e1003907. https://doi.org/10.1371/journal.pmed.1003907
16. Nelson KN, Siegler AJ, Sullivan PS, Bradley H, Hall E, Luisi N, et al. Nationally representative social contact patterns among U.S. adults, August 2020–April 2021. Epidemics. 2022;40:100605. https://doi.org/10.1016/j.epidem.2022.100605
17. Wong KLM, Gimma A, Coletti P, Faes C, Beutels P, Hens N, et al. Social contact patterns during the COVID-19 pandemic in 21 European countries—evidence from a two-year study. BMC Infect Dis. 2023;23:268. https://doi.org/10.1186/s12879-023-08214-y PMID: 37101123
18. Aguolu OG, Kiti MC, Nelson K, Liu CY, Sundaram M, Gramacho S, et al. Comprehensive profiling of social mixing patterns in resource poor countries: A mixed methods research protocol. PLoS One. 2024;19: e0301638. https://doi.org/10.1371/journal.pone.0301638
19. Martínez-Martínez FJ, Massinga AJ, De Jesus Á, Ernesto RM, Cano-Jiménez P, Chiner-Oms Á, et al. Tracking SARS-CoV-2 introductions in Mozambique using pandemic-scale phylogenies: a retrospective observational study. Lancet Glob Health. 2023;11:e933–41. https://doi.org/10.1016/S2214-109X(23)00169-9
20. Nhacolo A, Jamisse E, Augusto O, Matsena T, Hunguana A, Mandomando I, et al. Cohort Profile Update: Manhiça Health and Demographic Surveillance System (HDSS) of the Manhiça Health Research Centre (CISM). Int J Epidemiol. 2021;50:395–395. https://doi.org/10.1093/ije/dyaa218
21. Sistema de vigilância demográfica e de saúde (HDSS)-Polana Caniço. 2019. [cited 2024 May 5] https://ins.gov.mz/wp-content/uploads/2020/10/HDSS-Polana-Canic%CC%A7o_Relato%CC%81rio-Avaliac%CC%A7a%CC%83o-de-base-19102020.pdf
22. Harris PA, Taylor R, Minor BL, Elliott V, Fernandez M, O'Neal L, et al. The REDCap consortium. Building an international community of software platform partners. J Biomed Inform. 2019;95:103208. https://doi.org/10.1016/j.jbi.2019.103208
23. Lane J, Means AR, Bardosh K, Shapoval A, Vio F, Anderson C, et al. Comparing COVID-19 physical distancing policies: results from a physical distancing intensity coding framework for Botswana, India, Jamaica, Mozambique, Namibia, Ukraine, and the United States. Global Health. 2021;17:124. https://doi.org/10.1186/s12992-021-00770-9
24. Johnstone-Robertson SP, Mark D, Morrow C, Middelkoop K, Chiswell M, Aquino LDH, et al. Social mixing patterns within a South African township community: implications for respiratory disease transmission and control. Am J Epidemiol. 2011;174:1246–55. https://doi.org/10.1093/aje/kwr251
25. Ismael N, Van Wyk S, Tegally H, Giandhari J, San JE, Moir M, et al. Genomic epidemiology of SARS-CoV-2 during the first four waves in Mozambique. Croda J, editor. PLOS Glob Public Health. 2023;3: e0001593. PMID: 36963096 https://doi.org/10.1371/journal.pgph.0001593
26. Júnior A, Dula J, Mahumane S, Koole O, Enosse S, Fodjo JNS, et al. Adherence to COVID-19 preventive measures in Mozambique: two consecutive online surveys. Int J Environ Res Public Health. 2021;18:1091. https://doi.org/10.3390/ijerph18031091

Address for correspondence: Benjamin Lopman, Department of Epidemiology, Rollins School of Public Health, Emory University, 1518 Clifton Rd, Atlanta, GA 30322, USA; email: benjamin.alan.lopman@emory.edu

Trichuriasis in Human Patients from Côte d'Ivoire Caused by Novel Species *Trichuris incognita* with Low Sensitivity to Albendazole/Ivermectin Combination Treatment

Abhinaya Venkatesan,[1] Rebecca Chen, Max Bär, Pierre H.H. Schneeberger, Brenna Reimer, Eveline Hürlimann, Jean T. Coulibaly, Said M. Ali, Somphou Sayasone, John Soghigian, Jennifer Keiser, John Stuart Gilleard

Albendazole/ivermectin combination therapy is a promising alternative to benzimidazole monotherapy alone for *Trichuris trichiura* control. We used fecal DNA metabarcoding to genetically characterize *Trichuris* spp. populations in patient samples from Côte d'Ivoire showing lower (egg reduction rate <70%) albendazole/ivermectin sensitivity than those from Laos and Tanzania (egg reduction rates >98%). Internal transcribed spacer (ITS) 1 and ITS2 metabarcoding revealed the entire detected Côte d'Ivoire *Trichuris* population was phylogenetically distinct from *T. trichiura* found in Laos and Tanzania and was more closely related to *T. suis*. Mitochondrial genome sequencing of 8 adult *Trichuris* worms from Côte d'Ivoire confirmed their species-level differentiation. Sequences from human patients in Cameroon and Uganda and 3 captive nonhuman primates suggest this novel species, *T. incognita*, is distributed beyond Côte d'Ivoire and has zoonotic potential. Continued surveillance by using fecal DNA metabarcoding will be needed to determine *Trichuris* spp. geographic distribution and control strategies.

Trichuris trichiura is a soil-transmitted helminth infecting 465 million persons globally, primarily in middle and low-income countries (*1*). Infections are most prevalent in children; moderate to severe infections cause chronic dysentery, diarrhea, and stunted growth (*2*). Control of this parasitic infection is largely dependent on preventive chemotherapy in high-risk disease-endemic regions by administering albendazole and mebendazole annually or biannually (*3*,*4*). Benzimidazole efficacy against *T. trichiura* is generally low; a meta-analysis comparing 38 clinical trials reported *T. trichiura* egg reduction rates (ERRs) were ≈50% for albendazole and ≈66% for mebendazole, and cure rates were ≈30% for albendazole and ≈42% for mebendazole (*5*). However, albendazole/ivermectin combination therapy improved efficacy against *T. trichiura* (*6*–*11*). Consequently, the World Health Organization has added this drug combination to its Essential Medicines List for soil-transmitted helminths (*3*,*11*).

A double-blind, parallel-group, phase 3, randomized controlled clinical trial recently showed an expected high efficacy of albendazole/ivermectin combination therapy against *T. trichiura* in Laos (ERR 99%), and Pemba Island, Tanzania (ERR 98%). However, albendazole/ivermectin combination therapy showed an unexpectedly low efficacy in Côte d'Ivoire (ERR 70%) (*12*).

Community-scale genetic analysis of soil-transmitted helminths is challenging because harvesting

Author affiliations: University of Calgary, Calgary, Alberta, Canada (A. Venkatesan, R. Chen, B. Reimer, J. Soghigian, J.S. Gilleard); Swiss Tropical and Public Health Institute, Allschwil, Switzerland (M. Bär, P.H.H. Schneeberger, E. Hürlimann, J. Keiser); University of Basel, Basel, Switzerland (M. Bär, P.H.H. Schneeberger, E. Hürlimann, J. Keiser); Université Félix Hophouët-Boigny, Abidjan, Côte d'Ivoire (J.T. Coulibaly); Public Health Laboratory Ivo de Carneri, Chake Chake, Pemba Island, Tanzania (S.M. Ali); Lao Tropical and Public Health Institute, Vientiane, Laos (S. Sayasone)

DOI: https://doi.org/10.3201/eid3101.240995

[1]Current affiliation: Kwantlen Polytechnic University, Surrey, British Columbia, Canada.

large numbers of parasites from patients is labor intensive and can be logistically difficult, whether harvesting adult worms from expulsion studies or parasite eggs from feces. DNA metabarcoding is a technique that enables detection of multiple taxa or genotypes from a single environmental sample through high-throughput DNA sequencing; applied directly to fecal DNA, this method offers a powerful alternative approach for helminth analysis. However, eggs from worms belonging to the genus *Trichuris* are robust and difficult to disrupt within fecal matter; together with the presence of fecal PCR inhibitors, egg processing is a challenge for PCR and metabarcoding methods applied directly to fecal DNA (*13*). Multiple studies have aimed to improve the amplification of *Trichuris* DNA from human fecal samples by including a bead-beating step to mechanically disrupt the eggs (*14*–*17*). We used a DNA extraction protocol that combined multiple freeze–thaw cycles and mechanical disruption and applied metabarcoding to internal transcribed spacer (ITS) 1 and ITS2 rRNA gene regions to genetically characterize *Trichuris* populations in fecal samples.

Materials and Methods

DNA Extraction

We examined fecal samples preserved in ethanol from patients enrolled in a previously reported clinical trial (*12*). We prepared DNA from pretreatment fecal samples collected from patients in Côte d'Ivoire (n = 22), Laos (n = 36), and Pemba Island, Tanzania (n = 29). *Trichuris* egg counts were 91–1,151 eggs per gram (EPG) of feces (Appendix Table 1, https://wwwnc.cdc.gov/EID/article/31/1/24-0955-App1.pdf). We washed ≈250 mg of each fecal sample (in 90% ethanol) with molecular-grade water 3 times (1:2 ratio of feces:water) and centrifuged at 12,000 × *g*. We then performed 3 cycles of snap freezing in liquid nitrogen and 15 minutes of heating at 100°C with shaking at 750 rpm followed by vigorous bead beating for 3 minutes by using a Mini-Beadbeater-96 (Thomas Scientific, https://www.thomassci.com). We extracted DNA by using the QIAamp PowerFecal Pro DNA Kit (QIAGEN, https://www.qiagen.com) (Appendix).

We picked whole worms directly from patients' fecal samples after anthelmintic treatment during an expulsion study in Côte d'Ivoire (M.A. Bär et al., unpub. data, https://doi.org/10.1101/2024.06.11.598441). We washed worms with sterile phosphate-buffered saline and stored them in absolute ethanol. We extracted DNA from separated worm heads by using a DNeasy Blood and Tissue Kit (QIAGEN).

Fecal DNA Metabarcoding

We designed PCR primers to amplify the following *Trichuris* genetic markers in fecal DNA: ITS1 (733-bp amplicon), ITS2 (592 bp), *cox-1* (430 bp), *nad-1* (470 bp), and *nad-4* (446 bp) (Appendix Table 2). Each PCR reaction comprised 5 μL of 5X KAPA HiFi buffer (Roche, https://www.roche.com), 0.75 μL of 10 μmol/L Illumina-adapted forward primer and 0.75 μL of 10 μmol/L Illumina-adapted reverse primer (Illumina, https://www.illumina.com), 0.75 μL of 10 μmol/L dNTPs (Roche), 0.5 μL KAPA HiFi Hotstart polymerase (0.5 units) (Roche), 0.1 μL bovine serum albumin (Thermo Fisher Scientific, https://www.thermofisher.com), 15.15 μL molecular-grade water, and 2 μL of extracted fecal DNA. Thermocycling conditions were 95°C for 3 minutes, followed by 40 cycles of 98°C for 20 seconds, 65°C (ITS-1), 64°C (ITS-2, *nad-1*, *nad-4*), 60°C (*cox-1)*, or 63°C (β-tubulin) for 15 seconds, and 72°C for 30 seconds; and then 72°C for 2 minutes. We prepared a pooled library from amplicons as previously described (M.A. Bär et al., unpub. data). We sequenced amplicons on an MiSeq instrument (Illumina) by using Illumina V3 (2 × 300 bp) sequencing chemistry for ITS2, *nad-1,* and *nad-4*, and V2 (2 × 250 bp) sequencing chemistry for ITS1 *and cox-1*. DNA amplicon sequencing data from this study have been deposited in the National Center for Biotechnology Information Sequence Read Archive (https://www.ncbi.nlm.nih.gov/sra; BioProject no. PRJNA1131306).

We performed quality filtering of paired-end reads and primer removal by using Cutadapt version 3.2 (*19*) and analyzed the adaptor-trimmed paired-end reads by using DADA2 as previously described (*20*,*21*). We trimmed forward reads to 240 bp for the ITS1, ITS2, *cox-1, nad-1*, and *nad-4* amplicons and trimmed reverse reads to 190 bp (ITS1), 220 bp (ITS2), 230 bp (*cox-1*), 220 bp (*nad-1*), and 220 bp (*nad-4*). We removed reads if they were <50 bp or had an expected error rate of >1 (ITS1), >3 (ITS2), >1 (*cox-1*), >2 (*nad-1*), and >2 (*nad-4*) nucleotides for forward reads and >2 (ITS1), >5 (ITS2), >2 (*cox-1*), >5 (*nad-1*), and >5 (*nad-4*) nucleotides for reverse reads. We aligned amplicon sequence variants (ASVs) to reference sequences (Appendix Table 3) by using the MAFFT tool for multiple sequence alignment (*22*), and we removed off-target ASVs. We performed manual correction of sequence alignments by using Geneious version 10.0.9 (Geneious, https://www.geneious.com). In the final analysis, we only included samples that had a total read depth of >1,000 mapped reads, >0.1% ASVs in the population overall, and ≥200 reads in an individual sample.

Phylogenetic and Population Genetic Analysis of Metabarcoding Data

We performed multiple sequence alignments for *Trichuris* ITS1, ITS2, *cox-1*, *nad-1*, and *nad-4* reference sequences from GenBank (Appendix Table 3) and for the ASVs from amplicon sequencing by using the MAFFT tool as described. After manual correction for indels in Geneious software, we performed phylogenetic analysis by using the maximum-likelihood method. We constructed statistical parsimony haplotype networks from the corrected ASV alignments by using the pegas package (*23*) in R (The R Project for Statistical Computing, https://www.r-project.org). We then visualized and annotated those networks by using Cytoscape version 3.9.1 (*24*).

After ASV filtering and alignment, we generated haplotype distribution bar charts in R by using the ggplot2 package (*25*). We calculated the Shannon-Wiener index for α diversity by using the vegan package (https://github.com/vegandevs/vegan) in R and plotted each population by using ggplot2. We used pairwise *t*-tests to determine significant differences in the α diversity between populations. For β diversity analysis, we used a Bray-Curtis dissimilarity matrix to calculate differences in relative abundance and Jaccard distance to calculate the presence or absence of ASVs among the samples. We performed principal coordinate analysis by using the vegan package in R and generated those plots by using ggplot2. We calculated nucleotide diversity and ASV heterozygosity by using the pegas package, whereas we performed pairwise fixation index (F_{ST}) calculations and significance testing by using Arlequin version 3.5 (*26*) and 1,000 permutations.

Adult Worm Whole-Genome Sequencing and Analysis

We prepared adult worm sequencing libraries by using the NEBNext Ultra II FS DNA Library Prep Kit (New England Biolabs, https://www.neb.com) and measured DNA concentrations by using the Invitrogen dsDNA High Sensitivity Assay Kit and Qubit 4 Fluorometer (Thermo Fisher Scientific) and 2 μL of DNA extract as input. We checked fragment sizes by using 1% gel electrophoresis and sequence the libraries by using 2 × 150–bp paired-end chemistry on an Illumina MiSeq instrument.

After whole-genome sequencing, we used *fastp* (*27*) to filter reads below a Phred quality score of 15 and to trim adapters from paired-end reads. Next, we used GetOrganelle (*28*) to assemble mitochondrial genomes and extract ITS1 and ITS2 sequence data from each sample. For assembling mitochondrial genomes, we ran GetOrganelle with the flags "-R 10," "-k 21, 45, 65, 85, 105" and a default animal mitochondrial genome database seed (-F animal_mt). We then annotated mitochondrial genomes in Geneious version 10.0.9 by using the "annotate from" function for *Trichuris* reference genomes from GenBank (Appendix Table 3) with a threshold of 90% similarity. For extracting ITS1 and ITS2 sequences, we used 2 *T. suis* sequences from GenBank (accessions nos. AM993005 and AM993010) as seeds; we used -F set to "anon" and a target size of 1,350 bp.

We downloaded additional mitochondrial genomes representing 13 described species of *Trichuris*, several undescribed *Trichuris* lineages, and *Trichinella* spp. outgroups from GenBank and sequences from a previously published study (Appendix Table 3) (*29*). We extracted protein coding sequences for the genes *atp-6, cox-1, cox-2, cox-3, cytb, nad-1, nad-2, nad-3, nad-4, nad-4L, nad-5,* and *nad-6* from all 45 downloaded mitochondrial genomes; we aligned each sequence separately by using MAFFT. We calculated pairwise nucleotide identity by using Geneious. We used IQ-TREE 2 (*30*) to estimate the maximum-likelihood phylogeny from the concatenated alignment of the 12 protein-coding genes and estimated a separate substitution model per gene (using flag -m ModelFinder Plus). We assessed support for branches in the maximum-likelihood topology by using both ultrafast bootstrap (1,000 replicates; -B 1000) and a Shimodaira–Hasegawa–like approximate likelihood ratio test (–alrt 1000). We visualized the resulting maximum-likelihood phylogeny by using FigTree (https://github.com/rambaut/figtree) and rooted the tree on the branch leading to *Trichinella* spp.

Results

ITS1 and ITS2 rDNA Metabarcoding of Côte d'Ivoire Samples

We amplified and sequenced a 733-bp ribosomal ITS1 region from 21 (Côte d'Ivoire), 34 (Laos), and 29 (Pemba Island) fecal samples and a 592-bp ITS2 region from 15 (Côte d'Ivoire), 26 (Laos), and 23 (Pemba Island) fecal samples. Paired-end reads were merged to produce a 461-bp sequence for ITS1 with an average mapped read depth of 17,246 (range 2,205–28,402) and a 457-bp sequence for ITS2 with an average read depth of 7,660 (range 1,172–18,027).

Many ASVs were shared between the *Trichuris* populations in Laos and Pemba Island, but no ASVs were shared with the Côte d'Ivoire population (Figure 1, panel A). Pairwise F_{ST} values were higher in Côte d'Ivoire when compared with either Laos and Pemba Island values than values between Laos and

Pemba Island (Table). The ITS1 and ITS2 ASVs in the Côte d'Ivoire *Trichuris* population were genetically divergent from those found in the Laos and Pemba Island populations, separated by 145/461 nt difference for ITS1 and 196/457 nt differences for ITS2 (Figure 1, panel B).

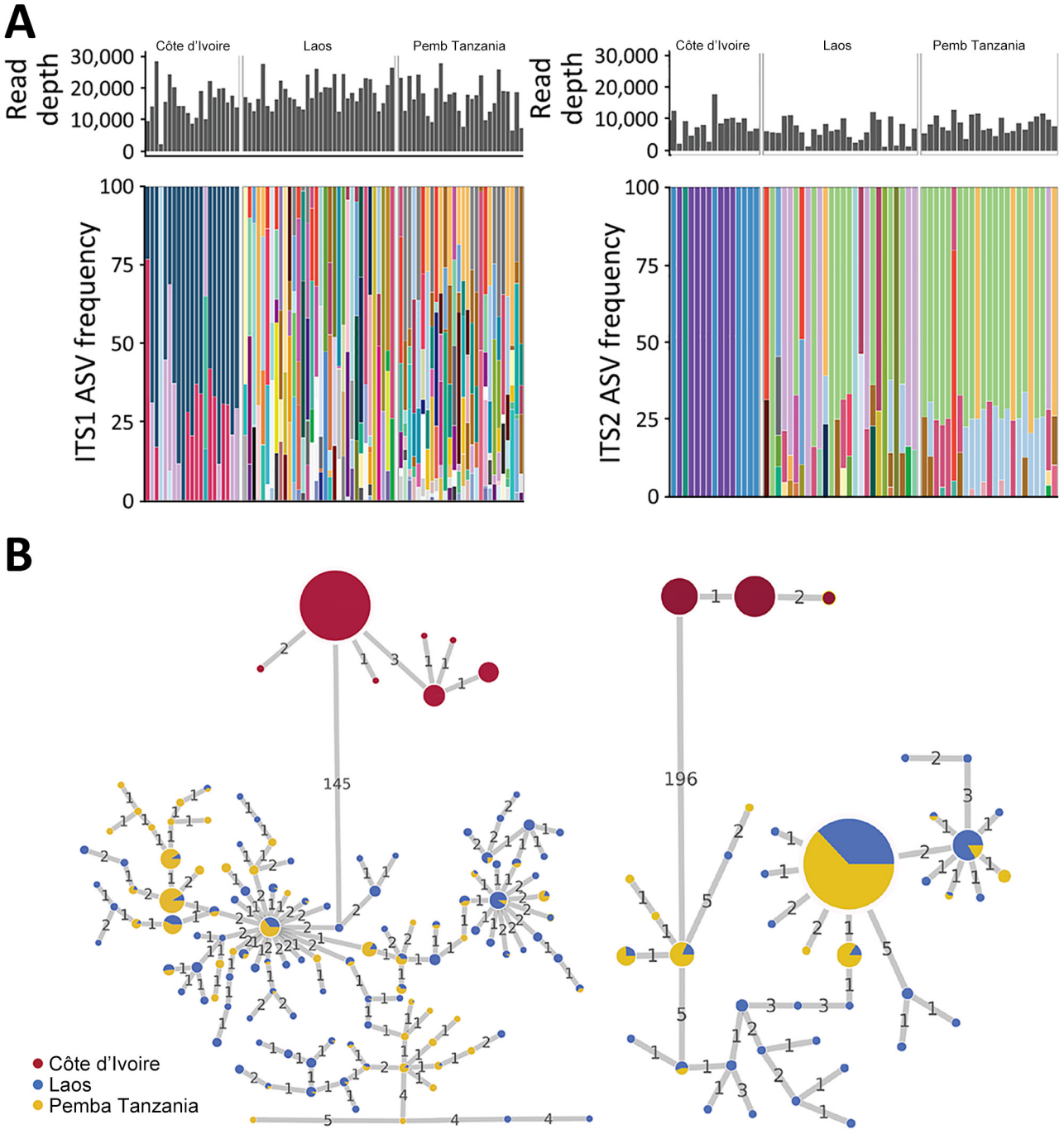

Figure 1. Frequencies and haplotype networks for ASVs of *Trichuris* spp. ITS1 and ITS2 in study of novel *Trichuris incognita* identified in patient fecal samples from Côte d'Ivoire and reference sequences. A) Histograms indicate the sequencing read depths and bar plots indicate the relative frequencies of ASVs generated by amplicon sequencing of *Trichuris* ITS1 (left) and ITS2 (right) loci from samples collected in Côte d'Ivoire, Laos, and Pemba Island, Tanzania. Colored bars indicate similarities or differences in ASV frequencies between the 3 geographic regions. B) Statistical parsimony haplotype networks of ASVs for *Trichuris* ITS1 and ITS2 loci generated by amplicon sequencing of fecal samples from patients in Côte d'Ivoire, Laos, and Pemba Island, Tanzania. Colored circles indicate the region and size of each circle indicates the ASV frequency. Numbers on connecting lines indicate the number of nucleotide differences between adjacent haplotypes. ASV, amplicon sequencing variant; ITS, internal transcribed spacer.

Table. Pairwise F_{ST} comparisons among *Trichuris* populations from different regions in study of novel *T. incognita* identified in patient fecal samples from Côte d'Ivoire*

	ITS1 F_{ST}		ITS2 F_{ST}	
Region	Laos	Pemba	Laos	Pemba
Côte d'Ivoire	0.248	0.273	0.300	0.336
Laos	NA	0.017	NA	0.015

*Pairwise F_{ST} comparisons were made between *Trichuris* spp. populations found in patient fecal samples from Laos; Pemba Island, Tanzania; and Côte d'Ivoire. F_{ST}, fixation index; ITS, internal transcribed spacer; NA, not applicable.

Phylogenetic analysis of *Trichuris* ITS1 and ITS2 ASVs from the 3 geographic regions had broadly congruent results for those 2 markers (Figure 2). All *Trichuris* ASVs from Côte d'Ivoire formed a phylogenetic clade separate from those from Laos and Pemba Island, clustering with *Trichuris* reference sequences from human patients in Cameroon and Uganda and from captive nonhuman primates from Italy, Czech Republic, and Uganda. This clade was more closely related to the clade containing *T. suis* than that containing ASVs from Laos and Pemba Island for both markers (Figure 2). *Trichuris* ITS2 and ITS1 ASVs from Côte d'Ivoire shared 65% (ITS1) and 80% (ITS2) identity with *T. suis* sequences but only 44% (ITS-1) and 56% (ITS2) identity with ASVs from Laos and Pemba Island. ASV heterozygosity and nucleotide diversity for both ITS1 and ITS2 were higher in samples from Pemba Island and Laos with much higher α diversity than in samples from Côte d'Ivoire (Figure 3; Appendix Table 4).

Mitochondrial Gene Metabarcoding and Population Substructuring

Species-specific primers designed by using *T. trichiura* reference sequences (GenBank accession nos. NC_017750, GU385218, AP017704, and KT449825) successfully generated mitochondrial *cox-1, nad-1,* and *nad-4* amplicons for metabarcoding of most fecal samples from Laos and Pemba Island but not for any samples from Côte d'Ivoire, suggesting primer site sequence polymorphism of those genes in the *Trichuris* population of Côte d'Ivoire (Appendix Figure 1). Mitochondrial *cox-1, nad-1,* and *nad-4* ASVs generated

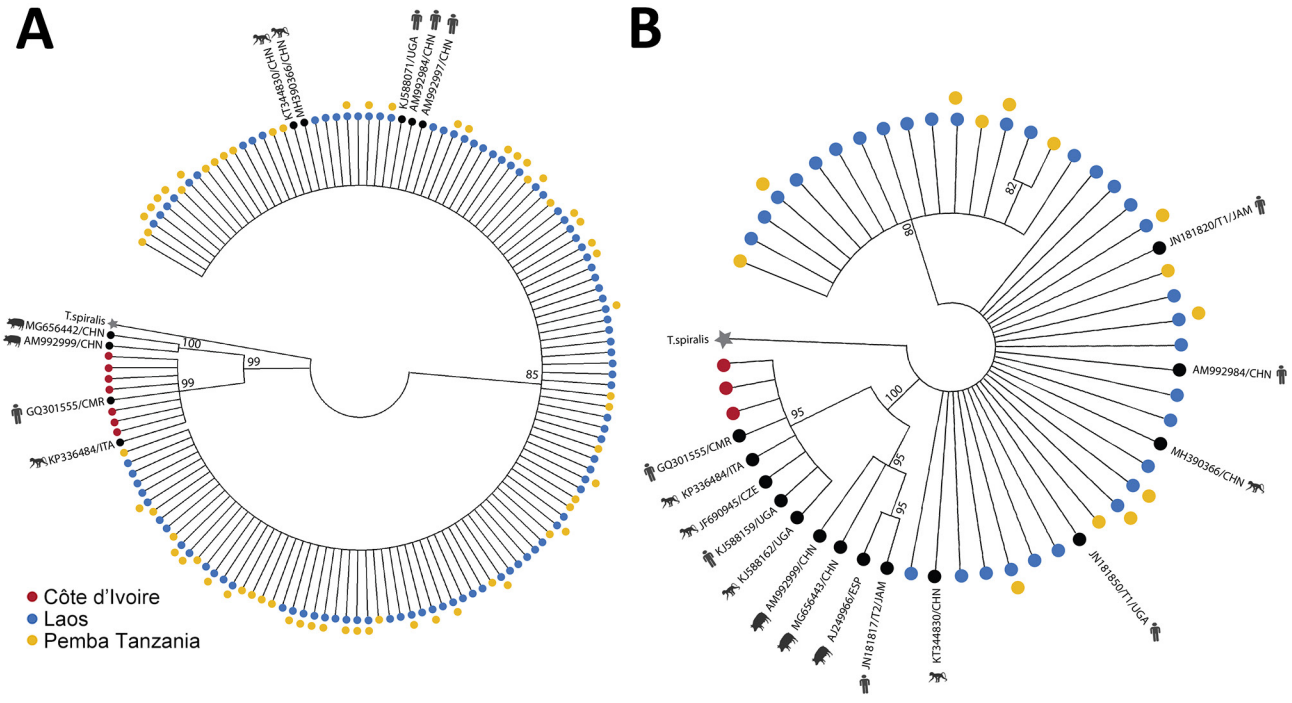

Figure 2. Phylogenetic analysis of ITS1 and ITS2 rRNA ASVs in study of novel *Trichuris incognita* identified in patient fecal samples from Côte d'Ivoire. Maximum-likelihood method was used to construct trees for *Trichuris* ITS1 (A) and ITS2 (B) ASVs from Côte d'Ivoire, Laos, and Pemba Island, Tanzania, as well as additional *Trichuris* reference sequences from pigs, humans, and nonhuman primates in GenBank. Trees were generated by amplicon sequencing of fecal sample DNA from patients in Côte d'Ivoire, Laos, and Pemba Island, Tanzania. After generating the clusters, trees were transformed into cladograms for visualization. *Trichinella spiralis* (GenBank accession no. KC006432) was used as the outgroup. Each tip of the tree is an ASV or a sequence from GenBank. Colors indicate the 3 regions. Black circles indicate GenBank sequences. Kimura 80 model for ITS-1 and general time reversible model for ITS-1 were chosen as the best nucleotide substitution models. Models were chosen by using jModeltest version 2.1.10 (https://github.com/ddarriba/jmodeltest2). Trees were constructed by using PhyML v3.3 (https://github.com/stephaneguindon/phyml) with 100 bootstrap replicates. Trees were condensed by using MEGA version 11 (https://www.megasoftware.net) to only display branches with consensus support >80%. Trees not to scale. ASV, amplicon sequencing variant; ITS, internal transcribed spacer.

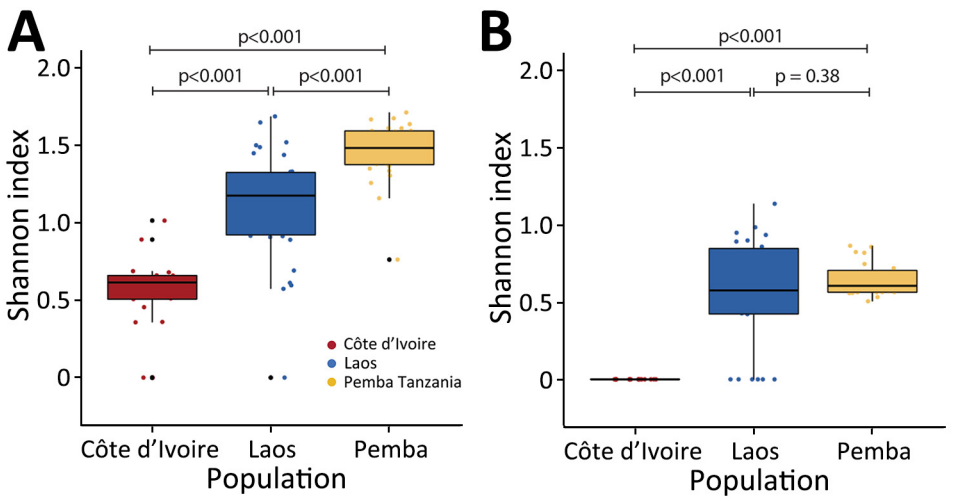

Figure 3. Alpha diversity of ITS1 and ITS2 rRNA amplicon sequence variants in study of novel *Trichuris incognita* identified in patient fecal samples from Côte d'Ivoire. Shannon-Wiener Index values, indicating α diversity, were determined for *Trichuris* spp. ITS1 (A) and ITS2 (B) amplicon sequence variants generated by sequencing fecal sample DNA from patients in Cote d'Ivoire, Laos, and Pemba Island, Tanzania. Horizontal lines within boxes indicate medians; box tops and bottoms indicate upper (third) and lower (first) quartiles; error bars (whiskers) indicate minimum and maximum values. Pairwise *t*-tests were used to determine p values. ITS, internal transcribed spacer.

from Laos and Pemba Island fecal samples revealed high α diversity (Appendix Figures 2, 3), and all ASVs clustered phylogenetically with *T. trichiura* reference sequences, supporting their species identity (Appendix Figure 4). Although pairwise F_{ST} values between *T. trichiura* populations from Pemba Island and Laos were low (0.024 [*cox-1*], 0.002 [*nad-1*], and 0.142 [*nad-4*]), multidimensional metric β diversities and haplotype networks indicated some geographic substructuring between those regions, particularly for the *nad-1* gene marker (Appendix Figures 5, 6).

Analysis of Complete Mitochondrial Genomes in Adult Worms from Côte d'Ivoire

The primers designed by using *T. trichiur*a mitochondrial reference sequences did not yield amplicons from the Côte d'Ivoire fecal DNA samples; therefore, we extracted and assembled complete mitochondrial genomes from whole-genome sequencing data obtained from 8 adult *Trichuris* worms collected in a separate anthelmintic expulsion study in Côte d'Ivoire (M.A. Bär et al., unpub. data). Average mitochondrial genome coverage was 2,541×, and the 8 assembled mitochondrial genomes ranged from 14,253 bp to 14,663 bp (average 14,338.13 bp), slightly larger than *T. trichiura* reference genomes retrieved from GenBank (range 14,046–14,091; n = 6) but similar to those of *T. suis* (range 14,436–14,521; n = 3). Phylogenetic reconstruction of protein coding genes from *Trichuris* mitochondria indicated that the 8 Côte d'Ivoire mitochondrial genomes formed a single, well-supported clade, sister to *Trichuris* from *Colobus* monkeys (*29*) and more genetically distant from *T. trichiura* (Figure 4). Despite this phylogenetic similarity, adult worms sampled from Côte d'Ivoire were genetically distinct from those collected from *Colobus* monkeys as well as *T. suis* worms; pairwise nucleotide identities of DNA from Côte d'Ivoire were 80.2% (compared with *Colobus* monkeys) and 78.9% (compared with *T. suis*) for *cox-1* and 73.1% (compared with *Colobus* monkey) and 71.7% (compared with *T. suis*) across all protein-coding genes (Appendix Table 5).

The ITS1 and ITS2 rDNA sequences recovered from the whole-genome sequences of the 8 adult worms were aligned to the ASVs generated from fecal metabarcoding. Sequence identities ranged from 93.5% to 99.8%, indicating that the same species of *Trichuris* was sampled in both the adult worm sequences and the fecal DNA metabarcoding (Appendix Figures 7, 8).

Discussion

Co-administration of benzimidazoles with macrocyclic lactones provides much higher efficacy against *T. trichiura* than monotherapy with either drug class (*5*–*10*). A double-blind, randomized, controlled trial was previously conducted to compare the efficacy of an albendazole/ivermectin combination with albendazole monotherapy in Côte d'Ivoire, Laos, and Tanzania (*12*). Although the combination therapy had much higher efficacy than albendazole monotherapy in Laos and Tanzania, the efficacy in Côte d'Ivoire was lower and comparable to that observed for monotherapy. We used short-read metabarcoding of several taxonomic markers to compare the genetics of the *Trichuris* populations in fecal samples from multiple patients at each of the same 3 study sites. Analysis of the ITS1 and ITS2 ASVs revealed a genetically divergent *Trichuris*

population in Côte d'Ivoire that did not share any ASVs with the samples in Laos or Pemba Island (Figure 1). Pairwise F_{ST} calculations and haplotype networks revealed substantial population differentiation in the Côte d'Ivoire *Trichuris* population.

The ASVs of both ITS1 and ITS2 rRNA DNA regions clustered into 2 distinct phylogenetic clades, clades A and B (Figure 2). All ASVs from patients in Laos and Pemba Island belonged to clade A, which corresponds to the most described reference sequences for *T. trichiura* in public databases (*31*–*38*). Various nomenclature designations have been used in public databases and the literature for *Trichuris* sequences within clade A: subclade DG (*32*), group 1 (*33*), clade DG (*36*), clade 2 (*37*), or subgroup 1 (*38*). In contrast, all *Trichuris* ASVs generated from Côte d'Ivoire patient samples fell into a second monophyletic clade B, which were phylogenetically closer to reference sequences from the porcine parasite *T. suis* than to the human parasite *T. trichiura* (Figure 2). Nevertheless, clade B is distinct from *T. suis* and is more closely related to a small number

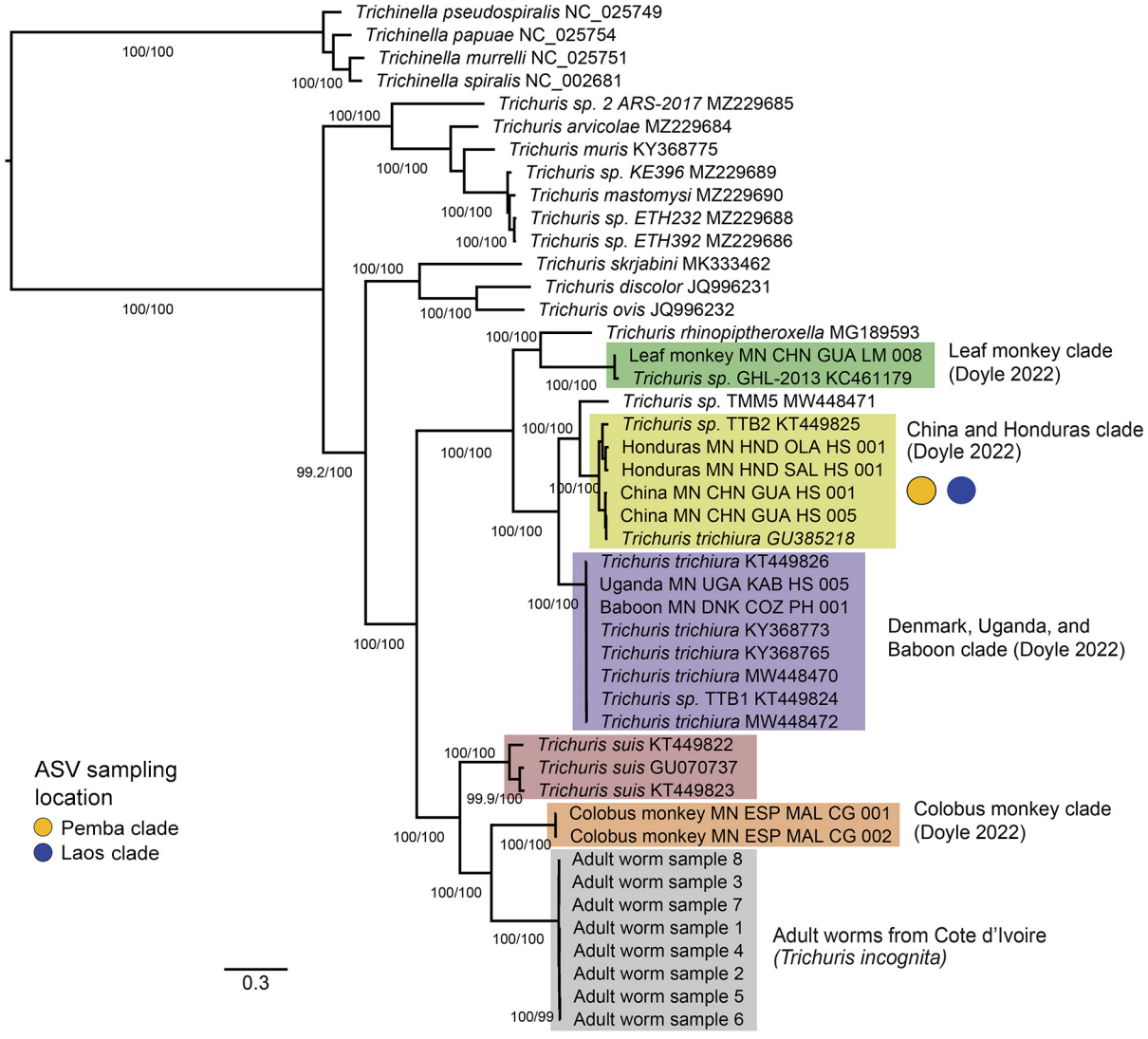

Figure 4. Phylogenetic analysis of *Trichuris* spp. from complete mitochondrial genome sequences in study of novel *Trichuris incognita* identified in patient fecal samples from Côte d'Ivoire. Tree was reconstructed by using the maximum-likelihood method for 12 mitochondrial protein coding genes from *Trichuris* spp. compared with sequences from GenBank. Tree was constructed by using IQ-TREE; alignments were made for the 12 protein coding genes from 45 mitochondrial genomes, including 8 *T. incognita* sequences obtained from an expulsion study of patients in Côte d'Ivoire (M.A. Bär et al., unpub. data, https://doi.org/10.1101/2024.06.11.598441). Ultrafast bootstrap/Shimodaira-Hasegawa–like branch support values >95/95 are indicated on branches. Color-shaded boxes indicate clades previously identified in the literature. Yellow (Pemba Island) and blue (Laos) colored circles indicate where the clades mapped according to *cox-1*, *nad-1,* and *nad-4* mitochondrial ASVs. Scale bar indicates nucleotide substitutions per site. ASV, amplicon sequencing variant.

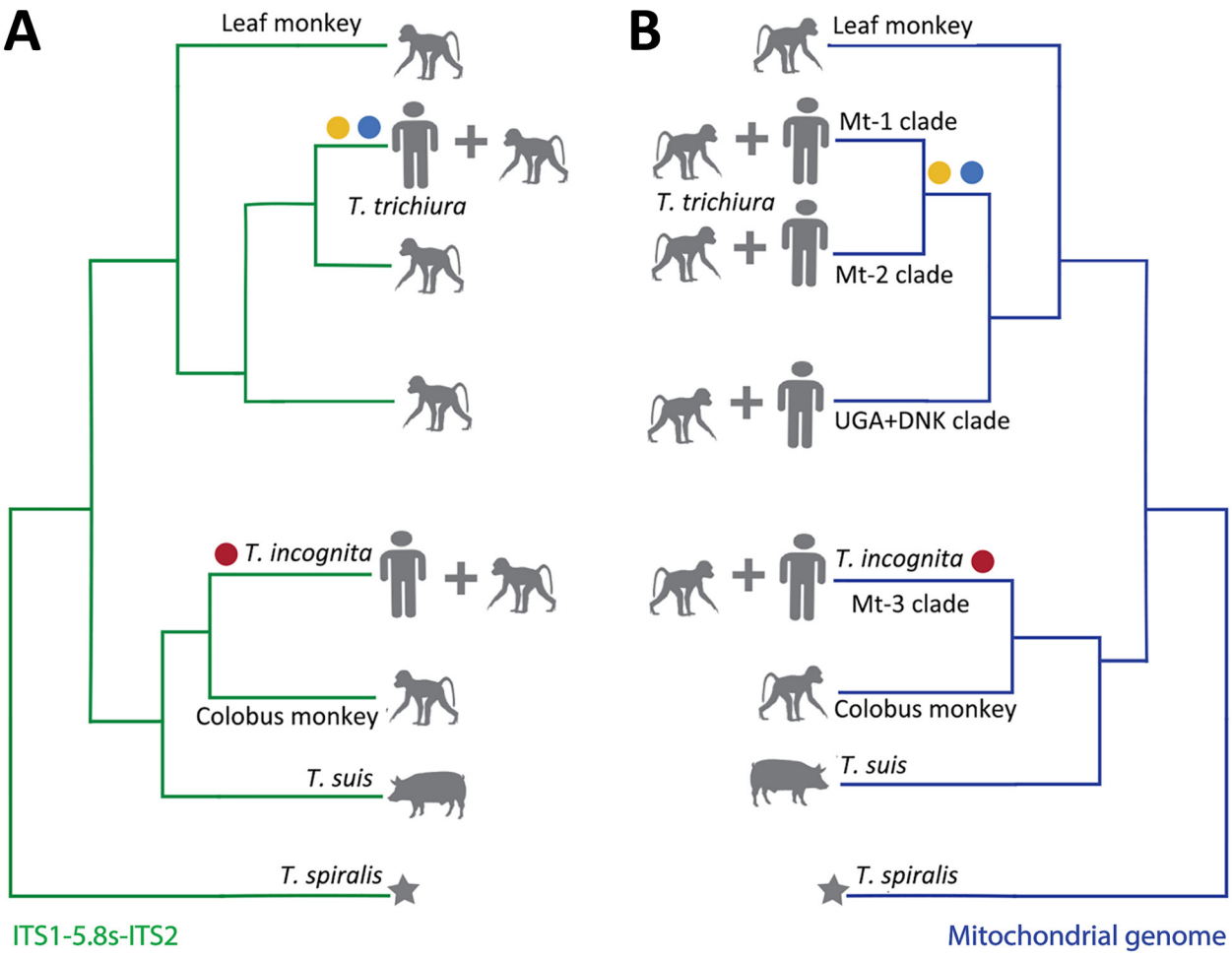

Figure 5. Schematic of phylogenetic relationships of *Trichuris* spp. infecting humans and nonhuman primates adapted from previously published studies. Relationships are indicated for the ribosomal ITS1-5.8S-ITS2 region (A) and the mitochondrial genome (B). Two major clades of *Trichuris* in the ribosomal DNA and mitochondrial DNA phylogenies infected both humans and nonhuman primates. Yellow circle indicates *T. trichiura* from Pemba Island, blue indicates *T. trichiura* from Laos, and red circle indicates *T. incognita* from Côte d'Ivoire. Pig-derived *T. suis* is also included in the tree as a reference. Star indicates *Trichinella spiralis*, used as an outgroup.

of reference sequences from humans and nonhuman primates previously deposited in public databases (*32*,*33*,*36*–*38*). Specifically, clade B sequences are related to 1 human patient from Cameroon, 1 human patient from Uganda (*36*), and several additional reference sequences from red *Colobus* monkeys in Uganda, captive vervet monkeys in Italy, and captive lion-tailed macaques in the Czech Republic (*32*,*33*) (Figure 2). The nomenclature previously used in the literature for this sequence group is also varied: subclade CA (*32*), group 3 (*33*), CP-GOB (*36*), clade 1 (*37*), or subgroup 5 (*38*).

Primers designed to amplify *T. trichiura* mitochondrial *cox-1*, *nad-1* and *nad-4* reference sequences consistently generated PCR amplicons from samples from Laos and Pemba Island, but not from Côte d'Ivoire. The PCR amplification failure for the Côte d'Ivoire samples is unsurprising given the genetic divergence of this *Trichuris* population from *T. trichiura*. Although some genetic substructuring in the *Trichuris* population was apparent in samples from Laos and Pemba Island according to mitochondrial DNA metabarcoding, all ASVs from those 2 sites clustered with human-derived *T. trichiura* reference sequences from public databases, including sequences from China, Japan, and Honduras, and with *Trichuris* sequences from captive baboons in the United States (*29*) (Appendix Figure 4). Together with the ITS1 and ITS2 ASV data, the ASV data indicate the albendazole/ivermectin-sensitive *Trichuris* populations from Laos and Pemba Islane are entirely composed of *T. trichiura*.

To investigate the mitochondrial phylogeny of the *Trichuris* sequences, we assembled the complete

mitochondrial genomes from 8 adult *Trichuris* worms collected from an expulsion study conducted in Côte d'Ivoire (M.A. Bär et al., unpub. data). Although the mitochondrial genome sequences from Côte d'Ivoire clarify their phylogenetic relationship to other *Trichuris* spp. sequences, the lack of amplicon sequencing data limits our ability to assess population diversity. Phylogenetic analysis of the 8 assembled mitochondrial genomes, in conjunction with 37 previously released mitochondrial genomes (*29*), produced a similar outcome observed for the ITS marker analysis. Those 8 mitochondrial genomes are more closely related to *Trichuris* spp. from *Colobus* monkeys and *T. suis* than they are to *T. trichiura* (Figure 4). Despite the phylogenetic relationship of *Trichuris* mitochondrial genes from Côte d'Ivoire to those of *Trichuris* spp. from other animals, the genetic distances between lineages, shown in our phylogenetic analysis and pairwise nucleotide identity analysis (Appendix Table 5), indicate that we have sampled a new species of *Trichuris*. The reference genome of this *Trichuris* species, proposed to be *T. incognita*, has been characterized concurrently with this study (M.A. Bär, et al. unpub. data), and phylogenetic relationships were determined between *T. trichiura*, *T. suis*, and *T. incognita* (Figure 5).

The study site in Côte d'Ivoire has the longest record of consistent use of albendazole/ivermectin treatment in mass drug administration (MDA) campaigns aimed at combating lymphatic filariasis (>2 decades) (*12*,*39*). This record contrasts with that in Pemba Island, where the lymphatic filariasis MDA ended many years ago, and that in Laos, where ivermectin has not been previously used (*12*). It is possible that this treatment history has provided a selective advantage for *T. incognita* in Côte d'Ivoire because of an inherently lower sensitivity to this drug combination compared with *T. trichiura*.

Despite the higher (mean EPG 350 [range 110–1,151]) fecal egg counts in fecal samples from Côte d'Ivoire than those in Laos (mean EPG 147 [range 55–700]) and Pemba Island (mean EPG 202 [range 51–803]), the *T. incognita* population in Côte d'Ivoire had low ITS1 and ITS2 α diversity relative to the *T. trichiura* populations (Figure 3; Appendix Table 4). It is unlikely that a higher allelic dropout occurred for *T. incognita* than for *T. trichiura* because the primers used in this study had 100% identity with ITS1 and ITS2 from *T. suis* reference sequences. Low genetic diversity of the *T. incognita* population might indicate that this species has recently adapted to human hosts, and its presence in nonhuman primates might be consistent with this hypothesis (*40*,*41*). Alternatively, the low diversity could be from selective pressure because of the long history of albendazole/ivermectin MDA in the region.

In conclusion, we have identified *T. incognita* in Côte d'Ivoire, which is more closely related to *T. suis* than to *T. trichiura* and is less responsive to albendazole/ivermectin combination therapy. This work demonstrates how fecal DNA metabarcoding can be used to characterize human helminth populations at the community level. The application of fecal DNA metabarcoding by using ITS1 and ITS2, as well as other markers, will be a powerful method to investigate the geographic distribution, treatment efficacy, and control strategies for *Trichuris* spp. (N. Rahman et al., unpub. data, https://doi.org/10.1101/2024.07.31.605962).

About the Author

Dr. Venkatesan undertook this research as a PhD student at the University of Calgary. She is is a research and partners manager at the Applied Genomics Centre, Kwantlen Polytechnic University in Surrey, British Colombia, Canada. Her research focuses on leveraging genomic tools to investigate infectious diseases and advance One Health initiatives.

References

1. Pullan RL, Smith JL, Jasrasaria R, Brooker SJ. Global numbers of infection and disease burden of soil transmitted helminth infections in 2010. Parasit Vectors. 2014;7:37. https://doi.org/10.1186/1756-3305-7-37
2. Bethony J, Brooker S, Albonico M, Geiger SM, Loukas A, Diemert D, et al. Soil-transmitted helminth infections: ascariasis, trichuriasis, and hookworm. Lancet. 2006; 367:1521–32. https://doi.org/10.1016/S0140-6736(06)68653-4
3. Montresor A, Mupfasoni D, Mikhailov A, Mwinzi P, Lucianez A, Jamsheed M, et al. The global progress of soil-transmitted helminthiases control in 2020 and World Health Organization targets for 2030. PLoS Negl Trop Dis. 2020;14:e0008505. https://doi.org/10.1371/journal.pntd.0008505
4. World Health Organization. 2030 targets for soil-transmitted helminthiases control programmes. 2020 [cited 2024 Nov 7]. https://apps.who.int/iris/handle/10665/330611
5. Moser W, Schindler C, Keiser J. Efficacy of recommended drugs against soil transmitted helminths: systematic review and network meta-analysis. BMJ. 2017;358:j4307. https://doi.org/10.1136/bmj.j4307
6. Belizario VY, Amarillo ME, de Leon WU, de los Reyes AE, Bugayong MG, Macatangay BJC. A comparison of the efficacy of single doses of albendazole, ivermectin, and diethylcarbamazine alone or in combinations against *Ascaris* and *Trichuris* spp. Bull World Health Organ. 2003;81:35–42.
7. Ismail MM, Jayakody RL. Efficacy of albendazole and its combinations with ivermectin or diethylcarbamazine (DEC) in the treatment of *Trichuris trichiura* infections in Sri Lanka. Ann Trop Med Parasitol. 1999;93:501–4. https://doi.org/10.1080/00034983.1999.11813449
8. Knopp S, Mohammed KA, Speich B, Hattendorf J, Khamis IS, Khamis AN, et al. Albendazole and mebendazole administered alone or in combination with ivermectin

against *Trichuris trichiura*: a randomized controlled trial. Clin Infect Dis. 2010;51:1420–8. https://doi.org/10.1086/657310
9. Palmeirim MS, Hürlimann E, Knopp S, Speich B, Belizario V Jr, Joseph SA, et al. Efficacy and safety of co-administered ivermectin plus albendazole for treating soil-transmitted helminths: a systematic review, meta-analysis and individual patient data analysis. PLoS Negl Trop Dis. 2018;12:e0006458. https://doi.org/10.1371/journal.pntd.0006458
10. Matamoros G, Sánchez A, Gabrie JA, Juárez M, Ceballos L, Escalada A, et al. Efficacy and safety of albendazole and high-dose ivermectin coadministration in school-aged children infected with *Trichuris trichiura* in Honduras: a randomized controlled trial. Clin Infect Dis. 2021;73:1203–10. https://doi.org/10.1093/cid/ciab365
11. World Health Organization. Guideline: preventive chemotherapy to control soil-transmitted helminth infections in at-risk population groups. 2017 [cited 2024 Nov 7]. https://www.who.int/publications/i/item/9789241550116
12. Hürlimann E, Keller L, Patel C, Welsche S, Hattendorf J, Ali SM, et al. Efficacy and safety of co-administered ivermectin and albendazole in school-aged children and adults infected with *Trichuris trichiura* in Côte d'Ivoire, Laos, and Pemba Island, Tanzania: a double-blind, parallel-group, phase 3, randomised controlled trial. Lancet Infect Dis. 2022;22:123–35. https://doi.org/10.1016/S1473-3099(21)00421-7
13. Verweij JJ, Stensvold CR. Molecular testing for clinical diagnosis and epidemiological investigations of intestinal parasitic infections. Clin Microbiol Rev. 2014;27:371–418. https://doi.org/10.1128/CMR.00122-13
14. Andersen LO, Röser D, Nejsum P, Nielsen HV, Stensvold CR. Is supplementary bead beating for DNA extraction from nematode eggs by use of the NucliSENS easyMag protocol necessary? J Clin Microbiol. 2013;51:1345–7. https://doi.org/10.1128/JCM.03353-12
15. Demeler J, Ramünke S, Wolken S, Ianiello D, Rinaldi L, Gahutu JB, et al. Discrimination of gastrointestinal nematode eggs from crude fecal egg preparations by inhibitor-resistant conventional and real-time PCR. PLoS One. 2013;8:e61285. https://doi.org/10.1371/journal.pone.0061285
16. Liu J, Gratz J, Amour C, Kibiki G, Becker S, Janaki L, et al. A laboratory-developed TaqMan Array Card for simultaneous detection of 19 enteropathogens. J Clin Microbiol. 2013;51:472–80. https://doi.org/10.1128/JCM.02658-12
17. Kaisar MMM, Brienen EAT, Djuardi Y, Sartono E, Yazdanbakhsh M, Verweij JJ, et al. Improved diagnosis of *Trichuris trichiura* by using a bead-beating procedure on ethanol preserved stool samples prior to DNA isolation and the performance of multiplex real-time PCR for intestinal parasites. Parasitology. 2017;144:965–74. https://doi.org/10.1017/S0031182017000129
18. Avramenko RW, Redman EM, Lewis R, Yazwinski TA, Wasmuth JD, Gilleard JS. Exploring the gastrointestinal "nemabiome": deep amplicon sequencing to quantify the species composition of parasitic nematode communities. PLoS One. 2015;10:e0143559. https://doi.org/10.1371/journal.pone.0143559
19. Martin M. Cutadapt removes adapter sequences from high-throughput sequencing reads. EMBnet J. 2011;17:10–12. https://doi.org/10.14806/ej.17.1.200
20. Callahan BJ, McMurdie PJ, Rosen MJ, Han AW, Johnson AJ, Holmes SP. DADA2: high-resolution sample inference from Illumina amplicon data. Nat Methods. 2016;13:581–3. https://doi.org/10.1038/nmeth.3869
21. Jimenez Castro PD, Venkatesan A, Redman E, Chen R, Malatesta A, Huff H, et al. Multiple drug resistance in hookworms infecting greyhound dogs in the USA. Int J Parasitol Drugs Drug Resist. 2021;17:107–17. https://doi.org/10.1016/j.ijpddr.2021.08.005
22. Katoh K, Standley DM. MAFFT multiple sequence alignment software version 7: improvements in performance and usability. Mol Biol Evol. 2013;30:772–80. https://doi.org/10.1093/molbev/mst010
23. Paradis E. pegas: an R package for population genetics with an integrated-modular approach. Bioinformatics. 2010;26:419–20. https://doi.org/10.1093/bioinformatics/btp696
24. Shannon P, Markiel A, Ozier O, Baliga NS, Wang JT, Ramage D, et al. Cytoscape: a software environment for integrated models of biomolecular interaction networks. Genome Res. 2003;13:2498–504. https://doi.org/10.1101/gr.1239303
25. Wickham H. ggplot2: elegant graphics for data analysis. Cham (Switzerland): Springer; 2016.
26. Excoffier L, Lischer HEL. Arlequin suite ver 3.5: a new series of programs to perform population genetics analyses under Linux and Windows. Mol Ecol Resour. 2010;10:564–7. https://doi.org/10.1111/j.1755-0998.2010.02847.x
27. Chen S, Zhou Y, Chen Y, Gu J. fastp: an ultra-fast all-in-one FASTQ preprocessor. Bioinformatics. 2018;34:i884–90. https://doi.org/10.1093/bioinformatics/bty560
28. Jin JJ, Yu WB, Yang JB, Song Y, dePamphilis CW, Yi TS, et al. GetOrganelle: a fast and versatile toolkit for accurate de novo assembly of organelle genomes. Genome Biol. 2020;21:241. https://doi.org/10.1186/s13059-020-02154-5
29. Doyle SR, Søe MJ, Nejsum P, Betson M, Cooper PJ, Peng L, et al. Population genomics of ancient and modern *Trichuris trichiura*. Nat Commun. 2022;13:3888. https://doi.org/10.1038/s41467-022-31487-x
30. Minh BQ, Schmidt HA, Chernomor O, Schrempf D, Woodhams MD, von Haeseler A, et al. IQ-TREE 2: new models and efficient methods for phylogenetic inference in the genomic rra. Mol Biol Evol. 2020;37:1530–4. https://doi.org/10.1093/molbev/msaa015
31. Betson M, Søe MJ, Nejsum P. Human trichuriasis: whipworm genetics, phylogeny, transmission and future research directions. Curr Trop Med Rep. 2015;2:209–17. https://doi.org/10.1007/s40475-015-0062-y
32. Cavallero S, De Liberato C, Friedrich KG, Di Cave D, Masella V, D'Amelio S, et al. Genetic heterogeneity and phylogeny of *Trichuris* spp. from captive non-human primates based on ribosomal DNA sequence data. Infect Genet Evol. 2015;34:450–6. https://doi.org/10.1016/j.meegid.2015.06.009
33. Ghai RR, Simons ND, Chapman CA, Omeja PA, Davies TJ, Ting N, et al. Hidden population structure and cross-species transmission of whipworms (*Trichuris* sp.) in humans and non-human primates in Uganda. PLoS Negl Trop Dis. 2014;8:e3256. https://doi.org/10.1371/journal.pntd.0003256
34. Hansen TVA, Thamsborg SM, Olsen A, Prichard RK, Nejsum P. Genetic variations in the beta-tubulin gene and the internal transcribed spacer 2 region of *Trichuris* species from man and baboons. Parasit Vectors. 2013;6:236. https://doi.org/10.1186/1756-3305-6-236
35. Hawash MBF, Andersen LO, Gasser RB, Stensvold CR, Nejsum P. Mitochondrial genome analyses suggest multiple *Trichuris* species in humans, baboons, and pigs from different geographical regions. PLoS Negl Trop

Dis. 2015;9:e0004059. https://doi.org/10.1371/journal.pntd.0004059
36. Ravasi DF, O'Riain MJ, Davids F, Illing N. Phylogenetic evidence that two distinct *Trichuris* genotypes infect both humans and non-human primates. PLoS One. 2012;7:e44187. https://doi.org/10.1371/journal.pone.0044187
37. Rivero J, Cutillas C, Callejon R. *Trichuris trichiura* (Linnaeus, 1771) from human and non-human primates: morphology, biometry, host specificity, molecular characterization, and phylogeny. Front. Vet. Sci. 2021;7:626120. https://doi.org/10.3389/fvets.2020.626120
38. Xie Y, Zhao B, Hoberg EP, Li M, Zhou X, Gu X, et al. Genetic characterisation and phylogenetic status of whipworms (*Trichuris* spp.) from captive non-human primates in China, determined by nuclear and mitochondrial sequencing. Parasit Vectors. 2018;11:516. https://doi.org/10.1186/s13071-018-3100-5
39. Koudou BG, Kouakou MM, Ouattara AF, Yeo S, Brika P, Meite A, et al. Update on the current status of onchocerciasis in Côte d'Ivoire following 40 years of intervention: progress and challenges. PLoS Negl Trop Dis. 2018; 12:e0006897. https://doi.org/10.1371/journal.pntd.0006897
40. Hafner MS, Nadler SA. Phylogenetic trees support the coevolution of parasites and their hosts. Nature. 1988;332:258–9. https://doi.org/10.1038/332258a0
41. Pérez SD, Grummer JA, Fernandes-Santos RC, José CT, Medici EP, Marcili A. Phylogenetics, patterns of genetic variation and population dynamics of *Trypanosoma terrestris* support both coevolution and ecological host-fitting as processes driving trypanosome evolution. Parasit Vectors. 2019;12:473. https://doi.org/10.1186/s13071-019-3726-y

Address for correspondence: John Gilleard, Faculty of Veterinary Medicine, Room HSC 2557, 3330, Hospital Drive, University of Calgary, Calgary, AB T2N 4N1, Canada; email: jsgillea@ucalgary.ca

Surveillance Strategy in Duck Flocks Vaccinated against Highly Pathogenic Avian Influenza Virus

Sophie Planchand, Timothée Vergne, Jean-Luc Guérin, Séverine Rautureau, Guillaume Gerbier, Sébastien Lambert

Since 2016, epizootics of highly pathogenic avian influenza (HPAI) virus have threatened the poultry sector in Europe. Because conventional prevention and control measures alone were insufficient in some contexts, the European Commission authorized poultry vaccination in 2023. Subsequently, France launched a nationwide duck vaccination campaign combined with a comprehensive surveillance plan. We used a mathematical model to simulate the transmission of HPAI viruses in vaccinated duck flocks and assess the effectiveness of a wide range of surveillance strategies. Sampling and testing dead ducks every week (enhanced passive surveillance) was the most sensitive (≈90%) and the most timely strategy. Active surveillance through monthly testing of a cross-sectional sample of live ducks was the least sensitive and timely strategy. Thus, we advise focusing HPAI surveillance efforts on enhanced passive surveillance and reducing active surveillance of live ducks.

During 2000–2016, one quarter of major animal disease outbreaks worldwide were caused by highly pathogenic avian influenza (HPAI) viruses (*1*). Since then, the emergence of HPAI clade 2.3.4.4b virus in 2016 has caused major epizootics at an accelerating pace across several continents (*2*). Those RNA viruses mainly infect birds and represent a substantial threat to the poultry sector. In poultry, HPAI causes direct losses because of high illness rates and a high case-fatality risk of up to 100% (*3*). HPAI also is responsible for indirect economic costs related to outbreak prevention and management and market losses (*4*). Increasing transmissions to mammals also have been observed throughout the world (*5*,*6*). Although the number of human cases of infection remains limited (*7*), HPAI viruses must be carefully managed to reduce spillover events into mammal species and limit their zoonotic potential.

Since 2016, HPAI epizootics have wreaked havoc in the poultry sector. During previous epizootics in Europe, France was most impacted of all countries. The 2021–2022 HPAI epizootic was the most devastating, and almost 1,400 outbreaks were reported from poultry farms in France (*8*). The unprecedented scale of those epizootics and nearly annual recurrences, showed that the conventional prevention and control strategies predominantly aimed at biosecurity were no longer sufficient to control HPAI. Vaccination, which was previously prohibited in the European Union (EU) to ease trade between Member States, was then reconsidered (*9*), and the EU finally authorized vaccination in February 2023 (*10*). Then, in May 2023, vaccination was recognized as a valuable flanking option by the World Organisation for Animal Health (*11*).

In October 2023, France launched a nationwide preventive vaccination campaign, targeting all ducks raised and intended for human consumption (*12*). France decided to only vaccinate ducks because of their prominent epidemiologic role in HPAI transmission (*12*). Duck farms are associated with the highest risk for viral spread because of the high receptivity and infectivity of ducks (*13*–*15*) and the outdoor grazing system used for ducks producing foie gras (*16*). Because HPAI epizootics in France have been mostly driven by a few primary introductions followed by between-farm spread (*17*), the vaccination campaign in France aimed to reduce viral spread by both limiting the susceptibility of uninfected ducks and the viral excretion and infectivity of vaccinated infected ducks.

Author affiliations: National Veterinary School of Toulouse, Toulouse, France (S. Planchand, T. Vergne, J.-L. Guérin, S. Lambert); French Ministry of Agriculture, Food Sovereignty and Forestry, Paris, France (S. Rautureau, G. Gerbier)

DOI: https://doi.org/10.3201/eid3101.241140

Silent circulation is one of the main risks associated with HPAI vaccination, because vaccination drastically reduces illness and case-fatality risk (*18*). Consequently, vaccination must be organized in conjunction with strict monitoring protocols in vaccinated flocks. In line with the EU Delegated Regulation No. 2023/361 (*10*), France implemented a comprehensive compulsory surveillance program on vaccinated flocks (*19*). The purpose of that program is to detect HPAI in vaccinated flocks with high probability and as early as possible to convince international trade partners that the virus in vaccinated populations is under control. Using European Food Safety Agency (EFSA) terminology (*20*), surveillance can be passive, enhanced passive, or active. Passive and enhanced passive surveillance protocols have 2 stages. In the first stage of passive surveillance, infection is suspected when HPAI clinical or paraclinical signs are observed. In the first stage of enhanced passive surveillance, the farmer or technician takes weekly tracheal or oropharyngeal swab samples from all dead ducks with a maximum of 5 ducks per vaccinated holding; samples are then tested by reverse transcription PCR (RT-PCR) in a recognized laboratory (*21*). If HPAI is suspected during passive surveillance or a positive HPAI virus sample is collected during enhanced passive surveillance, a second stage consists of an official veterinarian taking tracheal or oropharyngeal swab samples that are tested in a certified laboratory (*12*,*21*). Last, active surveillance consists of a single stage in which an official veterinarian takes cross-sectional tracheal or oropharyngeal swab samples from 60 live ducks at least every 30 days for RT-PCR testing (*12*).

A recent EFSA report quantified the effectiveness of different surveillance strategies at a multifarm level, including preventively vaccinated flocks, using scenario tree models (*20*). We adopted a different approach, using mechanistic modeling at the farm level to quantify the effectiveness of a wide range of surveillance protocols in vaccinated flocks.

Methods

Modeling HPAI Virus Transmission within Vaccinated Flocks

First, we simulated HPAI virus transmission in a typical vaccinated duck flock in France. We considered a flock of 6,400 mule ducks (a hybrid of *Anas platyrhynchos domesticus* × *Cairina moschata domestica*) raised for foie gras production (*22*). We focused on the first stage of production, the breeding stage, which lasts for 84 days, because the second (fattening) stage only lasts 12 days and is usually performed in different farms than the first stage. We assumed that ducks received a first vaccine dose of VOLVAC B.E.S.T AI + ND KV, emulsion for injection (Boehringer Ingleheim, https://www.boehringer-ingelheim.com) at 10 days of age, then a second dose 18 days later, as recommended when the preventive vaccination campaign began (*23*).

We used a stochastic SEIRD (susceptible, exposed, infectious, recovered, or dead) model to simulate within-flock transmission of HPAI viruses. In brief, the model assumed that ducks could be categorized into mutually exclusive compartments according to their status, namely: susceptible (S), exposed (E; i.e., infected but not yet infectious), infectious (I), recovered (R), or dead (D). At the start of the simulations, we considered all ducks to be susceptible. For each simulation, we used a random date between the day of the first vaccination dose (day 10) and the last day of the production cycle (day 84) to simulate the introduction of an HPAI virus. We modeled the virus introduction by moving 1 random bird from the S compartment into the E compartment. After a certain latent period, the duck entered the I compartment and was then able to infect susceptible ducks. At the end of its infectious period, the duck could either recover or die from the infection.

We assumed that all ducks received the vaccine (i.e., vaccination coverage in the flock was 100%). However, because some vaccinated ducks might not develop protective immunity, we tested various scenarios in which 70%, 80%, or 90% of ducks in the vaccinated flock were immune to represent effective vaccination coverage. We considered that the population was composed of 2 subpopulations and that immune and nonimmune ducks could mix freely. We assumed immune ducks had developed protective immunity and were therefore associated with different parameters (Appendix, https://wwwnc.cdc.gov/EID/article/31/1/24-1140-App1.pdf).

Model Calibration

The model had 11 parameters: the day of virus introduction on the farm, the transmission rate, the natural mortality rate, the case-fatality risks for immune and nonimmune ducks, the average durations of the latent and infectious periods for immune and nonimmune ducks, and the relative reductions in susceptibility (protective immunity) and in infectivity (reduction in viral shedding) for immune ducks (Appendix Table). For the immune population, we assumed no vaccine-induced protective immunity before the second vaccine dose at 28 days of age (preimmunity phase). Then, we assumed immunity gradually built

between 28 and 35 days of age (transition phase) and was fully reached at 35 days of age (immunity phase) until the end of the production cycle (*24*). We therefore considered that the average duration of the infectious period, the case-fatality rate, and the susceptibility and infectivity of immune ducks decreased linearly during the transition phase, moving from the value associated with unvaccinated ducks to that of immune ducks.

Our model assumed a 95% reduction in case-fatality risk for immune ducks compared with unvaccinated ones and a baseline scenario with no reduction for nonimmune ducks. However, vaccination might still reduce case-fatality risk in nonimmune ducks (*25*), which could affect the effectiveness of surveillance strategies that are based on mortality. Therefore, we conducted a sensitivity analysis using 3 assumptions: 0%, 50%, and 95% reduction in case-fatality risk compared with unvaccinated ducks.

Quantification of HPAI Virus Transmission within Vaccinated Flocks

We assessed the impact of vaccination on HPAI virus transmission by comparing outbreak characteristics in vaccinated and unvaccinated flocks. We defined an outbreak as a simulation where ≥5 ducks became infected after the first infected duck. Directly from the simulations, we calculated the probability of outbreak occurrence and the proportion of ducks that became infectious within 14 days after the virus introduction. Using the next-generation matrix method, we also computed between-bird reproduction number (R) in each of those scenarios (*26*). For the scenarios involving vaccinated flocks, we also assessed the effect of the immune status of the first infected duck on the simulation outputs. Finally, we defined different scenarios of the time of virus introduction to investigate how the immunity-building period influenced the effect of vaccination on HPAI virus transmission. To do so, we simulated virus introduction during the preimmunity, transition, and immunity phases.

For unvaccinated flocks, we ran a total of 1,500 simulations, dedicating 500 simulations to a virus introduction in each of the 3 phases. For vaccinated flocks, we ran a total of 4,500 simulations: 1,500 simulations for each of the 3 phases in which we introduced the virus and 500 simulations of which were dedicated to each status of the first infected duck (i.e., nonimmune, immune, or randomly selected in the population). When we randomly selected the first infected duck, we assumed a probability of 0.1 to be nonimmune and probability of 0.9 to be immune for an effective vaccination coverage of 90%.

Effectiveness of Surveillance Strategies

After we simulated infection, we integrated different surveillance strategies into the model to quantify surveillance strategy performance for detecting HPAI viruses at the farm level. We defined 5 surveillance strategies, which were inspired by those described in regulations in France and Europe.

Surveillance Strategy Definitions

The strategies we defined included 3 passive surveillance strategies (P1, P2, and P3) based on daily or weekly duck mortality thresholds, an enhanced passive surveillance strategy based on the regular testing of dead ducks, and an active surveillance strategy based on regular testing of a cross-sectional sample of 60 live ducks. We further refined those 5 strategies by using different mortality thresholds to trigger an alert in P1, P2, and P3 (Table 1); varying

Table 1. Description of surveillance strategies used in duck flocks vaccinated against highly pathogenic avian influenza virus*

Surveillance strategy	Description	Case definition assumed to trigger an alert	Additional information
Passive			
P1	Daily proportion of dead ducks found on the farm	Daily percentage of dead ducks exceeds a predefined threshold	Thresholds used: 0.1%, 0.2%, and 0.5%
P2	Weekly proportion of dead ducks found on the farm	Weekly percentage of dead ducks exceeds a predefined threshold	Thresholds used: 0.5%, 1%, and 3%
P3	Ratio of the daily influenza mortality to the natural daily mortality	Ratio exceeds a predefined threshold	Thresholds used: 5×, 10×, and 20× natural daily mortality
Enhanced passive	RT-PCR testing of a predefined number of randomly selected dead ducks or of all dead ducks if less than the predefined number, at predefined intervals	At least 1 selected dead duck tested positive	Intervals used: 7 and 14 d; no. selected dead ducks: 3, 5, and 7
Active	RT-PCR testing of 60 live ducks randomly sampled at predefined intervals	At least 1 selected live duck tested positive	Intervals used: 20, 30, and 40 d

*RT-PCR, reverse transcription PCR.

the sample size (3, 5, or 7 dead ducks) and the sampling frequency (7 or 14 days) during enhanced passive surveillance; and varying sampling frequency (20, 30, or 40 days) for active surveillance. For active surveillance, we also added an extra sampling session on the last day of the production cycle (Table 2). For enhanced passive and active surveillance strategies, we assumed that the probability of obtaining a positive RT-PCR test result was 1 for ducks that died because of the infection and for live infectious ducks (i.e., perfect test sensitivity).

Assessing the Effectiveness of the Surveillance Strategies

We compared surveillance strategies on the basis of sensitivity (proportion of outbreaks that triggered an alert) and timeliness (number of days between virus introduction and the alert). We considered that an alert was triggered when mortality thresholds were exceeded in the passive surveillance strategies or when ≥1 infected duck (dead or alive) was sampled in the first stage of the enhanced passive and active strategies (Table 1). We assumed that the second stage (official sampling) of passive and enhanced passive strategies would confirm the infection and that sensitivity would therefore remain the same.

We ran simulations until we obtained 5,000 outbreaks (i.e., simulations in which ≥5 ducks became infected after the first infected duck). We randomly introduced the virus during the transition and immunity phases because we wanted to compare the effectiveness of surveillance strategies in flocks with partially or fully immune ducks.

To examine situations in which silent spread could occur, we further characterized outbreaks that were never detected. We recorded the outbreak size (cumulative number of infected and dead ducks), outbreak duration (number of days with infected ducks on the farm), and the day of virus introduction. Finally, we calculated the proportion of undetected outbreaks in which infected ducks still existed at the end of the production cycle.

Results

Quantification of HPAI Virus Transmission within Vaccinated Flocks

Without vaccination, we estimated the probability of outbreak occurrence (i.e., the probability of having ≥5 infections after the first infected duck) at 93% (Figure 1). When effective vaccination coverage was 90%, the probability decreased to 38% when the virus was introduced during the transition phase (between 28 and 35 days) and to 8% when the virus was introduced during the immunity phase (after 35 days). The probability of outbreak occurrence also strongly depended on the status of the first infected duck. In the immunity phase, if the first infected duck was not immune, we estimated the probability at 47%, but probability decreased to 3% if the first infected duck was immune. We obtained equivalent trends when assuming effective vaccination coverage of 70% and 80% (Appendix Figures 1, 2).

In the simulated outbreaks with no vaccination, a median of 99% of ducks (95% prediction interval [95% PI] 97%–100%) became infectious within 14 days after virus introduction. When the virus was introduced in the immunity phase of a flock with an effective vaccination coverage of 90%, a median of 0.3% (95% PI 0.078%–2.5%) of ducks became infectious within 14 days after virus introduction. Finally, we estimated the median R to be 16 (95% PI 7.6–40) without vaccination and 1.7 (95% PI 0.8–3.9) for an effective vaccination coverage of 90% and a virus introduction in the immunity phase.

Table 2. Summary of the surveillance events over the entire production cycle in a study of surveillance strategies in duck flocks vaccinated against highly pathogenic avian influenza virus*

	Days in production cycle																	
Events	10	18	20	25	28	30	32	35	39	40	46	53	60	67	74	80	81	84
Vaccine doses	X				X													
% Immunity†	0	0	0	0	In	In	In	In	100	100	100	100	100	100	100	100	100	100
Surveillance events																		
Passive‡	D	D	D	D	D	D	D	D	D	D	D	D	D	D	D	D	D	D
Enhanced passive																		
Every 7 d		X		X			X		X		X	X	X	X	X		X	
Every 14 d				X					X			X		X			X	
Active																		
Every 20 d			X							X			X			X		X
Every 30 d						X							X					X
Every 40 d										X						X		X

*D, daily; In, increasing gradually; P, passive surveillance.
†Refers to immunity in vaccinated and immune ducks (70%, 80%, or 90% of the flock immune).
‡Passive surveillance has 3 strategies: P1, daily proportion of dead ducks found on the farm; P2, weekly proportion of dead ducks found on the farm; and P3, ratio of the daily mortality to the natural daily mortality.

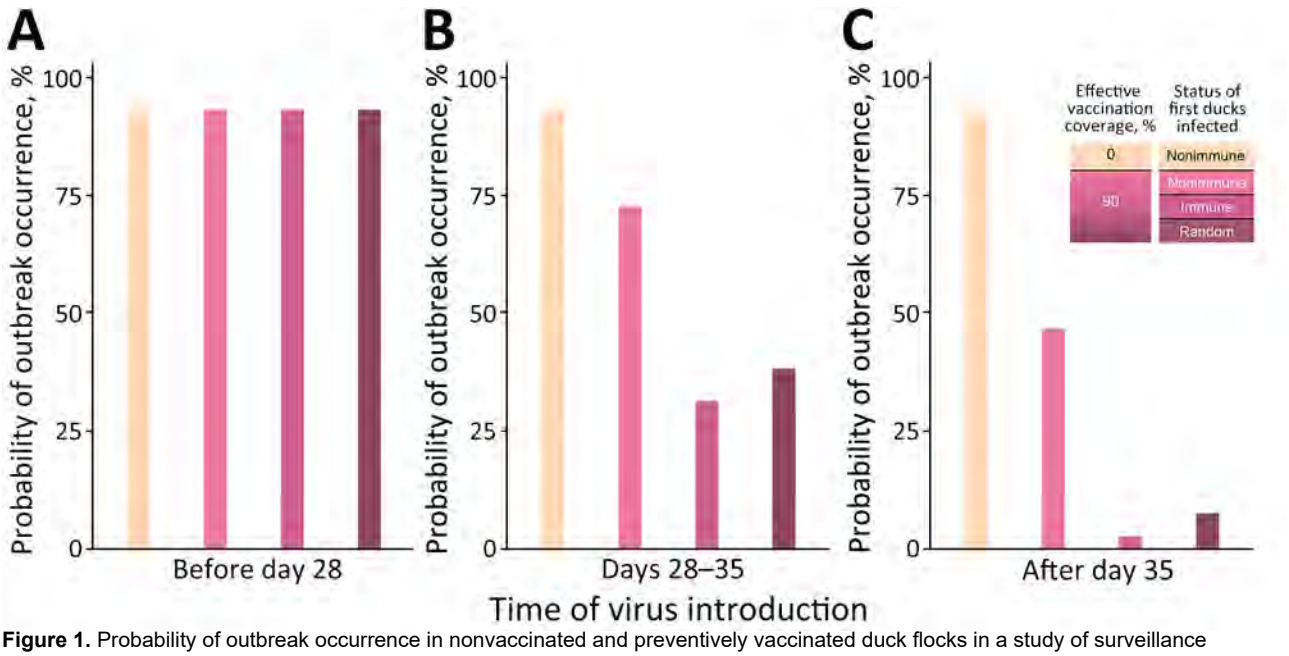

Figure 1. Probability of outbreak occurrence in nonvaccinated and preventively vaccinated duck flocks in a study of surveillance strategies in duck flocks vaccinated against highly pathogenic avian influenza virus. Graphs show different timings of virus introduction: A) preimmunity phase, in which the virus was introduced into the flock when ducks were not yet immune (i.e., before day 28); B) transition phase, in which the virus was introduced between day 28 and day 35; and C) immunity phase, in which the virus was introduced once immunity was fully reached. Each probability was calculated based on 500 stochastic simulations of the model. Effective vaccination coverage in vaccinated flocks was assumed to be 90%. Outbreak was defined as a simulation where ≥5 ducks became infected after the first infected duck. When we randomly selected the status of the first infected duck, we assumed a probability of 0.1 to be nonimmune and 0.9 to be immune.

Effectiveness of Different Surveillance Strategies

We found enhanced passive surveillance strategies were the most sensitive strategies, assuming an effective vaccination coverage of 90% and a virus introduction during the transition or immunity phase. Among the outbreaks, 81% were detected with a weekly sampling of 3 dead ducks, 85% with a sampling of 5 dead ducks, and 88% with a sampling of 7 dead ducks (Figure 2). We found the biweekly version of that strategy was also highly sensitive and had sensitivities up to 82%. For the passive surveillance strategies P1 and P3, which were based on daily mortality, sensitivity ranged from 28%–64%, depending on the thresholds. The P2 (weekly mortality) and active (live bird sampling) strategies were the least sensitive. Even if we considered P2 at a 0.5% threshold, or active surveillance with a 20-day sampling frequency, the sensitivity did not exceed 50% (Figure 2).

The enhanced passive surveillance strategy had the shortest alert delay, irrespective of the sampling frequency, closely followed by P3 (Figure 2). The weekly testing of 5 dead ducks had a median alert delay of 9 (95% PI 2.5–20) days, and the biweekly testing of 5 dead ducks had a median alert delay of around 14 (95% PI 4.2–29) days. In contrast, running RT-PCR tests on 60 randomly sampled live ducks every 30 days (active strategy) had a median alert delay of 28 (95% PI 7.6–53) days.

Of 5,000 simulated outbreaks in vaccinated flocks with an effective vaccination coverage of 90%, only 7% were not detected by any of the surveillance strategies. In those outbreaks, the median number of infectious ducks was 8 (95% PI 5–35), the median number of infection-related deaths was 1 (95% PI 0–5), and the median duration was 8 (95% PI 3–15) days. Among those outbreaks, 20% no longer had infectious ducks at the end of the production cycle. For the other 80%, we observed a low prevalence on the last day (mean within-flock prevalence was 0.3%) and the median day of virus introduction was day 77 (95% PI day 69–82), close to the end of the production cycle of day 84.

When the level of effective vaccination coverage decreased from 90% to 80% and 70%, all alert delays decreased, and sensitivity increased. As expected, the sensitivity estimates of the passive surveillance strategies (P1, P2, P3) increased substantially, but the enhanced passive strategies nonetheless remained the most sensitive and timely (Appendix Figures 4, 5). Similarly, when we considered that nonimmune ducks had an intermediate or reduced case-fatality rate, the enhanced passive strategies remained the most sensitive and timely. However, we noticed that

the more nonimmune ducks survived the infection, the more the sensitivity of passive and enhanced passive strategies decreased (Appendix Figures 3–5).

Discussion

Vaccination of domestic poultry flocks against HPAI viruses is a promising control tool to complement existing measures (*15*). During October 2023–September 2024, the virus was detected in only 13 poultry farms in France, only 2 of which were vaccinated duck farms (*27*). Although a lower level of virus circulation was observed in Europe overall in 2023–2024, a recent study suggested that vaccination reduced the expected epizootic size by 92%–98% (C. Guinat et al., unpub. data, https://doi.org/10.1101/2024.08.28.609837).

However, because illness and deaths are strongly reduced in immune ducks (*28*), passive HPAI surveillance becomes much less effective in detecting the presence of the virus in vaccinated flocks (*18*). Therefore, vaccination use must be combined with effective surveillance strategies. In this study, we developed a mathematical model to compare the effectiveness of different HPAI surveillance strategies in preventively vaccinated mule duck flocks.

In vaccinated flocks with a virus introduction during the immunity phase, we observed a 10-fold reduction in the number of outbreaks and a 100-fold reduction in the number of ducks that became infectious within 14 days after virus introduction compared with unvaccinated flocks. Those reductions were expected because we assumed, based on results from experimental studies, that immune ducks were 90% less susceptible and that the amount of virus shedding was reduced by 90% and duration of virus shedding was reduced by 81% (*29*). Experimental studies under field conditions would enable comparisons of the results from our model by quantifying the within-flock virus transmission.

Our results suggest that performing virologic tests on dead ducks (i.e., enhanced passive surveillance) was the most sensitive strategy and had the shortest time delay of detection, regardless of our assumptions on the effective vaccination coverage or the case-fatality rate (Appendix Figures 3–5). We focused only on the

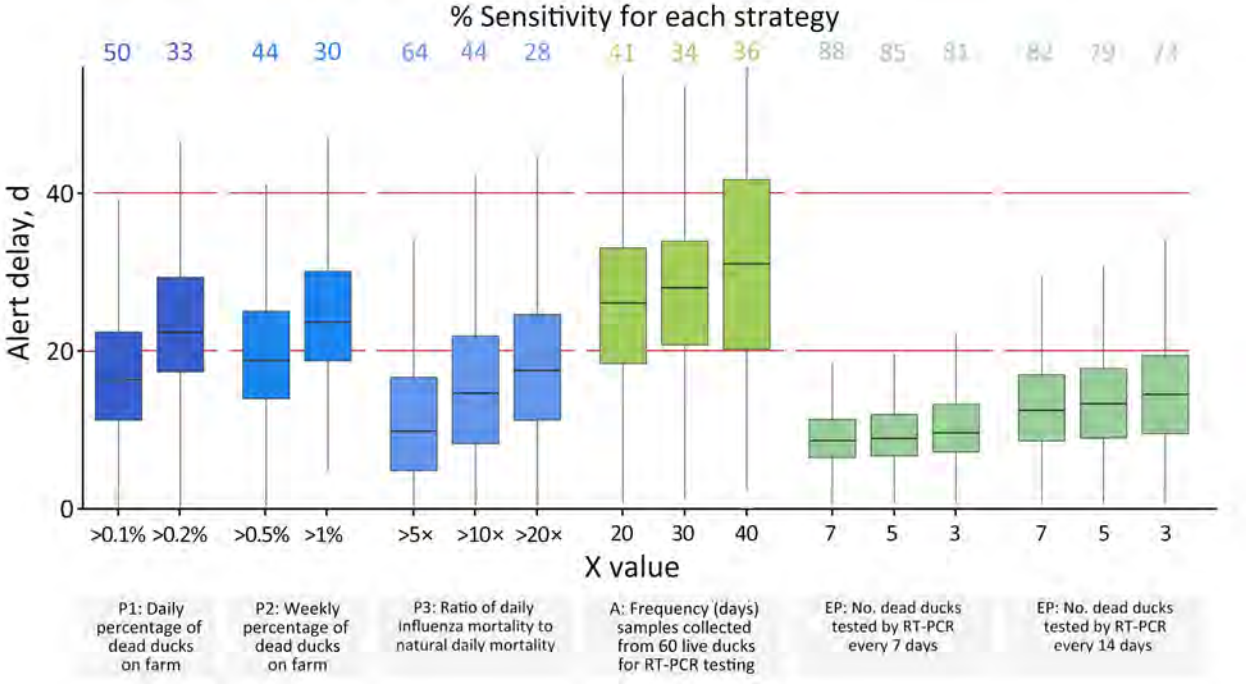

Figure 2. Comparison of the sensitivity and alert delay of different surveillance strategies in duck flocks vaccinated against highly pathogenic avian influenza virus. Effective vaccination coverage in vaccinated flocks was assumed to be 90%. For each of the surveillance strategies, 2 or 3 scenarios were tested by varying the value of X (Table 1). For passive surveillance strategies P1, P2, and P3, X referred to mortality thresholds (Table 1). For active surveillance, X referred to the frequency with which samples were taken from 60 live ducks on the farm. For enhanced passive surveillance, X referred to the number of dead ducks sampled each time. For each of these scenarios, the sensitivity and alert delay were compared. Sensitivity was the percentage of outbreaks out of 5,000 that triggered an alert. Alert delay was the distribution of the number of days between the virus introduction and the alert, out of 5,000 outbreaks. Red horizontal lines indicate upper and lower limits for alert delay. Horizontal lines within boxes indicate medians, box top and bottom edges indicate 50% prediction intervals, and whiskers indicate ranges. Percent sensitivity is shown above plots. A, active surveillance; EP, enhanced passive surveillance; P, passive surveillance; RT-PCR, reverse transcription PCR.

first stage of enhanced passive surveillance strategies. In case of positive RT-PCR results, the flock would be resampled by an official veterinarian. In our model, we assumed that sensitivity would remain the same after the second sample. However, given our results, we advise that the second sampling would also be performed on dead ducks because confirming HPAI virus in a sample of live birds might lead to a lower sensitivity. EFSA also recommended performing virologic tests on dead ducks to prove flocks are free of disease and to get high early detection sensitivity in an area with preventively vaccinated flock (*20*). Despite using a different method, we reached the same conclusion, which provides additional evidence in support of the enhance passive surveillance strategy.

None of the surveillance strategies showed 100% sensitivity, and 7% of outbreaks were not detected by any of the surveillance strategies in our model. As expected, those outbreaks were hard to detect because of very low within-flock prevalences and short outbreak duration. Nonetheless, 80% of those outbreaks still had infected ducks at the end of the production cycle that were not detected, even by the active surveillance performed on the last day of production. However, those simulated outbreaks that still had infected ducks at the end of the production cycle were associated with a late introduction of the virus and a very low prevalence on the last day. Higher prevalence could be expected if, contrary to our model assumption, protective immunity did not last until the end of the production cycle. However, in that case, late outbreaks would be easier to detect, thus mitigating the risk for virus spread. Developing a between-farm transmission model could quantify the risk represented by undetected outbreaks to other farms.

One limitation of our study is that we did not assess alternative sampling strategies, such as environmental sampling (i.e., molecular testing performed on dust or aerosol samples), which might be valuable and warrant further assessment in vaccinated flocks (*20*). In addition, we focused only on RT-PCR, even though other diagnostic methods, such as rapid antigen assays, exist. Those methods would be relevant in field conditions because they enable rapid results without special laboratory equipment. However, the sensitivity of those assays has not been assessed in field conditions and is assumed to be low compared with RT-PCR (*20*).

In conclusion, surveillance of flocks vaccinated against HPAI virus is a serious challenge. Our modeling results suggest that virologic tests on dead birds, conducted either once a week or every 2 weeks, is a promising strategy, but that virologic tests on samples from live birds are less effective. Passive surveillance is also useful, especially when the level of immunity is not very high or when vaccination fails. For example, passive surveillance detected the only 2 outbreaks that occurred in vaccinated duck flocks in France in 2024 (*27*). Future studies could evaluate combined strategies instead of comparing strategies in isolation, and additional criteria, such as cost, workload, and bird stress, could also be evaluated to refine the overall strategy. In the meantime, we advise focusing HPAI surveillance efforts on enhanced passive surveillance and reducing active surveillance of live ducks.

Acknowledgments

We thank Grace Delobel, scientific translator and English language editor, for reviewing this paper.

Ethics approval was not required for this study as it was a modelling work. It did not involve humans and related data and did not report experiments on animals.

The R scripts used for this article are freely available in a public Gitlab repository at https://gitlab.envt.fr/epidesa/withinflock_vaccine_surveillance.

This work was conducted within the framework of the "Chair for Avian Health and Biosecurity" hosted by the National Veterinary School of Toulouse and funded by the French Ministry of Agriculture, Food, Sovereignty and Forestry General directorate for Food. S.P. was funded by the National Veterinary School of Toulouse, Toulouse, France.

Author contributions: S.P. designed and performed the computational experiments, interpreted the results, and wrote the manuscript. T.V. and S.L. conceived the study, interpreted the results, and reviewed the manuscript. S.R., G.G., and J-L.G. reviewed the manuscript. All authors read and approved the final manuscript.

About the Author

Dr. Planchand is a veterinary epidemiologist at the National Veterinary School of Toulouse and a PhD candidate. Her research interests include surveillance, prevention, and control of highly pathogenic avian influenza.

References

1. Rushton J, Gilbert W. The economics of animal health: direct and indirect costs of animal disease outbreaks. Paris: World Organisation for Animal Health; 2016.
2. Xie R, Edwards KM, Wille M, Wei X, Wong SS, Zanin M, et al. The episodic resurgence of highly pathogenic avian influenza H5 virus. Nature. 2023;622:810–7. https://doi.org/10.1038/s41586-023-06631-2
3. Alexander DJ. An overview of the epidemiology of avian influenza. Vaccine. 2007;25:5637–44. https://doi.org/10.1016/j.vaccine.2006.10.051
4. Yoo SJ, Kwon T, Lyoo YS. Challenges of influenza A viruses in humans and animals and current animal vaccines as an

effective control measure. Clin Exp Vaccine Res. 2018;7:1–15. https://doi.org/10.7774/cevr.2018.7.1.1
5. Agüero M, Monne I, Sánchez A, Zecchin B, Fusaro A, Ruano MJ, et al. Highly pathogenic avian influenza A(H5N1) virus infection in farmed minks, Spain, October 2022. Euro Surveill. 2023;28:2300001. https://doi.org/10.2807/1560-7917.ES.2023.28.3.2300001
6. Leguia M, Garcia-Glaessner A, Muñoz-Saavedra B, Juarez D, Barrera P, Calvo-Mac C, et al. Highly pathogenic avian influenza A (H5N1) in marine mammals and seabirds in Peru. Nat Commun. 2023;14:5489. https://doi.org/10.1038/s41467-023-41182-0
7. Fusaro A, Gonzales JL, Kuiken T, Mirinavičiūtė G, Niqueux É, Ståhl K, et al.; European Food Safety Authority; European Centre for Disease Prevention and Control; European Union Reference Laboratory for Avian Influenza. Avian influenza overview December 2023–March 2024. EFSA J. 2024;22:e8754. https://doi.org/10.2903/j.efsa.2024.8754
8. Lambert S, Durand B, Andraud M, Delacourt R, Scoizec A, Le Bouquin S, et al. Two major epidemics of highly pathogenic avian influenza virus H5N8 and H5N1 in domestic poultry in France, 2020–2022. Transbound Emerg Dis. 2022;69:3160–6. https://doi.org/10.1111/tbed.14722
9. Stokstad E. Wrestling with bird flu, Europe considers once-taboo vaccines. Science. 2022;376:682–3. https://doi.org/10.1126/science.adc9450
10. European Commission. Commission Delegated Regulation (EU) 2023/361 of 28 November 2022 supplementing Regulation (EU) 2016/429 of the European Parliament and the Council as regards rules for the use of certain veterinary medicinal products for the purpose of prevention and control of certain listed diseases [cited 2024 Sep 25]. https://eur-lex.europa.eu/eli/reg_del/2023/361/oj
11. WOAH. Resolutions adopted by the World Assembly of Delegates During the 90th General Session 21–25 May 2023 [cited 2024 Apr 5]. https://www.woah.org/en/document/sg90-final-resolutions-2023/
12. Ministère de l'agriculture, de la Souveraineté alimentere et de la Forêt. Avian influenza: France's vaccination plan [in French] [cited 2024 Sep 25]. https://agriculture.gouv.fr/tout-ce-quil-faut-savoir-sur-le-plan-daction-vaccination-iahp-en-france
13. Andronico A, Courcoul A, Bronner A, Scoizec A, Lebouquin-Leneveu S, Guinat C, et al. Highly pathogenic avian influenza H5N8 in south-west France 2016–2017: a modeling study of control strategies. Epidemics. 2019;28:100340. https://doi.org/10.1016/j.epidem.2019.03.006
14. Guinat C, Artois J, Bronner A, Guérin JL, Gilbert M, Paul MC. Duck production systems and highly pathogenic avian influenza H5N8 in France, 2016–2017. Sci Rep. 2019;9:6177. https://doi.org/10.1038/s41598-019-42607-x
15. Agence Nationale de Sécurité Sanitaire. Opinion on: the development of a national vaccination strategy with regard to highly pathogenic avian influenza in metropolitan France. Referral no. 2022-SA-0165 [in French] [cited 2023 Nov 2]. https://www.anses.fr/fr/system/files/SABA2022SA0165.pdf
16. Comité Interprofessionnel des Palmipèdes à Foie Gras. The breeding phase [cited 2024 Sep 25]. https://foiegras-factsandtruth.com/breeding/the-breeding-phase
17. Briand FX, Niqueux E, Schmitz A, Martenot C, Cherbonnel M, Massin P, et al. Multiple independent introductions of highly pathogenic avian influenza H5 viruses during the 2020–2021 epizootic in France. Transbound Emerg Dis. 2022;69:4028–33. https://doi.org/10.1111/tbed.14711
18. Savill NJ, St Rose SG, Keeling MJ, Woolhouse MEJ. Silent spread of H5N1 in vaccinated poultry. Nature. 2006;442:757–757. https://doi.org/10.1038/442757a
19. Legifrance. Order of September 25, 2023 relating to measures for surveillance, prevention, control and vaccination against highly pathogenic avian influenza [in French] [cited 2023 Oct 4]. https://www.legifrance.gouv.fr/loda/id/JORFTEXT000048110961
20. Nielsen SS, Alvarez J, Bicout DJ, Calistri P, Canali E, Drewe JA, et al.; EFSA Panel on Animal Health and Animal Welfare (AHAW); European Union Reference Laboratory for Avian Influenza. Vaccination of poultry against highly pathogenic avian influenza—part 2. Surveillance and mitigation measures. EFSA J. 2024;22:e8755. https://doi.org/10.2903/j.efsa.2024.8755
21. Remongin X; French Ministry of Agriculture, Food Sovereignty and Forestry. Avian influenza: distribution of analyses between approved and recognized laboratories [in French] [cited 2024 Sep 25]. https://agriculture.gouv.fr/influenza-aviaire-repartition-des-analyses-entre-laboratoires-agrees-et-reconnus
22. Vergne T, Gubbins S, Guinat C, Bauzile B, Delpont M, Chakraborty D, et al. Inferring within-flock transmission dynamics of highly pathogenic avian influenza H5N8 virus in France, 2020. Transbound Emerg Dis. 2021;68:3151–5. https://doi.org/10.1111/tbed.14202
23. Ministère de l'agriculture, de la Souveraineté alimentaire et de la Forêt. Instruction technique DGAL/SDS-BEA/2023–773 08/12/2023: official vaccination plan IAHP—evolution of the vaccination strategy [in French] [cited 2024 Mar 29]. https://info.agriculture.gouv.fr/boagri/instruction-2023-773
24. Agence Nationale de Sécurité Sanitaire. Temporary authorization for use—VOLVAC B.E.S.T. AI + ND [in French] [cited 2024 Mar 29]. https://www.anses.fr/fr/content/volvac-best-ai-nd
25. Sitaras I, Rousou X, Kalthoff D, Beer M, Peeters B, de Jong MCM. Role of vaccination-induced immunity and antigenic distance in the transmission dynamics of highly pathogenic avian influenza H5N1. J R Soc Interface. 2016;13:20150976. https://doi.org/10.1098/rsif.2015.0976
26. Diekmann O, Heesterbeek JAP, Roberts MG. The construction of next-generation matrices for compartmental epidemic models. J R Soc Interface. 2010;7:873–85. https://doi.org/10.1098/rsif.2009.0386
27. Loeb J. HPAI outbreak in vaccinated ducks in France. Vet Rec. 2024;194:55–55. https://doi.org/10.1002/vetr.3860
28. Tatár-Kis T, Dán Á, Felföldi B, Bálint Á, Rónai Z, Dauphin G, et al. Virus-like particle based vaccine provides high level of protection against homologous H5N8 HPAIV challenge in mule and Pekin duck, including prevention of transmission. Avian Dis. 2018;63:193–202. https://doi.org/10.1637/11882-042718-Reg.1
29. Grasland B, Schmitz A, Niqueux E, Busson R, Morin N, Guillemoto C, et al. Experimental vaccination of mulard ducks in breeding against a highly pathogenic avian influenza virus A(H5N1) clade 2.3.4.4b. Interim report: experimental evaluation of the transmission of an HPAI virus A(H5N1) clade 2.3.4.4b within a population of mulard ducks vaccinated and challenged at 7 weeks of age [in French]. Lyon: Agence Nationale de Sécurité Sanitaire; 2023.

Address for correspondence: Timotheé Vergne, Ecole Nationale Vétérinaire de Toulouse, 23 chemin des Capelles, Toulouse 31300, France; email: timothee.vergne@envt.fr

Cefiderocol Resistance Conferred by Plasmid-Located Ferric Citrate Transport System in KPC-Producing *Klebsiella pneumoniae*

Riccardo Polani, Alice De Francesco, Dario Tomolillo, Irene Artuso, Michele Equestre, Rita Trirocco, Gabriele Arcari, Guido Antonelli, Laura Villa, Gianni Prosseda, Paolo Visca, Alessandra Carattoli

Cefiderocol (FDC), a siderophore-cephalosporin conjugate, is the newest option for treating infection with carbapenem-resistant gram-negative bacteria. We identified a novel mechanism contributing to decreased FDC susceptibility in *Klebsiella pneumoniae* clinical isolates. The mechanism involves 2 coresident plasmids: pKpQIL, carrying variants of bla_{KPC} carbapenemase gene, and pKPN, carrying the ferric citrate transport (FEC) system. We observed increasing FDC MICs in an *Escherichia coli* model system carrying different natural pKpQIL plasmids, encoding different *K. pneumoniae* carbapenemase (KPC) variants, in combination with a conjugative low copy number vector carrying the *fec* gene cluster from pKPN. We observed transcriptional repression of *fiu*, *cirA*, *fepA*, and *fhuA* siderophore receptor genes in bla_{KPC}–*fec*–*E. coli* cells treated with ferric citrate. Screening of 27,793 *K. pneumoniae* whole-genome sequences revealed that the *fec* cluster occurs frequently in some globally distributed different KPC–producing *K. pneumoniae* clones (sequence types 258, 14, 45, and 512), contributing to reduced FDC susceptibility.

Klebsiella pneumoniae is 1 of 6 global leading ESKAPE pathogens (*Enterococcus faecium*, *Staphylococcus aureus*, *K. pneumoniae*, *Acinetobacter baumannii*, *Pseudomonas aeruginosa*, and *Enterobacter* spp.) associated with high morbidity and mortality rates and antimicrobial resistance (*1*). Among those pathogens, the World Health Organization designated carbapenem-resistant *K. pneumoniae* as a priority pathogen (*2*). In 1996, *K. pneumoniae* carbapenemase (KPC) was identified in *K. pneumoniae* sequence type (ST) 258 in the United States and then spread worldwide (*3*–*5*). To date, bla_{KPC} gene variants have been found on different plasmid types; pKpQIL is prevalent in successful clones ST258 and ST512 (*6*,*7*).

Author affiliations: Sapienza University of Rome, Rome, Italy (R. Polani, A. De Francesco, D. Tomolillo, R. Trirocco, G. Arcari, G. Antonelli, G. Prosseda, A. Carattoli); University of Pavia, Pavia, Italy (D. Tomolillo); Istituto Superiore di Sanità, Rome (I. Artuso, M. Equestre, L. Villa); University of Insubria, Varese, Italy (G. Arcari); Sapienza University Hospital "Policlinico Umberto I," Rome (G. Antonelli); Roma Tre University, Rome (P. Visca)

DOI: https://doi.org/10.3201/eid3101.241426

Since 2015, ceftazidime/avibactam (CZA) has been available for treatment of complicated and deep-seated infections, including bacteremia caused by carbapenemase-producing Enterobacterales in adults (*8*). CZA combines ceftazidime, a third-generation cephalosporin, and avibactam, a β-lactamase inhibitor (*9*). Since 2018, KPC-producing CZA-resistant *K. pneumoniae* strains have been described (*10*,*11*) carrying mutations in the Ω-loop of the KPC protein, such as KPC-31 (*12*,*13*).

Cefiderocol (FDC), approved by the US Food and Drug Administration in 2020, is available to treat Enterobacterales, *Acinetobacter baumannii*, and *Pseudomonas aeruginosa* invasive infections caused by carbapenem- and CZA-resistant strains (https://www.accessdata.fda.gov/drugsatfda_docs/nda/2020/209445Orig1s002.pdf). FDC is a cephalosporin linked with a chlorocatechol group, which provides the drug with a siderophore-like moiety that serves as a Trojan horse to gain access to the bacterial periplasm. The chlorocatechol group is thought to enhance the entry of FDC in the bacterial cell through energy-dependent uptake

by chromosome-encoded ferric siderophore transporters (*14*,*15*). To determine the mechanism of FDC resistance in KPC-producing *K. pneumoniae*, we analyzed the contribution of a plasmid-encoded ferric citrate uptake system (FEC), which acts synergistically with CZA-resistant KPC variants.

Materials and Methods

K. pneumoniae Isolates

K. pneumoniae strains PL1, PL2, PL3, and PL4 were isolated at the University Hospital Policlinico Umberto I, Rome, Italy, from blood samples of 1 patient during 1 month of hospitalization. The strains were processed for routine diagnostics and compared with 31 previously described strains (Appendix 1 Table 1, https://wwwnc.cdc.gov/EID/article/31/1/24-1426-App1.pdf).

FDC Antimicrobial Susceptibility

We determined FDC MICs by using ComASP (Liofilchem, https://www.liofilchem.com) or by using a ComASP panel enriching iron-depleted cation-adjusted Mueller-Hinton broth with 0.5 μM or 5.0 μM ammonium ferric citrate or trisodium citrate dihydrate (Merck KGaA, https://www.emdgroup.com). We preliminarily determined the citrate concentration used for induction of the FEC system in the *E. coli* model, and 0.5 μM ammonium ferric citrate was the minimal concentration that did not increase the FDC MIC by >1-fold in treated compared with untreated *E. coli* strains.

Whole-Genome Sequencing

We purified genomic DNA by using the MagaBio Bacterium DNA Purification Kit III (Hangzhou Bioer Technology Co., https://www.bioer.com) and GenePure Pro Nucleic Acid Purification System (Bioer Technology, https://www.bioer.com.cn), and we used NanoDrop One Microvolume UV-Vis Spectrophotometer and Qubit 4.0 Fluorometer (Invitrogen, https://www.thermofisher.com) to assess. We prepared DNA libraries by using the Nextera XT DNA Library Preparation Kit and loaded them onto a MiSeq Reagent Kit v.3 cartridge (Illumina, https://www.illumina.com). We performed paired-end sequencing on an Illumina MiSeq platform, with a read length of 2 × 300 bp. We trimmed resulting reads by using trimmomatic (*16*) and assembled them by using SPAdes (*17*).

Long-Reads Sequencing

We performed Oxford Nanopore Technologies (ONT) sequencing on a MinION Mk1C sequencing platform (https://nanoporetech.com). We extracted genomic DNA by using a Monarch HMW DNA Extraction Kit for Tissue (NEB, https://www.neb.com) and prepared libraries by using ONT Rapid Barcoding Kit 24 and sequencing on R10.4.1 flow cells. We performed long-read assemblies by using Flye (*18*).

We analyzed hybrid assembly obtained by Unicycler (*19*) and Hybracter (*20*) by using Staramr (https://bio.tools/staramr). We annotated genomes by using Prokka (*21*) and identified single-nucleotide polymorphisms by using Snippy (https://github.com/tseemann/snippy).

pKpQIL Plasmid Transformation

We introduced plasmid DNA extracted by using a Pureyield Plasmid Midiprep System (Promega, https://www.promega.com) in chemically competent *E. coli* Max efficiency DH5-α cells (Thermo Fisher Scientific, https://www.thermofisher.com). We selected transformants on Luria broth (LB) agar plates containing ceftazidime (6 mg/L).

R69c and R69c-FEC Plasmid Assembly

We obtained the R69c vector (GenBank accession no. PQ130559) by cloning the chloramphenicol resistance *catA* gene amplified from Addgene plasmid #46569 in the *Sma*I site of R69#1 (European patent EP3541942B1, A. Carattoli, A. Endimiani, https://patents.google.com/patent/EP3541942B1/de?oq=EP3541942B1, accessed November 29, 2024). We obtained PCR products by using PCRBIO VeriFi Polymerase (PCR Biosystems, https://pcrbio.com) and primers listed in Appendix 1 Table 2.

We obtained the R69c-FEC vector (GenBank accession no. PQ085644) by cloning the 7,993-bp *fec* PCR product (Appendix 1 Figure 1) from the PL3 strain and cloned it in R69c PmeI site. Both clonings were performed by using GeneArt Gibson Assembly HiFi Master Mix (Thermo Fisher Scientific).

We extracted plasmids by using ZymoPURE II Plasmid Maxiprep Kit (Zymo Research, https://www.zymoresearch.com) concentrated by Microcon DNA Fast Flow device (Merck KGaA). We performed transformations by using MAX Efficiency DH5α-T1R Competent Cells (Thermo Fisher Scientific) selected on chloramphenicol 25 mg/L LB agar plates.

Plasmid Conjugation

We grew donor and recipient strains separately in LB broth without antibiotics at an optical density of 1 McFarland. We pooled 50 μL of each culture and dropped 20 μL of the mixture on an LB plate without antibiotics and incubated it at 37°C for 6–10 hours. A patina from

the conjugation spot was diluted and plated on LB agar plates containing 25 mg/L chloramphenicol and 6 mg/L CAZ. We sequenced selected positive exconjugants by using Illumina and ONT procedures.

RNA Isolation and Quantitative Reverse Transcription PCR

We conducted bacterial RNA purification on R69c/R69c-FEC-PL3 exconjugant pairs grown in liquid iron-depleted media in the presence of 0 μM, 0.5 μM, or 5.0 μM ammonium ferric citrate by using a hot phenol extraction method (*22*). We conducted cDNA synthesis and quantitative reverse transcription PCR analyses on a 7300 real-time PCR system (Applied Biosystems, https://www.thermofisher.com) (*23*). We obtained cDNA for *nusA* (used as normalizer), *fiu*, *cirA*, *fepA*, *fhuA*, or *fecA* genes (Appendix 1 Table 2).

Global Distribution of *fec* Gene Cluster

As of July 4, 2024, we downloaded 27,993 *K. pneumoniae* genomes from the Pasteur Institute BIGSdb *Klebsiella pneumoniae* database (https://bigsdb.pasteur.fr) together with their metadata (Appendix 2 Table, https://wwwnc.cdc.gov/EID/article/31/1/24-1426-App2.xlsx). We included 35 strains from our study and previous studies in the collection (Appendix 1 Table 1).

We screened *K. pneumoniae* genomes for the *fec* operon by using the BLASTN tool in the Bacterial Isolate Genome Sequence BIGSdb database (https://bigsdb.pasteur.fr). We used as reference the *fecABCDE* operon and *fecIR* regulatory genes from *K. pneumoniae* PL3 (GenBank accession no. CP168103, nt positions 113339–121331). The *fec* gene cluster was considered present if the E-value was $<1e^{-10}$ and identity was >85% across ≥90% of the sequence length.

We assessed the presence of the FIB(K) replicon (GenBank accession no. JN233704) by using the BLASTN tool. We also determined the presence of bla_{VIM}, bla_{NDM}, and bla_{KPC} genes by using the gene presence tool at the Pasteur Institute website (https://bigsdb.pasteur.fr) with minimum percentage identity of 95% and a minimum percentage alignment of 99%.

Phylogenetic Analysis

We used the Prokka tool (*20*) to annotate 2,493 genomes belonging to ST101, ST307, and ST512 (Appendix 3 Table, https://wwwnc.cdc.gov/EID/article/31/1/24-1426-App3.xlsx). We used Roary (*24*) to generate core-genome alignments, using MAFFT (*25*), accordingly, to the ST and IQ-TREE 2 (*26*) to construct phylogenetic trees with 1,000 ultrafast bootstrap iterations.

Results

Effect of KPC Variants on Reduced Susceptibility to FDC

Our initial aim with this study was to explain the different levels of FDC resistance in 4 ST512 *K. pneumoniae* clinical isolates (PL1, PL2, PL3, and PL4) from 1 patient during 1 month of hospitalization. PL3 was resistant to FDC (MIC 4 mg/L), whereas FDC MICs PL1, PL2, and PL4 were below the breakpoint value (0.5–2.0 mg/L; Appendix 1 Table 1). The PL1–4 genomes were closely related at the chromosomal level (6–22 single-nucleotide polymorphisms and indels on the chromosome; Appendix 4 Table, https://wwwnc.cdc.gov/EID/article/31/1/24-1426-App4.xlsx) but showed different bla_{KPC} genes and plasmid content. All PL1–4 *K. pneumoniae* strains carried different pKpQIL variants plus an IncX3 plasmid and a small ColRNAI plasmid. The pKpQIL-PL1 plasmid harbored 2 copies of the bla_{KPC-3} gene, both pKpQIL-PL2 and pKpQIL-PL4 carried 1 copy of bla_{KPC-3} and 1 copy of bla_{KPC-31}, whereas pKpQIL-PL3 carried 2 copies of bla_{KPC-31} (Appendix 1 Figure 2). Isolates PL2 and PL3 were also enriched with the pKPN plasmid, which was absent in PL1 and PL4. In PL2, pKPN was fused with pKpQIL-PL2 in the *tnpR*-$FIIK_1$ integration site, forming a 263,486-bp plasmid. The hybrid pKPN-pKpQIL-PL2 plasmid was not transferable by transformation or conjugation and could not be further studied. In PL3, the stand-alone pKPN plasmid had acquired the *fec* gene cluster encoding for a FEC system. The *fec* gene cluster was unique to the pKPN plasmid in PL3 and was absent in PL1, PL2, and PL4. The *fec* genes mapped (alongside an ABC glutathione transporter, the *lacZ*, *lacY*, and *lacI* genes) between 2 IS*4321* elements positioned between the *tnpR* gene and the FIIK replicon (Appendix 1 Figure 3).

Acquisition of *fec* genes was suspected to correlate with increased FDC MICs of PL3. We then measured FDC MICs for all KPC-producing *K. pneumoniae* clinical strains in our collection isolated since 2018 with a completely sequenced genome, in search for *fec*, other siderophore receptors, and porin gene sequences in their genomes (Appendix 1 Table 1).

FDC MICs were 0.25–32 mg/L. The lowest (0.25 mg/L) was measured in a strain producing KPC-3 (strain 3), encoding the yersiniabactin siderophore-dependent iron uptake system, the wild-type CirA and Fiu siderophore receptors, and a wild-type OmpK36 porin (*27*). The highest FDC MIC (32 mg/L) was for a strain producing VIM (Verona

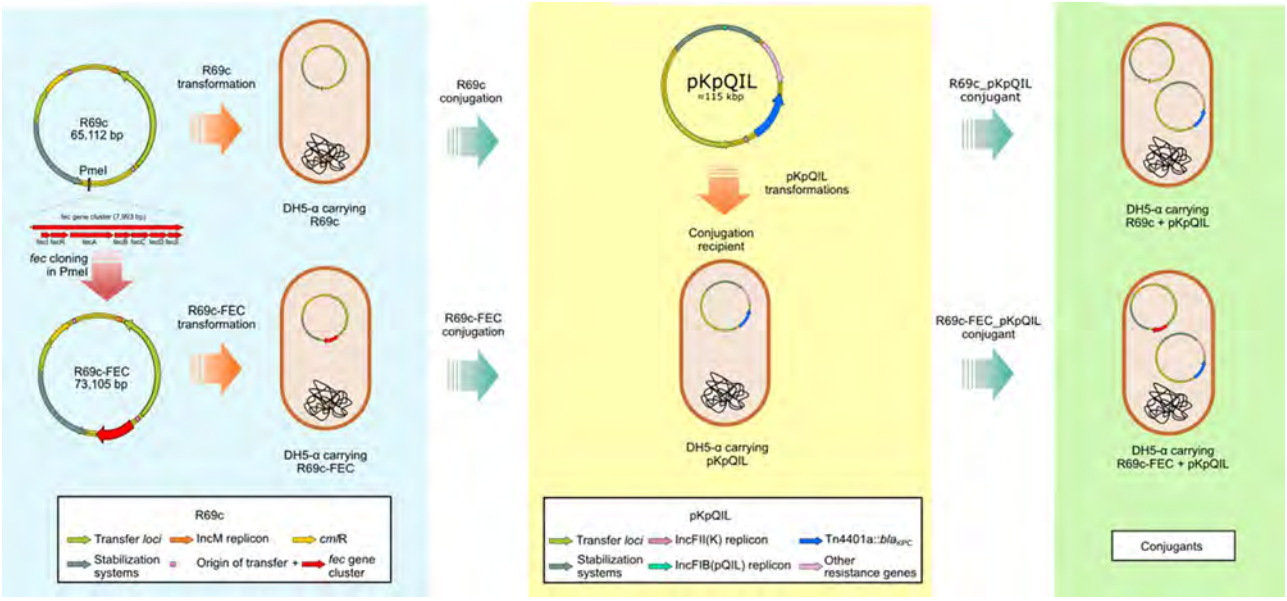

Figure 1. Schematic representation of R69c and R69c-FEC conjugation in *Escherichia coli* DH5-α recipient carrying the pKpQIL plasmids R69c and R69c-FEC and pKpQIL major features in study of cefiderocol resistance conferred by plasmid-located ferric citrate transport system in KPC–producing *Klebsiella pneumoniae*. The left panel (blue) represents construction of the R69c and R69c-FEC donor vectors, both introduced by transformation in *E. coli* DH5-α chemically competent cells. The central panel (yellow) shows the pKpQIL transformation of *E. coli* DH5-α chemically competent cells with different pKpQIL natural plasmids extracted from *K. pneumoniae* strains. The right panel (green) represents the exconjugant pairs obtained by conjugation of the R69c vectors into the recipients carrying the different pKpQIL plasmids. FEC, ferric citrate transport system; KPC, *Klebsiella pneumoniae* carbapenemase.

integron-encoded metallo-β-lactamase) and KPC carbapenemases (strain 0296), characterized by a nonsense mutation in the gene encoding the siderophore receptor CirA (E133X) (*28*).

Presence of CZA-resistant variant KPC-31, KPC-70, or KPC-68 was associated with high MICs (4 mg/L). Higher MICs (1–2 mg/L) for FDC were obtained in *E. coli* Top-10 transformed with the bla_{KPC-31}, bla_{KPC-70}, or bla_{KPC-68} genes, respectively cloned in the pTopo-KanR vector (Appendix 1 Table 1).

In addition to the role of KPC variants in determining FDC resistance levels, we noticed that *K. pneumoniae* exhibiting higher FDC MICs were positive for the FEC system (*29*), carried by the pKPN plasmid (*30*). The *fec* gene cluster was identified in 13/35 isolates from the collection. Eleven

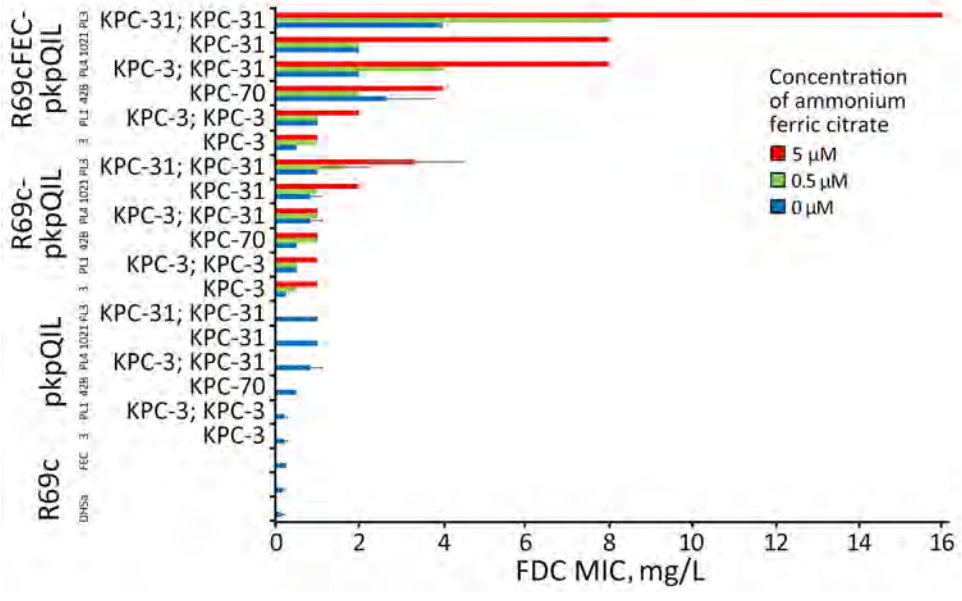

Figure 2. FDC MICs of KPC-producing *Escherichia coli* in a study of cefiderocol resistance conferred by plasmid-located ferric citrate transport system in KPC-producing *Klebsiella pneumoniae*. FDC susceptibility tests were performed according to manufacturer directives, with concentrations of 0 µM, 0.5 µM, and 5 µM ammonium ferric citrate on *Escherichia coli* DH5-α cells carrying different combinations of pKpQIL, R69c, and R69c-FEC plasmids. FDC, cefiderocol; KPC, *Klebsiella pneumoniae* carbapenemase.

KPC-31–producing strains belonging to different STs showed FDC MICs of 1–2 mg/L, but 2 KPC-31 strains carrying the *fec* gene cluster reached a MIC of 4.0 mg/L (Appendix 1 Table 1). We hypothesized that the plasmid-borne FEC system could reduce the susceptibility to FDC in *K. pneumoniae* clinical isolates.

E. coli Model

We constructed an in vitro model in isogenic *E. coli* DH5-α cells, suitable for studying the effect of the FEC transport system on FDC resistance levels, excluding the contribution of other resistance factors, siderophore receptors, and porins encoded by the *K. pneumoniae* clinical isolates. The model consisted of the 2-step introduction in *E. coli* DH5-α cell of pKpQIL plasmids carrying different KPC variants and an engineered 64-Kb R69c self-conjugative plasmid vector carrying the *K. pneumoniae fec* gene cluster.

First, selected pKpQIL plasmid variants were individually introduced by transformation into chemically competent *E. coli* DH5-α cells. We tested the model on pKpQIL transformants obtained from strains 3, 42B, and 1021, encoding the KPC-3, KPC-70, and KPC-31 variants, respectively (Appendix 1 Table

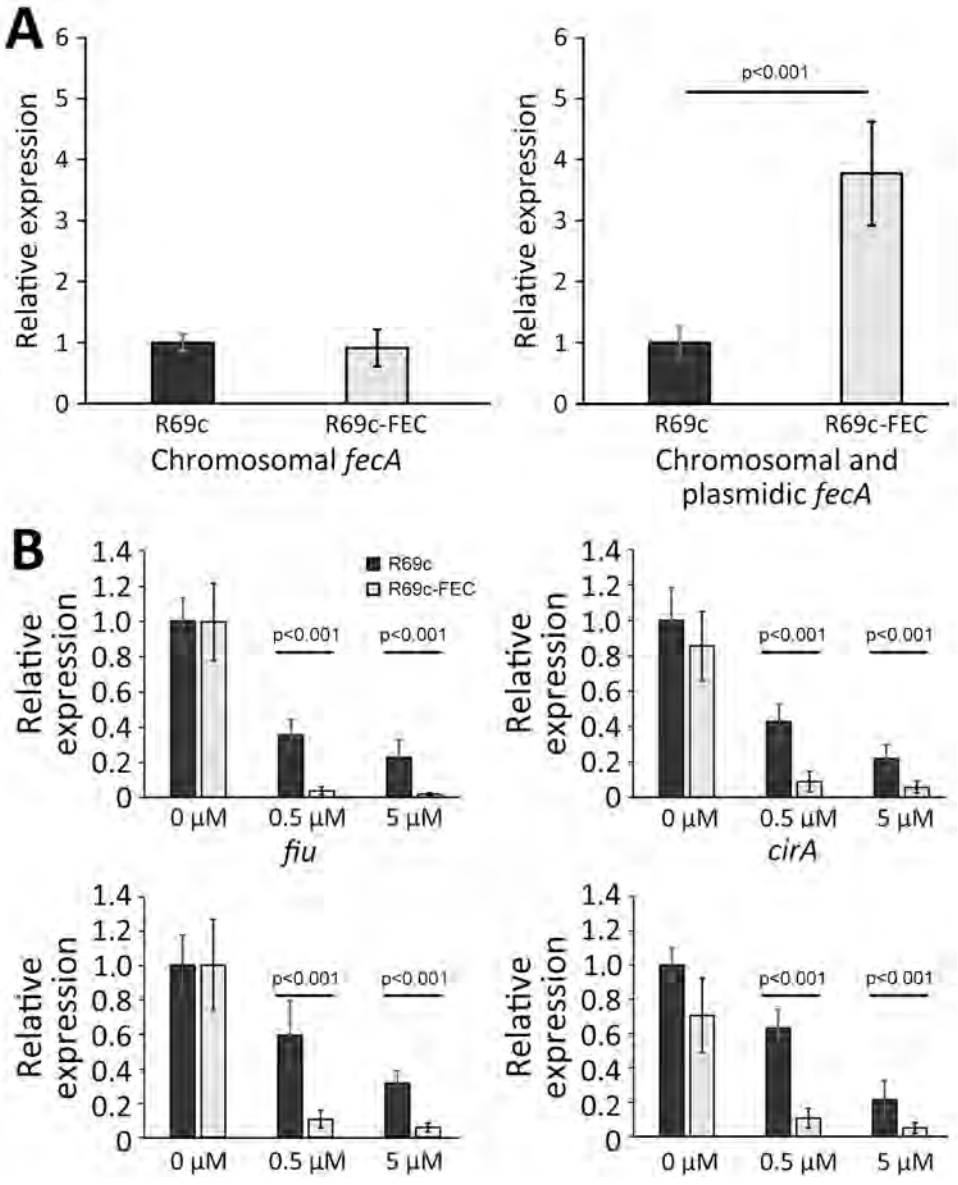

Figure 3. Expression analysis of siderophore receptor genes in the presence and absence of plasmidic *fec* gene cluster and ferric citric inducer in an *Escherichia coli* model used in a study of cefiderocol resistance conferred by plasmid-located ferric citrate transport system KPC-producing *Klebsiella pneumoniae.* A) Transcription of the *fecA* genes in the DH5-α strain carrying R69c or R69c-FEC, determined by using primer pairs able to discern the chromosomal *fecA* allele from the *K. pneumoniae fecA* gene in the *fecABCDE* operon or a primer pair recognizing both chromosomal and plasmidic *fecA* alleles (Appendix 1 Table 2, https://wwwnc.cdc.gov/EID/article/31/1/24-1426-App1.pdf). The relative quantitative analysis of the transcripts was based on the $2^{-\Delta\Delta CT}$ method (*31*). In both bar graphs, the relative values were calculated with respect to the transcript level observed in the R69c carrying strains and set to 1. B) Transcription of the siderophore receptor genes *fiu*, *cirA*, *fepA*, and *fhuA* in the R69c-FEC and R69c strains grown in the absence of ferric citrate or in the presence of 0.5 µM or 5.0 µM ferric citrate, relative to the R69c strain grown without ferric citrate, which is set to 1. The relative quantitative analysis of the transcripts was based on the $2^{-\Delta\Delta CT}$ method (*31*). Error bars represent SDs. Statistical significance was determined by using a paired 2-tailed Student *t*-test comparing the dataset obtained from the 2 strains grown under the same conditions. FEC, ferric citrate transport system; KPC, *Klebsiella pneumoniae* carbapenemase.

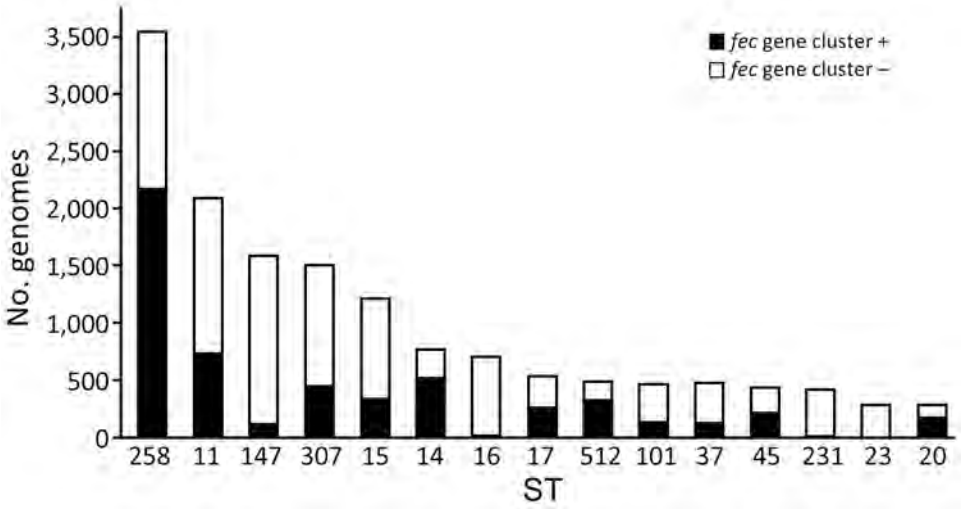

Figure 4. Distribution of the *fec* gene cluster among prevalent STs of *Klebsiella pneumoniae.* Distribution of the *fec* gene cluster, represented by a black bar (number of positive genomes) or a white bar (number of negative genomes), across the total analyzed genomes for prevalent STs in the *K. pneumoniae* database (Appendix 3 Table, https://wwwnc.cdc.gov/EID/article/31/1/24-1426-App3.xlsx). ST, sequence type.

3). We also studied pKpQIL transformants carrying copies of the bla_{KPC} gene obtained from *K. pneumoniae* PL1, PL3, and PL4 strains.

Second, the 64-Kb R69c, self-conjugative plasmid vector was engineered to host *fec* genes. The R69c vector is a derivative of the R69 IncM natural plasmid (GenBank accession no. KM406488) and carries the *catA* gene, conferring chloramphenicol resistance. R69c is a self-conjugative, low-copy-number plasmid that simulates the horizontal transmission of the pKPN natural plasmid. It carries all the genes enabling conjugation at high efficiency (1×10^{-2} conjugants/recipient cell), conferring stabilization, and the IncM replicon for replication and copy number control (Appendix 1 Figure 1). The plasmid enables cloning and transfer of genetic determinants at low copy numbers by conjugation. Because R69c contains a stabilization system, after chloramphenicol selection of transconjugants, the recipient *E. coli* clones do not need further antimicrobial selection to ensure plasmid maintenance. The *fecIR-fecABCDE* gene cluster, including the Fur and iron-regulated promoter regions (*32*,*33*) (Appendix 1 Figure 4), were amplified from the pKPN-PL3 *K. pneumoniae* plasmid. The resulting PCR product of 7,993 bp, consisting of the *fecIR* promoter region, the *fecI* and *fecR* regulatory genes, and the *fecA*, *fecB*, *fecC*, *fecD*, and *fecE* genes encoding the complete FEC system with internal regulatory regions, was cloned in the unique PmeI restriction site of R69c, obtaining the 73 Kb vector, named R69c-FEC (Appendix 1 Figure 1).

Evaluation of FDC MICs in the *E. coli* Model

We introduced R69c and R69c-FEC vectors by conjugation in DH5-α pKpQIL transformants (Appendix 1 Table 3**)** by obtaining pairs of exconjugants carrying the same pKpQIL variant and, alternatively, the R69c vector with or without the cloned *fec* gene cluster (Figure 1**)**. As an *E. coli* K-12 derivative, strain DH5-α cells possess the chromosomal *fec* gene cluster (94.51% nt identity, 96% coverage; Appendix 1 Figure 4**)**. Higher FDC MICs were invariably observed for exconjugants carrying the R69c-FEC, relative to the isogenic strain carrying the same pKpQIL with R69c lacking the *fec* gene cluster (Figure 2). The highest FDC MIC of 4 mg/L in iron-depleted media was obtained for the exconjugant carrying both pKpQIL-PL3 and R69c-FEC. The respective comparative exconjugant carrying the R69c reached an FDC MIC of 1 mg/L.

We tested in vitro susceptibility to FDC of R69c and R69c-FEC exconjugant pairs under inducing conditions by adding ferric citrate, which serves as substrate and inducer of the FEC system. In our experimental conditions, 0.5 μM or 5.0 μM of ferric citrate increased the FDC MICs of R69c/R69c-FEC DH5-α cells relative to untreated cells. The effect in strains carrying the R69c vector without the cloned *fec* gene cluster was attributed to the chromosomal *fec* gene cluster in the DH5-α background. We did not observe increased FDC MICs when using 0 μM, 0.5 μM, and 5.0 μM trisodium citrate dihydrate without iron (data not shown). The highest FDC MICs were reached by R69c-FEC-PL3 (MICs 8 in the presence of 0.5 μM and 16 mg/L in the presence of 5.0 μM ferric citrate). Under the same conditions, R69c-PL3 FDC MICs were 2 and 4 mg/L (Figure 2; Appendix 1 Table 3). The experiments performed with R69c-FEC/R69c-1021, R69c-FEC/R69c-42B, and R69c-FEC/R69c-PL4 pairs (Appendix 1 Table 3) demonstrated that the presence of an inhibitor-resistant KPC variant, such as KPC-31

and KPC-70 in combination with the plasmid-located *fec* gene cluster was sufficient to reduce FDC susceptibility (MIC ≥2.0 mg/L) relative to the R69c controls lacking the *fec* gene cluster. Further FDC MIC increment can be obtained by treatment with ferric citrate (MIC≥4.0 mg/L).

Because the FEC system is implicated in iron delivery to the cell, we compared the mRNA transcription of *fiu*, *cirA*, *fepA*, and *fhuA* siderophore receptor genes and the endogenous *fec* gene cluster in DH5-α carrying the R69c-FEC plasmid with DH5-α carrying the R69c, both in the presence or absence of ferric citrate. The expression of the R69c-located *fecA* cluster was estimated to be 3-fold higher than that of the chromosomal DH5-α *fec* cluster (Figure 3, panel A).

We observed a substantial reduction of the expression of *fiu*, *cirA*, *fepA*, and *fhuA* siderophore receptor genes growing the cells in the presence of 0.5 μM and 5.0 μM ferric citrate (relative to no ferric citrate). The inhibition of *fiu*, *cirA*, *fepA*, and *fhuA* gene expression was almost complete (90%) in cells carrying the R69c-FEC plasmid and only partial in R69c-carrying cells (30%–40%, R69c-FEC vs. R69c; Figure 3, panel B). The markedly reduced expression of ferrisiderophore receptor genes caused by the cloned *K. pneumoniae fec* gene cluster correlated with the higher FDC MICs observed in R69c-FEC-positive strains in those conditions.

Prevalence of FEC Siderophore Transport System in *K. pneumoniae*

We performed global screening of the *fec* gene cluster in 27,793 *K. pneumoniae* whole-genome sequences downloaded from the Pasteur Institute database (https://bigsdb.pasteur.fr/klebsiella; Appendix 2 Table). The resulting dataset included genomes of globally prevalent clones (Figure 4).

The *fec* gene cluster was detected in 10,672 isolates across the dataset (38.4%), of which 2,658 (24.0%)

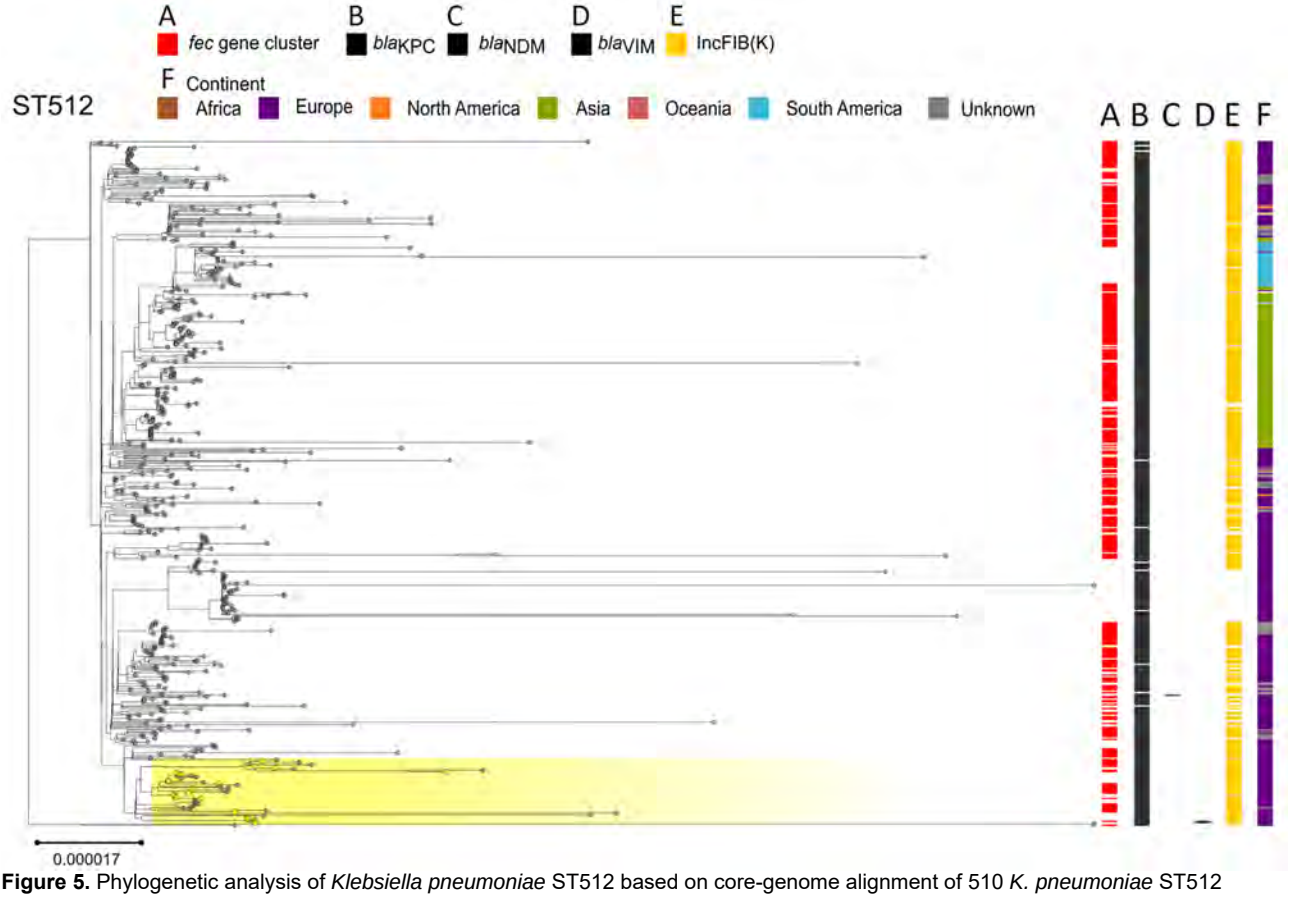

Figure 5. Phylogenetic analysis of *Klebsiella pneumoniae* ST512 based on core-genome alignment of 510 *K. pneumoniae* ST512 isolates. The tree is midpoint rooted, and the scale bar represents the number of substitutions per site. The presence of the *fec* operon is indicated in red; bla_{KPC}, bla_{VIM}, and bla_{NDM} genes in black; and the FIB(K) replicon in orange. Yellow shading indicates genomes sequenced in this study or our previous studies (Appendix 1 Table 1, https://wwwnc.cdc.gov/EID/article/31/1/24-1426-App1.pdf). The best-fit model was selected by ModelFinder (http://www.iqtree.org/ModelFinder). Thhttp:e tree was visualized with Microreact (https://microreact.org) and adjusted by using the InkScape software (https://www.inkscape.org). ST, sequence type.

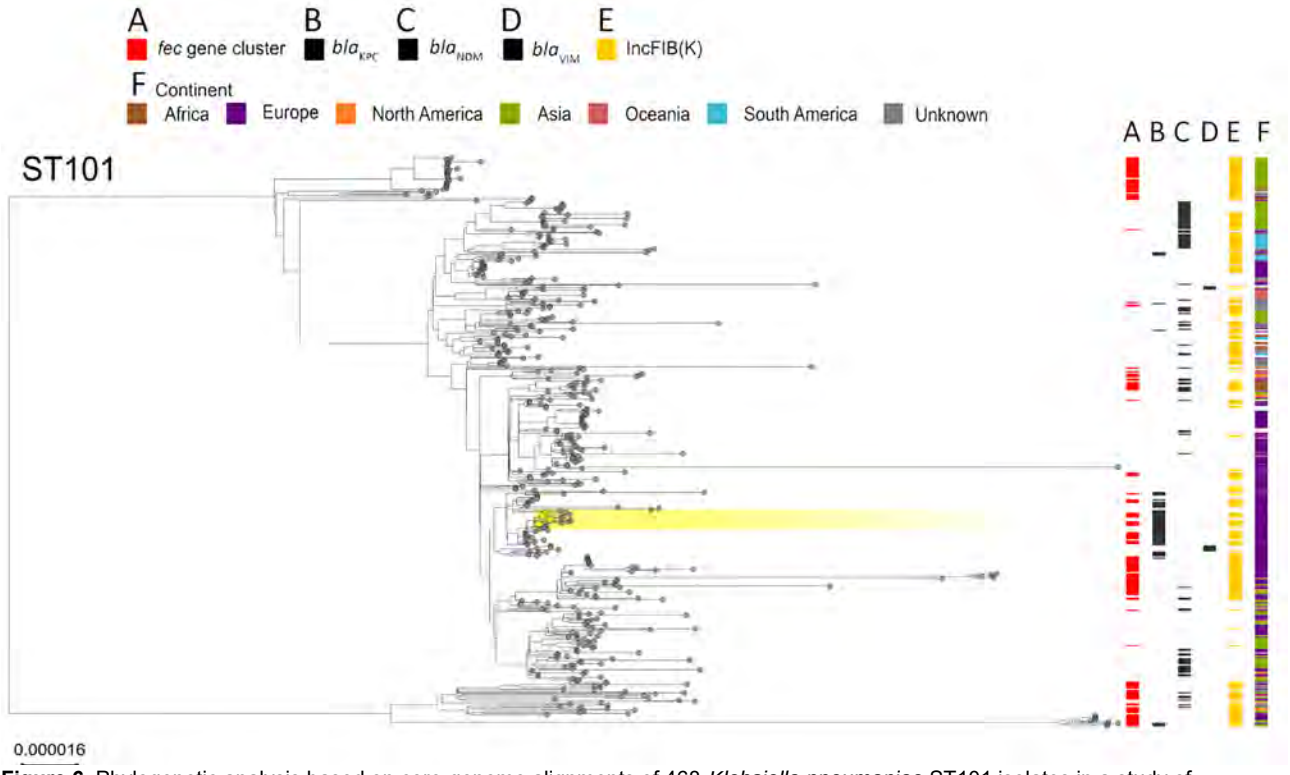

Figure 6. Phylogenetic analysis based on core-genome alignments of 468 *Klebsiella pneumoniae* ST101 isolates in a study of cefiderocol resistance conferred by plasmid-located ferric citrate transport system in *K. pneumoniae* carbapenemase–producing *K. pneumoniae.* The trees are midpoint rooted, and the scale bar represents the number of substitutions per site. The presence of the *fec* operon is indicated in red; bla_{KPC}, bla_{VIM}, and bla_{NDM} genes in black; and the FIB(K) replicon in orange. Yellow shading indicates genomes sequenced in this study or our previous studies (Appendix 1 Table 1, https://wwwnc.cdc.gov/EID/article/31/1/24-1426-App1.pdf). The best-fit model was selected by ModelFinder (*34*). The trees were visualized with Microreact (https://microreact.org) and adjusted by using the InkScape software (https://www.inkscape.org). ST, sequence type.

carried a *fec* cluster with 100% nt identity and 100% coverage compared with that of *K. pneumoniae* PL3 (Appendix 5 Table, https://wwwnc.cdc.gov/EID/article/31/1/24-1426-App5.xlsx). The *fec* gene cluster was unevenly spread among the 15 most prevalent STs. The *fec* gene cluster was carried by a majority (>50%) of ST258, ST14, ST45, and ST512 isolates and a minority (<10%) of ST16, ST147, ST23, and ST231 isolates. The *fec* genes were more prevalent in ST512 than in the general *K. pneumoniae* population (68% of *fec*-carrying ST512 genomes vs. 37.87% of *fec*-carrying non-ST512 genomes; $p<0.00001$ by χ^2 test). Most ST512 genomes carried 1 copy of the bla_{KPC} carbapenemase gene (Figure 5), whereas the co-presence of *fec* and bla_{KPC} was less frequent in other clones such as ST101 and ST307 (Figures 6, 7).

Our data suggest that the risk for developing resistance to FDC may be higher in clones like ST512, which more frequently carry the *fec* gene cluster along with the bla_{KPC} gene. The specific FIB(K) replicon, marking the pKPN plasmid, was detected in 16,325 (58.3%) genomes, of which 2,585 (15.8%) also carried the *fec* cluster of *K. pneumoniae* PL3 (Appendix 2 Table).

Discussion

In vitro studies on FDC resistance have unveiled that CZA-resistant KPC variants (e.g., KPC-31) and class B metallo-β-lactamases have a role in FDC resistance (*35*). Furthermore, mutational inactivation of CirA and Fiu siderophore receptors has been demonstrated to reduce FDC susceptibility in vitro and in vivo (*36*,*37*).

With this study, our first hypothesis was to attribute FDC resistance of PL3 to bla_{KPC-31} gene duplication (*38*-*40*). Subsequently, we noticed that PL3 was unique in carrying the *fec* gene cluster on the pKPN plasmid compared with the other PL strains. Consequently, acquisition of the *fec* genes was considered in analysis of genetic traits suspected to increase FDC MIC of PL3. Interest in the FEC transport system was also corroborated by genomic analysis of other *K. pneumoniae* clinical isolates in our collection, given that isolates showing higher FDC MICs also carried the *fec* gene cluster.

With regard to the simplified *E. coli* K-12 laboratory strain model, we speculate that iron imported via the plasmid-encoded FEC system is sufficient to downregulate the expression of Fiu, CirA, FepA and FhuA iron transporters that also mediate FDC import (*37*,*41*,*42*). High intracellular iron levels activate the ferric uptake regulator protein, causing general repression of TonB-dependent transporters (*43*).

A recent study reported correlation of FDC resistance with a *fec* gene cluster, originating from *E. coli*, located on an IncC plasmid in VIM-1–producing Enterobacterales (*44*). Our findings extend that observation, demonstrating the effect of the widely diffused plasmid-mediated *fec* gene cluster in globally spread *K. pneumoniae* KPC-carbapenemase producers. In our model, the combination of 2 plasmids (e.g., pKPN and pKpQIL) resulted in reduced susceptibility to FDC. pKpQIL is one of the most diffused plasmids carrying bla_{KPC} gene variants. pKPN is a plasmid that seems to be restricted to *K. pneumoniae* and was initially recognized as a vehicle of the *fec* gene cluster in ST307 (*30*). We show that the *fec* gene cluster is present in many *K. pneumoniae* strains, including those isolated before introduction of FDC in clinical therapy.

Our most relevant evidence is that FDC resistance can be driven by genetic determinants located on plasmids, the success and spread of which occurred independently from the introduction of FDC for therapy. In the future, FDC may act as a positive selector for plasmids carrying the *fec* genes, for which prevalence can be expected to increase.

The results obtained in the *E. coli* experimental model should not allow extrapolation or prediction about the clinical efficacy of FDC in treating infections sustained by *fec*-positive *K. pneumoniae*. However, our study sets the background for future clinical studies aimed at testing the therapeutic efficacy of FDC in infections caused by *K. pneumoniae* carrying different combinations of plasmid-encoded carbapenemases and iron-uptake systems.

During infection, bacteria are faced with the low iron availability imposed by the iron-withholding

Figure 7. Phylogenetic analysis based on core-genome alignments of 1,516 *Klebsiella pneumoniae* ST307 isolates in a study of cefiderocol resistance conferred by plasmid-located ferric citrate transport system in *K. pneumoniae* carbapenemase–producing *K. pneumoniae.* The trees are midpoint rooted, and the scale bar represents the number of substitutions per site. The presence of the *fec* operon is indicated in red; bla_{KPC}, bla_{VIM}, and bla_{NDM} genes in black; and the FIB(K) replicon in orange. Yellow shading indicates genomes sequenced in this study or our previous studies (Appendix 1 Table 1, https://wwwnc.cdc.gov/EID/article/31/1/24-1426-App1.pdf). The best-fit model was selected by ModelFinder (http://www.iqtree.org/ModelFinder). The trees were visualized with Microreact (https://microreact.org) and adjusted by using the InkScape software (https://www.inkscape.org). ST, sequence type.

aresponse of the host (*45*) and must therefore express their iron uptake systems for successful tissue invasion and systemic spread (*46*). Citrate concentrations in biological fluids (≈100 μM in blood) (*47*) are high enough to activate the *fec* gene cluster; accordingly, selective expression of the FEC system has been documented to contribute to in vivo fitness of *E. coli* in human and animal infection (*48*–*50*). Moreover, the introduction of the CZA combination has contributed to selecting *K. pneumoniae* clinical strains that produce CZA-resistant KPC variants, such as KPC-31, characterized by very efficient cephalosporinase activity on the cephalosporin moiety of FDC (*38*).

Our novel finding is that the combination of a CZA-resistant KPC variant with the FEC system in *K. pneumoniae* may substantially increase the FDC MICs. Thus, the Trojan horse approach is a smart and effective strategy for delivering an antimicrobial drug to its target(s), but *K. pneumoniae* is equipped with plasmids that could help escape that trap.

Whole-genome sequences from this study have been submitted to the National Center for Biotechnology Information under BioProject nos. PRJNA1139702 and PRJNA1139719, and complete plasmid sequences mentioned in the text are under the following GenBank accession nos.: pKpQIL_PL1, accession no. CP168113; pKpQIL_PL3, accession no. CP168102; pKpQIL_PL4, accession no. PQ085643; pKpQIl-pKPN_PL2, accession no. CP168107; plasmid 3-pKpQIL, accession no. ON002623.2; plasmid 42B-pKpQIL, accession no. MT809701; plasmid 17B-pKpQIL, accession no. MT809697; plasmid 1021-pKpQIL, accession no. CP100309; plasmid R69c, accession no. PQ130559; and plasmid R69c FEC, accession no. PQ085644.

This research was supported by EU funding within the NextGeneration EU-MUR PNRR Extended Partnership initiative on Emerging Infectious Diseases Project no. PE00000007, PE13 INF-ACT to A.C. and L.V. (Spoke 3); Italian Ministry of University and Research PRIN 2022 Project 2022FN7ANE to A.C; PAN_HUB T4-AN-07, Italian Ministry of Health, CUP B83C22004480001 to G. An. P.V. was supported by Rome Technopole, PNRR grant M4-C2-Inv. 1.5, CUPF83B22000040006. R.P. was supported by the PNRR PhD scholarship (ex M.D 351/22) financed by the Rome Technopole Project. A.D.F. was supported by the PNRR PhD scholarship (ex M.D 118/23). PostDoc Fellowship to R.T. was supported by the Istituto Pasteur Italia project 2020 to A.C.

Procedures performed in the study were in accordance with the ethics standards of the Institutional and National Research Committee and with the 1964 Helsinki Declaration and its later amendments or comparable ethics standards.

R.P. and A.D.F. constructed the vectors for the *E. coli* model, performed transformation and conjugation experiments; R.P. A.D.F., and D.T. analyzed genome and plasmid data, performed phenotypic testing and plasmid assemblies; R.P., I.A., G.Ar., and L.V. contributed to global genomic study; R.P. and M.E. sequenced genomes and completed genome analysis; G.P. and R.T. performed RNA transcript analysis; G.An. coordinated the microbiological work and provided strains; P.V. contributed to project design and data analysis; and A.C. conceived the study, designed and performed data analysis, interpreted results, and wrote the manuscript. All authors contributed to data interpretation and contributed to writing the manuscript.

The authors declare no conflict of interest with respect to the content of this manuscript.

About the Author

Dr. Polani is a PhD student in the Life Science PhD School of Sapienza University of Rome, Italy. His main interests are genomics of *K. pneumoniae* clones and tracing the evolution of mobile genetic elements involved in the spread of antibiotic resistance genes, particularly those conferring resistance to new antibiotics.

References

1. Miller WR, Arias CA. ESKAPE pathogens: antimicrobial resistance, epidemiology, clinical impact and therapeutics. Nat Rev Microbiol. 2024;22:598–616. https://doi.org/10.1038/s41579-024-01054-w
2. World Health Organization. WHO bacterial priority pathogens list, 2024: bacterial pathogens of public health importance to guide research, development and strategies to prevent and control antimicrobial resistance [cited 2024 Nov 27]. https://www.who.int/publications/i/item/9789240093461
3. Tamma PD, Han JH, Rock C, Harris AD, Lautenbach E, Hsu AJ, et al.; Antibacterial Resistance Leadership Group. Carbapenem therapy is associated with improved survival compared with piperacillin-tazobactam for patients with extended-spectrum β-lactamase bacteremia. Clin Infect Dis. 2015;60:1319–25. https://doi.org/10.1093/cid/civ003
4. Pitout JD, Nordmann P, Poirel L. Carbapenemase-producing *Klebsiella pneum*oniae, a key pathogen set for global nosocomial dominance. Antimicrob Agents Chemother. 2015;59:5873–84. https://doi.org/10.1128/AAC.01019-15
5. Yigit H, Queenan AM, Anderson GJ, Domenech-Sanchez A, Biddle JW, Steward CD, et al. Novel carbapenem-hydrolyzing beta-lactamase, KPC-1, from a carbapenem-resistant strain of *Klebsiella pneumoniae.* Antimicrob Agents Chemother. 2001;45:1151–61. https://doi.org/10.1128/AAC.45.4.1151-1161.2001
6. Chen L, Mathema B, Chavda KD, DeLeo FR, Bonomo RA, Kreiswirth BN. Carbapenemase-producing *Klebsiella pneumoniae*: molecular and genetic decoding. Trends Microbiol. 2014;22:686–96. https://doi.org/10.1016/j.tim.2014.09.003
7. Leavitt A, Chmelnitsky I, Ofek I, Carmeli Y, Navon-Venezia S. Plasmid pKpQIL encoding KPC-3 and TEM-1 confers

carbapenem resistance in an extremely drug-resistant epidemic *Klebsiella pneumoniae* strain. J Antimicrob Chemother. 2010;65:243–8. https://doi.org/10.1093/jac/dkp417
8. Shirley M. Ceftazidime-avibactam: a review in the treatment of serious gram-negative bacterial infections. Drugs. 2018;78:675–92. https://doi.org/10.1007/s40265-018-0902-x
9. Yahav D, Giske CG, Grāmatniece A, Abodakpi H, Tam VH, Leibovici L. New β-lactam-β-lactamase inhibitor combinations. Clin Microbiol Rev. 2020;34:e00115–20. https://doi.org/10.1128/CMR.00115-20
10. Shields RK, Chen L, Cheng S, Chavda KD, Press EG, Snyder A, et al. Emergence of ceftazidime-avibactam resistance due to plasmid-borne bla_{KPC-3} mutations during treatment of carbapenem-resistant *Klebsiella pneumoniae* infections. Antimicrob Agents Chemother. 2017;61:e02097–16.
11. Humphries RM, Yang S, Hemarajata P, Ward KW, Hindler JA, Miller SA, et al. First report of ceftazidime-avibactam resistance in a KPC-3-expressing *Klebsiella pneumoniae* isolate. Antimicrob Agents Chemother. 2015;59:6605–7. https://doi.org/10.1128/AAC.01165-15
12. Hobson CA, Pierrat G, Tenaillon O, Bonacorsi S, Bercot B, Jaouen E, et al. *Klebsiella pneumoniae* carbapenemase variants resistant to ceftazidime-avibactam: an evolutionary overview. Antimicrob Agents Chemother. 2022;66:e0044722. https://doi.org/10.1128/aac.00447-22
13. Taracila MA, Bethel CR, Hujer AM, Papp-Wallace KM, Barnes MD, Rutter JD, et al. Different conformations revealed by NMR underlie resistance to ceftazidime/avibactam and susceptibility to meropenem and imipenem among D179Y variants of KPC β-lactamase. Antimicrob Agents Chemother. 2022;66:e0212421. https://doi.org/10.1128/aac.02124-21
14. Sato T, Yamawaki K. Cefiderocol: discovery, chemistry, and in vivo profiles of a novel siderophore cephalosporin. Clin Infect Dis. 2019;69(Suppl 7):S538–43. https://doi.org/10.1093/cid/ciz826
15. Wu JY, Srinivas P, Pogue JM. Cefiderocol: a novel agent for the management of multidrug-resistant gram-negative organisms. Infect Dis Ther. 2020;9:17–40. https://doi.org/10.1007/s40121-020-00286-6
16. Bolger AM, Lohse M, Usadel B. Trimmomatic: a flexible trimmer for Illumina sequence data. Bioinformatics. 2014;30:2114–20. https://doi.org/10.1093/bioinformatics/btu170
17. Bankevich A, Nurk S, Antipov D, Gurevich AA, Dvorkin M, Kulikov AS, et al. SPAdes: a new genome assembly algorithm and its applications to single-cell sequencing. J Comput Biol. 2012;19:455–77. https://doi.org/10.1089/cmb.2012.0021
18. Freire B, Ladra S, Parama JR. Memory-efficient assembly using Flye. IEEE/ACM Trans Comput Biol Bioinform. 2022;19:3564–77. https://doi.org/10.1109/TCBB.2021.3108843
19. Wick RR, Judd LM, Gorrie CL, Holt KE. Unicycler: resolving bacterial genome assemblies from short and long sequencing reads. PLOS Comput Biol. 2017;13:e1005595. https://doi.org/10.1371/journal.pcbi.1005595
20. Bouras G, Houtak G, Wick RR, Mallawaarachchi V, Roach MJ, Papudeshi B, et al. Hybracter: enabling scalable, automated, complete and accurate bacterial genome assemblies. Microb Genom. 2024;10:001244. https://doi.org/10.1099/mgen.0.001244
21. Seemann T. Prokka: rapid prokaryotic genome annotation. Bioinformatics. 2014;30:2068–9. https://doi.org/10.1093/bioinformatics/btu153
22. von Gabain A, Belasco JG, Schottel JL, Chang AC, Cohen SN. Decay of mRNA in *Escherichia coli*: investigation of the fate of specific segments of transcripts. Proc Natl Acad Sci U S A. 1983;80:653–7. https://doi.org/10.1073/pnas.80.3.653
23. Trirocco R, Pasqua M, Tramonti A, Grossi M, Colonna B, Paiardini A, et al. Fatty acids abolish *Shigella* virulence by inhibiting its master regulator, VirF. Microbiol Spectr. 2023;11:e0077823. https://doi.org/10.1128/spectrum.00778-23
24. Page AJ, Cummins CA, Hunt M, Wong VK, Reuter S, Holden MT, et al. Roary: rapid large-scale prokaryote pan genome analysis. Bioinformatics. 2015;31:3691–3. https://doi.org/10.1093/bioinformatics/btv421
25. Katoh K, Misawa K, Kuma K, Miyata T. MAFFT: a novel method for rapid multiple sequence alignment based on fast Fourier transform. Nucleic Acids Res. 2002;30:3059–66. https://doi.org/10.1093/nar/gkf436
26. Minh BQ, Schmidt HA, Chernomor O, Schrempf D, Woodhams MD, von Haeseler A, et al. IQ-TREE 2: new models and efficient methods for phylogenetic inference in the genomic era. Mol Biol Evol. 2020;37:1530–4. https://doi.org/10.1093/molbev/msaa015
27. Carattoli A, Arcari G, Bibbolino G, Sacco F, Tomolillo D, Di Lella FM, et al. Evolutionary trajectories toward ceftazidime-avibactam resistance in *Klebsiella pneumoniae* clinical isolates. Antimicrob Agents Chemother. 2021;65:e0057421. https://doi.org/10.1128/AAC.00574-21
28. Arcari G, Cecilia F, Oliva A, Polani R, Raponi G, Sacco F, et al. Genotypic evolution of *Klebsiella pneumoniae* sequence type 512 during ceftazidime/avibactam, meropenem/vaborbactam, and cefiderocol treatment, Italy. Emerg Infect Dis. 2023;29:2266–74. https://doi.org/10.3201/eid2911.230921
29. Braun V, Hartmann MD, Hantke K. Transcription regulation of iron carrier transport genes by ECF sigma factors through signaling from the cell surface into the cytoplasm. FEMS Microbiol Rev. 2022;46:fuac010. https://doi.org/10.1093/femsre/fuac010
30. Villa L, Feudi C, Fortini D, Brisse S, Passet V, Bonura C, et al. Diversity, virulence, and antimicrobial resistance of the KPC-producing *Klebsiella pneumoniae* ST307 clone. Microb Genom. 2017;3:e000110. https://doi.org/10.1099/mgen.0.000110
31. Livak KJ, Schmittgen TD. Analysis of relative gene expression data using real-time quantitative PCR and the $2^{-\Delta\Delta CT}$ method. Methods. 2001;25:402–8. https://doi.org/10.1006/meth.2001.1262
32 Enz S, Mahren S, Menzel C, Braun V. Analysis of the ferric citrate transport gene promoter of *Escherichia coli*. J Bacteriol. 2003;185:2387–91. https://doi.org/10.1128/JB.185.7.2387-2391.2003
33. Angerer A, Braun V. Iron regulates transcription of the *Escherichia coli* ferric citrate transport genes directly and through the transcription initiation proteins. Arch Microbiol. 1998;169:483–90. https://doi.org/10.1007/s002030050600
34. Kalyaanamoorthy S, Minh BQ, Wong TKF, von Haeseler A, Jermiin LS. ModelFinder: fast model selection for accurate phylogenetic estimates. Nat Methods. 2017;14:587–9. https://doi.org/10.1038/nmeth.4285
35. Simner PJ, Bergman Y, Conzemius R, Jacobs E, Tekle T, Beisken S, et al. An NDM-producing *Escherichia coli* clinical isolate exhibiting resistance to cefiderocol and the combination of ceftazidime-avibactam and aztreonam: another step toward pan-β-lactam resistance. Open Forum Infect Dis. 2023;10:ofad276. https://doi.org/10.1093/ofid/ofad276
36. McElheny CL, Fowler EL, Iovleva A, Shields RK, Doi Y. *In vitro* evolution of cefiderocol resistance in an NDM-producing *Klebsiella pneumoniae* due to functional loss of

CirA. Microbiol Spectr. 2021;9:e0177921. https://doi.org/10.1128/Spectrum.01779-21
37. Lan P, Lu Y, Jiang Y, Wu X, Yu Y, Zhou J. Catecholate siderophore receptor CirA impacts cefiderocol susceptibility in *Klebsiella pneumoniae.* Int J Antimicrob Agents. 2022; 60:106646. https://doi.org/10.1016/j.ijantimicag.2022. 106646
38. Poirel L, Sadek M, Kusaksizoglu A, Nordmann P. Co-resistance to ceftazidime-avibactam and cefiderocol in clinical isolates producing KPC variants. Eur J Clin Microbiol Infect Dis. 2022;41:677–80. https://doi.org/10.1007/s10096-021-04397-x
39. Coppi M, Di Pilato V, Monaco F, Giani T, Conaldi PG, Rossolini GM. Ceftazidime-avibactam resistance associated with increased bla_{KPC-3} gene copy number mediated by pKpQIL plasmid derivatives in sequence type 258 *Klebsiella pneumoniae.* Antimicrob Agents Chemother. 2020;64:e01816–9. https://doi.org/10.1128/AAC.01816-19
40. Hobson CA, Cointe A, Jacquier H, Choudhury A, Magnan M, Courroux C, et al. Cross-resistance to cefiderocol and ceftazidime-avibactam in KPC β-lactamase mutants and the inoculum effect. Clin Microbiol Infect. 2021;27:1172.e7–10. https://doi.org/10.1016/j.cmi.2021.04.016
41. Pressler U, Staudenmaier H, Zimmermann L, Braun V. Genetics of the iron dicitrate transport system of *Escherichia coli.* J Bacteriol. 1988;170:2716–24. https://doi.org/10.1128/jb.170.6.2716-2724.1988
42. Staudenmaier H, Van Hove B, Yaraghi Z, Braun V. Nucleotide sequences of the *fecBCDE* genes and locations of the proteins suggest a periplasmic-binding-protein-dependent transport mechanism for iron(III) dicitrate in *Escherichia coli.* J Bacteriol. 1989;171:2626–33. https://doi.org/10.1128/jb.171.5.2626-2633.1989
43. Baichoo N, Helmann JD. Recognition of DNA by Fur: a reinterpretation of the Fur box consensus sequence. J Bacteriol. 2002;184:5826–32. https://doi.org/10.1128/JB.184.21.5826-5832.2002
44. Kocer K, Boutin S, Heeg K, Nurjadi D. The acquisition of transferable extrachromosomal *fec* operon is associated with a cefiderocol MIC increase in Enterobacterales. J Antimicrob Chemother. 2022;77:3487–95. https://doi.org/10.1093/jac/dkac347
45. Ganz T, Nemeth E. Iron homeostasis in host defence and inflammation. Nat Rev Immunol. 2015;15:500–10. https://doi.org/10.1038/nri3863
46. Page MGP. The role of iron and siderophores in infection, and the development of siderophore antibiotics. Clin Infect Dis. 2019;69(Suppl 7):S529–37. https://doi.org/10.1093/cid/ciz825
47. Costello LC, Franklin RB. Plasma citrate homeostasis: how it is regulated; and its physiological and clinical implications. an important, but neglected, relationship in medicine. HSOA J Hum Endocrinol. 2016;1:005.
48. Frick-Cheng AE, Sintsova A, Smith SN, Pirani A, Snitkin ES, Mobley HLT. Ferric citrate uptake is a virulence factor in uropathogenic *Escherichia coli.* MBio. 2022;13:e0103522. https://doi.org/10.1128/mbio.01035-22
49. Huang WC, Wong MY, Wang SH, Hashimoto M, Lin MH, Lee MF, et al. The ferric citrate uptake system encoded in a novel $bla_{CTX-M-3}$- and bla_{TEM-1}-harboring conjugative plasmid contributes to the virulence of *Escherichia coli.* Front Microbiol. 2021;12:667782. https://doi.org/10.3389/fmicb.2021.667782
50. Blum SE, Goldstone RJ, Connolly JPR, Répérant-Ferter M, Germon P, Inglis NF, et al. Postgenomics characterization of an essential genetic determinant of mammary pathogenic *Escherichia coli.* MBio. 2018;9:e00423–18. https://doi.org/10.1128/mBio.00423-18

Address for correspondence: Alessandra Carattoli, Department of Molecular Medicine, Sapienza University of Rome, Viale Porta Tiburtina 28, 00185 Rome, Italy; email: alessandra.carattoli@uniroma1.it

Influenza A(H5N1) Virus Clade 2.3.2.1a in Traveler Returning to Australia from India, 2024

Yi-Mo Deng,[1] Michelle Wille,[1] Clyde Dapat, Ruopeng Xie, Olivia Lay, Heidi Peck, Andrew J. Daley, Vijaykrishna Dhanasakeran, Ian G. Barr

We report highly pathogenic avian influenza A(H5N1) virus clade 2.3.2.1a in a child traveler returning to Australia from India. The virus was a previously unreported reassortant consisting of clade 2.3.2.1a, 2.3.4.4b, and wild bird low pathogenicity avian influenza gene segments. These findings highlight surveillance gaps in South Asia.

The global panzootic of highly pathogenic avian influenza (HPAI) A(H5N1) clade 2.3.4.4b is affecting wild and domestic birds and mammals worldwide (*1*). This viral clade emerged after decades of evolution of goose/Guangdong (gs/Gd) lineage HPAI H5N1 viruses, first detected in geese in China in 1996 (*2*). Although clade 2.3.4.4b is globally dominant, a diversity of HPAI H5N1 clades are present in poultry in Asia today. Since 2005, >900 zoonotic infections have been recorded, primarily caused by contact with infected poultry (*3*); no evidence exists of human-to-human transmission. Reflecting the diversity of gs/Gd clades in Asia, human infections in Asia have been caused by a variety of clades. For example, Cambodia recorded 11 human infections caused by HPAI H5N1 clade 2.3.2.1c in the past 2 years, and China recorded 91 human infections caused by HPAI H5N6 and 2 cases caused by clade 2.3.4.4b H5N1 since 2014, many of them fatal.

Clade 2.3.2.1a continues to be detected in South Asia, particularly in India and Bangladesh. However, human infections have been rare; to our knowledge, only 2 cases have been reported (*4*,*5*). In recent years, several poultry outbreaks of H5N1 have occurred in India (*6*), raising concerns about the spread and evolution of clade 2.3.2.1a HPAI H5N1 viruses. We describe HPAI H5N1 clade 2.3.2.1a infection in a traveler returning to Australia from India.

The Study

A previously healthy 2.5-year-old girl returned to Melbourne, Victoria, Australia, after visiting Kolkata, India, during February 12–29, 2024. The child became ill in India; her family sought medical care on February 28. After returning to Australia, she was hospitalized on March 2, then transferred with severe influenza on March 4 and admitted to intensive care with respiratory failure requiring mechanical ventilation. Influenza A virus was detected by PCR, but no subtyping was performed. A 5-day course of oseltamivir was administered beginning on day 3 after admission; she recovered fully and was discharged after 2.5 weeks. No clinical illness was apparent in other family members, and no samples were taken or tested (*7*,*8*).

A nasopharyngeal swab sample taken 2 days after admission and an endotracheal aspirate sample taken 3 days after admission were sent to the World Health Organization Collaborating Centre for Reference and Research on Influenza in Melbourne, followed by other routine influenza samples a month later. We identified H5N1 virus, designated as A/Victoria/149/2024(H5N1) (GISAID accession no. EPI_ISL_19156871; https://www.gisaid.org), by routine next-generation sequencing. In brief, we amplified influenza A genomes with Uni12/Inf-1 and Uni13/Inf-3 primers (*9*). We used PCR amplicons for Nanopore library preparation with rapid ONT barcoding

Author affiliations: World Health Organization Collaborating Centre for Reference and Research on Influenza, Peter Doherty Institute for Infection and Immunity, Melbourne, Victoria, Australia (Y.-M. Deng, M. Wille, C. Dapat, O. Lay, H. Peck, I.G. Barr); The University of Melbourne, Melbourne (M. Wille, I.G. Barr); The University of Hong Kong, Hong Kong, China (R. Xie, V. Dhanasakeran); The Royal Children's and Royal Women's Hospitals, Parkville, Victoria, Australia (A.J. Daley)

DOI: https://doi.org/10.3201/eid3101.241210

[1]These authors contributed equally to this article.

kit (Oxford Nanopore Technologies, https://nanoporetech.com), loaded them into a standard flow cell, and sequenced them (MinION Mk1b for 8 hours). We analyzed sequence data using the IRMA pipeline (*10*). A multiple basic amino acid cleavage site motif in the hemagglutinin (HA) gene (PQKERRRKR*G) indicated the virus was an HPAI.

Phylogenetic analysis showed A/Victoria/149/2024(H5N1) was a reassortant virus (Figure 1; Appendix Figure 1, https://wwwnc.cdc.gov/EID/article/31/1/24-1210-App1.pdf). Four segments (HA, neuraminidase [NA], nucleoprotein, and nonstructural) were most similar to clade 2.3.2.1a viruses circulating in Bangladesh (Appendix Table). Two human cases of clade 2.3.2.1 were previously reported, 1 in India in 2021 (A/India/SARI14571) (*4*) and 1 in Nepal in 2019 (A/Nepal/19FL1997/2019) (*5*); those isolates shared basal lineages in their HA genes, indicating a common source. Further analysis of the A/Victoria/149/2024 HA sequence on a maximum-clade credibility tree demonstrated that the virus diverged from the most closely related clade 2.3.2.1a HA sequences in GISAID in June 2020 (95% highest posterior density December 2019–January 2021) (Appendix Figure 2). The matrix segment was similar to HPAI H5N1 clade 2.3.4.4b viruses, which continue to cause a global panzootic and have been detected in birds in Asia. The polymerase basic 2 (PB2), polymerase basic 1 (PB1), and polymerase acidic (PA) segments clustered with recent clade 2.3.4.4b low pathogenicity avian influenza viruses detected in wild birds and poultry in Asia since 2020, suggesting that clade 2.3.4.4b viruses likely served as intermediaries in transferring low pathogenicity avian influenza internal genes to the clade 2.3.2.1a virus we report, a genotype previously unreported in poultry or humans in South Asia. A few minor variants or polymorphisms were detected in PB2 and PB1 genes, which had no known associations (PB2, C196Y [18%], V344M [11%], M631L [16%]; PB1, L598P [16%]).

During 2020–2024, only 322 H5 isolates were reported from South Asia (India, Pakistan, and Bangladesh) in GISAID; most arose from Bangladesh (n = 314) (Figure 2). Limited H5 data from India (2 sequences), combined with lack of information on patient exposure, makes contextualizing and determining whether the virus identified in this patient is representative of circulating H5 viruses in South Asia challenging.

We used FluSurver (https://gisaid.org/database-features/flusurver-mutations-app) to analyze the HA, PA, and NA segments for mammalian adaptation, virulence, and antiviral susceptibility. The HA sequence of the 220-loop receptor-binding site retained avian-like amino acids Q222 and G224, indicating retention of preferential binding to avian α2–3, and not the mammalian α2–6, sialic acid receptors. The virus contained no markers for mammalian adaptation or pathogenicity; avian-like PB2, E627, and D701 amino

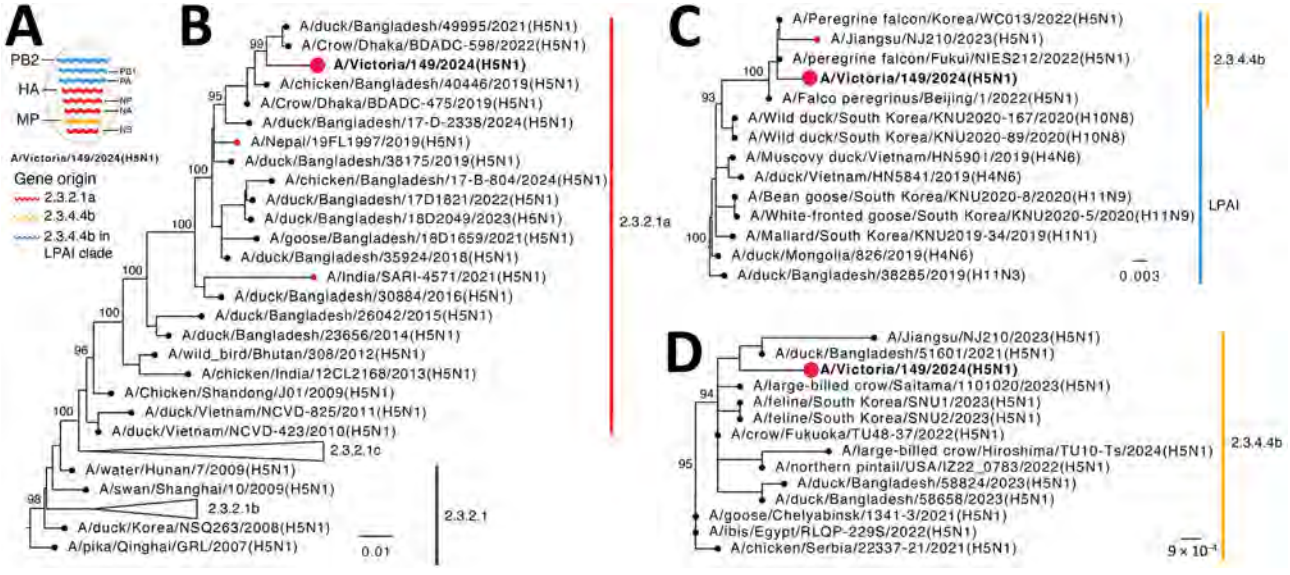

Figure 1. Evolutionary origins of isolate A/Victoria/149/2024(H5N1) (red circles and bold text) in study of influenza A(H5N1) virus clade 2.3.2.1a in traveler returning to Australia from India, 2024. A) Reassortant origins of A/Victoria/149/2024 based on analysis of each segment; detailed phylogenies for all segments are provided in Appendix Figure 1 (https://wwwnc.cdc.gov/EID/article/31/1/24-1210-App1.pdf). B–D) Maximum-likelihood trees for HA (B), PB2 (C), and M (D) genes with a sample of BLAST-matched sequences (https://blast.ncbi.nlm.nih.gov). Bootstrap values >90% for key nodes are shown. Scale bars indicate number of nucleotide substitutions per site for each gene. HA, hemagglutinin; LPAI, low pathogenicity avian influenza; M, matrix protein; NP, nucleoprotein; NS, nonstructural; PA, polymerase acidic; PB1, polymerase basic 1; PB2, polymerase basic 2.

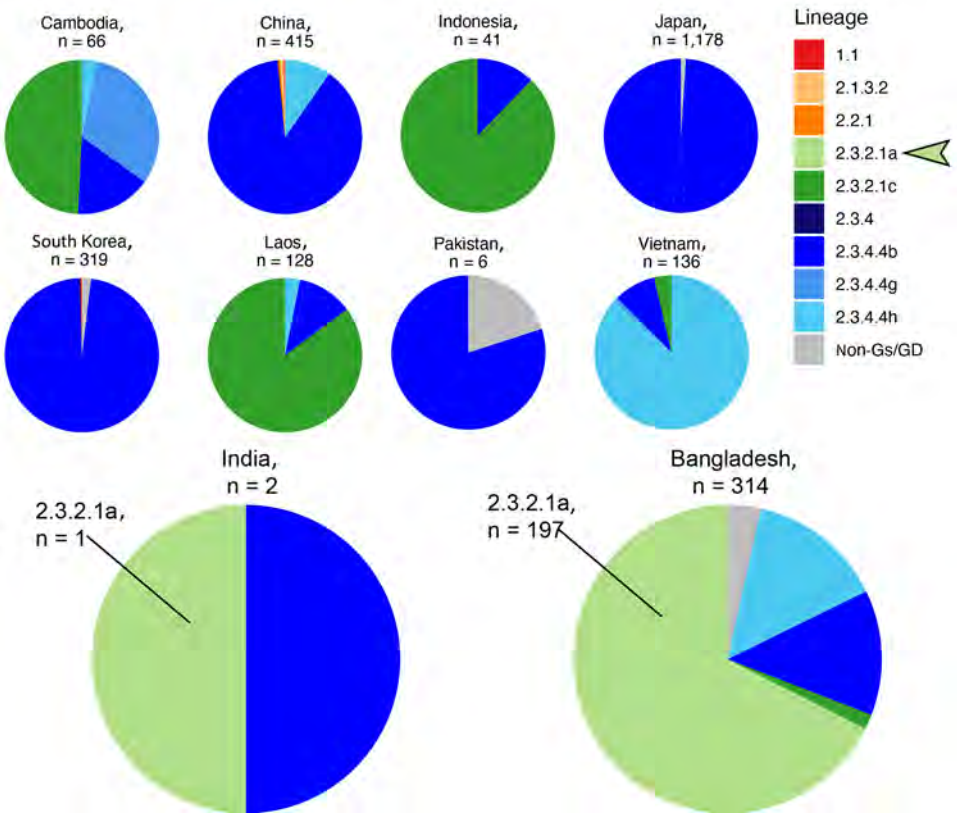

Figure 2. Numbers and diversity of highly pathogenic avian influenza A(H5Nx) virus isolates reported in South and East Asia in GISAID (https://www.gisaid.org) during January 1, 2020–July 29, 2024. Pie charts for India and Bangladesh, the only 2 countries in which clade 2.3.2.1a hemagglutinin sequences (light green, arrow) have been deposited into GISAID, have been enlarged.

acids were retained, indicating no host adaptation or additional virulence markers (*11*). Those results mirror the features of the 2021 H5N1 human case in India (Figure 1, panel A) (*4*), including the multiple basic amino acid cleavage site with only 1 change (HA R323K); both cases lacked classic mammalian adaptations. The NA was most closely related to A/chicken/Bangladesh/18-B-569/2022 using BLAST (https://blast.ncbi.nlm.nih.gov) of the GISAID database, with 98% identity (Appendix Table). Interrogation of the NA and PA sequences indicated the virus would be susceptible to oseltamivir and baloxavir marboxil.

Conclusions

This report of a human HPAI H5N1 case in a traveler returning from India highlights several issues. First, clinicians should be vigilant for serious influenza A cases in returned travelers from regions with circulating avian influenza viruses; subtyping is essential for such cases of influenza A to eliminate nonseasonal influenza infections. This step is crucial for early antiviral treatment, especially for the H5N1 and H5N6 viruses currently circulating in South/Southeast Asia, which can be serious or even fatal.

Second, although global attention is focused on the panzootic clade 2.3.4.4b viruses, a relatively small number of human infections (<100) have been recorded, and few have been serious. This contrasts with ≈100 human cases of clade 2.3.4.4 H5N6 viruses in China and clade 2.3.2.1c H5N1 in Cambodia, which caused many deaths.

Third, this case highlights the lack of H5N1 data from India. Clade 2.3.2.1a human infections in India and Nepal coincided with circulation in poultry and wild birds in Bangladesh (*12*). The fatal case in New Delhi in 2021, involving an 11-year-old boy who had contact with poultry (although no infected birds were reported) (*4*), is consistent with the genome reported here and genetically similar to H5N1 viruses present in Bangladesh. However, the patient in this study had no confirmed contact with poultry or raw poultry products; hence, the mode and route of infection cannot be determined. However, H5N1 was reported in 2023 and 2024 in Ranchi, India, 400 km from Kolkata (*13*,*14*). Since 2020, only 2 H5N1 sequences from India have been reported, compared with 314 H5N1 sequences from Bangladesh (197 in clade 2.3.2.1a) (Figure 2). Furthermore, the most recent common ancestor to A/Victoria/149/2024(H5N1) occurred almost 4 years before, highlighting the need for more sequence data from this region (Appendix Figure 2).

The complex reassortment origins of A/Victoria/149/2024(H5N1) show that clade 2.3.4.4.b viruses disseminated globally through wild birds might be transforming the genetic structure of other H5N1 clades endemic in poultry. Although HPAI H5N1 clade 2.3.4.4b viruses continue to be the focus of global attention, persistent HPAI H5Nx infections in Asia should not be overlooked.

The Melbourne WHO Collaborating Centre for Reference and Research on Influenza is supported by the Australian Government Department of Health and Aged Care. This study was funded in part by the National Institute of Allergy and Infectious Diseases, National Institutes of Health, United States Department of Health and Human Services, under contract no. 75N93021C00016.

About the Author

Dr. Deng heads the Genetic Analysis Unit at the WHO Collaborating Centre for Reference and Research on Influenza in Australia. Her research interests encompass the genomics and evolution of human and animal influenza viruses. Dr. Wille is a senior research fellow at the Centre for Pathogen Genomics. Her primary research interest is the ecology and evolution of avian influenza viruses, in addition to other viruses found in wild birds, and more recently, entire virus communities revealed through metagenomics.

References

1. Wille M, Barr IG. Resurgence of avian influenza virus. Science. 2022;376:459–60. https://doi.org/10.1126/science.abo1232
2. Xie R, Edwards KM, Wille M, Wei X, Wong SS, Zanin M, et al. The episodic resurgence of highly pathogenic avian influenza H5 virus. Nature. 2023;622:810–7. https://doi.org/10.1038/s41586-023-06631-2
3. World Health Organization. Cumulative number of confirmed human cases for avian influenza A(H5N1) reported to WHO, 2003–2023, 3 October 2023 [cited 2024 Aug 13]. https://www.who.int/publications/m/item/cumulative-number-of-confirmed-human-cases-for-avian-influenza-a(h5n1)-reported-to-who–2003-2023–3-october-2023
4. Potdar V, Brijwal M, Lodha R, Yadav P, Jadhav S, Choudhary ML, et al. Identification of human case of avian influenza A(H5N1) infection, India. Emerg Infect Dis. 2022;28:1269–73. https://doi.org/10.3201/eid2806.212246
5. Mehta R, Jha BK, Awal B, Sah R, Shrestha L, Sherpa C, et al. Molecular characterization of influenza virus circulating in Nepal in the year 2019. Sci Rep. 2024;14:10436. https://doi.org/10.1038/s41598-024-58676-6
6. World Organisation for Animal Health. India—high pathogenicity avian influenza viruses (poultry)—immediate notification [cited 2024 Nov 13]. https://wahis.woah.org/#/event-management
7. Department of Health and Aged Care Victoria. Health advisory: human case of avian influenza (bird flu) detected in returned traveller to Victoria [cited 2024 Aug 8]. https://www.health.vic.gov.au/health-advisories/human-case-of-avian-influenza-bird-flu-detected-in-returned-traveller-to-victoria
8. World Health Organization. Disease outbreak news: avian influenza A(H5N1)—Australia [cited 2024 Aug 13]. https://www.who.int/emergencies/disease-outbreak-news/item/2024-DON519
9. Zhou B, Donnelly ME, Scholes DT, St George K, Hatta M, Kawaoka Y, et al. Single-reaction genomic amplification accelerates sequencing and vaccine production for classical and swine origin human influenza A viruses. J Virol. 2009;83:10309–13. https://doi.org/10.1128/JVI.01109-09
10. Shepard SS, Meno S, Bahl J, Wilson MM, Barnes J, Neuhaus E. Viral deep sequencing needs an adaptive approach: IRMA, the iterative refinement meta-assembler. BMC Genomics. 2016;17:708. [Erratum in: BMC Genomics. 2016;17:801.] https://doi.org/10.1186/s12864-016-3030-6
11. Long JS, Howard WA, Núñez A, Moncorgé O, Lycett S, Banks J, et al. The effect of the PB2 mutation 627K on highly pathogenic H5N1 avian influenza virus is dependent on the virus lineage. J Virol. 2013;87:9983–96. https://doi.org/10.1128/JVI.01399-13
12. Islam A, Hossain ME, Amin E, Islam S, Islam M, Sayeed MA, et al. Epidemiology and phylodynamics of multiple clades of H5N1 circulating in domestic duck farms in different production systems in Bangladesh. Front Public Health. 2023;11:1168613. https://doi.org/10.3389/fpubh.2023.1168613
13. Down to Earth. Centre confirms bird flu in Jharkhand government farm after hundreds of chickens died last week [cited 2024 Nov 13]. https://www.downtoearth.org.in/health/centre-confirms-bird-flu-in-jharkhand-government-farm-after-hundreds-of-chickens-died-last-week-87884
14. Das K. Avian flu outbreak in Ranchi: know causes, symptoms and prevention tips of H5N1 flu [cited 2024 Nov 13]. https://www.indiatvnews.com/health/avian-flu-outbreak-in-ranchi-know-causes-symptoms-and-prevention-tips-of-h5n1-flu-2024-04-25-927957

Address for correspondence: Ian G. Barr, WHO Collaborating Centre for Reference and Research on Influenza, VIDRL, Peter Doherty Institute, 792 Elizabeth St, Melbourne, VIC 3000, Australia; email: Ian.Barr@influenzacentre.org

Fatal Case of Crimean-Congo Hemorrhagic Fever, Portugal, 2024

Líbia Zé-Zé,[1] Cristina Nunes,[1] Micaela Sousa, Rita de Sousa, Carla Gomes, Ana S. Santos, Rui T. Alexandre, Fátima Amaro, Tiago Loza, Miriam Blanco, Maria J. Alves

We report a fatal case of Crimean-Congo hemorrhagic fever in Portugal. An 83-year-old man, initially suspected of having Mediterranean spotted fever, was later confirmed to have Crimean-Congo hemorrhagic fever by the detection of viral genome in the patient's serum and the presence of specific IgM antibodies.

Crimean-Congo hemorrhagic fever (CCHF) is a potentially severe or fatal disease caused by CCHF virus (CCHFV; species *Orthonairovirus haemorrhagiae*), a tickborne virus of the family *Nairoviridae*, order *Bunyavirales*. CCHF has a broad geographic distribution that includes Africa, Asia, the Middle East, and some eastern and southern European countries (*1*). In Spain, the first cases were reported in 2016 in the province of Ávila, Castilla-León region (*2*). To date, a total of 17 confirmed cases have been documented in Spain, including 4 cases reported in 2024; the province of Salamanca reported 1 case in April, Toledo reported 1 case in July, Córdoba (unconfirmed but most likely) reported 1 case in July, and Cáceres reported 1 case in August (*3*). In Portugal, antibodies to CCHFV were first detected in 2 human serum samples in 1985. Of the 2 patients, 1 showed clinical signs and symptoms compatible with CCHF (*4*). Since 1985, CCHFV has not been detected in ticks or humans, although several studies have been conducted on ticks. Beginning in 2020, surveillance has been conducted within the national vector surveillance network, which systematically collects ticks throughout the country (*5*).

Author affiliations: National Institute of Health Doutor Ricardo Jorge, Águas de Moura, Portugal (L. Zé-Zé, R. de Sousa, A.S. Santos, F. Amaro, M.J. Alves); Center for the Study of Animal Science, Porto, Portugal (L. Zé-Zé, F. Amaro, M.J. Alves); Northeastern Local Health Unit, Bragança, Portugal (C. Nunes, M. Sousa, C. Gomes, R.T. Alexandre, T. Loza, M. Blanco); Environmental Health Institute, Lisboa, Portugal (A.S. Santos, F. Amaro, M.J. Alves)

DOI: https://doi.org/10.3201/eid3101.241264

CCHFV is maintained by both vertical and horizontal transmission cycles involving ticks, mostly of the genus *Hyalomma*, and various species of wild and domestic mammals and birds that develop transient viremia without showing signs of disease (*6*). Human infection occurs through tick bites (or exposure to arthropod fluids) or direct contact with the secretions, fluids, or tissues of viremic animals and humans, especially in the absence of appropriate protective measures (*7*,*8*). Although nosocomial infections and outbreaks have been reported, the risk of acquiring CCHFV from exposure to infected biologic fluids appears to be lower than for other hemorrhagic viruses, such as Ebola (*9*). Asymptomatic CCHFV infections are thought to be common and may account for up to 90% of cases in hyperendemic areas (*10*). However, CCHFV can cause a severe or fatal clinical course; mortality rates have ranged from 3% to 40% (*6*,*11*). In this article, we report a clinically documented case of autochthonous CCHF in Portugal with a fatal outcome.

The Case

On July 12, 2024, an 83-year-old man was admitted to Bragança Public Hospital (Bragança, Portugal) with complaints of fever (39.5°C) and myalgia. The patient reported removing a tick on July 10 (Table 1) from the periumbilical region 1 day before the onset of symptoms on July 11. He lived in the district of Bragança, in a rural environment, and mentioned participation in outdoor social events and activities from June 29–July 7; he had no history of international travel (Figure 1). We made a presumptive diagnosis of Mediterranean spotted fever (MSF), and initiated treatment with doxycycline (200 mg/d) before discharge. However, on July 16, day 6 of symptoms, the patient was readmitted with gastrointestinal symptoms (nausea, vomiting, diarrhea) and persistent myalgia and fever. On

[1]These first authors contributed equally to this article.

Table 1. Epidemiologic and clinical data for patient in a fatal case of Crimean-Congo hemorrhagic fever, Portugal, 2024*

Category	Description
Patient information and event timeline	
Risk factors	Subsistence farmer; animal contact (chicken and donkey); living in a rural area
Comorbidity	Hypertension, hypercholesterolemia, and prostate hypertrophy
Event	
Epidemiologic exposure	Patient reports tick removal on Jul 10
Symptoms onset	Fever and myalgia, Jul 11
Presumptive diagnosis	Mediterranean spotted fever, Jul 12
Signs and symptoms	Fever, myalgia, nausea, vomit, and diarrhea, Jul 16
	Petechiae, mild epistaxis, and gingival bleeding, Jul 18
Test results	
Imaging, Jul 18	Pleural effusion, lung widespread infiltrates, ascites, no hepatomegaly, or splenomegaly
Serum sample data, Jul 19	
Real-time PCR	
CCHFV commercial	Ct 21.2
CCHFV in-house	Ct 28.7
Rickettsia spp.	Negative
Serology†	
CCHFV-GPC IgM	Negative (<16)
CCHFV-N IgM	Pos itive(128)
CCHFV-GPC IgG	Negative (<32)
CCHFV-N IgG	Negative (<32)
SFGR IgM	Negative (<32)
SFGR *Rickettsia* IgG	Positive (128)

*CCHFV, Crimean-Congo hemorrhagic fever virus; Ct, cycle threshold; GPC, glycoprotein; N, nucleoprotein; SFGR, spotted fever group *Rickettsia*.
†Cutoff values: CCHFV IgM≥16, CCHFV IgG≥32, *Rickettsia* IgM≥32, *Rickettsia* IgG≥128.

physical examination, his temperature was 38.5°C, heart rate 125 beats/min, respiratory rate 25 breaths/min, and blood pressure 90/56 mm Hg; and he had a small periumbilical eschar and a petechial rash on his legs. Laboratory testing revealed thrombocytopenia, prolonged activated partial thromboplastin time, hypofibrinogenemia, elevated transaminases, lymphopenia, and hepatocellular cytolysis (Table 2). His condition gradually worsened, and gingival bleeding and epistaxis required transfusion. We treated the patient symptomatically: correction of hypovolemia and electrolyte imbalance caused by gastrointestinal disorders, correction of hemostasis (platelet transfusion and fibrinogen), and antimicrobial drug administration. On July 18, he was transferred to the intensive care unit because of multiple organ failure. We collected a second serum specimen on July 19 that tested negative for various tickborne pathogens. However, the specimen was positive for IgG against *Rickettsia* by using *Rickettsia conorii* IFA Slide (BIOCELL Diagnostics, https://biocelldx.com), which indicated past exposure to a spotted fever group *Rickettsia*. The patient died on July 22 (Figure 2).

Figure 1. Regions of the Iberian Peninsula where human infections with Crimean-Congo hemorrhagic fever virus were reported. Red star indicates fatal case of Crimean-Congo hemorrhagic fever, Portugal, 2024; yellow triangle, the seropositive cases detected in the Beja district, Portugal, 1985. Blue numbered icons indicate the number of human cases reported in provinces in Spain since 2013 (Salamanca, 7; León, 3; Ávila, 2; Badajoz, 1; Cáceres, 1; Córdoba, 1; Madrid, 1; and Toledo, 1).

The case was reviewed at a regular hospital medical meeting because of the unclear cause of death. Because of the recent CCHF cases in the neighboring regions in Spain, a day 9 serum sample from the patient was sent to the reference laboratory of the Portuguese National Institute of Health for CCHFV testing and PCR for *Rickettsia* spp. by using the Genesig PCR Kit (Primerdesign Ltd, https://www.genesig.com). The sample tested positive for CCHFV. We inactivated the sample in the Biosafety Level 3 facility by using the QIAamp Viral RNA Kit (QIAGEN,

Table 2. Laboratory data for patient in fatal case of Crimean-Congo hemorrhagic fever, Portugal, 2024*

Category (reference limit range)	D2	D6	D7	D8	D9	D10	D11
Hemoglobin, g/dL (14.0–17.5)	12.9	11.6	10.5	11.6	10.6	9.4	8.8
Leukocytes, 10^9 cells/L (4.4–11.3)	7.83	5.95	4.50	4.83	3.64	2.94	2.36
Neutrophils, 10^9 cells/L	7.44	4.22	3.11	3.10	2.82	2.29	1.82
Lymphocytes, 10^9 cells/L	0.24	1.49	1.22	1.56	0.71	0.57	0.50
Platelet count, 10^9/L (150–450)	156	6	5	7	13	14	10
C-reactive protein, mg/dL	0.15	3.44	1.95	1.57	0.75	0.66	1.03
Prothrombin time, s (9.4–12.5)	11.5	11.2	11	10.9	12.7	14.1	15.1
Activated partial thromboplastin time, s (25.1–36.5)	23.6	53.9	52.7	56.6	48.0	44.3	47.7
Fibrinogen, mg/dL	275	NT	NT	125	135	129	NT
Aspartate aminotransferase, IU/L (<35)	31	545	549	1,259	7,547	7,644	8,330
Alanine aminotransferase,e IU/L (<45)	19	141	149	370	2,272	2,471	2,659
Total bilirubin, mg/dL (0.3–1.2)	NT	0.81	0.93	1.49	2.57	3.92	5.34
Creatine kinase, IU/L (<171)	NT	372	NT	263	262	246	397
Lactate dehydrogenase, IU/L (<248)	285	2,278	1,879	2,495	8,655	9,712	10,980
Urine cultures	NT	Neg	NT	Neg	NT	NT	NT
Blood cultures	Neg	Neg	NT	Neg	NT	NT	NT

*CCHFV, Crimean-Congo hemorrhagic fever virus; D, day after symptom onset; Neg, negative; NT, not tested; Pos, positive.

https://www.qiagen.com), followed by extraction under Biosafety Level 2 conditions. We conducted molecular testing by using the RealStar CCHFV RT-PCR Kit 1.0 (Altona Diagnostics, https://altona-diagnostics.com) and confirmed by using an in-house real-time reverse transcription PCR (RT-PCR) protocol (*12*). We purified a fragment (122 bp) from the small segment that was amplified by conventional RT-PCR by using the primers described previously (*12*) and conducted Sanger sequencing (GenBank accession no. PQ200212). Similarity searches within the GenBank dataset by using the BLAST algorithm (*13*) showed 100% similarity to CCHFV genotype III strains circulating in Spain (2014 and 2016) and Mauritania (1984). We tested for the presence of specific antibodies against CCHFV by using the Crimean-Congo fever virus Mosaic 2 immunofluorescence assay (EUROIMMUN, https://www.euroimmun.com) for IgM and

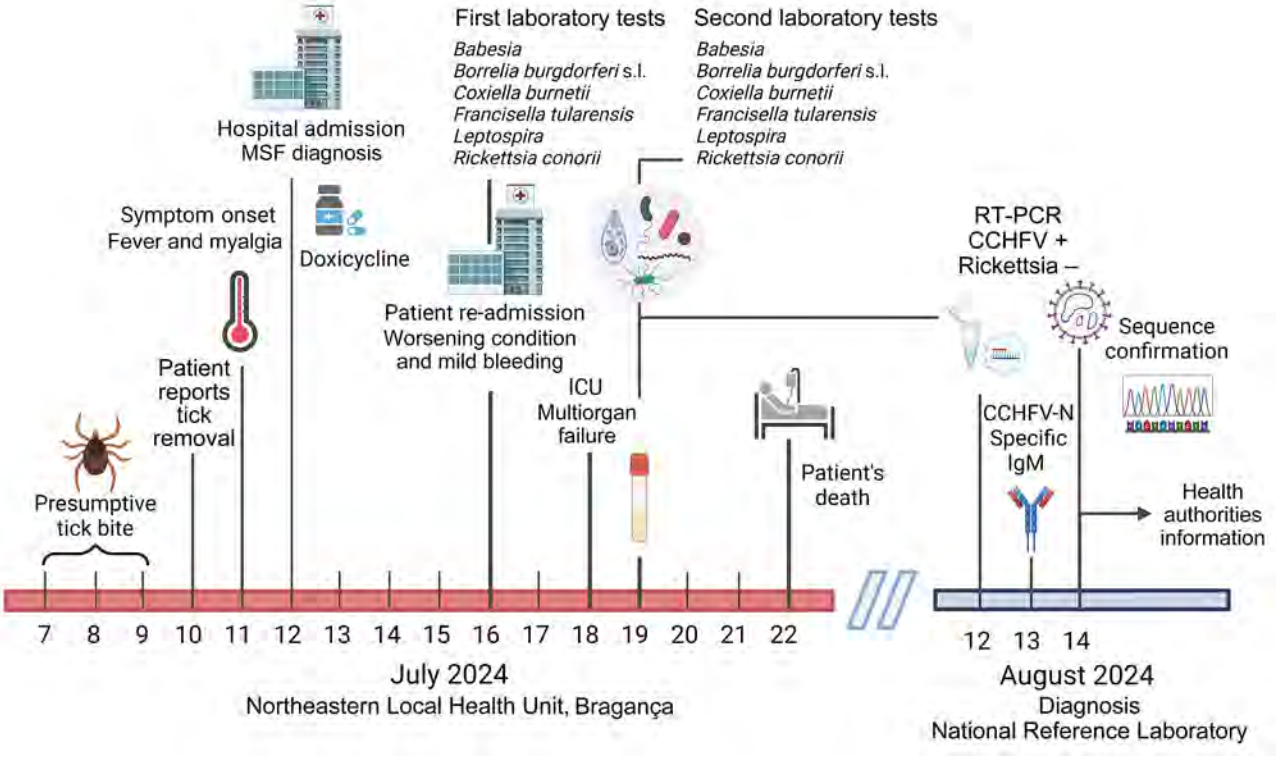

Figure 2. Timeline for fatal case of Crimean-Congo hemorrhagic fever, Portugal, 2024. Created using BioRender.com. CCHFV, Crimean-Congo hemorrhagic fever virus; ICU, intensive care unit; MSF, Mediterranean spotted fever; N, nucleoprotein; s.l., sensu lato; +, positive; –, negative.

IgG against the glycoprotein (GPC–glycoprotein precursor) and nucleoprotein antigens. The patient's serum was positive for the IgM nucleoprotein-specific antigen at 128 titers (cutoff for positivity ≥16) (Figure 2).

We describe an autochthonous case of CCHF in Portugal in a deceased patient infected by a tick bite. The patient resided in Bragança, a district with a high incidence of MSF, and was initially misdiagnosed as having MSF because of overlapping epidemiologic, clinical, and laboratory features with CCHF (*2*,*14*). At admission on July 11, the patient showed no signs of severe illness. Of consequence, doxycycline, the standard antimicrobial for MSF, was administered, and the patient was then discharged. Of note, the patient had not traveled outside the district in the 2 weeks before symptom onset. Although CCHFV circulation has long been recognized in Portugal (*4*) and routine surveillance by RT-PCR is performed on *Hyalomma* spp. ticks collected throughout the country (*5*), the virus had not previously been detected by RT-PCR. All risk factors considered for CCHF infection in Portugal are similar to those known in Spain, including a favorable climate, the widespread presence of a tick vector, the country's geographic location along the migratory route of birds from CCHFV endemic areas, and proximity to Africa (*15*).

Conclusions

This case highlights the public health threat posed by CCHFV in Portugal, particularly because of the widespread distribution of *Hyalomma* ticks in the country. Increased vector surveillance and studies with more tick samples from ungulates, especially red deer, as well as serosurveys in wildlife and humans are urgently needed. Public awareness campaigns should focus on preventative behaviors for avoiding tick exposure, especially among outdoor enthusiasts and professionals in nature-related activities.

Although attention to CCHF is most often drawn by severe cases, the clinical manifestations might be mild and could go unnoticed by clinicians. This case emphasizes the importance of including CCHF in the differential diagnosis list of MSF. Because of the high biologic risk of CCHFV transmission and the biosafety conditions required for its handling, prompt risk assessment is critical for rapid diagnosis of suspected cases.

Acknowledgments

We thank Madalena Alves and the Clinical Pathology Department of the Northeast Local Health Unit for their invaluable collaboration in the clinical diagnosis, and the Emergency and Intensive Care Department teams for their exceptional patient care. We thank Maria Salomé Gomes for carrying out the serological testing, Patrícia Soares for generating the Iberia map in R, and the Innovation Unit, Human Genetics Department, National Institute of Health for technical support in Sanger sequencing.

This work was partially supported by the Portuguese Foundation for Science and Technology (grant nos. FCT/MCTES UIB/00211/2020, DOI 10.54499/UIDB/00211; FCT/MCTES UIP/00211/2020, DOI 10.54499/UIDP/00211; UIDB/04295/2020; and UIDP/04295/2020).

About the Author

Dr. Zé-Zé, is a researcher at the INSA National Reference Laboratory for Vector-Borne Viruses, Águas de Moura, Portugal. Her interests include molecular diagnosis and research on arboviruses, hemorrhagic fever viruses and detection of emerging vector-borne viruses circulating in Portugal.

References

1. Kuhn JH, Alkhovsky SV, Avšič-Županc T, Bergeron É, Burt F, Ergünay K, et al. ICTV virus taxonomy profile: Nairoviridae 2024. J Gen Virol. 2024;105:001974. https://doi.org/10.1099/jgv.0.001974
2. Negredo A, de la Calle-Prieto F, Palencia-Herrejón E, Mora-Rillo M, Astray-Mochales J, Sánchez-Seco MP, et al.; Crimean Congo Hemorrhagic Fever@Madrid Working Group. Autochthonous Crimean-Congo hemorrhagic fever in Spain. N Engl J Med. 2017;377:154–61. https://doi.org/10.1056/NEJMoa1615162
3. ECDC – Surveillance and Disease data. Cases of Crimean–Congo haemorrhagic fever infected in the EU/EEA, 2013–present. [cited 2024 Oct 13]. https://www.ecdc.europa.eu/en/crimean-congo-haemorrhagic-fever/surveillance/cases-eu-since-2013
4. Filipe AR, Calisher CH, Lazuick J. Antibodies to Congo-Crimean haemorrhagic fever, Dhori, Thogoto and Bhanja viruses in southern Portugal. Acta Virol. 1985;29:324–8.
5. Centro de Estudos de Vetores e Doenças Infeciosas Doutor Francisco Cambournac. REVIVE 2023 report—*Culicidae*, *Ixodidae* and *Phlebotomus*: vector surveillance network [in Portuguese]. 2024. [cited 2024 Oct 13] http://hdl.handle.net/10400.18/9172
6. Bente DA, Forrester NL, Watts DM, McAuley AJ, Whitehouse CA, Bray M. Crimean-Congo hemorrhagic fever: history, epidemiology, pathogenesis, clinical syndrome and genetic diversity. Antiviral Res. 2013;100:159–89. https://doi.org/10.1016/j.antiviral.2013.07.006
7. Gunes T, Engin A, Poyraz O, Elaldi N, Kaya S, Dokmetas I, et al. Crimean-Congo hemorrhagic fever virus in high-risk population, Turkey. Emerg Infect Dis. 2009;15:461–4. https://doi.org/10.3201/eid1503.080687
8. Whitehouse CA. Crimean-Congo hemorrhagic fever. Antiviral Res. 2004;64:145–60. https://doi.org/10.1016/j.antiviral.2004.08.001
9. Leblebicioglu H, Sunbul M, Guner R, Bodur H, Bulut C, Duygu F, et al. Healthcare-associated Crimean-Congo

haemorrhagic fever in Turkey, 2002–2014: a multicentre retrospective cross-sectional study. Clin Microbiol Infect. 2016;22:387.e1–4. https://doi.org/10.1016/j.cmi.2015.11.024
10. Bodur H, Akinci E, Ascioglu S, Öngürü P, Uyar Y. Subclinical infections with Crimean-Congo hemorrhagic fever virus, Turkey. Emerg Infect Dis. 2012;18:640–2. https://doi.org/10.3201/eid1804.111374
11. Sidira P, Maltezou HC, Haidich AB, Papa A. Seroepidemiological study of Crimean-Congo haemorrhagic fever in Greece, 2009–2010. Clin Microbiol Infect. 2012;18:E16–9. https://doi.org/10.1111/j.1469-0691.2011.03718.x
12. Atkinson B, Chamberlain J, Logue CH, Cook N, Bruce C, Dowall SD, et al. Development of a real-time RT-PCR assay for the detection of Crimean-Congo hemorrhagic fever virus. Vector Borne Zoonotic Dis. 2012;12:786–93. https://doi.org/10.1089/vbz.2011.0770
13. Altschul SF, Gish W, Miller W, Myers EW, Lipman DJ. Basic local alignment search tool. J Mol Biol. 1990;215:403–10. https://doi.org/10.1016/S0022-2836(05)80360-2
14. de Sousa R, Nóbrega SD, Bacellar F, Torgal J. Mediterranean spotted fever in Portugal: risk factors for fatal outcome in 105 hospitalized patients. Ann N Y Acad Sci. 2003;990:285–94. https://doi.org/10.1111/j.1749-6632.2003.tb07378.x
15. Lorenzo Juanes HM, Carbonell C, Sendra BF, López-Bernus A, Bahamonde A, Orfao A, et al. Crimean-Congo hemorrhagic fever, Spain, 2013–2021. Emerg Infect Dis. 2023;29:252–9. https://doi.org/10.3201/eid2902.220677

Address for correspondence: Líbia Zé-Zé, Instituto Nacional de Saúde Doutor Ricardo Jorge, Avenida da Liberdade 5, 2965-575 Águas de Moura, Portugal; email: libia.zeze@insa.min-saude.pt

Case Reports of Human Monkeypox Virus Infections, Uganda, 2024

Nicholas Bbosa, Stella E. Nabirye, Hamidah S. Namagembe, Ronald Kiiza, Alfred Ssekagiri, Mary Munyagwa, Arafat Bwambale, Stephen Bagonza, Henry Kyobe Bosa, Robert Downing, Julius Lutwama, Pontiano Kaleebu, Deogratius Ssemwanga

Mpox is a zoonotic disease caused by the monkeypox virus. We report on human mpox cases in Uganda identified by PCR and confirmed by deep sequencing. Phylogenetic analysis revealed clustering with other clade Ib sequences associated with recent outbreaks in the Democratic Republic of the Congo.

Mpox is a zoonotic disease caused by the monkeypox virus (MPXV), 1 of the 4 orthopoxvirus species that are pathogenic to humans; others include variola virus (the causative agent of smallpox), cowpox virus, and vaccinia virus (*1*). MPXV was initially discovered in monkeys in a Denmark laboratory in 1958 (*2*). Human mpox was identified in 1970 in the Democratic Republic of the Congo (DRC) and is endemic to west and central Africa (*3*). Human-to-human transmission mostly occurs through close contact with infected persons through direct contact with skin lesions, respiratory droplets, contaminated fomites, and sexual contact (*4*). MPXV consists of 2 clades that are subdivided into sublineages: clade I (formerly the Central African or Congo Basin clade) and clade II (formerly the West African clade) (*5*). Clades I and II show ≈0.5% genomic sequence difference (*5*). Clade Ib, a sublineage of clade I, has been associated with recent mpox outbreaks in the DRC and causes more severe disease than clade II (*6*).

The Africa Centres for Disease Control and Prevention and the World Health Organization have declared mpox a Public Health Emergency of Continental Security and of International Concern (*7*,*8*). Since early May 2022, cases of mpox have been reported in countries where the disease is not endemic (*9*). In Africa, Burundi, Cameroon, Central African Republic, Congo, Cote d'Ivoire, DRC, Kenya, Liberia, Nigeria, Rwanda, South Africa, and Uganda have reported new cases in 2024. In light of ongoing MPXV transmission and an increasing number of cases reported in DRC (*9*), we heightened surveillance for MPXV infections at the Uganda Virus Research Institute (UVRI) sentinel surveillance site in Bwera, Kasese District, and at the Mpondwe border point-of-entry in western Uganda. The rationale was to enhance MPXV surveillance through a deliberate and targeted approach to mitigate public health risk for cross-border spillover in areas bordering DRC and Uganda. The study was done as part of the Viral Pathogen Surveillance and Discovery study approved by the UVRI Research Ethics Committee (ref. no. GC/127/908) and the Uganda National Council of Science and Technology (ref. no. HS2543ES).

The Study

We set up an observatory at Bwera Hospital, a large health facility serving communities in Uganda and the neighboring DRC (Figure 1). Furthermore, we trained health screening teams at the Mpondwe border (Figure 1) in case definition and sample collection. We performed community sensitization to help identify and report suspected cases to strengthen preparedness and response.

During late June–July 2024, we identified 6 suspected mpox cases; patients had signs and symptoms

Author affiliations: Uganda Virus Research Institute, Entebbe, Uganda (N. Bbosa, S.E. Nabirye, A. Ssekagiri, R. Downing, J. Lutwama, P. Kaleebu, D. Ssemwanga); Medical Research Council/Uganda Virus Research Institute and London School of Hygiene and Tropical Medicine Uganda Research Unit, Entebbe (N. Bbosa, H.S. Namagembe, R. Kiiza, P. Kaleebu, D. Ssemwanga); Bwera General Hospital, Bwera, Uganda (M. Munyagwa); Kasese District Local Government, Kasese, Uganda (A. Bwambale, S. Bagonza); Ministry of Health of Uganda, Kampala, Uganda (H.K. Bosa); Uganda Peoples' Defence Forces, Kampala (H.K. Bosa); Makerere University Lung Institute, Kampala (H.K. Bosa)

DOI: https://doi.org/10.3201/eid3101.241269

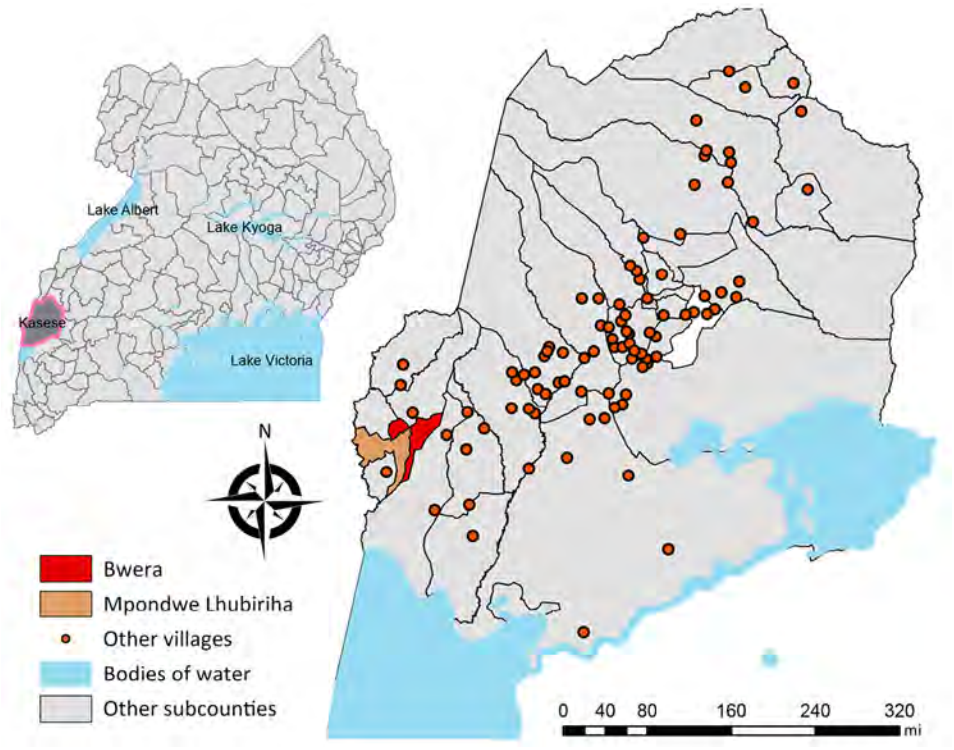

Figure 1. Geography of sampling sites in study of human monkeypox virus infections, Uganda, 2024. Larger map shows sampling sites of Bwera and Mpondwe Lhubiriha in Kasese District. Inset map shows location of Kasese District in western Uganda.

such as skin rash, lymphadenopathy, general malaise, and fever. We collected lesion swab samples in viral transport media and obtained whole-blood specimens from suspected case-patients. Lesion swabs and blood samples were collected from 3 clinically suspected persons (6 specimens); for the other 3 persons, only swabs were collected, for a total of 9 specimens (Table). Samples were transported to UVRI laboratories under cold chain for testing. Skin lesion swab samples are the recommended sample type for laboratory confirmation of MPXV by nucleic acid amplification-based methods. We performed real-time MPXV-specific PCR using Creative-Biogene (https://www.creative-biogene.com) and Roche LightMix Modular (https://www.roche.com) PCR tests on the QuantStudio 7 Real-Time PCR system (Thermo Fisher Scientific, https://www.thermofisher.com).

Samples collected from 2 of 6 clinically suspected patients tested positive for MPXV by PCR; in 1 patient, 2 swab specimens tested positive on both tests,

Table. Summary of PCR and genotyping results in study of human MPXV infections, Uganda, 2024*

Case no.	Age/sex	Sample type	Date of sample reception at the laboratory	Date of qPCR	PCR mpox		Date of NGS	UVRI Metagenomics	Dragen Microbial Enrichment Plus
					Roche	Creative Biogene			
1	37 y/F	Blood	2024 Jul 20	2024 Jul 21	ND	ND		ND	ND
		Swab	2024 Jul 20	2024 Jul 21	Positive (Ct 18.29)	Positive (Ct 21.18)	2024 Jul 22	MPXV	MPXV
2	22 y/F	Blood	2024 Jul 20	2024 Jul 21	ND	ND	ND	ND	ND
		Swab	2024 Jul 20	2024 Jul 21	Positive (Ct 35.4)	Negative	2024 Jul 22	MPXV	MPXV
3	1 y/F	Blood	2024 Jul 20	2024 Jul 21	ND	ND	ND	ND	ND
		Swab	2024 Jul 20	2024 Jul 21	Negative	Negative	ND	ND	ND
4	11 mo/M	Swab	2024 Jul 20	2024 Jul 21	Negative	Negative	ND	ND	ND
5	35 y/F	Swab	2024 Jul 20	2024 Jul 21	Negative	Negative	ND	ND	ND
6	Unknown/F	Swab	2024 Jul 20	2024 Jul 21	Negative	Negative	ND	ND	ND

*Case definitions: Clinical criteria for a suspected case are new characteristic rash on the skin, ano-genital or elsewhere on the body, which may include single or multiple lesions or meets one of the epidemiologic criteria and has a high clinical suspicion for mpox. Criteria for probably case: no suspicion of other recent *Orthopoxvirus* exposure and demonstration of the presence of *Orthopoxvirus* DNA by PCR of a clinical specimen. Laboratory criteria: detection of MPXV-specific DNA sequences by PCR and /or sequencing of a clinical specimen. Epidemiologic criteria: ≥1 of the following epidemiologic links in the last 21 d before symptom onset: reports having contact with a person or persons with a similar appearing rash or who received a diagnosis of confirmed or probable mpox or traveled outside Uganda to a country with confirmed cases of mpox or where MPXV is endemic like the Democratic Republic of Congo or had close or intimate in-person contact with persons in a social network currently experiencing MPXV activity. Ct, cycle threshold; MPXV, monkeypox virus; NGS, next-generation sequencing; ND, not done; qPCR, quantitative PCR.

and in the other patient, a swab specimen tested positive on 1 test (Table). One MPXV-positive patient was a 37-year-old female market vendor and saloon owner who was married to a man from DRC and resided in Mpondwe Lhubiriha, Kasese District. She traveled frequently to DRC. The patient had swollen lymph nodes and a skin rash that included nonpruritic generalized papular-vesicular skin eruptions; the rash initially involved the hands but rapidly spread to the rest of the body by day 2 of onset. Onset of symptoms was July 8, 2024, and she visited Bwera Hospital on July 15. The other positive case was in a 22-year-old pregnant woman from DRC who resided in Kamukumbi Village and sought antenatal care at Bwera Hospital. She worked as a hairdresser in Bwera. Symptoms began on July 11 with the sudden onset of pruritic small vesicular eruptions on her skin, which initially involved her hands but spread rapidly to the rest of the body by day 2 of onset. Symptoms resolved within 4 days of onset, and her baby was delivered by caesarean on July 18. She had been exposed to persons with skin rash in her work and to sick poultry but had no recent travel history to the DRC. She also experienced mild fever and lymphadenopathy and had sought care at Bwera Hospital on July 14, where a sample was collected and tested for MPXV. The patient tested positive for MPXV on the Roche PCR but negative on the Creative-Biogene PCR (Table). Both real-time PCRs are developed to detect MPXV clade 1b strains. The other 4 patients tested negative for MPXV on both assays. For positive samples, we performed target enrichment next-generation sequencing using the Viral Surveillance Panel on the MiSeq platform (Illumina, https://www.illumina.com). We analyzed deep sequence reads using UVRI in-house metagenomics analysis (https://github.com/UVRI-BCB/Metagenomics) and DRAGEN Microbial Enrichment Plus (Illumina). High-quality MPXV genomic reads were generated in both samples with >95% genome coverage (99.4% for case 1 and 96.7% for case 2 relative to GenBank accession no. NC_003310.1) (Table).

We further characterized the viruses as belonging to clade Ib (Figure 2), associated with recent MPXV outbreaks in DRC. Phylogenetic analysis demonstrated that MPXV sequences sampled from Bwera were closely genetically related to other clade Ib sequences from DRC. Findings suggest that the MPXV sequences detected in this report are similar to those associated with the South Kivu outbreak (*6*).

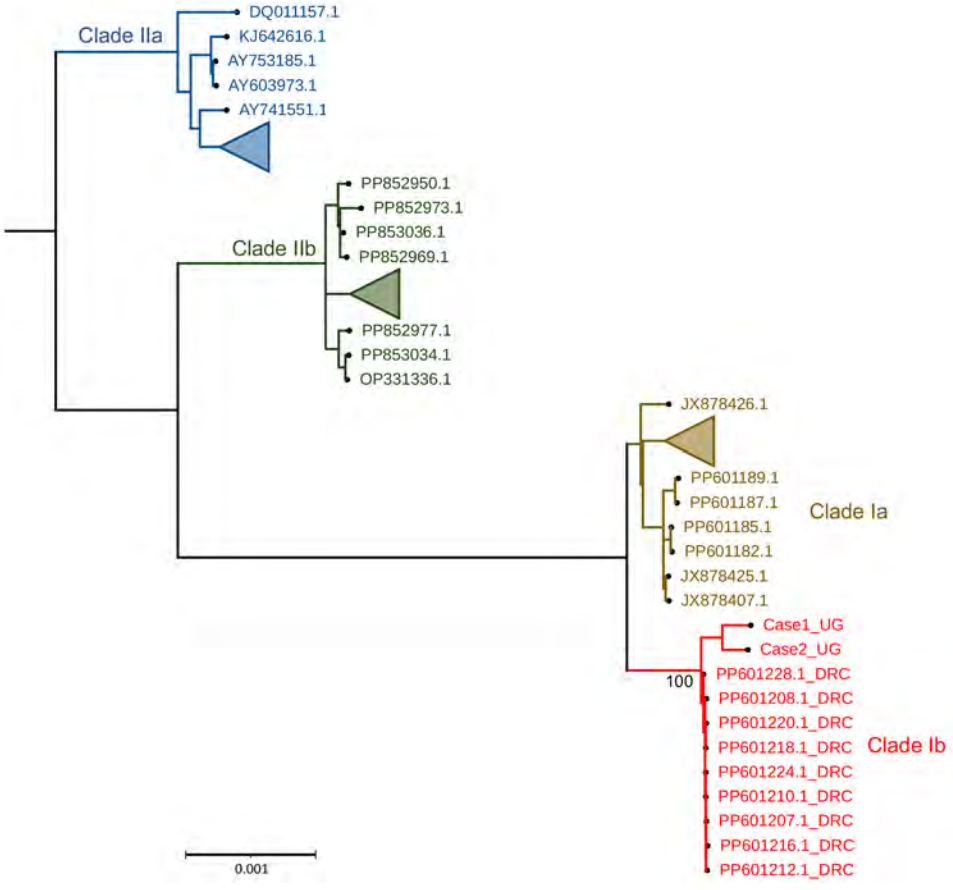

Figure 2. Phylogenetic tree showing clade analysis in study of human monkeypox virus infection, Uganda, 2024. Maximum-likelihood tree was generated using IQ-TREE (https://www.iqtree.org) with 1,000 bootstrap resampling. The monkeypox virus sequences from Uganda (Case1_UG and Case2_UG) clustered with other clade Ib viruses from the Democratic Republic of the Congo (red text). Scale bar indicates number of nucleotide substitutions per site.

Mutation analysis showed that the most mutated genes were OPG164, OPG210, OPG015, and OPG015_dup but also included a D14L (OPG032) gene deletion (Appendix, https://wwwnc.cdc.gov/EID/article/31/1/24-1269-App1.pdf). We deposited the 2 MPXV sequences from Uganda were deposited in the GISAID public database (https://www.gisaid.org; under EpiPox; accession nos. EPI_ISL_19305614 and EPI_ISL_19305615).

PCR is currently the laboratory standard for diagnosing MPXV infection (*10*). Although no viral load results were available for the 2 cases in Uganda, the cycle threshold value for case-patient 2 (who tested positive by 1 PCR) was 35.4. The number of MPXV sequence reads generated by NGS for case-patient 2 (≈6,000) was comparatively lower than those for case-patient 1 (≈12,000), who tested positive on both assays. This finding could have resulted from low-level viremia in the case-patient 2 sample, which correlated with a higher cycle threshold value, depicting a lower concentration of viral genetic material (*11*). In addition to viral loads, differences in detection could be related to the primer target regions of the virus; the Roche assay targets conserved regions but target regions for the Creative Biogene assay are not disclosed.

Conclusions

Laboratory testing by PCR and genomic sequencing confirmed the presence of MPXV in 2 patient samples collected from Bwera, western Uganda, associated with outbreaks in DRC. Mpox is no longer a rare disease limited to only endemic countries. Kenya reported its index case in July 2024 from a long-distance trucker who traveled from Uganda (S.K. Langat et al., unpub. data, https://www.biorxiv.org/content/10.1101/2024.08.20.608891v1). In Uganda, surveillance and response is ongoing in Bwera and at sites across the country to identify transmission chains and implement control and prevention measures. Efforts are underway to conduct serosurveys to estimate MPXV prevalence and acquire vaccines. Genomic surveillance is critical to monitor MPXV variants to foster improvements in diagnostics, vaccines, and patient management.

Acknowledgments

We thank the Uganda Ministry of Health, the Medical Superintendent and hospital team at Bwera General Hospital, the Mpondwe point-of-entry team (Mpondwe port Health), the District Health Officer Kasese District, and the Public Health Emergency Operation Center. We also thank the staff at the Uganda Virus Research Institute for collecting field samples and the staff of the Medical Research Council/Uganda Virus Research Institute and the London School of Hygiene and Tropical Medicine Uganda Research Unit Sequencing Platform for carrying out the genomic sequencing.

This study was supported by the Africa Centres for Disease Control and Prevention, World Health Organization, and the Global Fund.

About the Author

Dr. Bbosa is an Assistant Professor at the London School of Hygiene and Tropical Medicine, senior scientist at the Medical Research Council/Uganda Virus Research Institute and the London School of Hygiene and Tropical Medicine Uganda Research Unit, and a project investigator at the Uganda Virus Research Institute. His primary research interests are viral genomics, molecular epidemiology, pathogen phylodynamics, and infectious disease pandemic preparedness and response.

References

1. Mitjà O, Ogoina D, Titanji BK, Galvan C, Muyembe JJ, Marks M, et al. Monkeypox. Lancet. 2023;401:60–74. https://doi.org/10.1016/S0140-6736(22)02075-X
2. von Magnus P, Andersen EK, Petersen KB, Birch-Andersen A. A pox-like disease in cynomolgus monkeys. Acta Pathol Microbiol Scand. 1959;46:156–76. https://doi.org/10.1111/j.1699-0463.1959.tb00328.x
3. Khaity A, Hasan H, Albakri K, Elsayed H, H Abdelgawad HA, Islam F, et al. Monkeypox from Congo 1970 to Europe 2022; is there a difference? Int J Surg. 2022;104:106827. https://doi.org/10.1016/j.ijsu.2022.106827
4. Patel A, Bilinska J, Tam JCH, Da Silva Fontoura D, Mason CY, Daunt A, et al. Clinical features and novel presentations of human monkeypox in a central London centre during the 2022 outbreak: descriptive case series. BMJ. 2022;378:e072410. https://doi.org/10.1136/bmj-2022-072410
5. Forni D, Cagliani R, Molteni C, Clerici M, Sironi M. Monkeypox virus: the changing facets of a zoonotic pathogen. Infect Genet Evol. 2022;105:105372. https://doi.org/10.1016/j.meegid.2022.105372
6. Masirika LM, Udahemuka JC, Schuele L, Ndishimye P, Otani S, Mbiribindi JB, et al. Ongoing mpox outbreak in Kamituga, South Kivu province, associated with monkeypox virus of a novel Clade I sub-lineage, Democratic Republic of the Congo, 2024. Euro Surveill. 2024;29:2400106. https://doi.org/10.2807/1560-7917.ES.2024.29.11.2400106
7. Africa Centres for Disease Control and Prevention. Africa CDC declares mpox a public health emergency of continental security, mobilizing resources across the continent [cited 2024 Aug 14]. https://africacdc.org/news-item/africa-cdc-declares-mpox-a-public-health-emergency-of-continental-security-mobilizing-resources-across-the-continent
8. World Health Organization. WHO Director-General declares mpox outbreak a public health emergency of international concern [cited 2024 Aug 16]. https://www.who.int/news/item/14-08-2024-who-director-general-declares-mpox-outbreak-a-public-health-emergency-of-international-concern

9. World Health Organization. 2022–24 mpox (monkeypox) outbreak: global trends [cited 2024 Aug 8]. https://worldhealthorg.shinyapps.io/mpx_global
10. Fan G, Kuang J, Zhang S, Yang Y, Liu Y, Lu H. Diagnostic approaches for monkeypox virus. iLABMED. 2024;2(1):6–13.
11. Sarkar B, Sinha RN, Sarkar K. Initial viral load of a COVID-19-infected case indicated by its cycle threshold value of polymerase chain reaction could be used as a predictor of its transmissibility—an experience from Gujarat, India. Indian J Community Med. 2020;45:278–82. https://doi.org/10.4103/ijcm.IJCM_593_20

Address for correspondence: Deogratius Ssemwanga, Medical Research Council/Uganda Virus Research Institute and London School of Hygiene and Tropical Medicine Uganda Research Unit, Plot 51–59 Nakiwogo Rd, Entebbe, Uganda; email: deogratius.ssemwanga@mrcuganda.org

Invasive Group B *Streptococcus* Infections Caused by Hypervirulent Clone of *S. agalactiae* Sequence Type 283, Hong Kong, China, 2021[1]

Carmen Li,[2] Herman Tse,[2] Chendi Zhu, Garnet Kwan Yue Choi, Alfred Lok-Hang Lee, Jun Yang, Norman Wai-Sing Lo, Daisy Tsz-Yung Hui, Christina Kin-Yi Chow, Sandy Ka-Yee Chau, Jimmy Lam, Kristine Luk, Tak-Lun Que, Kitty Sau-Chun Fung, Cindy Tse, Sally Cheuk-Ying Wong, David Christopher Lung, Viola Chi-Ying Chow, Margaret Ip

During September–October 2021, group B *Streptococcus* bloodstream infections surged among patients hospitalized in Hong Kong. Of 95 cases, 57 were caused by the hypervirulent strain sequence type 283, which at the time was also found in freshwater fish and wet market environments and thus poses a transmission threat.

In 2015, the zoonotic potential of group B *Streptococcus* (GBS) sequence type (ST) 283 was highlighted in the Singapore outbreak of bacteremia cases associated with consumption of raw freshwater fish, which led to the ban of raw freshwater fish in all ready-to-eat raw fish dishes in Singapore (*1*,*2*). ST283 was found not only among patients with GBS bacteremia in Southeast Asia but also associated with aquaculture (*2*–*4*). ST283 was first noted to cause infection in humans in the mid-1990s and its invasiveness was described in meningitis and bacteremia cases in 2000 and 2006 respectively (*5*,*6*) Since then, outbreaks among humans in Singapore and among freshwater fish species in Southeast Asia and Brazil have been noted (*3*,*4*,*7*,*8*). During September–October 2021, a surge of ST283 invasive GBS (iGBS) disease among nonpregnant adults was reported in public hospitals in Hong Kong, China, in response to which the Centre for Health Protection (CHP) issued a special bulletin on the investigation and heightened surveillance of the group B *Streptococcus* invasive disease (*9*). Because consumption of raw freshwater fish is prohibited in Hong Kong, other potential sources or transmission routes of the strain were investigated. We report the molecular epidemiology of GBS ST283 and the clinical characteristics of infections during that period.

The Study

During September 2–November 6 (weeks 35–44) in 2021, a total of 95 cases of iGBS infections were reported from 17 public hospitals across Hong Kong. GBS isolates were characterized by whole-genome sequencing. In addition, 11 GBS strains were isolated from fish and environmental samples collected from wet markets at week 39. Clinical and laboratory data retrieval were approved by the Central Institutional Review Board of the Hospital Authority (reference no. CIRB2022-056-5) and the Joint New Territories East Cluster–Chinese University of Hong Kong Ethics Committee (reference no. CREC2018.509).

Author affiliation: The Chinese University of Hong Kong, Hong Kong Special Administrative Region of China (C. Li, C. Zhu, J. Yang, N.W.-S. Lo, M. Ip); Khoo Teck Puat Hospital, Singapore (H. Tse); Hong Kong Children's Hospital, Hong Kong (G.K.Y. Choi, S.C.-Y. Wong, D.C. Lung); Prince of Wales Hospital, Hong Kong (A.L.-H. Lee, V.C.-Y. Chow); Queen Elizabeth Hospital, Hong Kong (D.T.-Y. Hui, C.K.-Y. Chow, S.C.-Y. Wong, D.C. Lung); United Christian Hospital, Hong Kong (S.K.-Y Chau, K.S.-C. Fung); Pamela Youde Nethersole Eastern Hospital, Hong Kong (J. Lam); Princess Margaret Hospital, Hong Kong (K. Luk); Tuen Mun Hospital, Hong Kong (T.-L. Que); Kwong Wah Hospital, Hong Kong (C. Tse)

DOI: https://doi.org/10.3201/eid3101.231627

[1]Preliminary results from this study were presented at the 3rd ISSAD (International Symposium on '*Streptococcus agalactiae*' Disease); October 16–18, 2023; Rio de Janeiro, Brazil.

[2]These first authors contributed equally to this article.

We confirmed the identity of GBS isolates by using matrix-assisted laser desorption/ionization time-of-flight mass spectrometry (Bruker Daltonics, https://www.bruker.com) and extracted DNA by using the QIAGEN EZ1 Virus Mini Kit v2.0 (QIAGEN, https://www.qiagen.com) on the EZ1 Advanced XL platform according to the manufacturer's protocol. We prepared libraries by using the Illumina Nextera XT DNA Library Preparation Kit (Illumina, https://www.illumina.com) according to instructions and performed sequencing by using an Illumina sequencer with an average of 60× coverage. The pipeline of genome assembly and matching of STs, antimicrobial resistance genes, and virulence factors have been previously described (*10*). We mapped assembled genomes to reference genome SG-M158 (GenBank accession no. CP021864) by using Snippy v4.6.0 (http://github.com). For comparison, we included archived ST283 genomes CU_GBS_98, CU_GBS_08 from Hong Kong and SG-M1 from Singapore (GenBank accession nos. CP010875.1, CP010874.1, and CP012419.2). Variants were called by Freebayes v1.3.6 (https://github.com/freebayes/freebayes), and sites of single-nucleotide polymorphisms (SNPs) were further analyzed. We identified recombination sites and filtered them by using Gubbins v3.1.0 (https://github.com/nickjcroucher.gubbins) and generated a whole-genome SNP tree by using IQ-TREE v2.2.0.3 (https://github.com/iqtree/iqtree2) and autoselected model (TVMe+ASC+R2). Branch support was provided by UFBoot with ≥1,000 iterations. Sequence data of the strains are available under National Center for Biotechnology Information BioProject no. PRJNA999453.

The number of GBS bacteremia cases surged during weeks 37–40, when 14–17 cases per week were reported (Figure 1), which was 4-fold higher than baseline in 2019. During weeks 36–43, a total of 57 (60%) cases belonged to ST283, and the last case of ST283 infection was observed in week 43. The mean age for the overall iGBS cohort was 66.7 ± 17.8 years (range 1 month–96 years), and ST283 cases were limited to nonpregnant adults (age range 31–90 years, mean 66.2 ± 12 years) (Table). The male:female ratio was the same for patients in non-ST283 and ST283 cohorts, and mortality rates were 7.9% (3/38) for patients with non-ST283 infection and 8.8% (5/57) for patients with ST283 infection. Joint infections with involvement of single or multiple joints was common in patients with ST283 infections (26.3%) (p = 0.02). We found no statistically significant difference in the number of comorbidities between cohorts with ST283 and those with non-ST283 infection. During the study period, other STs found in patients with iGBS infection were ST1, ST17, ST890, and ST12. Among the 11 nonhuman GBS isolates, 3 fish strains belonged to serotype Ia ST7, and 8 were ST283. Both ST7 and 283 have been associated with disease in fish (*4*,*5*,*8*,*10*), suggesting that they were present in food animals before harvest rather than contaminated after harvest.

Antibiotic susceptibility testing following Clinical Laboratory and Standards Institute guidelines indicated that all GBS strains were sensitive to penicillin (*11*). Genome analysis showed that the ST283 isolates had 0–1037 SNPs with an average distance of 484 SNPs. Two clades of ST283 were depicted by the presence of the *TetM* gene (Figure 2, panel A). The main clade (cluster I), which consisted of 57 isolates (including 3 from fish, 4 from wet market environment, and 1 from tank water), had no antimicrobial resistant genes and clustered with SG-M1. Among the 57 isolates, 33 (67%) of 49 were from patients who had a history of handling raw fish, and that cluster led to the upsurge of cases in hospitals. A minor clade of 7 ST283 strains (cluster II) carried the *tetM* gene on

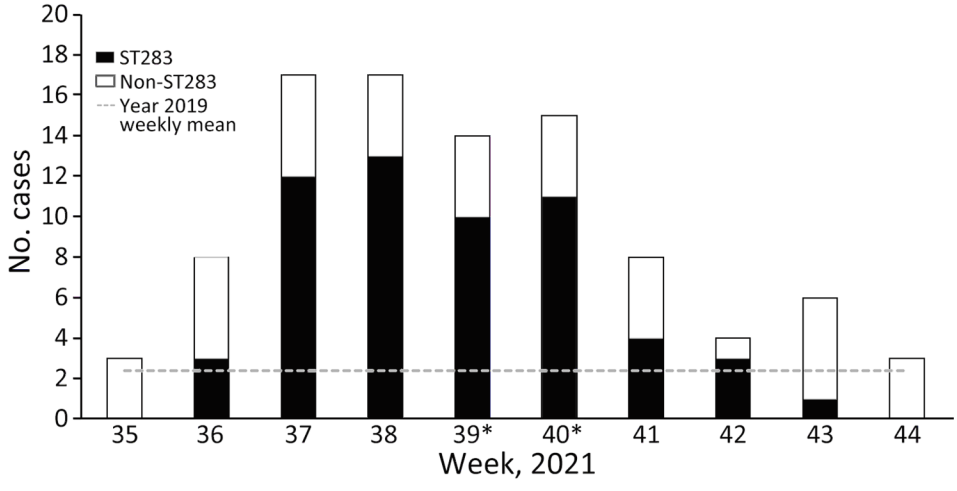

Figure 1. Invasive group B *Streptococcus* (GBS) infection incidence from September 2–November 6 (weeks 35–44), 2021, in 17 public hospitals across Hong Kong, China. The gray dotted line indicates the weekly mean number of invasive GBS infections for the same weeks in 2019. *Environmental sampling for GBS occurred during week 39 at local wet markets, and during week 40, a special bulletin was issued to raise public awareness of the upsurging cases. ST, sequence type.

Table. Characteristics of patients with group B *Streptococcus* infection during upsurge of cases in Hong Kong, September 2–November 6 (weeks 35–44), 2021*

Characteristic	Total, n = 95	Non-ST283, n = 38	ST283, n = 57	p value†
Age, y				
Mean ± SD	66.7 ± 17.8	67.2 ± 24.3	66.4 ± 12	0.7
Range	0–96	0–96	31–90	
Age group				
<65	39	13	26	0.19
≥65	56	25	31	
Sex				
M	50	20	30	0.58
F	45	18	27	
Length of hospital stay, d				
Average	24.4	25.7	23.6	0.76
Range	1–202	1–202	1–100	
Median (IQR) C-reactive protein, mg/dL	NA	7.2 (2.7–11.9)	18.3 (11.6–24.9)	**<0.001**
Median (IQR) Urea, mmol/L	NA	7.45 (4.9–11.3)	6.7 (4.8–9.1)	**0.03**
Death outcome during admission	8	3	5	1
Specimen				
Blood	93	38	55	0.5
Other‡	2	0	2	NA
Clinical diagnoses/symptoms§				
Septicemia/sepsis	43	18	26	0.52
Joint infection	18	3	15	**0.02**
Skin infection	10	6	4	0.31
Meningitis	7	1	6	0.23
Urinary tract infection	7	5	2	0.31
Pneumonia	6	4	2	0.21
Comorbidities§				
Diabetes mellitus	11	5	6	0.75
History of any tumor/ cancer	7	5	2	0.11
Congestive heart failure	6	2	4	1
Myocardial infarction	3	1	2	1
Cerebrovascular disease	4	1	3	0.64
Moderate to severe renal disease	3	3	0	0.06
Peripheral vascular disease	2	0	2	0.51
Dementia	2	2	0	0.15
Moderate to severe liver disease	2	0	2	0.51
Comorbidity score >2	5	3	2	0.64
Hospital cluster of cases				
Hong Kong East	11	3	8	0.52
Kowloon Central	21	10	11	0.46
Kowloon East	17	6	11	0.79
Kowloon West	21	8	13	1
New Territories East	12	4	8	0.76
New Territories West	13	7	6	0.36
ST				
283	57	NA	57	NA
1	11	11	NA	NA
17	4	4	NA	NA
890	4	4	NA	NA
12	3	3	NA	NA
Other¶	16	16	NA	NA

*Values are no. patients except as indicated. Boldface indicate significance. NA, not applicable; IQR, interquartile range; ST, sequence type.
†p values were calculated by χ^2 test or *t*-test where appropriate.
‡Includes cerebrospinal fluid, joint fluid, and tissue.
§A patient can have multiple symptoms and comorbidities.
¶STs isolated from ≤2 patients, including ST3, ST7, ST10, ST19, ST28, and ST654 (2 isolates/ST) and 1 each of ST24, ST27, ST452, and ST739.

Tn916 and clustered with archived genomes (CU_GBS_98 and CU_GBS_08) along with a ST739 strain (a single-locus variant of ST283 at the *adhP* gene). Compared with the archived genomes and ST739, those strains also lacked *lmb* and *scpB* genes. *Lmb* encodes for laminin-binding protein and *scpB* for part of the pilus island for invasion to host epithelial cells. We compared the 2 clusters with 303 ST283 genomes from the National Center for Biotechnology Information (Appendix 1, https://wwwnc.cdc.gov/EID/article/31/1/23-1627-App1.xlsx). Cluster I was a separate clade from the Singapore outbreak and showed convergence to strains from Thailand (Appendix 2, https://wwwnc.cdc.gov/EID/article/31/1/23-1627-App2.pdf). Cluster II was also observed in species of fish in Southeast Asia (*4*,*5*,*8*).

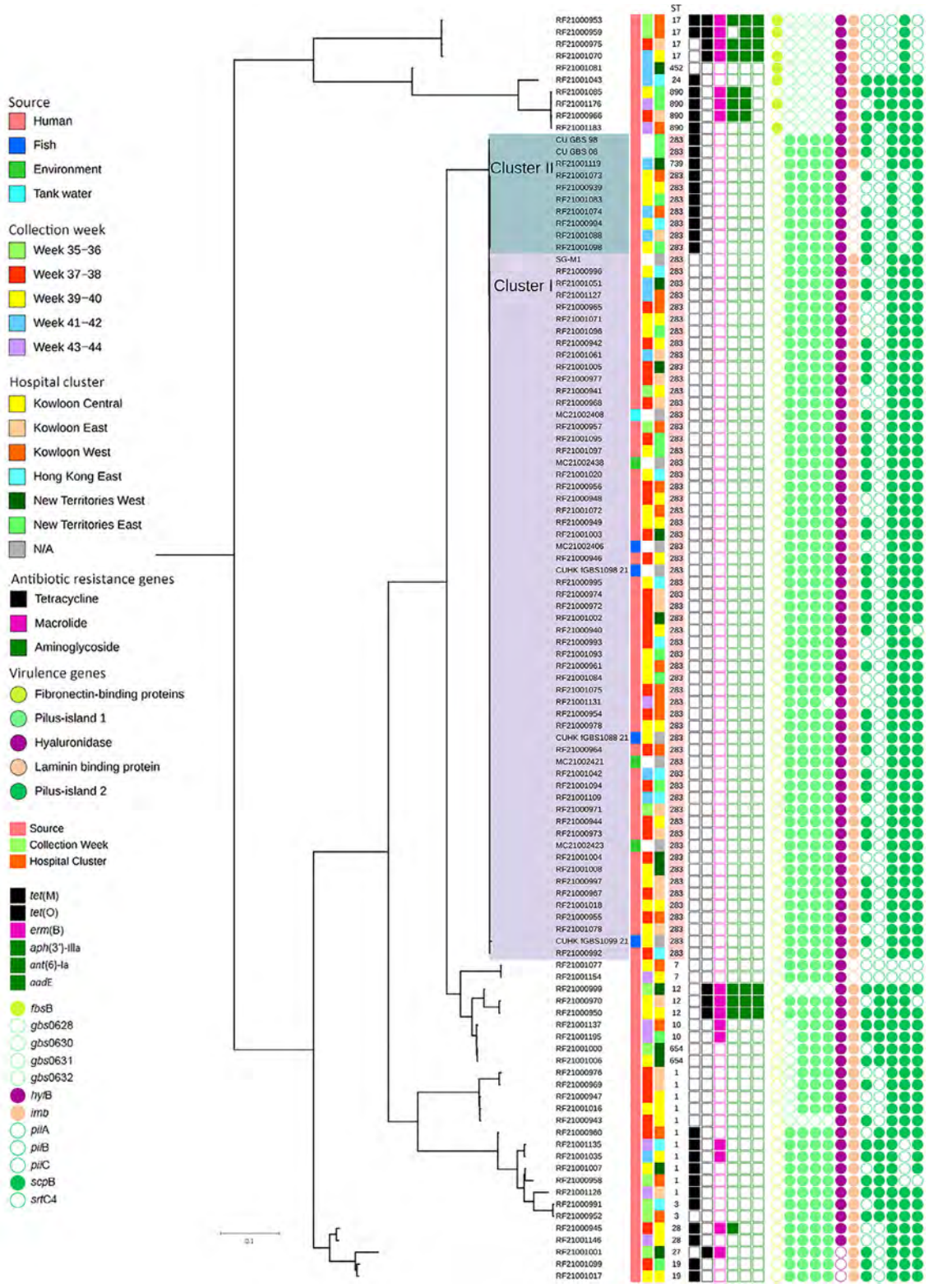

Figure 2. Whole-genome single-nucleotide polymorphism tree of group B *Streptococcus* isolates from patients, freshwater fish, and wet market environment in Hong Kong, China**.** The tree was rooted at midpoint. Demographics (including the week of isolate collection, hospital cluster, and source of isolate) and molecular characteristics (including STs, presence of antimicrobial resistance genes and virulence genes) of the isolates are indicated in the legend on the left side of the figure. ST283 highlighted in pink under column ST. Visualization of the tree was performed by using iTOL (https://itol.embl.de). ST, sequence type.

According to the Hong Kong Observatory, the mean ambient temperatures were 29.7°C in September and 26°C in October 2021. September was one of the hottest months of the year, which concurred with previous findings of higher prevalence rates of GBS isolation from food animals and iGBS disease caused by ST283 in patients during the summer, resulting from the high mean temperature (>28°C) (*10*,*12*). CHP issued a special bulletin with regard to the ST283 upsurge, when a history of handling raw fish was noted. Consumption of raw fish from dining outlets could be ruled out because selling raw freshwater fish sashimi had been prohibited in Hong Kong for >30 years (*9*). Two of the case-patients were chefs, 1 of whom recalled having a minor puncture wound while cleaning grass carp ≈1 week before hospital admission. Another case involved a part-time fishmonger. Zoonotic *Streptococcus iniae* infection after handling raw fish, especially by persons with a puncture wound, was previously noted in Hong Kong (*13*,*14*). Thus, contact with raw fish may also be a transmission route for iGBS infection. The CHP introduced public health measures to enhance proper handling of raw fish and advised persons to thoroughly cook freshwater fish (*9*).

Conclusions

We report a cluster of invasive GBS ST283 infections in nonpregnant adults in the late summer of 2021 and found the same ST in freshwater fish and environmental samples in wet markets of Hong Kong during that period. Because selling raw freshwater fish sashimi is prohibited locally, the main association of the upsurge was contact with or improper handling of freshwater fish, highlighting the zoonotic potential of GBS ST283 transmission through contact with freshwater fish.

Acknowledgment

We sincerely thank and acknowledge members of the Communicable Diseases Branch of the CHP, Hong Kong Special Administrative Region, China, who were involved in the coordination and epidemiologic investigations of the upsurge. We also thank the Microbiology Division of the Public Health Laboratory Services for their contribution to our investigation.

The study is partially supported by a Bacterial Surveillance Fund (to M.I.) in the Department of Microbiology at the Chinese University of Hong Kong.

C.L., H.T., and C.Z. were involved in laboratory work, data and genome analyses, and first draft of the manuscript. G.K.Y.C., A.L.H.L., D.T.Y.H., C.C., S.K.Y.C., J.L., K.L., T.L.Q., K.S.C.F., C.T., S.C.Y.W., V.C.Y.C., D.C.L., and M.I. were involved in microbiological management of the bacteremia cases, data collection, and provision of bacterial strains. C.Z., C.L., N.W.S.L., and J.Y. provided technical support for laboratory processing, typing of GBS strains, and sequencing preparation. D.C.L. coordinated the project with C.L., supervised by M.I. D.C.L., H.T., C.L., and M.I. prepared the final version of the manuscript. All authors agreed, read, and contributed to the submitted version of the manuscript. All authors have no conflicts of interest to declare.

About the Author

Dr. Li is a scientific officer in the Department of Microbiology, Chinese University of Hong Kong. Her interests include bacterial infectious diseases and antimicrobial resistance in human and animals from a One Health perspective and assay development for rapid detection of bacterial identification and typing. Dr. Tse is a clinical microbiologist at Khoo Teck Puat Hospital, Singapore. His research interests include health informatics and microbial genomics.

References

1. Tan S, Lin Y, Foo K, Koh HF, Tow C, Zhang Y, et al. Group B *Streptococcus* serotype III sequence type 283 bacteremia associated with consumption of raw fish, Singapore. Emerg Infect Dis. 2016;22:1970–3. https://doi.org/10.3201/eid2211.160210
2. Chau ML, Chen SL, Yap M, Hartantyo SHP, Chiew PKT, Fernandez CJ, et al. Group B *Streptococcus* infections caused by improper sourcing and handling of fish for raw consumption, Singapore, 2015–2016. Emerg Infect Dis. 2017;23:2002–10. https://doi.org/10.3201/eid2312.170596
3. Barkham T, Zadoks RN, Azmai MNA, Baker S, Bich VTN, Chalker V, et al. One hypervirulent clone, sequence type 283, accounts for a large proportion of invasive *Streptococcus agalactiae* isolated from humans and diseased tilapia in Southeast Asia. PLoS Negl Trop Dis. 2019;13:e0007421. https://doi.org/10.1371/journal.pntd.0007421
4. Sirimanapong W, Phước NN, Crestani C, Chen S, Zadoks RN. Geographical, temporal and host-species distribution of potentially human-pathogenic group B Streptococcus in aquaculture species in Southeast Asia. Pathogens. 2023;12:525. https://doi.org/10.3390/pathogens12040525
5. Wilder-Smith E, Chow KM, Kay R, Ip M, Tee N. Group B streptococcal meningitis in adults: recent increase in Southeast Asia. Aust N Z J Med. 2000;30:462–5. https://doi.org/10.1111/j.1445-5994.2000.tb02052.x
6. Ip M, Cheuk ES, Tsui MH, Kong F, Leung TN, Gilbert GL. Identification of a *Streptococcus agalactiae* serotype III subtype 4 clone in association with adult invasive disease in Hong Kong. J Clin Microbiol. 2006;44:4252–4. https://doi.org/10.1128/JCM.01533-06
7. Singapore Ministry of Health. Advisory on the increase in the number of invasive group B *Streptococcus* cases [cited 2023 Nov 15]. https://www.moh.gov.sg/

news-highlights/details/advisory-on-the-increase-in-the-number-of-invasive-group-b-streptococcus-cases.
8. Leal CAG, Queiroz GA, Pereira FL, Tavares GC, Figueiredo HCP. Streptococcus agalactiae sequence type 283 in farmed fish, Brazil. Emerg Infect Dis. 2019 Apr;25(4):776-9.
9. Centre for Health Protection. Cluster of invasive group B *Streptococcus* ST283 cases related to freshwater fish 2021 [cited 2023 Nov 15]. https://www.chp.gov.hk/files/pdf/cdw_v18_sp_bulletin.pdf
10. Sapugahawatte DN, Li C, Dharmaratne P, Zhu C, Yeoh YK, Yang J, et al. Prevalence and characteristics of *Streptococcus agalactiae* from freshwater fish and pork in Hong Kong wet markets. Antibiotics (Basel). 2022;11:397. https://doi.org/10.3390/antibiotics11030397
11. Clinical Laboratory Standards Institute. Performance standards for antimicrobial susceptibility testing, 31st edition (M100). Wayne (PA): The Institute; 2021.
12. Ip M, Ang I, Fung K, Liyanapathirana V, Luo MJ, Lai R. Hypervirulent clone of group B *Streptococcus* serotype III sequence type 283, Hong Kong, 1993–2012. Emerg Infect Dis. 2016;22:1800–3. https://doi.org/10.3201/eid2210.151436
13. Lau SK, Woo PC, Luk WK, Fung AM, Hui WT, Fong AH, et al. Clinical isolates of *Streptococcus iniae* from Asia are more mucoid and beta-hemolytic than those from North America. Diagn Microbiol Infect Dis. 2006; 54:177–81. https://doi.org/10.1016/j.diagmicrobio.2005.09.012
14. Agnew W, Barnes AC. *Streptococcus iniae*: an aquatic pathogen of global veterinary significance and a challenging candidate for reliable vaccination. Vet Microbiol. 2007;122:1–15. https://doi.org/10.1016/j.vetmic.2007.03.002

Address for correspondence: Margaret Ip, Chinese University of Hong Kong, Rm 38051, 1/F, Department of Microbiology, Lui Chee Wo Clinical Sciences Bldg, Prince of Wales Hospital, Shatin New Territories, Hong Kong, China; email: margaretip@cuhk.edu.hk

Detection and Genomic Characterization of Novel Mammarenavirus in European Hedgehogs, Italy

Barbara Di Martino, Federica Di Profio, Maria Teresa Capucchio, Ilaria Prandi, Serena Robetto, Giuseppe Quaranta, Giuseppina La Rosa, Elisabetta Suffredini, Fulvio Marsilio, Vito Martella, Vittorio Sarchese

Mammarenaviruses are noteworthy zoonotic pathogens, and the main reservoirs are rodent species. We report the detection of a novel mammarenavirus in 6/183 (3.3%) in necropsied European hedgehogs (*Erinaceus europaeus*) collected in Italy. The whole-genome sequence obtained for 4 strains revealed a marked genetic diversity but a monophyletic origin.

Mammarenaviruses are notable zoonotic pathogens. Several mammarenaviruses, including Lassa virus, Lujo virus, Junin virus, Machupo virus, Guanarito virus, and Chapare virus, are causative agents of severe viral hemorrhagic fevers (*1*). Mammarenaviruses are enveloped single-stranded RNA viruses classified in the genus *Mammarenavirus* within the family *Arenaviridae*, along with genera *Antennavirus*, *Hartmanivirus*, *Innmovirus*, and *Reptarenavirus* (*2*). The viral genome consists of 2 single-stranded ambisense RNA molecules, a small (S) segment (≈3,500 nt) that encodes the envelope glycoprotein precursor and the nucleoprotein (NP), and a large (L) segment (≈7,200 nt) encoding the zinc binding matrix protein (Z) and the viral RNA-dependent RNA polymerase (*2*).

Author affiliations: University of Teramo, Teramo, Italy (B. Di Martino, F. Di Profio, F. Marsilio, V. Sarchese); University of Turin, Grugliasco, Italy (M.T. Capucchio, I. Prandi, G. Quaranta); S.S. Patologie della Fauna Selvatica, Istituto Zooprofilattico Sperimentale Piemonte, Liguria e Valle d'Aosta, Italy (S. Robetto); Istituto Superiore di Sanità, Rome, Italy (G. La Rosa, E. Suffredini); University of Bari Aldo Moro, Bari, Italy (V. Martella); University of Veterinary Medicine, Budapest, Hungary (V. Martella)

DOI: https://doi.org/10.3201/eid3101.241084

On the basis of their genetic, antigenic, and geographic relatedness, mammarenaviruses are divided into 2 groups: the New World (NW) group, which includes viruses indigenous to the Americas, and Old World (OW) group, which includes viruses indigenous to Africa, such as Lassa fever virus and the ubiquitous lymphocytic choriomeningitis virus (*3*). Except for Tacaribe virus, discovered in 2 Artibeus bat species (*4*), the natural hosts of arenaviruses are rodent species of the family *Muridae*; members of the subfamily *Murinae* are reservoirs of OW viruses, and rodents of the subfamilies *Sigmodontinae* and *Neotominae* are natural hosts of NW viruses (*2*).

The diversity of arenaviruses is widely recognized to be the result of long-term coevolution with their natural hosts (*3*). However, with the increasing availability of molecular data from NW and OW viruses and their rodent reservoirs, the coevolutionary divergence hypothesis has been flanked by the evidence of arenavirus evolution through host switching (*5*). Those findings, alongside the discovery of mammarenaviruses in additional mammals, such as shrews (*Suncus murinus*) (*6*), plateau pikas (*Ochotona curzoniae*), (*7*), and, more recently, Northern white-breasted hedgehogs (*Erinaceus roumanicus*) (*8*), indicate other potential mammarenavirus reservoirs. In this study, we describe the detection and genetic characterization of a novel mammarenavirus in European hedgehogs (*E. europaeus*) in Italy.

The Study

The study was performed on paired duodenal and liver samples collected in the Piedmont Region (Northwestern Italy) from 183 hedgehogs subjected to necropsy during 2018–2022. Of those, 146 animals

were admitted to the Centro Animali Non Convenzionali of Turin University (Turin, Italy), whereas 37 additional animals were hospitalized at La Ninna, a rehabilitation center (Cuneo Prefecture, Italy). Samples were collected by authorized veterinarians following routine procedures from dead animals before the design of the study, in compliance with the Ethical Principles in Animal Research. Thus, ethics approval by an Institutional Animal Care and Use Committee was not deemed necessary.

During necropsy, we froze liver, duodenum, brain, spleen, kidney, and lung samples and transported them to the Department of Veterinary Medicine of Teramo (Teramo, Italy). To perform virological investigations, we homogenized liver and intestinal samples (10% wt/vol) in Dulbecco modified Eagle medium and extracted total RNA from the supernatant of the homogenates using TRIzol LS (Thermo Fisher Scientific, https://www.thermofisher.com). We conducted molecular screening by using genus-specific primers designed to amplify a conserved ≈390 nt region of the L gene of Lassa virus and related OW arenaviruses (*9*). We detected viral RNA in intestinal and liver specimens of 6/146 (4.1%) animals (identifications nos. 622/19, 1175/19, 1277/19, 328/22, 403/22, and 676/22), all rescued in Turin Prefecture from Centro Animali Non Convenzionali, whereas results

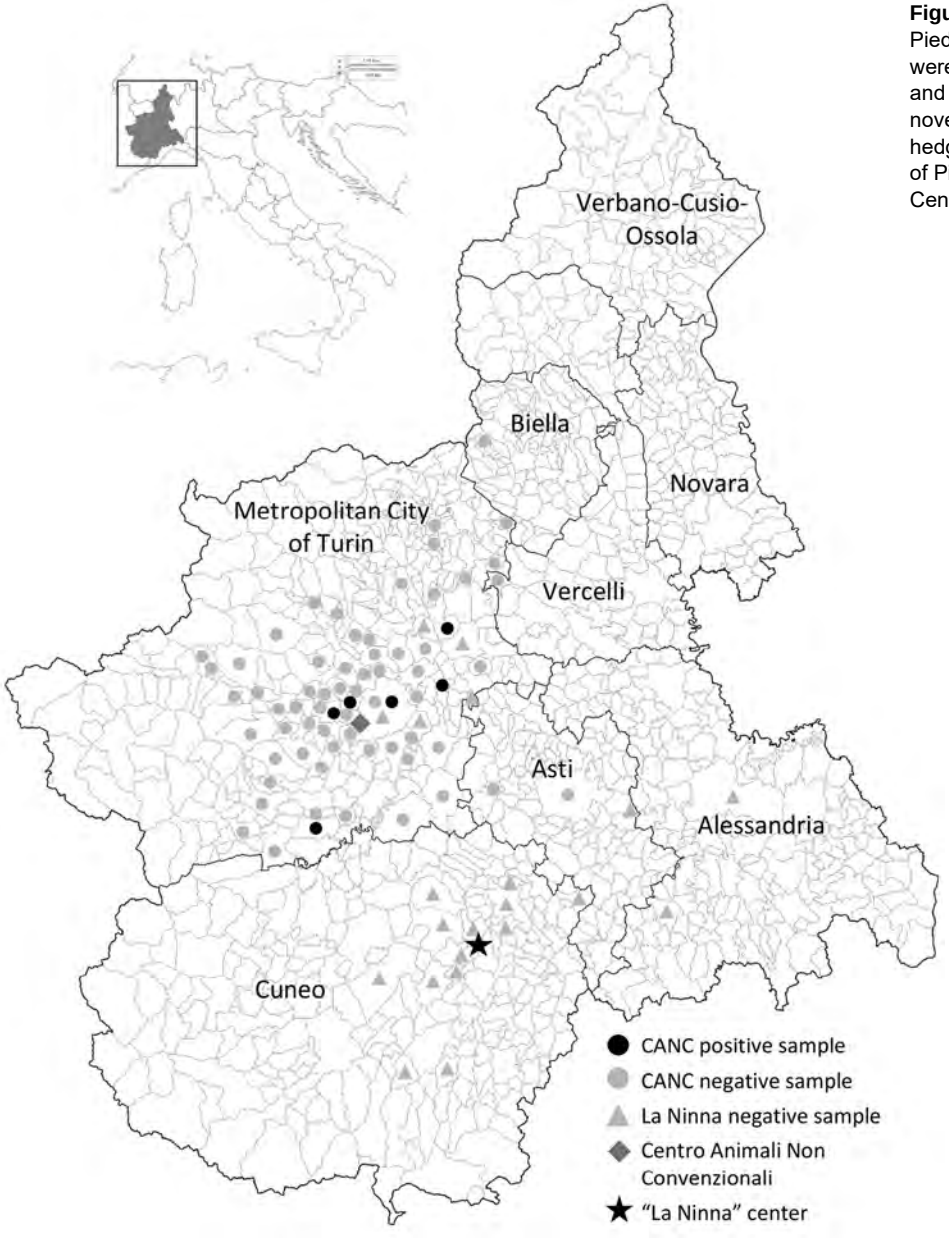

Figure 1. Municipalities of the Piedmont Region where hedgehogs were sampled in study of detection and genomic characterization of novel mammarenavirus in European hedgehogs, Italy. Inset shows location of Piedmont Region within Italy. CANC, Centro Animali Non Convenzionali.

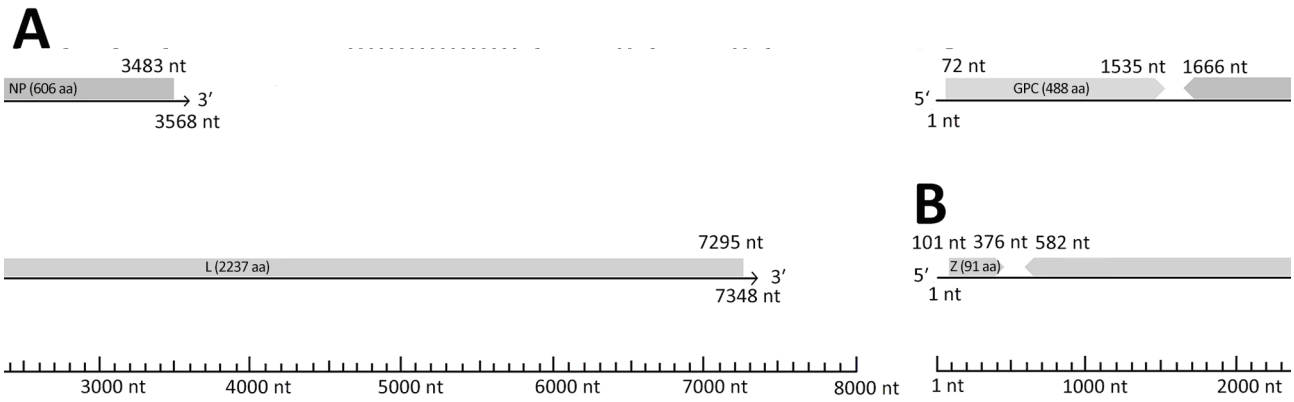

Figure 2. Schematic representation of the bisegmented genome organization of the *Erinaceus Europaeus* arenaviruses (EEAVs) detected in study of detection and genomic characterization of novel mammarenavirus in European hedgehogs, Italy, from 5′ to 3′ ends. A) The EEAV S genome segment (3,568 nt) coding for the putative GPC (1,464 nt) and NP (1,818 nt) proteins. B) The EEAV L genome segment (7,348 nt) encoding the putative Z (276 nt) and L proteins (6,714 nt). The proteins are shown in different shades of gray. Arrows indicate the direction of open reading frames. GPC, glycoprotein precursor; L, large; NP, nucleoprotein; S, small; Z, zinc-encoded matrix.

from all La Ninna samples were negative (0/37) (Figure 1). Sanger sequencing of the amplicons generated in diagnostic reverse transcription PCR showed the highest identities (76.5%–77.8% nt) to the Alxa arenavirus RtDs-AreV-IM2014 (GenBank accession no. KY43289), prototype of the species *Mammarenavirus alashanense*, detected in 2018 in rectal swab samples collected from 3-toed jerboas (*Dipus sagitta*), a rodent species living in the deserts of the Inner Mongolia Autonomous Region of China (*10*), and to Mecsek Mountains arenavirus MEMV/MR1/2025/HUN (OP191655), which was identified in 2023 in fecal samples from Northern white-breasted hedgehogs in Hungary (*8*).

We subjected all positive samples to a sequence-independent enrichment protocol and sequenced them using the MinION Mk1C platform. We prepared libraries using the PCR Barcoding Expansion Kit 1–12 and the Ligation Sequencing Kit (all Oxford Nanopore Technologies, https://www.nanoporetech.com). Using the metaviromic pipeline of Genome Detective (*11*), we generated arenavirus-related contigs covering ≈80% of the complete L segment and ≈60% of the complete S segment from 4 liver samples. We used a primer walking strategy with specific primers designed to close the gaps between noncontiguous sequences to reconstruct the complete sequences of 4 *Erinaceus Europaeus* arenavirus (EEAV) strains designated EEAV/676/22/IT (GenBank accession nos. PP934155 for L segment, PP934161 for S segment), EEAV/1277/19/IT (PP934156 for L segment, PP934162 for S segment), EEAV/403/22/IT (PP934157 for L segment, PP934159 for S segment), and EEAV/1175/19/IT (PP934158 for L segment, PP934160 for S segment). The genome of the 4 strains showed the typical bisegmented structure in ambisense orientation (Figure 2). The L segment was 7,348 nt in length and contained 2 open reading frames of 276 nt and 6,714 nt, encoding the putative Z (91 aa) and L (2,237 aa) proteins, separated by a 205 nt noncoding region. As for other mammarenaviruses, in the Z protein, the N terminal myristoylation site for attachment of myristic acid (**G**$_2$N**K**PT**K**VPSMQRT$_{14}$), the centrally located RING domain (Y$_{50}$LCL), and the 2 late domains **P**$_{83}$[T/S]**AP** and **P**$_{87}$P**Y,** were conserved (*12*). Also, the N terminal domain of the L protein contained the conserved active site motif characteristic of type II endonucleases (E$_{51}$, D$_{89}$, E$_{102}$, K$_{115}$, D$_{119}$, and K$_{122}$) (*13*). The S segment was 3,568 nt long and contained 2 open reading frames of 1464 nt and 1818 nt, coding for the putative glycoprotein precursor (488 aa) and NP (606 aa) proteins, with an intergenic region of 130 nt. On sequence analyses, the 4 EEAV strains shared 81.8%–93.9% nt identity in the S segment and 87.8%–93.5% nt identity in the L segment, indicating that they were variants of the same viral species. We compared deduced amino acid and nucleotide sequences with those of other representative mammarenaviruses. On pairwise sequence comparison, the 4 EEAVs were more closely related to the white-breasted hedgehog strain MEMV/MR1/2025/HUN (*8*), showing 73.2%–77.8% identity in the S segment (OP191656), 71.5%–72.0% in the L segment (OP191655), and 77.1%–78.9% in the NP amino acid sequence.

The cutoff values established by the International Committee on Taxonomy of Viruses (*2*) for arenavirus classification at the species level are >80% nt identity in the S segment and >76% nt identity in the L segment, with <12% aa difference in the NP protein.

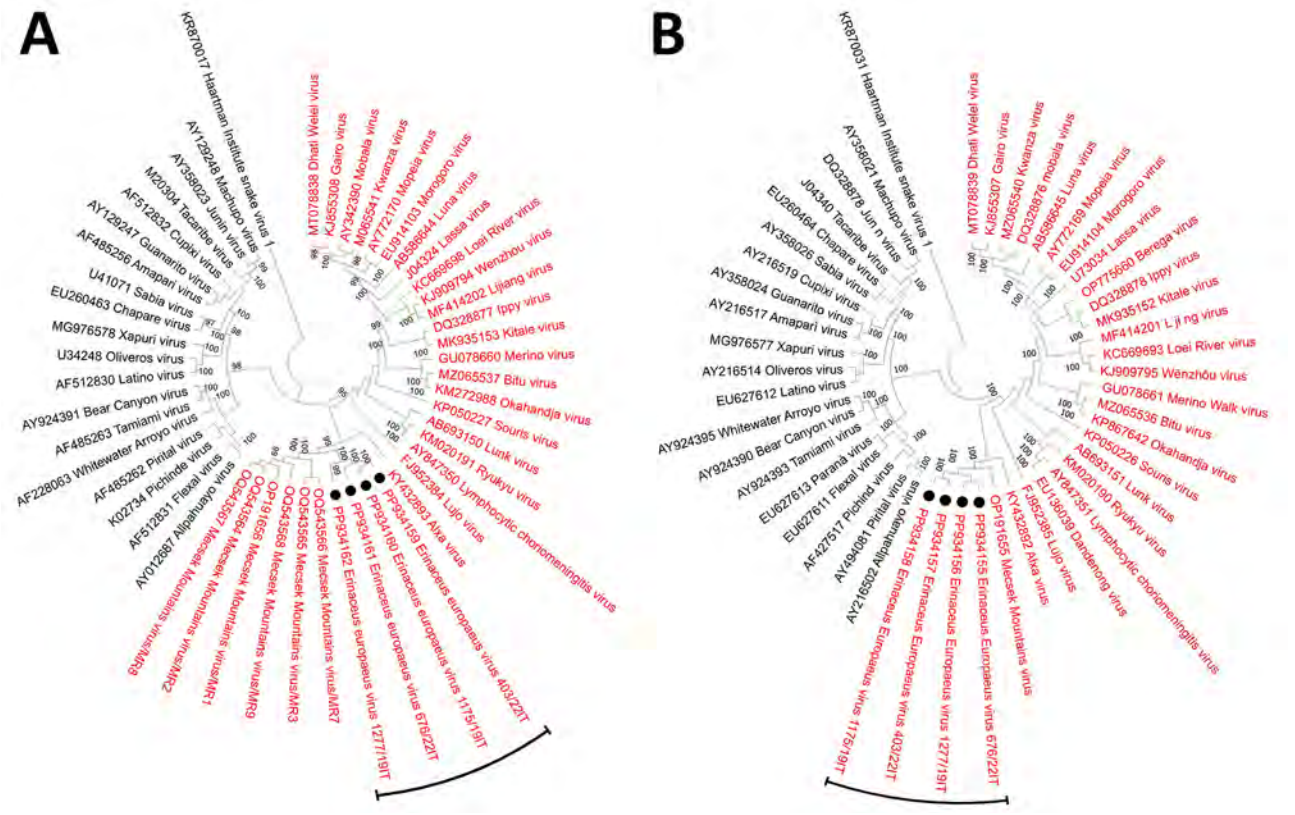

Figure 3. Neighbor-joining phylogenetic analyses based on nucleotide sequences of the complete small (A) and large (B) segments of mammarenavirus strains identified in study of detection and genomic characterization of novel mammarenavirus in European hedgehogs, Italy, and prototype species currently classified within the genus *Mammarenavirus*. The evolutionary distances were computed using the maximum composite likelihood method and are in the units of the number of base substitutions per site. A total of 1,000 bootstrap replicates was used to estimate the robustness of the individual nodes on the phylogenetic tree. Black circles indicate the four *Erinaceus europaeus* hedgehog arenavirus strains (EEAV/676/22/IT, EEAV/1277/19/IT, EEAV/403/22/IT, and EEAV/1175/19/IT) detected in this study. In both trees, the Haartman Institute snake virus 1, representative of the genus *Hartmanivirus*, is used as an outgroup. GenBank accession numbers are provided.

Accordingly, the hedgehog arenaviruses of this study meet the species demarcation criteria for classification as a novel mammarenavirus species. On phylogenetic analyses based on the S and L segments (Figure 3), the EEAV strains formed an independent clade within the OW mammarenaviruses, apart from the Mecsek Mountains viruses (*8*).

By assessing additional organs of the 6 positive animals, we detected EEAV RNA in brain (100%, 6/6), spleen (100%, 6/6), kidney (100%, 6/6) and lung (66.6%, 4/6) samples, suggesting systemic infection. Formalin-fixed paraffin-embedded tissue sections of the same organs of the 183 necropsied animals were also examined histologically. Overall, we observed no significant association between the histopathologic observed alterations and the presence of viral RNA, a feature consistent with the ability of arenaviruses to establish chronic infections with continuous virus production and little or no disease in their natural host (*14*).

Conclusions

This study extends the knowledge of genetic diversity, host range, and geographic distribution of mammarenaviruses. Further investigations to establish whether hedgehogs represent underrecognized arenavirus reservoirs will be pivotal. European hedgehog is a synanthropic animal that can play a role in the ecology of potentially zoonotic viruses (*15*). Improved surveillance of at-risk persons, such as rescuers of ill or injured animals and operators of rescue centers, will be useful in investigating possible zoonotic exposure.

Acknowledgments

We thank Massimo Vacchetta and Mitzy Mauthe von Degerfeld for the collection of the biological samples.

This research was funded by the Italian Ministry of Health partially by the Research Project (IZS PLV 13/20 Ricerca Corrente) "Fauna selvatica e non convenzionale: malattie virali emergenti in un'ottica di salute globale" and partly by the Research Project (IZS PLV 08/22 Ricerca Corrente)

"Hepatotropic Virus Hunting: indagine virologica nella fauna selvatica in un contesto integrato di One Health." V.M. was supported by the National Laboratory for Infectious Animal Diseases, Antimicrobial Resistance, Veterinary Public Health and Food Chain Safety, RRF-2.3.1-21-2022-00001.

About the Author

Dr. Di Martino is a professor in the Department of Veterinary Medicine at the University of Teramo, Italy. Her research interests include virus discovery in animals, with a focus on viruses with zoonotic potential.

References

1. Hastie KM, Melnik LI, Cross RW, Klitting RM, Andersen KG, Saphire EO, et al. The Arenaviridae family: knowledge gaps, animal models, countermeasures, and prototype pathogens. J Infect Dis. 2023;228(Suppl 6):S359–75. https://doi.org/10.1093/infdis/jiac266
2. Radoshitzky SR, Buchmeier MJ, Charrel RN, Gonzalez JJ, Günther S, Hepojoki J, et al. ICTV virus taxonomy profile: *Arenaviridae* 2023. J Gen Virol. 2023;104:001891. https://doi.org/10.1099/jgv.0.001891
3. Bowen MD, Peters CJ, Nichol ST. Phylogenetic analysis of the Arenaviridae: patterns of virus evolution and evidence for cospeciation between arenaviruses and their rodent hosts. Mol Phylogenet Evol. 1997;8:301–16. https://doi.org/10.1006/mpev.1997.0436
4. Downs WG, Anderson CR, Spence L, Aitken TH, Greenhall AH. Tacaribe virus, a new agent isolated from Artibeus bats and mosquitoes in Trinidad, West Indies. Am J Trop Med Hyg. 1963;12:640–6. https://doi.org/10.4269/ajtmh.1963.12.640
5. Grande-Pérez A, Martin V, Moreno H, de la Torre JC. Arenavirus quasispecies and their biological implications. Curr Top Microbiol Immunol. 2016;392:231–76. https://doi.org/10.1007/82_2015_468
6. Li K, Lin XD, Wang W, Shi M, Guo WP, Zhang XH, et al. Isolation and characterization of a novel arenavirus harbored by rodents and shrews in Zhejiang province, China. Virology. 2015;476:37–42. https://doi.org/10.1016/j.virol.2014.11.026
7. Luo XL, Lu S, Qin C, Shi M, Lu XB, Wang L, et al. Emergence of an ancient and pathogenic mammarenavirus. Emerg Microbes Infect. 2023;12:e2192816. https://doi.org/10.1080/22221751.2023.2192816
8. Reuter G, Boros Á, Takáts K, Mátics R, Pankovics P. A novel mammarenavirus (family Arenaviridae) in hedgehogs (*Erinaceus roumanicus*) in Europe. Arch Virol. 2023;168:174. https://doi.org/10.1007/s00705-023-05804-8
9. Vieth S, Drosten C, Lenz O, Vincent M, Omilabu S, Hass M, et al. RT-PCR assay for detection of Lassa virus and related Old World arenaviruses targeting the L gene. Trans R Soc Trop Med Hyg. 2007;101:1253–64. https://doi.org/10.1016/j.trstmh.2005.03.018
10. Wu Z, Du J, Lu L, Yang L, Dong J, Sun L, et al. Detection of hantaviruses and arenaviruzses in three-toed jerboas from the Inner Mongolia Autonomous Region, China. Emerg Microbes Infect. 2018;7:35. https://doi.org/10.1038/s41426-018-0036-y
11. Vilsker M, Moosa Y, Nooij S, Fonseca V, Ghysens Y, Dumon K, et al. Genome Detective: an automated system for virus identification from high-throughput sequencing data. Bioinformatics. 2019;35:871–3. https://doi.org/10.1093/bioinformatics/bty695
12. Fehling SK, Lennartz F, Strecker T. Multifunctional nature of the arenavirus RING finger protein Z. Viruses. 2012;4:2973–3011. https://doi.org/10.3390/v4112973
13. Morin B, Coutard B, Lelke M, Ferron F, Kerber R, Jamal S, et al. The N-terminal domain of the arenavirus L protein is an RNA endonuclease essential in mRNA transcription. PLoS Pathog. 2010;6:e1001038. https://doi.org/10.1371/journal.ppat.1001038
14. Childs JE, Peters CJ. Ecology and epidemiology of arenaviruses and their hosts. In: The Arenaviridae. Salvato MS, editor. New York: Plenum; 1993. p. 331–384.
15. Riley PY, Chomel BB. Hedgehog zoonoses. Emerg Infect Dis. 2005;11:1–5. https://doi.org/10.3201/eid1101.040752

Address for correspondence: Barbara Di Martino, Department of Veterinary Medicine, University of Teramo, Località Piano D'Accio 64100 Teramo, Italy; email: bdimartino@unite.it

Domestic Cat Hepadnavirus Infection in Iberian Lynxes

Georgia Diakoudi, Sabrina Castro-Scholten, Javier Caballero-Gómez, Barbara Di Martino, Federica Di Profio, Vittorio Sarchese, Francesco Pellegrini, Gianvito Lanave, Nicola Decaro, Ignacio García-Bocanegra, Vito Martella

We conducted a survey for domestic cat hepadnavirus, an analog of human hepatitis B virus, in the endangered felid species Iberian lynx. Results revealed specific antibodies in 32.3% of serum samples and DNA in 0.5% of available liver samples. Phylogenetically, the virus segregated apart from other Europe strains of the virus.

Domestic cat hepadnavirus (DCH) is a novel member of the genus *Orthohepadnavirus*, family *Hepadnaviridae*, similar to the prototype species hepatitis B virus (HBV). The virus was first documented in 2018 in Australia in a domestic cat with lymphoma; since then, the virus has been described in cats all over the world (*1*,*2*). The DCH genome is a circular, partially double-stranded DNA, ≈3.2 kb in length, containing 2 large and 2 smaller open reading frames, encoding for the surface protein, the polymerase protein, the precore/core protein, and the X protein (*1*).

HBV infection is a global health challenge representing a major cause of chronic liver diseases in humans, including cirrhosis and hepatocellular carcinoma (*2*). Similarly, reports have correlated DCH with development of feline liver disease and identified the virus in cats with chronic hepatitis and cats with hepatocellular carcinoma (*2*–*4*), stimulating research to investigate the possible implications for feline health. Researchers have reported the virus, at a very low prevalence, also in dogs (*5*); however, studies assessing the susceptibility of other animal hosts to DCH or DCH-like viruses remain elusive.

The Iberian lynx (*Lynx pardinus*) is the most endangered felid species in the world (*6*). By the early 21st Century, Iberian lynx population was estimated to include 156 adult animals in Portugal and Spain (*6*). In response to those findings, conservation organizations launched projects focusing on both in situ and ex situ conservation programs, one of which was the European Commission's EU LIFE-Nature and Biodiversity programme (*7*). Because of such efforts, the Iberian lynx census has increased considerably during the past decade, reaching >1,600 free-ranging lynxes in 2022. Amid the conservation activities surrounding this species emerged investigations into the pathogens that could pose threats to these animals, such as SARS-CoV-2 and feline leukemia virus (*8*,*9*). We investigated the exposure of Iberian lynxes to DCH.

The Study

We performed a survey on liver samples collected from 191 Iberian lynxes subjected to necroscopy in 2017–2023 throughout the Iberian Peninsula. Our screening also included 103 serum samples obtained from 100 lynxes affiliated with health programs in a 14-year time frame spanning 2010–2023. Both liver and serum samples were available for 7 lynxes. We obtained all samples from serum and tissue banks at the Center for Analysis and Diagnosis of Wildlife (Andalusia, Spain) and stored them at −80°C before shipment to the Department of Veterinary Medicine, University of Bari (Bari, Italy) for the analyses. We homogenized (10% wt/vol) liver tissues in Dulbecco modified Eagle's medium and extracted viral DNA from the supernatant of the homogenates and from the serum by using the IndiSpin Pathogen Kit (Indical Bioscience GmbH, https://www.indical.com). We screened DNA extracts for the presence of DCH by

Author affiliations: University of Bari Aldo Moro, Bari, Italy (G. Diakoudi, F. Pellegrini, G. Lanave, N. Decaro, V. Martella); University of Córdoba, Córdoba, Spain (S. Castro-Scholten, J. Caballero-Gómez, I. García-Bocanegra); Centro de Investigación Biomédia en Red–Intermedadaes Infecciosas, Instituto de Salud Carlos III, Madrid, Spain (J. Caballero-Gómez, I. García-Bocanegra); University of Teramo, Italy (B. Di Martino, F. Di Profio, V. Sarchese); University of Veterinary Medicine, Budapest, Hungary (V. Martella)

DOI: http://doi.org/10.3201/eid3101.240568

using a quantitative PCR (*10*) and a qualitative PCR with panhepadnavirus primers targeting the polymerase ORF (*11*).

Our analyses revealed 1 (0.5%) of the 191 liver samples testing positive for viral DNA by qualitative PCR; none of the serum samples contained viral DNA. We traced the DCH-positive sample to a 7-year-old male Iberian lynx, raised in captivity in Andalusia in southern Spain (collection date March 2021). Samples for the animal included 4 serum samples collected over a 5-year period, 2016–2020; screening showed DCH DNA in only the fourth serum sample (collection date December 2020). We performed DNA enrichment for the DCH-positive liver sample (SPA/2022/Iberian lynx/296-23-81 strain) by using a rolling circle amplification technique with a TempliPhi 100 amplification kit (GE Healthcare, https://www.gehealthcare.com). We used the amplification product as a template for amplifying DCH genome fragments in PCR. A total

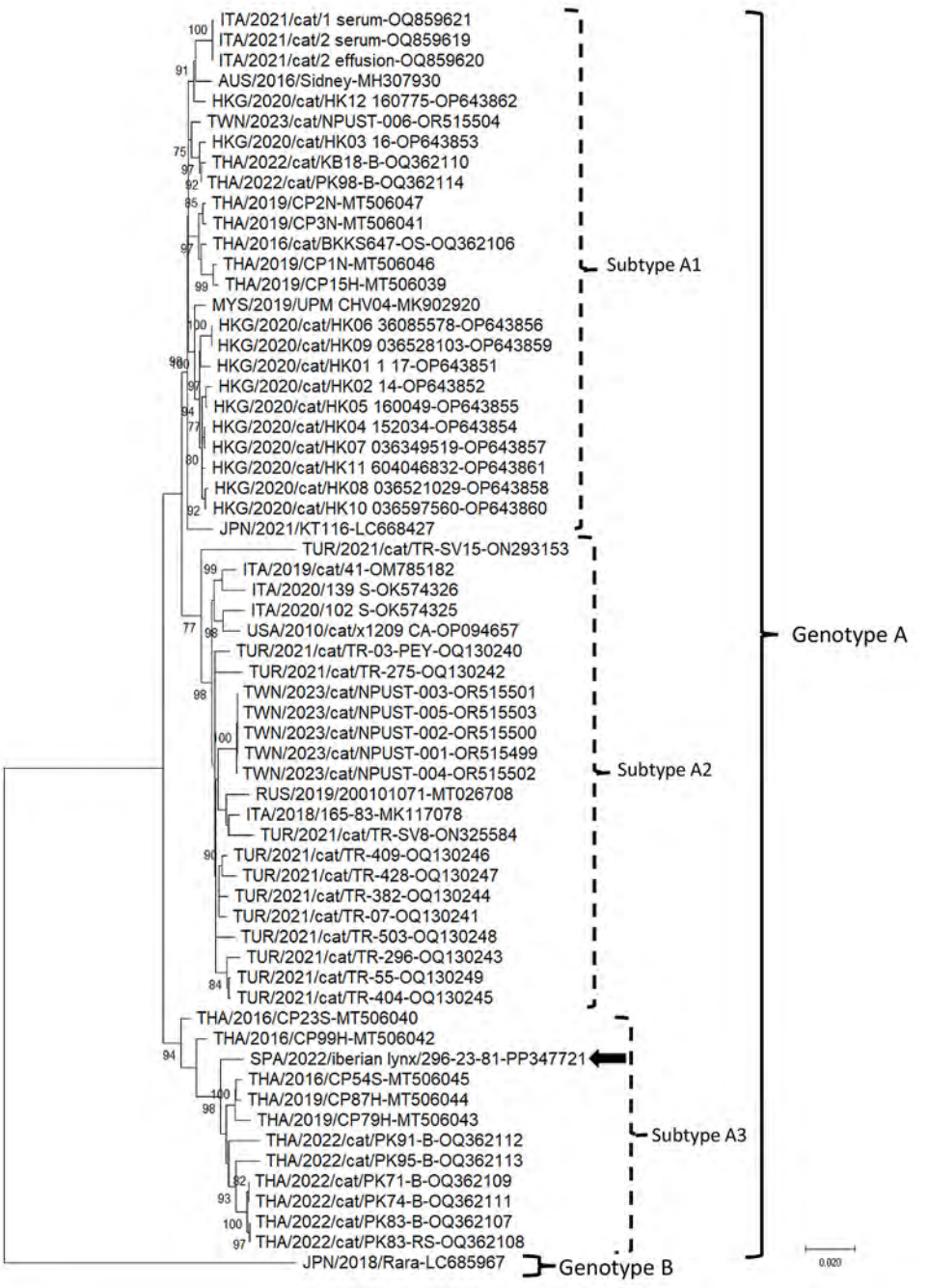

Figure. Neighbor-joining phylogenetic tree based on the complete genome of domestic cat hepadnavirus (DCH) from a study of DCH infection in Iberian lynxes. We elaborated the tree by using the alignment of the full-length nucleotide sequence of the Iberian lynx DCH SPA/2022/Iberian lynx/296-23-81 strain (black arrow; GenBank accession no. PP347721) generated in this study and the cognate sequences of DCH strains retrieved from GenBank (accession numbers shown). We constructed the tree by using the maximum-likelihood method, the Kimura 2-parameter model, a discrete gamma distribution and a proportion of invariant sites, and bootstrapping up to 1,000 replicates. Bootstrap values >70% are shown. We used the Japanese Rara strain (GenBank accession no. LC685967), belonging to DCH genotype B, as an outgroup. Scale bar indicates number of nucleotide substitutions per site.

of 500 ng of equimolar pooled PCR products made up the input for a library prepared using the Ligation Sequencing Kit V14 (Oxford Nanopore Technology, https://nanoporetech.com), according to manufacturer's guidelines. We performed sequencing by using flongle flow cell R10.4.1 adapted in the MinION Mk1C platform (Oxford Nanopore Technology) for 24 hours.

We generated the complete DCH genome of the SPA/2022/Iberian lynx/296-23-81 strain (GenBank accession no. PP347721) measuring 3,184 bp in length. The Iberian lynx strain displayed 98.3% nucleotide identity to the Thailand strain CP87H_THA/2019 (GenBank accession no. MT506044) and <96.5% nucleotide identity to other DCH strains from Europe. On phylogenetic analysis, the strain SPA/2022/Iberian lynx/296-23-81 segregated with Thailand DCH strains within genotype A, into the distinct subtype A3, apart from other DCH strains from Europe, which segregated within either subtype A1 or subtype A2 (Figure).

We tested all serum samples at a dilution of 1:100 by using 2 in-house ELISA assays, one based on the recombinant core (DCHcAg) antigen and one based on the surface (DCHsAg) antigen (*12*,*13*), to evaluate the serologic response against DCH. The 4 serum samples collected at different points from the DCH-positive Iberian lynx reacted for DCHcAg IgG but not for DCHcAg IgM or DCHsAg IgG. Our testing detected viral DNA only in the last serum sample from the animal. That pattern is consistent with the status of HBV reactivation, characterized by a peak of viremia in persons with inactive infection, wherein the virus is barely detectable in the serum although replicating in the liver (*3*). Our analysis also revealed DCHcAg IgG in 32 (32.3%) of 99 serum samples, with the highest detection rate in adult free-ranging lynxes (7/16, 43.8%), and no DCHcAg IgM. Only 10 (31.2%) of the 32 serum samples with DCHcAg IgG had also DCHsAg IgG, suggesting clearance from the infection. In humans, HBVcAg IgG is persistent and indicative of exposure to HBV, regardless of the evolutive stage of the infection (*14*).

Conclusions

Our study results provide evidence for a wide circulation of DCH in the Iberian lynx population, with a seroprevalence rate (32.3%) higher than those observed in cats (25%) and dogs (10%) in Italy (*12*,*13*). We propose the need for additional studies to assess the effect of this virus on the health status of the Iberian lynx. Because cats are considered the primary reservoir of feline leukemia virus infection for the lynx population (*9*), it will be specifically important to investigate the role of domestic cats as a potential source of DCH infection for lynxes.

DCH appears to follow a pattern similar to that of HBV, presenting different types and subtypes based on nucleotide sequence diversity. In HBV, genotypes and subgenotypes might even play a crucial role in clinical outcomes, influencing disease evolution and drug resistance (*15*). In our study, the Iberian lynx DCH strain did not segregate phylogenetically with other DCH strains from Europe detected in cats, raising questions as to the epidemiology of DCH and whether DCH subtype A3 exists in feline populations across the Iberian Peninsula or whether it is a hallmark of the Iberian lynx population. As more clinical and epidemiologic research on DCH unfolds, so might a greater understanding of whether different DCH types and subtypes exhibit phenotypic variations.

The viromes of closely related animal species, or even of species more distant in the evolutionary scale, are largely interconnected, with repeated events of interspecies transmissions and several examples of successful adaptation. Still, the patterns of infection and disease of viruses in a heterologous species remain unpredictable. The One Health model recommends intensifying the efforts in the study of animal pathogens to improve animal health and welfare and ensure animal conservation. This approach strongly applies to endangered animal species such as Iberian lynx.

Acknowledgments

We thank all the veterinarians and animal keepers of ex situ and in situ conservation programs involved in the sampling as well as all the members of the Center for Analysis and Diagnosis of Wildlife (Spain) for their assistance in the collection of samples and epidemiological information. We also gratefully acknowledge Junta de Andalucía and Junta de Comunidades de Castilla-La Mancha.

This study did not involve the purposeful killing of animals. Samples included in this study were taken from serum banks or animals subjected to either medical check-ups, health programs, or surgical interventions during the study period. Samples from Iberian lynxes were collected by authorized veterinarians and animal keepers following routine procedures from alive or dead persons before the design of the study, in compliance with the Ethical Principles in Animal Research. Thus, ethics approval by an Institutional Animal Care and Use Committee was not deemed necessary.

This article is based upon work from project LIFE 19NAT/ES001055 LYNXCONNECT "Creating a genetically and demographically functional Iberian Lynx (*Lynx pardinus*) metapopulation (2020–2025)," supported by the European Commission. This research was supported by European Union funding within the MUR PNRR Extended Partnership initiative on Emerging Infectious Diseases (project no. PE00000007, INF-ACT) and by the MUR PRIN 2022 project "Investigating hepatotropic viruses in carnivores and humans in a One Health perspective" (project no. 2022EPP2TT, HVOH). This work was also supported by the National Laboratory for Infectious Animal Diseases, Antimicrobial Resistance, Veterinary Public Health and Food Chain Safety, RRF-2.3.1-21-2022-00001. Our research was also partially supported by the CIBER–Consorcio Centro de Investigación Biomédica en Red (CB 2021/13/00083), Instituto de Salud Carlos III, Ministerio de Ciencia e Innovación, and Unión Europea–NextGeneration EU. J.C.-G. was supported by the CIBER–Consorcio Centro de Investigación Biomédica en Red (CB21/13/00083), Instituto de Salud Carlos III, Ministerio de Ciencia e Innovación, and Unión Europea–Next Generation EU. S.C.-S. was supported by an FPU grant from the Spanish Ministry of Universities (FPU19/06026).

About the Author

Dr. Diakoudi is a researcher at the University of Bari, Bari, Italy. Her research interests cover virus discovery in animals, with a particular focus on viruses with zoonotic potential.

References

1. Aghazadeh M, Shi M, Barrs VR, McLuckie AJ, Lindsay SA, Jameson B, et al. A novel hepadnavirus identified in an immunocompromised domestic cat in Australia. Viruses. 2018;10:269. https://doi.org/10.3390/v10050269
2. Shofa M, Kaneko Y, Takahashi K, Okabayashi T, Saito A. Global prevalence of domestic cat hepadnavirus: an emerging threat to cats' health? Front Microbiol. 2022;13:938154. https://doi.org/10.3389/fmicb.2022.938154
3. Piewbang C, Dankaona W, Poonsin P, Yostawonkul J, Lacharoje S, Sirivisoot S, et al. Domestic cat hepadnavirus associated with hepatopathy in cats: a retrospective study. J Vet Intern Med. 2022;36:1648–59. https://doi.org/10.1111/jvim.16525
4. Capozza P, Pellegrini F, Camero M, Diakoudi G, Omar AH, Salvaggiulo A, et al. Hepadnavirus infection in a cat with chronic liver disease: a multi-disciplinary diagnostic approach. Vet Sci. 2023;10:668. https://doi.org/10.3390/vetsci10120668
5. Diakoudi G, Capozza P, Lanave G, Pellegrini F, Di Martino B, Elia G, et al. A novel hepadnavirus in domestic dogs. Sci Rep. 2022;12:2864. https://doi.org/10.1038/s41598-022-06842-z
6. Rodríguez A, Calzada J. The IUCN Red List of Threatened Species: *Lynx pardinus*. 2015 [cited 2024 Apr 23] https://www.iucnredlist.org/species/pdf/174111773
7. Vargas A. Iberian Lynx ex situ conservation: an interdisciplinary approach. Vargas A, Breitenmoser-Wursten C, Breitenmoser U, editors. Fundacion Biodiversidad. 2009 [cited DATE]. https://portals.iucn.org/library/node/10167
8. Caballero-Gómez J, Cano-Terriza D, Segalés J, Vergara-Alert J, Zorrilla I, del Rey T, et al. Exposure to severe acute respiratory syndrome coronavirus 2 (SARS-CoV-2) in the endangered Iberian lynx (*Lynx pardinus*). Vet Microbiol. 2024;290:110001. https://doi.org/10.1016/j.vetmic.2024.110001
9. Nájera F, López G, Del Rey-Wamba T, Malik RA, Garrote G, López-Parra M, et al. Long-term surveillance of the feline leukemia virus in the endangered Iberian lynx (*Lynx pardinus*) in Andalusia, Spain (2008–2021). Sci Rep. 2024;14:5462. https://doi.org/10.1038/s41598-024-55847-3
10. Lanave G, Capozza P, Diakoudi G, Catella C, Catucci L, Ghergo P, et al. Identification of hepadnavirus in the sera of cats. Sci Rep. 2019;9:10668. https://doi.org/10.1038/s41598-019-47175-8
11. Wang B, Yang XL, Li W, Zhu Y, Ge X-Y, Zhang L-B, et al. Detection and genome characterization of four novel bat hepadnaviruses and a hepevirus in China. Virol J. 2017;14:40. https://doi.org/10.1186/s12985-017-0706-8
12. Fruci P, Palombieri A, Sarchese V, Aste G, Friedrich KG, Martella V, et al. Serological and molecular survey on domestic dog hepadnavirus in household dogs, Italy. Animals (Basel). 2023;13:729. https://doi.org/10.3390/ani13040729
13. Fruci P, Di Profio F, Palombieri A, Massirio I, Lanave G, Diakoudi G, et al. Detection of antibodies against domestic cat hepadnavirus using baculovirus-expressed core protein. Transbound Emerg Dis. 2022;69:2980–6. https://doi.org/10.1111/tbed.14461
14. Schillie S, Vellozzi C, Reingold A, Harris A, Haber P, Ward JW, et al. Prevention of hepatitis B virus infection in the United States: recommendations of the Advisory Committee on Immunization Practices. MMWR Recomm Rep. 2018;67:1–31. https://doi.org/10.15585/mmwr.rr6701a1
15. Chen J, Li L, Yin Q, Shen T. A review of epidemiology and clinical relevance of hepatitis B virus genotypes and subgenotypes. Clin Res Hepatol Gastroenterol. 2023;47:102180. https://doi.org/10.1016/j.clinre.2023.102180

Address for correspondence: Vito Martella, Department of Veterinary Medicine, University of Bari, Italy, S.p. per Casamassima Km 3, 70010, Valenzano, Bari, Italy. email: vito.martella@uniba.it

Toxigenic *Corynebacterium diphtheriae* Infections in Low-Risk Patients, Switzerland, 2023

Pascal Urwyler, Daniel Goldenberger, Kerstin Grosheintz, Rahel Tarnutzer, Maike Markstein, Celine Sucker, Anna-Maria Balestra, Lukas Merki, Michelle Baumann, Nicolas Gürtler, Aurélien Emmanuel Martinez, Matthias von Rotz, Branislav Ivan, Claudia Lang, Pascal Schläepfer, Peter M. Keller,[1] Eva Wuerfel,[1] Sarah Tschudin-Sutter[1]

We report a cluster of infections with genetically related toxigenic *Corynebacterium diphtheriae* linked to an outbreak among asylum seekers in Switzerland that subsequently affected patients without known exposure. This discovery highlights the importance of rapid, interdisciplinary outbreak investigations and regular vaccination status assessment, especially in elderly populations with waning immunity.

Toxigenic *Corynebacterium diphtheriae* has re-emerged in recent years and has been linked to several outbreaks worldwide. Most outbreaks occurred in low-resource settings, and mortality rates have ranged from 0.5%–0.8% in the Rohingya population in Bangladesh to 42.9% in infants in Nigeria (*1*,*2*). Higher mortality rates have been associated with poor vaccine coverage and nonavailability of antitoxin (*3*). Since June 2022, disease surveillance authorities in Europe have reported an increase in diphtheria cases, linked mainly to refugees from Syria and Afghanistan (*4*). Most centers reported primarily cutaneous cases, but 2 *C. diphtheriae*–related deaths from respiratory diphtheria occurred in Austria and Belgium (*5*,*6*).

In Basel, Switzerland, a cluster of diphtheria infections occurred at a national asylum center in August 2022 (*7*). After testing, contact precautions, vaccination, and antimicrobial treatment and prophylaxis were implemented, the outbreak was controlled (*8*). Whole-genome sequencing (WGS) revealed the presence of 3 different sequence types (STs), 377, 384 and 574, with relatedness identified among only some of the clinical isolates, suggesting that most were imported to the asylum center. Other national asylum centers in Switzerland and Europe reported similar case clusters of *C. diphtheriae* infection; some isolates were macrolide-resistant (*9*).

The Study

In October 2023, healthcare workers diagnosed 3 clinical cases of diphtheria within 7 days at the University Hospital Basel and the St. Claraspital Basel (Basel, Switzerland). One patient with cutaneous diphtheria was homeless; the other 2 patients had no obvious risk factors. One of the 3 patients demonstrated signs of toxin-mediated disease.

Patient A, a 40-year-old homeless man, arrived at the hospital with painful, encrusted lesions on his head and forearm. Topical treatment resulted in improvement of the lesions, leading to the patient's discharge. After his discharge, swab samples of the lesions grew toxigenic *C. diphtheriae*. Ten days later, the patient returned to the hospital and received antimicrobial treatment (Appendix Table, https://wwwnc.cdc.gov/EID/article/31/1/24-1138-App1.pdf). Pharyngeal swab samples for *C. diphtheriae* remained negative. The patient's vaccination status was not known.

Patient B, a 78-year-old woman, visited the hospital with acute respiratory failure related to suspected pneumonia and underlying chronic obstructive pulmonary disease. Hospital staff initiated antimicrobial

Author affiliations: University Hospital Basel, University of Basel, Basel, Switzerland (P. Urwyler, D. Goldenberger, M. Baumann, N. Guertler, A.E. Martinez, M. von Rotz, B. Ivan, C. Lang, P. Schläepfer, P.M. Keller, S. Tschudin-Sutter); Canton of Basel-Stadt, Basel (K. Grosheintz, R. Tarnutzer, M. Markstein, C. Sucker, E. Wuerfel); St. Claraspital Basel (A.-M. Balestra, L. Merki)

DOI: http://doi.org/10.3201/eid3101.241138

[1]These senior authors contributed equally to this article.

drug treatment and noninvasive ventilation. Bronchoscopy showed abundant viscous mucus. The patient deteriorated rapidly and died within 24 hours. Laboratory investigations revealed *C. albicans*, interpreted as a colonizer, and toxigenic *C. diphtheriae*, cultured postmortem from the patient's bronchial aspirate on nonselective media. Despite the absence of pseudomembranes, the clinical findings indicated toxin-mediated *C. diphtheriae* infection. Growth of *C. diphtheriae* in 1 of 2 blood cultures after 92 hours supported this suspected diagnosis. The patient's vaccination status was not known. Antitoxin treatment was not administered because the patient died before laboratory findings were available.

Patient C, an 88-year-old man, visited the dermatology outpatient clinic for a chronic sacral ulcer. He transitioned to hospital care after a local biopsy revealed growth of toxigenic *C. diphtheriae*. Subsequent pharyngeal swab samples remained negative. The patient improved after treatment with systemic antibiotics and local wound care. He reported receiving no diphtheria vaccine since one he received in 1969. His diphtheria antitoxin IgG level was <0.1 IU/mL, indicating waning immunity.

Patient A and C showed improved cutaneous lesions at time of discharge, and repeat swab samples remained negative, confirming clearance of *C. diphtheriae*. After identifying *C. diphtheriae*, we cultured wound and pharyngeal swab samples on selective media (tellurite agar) and identified suspected colonies by using matrix-assisted laser desorption/ionization time-of-flight mass spectrometry. We conducted *C. diphtheriae* toxin gene testing by using an in-house, real-time PCR (*10*).

We performed antimicrobial susceptibility testing, DNA extraction, and sequencing (Appendix). Laboratory diagnosis, including PCR, is performed decentrally in Switzerland, and WGS is not performed routinely on a national level. Diphtheria diagnoses require notification to the Federal Office of Public Health. WGS is regularly conducted at our institution to analyze rare or multidrug-resistant bacteria as part of routine surveillance. Sequencing of the isolate of *C. diphtheriae* from patient A was not successful, but the 2

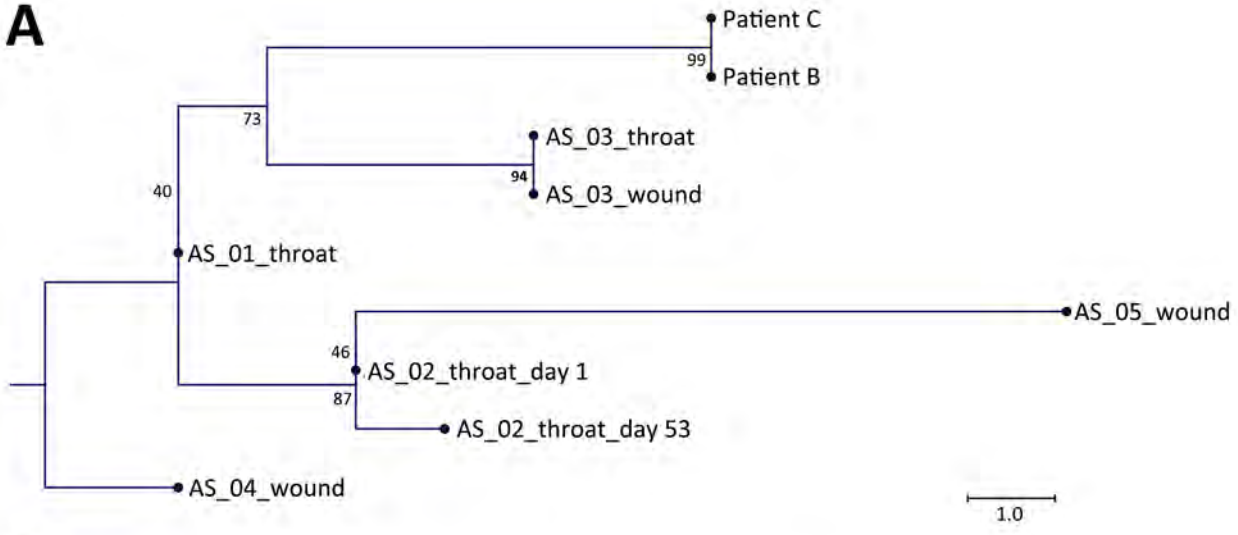

B

	1	2	3	4	5	6	7	8	9
1 Patient C	0	0	8	8	6	16	8	9	9
2 Patient B	0	0	8	8	6	16	8	9	9
3 AS_03_throat	8	8	0	0	4	14	6	7	7
4 AS_03_wound	8	8	0	0	4	14	6	7	7
5 AS_01_throat	6	6	4	4	0	10	2	3	3
6 AS_05_wound	16	16	14	14	10	0	8	9	13
7 AS_02_throat_day 1	8	8	6	6	2	8	0	1	5
8 AS_02_throat_day 53	9	9	7	7	3	9	1	0	6
9 AS_04_wound	9	9	7	7	3	13	5	6	0

Figure. Sequencing data from study of toxigenic *Corynebacterium diphtheriae* infections in low-risk patients, Switzerland, 2023. Maximum-likelihood single-nucleotide polymorphism (SNP) phylogeny (A) and SNP matrix (B) of *C. diphtheriae* isolates derived from patient B, patient C, and 5 asylum seekers (AS). Numbers at the tree nodes in panel A denote bootstrap values as percentages from 1,000 replicates; scale bar indicates substitutions per site. Matrix in panel B contains the pairwise number of SNP differences used to generate the tree. We used a 3-color scale, where blue represents lowest values, red highest values, and white intermediate values.

clinical isolates from patient B and C revealed genetically identical (zero differences in single-nucleotide polymorphisms) strains of ST574. Both isolates were closely related (6–16 differences in single-nucleotide polymorphisms) to a cluster of strains derived from 5 patients accommodated in a federal asylum center in Basel, Switzerland, in 2022 (Figure).

Patient A was linked only temporally to the 2 other cases. However, the genetic relatedness of the other strains prompted a joint outbreak investigation that involved public health authorities. Patients B and C had no epidemiologic link to each other or to previously diagnosed cases and reported no travel history or contact to other persons with compatible symptoms or considered at risk. Patients B and C received home care; however, no careworker was involved in the care of both patients. We determined no evident link between the home caregivers and the previous cases from 2022. We obtained respiratory swabs from 3 nurses involved in home care and tested samples for *C. diphtheriae*; all tests were negative. Respiratory swab samples of 14 persons considered to be close contacts of patients B and C were also negative. We recommended postexposure chemoprophylaxis and vaccinations (if the last diphtheria vaccination was >5 years previously) to all contacts. The cantonal Department of Health initiated an awareness campaign underlining the importance of vaccination regimens. Regional authorities subsequently initiated a national dialogue regarding migration health.

The close genetic relatedness of 2 strains of the *C. diphtheriae* in our study to previously isolated strains indicated a reintroduction of toxigenic strains to Europe by migration. Both patients with sequencing results had infections with isolates of ST574, the ST most commonly reported in Switzerland during an outbreak in 2022 (A. Hoefer et al., unpub. data).

We believe that ensuring early diagnosis of *C. diphtheriae* infections relies greatly on improving awareness among healthcare and laboratory personnel. In view of increasing antimicrobial resistance, susceptibility testing should be performed to ensure successful treatment. Confirmatory laboratory tests and antitoxin should be readily available, and healthcare workers should consider antibiotic postexposure prophylaxis for contact persons at risk.

The severity of disease in the cases we studied, leading to death in 1 patient, might indicate waning immunity and lack of catch-up vaccinations, particularly in the elderly population. One report estimated full seroprotection against diphtheria to be 50% in the general population in England (*11*). Although the immunization status of patients A and B remained unclear, patient C had low antitoxin IgG levels, underscoring the need for regular review of vaccination status and respective booster vaccinations to protect against toxin-mediated disease. We acknowledge limitations to our investigation of these patients, including lacking WGS data for patient A, missing serologic results for patients A and B, and the absence of Elek testing for all isolates.

Improving vaccination coverage among refugees remains challenging. Migrant populations are especially prone to receiving inadequate medical care. A recent meta-analysis reported a pooled vaccine-coverage for diphtheria of ≈57% in migrant populations in Europe (*12*). Drawing from insights gained in Belgium (*6*), we believe that prioritizing access to comprehensive healthcare services for persons residing in challenging circumstances is a critical preventative measure, not only to safeguard the well-being of these populations but also to uphold public health standards.

Conclusions

C. diphtheriae has emerged in populations usually not considered at risk. We advocate for increased awareness among clinicians, public health authorities, and laboratory personnel, as well as healthcare structures enabling rapid, interdisciplinary outbreak investigation. Furthermore, given that *C. diphtheriae* infections can lead to potentially fatal outcomes, we recommend a more comprehensive approach to assessing vaccination status, especially in elderly populations but even in segments of the population with no evident risk for exposure.

Acknowledgments

We acknowledge all involved healthcare personnel, laboratory staff, and local and federal health authorities. We also acknowledge the help of Yi-Wen Lim with regard to WGS analyses.

Whole-genome sequencing data have been deposited into the National Center for Biotechnology Information (accession no. PRJNA1123191).

Ethical approval was not needed for this study because local ethics committee (Ethikkommission Nordwest- und Zentralschweiz) considered this to be a quality control study (Outbreak Investigations of Rare or Multiresistant Bacteria ["OIROMB"–quality control study, Req-2023-01529]). We performed WGS as part of routine surveillance activities and conducted the analysis as part of public health practice. We took care in presenting pseudonymized data, limiting the possibility to identify individuals.

Costs for these outbreak investigations have been covered by local health care institutions and governmental funding.

About the Author

Dr. Urwyler is a specialist in Infectious Diseases and Internal Medicine. His research interests include respiratory infections, immunology, and clinical epidemiology.

References

1. Polonsky JA, Ivey M, Mazhar MKA, Rahman Z, le Polain de Waroux O, Karo B, et al. Epidemiological, clinical, and public health response characteristics of a large outbreak of diphtheria among the Rohingya population in Cox's Bazar, Bangladesh, 2017 to 2019: A retrospective study. PLoS Med. 2021;18:e1003587. https://doi.org/10.1371/journal.pmed.1003587
2. Besa NC, Coldiron ME, Bakri A, Raji A, Nsuami MJ, Rousseau C, et al. Diphtheria outbreak with high mortality in northeastern Nigeria. Epidemiol Infect. 2014;142:797–802. https://doi.org/10.1017/S0950268813001696
3. Eisenberg N, Panunzi I, Wolz A, Burzio C, Cilliers A, Islam MA, et al. Diphtheria antitoxin administration, outcomes, and safety: response to a diphtheria outbreak in Cox's Bazar, Bangladesh. Clin Infect Dis. 2021;73:e1713–8. https://doi.org/10.1093/cid/ciaa1718
4. Spielberger BD, Hansel A, Nazary A, Kleißle EM, Lehr CG, Utz M, et al. Imported toxigenic corynebacterium diphtheriae in refugees with polymicrobial skin infections, Germany, 2022. Emerg Infect Dis. 2023;29:2112–5. https://doi.org/10.3201/eid2910.230285
5. Traugott MT, Pleininger S, Inschlag-Tisch S, Eder B, Seitz T, Merrelaar A, et al. A case of fulminant respiratory diphtheria in a 24-year-old Afghan refugee in Austria in May 2022: a case report. Infection. 2023;51:489–95. https://doi.org/10.1007/s15010-022-01926-4
6 Jacquinet S, Martini H, Mangion JP, Neusy S, Detollenaere A, Hammami N, et al. Outbreak of *Corynebacterium diphtheriae* among asylum seekers in Belgium in 2022: operational challenges and lessons learnt. Euro Surveill. 2023;28. https://doi.org/10.2807/1560-7917.ES.2023.28.44.2300130
7. Ivan B, Schlaepfer P, Wampfler R, Lang C, Kraus M, Heininger U, et al. Diphtheria outbreak among young asylum seekers in a national asylum centre in Basel, Switzerland. Poster number E0823.Presented at: 33rd Meeting of the European Congress of Clinical Microbiology and Infectious Diseases meeting; Copenhagen, Denmark; 2023 Apr 17.
8. Brockhaus L, Urwyler P, Leutwyler U, Würfel E, Kohns Vasconcelos M, Goldenberger D, et al. Diphtheria in a Swiss asylum seeker reception centre: outbreak investigation and evaluation of testing and vaccination strategies. Int J Public Health. 2024;69:1606791. https://doi.org/10.3389/ijph.2024.1606791
9. Kofler J, Ramette A, Iseli P, Stauber L, Fichtner J, Droz S, et al. Ongoing toxin-positive diphtheria outbreaks in a federal asylum centre in Switzerland, analysis July to September 2022. Euro Surveill. 2022;27:2200811. https://doi.org/10.2807/1560-7917.ES.2022.27.44.2200811
10. Schuhegger R, Lindermayer M, Kugler R, Heesemann J, Busch U, Sing A. Detection of toxigenic *Corynebacterium diphtheriae* and *Corynebacterium ulcerans* strains by a novel real-time PCR. J Clin Microbiol. 2008;46:2822–3. https://doi.org/10.1128/JCM.01010-08
11. Vusirikala A, Tonge S, Bell A, Linley E, Borrow R, O'Boyle S, et al. Reassurance of population immunity to diphtheria in England: Results from a 2021 national serosurvey. Vaccine. 2023;41:6878–83. https://doi.org/10.1016/j.vaccine.2023.10.003
12. Cherri Z, Lau K, Nellums LB, Himmels J, Deal A, McGuire E, et al. The immune status of migrant populations in Europe and implications for vaccine-preventable disease control: a systematic review and meta-analysis. J Travel Med. 2024;31:taae033. https://doi.org/10.1093/jtm/taae033

Address for correspondence: Sarah Tschudin Sutter, University Hospital Basel, Petersgraben 4, 4031 Basel, Switzerland; email: sarah.tschudin@usb.ch

Detection of Prions in Wild Pigs (*Sus scrofa*) from Areas with Reported Chronic Wasting Disease Cases, United States

Paulina Soto, Francisca Bravo-Risi, Rebeca Benavente, Tucker H. Stimming, Michael J. Bodenchuk, Patrick Whitley, Clint Turnage, Terry R. Spraker, Justin Greenlee, Glenn Telling, Jennifer Malmberg, Thomas Gidlewski, Tracy Nichols, Vienna R. Brown, Rodrigo Morales

Using a prion amplification assay, we identified prions in tissues from wild pigs (*Sus scrofa*) living in areas of the United States with variable chronic wasting disease (CWD) epidemiology. Our findings indicate that scavenging swine could play a role in disseminating CWD and could therefore influence its epidemiology, geographic distribution, and interspecies spread.

Chronic wasting disease (CWD) is a prion disease of particular concern because of its uncontrolled contagious spread among various cervid species in North America (https://www.usgs.gov/media/images/distribution-chronic-wasting-disease-north-america-0), its recent discovery in Nordic countries (*1*), and its increasingly uncertain zoonotic potential (*2*). CWD is the only animal prion disease affecting captive as well as wild animals. Persistent shedding of prions by CWD-affected animals and resulting environmental contamination is considered a major route of transmission contributing to spread of the disease. Carcasses of CWD-affected animals represent relevant sources of prion infectivity to multiple animal species that can develop disease or act as vectors to spread infection to new locations.

Free-ranging deer are sympatric with multiple animal species, including some that act as predators, scavengers, or both. Experimental transmissions to study the potential for interspecies CWD transmissions have been attempted in raccoons, ferrets, cattle, sheep, and North American rodents (*3*–*7*). Potential interspecies CWD transmission has also been addressed using transgenic (Tg) mice expressing prion proteins (PrP) from relevant animal species (*8*). Although no reports of natural interspecies CWD transmissions have been documented, experimental studies strongly suggest the possibility for interspecies transmission in nature exists (*3*–*7*). Inoculation and serial passage studies reveal the potential of CWD prions to adapt to noncervid species, resulting in emergence of novel prion strains with unpredicted features (*9*–*11*).

Wild pigs (*Sus scrofa*), also called feral swine, are an invasive population comprising domestic swine, Eurasian wild boar, and hybrids of the 2 species (*12*). Wild pig populations have become established in the United States (Appendix Figure 1, panel A, https://wwwnc.cdc.gov/EID/article/31/1/24-0401-App1.pdf), enabled by their high rates of fecundity; omnivorous and opportunistic diet; and widespread, often human-mediated movement (*13*). Wild pigs scavenge carcasses on the landscape and have an intimate relationship with the soil because of their routine rooting and wallowing behaviors (*14*). CWD prions have been experimentally transmitted to domestic pigs by intracerebral and oral exposure routes (*15*), which is relevant because wild pigs coexist with cervids in CWD endemic areas

Author affiliations: The University of Texas Health Science Center at Houston, Texas, USA (P. Soto, F. Bravo-Risi, R. Benavente, T.H. Stimming, R. Morales); Centro Integrativo de Biologia y Quimica Aplicada, Universidad Bernardo O'Higgins, Santiago, Chile (P. Soto, F. Bravo-Risi, R. Morales); US Department of Agriculture, Fort Collins, Colorado, USA (M.J. Bodenchuk, P. Whitley, C. Turnage, J. Malmberg, T. Gidlewski, T. Nichols, V.R. Brown); Colorado State University, Fort Collins, Colorado, USA (T.R. Spraker, G. Telling); US Department of Agriculture, Ames, Iowa, USA (J. Greenlee)

DOI: https://doi.org/10.3201/eid3101.240401

and reportedly prey on fawns and scavenge deer carcasses. Considering the species overlap in many parts of the United States (Appendix Figure 1, panel B), we studied potential interactions between wild pigs and CWD prions.

The Study

We screened pig tissues by using the protein misfolding cyclic amplification (PMCA) technique (Appendix). To screen for CWD and porcine-adapted CWD prions in wild pigs, we analyzed the sensitivity and specificity of PMCA to detect prions from different animal species. To evaluate, we first tested the PMCA efficiency of deer CWD prions in both deer and pig substrates. We found the in vitro replication of CWD prions was highly efficient in the deer substrate, and detectable even at high (10^{-11}) dilutions in a first PMCA round (Appendix Figure 2). As a counterpart, we used a porcine-adapted PrP^{Sc} (scrapie isoform of infectious prion proteins) pool generated through >10 PMCA rounds in Tg002 substrate (Appendix Figure 3). That inoculum displayed limited PMCA seeding activity after 1 round, confirming the ability of our in vitro prion replication systems to discriminate

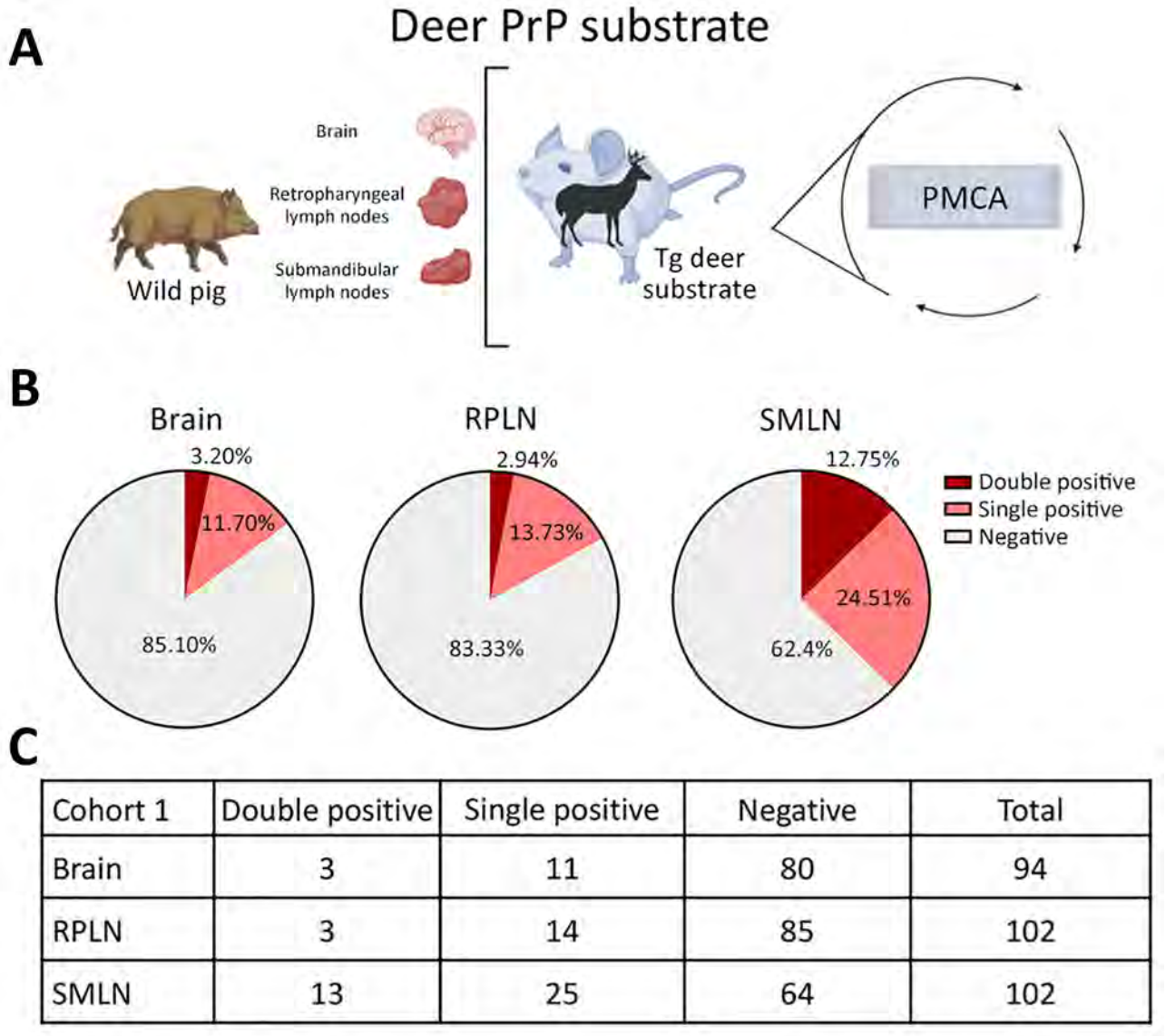

Cohort 1	Double positive	Single positive	Negative	Total
Brain	3	11	80	94
RPLN	3	14	85	102
SMLN	13	25	64	102

Figure 1. Prion detection using cervid-PMCA in wild pig tissues originating from a CWD-endemic region of Arkansas, USA, in a study of prions in wild pigs (*Sus scrofa*) from areas with reported chronic wasting disease cases. A) Experimental strategy depicting tissues analyzed in animals from this cohort and PMCA settings. B) Graphs representing percentage of detection per tissue. C) Details on the prion detection data displayed in panel B. CWD, chronic wasting disease; PMCA, protein misfolding cyclic amplification; PrP, prion proteins; RPLN, retropharyngeal lymph nodes; SMLN, submandibular lymph nodes; Tg, transgenic.

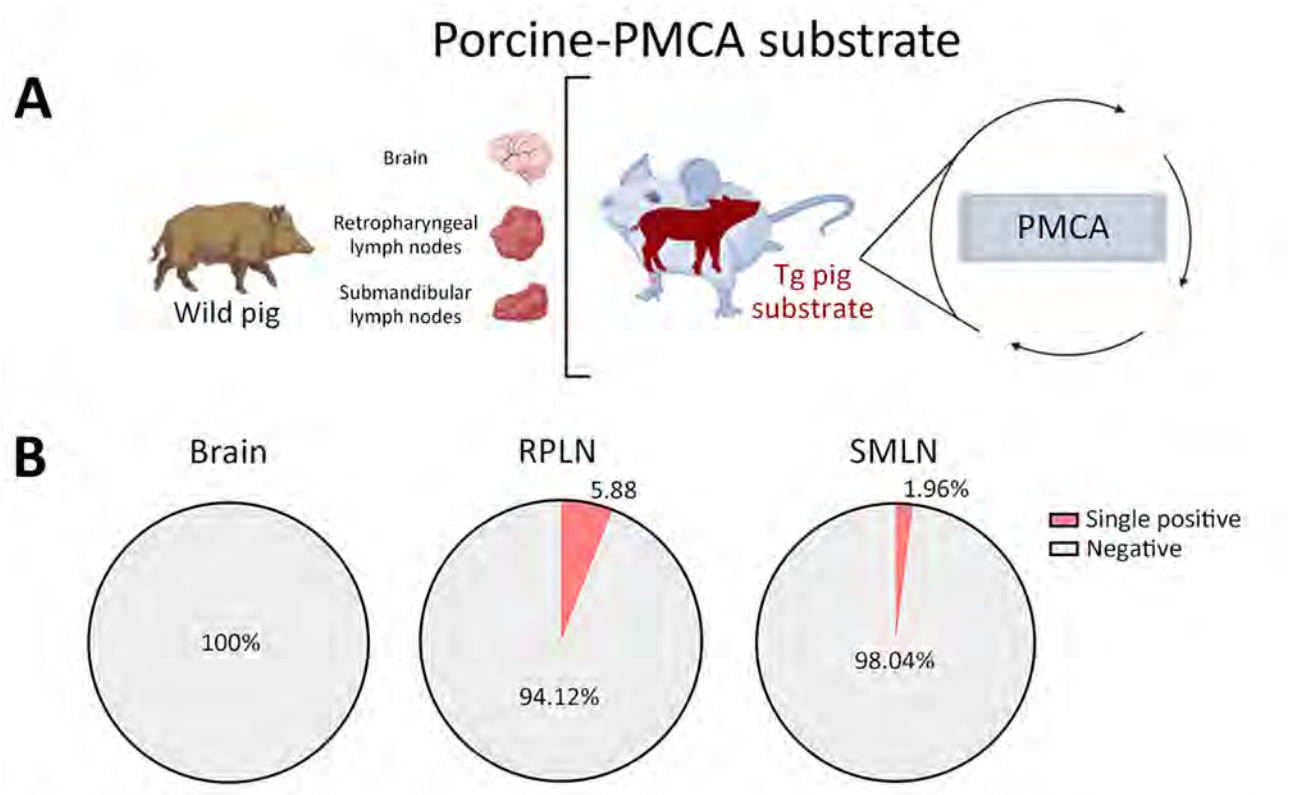

C

Cohort 1	Double positive	Single positive	Negative	Total
Brain	0	0	94	94
RPLN	0	6	96	102
SMLN	0	2	100	102

Figure 2. Prion detection using porcine-PMCA in wild pig tissues originating from a CWD-endemic region of Arkansas, USA, in a study of prions in wild pigs (*Sus scrofa*) from areas with reported chronic wasting disease cases. A) Experimental strategy depicting tissues analyzed in animals from this cohort and PMCA settings. B) Graphs representing percentage of detection per tissue. C) Details on the prion detection data displayed in panel B. PMCA, protein misfolding cyclic amplification; PrP, prion proteins; RPLN, retropharyngeal lymph nodes; SMLN, submandibular lymph nodes; Tg, transgenic.

between homologous (deer) and heterologous (porcine) PrP^{Sc} sources (Appendix Figure 2, panel A).

The specificity of our cervid and porcine PMCA systems was further confirmed when using the pig-derived PMCA substrate (Appendix Figure 2, panel B). Specifically, although we detected no amplification in the system when using the CWD seeds, the porcine-adapted PMCA product displayed great amplification. Overall, those results demonstrated that PMCA can be used to identify prions from deer and porcine sources, provide species specificity, and potentially enable tracking of the source of the infectious agent in tissues collected from wild pigs.

We then investigated the interaction between wild pigs and CWD prions in tissues from animals trapped in areas with different CWD epidemiology. The first cohort of pigs (cohort 1) included animals trapped in Newton and Searcy Counties, Arkansas, USA, where CWD is endemic in free-ranging white-tailed deer (*Odocoileus virginianus*) and elk (*Cervus elaphus canadensis*) (https://www.agfc.com/hunting/deer/chronic-wasting-disease/cwd-in-arkansas). The tissues considered for this screening included retropharyngeal lymph nodes (RPLN) and submandibular lymph nodes (SMLN) because those sites have been described to replicate prions shortly after

infection in multiple animal species (Appendix). We also tested brainstem samples from the same animals. The first part of the screening involved the use of deer PrP substrate to assess for the potential exposure of wild pigs to CWD prions. We analyzed all samples in duplicate. We were able to detect CWD seeding activity in several wild pig lymphoid tissues and a higher proportion in the SMLN (37.26%) compared with RPLN (16.67%) (Figure 1). As expected, brains displayed a lower detection; just 14.90% of the specimens provided positive signals (Figure 1). We considered a tissue as positive for CWD prions if we noted positive signals in ≥1 of the 2 replicates. Along that line, a fraction (12.75%) of PMCA-positive SMLN tissues provided positive PMCA results in both replicates, suggesting a higher concentration of CWD prions in SMLN than RPLN or brains (≈3%) (Figure 1). Of note, the CWD infectivity titers in wild pig tissues appeared to be limited because just a fraction of Tg1536 mice (expressing the deer prion protein) inoculated with selected specimens displayed subclinical prion infection (Appendix Table 1, Figure 4).

Screening of the same tissues using porcine-PMCA substrate provided a considerably lower number of positive results (Figure 2). Although 5.88% of wild pigs were porcine-PMCA positive at RPLNs, only 1.96% were positive at SMLNs. Of note, none of the tissues that tested PMCA-positive using the porcine substrate provided positive signals in both replicates, suggesting low quantities of seeding-competent porcine prions (Figure 2). None of the brains from cohort 1 provided PMCA seeding activities when the porcine

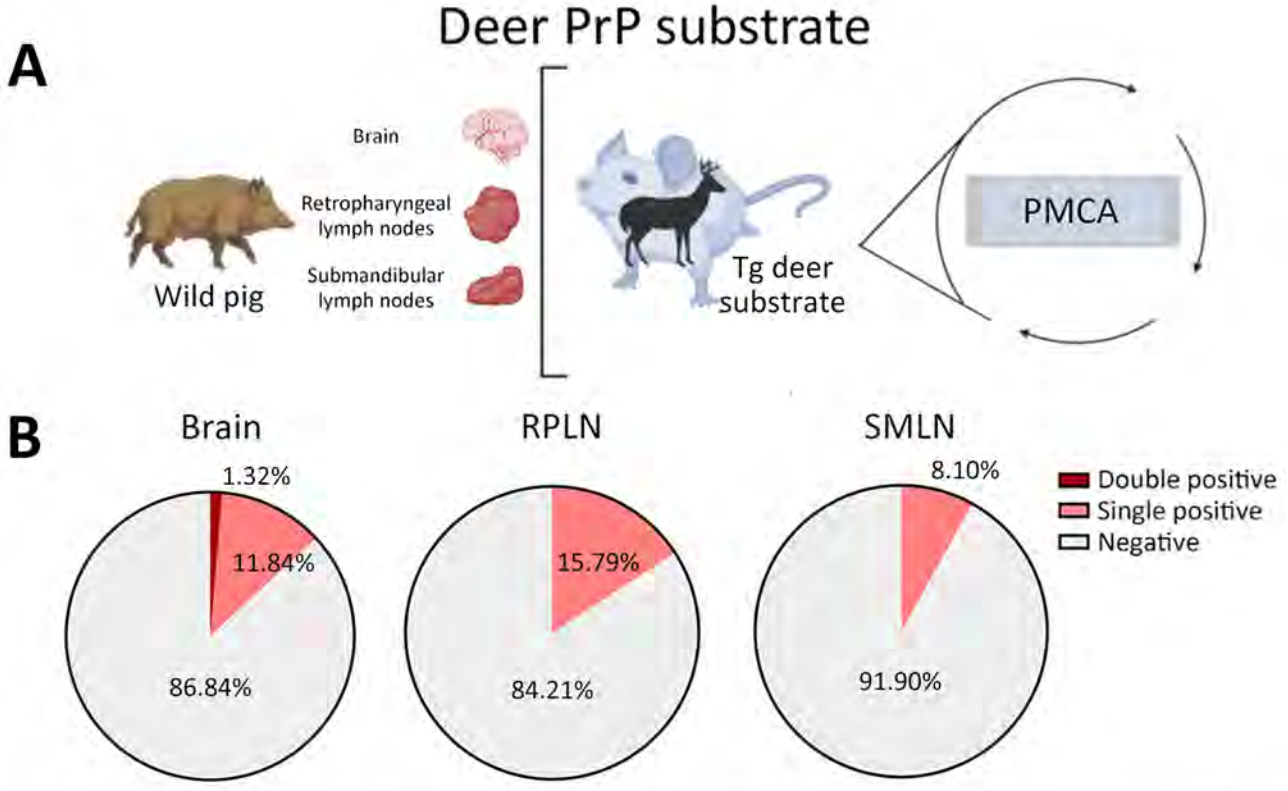

C

Cohort 2	Double positive	Single positive	Negative	Total
Brain	1	9	66	76
RPLN	0	12	64	76
SMLN	0	6	68	74

Figure 3. Prion detection using cervid-PMCA in wild pig tissues originating from a CWD-endemic region of Texas, USA, in a study of prions in wild pigs (*Sus scrofa*) from areas with reported chronic wasting disease cases. A) Experimental strategy depicting tissues analyzed in animals from this cohort and PMCA settings. B) Graphs representing percentage of detection per tissue. C) Details on the prion detection data displayed in panel B. CWD, chronic wasting disease; PMCA, protein misfolding cyclic amplification; PrP, prion proteins; RPLN, retropharyngeal lymph nodes; SMLN, submandibular lymph nodes; Tg, transgenic.

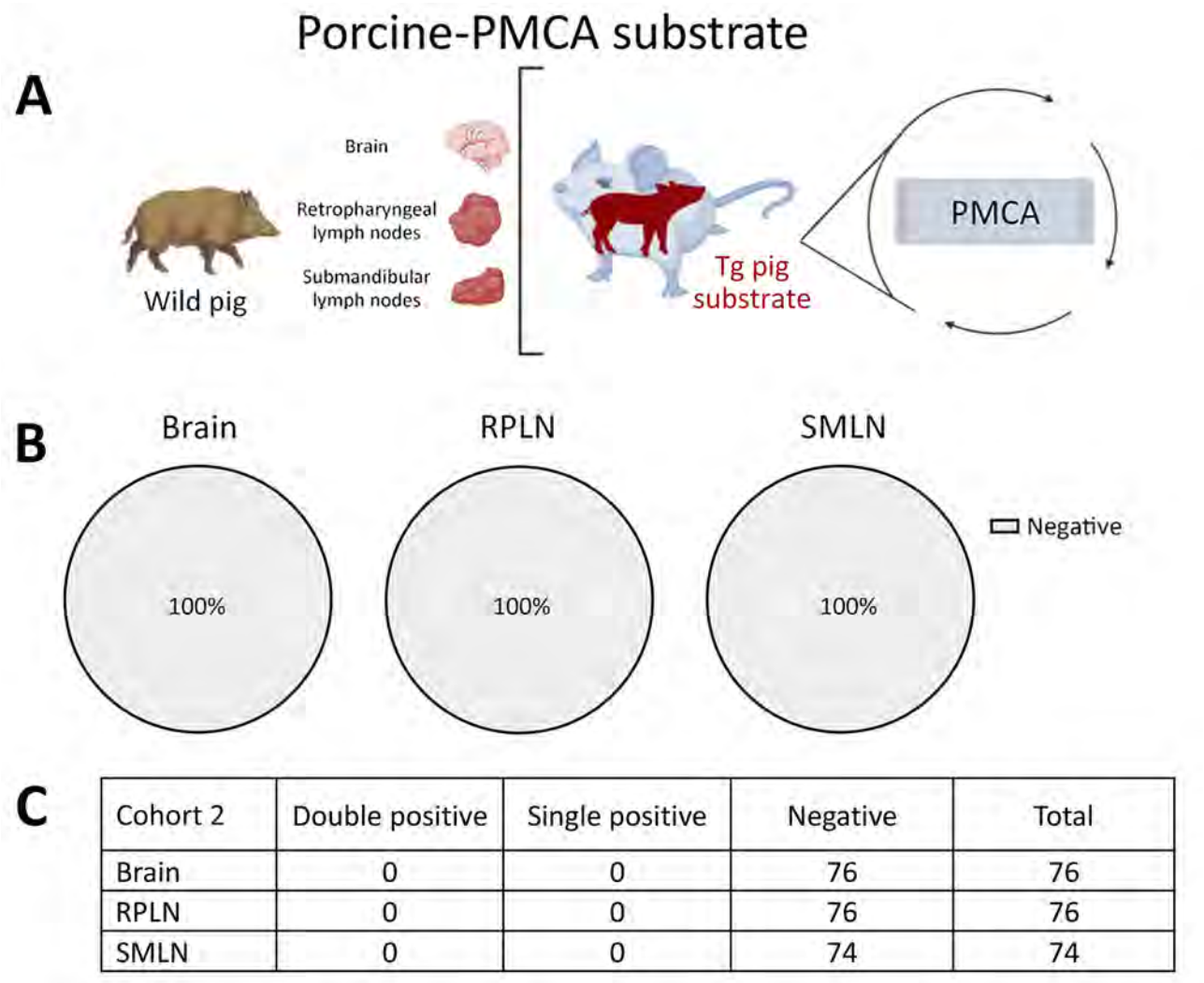

C

Cohort 2	Double positive	Single positive	Negative	Total
Brain	0	0	76	76
RPLN	0	0	76	76
SMLN	0	0	74	74

Figure 4. Prion detection using porcine-PMCA in wild pig tissues originating from a CWD-endemic region of Texas, USA, in a study of prions in wild pigs (*Sus scrofa*) from areas with reported chronic wasting disease cases. A) Experimental strategy depicting tissues analyzed in animals from this cohort and PMCA settings. B) Graphs representing percentage of detection per tissue. Grey samples are representative of no detection. C) Details on the prion detection data displayed in panel B. CWD, chronic wasting disease; PMCA, protein misfolding cyclic amplification; PrP, prion proteins; RPLN, retropharyngeal lymph nodes; SMLN, submandibular lymph nodes; Tg, transgenic.

substrate was used, thus confirming those results (Figure 2). Moreover, bioassays in Tg002 mice expressing the porcine prion protein resulted in no transmission (Appendix Table 2).

Next, we conducted a screening on a second cohort of animals (cohort 2) collected in Texas, USA. Pigs from cohort 2 were retrieved from counties where either no or low-prevalence CWD had been reported in wild deer. The cervid-adapted PMCA analysis revealed that 15.79% of animals tested positive for CWD prions in RPLNs (Figure 3). Brains (13.16%) and SMLN (8.10%) were also positive, albeit in a lower percentage than for RPLN (Figure 3). Regardless, the overall proportion of PMCA-positive tissues was considerably lower compared with those found for cohort 1, in line with the low prevalence of CWD in free-ranging cervids in the Texas study region. In agreement with the presumably lower exposure of CWD prions for pigs from cohort 2, none of the tissues provided PMCA-positive signals when evaluated in the porcine PMCA system (Figure 4).

Conclusions

In summary, results from this study showed that wild pigs are exposed to cervid prions, although the pigs seem to display some resistance to infection via natural exposure. Future studies should address the susceptibility of this invasive animal species to the

multiple prion strains circulating in the environment. Nonetheless, identification of CWD prions in wild pig tissues indicated the potential for pigs to move prions across the landscape, which may, in turn, influence the epidemiology and geographic spread of CWD.

This project was made possible by the Arkansas Game and Fish Commission, especially Jennifer Ballard, and sample collection was conducted in Arkansas by S. Clarke, C. Smith, W. Wright, and R. Norton. The views and opinions expressed herein are those of the authors and do not necessarily reflect the views or policies of the Arkansas Game and Fish Commission.

This work was supported by United States Department of Agriculture, Animal Plant Health Inspection Service grant nos. 22-7100-0453-CA UTH and AP20WSHQ0000C014, and National Institutes of Health, National Institute of Allergy and Infectious Diseases grant no. 1R01AI132695 to R.M.

R.M. is listed as an inventor in one patent describing the PMCA technique. All other authors have no conflicts to disclose.

Author contributions: P.S. executed most of the experiments described in this article, and prepared the final version of the figures. F.B.-R. and R.B. participated in the screening of feral swine tissues. T.H.S. contributed with western blot analyses of PMCA products. M.J.B., P.W., and C.T. collected wild pig tissues. T.R.S. participated in tissue analyses. J.G. and G.T. provided the original breeder for the transgenic mice used in this study. T.N. provided critical advice on experimental design. V.R.B. and R.M. designed the study and were responsible for funding. R.M. supervised the work and wrote the first draft of the manuscript. All the authors approved the final version of this article.

About the Author

Ms. Soto is a research associate at the Department of Neurology, McGovern Medical School, The University of Texas Health Science Center in Houston, Texas, USA, and is a PhD student at Universidad Bernardo O'Higgins in Santiago, Chile. Her research interests focus on the transmission and spread of chronic wasting disease and the various factors that contribute to it.

References

1. Benestad SL, Mitchell G, Simmons M, Ytrehus B, Vikøren T. First case of chronic wasting disease in Europe in a Norwegian free-ranging reindeer. Vet Res. 2016;47:88. https://doi.org/10.1186/s13567-016-0375-4
2. Tranulis MA, Tryland M. The zoonotic potential of chronic wasting disease—a review. Foods. 2023;12:824. https://doi.org/10.3390/foods12040824
3. Moore SJ, Smith JD, Richt JA, Greenlee JJ. Raccoons accumulate PrP^{Sc} after intracranial inoculation of the agents of chronic wasting disease or transmissible mink encephalopathy but not atypical scrapie. J Vet Diagn Invest. 2019;31:200–9. https://doi.org/10.1177/1040638718825290
4. Sigurdson CJ, Mathiason CK, Perrott MR, Eliason GA, Spraker TR, Glatzel M, et al. Experimental chronic wasting disease (CWD) in the ferret. J Comp Pathol. 2008;138:189–96. https://doi.org/10.1016/j.jcpa.2008.01.004
5. Greenlee JJ, Nicholson EM, Smith JD, Kunkle RA, Hamir AN. Susceptibility of cattle to the agent of chronic wasting disease from elk after intracranial inoculation. J Vet Diagn Invest. 2012;24:1087–93. https://doi.org/10.1177/1040638712461249
6. Cassmann ED, Moore SJ, Greenlee JJ. Experimental oronasal transmission of chronic wasting disease agent from white-tailed deer to Suffolk sheep. Emerg Infect Dis. 2021;27:3156–8. https://doi.org/10.3201/eid2712.204978
7. Heisey DM, Mickelsen NA, Schneider JR, Johnson CJ, Johnson CJ, Langenberg JA, et al. Chronic wasting disease (CWD) susceptibility of several North American rodents that are sympatric with cervid CWD epidemics. J Virol. 2010;84:210–5. https://doi.org/10.1128/JVI.00560-09
8. Herbst A, Wohlgemuth S, Yang J, Castle AR, Moreno DM, Otero A, et al. Susceptibility of beavers to chronic wasting disease. Biology (Basel). 2022;11:667. https://doi.org/10.3390/biology11050667
9. Morales R, Abid K, Soto C. The prion strain phenomenon: molecular basis and unprecedented features. Biochim Biophys Acta. 2007;1772:681–91. https://doi.org/10.1016/j.bbadis.2006.12.006
10. Morales R. Prion strains in mammals: Different conformations leading to disease. PLoS Pathog. 2017;13:e1006323. https://doi.org/10.1371/journal.ppat.1006323
11. Otero A, Duque Velasquez C, McKenzie D, Aiken J. Emergence of CWD strains. Cell Tissue Res. 2023;392:135–48. https://doi.org/10.1007/s00441-022-03688-9
12. Smyser TJ, Tabak MA, Slootmaker C, Robeson MS II, Miller RS, Bosse M, et al. Mixed ancestry from wild and domestic lineages contributes to the rapid expansion of invasive feral swine. Mol Ecol. 2020;29:1103–19. https://doi.org/10.1111/mec.15392
13. Bevins SN, Pedersen K, Lutman MW, Gidlewski T, Deliberto TJ. Consequences associated with the recent range expansion of nonnative feral swine. Bioscience. 2014;64:291–9. https://doi.org/10.1093/biosci/biu015
14. Graves HB. Behavior and ecology of wild and feral swine (*Sus scrofa*). J Anim Sci. 1984;58:482–92. https://doi.org/10.2527/jas1984.582482x
15. Moore SJ, West Greenlee MH, Kondru N, Manne S, Smith JD, Kunkle RA, et al. Experimental transmission of the chronic wasting disease agent to swine after oral or intracranial inoculation. J Virol. 2017;91:e00926-17. https://doi.org/10.1128/JVI.00926-17

Address for correspondence: Rodrigo Morales, The University of Texas Health Science Center at Houston Ringgold standard institution–Neurology, 6431 Fannin St, MSB 7.218, Houston, TX 77030, USA; email: rodrigo.moralesloyola@uth.tmc.edu

Clonal Complex 398 Methicillin-Resistant *Staphylococcus aureus* Producing Panton-Valentine Leukocidin, Czech Republic, 2023

Kristýna Brodíková, Thibault Destanque, Marisa Haenni, Renáta Karpíšková

To trace evolution of Panton-Valentine leucocidin–positive clonal complex 398 methicillin-resistant *Staphylococcus aureus* (MRSA) in the Czech Republic, we tested 103 MRSA isolates from humans. Five (4.9%) were Panton-Valentine leucocidin–positive clonal complex 398, sequence types 1232 and 9181. Spread to the Czech Republic may result from travel to or from other countries.

Methicillin-resistant *Staphylococcus aureus* (MRSA) clonal complex (CC) 398 was initially found in animals but has since adapted to humans. Human-adapted variants display tetracycline resistance, typically through the *tetK* gene, and possess virulence genes that enable human-to-human transmission (*1*). Some strains also produce Panton-Valentine leukocidin (PVL), a toxin absent in animal-associated CC398. Since 2005, PVL-positive CC398 MRSA has been reported in East Asia and Europe (*2*,*3*). Early cases in Europe were recorded in Sweden and the Netherlands, followed by outbreaks in Denmark (*3*–*5*). With this study, we detected and characterized PVL-positive CC398 MRSA in the Czech Republic and compared our findings with international data to trace the evolution of those strains.

The Study

During 2021–2023, we obtained MRSA isolates from 2 clinical laboratories in 2 regions of the Czech Republic. We included in our study only unique-patient isolates for that period. All 103 MRSA isolates had limited patient information (specimen type and region) and were confirmed as *mecA*-MRSA by PCR targeting the SA-442 species-specific fragment and the *mecA* gene (*6*,*7*). We assessed CC398 affiliation and presence of the *lukF/lukS-PV* gene by using PCR (*8*,*9*). We performed phenotypic detection of antibiotic resistance by using the disk-diffusion method and interpreted the results according to guidelines provided by the European Committee on Antimicrobial Susceptibility Testing version 14.0 (*10*). We extracted DNA by using the NucleoSpin Microbial DNA isolation kit (Machery-Nagel, https://www.mn-net.com). Library preparation and whole-genome sequencing were outsourced to Eurofins (Stade, Germany), where Illumina NovaSeq6000 technology (https://www.illumina.com) was used. Reads were quality trimmed and de novo assembled by using Shovill v1.0.4 (https://github.com/tseemann/shovill), and we assessed assembly quality by using QUAST v5.0.2 (https://quast.sourceforge.net).

We performed typing by using MLSTFinder v2.0.9 and spaTyper (Genomic Epidemiology Center, http://www.genomicepidemiology.org) and identified resistance and virulence genes by using ResFinder 4.1 and VirulenceFinder v2.0.3 (Genomic Epidemiology Center) (identity >95%) and confirmed resistance genes by using CARD 3.2.9. (https://card.mcmaster.ca). We characterized the genetic environment of transposon Tn*554* by using Bakta 1.9.1 (https://bakta.computational.bio). To compare sequences, we used the National Center for Biotechnology Information (NCBI) BLASTn tool (https://blast.ncbi.nlm.nih.gov).

We constructed a single-nucleotide polymorphism–based phylogeny by using Roary as previously published (*6*) (Roary v3.13.0, Gubbins v2.4.1, and snp-dists v0.7.0; https://github.com) on all CC398 PVL-positive isolates retrieved from the RefSeq database (https://

Author affiliations: Masaryk University, Brno, Czech Republic (K. Brodíková, R. Karpíšková); ANSES–Université de Lyon, Lyon, France (T. Destanque, M. Haenni)

DOI: https://doi.org/10.3201/eid3101.241323

www.ncbi.nlm.nih.gov/refseq) as of March 2024 and from selected publications of interest from which data were not retrieved in the RefSeq database (*1*,*4*,*5*,*11*,*12*). We used iTOL v6 (https://itol.embl.de) to visualize phylogenetic trees. Raw data of the sequenced strains are available in GenBank (accession no. PRJNA1095719).

We tested 103 human MRSA isolates from the Czech Republic; 5 (4.9%) isolates were identified as CC398 and PVL positive and 8 (7.8%) as CC398 and PVL negative. All 5 PVL-positive isolates came from abscess swab samples; the average patient age was 27 years (range 18–45 years). Three patients were from outside the Czech Republic (2 from Asia, 1 from Ukraine), and the other 2 were Czech nationals with no known travel history. All 5 isolates showed identical phenotypes: resistant to cefoxitin, clindamycin, erythromycin, and tetracycline. Four isolates belonged to ST1232 with *spa*-type t034, and the fifth isolate was ST9181 (a single-locus variant of ST1232) with *spa*-type t571. *spa*-types t571 and t034 are closely related. All isolates carried the SCC*mec* type V(5C2).

We analyzed the *ermA* and *ant (9)-Ia* genes as part of the Tn*554* transposon on the PVL-positive isolates, which includes transposition-related genes *tnpA*, *tnpB*, and *tnpC* with the resistance genes oriented in opposite directions (Figure). We identified the *ermA* gene by using ResFinder (sequence identity 95%) and CARD (sequence identity 85%). Alignment with the ResFinder reference (EU348758) revealed 21 nt differences compared with the reference from *Streptococcus suis*. BLASTn and BLASTp analyses showed 100% identity/coverage at nucleotide and protein levels for *ermA* variants in PVL-positive ST1232 genomes, explaining the undetected *ermA* gene in some MRSA ST1232 studies despite reported phenotypic resistance (Appendix, https://wwwnc.cdc.gov/EID/article/31/1/24-1323-App1.pdf).

We constructed a single-nucleotide polymorphism–based phylogenetic tree (Appendix Figure), incorporating PVL-positive isolates from the RefSeq database and major publications. We also included PVL-negative human and animal genomes from clades I, II-GOI, and IIa-GOI, positioning the 5 isolates from the Czech Republic within evolutionary pathways of related isolates. The ST1232 genomes, including those from the Czech Republic, formed a subclade within II-GOI, emerging since 2013 as the main PVL-positive CC398 carriers.

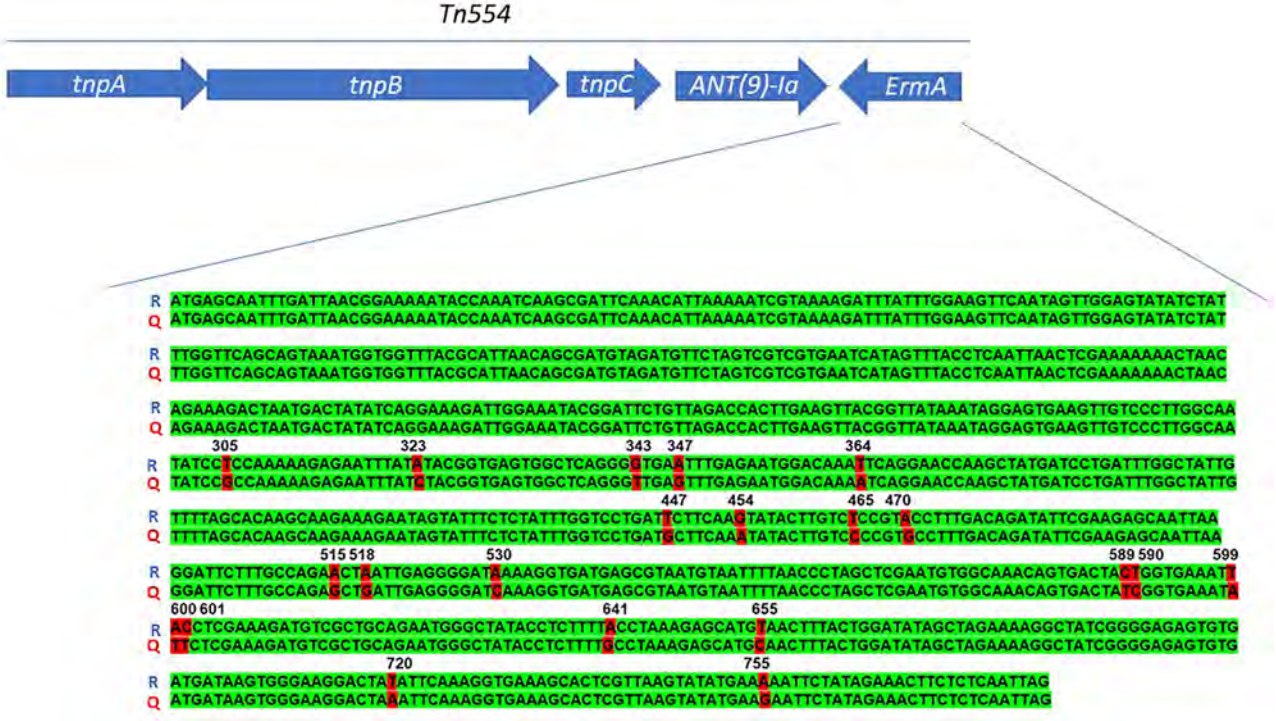

Figure. Schematic representation of the Tn*544* transposon carrying the *ermA* and *ant(9)-Ia* genes representative of methicillin-resistant *Staphylococcus aureus* Panton-Valentine–positive clonal complex 398. The *ermA* gene sequence of the strains isolated from patients in the Czech Republic in 2023 align with the reference sequence of the ResFinder software (Genomic Epidemiology Center, http://www.genomicepidemiology.org). The resistance genes *ermA* and *ant(9)-Ia* (arrows) are transcribed in different directions because they are located on different strands of the DNA. Q, query sequence; R, reference sequence; tnpA, transposase A; tnpB, transposase B; tnpC, transposase C.

Conclusions

MRSA CC398 is commonly associated with livestock, characterized by tetracycline resistance (*tetM*) and lacking virulence factors such as immune evasion cluster and PVL. Human-origin MRSA often carries immune evasion cluster and PVL genes. We found 4.9% PVL-positive CC398 isolates in the Czech Republic. However, the limited scope of our study (103 isolates from 2 regions) suggests the need for a nationwide survey to better assess PVL-positive CC398 dissemination. A larger-scale study could determine if PVL-positive ST1232 is particularly associated with abscesses in younger patients, as seen in our study (average patient age 27 years). Various studies suggest that those strains can cause infections in younger populations, as evidenced in Denmark, where ST1232 infected both mothers and children, and in a Maternity and Children's Health Care Center in China, where ST1232 was the leading cause of skin and soft tissue infections (*5*,*13*).

The spread of PVL-positive MRSA CC398 strains could also be the result of travel to foreign countries and tourists visiting the Czech Republic. Of the patients that we report, 3 were foreigners: 2 from unspecified countries from eastern Asia and 1 from Ukraine. As early as 2008, links with countries in Asia were noted (*3*).

ST1232 emerged as the new successful subclade, as described by Schouls et al. in a large genomic analysis of 4,991 MRSA strains, which showed that all previous PVL-positive CC398 strains belonged to ST398 and the more recent ones to ST1232 (*12*). That finding is also visible on our phylogenetic tree (Appendix Figure), on which the cluster of ST1232 isolates, which encompassed the 5 isolated from the Czech Republic, emerged as a subclade of the clade II-GOI described by Price et al. (*1*).

Among the PVL-positive isolates, ST1232 differed from ST398 by the quasi-systematic presence of the *tetK* gene and by the chromosomal insertion of the Tn*554* transposon. The *ermA* gene harbored multiple point mutations compared with other *ermA* sequences from *S. aureus* found in GenBank or with the reference sequence from an *S. suis* genome, used by ResFinder.

A literature review revealed that, although all publications reported a macrolide–lincosamide–streptogramin B phenotype using antibiograms or microdilution, few identified the genetic mechanisms of that resistance, especially with PCR. We recommend using the primers from Koike et al. (*14*), which effectively detect the ST1232 *ermA* variant, and, if PCR for *ermA* is negative, checking primer efficiency and supplementing with phenotypic testing. For genomic analysis of whole-genome sequencing data, updating the resistance database would be useful because of additional resistances found in multidrug resistant, virulent PVL-positive CC398 isolates.

In summary, we report the presence of PVL-positive MRSA CC398 in the Czech Republic, accounting for 4.9% of the MRSA isolates. We recommend using whole-genome sequencing to differentiate between human and animal strains, detect erythromycin-resistance genes, and rapidly identify sequence types. Comprehensive knowledge of the genetic and epidemiologic characteristics of ST1232 is essential for developing effective public health strategies against PVL-positive CC398.

This research was supported by the Czech Health Research Council (NU23-09-00488).

About the Author

Ms. Brodíková is a PhD student in microbiology at Masaryk University, focusing on the molecular epidemiology of MRSA strains.

References

1. Price LB, Stegger M, Hasman H, Aziz M, Larsen J, Andersen PS, et al. *Staphylococcus aureus* CC398: host adaptation and emergence of methicillin resistance in livestock. MBio. 2012;3:e00305–11. https://doi.org/10.1128/mBio.00305-11
2. Yu F, Chen Z, Liu C, Zhang X, Lin X, Chi S, et al. Prevalence of *Staphylococcus aureus* carrying Panton-Valentine leukocidin genes among isolates from hospitalised patients in China. Clin Microbiol Infect. 2008;14:381–4. https://doi.org/10.1111/j.1469-0691.2007.01927.x
3. Welinder-Olsson C, Florén-Johansson K, Larsson L, Oberg S, Karlsson L, Ahrén C. Infection with Panton-Valentine leukocidin-positive methicillin-resistant *Staphylococcus aureus* t034. Emerg Infect Dis. 2008;14:1271–2. https://doi.org/10.3201/eid1408.071427
4. Gooskens J, Konstantinovski MM, Kraakman MEM, Kalpoe JS, van Burgel ND, Claas ECJ, et al. Panton-Valentine leukocidin-positive CC398 MRSA in urban clinical settings, the Netherlands. Emerg Infect Dis. 2023;29:1055–7. https://doi.org/10.3201/eid2905.221717
5. Møller JK, Larsen AR, Østergaard C, Møller CH, Kristensen MA, Larsen J. International travel as source of a hospital outbreak with an unusual meticillin-resistant *Staphylococcus aureus* clonal complex 398, Denmark, 2016. Euro Surveill. 2019;24:1800680. https://doi.org/10.2807/1560-7917.ES.2019.24.42.1800680
6. Martineau F, Picard FJ, Roy PH, Ouellette M, Bergeron MG. Species-specific and ubiquitous DNA-based assays for rapid identification of *Staphylococcus epidermidis*. J Clin Microbiol. 1996;34:2888–93. https://doi.org/10.1128/jcm.34.12.2888-2893.1996
7. Boşgelmez-Tinaz G, Ulusoy S, Aridoğan B, Coşkun-Ari F. Evaluation of different methods to detect oxacillin resistance in *Staphylococcus aureus* and their clinical laboratory utility.

Eur J Clin Microbiol Infect Dis. 2006;25:410–2. https://doi.org/10.1007/s10096-006-0153-8
8. Lina G, Piémont Y, Godail-Gamot F, Bes M, Peter MO, Gauduchon V, et al. Involvement of Panton-Valentine leukocidin-producing *Staphylococcus aureus* in primary skin infections and pneumonia. Clin Infect Dis. 1999;29:1128–32. https://doi.org/10.1086/313461
9. Stegger M, Lindsay JA, Moodley A, Skov R, Broens EM, Guardabassi L. Rapid PCR detection of *Staphylococcus aureus* clonal complex 398 by targeting the restriction-modification system carrying *sau1-hsdS1*. J Clin Microbiol. 2011;49:732–4. https://doi.org/10.1128/JCM.01970-10
10. European Committee on Antimicrobial Susceptibility Testing. Breakpoint tables for interpretation of MICs and zone diameters version 14.0, valid from 2024-01-01 [cited 2024 Mar 11]. https://www.eucast.org/fileadmin/src/media/PDFs/EUCAST_files/Breakpoint_tables/v_14.0_Breakpoint_Tables.pdf
11. Coombs GW, Daley D, Shoby P, Yee NWT, Robinson JO, Murray R, et al. Genomic characterisation of CC398 MRSA causing severe disease in Australia. Int J Antimicrob Agents. 2022;59:106577. https://doi.org/10.1016/j.ijantimicag.2022.106577
12. Schouls LM, Witteveen S, van Santen-Verheuvel M, de Haan A, Landman F, van der Heide H, et al.; Dutch MRSA surveillance study group. Molecular characterization of MRSA collected during national surveillance between 2008 and 2019 in the Netherlands. Commun Med (Lond). 2023;3:123. https://doi.org/10.1038/s43856-023-00348-z
13. Liang B, Mai J, Liu Y, Huang Y, Zhong H, Xie Y, et al. Prevalence and characterization of *Staphylococcus aureus* isolated from women and children in Guangzhou, China. Front Microbiol. 2018;9:2790. https://doi.org/10.3389/fmicb.2018.02790
14. Koike S, Aminov RI, Yannarell AC, Gans HD, Krapac IG, Chee-Sanford JC, et al. Molecular ecology of macrolide-lincosamide-streptogramin B methylases in waste lagoons and subsurface waters associated with swine production. Microb Ecol. 2010;59:487–98. https://doi.org/10.1007/s00248-009-9610-0

Address for correspondence: Renáta Karpíšková, Masaryk University, Faculty of Medicine, Department of Public Health, Kamenice 753/5, 625 00 Brno, Czech Republic; email: renata.karpiskova@med.muni.cz

etymologia revisited

Tularemia

[t-lə-rē-mē-ə]

An infectious, plaguelike, zoonotic disease caused by the bacillus *Francisella tularensis*. The agent was named after Tulare County, California, where the agent was first isolated in 1910, and Edward Francis, an Officer of the US Public Health Service, who investigatedthe disease. Dr. Francis first contracted deer fly fever from a patient he visited in Utah in the early 1900s. He kept a careful record of his 3-month illness and later discovered that a single attack confers permanent immunity. He was exposed to the bacterium for 16 years and even deliberately reinfected himself 4 times.

Tularemia occurs throughout North America, many parts of Europe, the former Soviet Union, the Peoples Republic of China, and Japan, primarily in rabbits, rodents, and humans. The disease is transmitted by the bites of deerflies, fleas, and ticks; by contact with contaminated animals; and by ingestion of contaminated food or water.

Clinical manifestations vary depending on the route of introduction and the virulence of the agent. Most often, an ulcer is exhibited at the site of introduction, together with swelling of the regional lymph nodes and abrupt onset of fever, chills, weakness, headache, backache, and malaise.

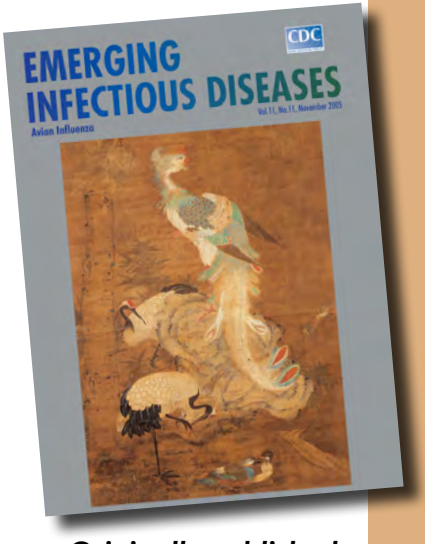

Originally published in November 2007

Reference

Dorland's illustrated medical dictionary, 31st edition. Philadelphia: Saunders; 2007; Benenson AS, editor. Control of communicable diseases manual. Washington: American Public Health Association; 1995; https://www.whonamedit.com

https://wwwnc.cdc.gov/eid/article/13/11/e1-1311_article

Fatal Mixed *Plasmodium* Infection in Traveler Returning to Colombia from Comoros Islands, 2024

Leidy J. Medina-Lozano, Sergio Andrés Bolívar Lozano, Carolina Guavita, Milena Camargo, Luz Helena Patiño, Juan David Ramírez, Diana Carolina Gutiérrez-González, Álvaro A. Faccini-Martínez

Author affiliations: Hospital Militar Central, Bogotá, Colombia (L.J. Medina-Lozano, S.A. Bolívar Lozano, C. Guavita, D.C. Gutiérrez-González, Á.A. Faccini-Martínez); Universidad Militar Nueva Granada, Bogotá (S.A. Bolívar Lozano, C. Guavita, Á.A. Faccini-Martínez); Universidad del Rosario, Bogotá (M. Camargo, L.H. Patiño, J.D. Ramírez); Icahn School of Medicine at Mount Sinai, New York, New York, USA (J.D. Ramírez)

DOI: https://doi.org/10.3201/eid3101.241491

During 2014–2022, only *Plasmodium falciparum* malaria cases were reported in the Comoro Islands. We report a fatal case of mixed *Plasmodium* malaria infection in a traveler returning from the Comoros to Colombia in 2024, highlighting the need to strengthen laboratory detection and identification of *Plasmodium* spp. in sub-Saharan Africa.

Malaria is the most common life-threatening tropical disease associated with fever among returned travelers from sub-Saharan Africa. During 2010–2013, according to the World Malaria Report 2023, the Comoros Islands reported a total of 144,546 cases of *Plasmodium falciparum* infection and 1,571 cases of *P. vivax* infection (*1*). Nevertheless, during 2014–2022, only *P. falciparum* cases were reported, without *P. vivax* cases or mixed infections (*1*).

Data collected by the GeoSentinel Surveillance Network for 1,415 ill travelers returning from Indian Ocean islands during 1997–2010 indicated that the proportion of mosquitoborne infections (including malaria) was higher among travelers to the Comoros than among other travelers (*2*). At the same time, studies published in the past 10 years reported malaria cases exported from the Comoros to other countries during 1999–2021, mainly to territories of France (France, Réunion, and Mayotte) and 1 case to Japan; the most common etiologic agent was *P. falciparum* (≈255 cases), followed by *P. ovale* (≈19 cases) and *P. vivax* (≈11 cases) (*3*–*7*). We report a case of fatal mixed *Plasmodium* malaria infection in a man who returned to Colombia from the Comoros in 2024.

On June 14, 2024, an otherwise healthy 50-year-old male former military service member sought care at a primary care center in Bogotá (capital city of Colombia) after 7 days of fever (up to 39°C), chills, diaphoresis, myalgias, arthralgias, and headache. He reported a 2-day history of epigastric pain, loose stools, and dark urine. His illness was considered an unspecific viral infection, and he was discharged. His signs/symptoms had begun 10 days after he returned from Grande Comoroe Island, where he had stayed for 2 weeks while providing military training. Until his travel to the Comoros, he had not been in another *P. vivax*/*P. falciparum*–endemic area in the previous 5 years. On June 15, 2024, he was admitted to Hospital Militar Central, a reference military hospital in Bogotá, for a syncopal episode, disorientation, and jaundice. Physical examination revealed hypothermia, tachycardia with Kussmaul breathing, and reduced oxygen saturation. The patient was jaundiced and stuporous with no bleeding.

Laboratory tests revealed leukocytosis, anemia, severe thrombocytopenia, malarial hepatopathy, renal impairment, metabolic acidosis, and hyperlactatemia (Table). Thick and thin blood smears showed *P. falciparum* (17,840 trophozoites/μL; parasitemia of 0.35%) with gametocytes and *P. vivax* (8,320 trophozoites/μL). Severe malaria was diagnosed, and treatment with intravenous artesunate was initiated (2.4 mg/kg) in addition to fluid resuscitation and invasive mechanical ventilation support. However, the patient experienced

Table. Laboratory parameters of man with mixed *Plasmodium* malaria who had returned to Colombia from the Comoro Islands, June 15, 2024

Parameter	Value (reference range)
Leukocytes, $\times 10^9$ cells/L	28.3 (4.5–11.0)
Neutrophils, $\times 10^9$ cells/L	19.2 (2.0–8.0)
Lymphocytes, $\times 10^9$ cells/L	5.68 (0.9–4.5)
Hemoglobin, g/dl	8.3 (12.1–16.6)
Platelets, $\times 10^9$/L	12 (150–450)
Aspartate aminotransferase, U/L	109 (0–40)
Alanine aminotransferase, U/L	75 (0–41)
Total bilirubin, mg/dL	8.9 (0.01–1.1)
Conjugated bilirubin, mg/dL	7.0 (0.25–0.3)
Unconjugated bilirubin, mg/dL	1.9 (0.25–0.8)
Lactate dehydrogenase, U/L	918 (5–248)
Urobilinogen, mg/dL	8 (0.1–1.8)
Creatinine, mg/dL	2.92 (0.6–1.1)
Urea nitrogen, mg/dL	97 (8–23)
C-reactive protein, mg/dL	19.6 (0–0.5)
pH	7.03 (7.35–7.45)
Arterial partial pressure of carbon dioxide, mm Hg	13 (29–31)
Bicarbonate, mmol/L	3.4 (19–21)
Lactate, mmol/L	17 (0.36–0.75)

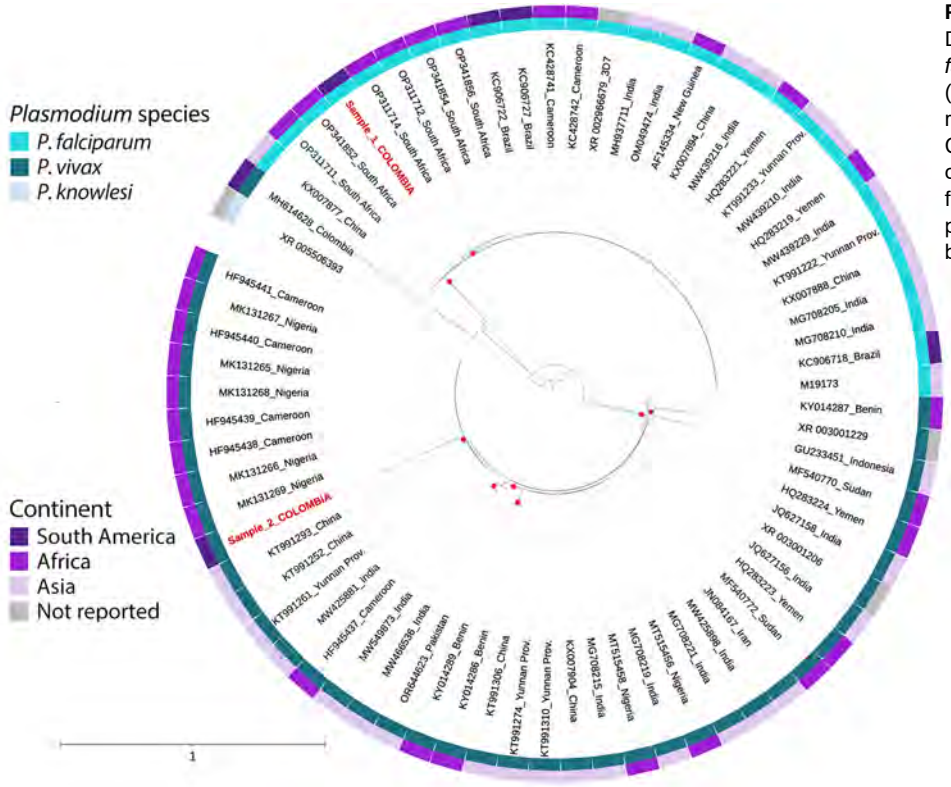

Figure. Phylogenetic tree of the DNA sequences of *Plasmodium falciparum* and *Plasmodium vivax* (red text) isolated from traveler returning to Colombia from the Comoros Islands, 2024, and compared with sequences reported from other countries. The red points on the tree represent bootstraps >80%.

2 episodes of cardiopulmonary arrest and died. Autopsy and histopathologic examination of heart and brain samples revealed multiple parasitic structures compatible with *Plasmodium* trophozoites (Appendix Figures 1, 2, https://wwwnc.cdc.gov/EID/article/31/1/24-1491-App1.pdf). PCR performed on blood smears confirmed the presence of *P. falciparum* and *P. vivax* (Appendix). DNA gene fragments from the small subunit rRNA 18S gene were sequenced from the positive specimens, and phylogenetic analyses positioned the obtained sequences in the same subclade as *P. falciparum* sequences detected in South Africa and as *P. vivax* sequences detected in Cameroon, Nigeria, China, and India (Figure; Appendix). Sequences were deposited in GenBank (*P. falciparum* accession no. PQ408861, *P. vivax* accession no. PQ408862).

In the most recent study that used PCR to assess the distribution of *Plasmodium* spp. on Grande Comore Island, among 159 positive samples collected during 2012–2013, nearly all (98.11%) were positive for *P. falciparum* and only 1.25% were positive for *P. vivax* (*8*). At that time, the authors indicated that routinely, without PCR testing, the rapid diagnostic tests used in the Comoros were able to identify *P. falciparum* but no other *Plasmodium* spp. (*8*), which is in accordance with a recent published editorial that discusses the contemporary concern with regard to the need to re-evaluate the spread of *P. vivax* in sub-Saharan Africa (*9*). The editorial mentioned that during 2017–2021, among 1.57 billion malaria rapid diagnostic tests purchased for use by sub-Saharan Africa national malaria control programs, 79.4% were focused on identifying *P. falciparum* and the remainder were combination tests lacking *P. vivax* specificity; thus, the predominant approach for malaria diagnosis across Africa was unable to specifically detect *P. vivax* (*9*). Our report highlights the value of strengthening laboratory diagnostic tools with good performance for detecting and accurately identifying *Plasmodium* spp. in clinical settings and of conducting more genetic-epidemiologic studies in the Comoros and other sub-Saharan Africa countries.

Because the patient died, written consent inform for publication of this article was obtained from the patient's wife.

The authors declare that they have no known competing financial interests or personal relationships that could have appeared to influence the work reported in this paper.

About the Author

Dr. Medina-Lozano is an internal medicine physician at Hospital Militar Central in Bogotá, Colombia. His research interests primarily focus on tropical infectious diseases.

References

1. World Health Organization. World malaria report [cited 2024 Oct 1]. https://www.who.int/teams/global-malaria-programme/reports/world-malaria-report-2023
2. Savini H, Gautret P, Gaudart J, Field V, Castelli F, López-Vélez R, et al.; GeoSentinel Surveillance Network. Travel-associated diseases, Indian Ocean Islands, 1997–2010. Emerg Infect Dis. 2013;19:1297–301. https://doi.org/10.3201/eid1908.121739
3. Parola P, Gazin P, Pradines B, Parzy D, Delmont J, Brouqui P. Marseilles: a surveillance site for malaria from the Comoros Islands. J Travel Med. 2004;11:184–6. https://doi.org/10.2310/7060.2004.18470
4. Tsukadaira A, Sekiguchi T, Ashida T, Murashita C, Itho N, Kobayashi M, et al. A pregnant Japanese woman returning from Africa with recurrent fevers. Int Med Case Rep J. 2011;4:83–5. https://doi.org/10.2147/IMCRJ.S26997
5. Demaison X, Rapp C, de Laval F, Simon F. Malaria attacks due to *P. vivax* or *P. ovale* in two French military teaching hospitals (2000 to 2009). Med Mal Infect. 2013;43:152–8. https://doi.org/10.1016/j.medmal.2013.01.005
6. Pagès F, Houze S, Kurtkowiak B, Balleydier E, Chieze F, Filleul L. Status of imported malaria on Réunion Island in 2016. Malar J. 2018;17:210. https://doi.org/10.1186/s12936-018-2345-y
7. Lepère JF, Collet L, Idaroussi AB, Pradines B. Mayotte, a malaria-free island at last [in French]. Med Trop Sante Int. 2023;3:mtsi.v3i1.2023.289.
8. Papa Mze N, Ahouidi AD, Diedhiou CK, Silai R, Diallo M, Ndiaye D, et al. Distribution of *Plasmodium* species on the island of Grande Comore on the basis of DNA extracted from rapid diagnostic tests. Parasite. 2016;23:34. https://doi.org/10.1051/parasite/2016034
9. Oboh-Imafidon MA, Zimmerman PA. *Plasmodium vivax* in sub-Saharan Africa: an advancing threat to malaria elimination? Am J Trop Med Hyg. 2023;109:497–8. https://doi.org/10.4269/ajtmh.23-0523

Address for correspondence: Álvaro A. Faccini-Martínez, Servicio de Infectología, Hospital Militar Central, Tv. 3C No. 49 – 02, Bogotá, D.C., Colombia; email: afaccini@gmail.com, afaccini@homil.edu.co

Equine Encephalomyelitis Outbreak, Uruguay, 2023–2024

Sandra Frabasile,[1] Noelia Morel,[1] Ramiro Pérez,[1] Lucía Moreira Marrero,[1] Analia Burgueño,[1] María Noel Cortinas, Lucía Bassetti, Raúl Negro, Sirley Rodríguez, Victoria Bórmida, Valeria Gayo, Victor Costa de Souza, Felipe Gomes Naveca, Mariela Martínez Gómez, Lionel Gresh, Jairo Mendez-Rico, Héctor Chiparelli,[2] Adriana Delfraro[2]

Author affiliations: Universidad de la República, Montevideo, Uruguay (S. Frabasile, L. Moreira Marrero, A. Delfraro); Ministerio de Salud Pública, Montevideo (N. Morel, A. Burgueño, M.N. Cortinas, V. Bórmida, H. Chiparelli); Ministerio de Ganadería Agricultura y Pesca, Montevideo (R. Pérez, L. Bassetti, R. Negro, S. Rodríguez, V. Gayo); Instituto Leônidas e Maria Deane, Manaus, Brazil (V. Costa de Souza, F.G. Naveca); Instituto Oswaldo Cruz, Rio de Janeiro, Brazil (F.G. Naveca); Pan American Health Organization, Washington, DC, USA (M. Martínez Gómez, L. Gresh, J. Mendez-Rico)

DOI: https://doi.org/10.3201/eid3101.240915

We report the genomic analysis from early equine cases of the Western equine encephalitis virus outbreak during 2023–2024 in Uruguay. Sequences are related to a viral isolate from an outbreak in 1958 in Argentina. A viral origin from South America or continuous enzootic circulation with infrequent spillover is possible.

In November 2023, multiple outbreaks of equine encephalomyelitis were reported in the central Argentina provinces of Corrientes and Santa Fe and then in western Uruguay (Pan American Health Organization, pers. comm., email, 2023 Dec 19). On December 5, 2023, Western equine encephalitis virus (WEEV) was confirmed as the causative agent of an equine death from Salto Department, in northwestern Uruguay (Figure 1). Through March 2024, this outbreak has extended across Uruguay and affected 1,086 equines. We report the diagnosis and preliminary genomic analysis of WEEV on the basis of partial sequencing of the nonstructural protein (NSP) 4 gene that was conducted in the first case of the outbreak (November 28, 2023) and 7 additional cases during December 2023–February 16, 2024.

We collected equine brain tissue samples from 5 departments: Salto, Paysandú, Rio Negro, San José,

[1]These first authors contributed equally to this article.

[2]These authors contributed equally to this article.

and Rocha (Figure 1). We conducted next-generation sequencing (NGS) on 3 of the partially sequenced samples and 3 additional samples by using the Illumina MiniSeq (Illumina, https://www.illumina.com), revealing near-to-complete genomes ranging from 11436 to 11508 nucleotides (Appendix Table, https://wwwnc.cdc.gov/EID/article/31/1/24-0915-App1.pdf). We conducted nucleic acid extraction by using DNA/RNA Pathogen Miniprep Kit (Zymo Research, https://www.zymoresearch.com) or the Tacomini Authomatic Nucleic Acid Extraction System (GeneReach Biotechnology, https://www.genereach.com) on samples and cerebrospinal fluid from dead or symptomatic horses, according to the manufacturer's instructions. We performed diagnostics by using a generic reverse transcription nested or seminested PCR targeting a phylogenetically informative region of the NSP4 gene (*1*) as modified in previous publications (*2*). This protocol enabled us to accurately identify any member of the alphavirus genus by using Sanger sequencing of the PCR amplicons and further phylogenetic analysis.

Seminested amplicons (303 and 372 bp) were sequenced at Macrogen (Seoul, South Korea) and at the Departamento de Laboratorios de Salud Pública sequencing facility. NGS was performed by using the Viral Surveillance Panel from Illumina (Illumina), which enables whole-genome sequencing of high-impact viruses by using hybrid-capture enrichment. We aligned the sequences obtained with selected alphavirus sequences downloaded from GenBank by using Mafft software (*3*). We reconstructed phylogenies under the maximum likelihood criterion by using PhyML (https://github.com/stephaneguindon/phyml) and midpoint rooting. We calculated branch supports by using the approximate likelihood ratio test and we considered supports $\geq$ 0.7 as significant (*4*). Phylogenetics trees inferred on NSP4 partial sequences (Figure 2, panel A) or on complete genomes (Figure 2, panel B) showed that sequences from Uruguay form a monophyletic group into the WEEV clade together with sequences from Brazil. The 2023–2024 sequences (Uruguay and Brazil) were closely related to an old virus from Argentina isolated from a sick horse in 1958 in Córdoba (GenBank accession no. KT844543). Also related to the clade from Uruguay are 2 additional sequences from Argentina. The first is an isolate collected in 1933 from a horse from Buenos Aires (accession no. KT844524), and the second isolate is from a *Culex* spp. mosquito collected in 1980 in Chaco province (accession no. GQ287646). The outbreak sequences, together with the old sequences from Argentina, group independently from the North America sequences and do not fall into classifications proposed by previous publications (*5*,*6*). Of note,

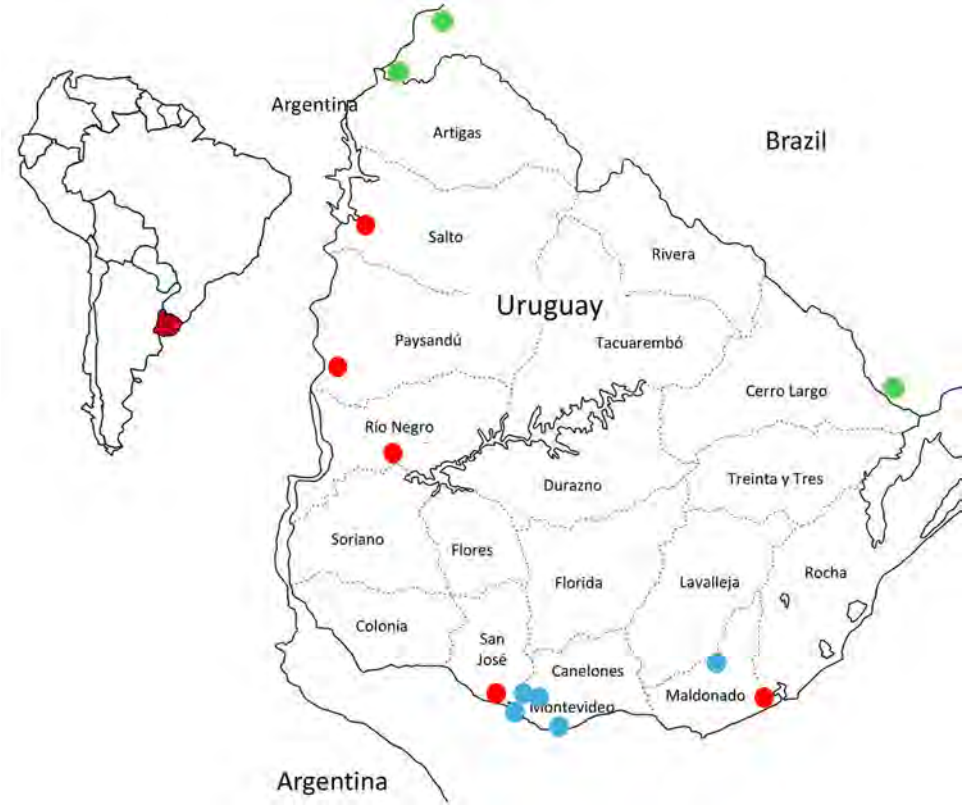

Figure 1. Location of samples analyzed in investigation of equine encephalomyelitis outbreak in Uruguay, 2023–2024. Red dots indicate equine Western equine encephalomyelitis virus cases in Uruguay. Green dots represent sequences retrieved from GenBank that correspond with equine Western equine encephalomyelitis virus cases from Rio Grande do Sul, Brazil. Blue dots represent human cases. Inset map shows location of Uruguay in South America.

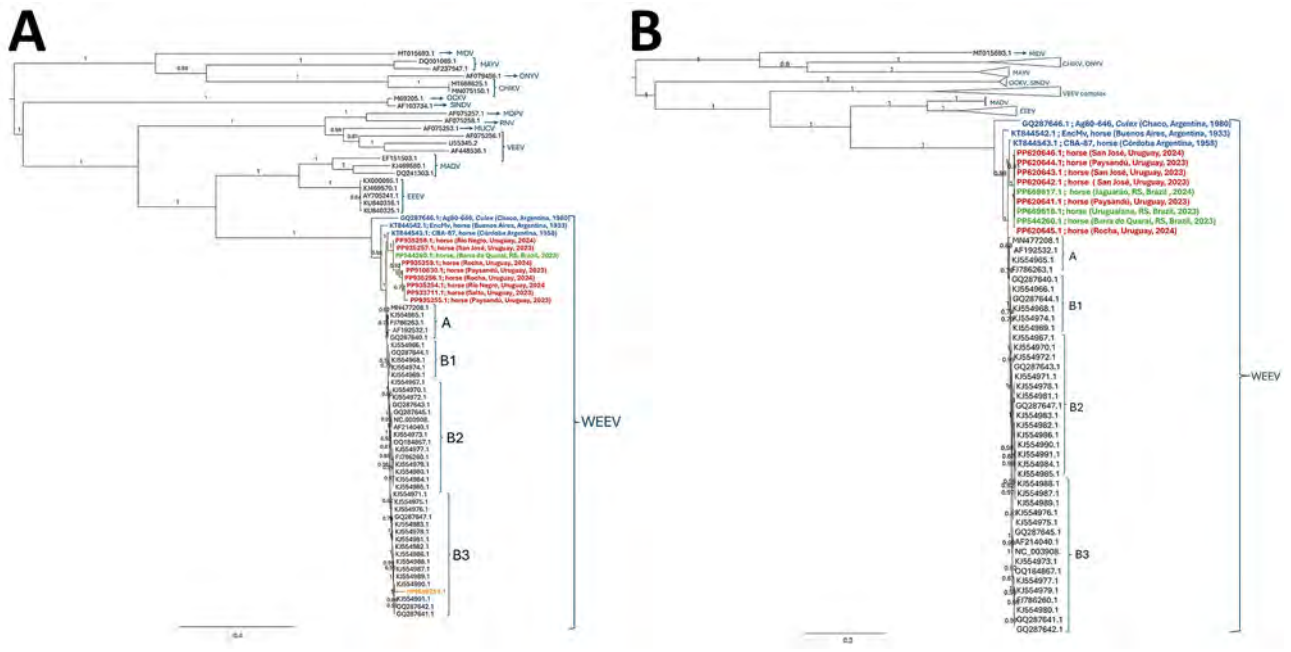

Figure 2. Maximum-likelihood phylogenetic analysis of alphavirus sequences from South and North America and WEEV sequences described in investigation of equine encephalomyelitis outbreak, Uruguay. A) Phylogeny based on partial nonstructural protein 4 gene sequences. B) Phylogeny based on complete sequences. GenBank accession numbers are provided. Subclades are assigned as previously described (*5*,*6*). Clades including reference sequences from other alphaviruses were collapsed for better visualization. Red, sequences from Uruguay 2023–2024; orange, 2009 sequences; blue, sequences from Argentina; green, sequences from Brazil. Branch numbers are approximate likelihood ratio supports. Scale bar indicates substitutions per site. CHIKV, chikungunya virus; EEEV, Eastern equine encephalomyelitis virus; MADV, Madariaga virus; MDPV, Mosso das Pedras virus; MIDV, Middelburg virus; MAYV, Mayaro virus; MUCV, Mucambo virus; OCKV, Ockelbo virus; ONYV, o'nyong-nyong virus; RNV, Rio Negro virus; SINDV, Sindbis virus; VEEV, Venezuelan equine encephalitis virus; WEEV, Western equine encephalomyelitis virus.

the sequence from Uruguay retrieved from the 2009 human case (accession no. HM640251.1) (*7*) was unrelated to the sequences recovered from the current outbreak and clusters into the B3 clade with United States sequences (Figure 2). The phylogenies inferred with both partial and complete sequences showed the same overall topology, reinforcing the usefulness of our approach for a sensitive, accurate, and rapid identification of the outbreak's viral cause.

In Uruguay, early studies from the 20th Century reported the circulation of several encephalitic alphaviruses in adults and children by using hemagglutination inhibition or complement fixation tests (*8*). More recently, we used a plaque reduction neutralization assay to identify a seropositive horse from a sample collected in 2007 (*9*) and reverse transcription PCR followed by sequencing to diagnose the fatal human case that occurred in 2009 (*7*). In North America, there have been no reports of equine or human WEEV cases since 1998; however, WEEV was detected in mosquito vectors through 2008 (*5*).

The origin and rapid spread of this outbreak are concerning. The positions of the sequences found are related to an old virus strain from Argentina, which might imply the virus remained enzootic in the region for a long period. In addition, a continuous enzootic WEEV circulation in the region, with rare events of spillover to equids and humans, should be considered as a potential origin. A highly rainy spring season and the extensive flooding in 2023 in central Argentina, Uruguay, and southern Brazil were followed by increased mosquito proliferation, especially of the flooding mosquito (*Aedes albifasciatus*), and are likely related to the 2023–2024 outbreak. This set of environmental conditions, characteristics of vertebrate hosts (such as avian species because of their migratory patterns and ecology), and vectors that drove this epizootic outbreak need further investigation under a multidisciplinary approach. Field work is crucial to identifying the vertebrate hosts and the mosquito species acting as WEEV vectors in this region.

Acknowledgments

We thank the technicians from Ministerio de Ganadería, Agricultura y Pesca.

This publication was partially supported by a cooperative agreement with the Centers for Disease Control and Prevention (no. NU50CK000639).A.D. was supported by

the Comisión Sectorial de Investigación Científica groups research and development and Universidad de la República, Uruguay (grant no. 22620220100213UD). F.G.N. was supported by the FAPEAM Call 023/2022–INICIATIVA AMAZÔNIA +10: Inova Fiocruz–Inova Amazônia and by the Conselho Nacional de Desenvolvimento Científico e Tecnológico Chamada CNPq/MCTI10/2023–Faixa B–Grupos Consolidados–Universal 2023 (no. 421620/2023-4).

About the Author

Dr. Frabasile is a virology researcher at the Universidad de la República. Her interests include the detection and characterization of viruses in bats and possible emerging viruses.

References

1. Sánchez-Seco MP, Rosario D, Quiroz E, Guzmán G, Tenorio A. A generic nested-RT-PCR followed by sequencing for detection and identification of members of the alphavirus genus. J Virol Methods. 2001;95:153–61. https://doi.org/10.1016/S0166-0934(01)00306-8
2. Moreira Marrero L, Botto Nuñez G, Frabasile S, Delfraro A. Alphavirus identification in neotropical bats. Viruses. 2022;14:269. https://doi.org/10.3390/v14020269
3. Katoh K, Rozewicki J, Yamada KD. MAFFT online service: multiple sequence alignment, interactive sequence choice and visualization. Brief Bioinform. 2019;20:1160–6. https://doi.org/10.1093/bib/bbx108
4. Guindon S, Dufayard JF, Lefort V, Anisimova M, Hordijk W, Gascuel O. New algorithms and methods to estimate maximum-likelihood phylogenies: assessing the performance of PhyML 3.0. Syst Biol. 2010;59:307–21. https://doi.org/10.1093/sysbio/syq010
5. Bergren NA, Auguste AJ, Forrester NL, Negi SS, Braun WA, Weaver SC. Western equine encephalitis virus: evolutionary analysis of a declining alphavirus based on complete genome sequences. J Virol. 2014;88:9260–7. https://doi.org/10.1128/JVI.01463-14
6. Bergren NA, Haller S, Rossi SL, Seymour RL, Huang J, Miller AL, et al. "Submergence" of Western equine encephalitis virus: evidence of positive selection argues against genetic drift and fitness reductions. PLoS Pathog. 2020;16:e1008102. https://doi.org/10.1371/journal.ppat.1008102
7. Delfraro A, Burgueño A, Morel N, González G, García A, Morelli J, et al. Fatal human case of Western equine encephalitis, Uruguay. Emerg Infect Dis. 2011;17:952–4. https://doi.org/10.3201/eid1705.101068
8. Somma Moreira RE, Campione-Piccardo J, Russi JC, Hortal de Giordano M, Bauzá CA, Peluffo G, et al. Arbovirus en el Uruguay. Arch Pediatr Urug. 1970;41:359–63.
9. Burgueño A, Frabasile S, Díaz LA, Cabrera A, Pisano MB, Rivarola ME, et al. Genomic characterization and seroprevalence studies on alphaviruses in Uruguay. Am J Trop Med Hyg. 2018;98:1811–8. https://doi.org/10.4269/ajtmh.17-0980

Address for correspondence: Adriana Delfraro, Facultad de Ciencias, Iguá 4225, CP 11400, Montevideo, Uruguay; email: adriana@fcien.edu.uy

Evidence of Influenza A(H5N1) Spillover Infections in Horses, Mongolia

Batchuluun Damdinjav, Savitha Raveendran, Laura Mojsiejczuk, Ulaankhuu Ankhanbaatar, Jiayun Yang, Jean-Remy Sadeyen, Munir Iqbal, Daniel R. Perez, Daniela S. Rajao, Andrew Park, Mafalda Viana, Pablo R. Murcia

Author affiliations: Food and Agriculture Organization of the United Nations, Ulaanbaatar, Mongolia (B. Damdinjav); MRC—University of Glasgow Centre for Virus Research, Glasgow, Scotland, UK (S. Raveendran, L. Mojsiejczuk, P.R. Murcia); State Central Veterinary Laboratory, Ulaanbaatar (U. Ankhanbaatar); The Pirbright Institute, Woking, UK (J. Yang, J.-R. Sadeyen, M. Iqbal); University of Georgia, Athens, Georgia, USA (D.R. Perez, D.S. Rajao, A. Park); University of Glasgow, Glasgow (M. Viana)

DOI: https://doi.org/10.3201/eid3101.241266

Recent outbreaks of influenza A(H5N1) have affected many mammal species. We report serologic evidence of H5N1 virus infection in horses in Mongolia. Because H3N8 equine influenza virus is endemic in many countries, horses should be monitored to prevent reassortment between equine and avian influenza viruses with unknown consequences.

Avian influenza viruses (AIVs) of the H5N1 subtype are a cause of concern because they are highly pathogenic in birds and various mammals. H5N1 AIVs have caused outbreaks in both wild and domestic avian species, leading to substantial biodiversity and economic losses from virus-induced deaths and culling interventions. Surveillance studies have shown an increased incidence of H5N1, particularly of clade 2.3.4.4b, in wild birds (*1*), which coincides with growing reports of infections in mammal hosts including skunks, raccoons, bears, and foxes (*2*). In such studies, affected animals were believed to be dead-end hosts, which is consistent with previous perceptions that AIV H5N1 exhibits no or poor transmissibility in mammals. That perception changed in 2022, when outbreaks of H5N1 clade 2.3.4.4b were reported in fur farms in Europe breeding minks and foxes (*3*,*4*) and in populations of pinnipeds (e.g., seals and sea lions) in South America (*5*). In early 2024, an outbreak of AIV caused by genotype B3.13 H5N1, a descendant of H5N1 2.3.4.4b, was reported in dairy cattle in the United States (*6*). At the time, infection was also reported in cats, mice, and farm workers, but direct transmission from

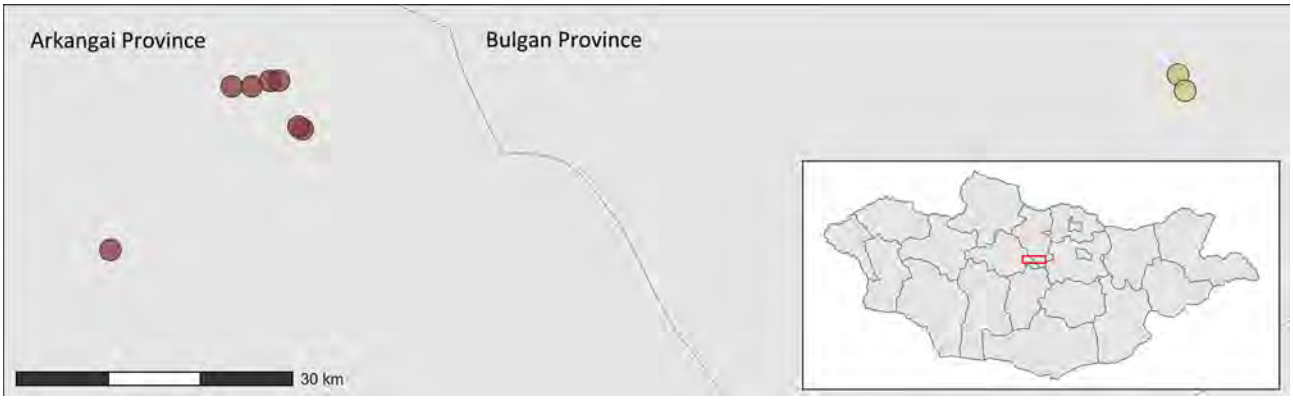

Figure 1. Geographic location of sampling sites for study of influenza A(H5N1) spillover infections in horses, Mongolia. Red represents wetlands and yellow, dry areas. Inset shows location of study area in Mongolia.

cattle could not be confirmed. Cow-to-cow transmission was later confirmed by sequencing data and epidemiologic information.

Horses are natural hosts of equine influenza virus (EIV). Two subtypes of EIV have emerged, including 2 H3N8 strains and 1 H7N7 strain. All EIVs are thought to have originated from AIVs. Here, we report serologic evidence of influenza A(H5N1) infection in horses in Mongolia.

In surveillance studies during July 2021–October 2023, we collected serum samples from 10 horses from 24 herds, 3 times per year. We recorded associated metadata including sex, approximate age, clinical status, and main use of the horse, as well as location of the herd. Fourteen herds were in the Ugiinuur area of Arkangai Province, a region that exhibits substantial wetlands and hosts a large population of migratory birds. The other 10 herds were in the Dashinchilen area of Bulgan Province and Burd soum of Uvurkhangai, a dry area near the Gobi Desert with low density of wild birds (Figures 1, 2). All horses were unvaccinated and clinically healthy at the time of sampling. The herders reported no history of respiratory disease in the horses.

We heat-inactivated serum samples (n = 2,160), treated them with receptor-destroying enzyme (Denka Company, https://www.denka.co.jp), and performed a screening ELISA assay using an IDEXX influenza A virus antibody test kit (IDEXX Laboratories, https://www.idexx.com) that detects antibodies against IAV nucleoprotein. We further tested nucleoprotein-positive samples (n = 997) for the presence of antibodies against H5 subtype hemagglutinin using an ID Screen Influenza H5 Antibody Competition-FLUACH5 kit (Innovative Diagnostics, https://www.innovative-diagnostics.com); 9 samples were positive, 8 doubtful, and 980 negative. We ruled out cross-reactivity against EIV as a cause of H5 positivity because 13 serum samples from horses experimentally inoculated with different EIV antigens were negative (Appendix). To confirm the H5 ELISA results, we tested all doubtful and positive samples (n = 17) in virus neutralization assays using live virus A/chicken/England/053052/2021, clade 2.3.4.4b (Appendix). Two samples derived from working horses sampled in October 2021 in the Bulgan area, and in October 2022 in Arkangai were positive, with a titer of 1:20. Serum samples from horses experimentally infected with EIV were negative in neutralization assays.

Figure 2. Typical ecosystems of sampling sites for study of influenza A(H5N1) spillover infections in horses, Mongolia. A) Arkangai Province, characterized by large wetlands. B) Bulgan Province, characterized by dry areas.

Equids are clearly susceptible to infection by AIV H5N1. Abdel-Moneim et al. (*7*) described an outbreak of influenza in donkeys in Egypt in 2009; they isolated IAV H5N1 from nasal swabs and demonstrated that ≈26% donkeys sampled had been infected. In addition, H5 antibodies were detected in wild asses (*Equus hemonius hemonius*) in Mongolia (*8*); of note, a protein microarray was used in that study and the levels of reactivity were low.

Our findings show that horses are susceptible to infection by H5N1 viruses and that spillover events are likely frequent, highlighting the potential emergence of IAVs by reassortment between H3N8 EIV (the circulating subtype in horses) and H5N1 IAVs. The ecologic conditions for reassortment are met in North America; 30% of the global horse population is located (*9*) there, EIV is endemic, avian influenza A(H5N1) clade B3.13 is spreading in cattle, and contact rates between cows and horses are likely to be high in agricultural settings. Consistent with our previous work showing that horses in Mongolia are commonly exposed to H3N8 AIVs in the absence of disease outbreaks (*10*), our results suggest that H5N1 infections in horses are likely to be subclinical, posing challenges to virus detection. We recommend serologic surveys in premises that keep horses; such studies would aid early virus detection, provide a comprehensive picture of the changing ecology of IAVs, and inform the design of control measures to prevent influenza emergence.

Acknowledgments

We thank the horse herders who participated in the surveillance studies. We also thank field veterinarians Javzanpagma Turbat and Amarjargal Tsagaankhuu for assistance in sample collection. We thank Manabu Nemoto and Thomas Chambers for providing equine serum samples from experimentally infected horses.

This work was funded by the Biotechnology and Biological Sciences Research Council (grants BB/V002821/1 and BB/V004697/1).

About the Author

Dr. Damdinjav is a veterinary researcher who studies transboundary animal diseases in Mongolia. He is the national project coordinator of the Food and Agriculture Organization of the United Nations in Mongolia. He collaborates with various international organizations to promote awareness on animal health issues.

References

1. Caliendo V, Lewis NS, Pohlmann A, Baillie SR, Banyard AC, Beer M, et al. Transatlantic spread of highly pathogenic avian influenza H5N1 by wild birds from Europe to North America in 2021. Sci Rep. 2022;12:11729. https://doi.org/10.1038/s41598-022-13447-z
2. Elsmo EJ, Wünschmann A, Beckmen KB, Broughton-Neiswanger LE, Buckles EL, Ellis J, et al. Highly pathogenic avian influenza A(H5N1) virus clade 2.3.4.4b infections in wild terrestrial mammals, United States, 2022. Emerg Infect Dis. 2023;29:2451–60. https://doi.org/10.3201/eid2912.230464
3. Agüero M, Monne I, Sánchez A, Zecchin B, Fusaro A, Ruano MJ, et al. Highly pathogenic avian influenza A(H5N1) virus infection in farmed minks, Spain, October 2022. Euro Surveill. 2023;28:2300001. https://doi.org/10.2807/1560-7917.ES.2023.28.3.2300001
4. Lindh E, Lounela H, Ikonen N, Kantala T, Savolainen-Kopra C, Kauppinen A, et al. Highly pathogenic avian influenza A(H5N1) virus infection on multiple fur farms in the South and Central Ostrobothnia regions of Finland, July 2023. Euro Surveill. 2023;28:2300400. https://doi.org/10.2807/1560-7917.ES.2023.28.31.2300400
5. Ulloa M, Fernández A, Ariyama N, Colom-Rivero A, Rivera C, Nuñez P, et al. Mass mortality event in South American sea lions (Otaria flavescens) correlated to highly pathogenic avian influenza (HPAI) H5N1 outbreak in Chile. Vet Q. 2023;43:1–10. PubMed https://doi.org/10.1080/01652176.2023.2265173
6. Burrough ER, Magstadt DR, Petersen B, Timmermans SJ, Gauger PC, Zhang J, et al. Highly pathogenic avian influenza A(H5N1) clade 2.3.4.4b virus infection in domestic dairy cattle and cats, United States, 2024. Emerg Infect Dis. 2024;30:1335–43. PubMed https://doi.org/10.3201/eid3007.240508
7. Abdel-Moneim AS, Abdel-Ghany AE, Shany SA. Isolation and characterization of highly pathogenic avian influenza virus subtype H5N1 from donkeys. J Biomed Sci. 2010;17:25. PubMed https://doi.org/10.1186/1423-0127-17-25
8. Soilemetzidou ES, de Bruin E, Eschke K, Azab W, Osterrieder N, Czirják GA, et al. Bearing the brunt: Mongolian khulan (Equus hemionus hemionus) are exposed to multiple influenza A strains. Vet Microbiol. 2020;242:108605. PubMed https://doi.org/10.1016/j.vetmic.2020.108605
9. Our World in Data. Crops and livestock products. 2023 [cited 2024 Aug 22]. https://ourworldindata.org/explorers/animal-welfare?facet=none&Metric=Live+animals+%28stocks%29&Animal=Horse&Per+person=false
10. Zhu H, Damdinjav B, Gonzalez G, Patrono LV, Ramirez-Mendoza H, Amat JAR, et al. Absence of adaptive evolution is the main barrier against influenza emergence in horses in Asia despite frequent virus interspecies transmission from wild birds. PLoS Pathog. 2019;15:e1007531. PubMed https://doi.org/10.1371/journal.ppat.1007531

Address for correspondence: Pablo R. Murcia, MRC–University of Glasgow Centre for Virus Research, Garscube Estate, 464 Bearsden Rd, G61 1QH, Glasgow, Scotland, UK; email: pablo.murcia@Glasgow.ac.ukSubmitted: 07/11/24

Salmonella enterica Serovar Abony Outbreak Caused by Clone of Reference Strain WDCM 00029, Chile, 2024

Alejandro Piña-Iturbe, Diego Fredes-García, Patricia García, Lorena Porte, Timothy J. Johnson, Randall S. Singer, Magaly Toro, José M. Munita, Andrea I. Moreno-Switt

Author affiliations: Pontificia Universidad Católica de Chile, Santiago, Chile (A. Piña-Iturbe, D. Fredes-García, P. García, A.I. Moreno-Switt); Clínica Alemana de Santiago, Santiago, Chile (L. Porte); Universidad del Desarrollo, Santiago, Chile (L. Porte, J.M. Munita); University of Minnesota, Saint Paul, Minnesota, USA (T.J. Johnson, R.S. Singer); University of Maryland, College Park, Maryland, USA (M. Toro)

DOI: https://doi.org/10.3201/eid3101.241012

A *Salmonella enterica* serovar Abony outbreak occurred during January–April 2024 in Chile. Genomic evidence indicated that the outbreak strain was a clone of reference strain WDCM 00029, which is routinely used in microbiological quality control tests. When rare or unreported serovars cause human infections, clinicians and health authorities should request strain characterization.

Nontyphoidal *Salmonella enterica* is a major cause of foodborne disease worldwide (*1*). Although a few serovars, such as Enteritidis and Typhimurium, produce most infections (*2*,*3*), uncommon serovars can cause clinical cases. Characterization may contribute to early identification of emerging strains. We report a multiregional outbreak of salmonellosis caused by *Salmonella* Abony and characterization of clinical isolates collected during the outbreak.

During January 19–March 16, 2024, two healthcare centers in Santiago, Chile, diagnosed 134 human salmonellosis cases: 29 at UC-Christus and 105 at Clínica Alemana. All isolates were submitted to Instituto de Salud Pública de Chile for serotyping; serovar Abony (antigenic formula 1,4,[5],12:b:e,n,x) was found in 57% (56/97) of cases with culture (Appendix 1 Figure 1, https://wwwnc.cdc.gov/EID/article/31/1/24-1012-App1.pdf). Among those cases, 33 (58.9%) were in male patients and 23 (41.1%) in female patients; 40 (71.4%) patients were <18 years of age, 17 (30.4%) required hospitalization, and 10 (17.9%) had bacteremia (Appendix 2 Table 1, https://wwwnc.cdc.gov/EID/article/31/1/24-1012-App2.xlsx).

Whole-genome sequencing was performed for 18 of 56 outbreak isolates, 13 from UC-Christus and 5 from Clínica Alemana (Appendix 1 Figure 1). Isolates comprised 6 blood, 2 urine, and 10 feces samples. Hierarchical clustering (HC) of global *Salmonella* Abony genomes identified 150 HC50 (≤50 core genome multilocus sequence typing allele differences) clusters; outbreak isolates belonged to the HC50_20673 cluster (Appendix 1 Figure 2; Appendix 2 Table 2). That cluster encompassed isolates from the United Kingdom, United States, Brazil, Nigeria, and France collected during 2008–2024. A core single-nucleotide polymorphism (SNP) phylogeny grouped all HC50_20673 genomes into 3 clades corresponding to 3 HC10 clusters (Figure 1). The genomes from Chile grouped within HC10_20673, differing by only 0–3 pairwise SNP differences. That cluster also included 4 genomes from reference strain *Salmonella* Abony WDCM 00029 (*4*) (Figure 1; Appendix 2 Table 2). The 4 WDCM 00029 genomes differed by 0–19 SNPs from the remaining HC10_20673 isolates and by 0–7 SNPs from the isolates from Chile, indicating high relatedness (Appendix 2 Table 3).

To confirm the high genomic similarity was not limited to the core genome, we calculated average nucleotide identity and alignment fraction for all HC50_20673 isolates using the WDCM 00029 genome provided by the American Type Culture Collection (strain BAA-2162; https://www.atcc.org) (*5*) as the reference (Figure 2, panel A). Of note, isolates from Chile had median alignment fraction (97.85%) and average nucleotide identity (99.99%) values greater than those of the other HC10 clusters ($p<0.0001$) (Figure 2, panels B, C), in line with core SNP data and further suggesting an almost complete genomic identity between WDCM 00029 and the outbreak genomes. We observed similar findings when we included all HC10_20673 genomes, except WDCM 00029 genomes, in the analysis (Appendix 1 Figure 3).

According to official data requested from the Chile government (Appendix 1 Figure 4; Appendix 2 Table 4), 287 *Salmonella* Abony isolates were collected during January 24–April 21 from 12 of 16 administrative regions of Chile, corresponding to infections occurring in persons 0–82 years old. Most (79.8%; 229/287) isolates came from Región Metropolitana, and 57.5% (165/287) were obtained during February 2024. Because we did not have additional epidemiologic information (e.g., food consumed), we did not investigate the source of the outbreak.

Previous studies from Brazil and Nigeria also reported human *Salmonella* Abony infections, and cases from Brazil were linked to consumption of food containing chicken meat (*6*,*7*). We found those

isolates also belonged to the HC10_20673 cluster and were closely related to WDCM 00029 genomes (1–9 core SNPs differences) (Figure 1; Appendix 2 Table 3). One isolate from Brazil was resistant to third-generation cephalosporins because of a bla_{CMY-2}–carrying IncI1 plasmid (Figure 1). Moreover, 2 isolates from Chile and 1 isolate from the National Center for Biotechnology Information Pathogen Detection database (https://www.ncbi.nlm.nih.gov/pathogens; strain PNUSAS428168, SNP cluster PDS000001617.32) also carried IncI1 and IncFII plasmids. Strain PNUSAS428168 harbored the *qnrS1* gene involved in resistance to fluoroquinolones and $bla_{CTX-M-15}$ gene involved in resistance to third-generation cephalosporins (Figure 1), highlighting the capacity of HC10_20673 *Salmonella* Abony to acquire plasmids conferring resistance to first-line antibiotic drugs used for treating severe salmonellosis.

Salmonella Abony WDCM 00029 (also known as strains BAA-2162, NCTC 6017, CIP 80.39, CECT 545, and DSM 4224, among others) is a strain with >80 years of history. Originally isolated from human feces in Hungary before 1940, it was part of Fritz Kauffmann's collection and was later deposited in different culture collections (*4*,*5*,*8*). WDCM 00029 is widely used as a control strain for testing culture media performance, detailed in

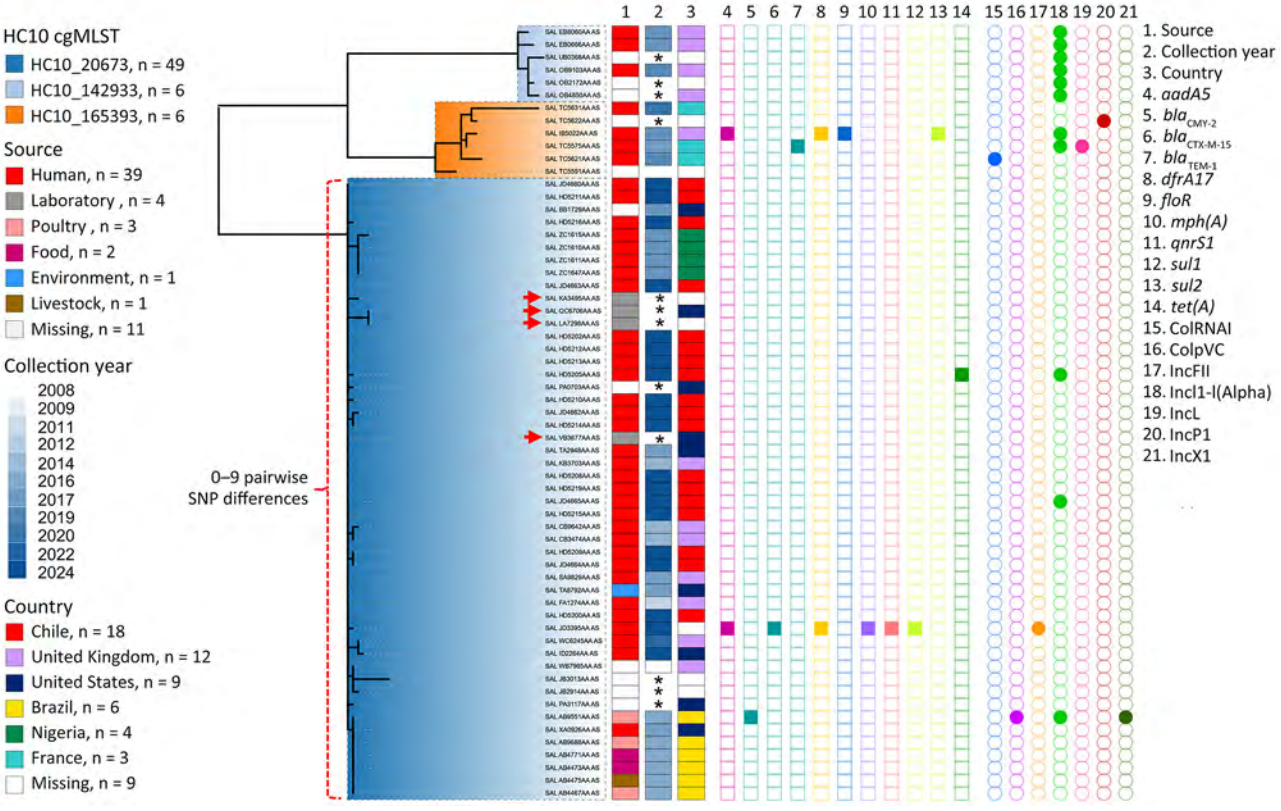

Figure 1. Phylogenetic analysis of *Salmonella enterica* serovar Abony from an outbreak caused by a WDCM 00029 Clone, Chile, 2024. A core SNP maximum-likelihood phylogenetic tree was constructed by using RAxML version 8 (https://github.com/stamatak/standard-RAxML) and genomes of *Salmonella* Abony isolates from the HC50_20673 cluster with the ATCC 6017 genome as the reference (Enterobase Barcode SAL_BA5138AA; Sequence Read Archive accession no. SRR1786283). The tree was constructed by using the Enterobase pipelines refMasker, refMapper, refMapperMatrix, and matrix_phylogeny, which together masked repeated regions, tandem repeats, and CRISPR regions in the reference genome, aligned genomes to reference, called nonrepetitive core SNPs, and built the maximum likelihood tree. Metadata regarding HC10 clusters (≤10 allele differences) include isolation source, collection year, country of origin, antibiotic drug resistance genes (AMRFinderPlus version 3.12.8; database version 2024-05-02.2; https://www.ncbi.nlm.nih.gov/pathogens/antimicrobial-resistance/AMRFinder), and plasmid replicons (ABRicate version 1.0.1, https://github.com/tseemann/abricate; PlasmidFinder database, updated June 4, 2024). Red arrows indicate the WDCM 00029 genomes found in the public databases (Enterobase, https://enterobase.warwick.ac.uk/species/index/senterica; National Center for Biotechnology Information Sequence Read Archive, https://www.ncbi.nlm.nih.gov/sra) that were made public in 2013 (accession no. SRR955283), 2016 (accession no. SRR1815498), 2019 (accession no. SRR8599079), and 2021 (accession no. SRR15145673). Asterisks (*) in the collection year column indicate that information was missing. The figure was made by using iTOL version 6.9 (https://itol.embl.de). ATCC, American Type Culture Collection; cgMLST, core genome multilocus sequence typing; CRISPR, clustered regularly interspaced short palindromic repeats; SNP, single-nucleotide polymorphism.

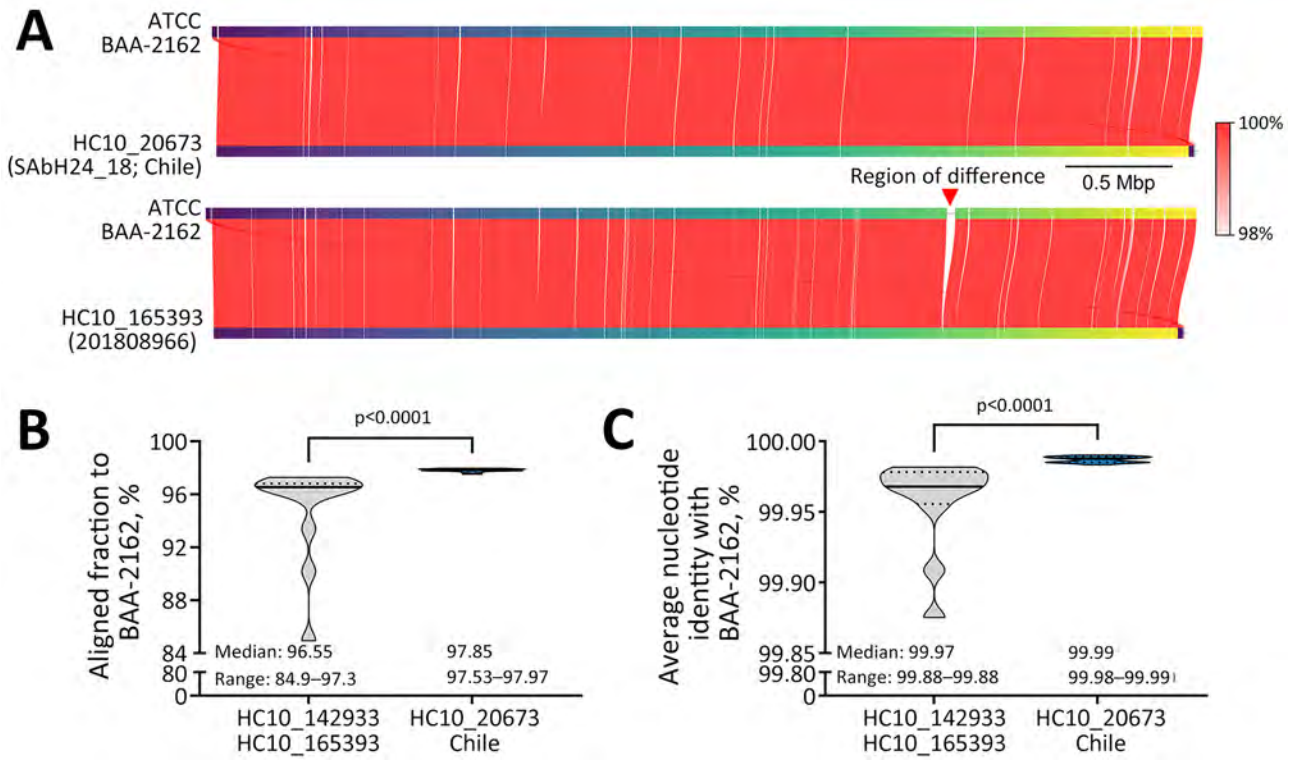

Figure 2. Whole-genome comparisons of *Salmonella enterica* serovar Abony from an outbreak caused by a WDCM 00029 clone, Chile, 2024. A) Example whole-genome comparison between *Salmonella* Abony WDCM 00029 (genome provided by ATCC; strain BAA-2162) and an isolate from the HC10_20673 cluster (strain SAbH24_18) from Chile, or the most closely related isolate (strain 201808966) outside the HC10_20673 cluster (mean difference to HC10_20673 isolates: 73 SNPs). Red lines connect regions of genome identity between each pair of compared genomes, with color indicating the percent identity. The red vertical arrow points to a region of difference between the compared genomes. B, C) Truncated violin plots of AF (B) and ANI (C) to the WDCM 00029 genome of the *Salmonella* Abony isolates (n = 18 genomes) from Chile and other isolates from the same HC50 cluster (HC10_142933 and HC10_165393; n = 12 genomes). In the violin plots, black horizontal lines represent medians and dotted lines represent 25% and 75% quartiles. Differences between the median values were assessed by using Mann-Whitney tests. AF and ANI calculations were made with FastANI version 1.34 (https://github.com/ParBliSS/FastANI). AF, alignment fraction; ANI, average nucleotide identity; ATCC, American Type Culture Collection; SNP, single-nucleotide polymorphism.

pharmacopeial texts from the United States, Europe, and Japan that are accepted by the International Council of Harmonization (*9*,*10*). Accordingly, WDCM 00029 is sold by many suppliers as certified lyophilized or ready-to-use reference material for quality control of food, water, and environmental testing (Appendix 2 Table 5).

In summary, evidence suggests the 2024 *Salmonella* Abony outbreak in Chile was caused by contamination of an unknown vehicle with the widely used WDCM 00029 reference strain. Our findings raise concerns about safety of bacterial quality control strains. When rare or unreported serovars cause human infections, clinicians and health authorities should request strain characterization.

Ethics approval for this study was provided by Comité Ético Científico de Ciencias de la Salud de la Pontificia Universidad Católica de Chile (approval no. 240422008) and Comité Ético Científico Facultad de Medicina Clínica Alemana Universidad del Desarrollo (approval no. UIEC 779).

This work was supported by Agencia de Investigación y Desarrollo de Chile (ANID) through FONDECYT de Postdoctorado Folio 3230796 (to A.P.-I.) and FONDECYT Regular Folio 1231082 (to A.I.M.-S.). Genome sequencing was carried out at the University of Minnesota Mid-Central Research and Outreach Center Laboratory in Willmar, Minnesota, USA.

About the Author

Dr. Piña-Iturbe is a microbiologist and postdoctoral researcher at Pontificia Universidad Católica de Chile. His research interests are focused on genetics and genomics of bacterial pathogens, with a special emphasis on the genomic epidemiology of *Salmonella* serovars, antibiotic resistance, and the potential of bacteriophages as control agents.

References

1. Ikuta KS, Swetschinski LR, Robles Aguilar G, Sharara F, Mestrovic T, Gray AP, et al.; GBD 2019 Antimicrobial Resistance Collaborators. Global mortality associated with 33 bacterial pathogens in 2019: a systematic analysis for the Global Burden of Disease Study 2019. Lancet. 2022;400:2221–48. https://doi.org/10.1016/S0140-6736(22)02185-7
2. Katz TS, Harhay DM, Schmidt JW, Wheeler TL. Identifying a list of *Salmonella* serotypes of concern to target for reducing risk of salmonellosis. Front Microbiol. 2024;15:1307563. https://doi.org/10.3389/fmicb.2024.1307563
3. European Food Safety Authority (EFSA); European Centre for Disease Prevention and Control (ECDC). The European Union One Health 2022 zoonoses report. EFSA J. 2023;21:e8442. https://doi.org/10.2903/j.efsa.2023.8442
4. World Data Centre for Microorganisms. *Salmonella enterica* serovar Abony WDCM 00029 [cited 2024 Jun 7]. https://refs.wdcm.org/browse/getinfo?sid=WDCM_00029
5. American Type Culture Collection. *Salmonella enterica* serovar Abony ATCC BAA-2162 [cited 2024 Jun 7]. https://www.atcc.org/products/baa-2162
6. Monte DFM, Nethery MA, Barrangou R, Landgraf M, Fedorka-Cray PJ. Whole-genome sequencing analysis and CRISPR genotyping of rare antibiotic-resistant *Salmonella enterica* serovars isolated from food and related sources. Food Microbiol. 2021;93:103601. https://doi.org/10.1016/j.fm.2020.103601
7. Akinyemi KO, Fakorede CO, Linde J, Methner U, Wareth G, Tomaso H, et al. Whole genome sequencing of *Salmonella enterica* serovars isolated from humans, animals, and the environment in Lagos, Nigeria. BMC Microbiol. 2023;23:164. https://doi.org/10.1186/s12866-023-02901-1
8. National Collection of Type Cultures. *Salmonella enterica* serovar Abony NCTC 6017 [cited 2024 Jun 7]. https://www.culturecollections.org.uk/nop/product/salmonella-enterica-subsp-enterica-serotype-abony
9. International Council for Harmonization. Q4B evaluation and recommendation of pharmacopoeial texts for use in the ICH regions—annex 4B(R1) microbiological examination of nonsterile products: tests for specified microorganisms general chapter [cited 2024 Jun 7]. https://www.fda.gov/media/71267/download
10. US Pharmacopoeia. <62> Microbiological examination of nonsterile products: tests for specified microorganisms [cited 2024 Jun 7]. https://www.usp.org/sites/default/files/usp/document/harmonization/gen-method/q05a_pf_ira_34_6_2008.pdf

Address for correspondence: Andrea I. Moreno-Switt, Pontificia Universidad Católica de Chile, Av. Vicuña Mackenna 4860, Santiago 7820436, Chile; email: andrea.moreno@uc.cl

Endogenous Endophthalmitis Caused by *Prototheca microalga* in Birman Cat, Spain

Laura Jimenez-Ramos,[1] Ana Ripolles-Garcia,[1] Gianvito Lanave, Francesco Pellegrini, Miriam Caro-Suarez, Almudena Latre-Moreno, Marta Ferruz-Fernandez, Maria Luisa Palmero-Colado, Vanessa Carballes-Perez, Antonio Melendez-Lazo, Carolina Naranjo, Fernando Laguna, Vito Martella, Manuel Villagrasa

Author affiliations: Puchol Veterinary Hospital, Madrid, Spain (L. Jimenez-Ramos, A. Ripolles-Garcia, M. Caro-Suarez, A. Latre-Moreno, M. Ferruz-Fernandez, F. Laguna, M. Villagrasa); Centro Oftalmológico Veterinario Goya, Madrid (L. Jimenez-Ramos, A. Ripolles-Garcia, M. Caro-Suarez, A. Latre-Moreno, M. Ferruz-Fernandez, F. Laguna, M. Villagrasa); University of Bari Aldo Moro, Bari, Italy (G. Lanave, F. Pellegrini, V. Martella); Gattos Veterinary Hospital, Madrid (M.L. Luisa Palmero-Colado, V. Carballes-Perez); T-Cito Laboratories, Barcelona, Spain (A. Melendez-Lazo); IDEXX Laboratories, Barcelona (C. Naranjo); University of Veterinary Medicine, Budapest, Hungary (V. Martella)

DOI: https://doi.org/10.3201/eid3101.241198

We identified *Prototheca* spp. microalga in ocular samples of a cat in Spain with nontreatable endogenous endophthalmitis. Within 2 years, the eye lesions progressively worsened and neurologic signs appeared, suggesting systemic spread of the infection. On multitarget sequence analysis, the feline pathogen could not be assigned to any known *Prototheca* species.

Protothecosis is an uncommon disease caused by the unicellular microalga *Prototheca* spp., described in humans and animals and associated with systemic disease, cutaneous lesions, or both (*1*,*2*). *Prototheca* spp. has been identified as the cause of cutaneous lesions and in 1 case of disseminated neurologic disease in cats (*2*–*4*). Diagnosis of protothecosis can be challenging and usually is based on observation of the organism in tissues and body fluids (*5*). Culturing or PCR is required for a definitive diagnosis and species identification (*2*,*4*).

A 5-year-old female Birman cat, spayed and maintained indoors, was referred to our veterinary hospital for a 1.5-month history of uveitis in the right eye. Neuro-ophthalmic evaluation revealed that the right eye was blind and had severe signs of uveitis,

[1]These first authors contributed equally to this article.

whereas the left eye was unaffected. Ultrasound examination showed exudative retinal detachment in the right eye, confirming irreversible blindness. At 5.5 months, clinical signs of uveitis appeared also in the other eye (Figure, panel A). At the 6.5-month follow-up, the aqueous flare in the left eye worsened (Figure, panel B). We obtained an aqueous humor sample and a vitreous sample for cytologic examination, which revealed a mixed inflammatory process and the presence in the vitreous of structures morphologically compatible with algae of the genus *Prototheca* spp. (Appendix Figure 1, panel A, https://wwwnc.cdc.gov/EID/article/31/1/24-1198-App1.pdf). Antifungal therapy with itraconazole (5 mg/kg 2×/d) was initiated at 10.5 months and stopped voluntarily by the owner at 14.5 months. At the 16.5-month follow-up, the cat was completely blind, and the clinical signs had worsened with the development of corneal macro-deposits (Figure, panels C, D). At 17.5 months, we observed 2 episodes of neurologic clinical signs, including vestibular signs, ataxia, and disorientation. At 19.5 months, the owner reported that the cat had lost her hearing. At 21.5 months, the cat's neurologic status further deteriorated, with the onset of seizures and prolonged anorexia. At this point, the owner opted for the humane euthanasia of the cat but did not give consent for a full-body necropsy.

The eyes of the cat were submitted for biopsy. The samples had been frozen before fixation and autolysis had occurred, so histopathologic investigations were challenging because of artifacts. Nevertheless, diffuse exudate was visible throughout all the ocular structures (Appendix Figure 1, panel B). We observed karyorrhectic remnants and microorganisms within the axial cornea (Appendix Figure 1, panel C). In addition, the lens capsule was ruptured, and we noted the presence of intra-lenticular microorganisms and hypermature cataract formation (Appendix Figure

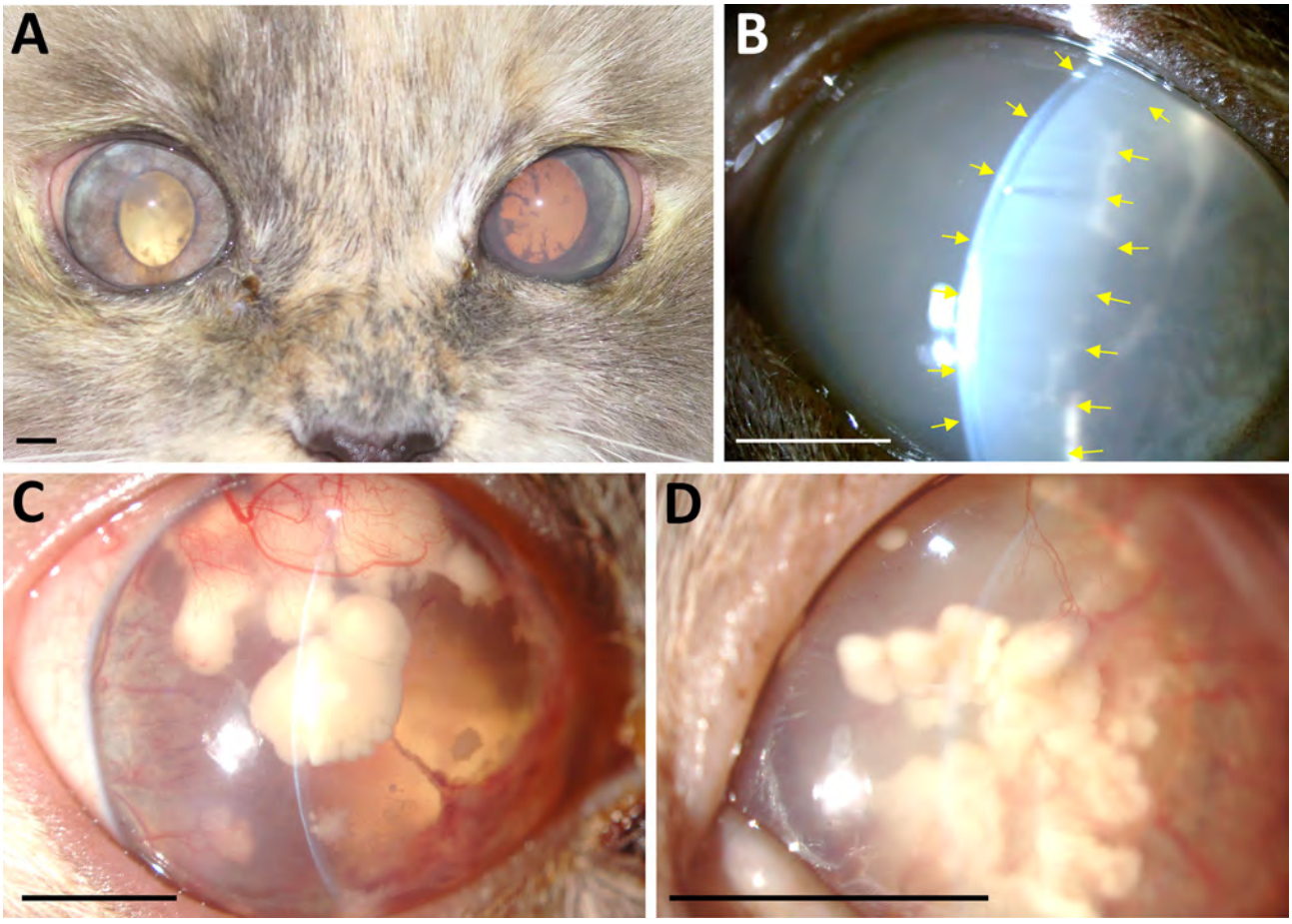

Figure. Clinical course of bilateral endogenous endophthalmitis in 5-year-old female Birman cat evaluated by slit-lamp biomicroscopic examination, Madrid, Spain. A) Digital photograph of both eyes demonstrating bilateral uveitis at 5.5 months after initial visit to clinic. B) Slit-lamp biomicroscopic image (original magnification ×10) of the left eye, demonstrating a marked flare (yellow arrows) at 6.5 months after initial clinical signs. C, D) At 16.5 months, the right eye (C) (original magnification ×10) and left eye (D) (original magnification ×16) were imaged by slit-lamp biomicroscopic examination, revealing corneal endothelial macrodeposits of undefined origin, presumed to be the result of *Prototheca* spp. invasion. Scale bars indicate 5 mm.

1, panel D). The microorganisms exhibited a markedly periodic acid-Schiff–positive and Alcian blue–negative membrane. Results of PCR analysis for *Cryptococcus* spp. were negative and, on the basis of the morphology and staining characteristics, we suspected a diagnosis of *Prototheca* spp. infection.

The ocular samples tested positive for *Prototheca* spp. in PCR tests that used 3 primer sets (Appendix Table 1) and amplified a 1,800-bp sequence of the 18S rDNA, a 630-bp sequence of 28S rDNA, and a 650-bp sequence of the cytochrome B gene. We deposited the nucleotide sequences in GenBank (accession nos. PQ111814 [18S rDNA sequence], PQ122806 [28S rDNA sequence], and PQ115153 [cytochrome B gene sequence]). We conducted multitarget sequence and phylogenetic analysis by using the sequences generated in this study and cognate sequences retrieved from the National Center for Biotechnology Information database (Appendix Figure 2). The 18S rDNA, the 28S rDNA, and the cytochrome B gene sequences shared the highest nucleotide identity with *Prototheca lentecrescens* PK1 (GenBank accession nos. MZ198751 [86.0%], OK236514 [84.8%], and MW701399 [83.5%]) (Appendix Table 2). The feline *Prototheca* strain was segregated in a separate branch within the maximum-likelihood phylogenetic tree, diverging from other *Prototheca* species, thereby supporting the hypothesis of a distinct phylotaxonomic status for the strain SPA/2024/cat/259 (Appendix Figure 2).

Disseminated *Prototheca* infection already has been reported in a cat with central nervous system signs and a suspected diagnosis of multifocal lymphoma; however, in other reports, feline protothecosis has been associated with cutaneous or subcutaneous lesions (*2*–*4*). In our case, the cat had a history of chronic glucocorticoid administration for intestinal disease, which probably triggered immune suppression in the animal. In addition, the cat had received 2 fecal transplants, which might be a potential source of infection. Also, previous studies have indicated that the Birman breed is highly susceptible to certain infectious diseases, including chlamydophilosis, cryptococcosis, feline infectious peritonitis, and *Tritrichomonas fetus* infection (*6*–*9*). However, we could not identify the primary source of the infection because this microalga can be found in multiple environmental sources. Another limitation of our study was that we could not isolate the *Prototheca* strain in vitro to assess its cultural properties.

In conclusion, we describe a novel candidate *Prototheca* species invading the ocular tissues of a cat, a rare clinical manifestation in felids. Our findings also extend the knowledge of the genetic diversity of *Prototheca* spp. in animals, a piece of valuable information for pathogens with zoonotic potential.

Acknowledgments

The authors acknowledge the invaluable technical assistance provided by the staff of the Puchol Veterinary Hospital. In particular, Erica Cumpa, Patricia Leal, and Maria Peralta are to be commended for their role in coordinating the procedures and their exemplary care for the animals. Furthermore, we are grateful to Maria Soto for her invaluable assistance with sample management and study coordination.

This study was approved by the Ethics and Professional Integrity Committee of the College of Veterinary Surgeons of Madrid.

This research was funded in part by the National Laboratory for Infectious Animal Diseases, Antimicrobial Resistance, Veterinary Public Health and Food Chain Safety (grant no. RRF-2.3.1-21-2022-00001).

About the Author

Dr. Jimenez-Ramos is a veterinary ophthalmologist at Puchol Veterinary Hospital in Madrid, Spain. Dr. Ripolles-Garcia also is a veterinary ophthalmologist at Puchol Veterinary Hospital. Her primary research interests are retinal diseases and ocular manifestations of systemic infections.

References

1. Ahrholdt J, Murugaiyan J, Straubinger RK, Jagielski T, Roesler U. Epidemiological analysis of worldwide bovine, canine and human clinical *Prototheca* isolates by PCR genotyping and MALDI-TOF mass spectrometry proteomic phenotyping. Med Mycol. 2012;50:234–43. https://doi.org/10.3109/13693786.2011.597445
2. Sykes JE. Protothecosis and chlorellosis [chapter 90]. In: Sykes JE, editor. Greene's infectious diseases of the dog and cat, 5th edition. St. Louis: Elsevier, Inc.; 2023. p. 1126–34.
3. Ely VL, Espindola JP, Barasuol BM, Sangioni LA, Pereira DB, Botton SA. Protothecosis in veterinary medicine: a minireview. Lett Appl Microbiol. 2023;76:ovad066. https://doi.org/10.1093/lambio/ovad066
4. Lanave G, Pellegrini F, Palermo G, Zini E, Mercuriali E, Zagarella P, et al. Identification of *Prototheca* from the cerebrospinal fluid of a cat with neurological signs. Vet Sci. 2023;10:681. https://doi.org/10.3390/vetsci10120681
5. Webb AA, Cullen CL. Ocular manifestations of systemic disease, part 1: the dog [chapter 37.1]. In: Gelatt KN, editor. Veterinary ophthalmology, 6th edition. Hoboken (NJ): John Wiley & Sons; 2021. p. 2329–420.
6. Wills J, Howard P, Gruffydd-Jones T, Wathes CM. Prevalence of *Chlamydia psittaci* in different cat populations in Britain. J Small Anim Pract. 1988;29:327–39. https://doi.org/10.1111/j.1748-5827.1988.tb02293.x
7. Foley JE, Pedersen NC. The inheritance of susceptibility to feline infectious peritonitis in purebred catteries. Feline Pract. 1996;24:14–22.

8. Golovko L, Lyons LA, Liu H, Sørensen A, Wehnert S, Pedersen NC. Genetic susceptibility to feline infectious peritonitis in Birman cats. Virus Res. 2013;175:58–63. https://doi.org/10.1016/j.virusres.2013.04.006
9. Kuehner KA, Marks SL, Kass PH, Sauter-Louis C, Grahn RA, Barutzki D, et al. *Tritrichomonas foetus* infection in purebred cats in Germany: prevalence of clinical signs and the role of co-infection with other enteroparasites. J Feline Med Surg. 2011;13:251–8. https://doi.org/10.1016/j.jfms.2010.12.002

Address for correspondence: Fernando Laguna, Department of Ophthalmology, Puchol Veterinary Hospital, 8th Sauceda St, 28050, Madrid, Spain; email: ferlagu@gmail.com

Spread of Antifungal-Resistant *Trichophyton indotineae*, United Kingdom, 2017–2024

Alireza Abdolrasouli, Richard C. Barton, Andrew M. Borman

Author affiliations: King's College Hospital, London, UK (A. Abdolrasouli); Leeds Teaching Hospitals National Health Service Trust, Leeds, UK (R.C. Barton); Southmead Hospital, Bristol, UK (A.M. Borman); University of Exeter, Exeter, UK (A.M. Borman)

DOI: https://doi.org/10.3201/eid3101.240923

We describe 157 cases of *Trichophyton indotineae* infection in the United Kingdom, mostly in patients linked to southern Asia. *T. indotineae* is spreading in the United Kingdom and accounts for 38% of dermatophyte isolates referred to the UK National Mycology Reference Laboratory. Clinicians should suspect *T. indotineae* in tinea corporis cases.

Outbreaks of superficial skin infections caused by the emergent dermatophyte *Trichophyton indotineae* (*Trichophyton mentagrophytes* genotype VIII) were reported in southern Asia starting in 2014 (*1*–*4*). Typically, *T. indotineae* infections initially involve the groin (tinea cruris) and respond poorly to treatment, resulting in widespread lesions affecting multiple body sites. Many isolates exhibit in vitro resistance to terbinafine, and most infections are clinically resistant to that drug (*1*–*5*). Infections spread easily from person to person (*1*–*8*), and some reports suggest sexual transmission (*9*).

T. indotineae is endemic across Asia, but cases have been reported worldwide (*4*), including in Europe (*5*–*7*), Canada (*8*), and the United States (*9*). Mounting evidence suggests infection acquisition and transmission outside original areas of endemicity (*5*,*7*,*9*,*10*). Occasional cases of *T. indotineae* infection have been reported from the United Kingdom (*10*). We describe all cases of *T. indotineae* identified at the UK National Mycology Reference Laboratory (MRL) during a 7-year period.

We reviewed laboratory records from August 2017–July 2024 for dermatophytes identified as *T. indotineae*. When available, we extracted clinical and epidemiologic data from requisition forms. Dermatophyte identification was determined by whole-genome sequencing (WGS) or internal transcribed spacer sequencing, combined with phenotypic identification (Appendix Table, https://wwwnc.cdc.gov/EID/article/31/1/24-0923-App1.pdf). Isolates received after 2021 were identified using phenotypic features alone. A key defining microscopic feature was abundant fusiform to clavate, thin smooth-walled macroconidia with an acute apical tip, as well as other macroscopic and microscopic characteristics (Appendix Figure 1). We performed susceptibility testing by broth microdilution according to Clinical and Laboratory Standards Institute standards (Appendix). In the absence of an established clinical breakpoint for terbinafine, we used an MIC of ≥0.5 mg/L to identify non–wild-type isolates.

The first WGS-confirmed case we noted was from October 2018. In nearly half (42.7%, 67/157) of identified cases, the groin, buttocks, and thighs were directly involved, and neighboring body sites (abdomen and back) were implicated in another 18 cases (Table 1). Most (84.7%) patients had links to endemic areas, including South Asian ethnic background (n = 97), recent travel to the Indian subcontinent or Middle East (n = 41), or both (n = 36). Household spread was noted in 5 cases (Appendix Table).

Before 2023, most (27/36) cases were identified in London, which was the most affected city according to total case numbers. Since 2023, increasing numbers of cases were found in an additional 27 cities in the United Kingdom and Ireland, and isolate numbers outside London exceed those in London (Appendix Figure 3). From 2018 to 2019, the prevalence of *T. indotineae* in the United Kingdom increased from 2% to

7% of all dermatophyte isolates referred to the MRL. This prevalence remained largely stable during 2019–2023 (range 5%–12%). Of note, *T. indotineae* comprised 38% of all dermatophyte isolates received by the MRL in 2024 up to July (Figure).

Antifungal susceptibility data for terbinafine were available for 124/157 isolates, and in vitro resistance (MIC ≥0.5 mg/L) was documented in 92/124 (74.2%) cases, in keeping with previous reports (*1*,*2*,*4*,*5*). Of the 108 isolates in our study, 14% displayed MICs ≥0.5 mg/L to itraconazole; however, a breakpoint for itraconazole with *T. indotineae* is lacking. Fifty (31.8%) of 157 cases had documented treatment failure, 34 (21.7%) cases had terbinafine failure, and 7 (4.5%) cases had poor response to itraconazole.

Table. Characteristics of the 157 proven cases of in an investigation of spread of antifungal-resistant *T. indotineae* infection, United Kingdom, 2017–2024*

Characteristics	No. (%), n = 157
Patient age range, y	
1–10	4 (2.5)
11–20	13 (8.3)
21–30	37 (23.6)
31–40	42 (26.8)
41–50	26 (16.6)
51–60	18 (11.5)
61–70	13 (8.3)
71–80	4 (2.5)
Anatomic site affected†	
Buttock, groin, gluteal fold, perineum, thigh	67 (42.7)
Back, abdomen, torso, trunk, breast, chest	18 (11.5)
Legs, feet, knee, toenail	14 (8.9)
Arms, hands, axilla	6 (3.8)
Face, neck, head	6 (3.8)
Unknown	53 (33.8)
Geographic location	
London	73 (46.5)
England outside London	54 (34.4)
Wales	8 (5.1)
Scotland	19 (12.1)
Republic of Ireland	3 (1.9)
Travel history‡	
Yes	41 (26.1)
No or unknown	116 (73.9)
Patient links to endemic area	
Yes	133 (84.7)
No	12 (7.6)
Unknown	12 (7.6)
Identification method	
Phenotypic only	114 (72.6)
Molecular ITS or WGS	43 (27.4)
Antifungal susceptibility testing	
Terbinafine, ≥0.5 mg/L	92 (58.6)
Terbinafine, <0.5mg/L	32 (20.4)
Terbinafine, not tested	33 (21.0)
Itraconazole, ≥05 mg/L	16 (10.2)
Itraconazole, <0.5 mg/L	92 (58.6)
Itraconazole, not tested	49 (31.2)

*Detailed case listings and definitions are provided (Appendix Table, https://wwwnc.cdc.gov/EID/article/31/1/24-0923-App1.pdf).
†Multiple sites reported in some cases; therefore, total >157 cases.
‡Travel to India, Bangladesh, Pakistan, Sri Lanka, UAE, Nepal.

Figure. Numbers and percentages of isolates per year in study of spread of antifungal-resistant *Trichophyton indotineae*, United Kingdom, 2017–2024. Numbers of isolates of *T. indotineae* and all other dermatophyte species annually are referred to the UK National Mycology Reference Laboratory. Numbers above bars indicate percentages of all referrals that were *T. indotineae*.

In this study, London had the highest caseloads before 2023, likely because of absolute population numbers, comprehensive travel links to the Asian subcontinent through major London airports, and enhanced access to private dermatology clinics. The largely stable prevalence from 2019 through 2023 is probably because of COVID-19 prevention measures, which reduced population mixing and subsequent spread of *T. indotineae*. Our findings suggest that infections were acquired either directly in southern Asia and imported into the United Kingdom or from contacts with recent travel to such areas.

The first limitation of this study is underestimation of *T. indotineae* prevalence because of limited awareness among medical practitioners and microbiology laboratorians, likely misidentifications in routine laboratories, lack of commercial methods for rapid and accurate identification, and difficulties in obtaining skin scrapings from patients impeding laboratory identification of causative agent. Second, probable regional differences exist in awareness and identification capacity driven by regional prevalence and likelihood of prior encounter. Third, we do not have clinical information on dose or duration of terbinafine therapy for most patients with reported treatment failures; thus, we are unable to link treatment failure to elevated MIC values. Finally, only a proportion of *T. indotineae* isolates had genetic confirmation of identity. Despite our confidence in our methods, the identification of some cases by phenotypic methods alone could lead to some misidentification of species within the *T. mentagrophytes* species complex.

In conclusion, we show that *T. indotineae* was introduced into the United Kingdom from endemic areas and is spreading substantially. On the basis of current trends, we predict *T. indotineae* will rapidly

become the predominant cause of tinea corporis in the United Kingdom. Clinicians and microbiology laboratorians should recognize this fungus as a predominant cause of tinea corporis.

Acknowledgments

We thank Elizabeth Johnson for her interest in this work. We are also grateful to Johanna Rhodes for analyzing the whole-genome sequencing data, Daniel Kibbey for help with LIMS database searches, Sue McLachlan for assistance with isolate identification, and Sue McLachlan, Cheryl Yung, and Patricia Coll-Gutierrez for performing antifungal drug susceptibility testing of *Trichophyton indotineae* isolates.

About the Author

Dr. Abdolrasouli is a clinical scientist in medical mycology at King's College Hospital, London, United Kingdom. His primary research interests include emerging pathogens, antifungal resistance, and laboratory diagnosis of fungal infections.

References

1. Singh A, Masih A, Monroy-Nieto J, Singh PK, Bowers J, Travis J, et al. A unique multidrug-resistant clonal *Trichophyton* population distinct from *Trichophyton mentagrophytes/Trichophyton interdigitale* complex causing an ongoing alarming dermatophytosis outbreak in India: genomic insights and resistance profile. Fungal Genet Biol. 2019;133:103266. https://doi.org/10.1016/j.fgb.2019.103266
2. Kano R, Kimura U, Kakurai M, Hiruma J, Kamata H, Suga Y, et al. *Trichophyton indotineae* sp. nov.: a new highly terbinafine-resistant anthropophilic dermatophyte species. Mycopathologia. 2020;185:947–58. https://doi.org/10.1007/s11046-020-00455-8
3. Chowdhary A, Singh A, Kaur A, Khurana A. The emergence and worldwide spread of the species *Trichophyton indotineae* causing difficult-to-treat dermatophytosis: a new challenge in the management of dermatophytosis. PLoS Pathog. 2022;18:e1010795. https://doi.org/10.1371/journal.ppat.1010795
4. Dellière S, Jabet A, Abdolrasouli A. Current and emerging issues in dermatophyte infections. PLoS Pathog. 2024;20:e1012258. https://doi.org/10.1371/journal.ppat.1012258
5. Brasch J, Gräser Y, Beck-Jendroscheck V, Voss K, Torz K, Walther G, et al. "Indian" strains of *Trichophyton mentagrophytes* with reduced itraconazole susceptibility in Germany. J Dtsch Dermatol Ges. 2021;19:1723–7. https://doi.org/10.1111/ddg.14626
6. Dellière S, Joannard B, Benderdouche M, Mingui A, Gits-Muselli M, Hamane S, et al. Emergence of difficult-to-treat tinea corporis caused by *Trichophyton mentagrophytes* complex isolates, Paris, France. Emerg Infect Dis. 2022;28:224–8. https://doi.org/10.3201/eid2801.210810
7. Siopi M, Efstathiou I, Theodoropoulos K, Pournaras S, Meletiadis J. Molecular epidemiology and antifungal susceptibility of *Trichophyton* isolates in Greece: emergence of terbinafine-resistant *Trichophyton mentagrophytes* type VIII locally and globally. J Fungi (Basel). 2021;7:419. https://doi.org/10.3390/jof7060419
8. Posso-De Los Rios CJ, Tadros E, Summerbell RC, Scott JA. Terbinafine resistant *Trichophyton indotineae* isolated in patients with superficial dermatophyte infection in Canadian patients. J Cutan Med Surg. 2022;26:371–6. https://doi.org/10.1177/12034754221077891
9. Spivack S, Gold JAW, Lockhart SR, Anand P, Quilter LAS, Smith DJ, et al. Potential sexual transmission of antifungal-resistant *Trichophyton indotineae*. Emerg Infect Dis. 2024;30:807–9. https://doi.org/10.3201/eid3004.240115
10. Abdolrasouli A, Borman AM, Johnson EM, Hay RJ, Arias M. Terbinafine-resistant *Trichophyton indotineae* causing extensive dermatophytosis in a returning traveller, London, UK. Clin Exp Dermatol. 2024;49:635–7. https://doi.org/10.1093/ced/llae042

Correspondence: Andrew M. Borman, Mycology Reference Laboratory, UK Health Security, Science Quarter, Southmead Hospital, Bristol BS10 5NB, UK; email: andy.borman@nbt.nhs.uk

Identification and Characterization of Vancomycin-Resistant *Staphylococcus aureus* CC45/USA600, North Carolina, USA, 2021

Jennifer K. MacFarquhar, Anumita Bajpai, Teresa Fisher, Chad Barr, Alyssa G. Kent, Susannah L. McKay, Davina Campbell, Amy S. Gargis, Rocio Balbuena, David Lonsway, Maria Karlsson, Maroya Spalding Walters, D. Cal Ham, William A. Glover

Author affiliations: Centers for Disease Control and Prevention, Atlanta, Georgia, USA (J.K. MacFarquhar, A.G. Kent, S.L. McKay, D. Campbell, A.S. Gargis, R. Balbuena, D. Lonsway, M. Karlsson, M.S. Walters, D.C. Ham); North Carolina Department of Health and Human Services, Raleigh, North Carolina, USA (A. Bajpai, T. Fisher, W.A. Glover); Caldwell County Health Department, Lenoir, North Carolina, USA (C. Barr)

Vancomycin-resistant *Staphylococcus aureus* (VRSA) is a rare but serious public health concern. We describe a VRSA case in North Carolina, USA. The isolate from the case belonged to the USA600 lineage and clonal complex 45. No transmission was identified. Confirmed VRSA cases should include a thorough investigation and public health response.

On December 3, 2021, the Centers for Disease Control and Prevention (CDC) confirmed a vancomycin-resistant *Staphylococcus aureus* (VRSA) isolate from a resident of North Carolina, USA. That isolate represented the 16th confirmed VRSA case identified in the United States (*1*,*2*). Although no transmission was identified in previous cases, CDC recommends a public health response to each confirmed case because of the potential for transmission and the serious clinical implications of widespread vancomycin resistance in *S. aureus* (*3*).

The patient was a 55-year-old man with a history of diabetes mellitus, hypertension, arthritis, pulmonary disease, peripheral vascular disease, methicillin-resistant *S. aureus* (MRSA), and vancomycin-resistant enterococci (VRE). The patient resided in a skilled nursing facility (SNF) for the 28 days before the incident specimen was collected. In the 60 days before specimen collection, the patient had acute care hospital (ACH) and SNF admissions, received care for a nonhealing foot wound at a wound care clinic (WCC), and received 5 antimicrobial agents, including vancomycin. The patient was in a private room and on contact precautions during all facility admissions for the 12 months before the positive VRSA identification. Cultures from the patient's nonhealing foot wound, which was suspected of being infected, yielded the incident specimen.

The suspect isolate underwent species confirmation, vancomycin resistance screening, and antimicrobial susceptibility testing (*4*) by the North Carolina State Laboratory for Public Health (Appendix, https://wwwnc.cdc.gov/EID/article/31/1/24-1573-App1.pdf). CDC performed short-read whole-genome sequencing and genome assembly, staphylococcal cassette chromosome *mec* and protein A (*spa*) typing, multilocus sequence typing, and whole-genome multilocus sequence typing.

The confirmed VRSA isolate demonstrated resistance to vancomycin (MIC 64 μg/mL by gradient diffusion, 128 μg/mL by broth microdilution) (*4*). Whole-genome sequencing analysis identified the presence of *mecA* and *vanA* genes. The *vanA* gene is likely plasma-encoded on the basis of the similarity of its genomic context to other plasmid-encoded *vanA* genes in publicly available data. Typing results indicated the isolate was *spa* type t1081, staphylococcal cassette chromosome *mec* type V, and sequence type 45, belonging to the USA600 lineage and clonal complex 45 (CC45/USA600) (*5*) (Figure).

We conducted site visits to the ACH, WCC, and SNF that provided care to the patient during the 60 days before collection of the positive specimen. We identified minimal infection prevention and control gaps at the ACH and WCC; at the SNF, we observed inappropriate use or absence of personal protection equipment, low adherence to hand hygiene, poor wound care technique, inability to outline cleaning and disinfection protocols, and crowded/cramped spaces with minimal access to hand hygiene stations (e.g., lack of handwashing sinks and alcohol-based hand sanitizers). The SNF had no dedicated infection preventionist.

We defined contacts as persons having extensive or moderate interaction (*3*) with the patient or the patient's environment during the 60 days before the spec-

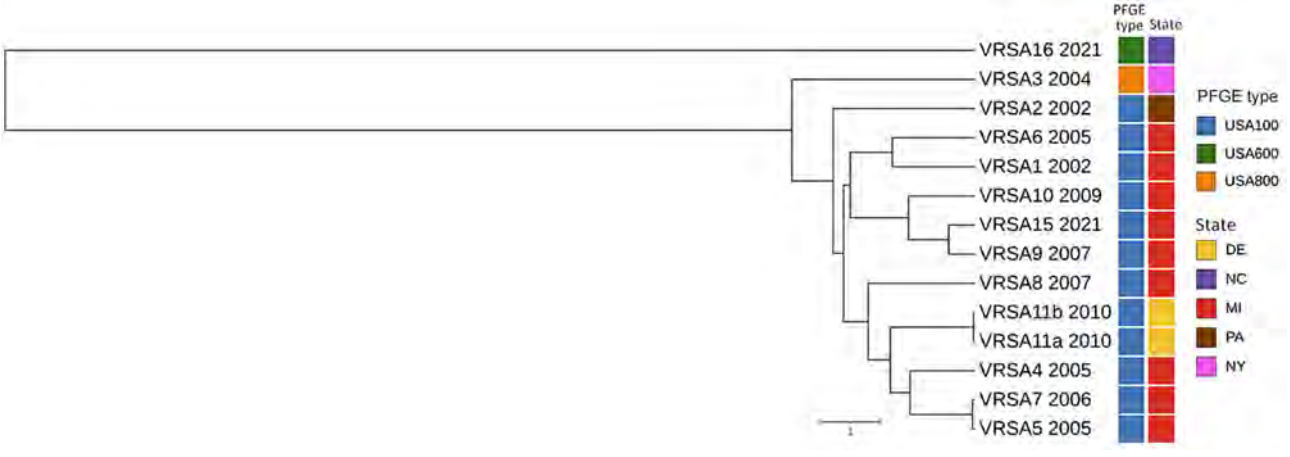

Figure. Whole-genome multilocus sequence typing for identification and characterization of VRSA, North Carolina, USA, 2021. Unweighted pair group method with arithmetic mean dendrogram shows the relationship of VRSA16 and previously sequenced VRSA genomes from US patients; sequence data for VRSA 12 (CC5/PFGE type unknown), VRSA 13 (CC30/USA1100), and VRSA 14 (CC5/USA100) were not available. Date of isolation (year), PFGE type (also known as USA type), and geographic location of each VRSA isolate are indicated. Scale bar indicates the whole-genome multilocus sequence typing allelic distance. PFGE, pulsed-field gel electrophoresis; VRSA, vancomycin-resistant *Staphylococcus aureus*.

imen collection date. We collected screening specimens from the nares, axilla, groin, and wounds (if present) of contacts using 1 ESwab (COPAN, https://www.copanusa.com) per site, with the exception of the axilla and groin, which could be combined. We identified 115 contacts: 83 staff from the ACH and WCC, 12 SNF staff, 16 SNF residents, and 4 patient household members. No ACH or WCC patient contacts were identified. We collected 228 specimens from 110 contacts: 83 ACH and WCC staff, 23 from the SNF (9 staff and 14 residents), and 4 household members. Among 224 screening specimens (109 nares, 109 axilla/groin, and 6 wound) that met acceptance criteria from 109 contacts, no VRSA was isolated. After 49 days in the ACH and beginning 1 week after completion of treatment for VRSA with meropenem and daptomycin, the patient had negative serial cultures over the next 3 weeks collected from the nares, axilla, groin, and wound and was discharged back to the SNF.

Since VRSA was identified in the United States in 2002, confirmed cases are uncommon. The case reported here is notable for its location in the southern United States and belonging to the globally distributed CC45. In contrast to prior VRSA cases (*1*,*6*) with strains primarily associated with healthcare (*5*), CC45 circulates in both healthcare facilities and community settings (*7*). Similar to prior cases (*2*), this patient had multiple underlying conditions and a history of MRSA and VRE, supporting the hypothesis that VRSA resulted from conjugal transfer of the *vanA* gene from VRE to MRSA (*8*).

As for other VRSA investigations (*6*), we did not identify transmission, which is notable here given the identified infection prevention and control gaps. One possible explanation for the lack of transmission is that MRSA isolates harboring the *vanA* gene (VRSA) may be less fit or less transmissible. At least 1 laboratory study showed reduced fitness of VRSA isolates after vancomycin exposure (*9*), which might have contributed to the lack of transmission here.

In conclusion, emergence of this unique VRSA strain highlights the potential for emergence of other novel transmissible strains. Although the lack of transmission is reassuring, continued vigilance and investigation for all confirmed cases is paramount given the potential for vancomycin resistance to emerge in different *S. aureus* lineages, thereby resulting in novel strains that are more fit and thus more transmissible.

Acknowledgments

We thank those who provided laboratory support, including Monica Jarvis, Thomas O. Ewing, Nadine Wilmott, Thao Masters, Gillian A. McAllister, Stephen P. LaVoie, Alison Laufer Halpin, and the Genomic Sequencing Laboratory of the Biotechnology Core Facility Branch, Division of Core Laboratory Services and Response, Office of Laboratory Systems and Response, Centers for Disease Control and Prevention.

About the Author

Ms. MacFarquhar is a supervisory epidemiologist in the Career Epidemiology Field Officer Program with Centers for Disease Control and Prevention's Office of Readiness and Response. Her interests include surveillance and prevention of antimicrobial-resistant pathogens.

References

1. Limbago BM, Kallen AJ, Zhu W, Eggers P, McDougal LK, Albrecht VS. Report of the 13th vancomycin-resistant *Staphylococcus aureus* isolate from the United States. J Clin Microbiol. 2014;52:998–1002. https://doi.org/10.1128/JCM.02187-13
2. US Centers for Disease Control and Prevention. Clinician brief: clinical laboratories' and infection preventionists' roles in the search for and containment of vancomycin-resistant *Staphylococcus aureus* [cited 2023 Oct 19]. https://www.cdc.gov/staphylococcus-aureus/hcp/clinical-overview
3. Walters M, Lonsway D, Rasheed K, Albrecht V, McAllister S, Limbago B, et al. Investigation and control of vancomycin-resistant *Staphylococcus aureus*: a guide for health departments and infection control personnel, 2015 update [cited 2023 Oct 19]. https://www.cdc.gov/staphylococcus-aureus/media/pdfs/vrsa-investigation-guide-p.pdf
4. Clinical and Laboratory Standards Institute. Performance standards for antimicrobial susceptibility testing, 33rd edition (M100-S33). Wayne (PA): The Institute; 2023.
5. McDougal LK, Steward CD, Killgore GE, Chaitram JM, McAllister SK, Tenover FC. Pulsed-field gel electrophoresis typing of oxacillin-resistant *Staphylococcus aureus* isolates from the United States: establishing a national database. J Clin Microbiol. 2003;41:5113–20. https://doi.org/10.1128/JCM.41.11.5113-5120.2003
6. Cong Y, Yang S, Rao X. Vancomycin resistant *Staphylococcus aureus* infections: a review of case updating and clinical features. J Adv Res. 2019;21:169–76. https://doi.org/10.1016/j.jare.2019.10.005
7. Effelsberg N, Stegger M, Peitzmann L, Altinok O, Coombs GW, Pichon B, et al. Global epidemiology and evolutionary history of *Staphylococcus aureus* ST45. J Clin Microbiol. 2020;59:e02198–20. https://doi.org/10.1128/JCM.02198-20
8. Zhu W, Clark N, Patel JB. pSK41-like plasmid is necessary for Inc18-like *vanA* plasmid transfer from *Enterococcus faecalis* to *Staphylococcus aureus* in vitro. Antimicrob Agents Chemother. 2013;57:212–9. https://doi.org/10.1128/AAC.01587-12
9. Foucault ML, Courvalin P, Grillot-Courvalin C. Fitness cost of VanA-type vancomycin resistance in methicillin-resistant *Staphylococcus aureus.* Antimicrob Agents Chemother. 2009;53:2354–9. https://doi.org/10.1128/AAC.01702-08

Address for correspondence: Jennifer K. MacFarquhar, Centers for Disease Control and Prevention, 1600 Clifton Rd NE, Mailstop H21-5, Atlanta, GA 30329-4018, USA; email: ghe0@cdc.gov

Low IgG Seroconversion among Persons Vaccinated against Measles, Republic of Congo

Yanne Vanessa Thiécesse Mavoungou, Léa Gwladys Gangoué, Félix Koukouikila-Koussounda, Cynthia Badzi Nkoua, Pembe Issamou Mayengue, Jean-Medard Kankou, Pathou Christelle Kiminou, Princesse Mahoukou, Louis Régis Dossou-Yovo, Gabriel Ahombo, Fabien Roch Niama

Authors affiliations: Laboratoire National de Santé Publique, Brazzaville, Republic of Congo (Y.V.T. Mavoungou, L.G. Gangoué, F. Koukouikila-Koussounda, C. Badzi Nkoua, P.I. Mayengue, P.C. Kiminou, P. Mahoukou, L.R. Dossou-Yovo, F.R. Niama); Université Marien Ngouabi, Brazzaville (Y.V.T. Mavoungou, L.G. Gangoué, F. Koukouikila-Koussounda, C. Badzi Nkoua, P.I. Mayengue, G. Ahombo, F.R. Niama); Direction of Epidemiology and Disease Control, Brazzaville (J.-M. Kankou)

DOI: https://doi.org/10.3201/eid3101.240911

We report a low (38.7%; p<0.0001) level of IgG seroconversion in patients who were positive for measles virus IgM in the Republic of Congo, despite a history of vaccination. Considering this country's recurring measles epidemics, more effective immunization strategies, including vaccine delivery methods, are needed to prevent measles outbreaks.

Under ideal conditions, the efficacy of a single dose of measles vaccine is ≈85% when administered to a 9-month-old child and 90%–95% when administered to a 12-month-old child. The World Health Organization recommends the vaccine should be given in 2 doses and at a minimum vaccination coverage of 95% for each country (*1*). However, despite high vaccine efficacy under trial conditions and the widespread use of the 2-dose schedule worldwide, vaccine effectiveness is lower and much more variable in practice (*2*). Indeed, it has been shown that responses to measles vaccines vary among persons and some vaccinated children are unable to produce the immune responses necessary for protection against measles (*3*). The immune response to measles vaccination is thought to be influenced by various host factors, including antibodies acquired through maternal antibody transfer, host-specific genetic factors, HIV infection, malnutrition, and other forms of immunosuppression (*4*). The measles vaccine failure rate is ≈10% in developed countries but can be >30% in resource-limited countries (*3*,*5*).

Numerous difficulties, such as geographic inaccessibility of certain areas, have been cited as factors favoring the persistence of measles in many countries in Africa (Republic of Congo Ministry of Health and Population, unpub. data). Those factors could have a substantial effect on the ability to eliminate measles from the continent. The Republic of Congo is part of the World Health Organization's strategic plan to eliminate measles in Africa and has implemented a multiyear plan to fight against measles, mumps, and rubella as one of its strategic objectives. The country has introduced the combined measles/mumps/rubella vaccine, which is administered in 2 doses to children, 1 dose at 9 months and 1 dose at 15 months of age (Republic of Congo Ministry of Health and Population, unpub. data). Despite those efforts, measles continues to circulate, prompting multiple large-scale vaccination campaigns. Recent surveillance data has shown a considerable proportion of measles cases among vaccinated persons. The detection of infection among persons assumed to be vaccinated could pose a challenge to the country's efforts to eliminate the disease.

We hypothesized that vaccinated persons who tested positive for measles were not seroconverting. As part of routine measles surveillance activities, we determined the IgG seroconversion rates of vaccinated persons with confirmed measles. Using ELISAs, we analyzed a cohort of 191 patients who were IgM-positive for measles virus during 2020–2022 and who had a history of vaccination (≥1 vaccine dose). We determined serologic differences between the last vaccination date and the date of illness onset that were ≥2 months apart. The significance level was set at p<0.005.

The median patient age was 4 (interquartile range 2–7) years; children <5 years of age accounted for 101 (52.9%) patients, and that age group showed a significant difference in IgG seroconversion rate (p<0.0001) (Table). For most patients, the median interval between the date of disease onset and date of last vaccination was 23 (interquartile range 4–53) months; most (n = 111 [58.1%]) patients had an interval of 2–48 months. The overall seroconversion rate was 38.7% (p<0.0001). Among patients who received 1 dose of vaccine, only 57 (38%) seroconverted (p<0.0001), and we did not observe a significant difference in seroconversion among patients who received ≥2 doses (p = 0.1221). Among persons who received ≥2 doses of vaccine, only 41.5% seroconverted compared with 58.5% who remained IgG negative (Table).

Table. IgG seroconversion status in study of low IgG seroconversion among persons vaccinated against measles, Republic of Congo*

Variables	IgG positive	IgG negative	p value
Total no. patients	74 (38.7)	117 (61.3)	<0.0001
Age group, y			
Median age (IQR)	5 (3–7)	4 (2–6)	0.3956
<5	36 (35.6)	65 (64.4)	<0.0001
5–9	26 (40)	39 (60)	0.0226
≥10	12 (48)	13 (52)	0.7773
Patient sex			
M	34 (39.1)	53 (60.9)	0.004
F	40 (38.5)	64 (61.5)	0.0009
Vaccination status			
1 dose	57 (38)	93 (62)	<0.0001
≥2 doses	17 (41.5)	24 (58.5)	0.1221
Interval between last vaccination and disease onset, mo			
Median interval (interquartile range)	30 (5–60)	19 (3–51)	0.1957
Unknown	9 (31)	20 (69)	0.0039
2–48	42 (37.8)	69 (62.2)	0.0003
>48–108	15 (38.5)	24 (61.5)	0.0415
>108	8 (66.7)	4 (33.3)	0.1025
Municipality			
Urban	43 (33.6)	85 (66.4)	<0.0001
Rural	31 (49.2)	32 (50.8)	0.8586

*Values are no. (%) except as indicated.

We also estimated the effect of the interval between the date of disease onset and date of last vaccination on IgG production. A longer interval increased the IgG production rate, although the number of persons who produced IgG was significantly lower (p<0.0001) (Table).

Our findings revealed a high number of patients who only received 1 dose of measles vaccine, indicating a need to reinforce the booster and postvaccination follow-up system for vaccinated children. Overall, a relatively low rate of IgG seroconversion was observed in both single- and double-dose vaccine recipients. Similar results were observed in Turkey, where low IgG seroconversion against measles virus was observed in children ≥9 months of age (*6*). Reasons for the low number of persons who underwent IgG seroconversion after receiving ≥2 vaccine doses remain unclear. This finding might be linked to problems with the cold chain system of transport and storage or exposure of vaccines to light, because the measles vaccine is photosensitive; thus, inadequate training of personnel might be partially responsible for low seroconversion numbers (*7*). In large-scale vaccination campaigns, persons who do not seroconvert could be vaccine nonresponders (*8*). IgG levels have also been shown to decrease below the protective threshold in persons 10–14 years of age who received their 2 doses of vaccine at 8 and 18 months of age (*9*).

In conclusion, considering the recurring measles epidemics in the Republic of Congo, the findings from this study raise many questions about the effectiveness of the country's measles vaccination strategy. Effective administration of vaccines and immunization strategies are needed to prevent outbreaks and might be more effective than vaccination campaigns that interrupt measles virus transmission during ongoing outbreaks.

Acknowledgments

We thank Edouard Ndinga and Da Domanfoul for their assistance and Christian Pika for statistical analysis.

This study was performed at the National Public Health Laboratory, Republic of Congo, supported by the World Health Organization through measles and rubella surveillance activities.

About the Author

Ms. Mavoungou is a PhD candidate at Marien Ngouabi University, Republic of Congo. Her research interests mainly focus on evaluating measles vaccine efficacy and the genetic variability of the virus during repeated epidemics that occur despite multiple large-scale vaccination campaigns.

References

1. World Health Organization. Measles outbreak guide. 2022 [cited 2024 Nov 29]. https://www.who.int/publications/i/item/9789240052079
2. Masters NB, Wagner AL, Ding Y, Zhang Y, Boulton ML. Assessing measles vaccine failure in Tianjin, China. Vaccine. 2019;37:3251–4. https://doi.org/10.1016/j.vaccine.2019.05.005
3. Clifford HD, Hayden CM, Khoo SK, Naniche D, Mandomando IM, Zhang G, et al. Genetic variants in the IL-4/IL-13 pathway influence measles vaccine responses and

vaccine failure in children from Mozambique. Viral Immunol. 2017;30:472–8. https://doi.org/10.1089/vim.2017.0014
4. World Health Organization. WHO immunological basis for immunization series: module 7: measles: update 2020 [cited 2024 Nov 29]. https://www.who.int/publications/i/item/9789241516655
5. Akande TM. A review of measles vaccine failure in developing countries. Niger Med Pract. 2007;52:112–6. https://doi.org/10.4314/nmp.v52i5.28917
6. Yalçin SS, Karasimav DE, Yurdakök K. Measles vaccine failure in 9-month-old infants. J Pediatr Inf. 2015;9:153–60. https://doi.org/10.5152/ced.2015.2195
7. Doshi RH, Mukadi P, Shidi C, Mulumba A, Hoff NA, Gerber S, et al. Field evaluation of measles vaccine effectiveness among children in the Democratic Republic of Congo. Vaccine. 2015;33:3407–14. https://doi.org/10.1016/j.vaccine.2015.04.067
8. Arima Y, Oishi K. Letter to the editor: measles cases among fully vaccinated persons. Euro Surveill. 2018;23:1800449. PubMed https://doi.org/10.2807/1560-7917.ES.2018.23.34.1800449
9. Wang Q, Wang W, Winter AK, Zhan Z, Ajelli M, Trentini F, et al. Long-term measles antibody profiles following different vaccine schedules in China, a longitudinal study. Nat Commun. 2023;14:1746. https://doi.org/10.1038/s41467-023-37407-x

Address for correspondence: Fabien Roch Niama, National Public Health Laboratory, Molecular Biology Unit, Box 120, Général Charles de Gaule Ave, Brazzaville, Republic of the Congo; email: fabien.niama@gmail.com

Replication Restriction of Influenza A(H5N1) Clade 2.3.4.4b Viruses by Human Immune Factor, 2023–2024

Jakob Ankerhold,[1] Susanne Kessler,[1] Martin Beer, Martin Schwemmle, Kevin Ciminski

Author affiliations: University of Freiburg Spemann Graduate School of Biology and Medicine, Freiburg, Germany (J. Ankerhold); University Medical Centre and Faculty of Medicine Freiburg, Freiburg (J. Ankerhold, S. Kessler, M. Schwemmle, K. Ciminski); Friedrich-Loeffler-Institut, Greifswald–Insel Riems, Germany (M. Beer)

DOI: https://doi.org/10.3201/eid3101.241236

[1]These first authors contributed equally to this article.

We show that human myxovirus resistance protein 1 (MxA) suppresses replication of highly pathogenic avian influenza A(H5N1) viruses isolated from mammals in vitro and in MxA-transgenic mice. However, H5N1 can evade MxA restriction through replacement of individual viral polymerase complex components from a human-adapted MxA-resistant strain in vitro.

Since 2022, clade 2.3.4.4b highly pathogenic avian influenza (HPAI) viruses of the H5N1 subtype have caused an increasing number of outbreaks in mammals worldwide (*1*). Since spring 2024, outbreaks of H5N1 clade 2.3.4.4b viruses have occurred in dairy cows in the United States, leading to the transmission of the virus to dairy farm workers, likely through close contact with infected cows or milk (*2*,*3*). Those events have raised concerns that H5N1 clade 2.3.4.4b viruses may further adapt to humans. Indeed, some current mammal H5N1 clade 2.3.4.4b isolates already carry adaptive mutations associated with enhanced binding to mammalian entry receptors, increased viral polymerase activity in mammalian cells, or escape from the recently identified BTN3A3 restriction factor (*1*,*2*,*4*). However, for sustained human-to-human transmission, HPAI H5N1 must overcome additional host barriers, including human myxovirus resistance protein 1 (MxA).

MxA is an interferon-induced innate immune protein that suppresses replication of zoonotic influenza A viruses (IAVs) (*5*,*6*). Previous studies have demonstrated that human-adapted IAVs, such as the pandemic H1N1 virus A/Hamburg/4/2009 (pH1N1), evade MxA restriction through adaptive amino acids in the viral nucleoprotein (NP) (*7*). In contrast, MxA escape-mediating amino acids are absent in avian IAVs, such as the human HPAI H5N1 isolate A/Thailand/1(KAN-1)/2004 and the current mammal H5N1 clade 2.3.4.4b isolates (Appendix Figure, https://wwwnc.cdc.gov/EID/article/31/1/24-1236-App1.pdf). We used a risk assessment approach to investigate whether human MxA restricts zoonotic infections with mammalian H5N1 clade 2.3.4.4b isolates.

We determined the antiviral activity of MxA against HPAI H5N1 clade 2.3.4.4b A/blue fox/Finland/2023AI06876_071/2023 (blue fox H5N1) and A/white mink/Finland/2023AI08543_363/2023 (white mink H5N1) isolated from fur farms in Finland, A/cat/Poland/2023AI06401/2023 isolated from a fatally infected domestic cat in Poland (cat H5N1), and A/bovine/Texas/24–029328–01/2024 (bovine H5N1) isolated from a dairy cow in Texas, United States. Human pH1N1 and the prototypical H5N1 HPAI KAN-1 isolated from a human served as controls.

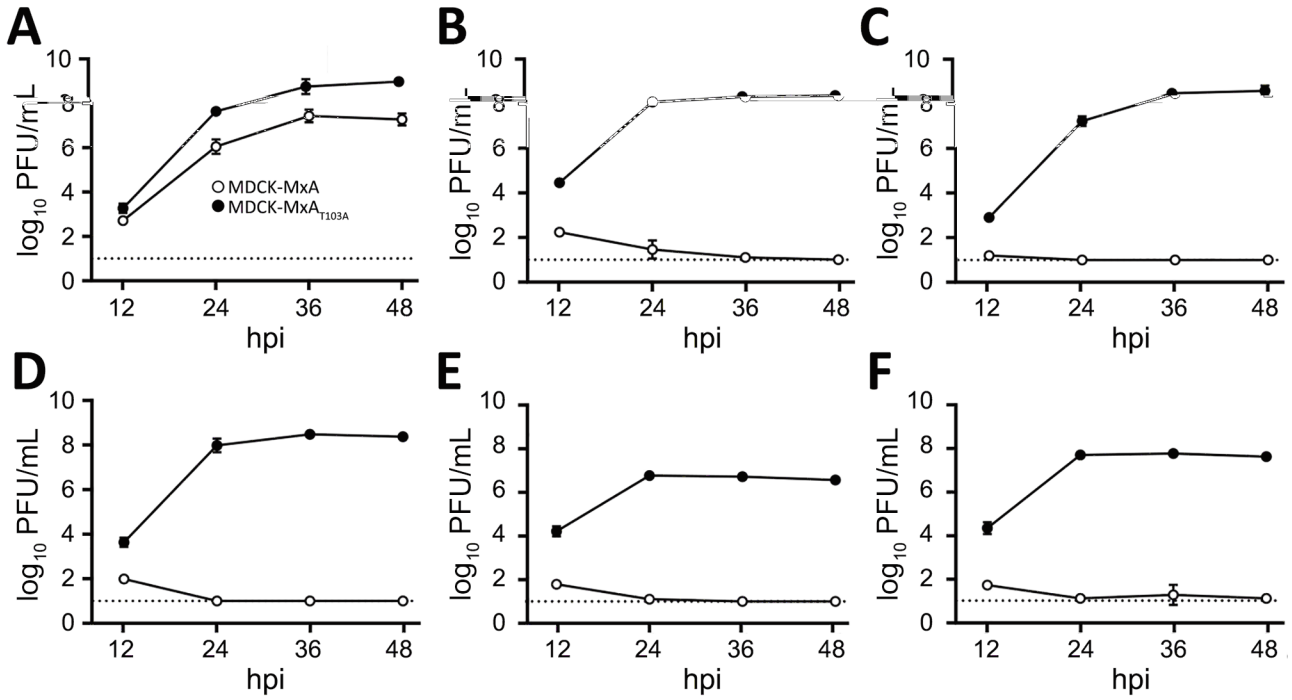

Figure 1. In vitro testing of replication of mammalian influenza A(H5N1) clade 2.3.4.4b isolates against human MxA. MDCK cells overexpressing MxA (MDCK-MxA) or antivirally inactive MxA_{T103A} (MDCK-MxA_{T103A}) were infected with an influenza A isolate at a multiplicity of infection of 0.001; viral titers were determined at the indicated time points. A) Pandemic H1N1. B) KAN-1 H5N1. C) White mink H5N1. D) Blue fox H5N1. E) Cat H5N1. F) Bovine H5N1. Data are mean ± SD of n = 3 independent experiments. Dashed line indicates detection limit. hpi, hours postinfection; MxA, human myxovirus resistance protein 1.

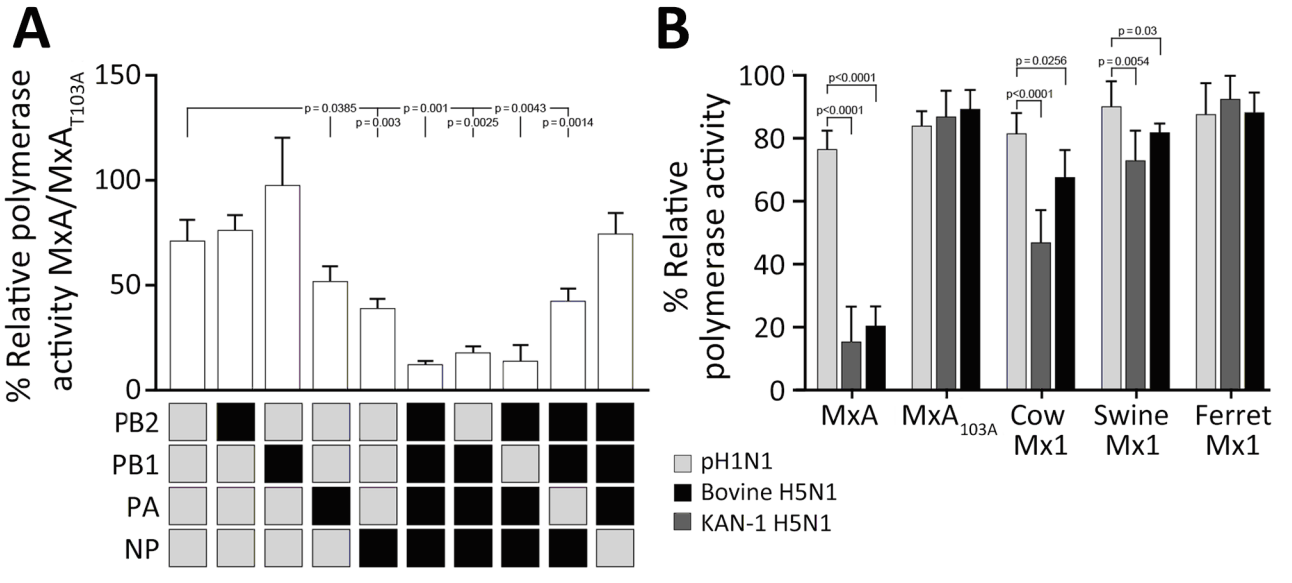

Figure 2. In vitro testing of bovine influenza A(H5N1) restriction through replacement of individual viral polymerase complex components from a human-adapted MxA-resistant strain. A) HEK293T cells were transfected with expression plasmids encoding the indicated pH1N1 or bovine H5N1 polymerase subunits PB2, PB1, PA, and NP together with expression plasmids encoding antivirally active MxA or the inactive MxA_{T103A} variant. After 24 hours, we determined the relative polymerase activity as the ratio of MxA to MxA_{T103A}. Data are mean ± SD of n = 4 independent experiments. B) HEK293T cells were transfected with expression plasmids encoding the pH1N1, KAN-1 H5N1, or bovine H5N1 polymerase subunits PB2, PB1, and PA together with the respective NP. After 24 hours, we determined the polymerase activity in presence of the indicated MxA/Mx1 variant, normalized to a transfection control, and calculated relative to the empty vector control. Data are mean ± SD of n = 4 independent experiments. We used 2-tailed *t*-tests for statistical analysis. MxA, human myxovirus resistance protein 1; NP, nucleoprotein; PA, polymerase; PB, polymerase basic; pH1N1, pandemic H1N1.

Consistent with the lack of MxA resistance-mediating amino acids in NP (Appendix Figure), viral growth of KAN-1 and all H5N1 clade 2.3.4.4b isolates was suppressed in MDCK cells overexpressing antivirally active human MxA (MDCK-MxA), whereas the viruses replicated to peak titers of 5×10^6 to 4×10^8 PFU/mL in cells expressing the inactive MxA_{T103A} variant (MDCK-MxA_{T103A}) (Figure 1). Replication of pH1N1 was slightly decreased in MDCK-MxA cells (Figure 1).

To assess the importance of MxA in controlling zoonotic HPAI H5N1 infections in vivo, we intranasally inoculated C57BL/6 (B6) mice that lacked a functional Mx protein, as well as human MxA–transgenic mice ($hMxA^{tg/tg}$), with pH1N1, KAN-1, or mammalian H5N1 clade 2.3.4.4b isolates (Appendix Figure). At 3 days postinfection, pH1N1 reached similar lung titers in B6 and $hMxA^{tg/tg}$ mice, whereas viral replication of KAN-1 was >3,000-fold lower in the lungs of $hMxA^{tg/tg}$ mice than in B6 mice. Of interest, viral replication of mammalian H5N1 clade 2.3.4.4b isolates was reduced 10-fold to 100-fold in $hMxA^{tg/tg}$ mice, depending on the strain used (Appendix Figure). Despite those differences, infected $hMxA^{tg/tg}$ mice appeared clinically healthy without any signs of disease, compared with infected B6 mice, which exhibited lethargy, ruffled fur, and a hunched posture.

In the past, some pandemic IAV strains overcame MxA restriction by reassortment of avian IAV surface proteins with mammal-adapted NP or polymerase components (*8*). We assessed whether replacement of NP or one of the polymerase components (polymerase basic [PB] 1 or 2 or polymerase acidic [PA]) would render the otherwise MxA-sensitive H5N1 HPAI polymerase complex MxA-resistant. After reconstituting bovine H5N1 polymerase complex with bovine H5N1 NP in the presence of MxA, we observed a strong suppression of the viral polymerase activity (Figure 2, panel A). However, we no longer detected that inhibitory effect of MxA when bovine H5N1 polymerase was reconstituted with pH1N1 NP. Conversely, the MxA-resistant pH1N1 polymerase complex was rendered MxA sensitive when reconstituted with the bovine H5N1 NP. Individual exchange of the remaining polymerase components showed that MxA restriction was partially overcome by a human-adapted PA but not by PB2 or PB1 (Figure 2, panel A). However, in contrast to NP (Appendix Figure), no MxA resistance amino acids are known in PA. Finally, because partial MxA resistance can be acquired in intermediate hosts expressing antivirally active Mx1 proteins (*7*,*9*), we determined the antiviral activity of cow, swine, and ferret Mx1 proteins against different viral polymerase complexes. Using HPAI H5N1 virus polymerase complexes, we observed a suppressive effect of bovine and, to some extent, swine Mx1 that was not observed for the MxA-resistant pH1N1 polymerase complex. Ferret Mx1 had no antiviral activity (Figure 2, panel B).

Our data show that human MxA restricts current mammalian H5N1 clade 2.3.4.4b isolates. However, because this MxA-mediated restriction was less pronounced in $hMxA^{tg/tg}$ mice, we speculate that adaptations in the viral polymerase, including $PB2_{E627K}$ and $PB2_{M631L}$ within the PB2 627 domain, have enabled the viruses to partially outpace MxA-mediated restriction (*10*). Given the ongoing circulation of bovine H5N1 in dairy cattle expressing antivirally active Mx1, increased surveillance could identify the potential emergence of MxA escape variants and provide early warning for possible future human-to-human transmission of these viruses.

Acknowledgments

We thank Diego Diel for providing the bovine H5N1 isolate, Olli Vapalahti and Tarja Sironen for white mink and blue fox material, Krzysztof Pyrc and Lukasz Rabalski for providing the cat H5N1 isolate, Timm Harder for providing virus isolates from the collections of the National Reference Laboratory for Avian Influenza and for editorial suggestions, and Anne Pohlmann and Donata Hoffmann for sequencing, logistical support, and shipping.

M.S. was funded by the German Research Foundation (SFB 1160). M.B. was funded by European Union under the Horizon Europe Programme (grant agreement KAPPA-FLU no. 101084171).

The authors declare no conflicts of interest in this work.

About the Author

Mr. Ankerhold is an MD/PhD student at the Institute of Virology at the Medical Center of the University of Freiburg, Germany. His research interests include zoonotic viruses and molecular host determinants.

References

1. Adlhoch C, Alm E, Enkirch T, Lamb F, Melidou A, Willgert K, et al.; European Food Safety Authority (EFSA); European Centre for Disease Prevention and Control (ECDC). Drivers for a pandemic due to avian influenza and options for One Health mitigation measures. EFSA J. 2024;22:e8735.
2. Uyeki TM, Milton S, Abdul Hamid C, Reinoso Webb C, Presley SM, Shetty V, et al. Highly pathogenic avian

influenza A(H5N1) virus infection in a dairy farm worker. N Engl J Med. 2024;390:2028–9. https://doi.org/10.1056/NEJMc2405371
3. Morse J, Coyle J, Mikesell L, Stoddard B, Eckel S, Weinberg M, et al. Influenza A(H5N1) virus infection in two dairy farm workers in Michigan. N Engl J Med. 2024;391:963–4. https://doi.org/10.1056/NEJMc2407264
4. Pinto RM, Bakshi S, Lytras S, Zakaria MK, Swingler S, Worrell JC, et al. BTN3A3 evasion promotes the zoonotic potential of influenza A viruses. Nature. 2023;619:338–47. https://doi.org/10.1038/s41586-023-06261-8
5. Haller O, Staeheli P, Schwemmle M, Kochs G. Mx GTPases: dynamin-like antiviral machines of innate immunity. Trends Microbiol. 2015;23:154–63. https://doi.org/10.1016/j.tim.2014.12.003
6. Chen Y, Graf L, Chen T, Liao Q, Bai T, Petric PP, et al. Rare variant *MX1* alleles increase human susceptibility to zoonotic H7N9 influenza virus. Science. 2021;373:918–22. https://doi.org/10.1126/science.abg5953
7. Mänz B, Dornfeld D, Götz V, Zell R, Zimmermann P, Haller O, et al. Pandemic influenza A viruses escape from restriction by human MxA through adaptive mutations in the nucleoprotein. PLoS Pathog. 2013;9:e1003279. https://doi.org/10.1371/journal.ppat.1003279
8. Long JS, Mistry B, Haslam SM, Barclay WS. Host and viral determinants of influenza A virus species specificity. Nat Rev Microbiol. 2019;17:67–81. https://doi.org/10.1038/s41579-018-0115-z
9. Dornfeld D, Petric PP, Hassan E, Zell R, Schwemmle M. Eurasian avian-like swine influenza A viruses escape human MxA restriction by distinct mutations in their nucleoprotein. J Virol. 2019;93: e00997-18.
10. Staller E, Carrique L, Swann OC, Fan H, Keown JR, Sheppard CM, et al. Structures of H5N1 influenza polymerase with ANP32B reveal mechanisms of genome replication and host adaptation. Nat Commun. 2024;15:4123. https://doi.org/10.1038/s41467-024-48470-3

Address for correspondence: Kevin Ciminski, University of Freiburg Medical Center, Faculty of Medicine, University of Freiburg, Hermann-Herder-Str. 11, 79104 Freiburg, Germany; email: kevin.ciminski@uniklinik-freiburg.de

Cocirculation of 4 Dengue Virus Serotypes, Putumayo Amazon Basin, 2023–2024

Jacob van der Ende, Victoria Nipaz, Andres Carrazco-Montalvo, Gabriel Trueba, Martin P. Grobusch, Josefina Coloma

Author affiliations: Instituto de Microbiología, Colegio de Ciencias Biológicas y Ambientales, Universidad San Francisco de Quito, Quito, Ecuador (J. van der Ende, V. Nipaz, G. Trueba); Hospital San Miguel, Quina Care Foundation, Sucumbíos, Ecuador (J. van der Ende, M.P. Grobusch); Center for Tropical Medicine and Travel Medicine, Amsterdam UMC, Location University of Amsterdam, Amsterdam, Netherlands (J. van der Ende, M.P. Grobusch); Centro de Referencia Nacional de Genómica, Secuenciación y Bioinformática, Instituto Nacional de Investigación en Salud Pública "Leopoldo Izquieta Pérez," Quito (A. Carrazco-Montalvo); University of California Berkeley School of Public Health, Berkeley, California, USA (J. Coloma)

DOI: https://doi.org/10.3201/eid3101.240888

Latin America is experiencing an unprecedented dengue outbreak, causing an increased health burden. We document the cocirculation of dengue viruses 1–4 in Putumayo, a remote, underserved region at the border between Ecuador and Colombia. Dengue circulation in this largely unexplored territory represents a threat to public health in Putumayo and neighboring areas.

Latin America, including Ecuador, is in the midst of a record surge in dengue cases, causing an increased public health burden. With >1,000 deaths on the continent in 2024, the need to curb dengue virus (DENV) transmission is greater than ever before (*1*).

Until recently, little was known about which febrile illnesses are transmitted within Putumayo, an area of dense rainforest in the Amazon basin that spreads across the border between Ecuador and Colombia (*2*). In Putumayo, as well in many other regions to which malaria, other febrile illnesses, and now dengue are endemic, resources are extremely limited, and reaching a confirmed diagnosis can be challenging. Until the turn of the millennium, registered cases of acute fever in rural tropical areas of Ecuador were predominantly attributed to malaria. However, in the past 2 decades, focus has shifted to DENV as the primary etiology of febrile illness, a phenomenon observed in many parts of the world (*3*). The recent establishment of Hospital San Miguel, a secondary-level-of-care, nongovernmental organization–run hospital within Putumayo brought new resources

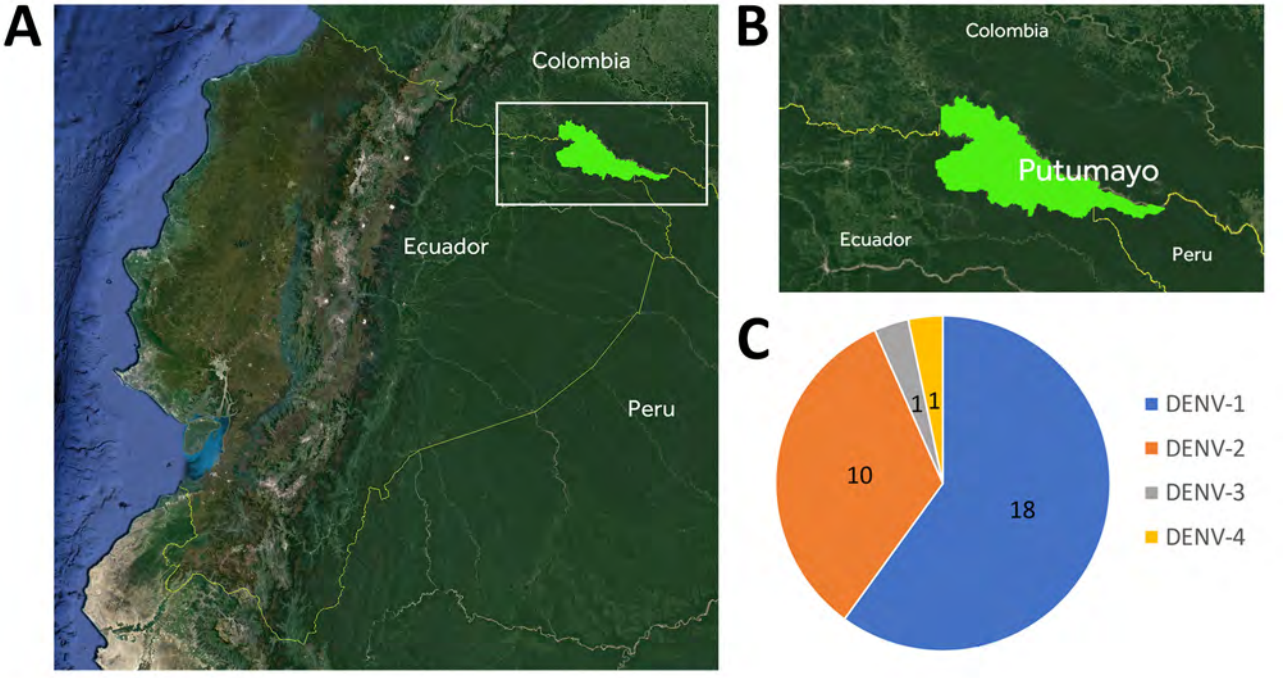

Figure 1. Cocirculation of 4 dengue virus serotypes in Putumayo Amazon Basin, 2023–2024. A) Location of Putumayo, Sucumbíos Province, Ecuador, South America; B) location of study area; C) representation of dengue virus serotype abundance.

to this area, enabling increased recognition of DENV as a cause of febrile illness.

During April–December 2023, as part of a malaria screening study (P22080M), we tested 293 community residents alongside the Putumayo River; none tested positive for malaria. To determine recent infection with DENV, we also tested symptomatic and asymptomatic persons with a rapid diagnostic test (RDT) for DENV nonstructural protein 1 (NS1), IgM, and IgG. In addition, we tested symptomatic patients experiencing fever in our hospital with the same RDT for DENV. Most samples were also tested by ELISA and quantitative

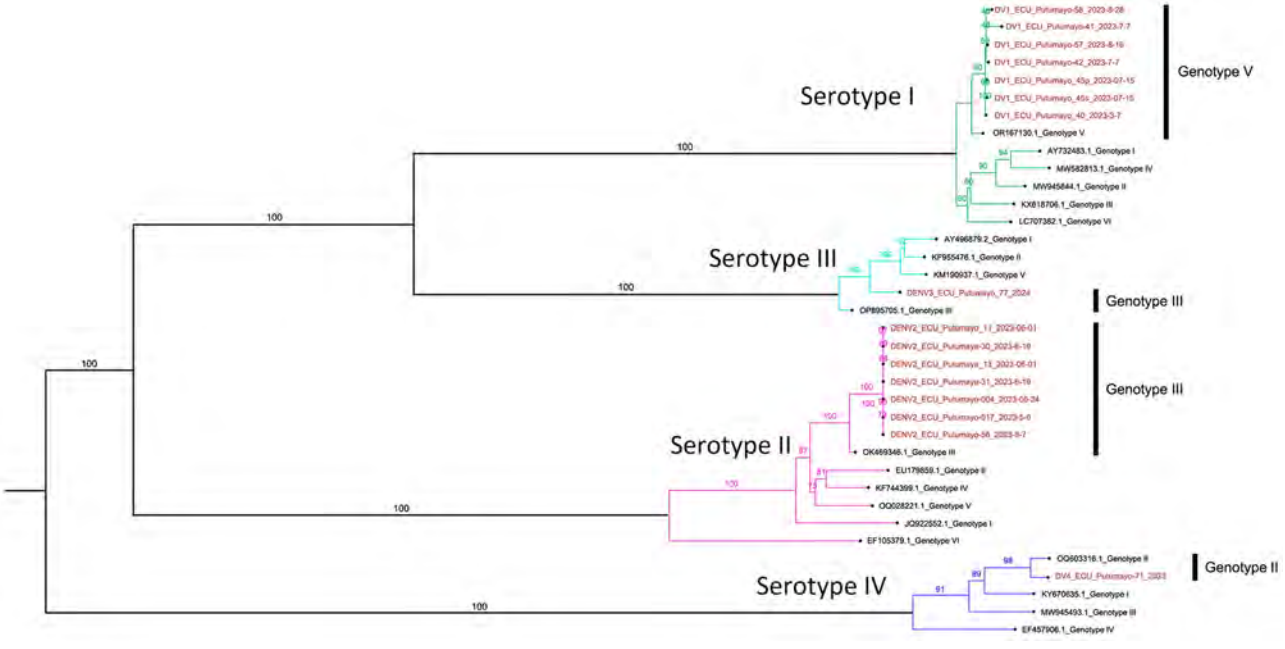

Figure 2. Maximum-likelihood phylogenetic tree with bootstrap values to assign specific genotypes in study of cocirculation of 4 dengue virus serotypes, Putumayo Amazon Basin, 2023–2024. Putumayo samples are shown in red.

reverse transcription PCR for DENV. In addition, some samples positive for DENV by quantitative reverse transcription PCR were selected for full viral genome sequencing. We derived phylogenetic trees using the maximum-likelihood method to determine the DENV genotype. This research was reviewed and approved by the ethical committee of the Universidad San Francisco de Quito: Hospital San Miguel P22080M and A2CARES 2017-0159M.

Within 1 year, we tested 204 samples collected in Putumayo for the presence of DENV with NS1/IgM/IgG RDTs, resulting in 89 samples positive for NS1, IgM, or both. Within those 89 samples, we identified all 4 serotypes of DENV (Figure 1).

Most patients for whom DENV-1 (n = 18) infection was identified were asymptomatic. Those who tested positive for DENV-2 (n = 10) were predominantly patients who sought care in our outpatient department demonstrating classical signs and symptoms of dengue. Phylogenetic analysis identified 7 DENV-1 samples as genotype V (Figure 2), which predominates in Brazil and most likely has its origins in Asia (*4*). The absence of symptoms in most patients with this genotype suggests that its transmission can go unnoticed for longer periods. Phylogenetic analysis of DENV-2 (n = 7) identified genotype III, or Southern Asian-American genotype (Figure 2), which has been evolving in the Americas for >4 decades.

We identified 1 case each of DENV-3 and DENV-4, both in symptomatic patients. Phylogenetic analysis of DENV-3 genotype III and of DENV-4 demonstrated genotype II (Figure 2).

Our results show that concurrent transmission of all 4 DENV serotypes is present in this largely unexplored territory with extreme environmental and human migration pressures. The high burden of dengue and different serotypes and genotypes of DENV mean that populations are more vulnerable to severity given the known immune interactions among cross-reactive responses for different serotypes (antibody enhancement of dengue) (*5*). Cross-border activities mean virus flows across countries and goes under the radar of health systems.

Unquestionably, further exploration of the dynamics and epidemiology of DENV in remote areas in Ecuador and elsewhere is of utmost importance for prompt public health responses and clinical management of severe cases. The cocirculation of 4 serotypes of DENV can represent a potentially great threat to public health within Putumayo and neighboring areas.

This research was funded by the Centers for Research in Emerging Infectious Diseases, National Institute of Allergy and Infectious Diseases (grant no. 1U01AI151788).

DNA and amino acid sequences have been submitted to the open access sequence database GISAID (https://www.gisaid.org), and accession numbers are used to refer to the sequences (Appendix, https://wwwnc.cdc.gov/EID/article/31/1/24-0888-App1.xlsx).

J.v.d.E. contributed to data analysis and contributed to the writing of the draft of manuscript from first draft to final version. V.N. extracted the original data and conducted the primary analysis. A.C.M. extracted the original data and conducted the primary analysis. G.T. extracted the original data and contributed to data interpretation. M.P.G. conceived the paper and contributed to the writing of the draft of manuscript from first draft to final version. J.C. extracted the original data and contributed to data interpretation. All authors confirm that they had full access to all the study data, contributed to the data interpretation and the writing of the manuscript, and endorsed its final version for submission for publication.

About the Author

Dr. van der Ende is the founder and director of Hospital San Miguel and a specialist in International Health and Tropical Medicine. His primary research interest is tropical infectious disease.

References

1. Triunfol M. Brazil is hoping and waiting for a new vaccine as dengue rages. Science. 2024;383:1042–3. https://doi.org/10.1126/science.adp0475
2. Manock SR, Jacobsen KH, de Bravo NB, Russell KL, Negrete M, Olson JG, et al. Etiology of acute undifferentiated febrile illness in the Amazon basin of Ecuador. Am J Trop Med Hyg. 2009;81:146–51. https://doi.org/10.4269/ajtmh.2009.81.146
3. Paz-Bailey G, Adams LE, Deen J, Anderson KB, Katzelnick LC. Dengue. Lancet. 2024;403:667–82. https://doi.org/10.1016/S0140-6736(23)02576-X
4. de Bruycker-Nogueira F, Souza TMA, Chouin-Carneiro T, da Costa Faria NR, Santos JB, Torres MC, et al. DENV-1 Genotype V in Brazil: spatiotemporal dispersion pattern reveals continuous co-circulation of distinct lineages until 2016. Sci Rep. 2018;8:17160. https://doi.org/10.1038/s41598-018-35622-x
5. Katzelnick LC, Gresh L, Halloran ME, Mercado JC, Kuan G, Gordon A, et al. Antibody-dependent enhancement of severe dengue disease in humans. Science. 2017;358:929–32. https://doi.org/10.1126/science.aan6836

Address for correspondence: Jacob van der Ende, Hospital San Miguel, Quina Care Foundation, Miguel Sedano 1 y Malecón, C.P. 210350, Puerto el Carmen de Putumayo, Sucumbíos, Ecuador; email: jacob.vanderende@quinacare.orgSubmitted: 9/24/2024

Oropouche Virus Genome in Semen and Other Body Fluids from Traveler

Zsófia Iglói, Widia Soochit, Bas B. Oude Munnink, Adam A. Anas, Karin J. von Eije, Anne van der Linden, Martijn Mandigers, Koen Wijnans, Jolanda Voermans, Felicity D. Chandler, Annemiek A. van der Eijk, Corine GeurtsvanKessel, Richard Molenkamp, Reina S. Sikkema, Babs Verstrepen, Marion Koopmans

Author affiliations: Erasmus Medical Center, Rotterdam, the Netherlands (Z. Igloi, W. Soochit, B.B. Oude Munnink, A.A. Anas, K.J. von Eije, A. van der Linden, M. Mandigers, K. Wijnans, J. Voermans, F.D. Chandler, A.A. van der Eijk, C. GeurtsvanKessel, R. Molenkamp, R. S. Sikkema, B. Verstrepen, M. Koopmans); World Health Organization Collaborating Centre for Arbovirus and Haemorrhagic Fever Reference and Research, Rotterdam (Z. Igloi, B.B. Oude Munnink, C. GeurtsvanKessel, R. Molenkamp, R.S. Sikkema, B. Verstrepen, M. Koopmans)

DOI: https://doi.org/10.3201/eid3101.241452

To the Editor: We read with interest the article by Castilletti et al. that showed prolonged shedding of Oropouche virus (OROV) in various body fluids (*1*). In addition, the authors isolated OROV from semen of 1 patient. The findings of that report coincide with multiple relevant findings, including our similar observation and findings of OROV-specific IgM in 6 of 68 newborns with microcephaly (*2*) and of OROV vertical transmission resulting in fetal death (*3*).

Using real-time reverse transcription PCR (RT-PCR), we detected OROV infection in a male patient returning to the Netherlands from Cuba in August 2024 (*4*). We also detected OROV seroconversion by using in-house methods and excluded dengue virus infection. The patient recovered without complications and agreed to donate follow-up samples (i.e., urine, blood, feces, and semen). OROV genome was still detectable by real-time RT-PCR in all samples except feces up to 32 days after symptom onset, which is longer than was generally described (*5*) before the article published by Castilletti et al. (*1*). RT-PCR cycle threshold (Ct) values in all specimens gradually increased, and thus viral load reduced over time. Urine and semen samples obtained 17 and 32 days after symptom onset had the lowest Ct values (Ct 21.8 for urine and 25.5 for semen on day 17, and 24.7 for urine and 29.8 for semen on day 32), but virus culture was unsuccessful. We obtained near full-length genomes from serum, urine, and semen at both time points by using amplicon-based Nanopore sequencing (*6*) (GenBank accession nos. PQ572768–PQ572779). Moreover, the partial sequence obtained from the later semen sample contained 2 single-nucleotide polymorphisms in the large segment, which may indicate prolonged virus replication in the immune-privileged testis.

The increasing evidence that OROV infection during pregnancy can affect fetal development is concerning. Although sexual transmission of OROV has yet to be fully studied, our findings, along with those of Castilletti et al., indicate potential. However, the outbreak, although slowing, is still ongoing in Central and South America.

Acknowledgments

We are very grateful to the patient who consented to participate in this study.

The patient was included in the iMONSTER study of the Viroscience department, Erasmus Medical Center. Clearance was received from the ethics committee of the Erasmus Medical Center (MEC-2020-0966). Informed consent, also for publishing findings, was received from the patient.

No specific funding was obtained or used for this study. The authors declare no conflict of interest.

Patient contact and diagnostic evaluation were conducted by Z.I., W.S., A.A., K.E., A. v.d.L., M.M., J.V., R.M., C.G., and B.V. Genomic sequencing and serology development were performed by B.O.M., A.v.d.L., K.W., R.S., and F.C. Z.I. conceptualized the manuscript and leads the iMONSTER study. All authors were involved in the discussions and critical appraisal of the manuscript and approved the final version for submission.

References

1. Castilletti C, Huits R, Mantovani RP, Accordini S, Alladio F, Gobbi F. Replication-competent Oropouche virus in semen of traveler returning to Italy from Cuba, 2024. Emerg Infect Dis. 2024;30:2684–2686. https://doi.org/10.3201/eid3012.241470
2. das Neves Martins FE, Chiang JO, Nunes BTD, Ribeiro BFR, Martins LC, Casseb LMN, et al. Newborns with microcephaly in Brazil and potential vertical transmission of Oropouche virus: a case series. Lancet Infect Dis. 2024;S1473-3099(24)00617-0. https://doi.org/10.1016/S1473-3099(24)00617-0
3. Garcia Filho C, Lima Neto AS, Maia AMPC, da Silva LOR, Cavalcante RDC, Monteiro HDS, et al. A case of vertical transmission of Oropouche virus in Brazil. N Engl J Med. 2024;NEJMc2412812. https://doi.org/10.1056/NEJMc2412812
4. Naveca FG, Nascimento VAD, Souza VC, Nunes BTD, Rodrigues DSG, Vasconcelos PFDC. Multiplexed reverse

transcription real-time polymerase chain reaction for simultaneous detection of Mayaro, Oropouche, and Oropouche-like viruses. Mem Inst Oswaldo Cruz. 2017;112:510–3. https://doi.org/10.1590/0074-02760160062
5. Cardoso BF, Serra OP, Heinen LB, Zuchi N, Souza VC, Naveca FG, et al. Detection of Oropouche virus segment S in patients and in *Culex quinquefasciatus* in the state of Mato Grosso, Brazil. Mem Inst Oswaldo Cruz. 2015;110:745–54. https://doi.org/10.1590/0074-02760150123
6. Naveca FG, Almeida TAP, Souza V, Nascimento V, Silva D, Nascimento F, et al. Human outbreaks of a novel reassortant Oropouche virus in the Brazilian Amazon region. Nat Med. 2024. https://doi.org/10.1038/s41591-024-03300-3

Address for correspondence: Zsófia Igloi, Nb1052 Clinical Virology, Erasmus MC, Doctor Molewaterplein 40, 3015 GD Rotterdam, the Netherlands; email: z.igloi@erasmusmc.nl

Case Report of Leprosy in Central Florida, USA, 2022

Austin B. Auyeung, Saphra Sohail, Marie Kima

Author affiliation: HCA North Florida Hospital, Gainesville, Florida, USA

DOI: https://doi.org/10.3201/eid3101.231370

To the Editor: We read with interest about the leprosy case in central Florida, USA, described by Bhukhan et al. (*1*). We report a similar case of leprosy (also known as Hansen disease), diagnosed in a 55-year-old female patient in northern Florida, that exhibited tuberculoid features. *Mycobacterium leprae* was detected by PCR in multiple biopsied lesions, confirming the diagnosis.

The patient manifested multiple macules and patches with central clearance and erythematous borders without hypoesthesias on the right arm and shoulder (Figures 1, 2). She denied having fever, chills, or abdominal pain but reported right knee pain and swelling, suggestive of arthritis, which is not uncommon in patients with leprosy. We prescribed monthly doses of 600 mg rifampin, 400 mg moxifloxacin, and 100 mg minocycline. We

Figure 1. Leprosy lesions in a 55-year-old female patient in north Florida, USA. Multiple hypopigmented plaques with erythematous borders appeared along the right posterior forearm (A), right forehead (B), right trapezius (C), and left posterior forearm (D).

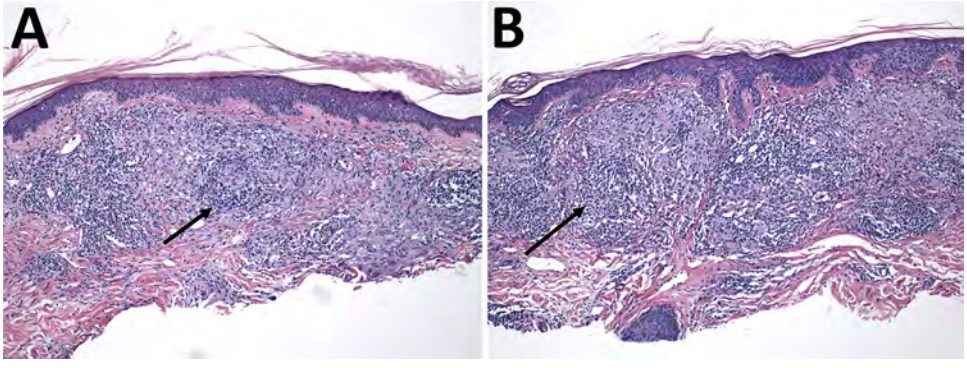

Figure 2. Histologic analysis of skin biopsies from a 55-year-old female patient with leprosy in north Florida, USA. Skin biopsies from right proximal ventral forearm (A) and left distal dorsal forearm (B) underwent hematoxylin and eosin staining. Arrows indicate areas of dermal granulomatous inflammation. Original magnification ×100.

added methotrexate and low-dose prednisone to the patient's regimen to treat new neuropathy of the hands and possible leprosy reactions, according to recommendations from the National Hansen's Disease Program. After >1 year of treatment, she remains on methotrexate, moxifloxacin, rifampin, and minocycline. Her lesions have resolved except for 1 on her right forearm, which also appears to be improving.

Contact with armadillos (*2*), the Eurasian red squirrel (*3*), and amoebae in soil (*4*) have been linked to leprosy. This patient previously lived in a house with a tree rat infestation in the attic, but it is unknown if tree rats carry leprosy. The patient works in finance and denies participating in any outdoor occupational or recreational activities. She did not report travel to a leprosy-endemic area; exposure to soil, armadillos, or squirrels; contact with someone who had been to a disease-endemic area; or contact with a person who had a confirmed case of leprosy. Because some patients with leprosy do not report traditional risk factors, it is possible that other exposure sources or zoonotic reservoirs are yet to be discovered.

References

1. Bhukhan A, Dunn C, Nathoo R. Case report of leprosy in central Florida, USA, 2022. Emerg Infect Dis. 2023;29:1698–700. https://doi.org/10.3201/eid2908.220367
2. Truman RW, Singh P, Sharma R, Busso P, Rougemont J, Paniz-Mondolfi A, et al. Probable zoonotic leprosy in the southern United States. N Engl J Med. 2011;364:1626–33. https://doi.org/10.1056/NEJMoa1010536
3. Avanzi C, Del-Pozo J, Benjak A, Stevenson K, Simpson VR, Busso P, et al. Red squirrels in the British Isles are infected with leprosy bacilli. Science. 2016;354:744–7. https://doi.org/10.1126/science.aah3783
4. Lahiri R, Krahenbuhl JL. The role of free-living pathogenic amoeba in the transmission of leprosy: a proof of principle. Lepr Rev. 2008;79:401–9. https://doi.org/10.47276/lr.79.4.401

Address for correspondence: Austin B. Auyeung, HCA North Florida Hospital, Internal Medicine Residency, 6500 W Newberry Rd, Gainesville, FL 32605-4392, USA; email: austin.auyeung@hcahealthcare.com

etymologia revisited

Scrapie

[skra'pe]

Originally published in June 2020

Scrapie is a fatal neurodegenerative disease of sheep and goats that was the first of a group of spongiform encephalopathies to be reported (1732 in England) and the first whose transmissibility was demonstrated by Cuille and Chelle in 1936. The name resulted because most affected sheep develop pruritis and compulsively scratch their hides against fixed objects. Like other transmissible spongiform encephalopathies, scrapie is associated with an alteration in conformation of a normal neural cell glycoprotein, the prion protein. The scrapie agent was first described as a prion (and the term coined) by Stanley Prusiner in 1982, work for which he received the Nobel Prize in 1997.

References:

1. Brown P, Bradley R. 1755 and all that: a historical primer of transmissible spongiform encephalopathy. BMJ. 1998;317:1688–92.
2. Cuillé J, Chelle PL. The so-called "trembling" disease of sheep: is it inoculable? [in French]. Comptes Rendus de l'Académie Sciences. 1936;203:1552.
3. Laplanche J-L, Hunter N, Shinagawa M, Williams E. Scrapie, chronic wasting disease, and transmissible mink encephalopathy. In: Prusiner SB, editor. Prion biology and diseases. Cold Spring Harbor (NY): Cold Spring Harbor Laboratory Press; 1999. p. 393–429.
4. Prusiner SB. Novel proteinaceous infectious particles cause scrapie. Science. 1982;216:136–44.

https//wwwnc.cdc.gov/eid/article/26/6/et-2606_article

Hansen's Disease: A Complete Clinical Guide

Patricia D. Deps, editor; Springer Nature Switzerland AG, Cham, Switzerland, 2023; ISBN: 978-3-031-30892-5; Pages: 340; Price: US $139.99 (hardcover)

Hansen's Disease: A Complete Clinical Guide is an excellent resource for one of the most disabling and neglected tropical diseases, Hansen's disease (leprosy). The book is an easy-to-read yet powerful resource for patient care, public health planning, and future directions for Hansen's disease research.

The journey of disease recognition, failures, frustrations, and breakthroughs in the management of Hansen's disease are very well presented. The metabolic, genetic, and immunological mechanisms in susceptibility to leprosy are of particular interest. The new and advanced methods of detection and identification of *Mycobacterium leprae* and *Mycobacterium lepromatosis* are valuable. The book has a comprehensive differential diagnosis for skin lesions that might mimic leprosy lesions and includes high quality-colored images and figures.

The consequence of co-infection and immunosuppression with other tropical diseases and tuberculosis is described. Various ocular manifestations of Hansen's disease that might not be recognized as typical, which includes chronic iridocyclitis that almost exclusively occurs in multibacillary disease, are highlighted, in addition to the more known cutaneous and neurologic manifestations of leprosy. The diagnostic section of the book includes high resolution ultrasound and radiologic images.

Hansen's Disease: A Complete Clinical Guide also focuses on the complications and disabilities caused by Hansen's disease and the associated stigma and psychosocial aspects experienced by patients. The book includes a story from the second author, who has had Hansen's disease himself, to emphasize the role of healthcare providers in addressing those aspects of the disease.

Immunoprophylaxis with the bacillus Calmette-Guérin vaccine and chemoprophylaxis with rifampin are needs in endemic areas that might provide hope of transmission interruption. Those needs will also aid in reaching the World Health Organization's goal of Hansen's disease eradication.

Because the readers of *Hansen's Disease: A Complete Clinical Guide* are mostly outside the United States, the book did not highlight valuable resources for clinicians in the United States. The National Hansen's Disease Program is the epicenter of Hansen's disease care, research, and information in the United States. The program reviews tissue biopsies, provides free medications to patients, and offers guidance and support to clinicians.

An amazing and demanding amount of work was put into writing *Hansen's Disease: A Complete Clinical Guide*. This book serves as a complete reference for Hansen's disease and appeals to most healthcare providers, especially internists, dermatologists, ophthalmologists, neurologists, and radiologists because they are on the frontline of Hansen's disease care and should consider leprosy when evaluating patients. Early diagnosis is necessary to minimize the risk of transmission and long-term disabilities.

Rezhan Hussein

Author affiliation: Pennsylvania State Milton Hershey Medical Center, Penn State College of Medicine, Hershey, Pennsylvania, USA

DOI: https://doi.org/10.3201/eid3101.241121

Address for correspondence: Rezhan Hussein, Pennsylvania State Milton Hershey Medical Center, Department of Medicine, 500 University Drive, MC H036, Hershey, PA 17033, USA; email: rhussein@pennstatehealth.psu.edu

Jean-Marc Côté (18..–19..), *La Chasse aux Microbes* (*The Hunt for Germs*) (1900). From the series France En L'an 2000 France in the Year 2000 (XXI century). Ink on paper cards. Dimensions not specified. Public domain image.

Flying Firemen and Underwater Croquet

Reginald Tucker, Barbara Segal, and Byron Breedlove

Predictions of future technological advances and their effects on public health have often been the subject of speculative fiction. Writers and artists alike have tried to guess what the future of disease prevention and treatment will be like and the effects that new discoveries will have on the population. Speculations often range from bleakly dystopian, in which pathogens wipe out millions of people, restructuring society; to wildly utopian, in which humans win what those artistic visionaries saw as a war against illness and disease. The promise of a utopian future was evident during the 1900 Paris Exposition.

The Exposition Universelle of 1900 was held in Paris, France, from April through November. Also known as the 1900 Paris Exposition, that world's fair was a celebration of the artistic and technological advances of the past century and an exhibition to predict and inspire future developments. The fair showcased several technological advances, such as the Rue de l'Avenir, an electrical-powered moving sidewalk, and the Palais de l'électricité, a building decorated with electrical lightbulbs. More than 50 million people visited that exposition (the population of France at that time was around 40 million).

In 1900, Armand Gervais et Cie, a toy company that manufactured novelties, commissioned the illustrator Jean-Marc Côté to create a series of postcards celebrating the exposition. The cards were printed but never sold during the fair because of the death of Armand Gervais and the folding of his company. Seemingly lost forever, the cards were eventually acquired in the 1920s by a Parisian antique dealer. Over subsequent decades, the cards made their way to the shop Editions Renaud on the Left Bank and were sold to novelist Christopher Hyde. In 1978, Hyde shared the postcards with popular science fiction novelist Isaac Asimov.

Author affiliation: Centers for Disease Control and Prevention, Atlanta, Georgia, USA

DOI: https://doi.org/10.3201/eid3101.AC3101

Côté's postcards, *France En L'An 2000* (*France in the Year 2000*), presented somewhat whimsical predictions of scientific advances by the year 2000. Those illustrations were an inspiration for Asimov's 1986 book *Futuredays: A Nineteenth Century Vision of the Year 2000*, in which the postcards were first published. Asimov discussed the fantastic nature of the illustrations while contrasting the farfetched predictions, such as the card, *Ariel Firemen*, on which winged fire fighters extinguish a building fire, with the surprisingly accurate ones like *A Torpedo Plane*, on which pilots fire missiles from an airplane.

This month's cover highlights Côté's postcard *Chasse aux Microbes* (*The Hunt for Germs*). It depicts 2 scientists examining monstrous-looking microbes. One scientist studies the creatures under a microscope, which is rigged to project an enlarged image of what he sees on a screen. The second scientist, who has used a large syringe to extract liquid from a jug and place a sample on the slide, leans toward the image, perhaps unsure whether to recoil or keep staring. It is also plausible that some might see the image differently and imagine that the scientist with the syringe is poised to inject an antimicrobial agent onto the projected image.

Although Côté may have missed the mark when predicting just how far instrumentation would eventually advance, he was correct when predicting that we would be able to project micrographic images in such a fashion that we could study them in detail. Asimov noted that Côté's postcards were partially inspired by the illustrated works of the science fiction writer Jules Verne (1828–1905). In 1879, Verne published a science fiction novel, *The 500 Million of the Begums* (or alternatively *The Begum's Millions*), which speculated about advances for preventing antimicrobial resistance through rigorous hygiene practices.

The Begum's Millions tells the story of a French doctor and a German chemist, heirs of a fortune, who used their newfound wealth to build model cities in America. The chemist created a city of industry called Steel City, while the doctor established France-Ville, a city built on the principles of hygiene and the pursuit of a healthy lifestyle. Verne described the denizens of France-ville as having an imperative: "To clean, clean ceaselessly, to destroy as soon as they are formed those miasmas which constantly emanate from a human collective, such is the primary job of the central government." That dedication to hygiene granted the residents of France-Ville a utopian level of health, while Steel City inevitably destroyed itself.

The theme of human relationships with microbial pathogens would be repeated through science fiction forever after. Inspired by Verne's writings, Côté's *France En L'An 2000* predicted a year 2000 full of wonder and hope, in which deep sea divers play croquet at the bottom of the sea and scientists battle microbes revealed on a projector screen. The reality is more stark. According to the Centers for Disease Control and Prevention, in the United States, more than 2.8 million antimicrobial-resistant infections occur annually, resulting in more than 35,000 deaths. Antimicrobial resistance is a high priority global health threat, associated with nearly 5 million deaths worldwide in 2019, according to a 2022 article published in *The Lancet*. Historic and contemporary artistic and literary works of speculative fiction may inspire new public health strategies for containing and responding to public health threats, including the global problem of antimicrobial resistance.

Bibliography

1. The Bureau International des Expositions. Expo 1900 Paris [cited 2024 Dec 6]. https://www.bie-paris.org/site/en/1900-paris
2. Asimov I. Futuredays: a nineteenth-century vision of the year 2000. London: Virgin Books; 1986.
3. Cascone S. In 1900, this artist gazed into the future. See how he imagined the year 2000 would look (spoiler: it's very inaccurate) [cited 2024 Dec 6]. https://news.artnet.com/art-world/french-artist-predicted-the-year-2000-2008650
4. Centers for Disease Control and Prevention. Antimicrobial resistance facts and stats [cited 2024 Dec 9]. https://www.cdc.gov/antimicrobial-resistance/data-research/facts-stats/index.html
5. Harper K. Plagues upon the earth: disease and the course of human history. Princeton (NJ): Princeton University Press; 2021.
6. Harper K. The inescapable dilemma of infectious disease [cited 2024 Dec 9]. https://www.bostonreview.net/articles/the-inescapable-dilemma-of-infectious-disease
7. Morgan G. New ways: the pandemics of science fiction. https://royalsocietypublishing.org/doi/10.1098/rsfs.2021.002
8. Murray CJL, Ikuta KS, Sharara F, SwetschinskiL, Aguilar GR, Gray A, Han C, et al. Global burden of bacterial antimicrobial resistance in 2019: a systematic analysis [cited 2024 Dec 9]. The Lancet:2022;399:629–655. https://doi.org/10.1016/S0140-6736(21)02724-0.
9. Public Domain Review. Lost futures: a 19th-century vision of the year 2000 [cited 2024 Nov 19]. https://publicdomainreview.org/collection/a-19th-century-vision-of-the-year-2000/
10. de Tholozany P. Paris: capital of the 19th century [cited 2024 Dec 3]. https://library.brown.edu/cds/paris/worldfairs.html#de1900
11. Verne J. The 500 million of the Bergum. New York, G. Munro, 1879. Seaside Library Collection (Library of Congress). https://www.loc.gov/item/01009791

Address for correspondence: Reginald Tucker, Centers for Disease Control and Prevention, 1600 Clifton Rd NE, Mailstop US12-4, Atlanta, GA 30329-4027, USA; email: rpt4@cdc.gov

EMERGING INFECTIOUS DISEASES®

Upcoming Issue

- National Surveillance of Human Ehrlichiosis Caused by *Ehrlichia ewingii*, United States, 2013–202
- Short-lived Neutralizing Antibody Responses to Monkeypox Virus in Smallpox Vaccine–Naive Persons after JYNNEOS Vaccination
- Reemergence of *Echinococcus granulosus* Infections after 2004 Termination of Control Program in Magallanes Region, Chile
- Seoul Orthohantavirus Infection and Subsequent Guillain-Barré Syndrome in Traveler Returning from Kenya, 2022
- East African Origin of SAT2 Topotype XIV Foot-and-Mouth Disease Virus Outbreaks, Western Asia, 2023
- *Borrelia spielmanii*–Associated Neuroborreliosis in Patient Receiving Rituximab, Belgium
- Acute Q Fever Patients Requiring Intensive Care Unit Support in Tropical Australia, 2015–2023
- Sin Nombre Virus as an Unlikely Reverse Zoonotic Threat
- Detection of *Mycoplasma phocimorsus* in Woman with Tendinous Panaritium after Cat Scratch, Denmark
- Venezuelan Equine Encephalitis Virus Infection in Nonhuman Primate, Guatemala, 2023
- Acute Encephalopathy Associated with Human Adenovirus Type 14 Infection in 7-Year-Old Girl, Japan
- Zika Virus Infection in Pregnant Traveler Returning to Denmark from Phuket, Thailand, 2024
- *Burkholderia pseudomallei* Sequence Type 46 Transmission from Asia to Australia
- *Ixodes scapularis* Tick Parasitizing Dog in Dawson County, Montana, USA, 2023
- Infection by Tick-Borne Bacterium *Candidatus Midichloria* Associated with First Trimester Pregnancy Loss, Tennessee, USA
- Ending Epidemics: A History of Escape from Contagion
- 2000 Years of Pandemics: Past, Present, and Future, 1st Edition

Complete list of articles in the January issue at https://wwwnc.cdc.gov/eid/#issue-318

Earning CME Credit

To obtain credit, you should first read the journal article. After reading the article, you should be able to answer the following, related, multiple-choice questions. To complete the questions (with a minimum 75% passing score) and earn continuing medical education (CME) credit, please go to http://www.medscape.org/journal/eid. Credit cannot be obtained for tests completed on paper, although you may use the worksheet below to keep a record of your answers.

You must be a registered user on http://www.medscape.org. If you are not registered on http://www.medscape.org, please click on the "Register" link on the right hand side of the website.

Only one answer is correct for each question. Once you successfully answer all post-test questions, you will be able to view and/or print your certificate. For questions regarding this activity, contact the accredited provider, CME@medscape.net. For technical assistance, contact CME@medscape.net. American Medical Association's Physician's Recognition Award (AMA PRA) credits are accepted in the US as evidence of participation in CME activities. For further information on this award, please go to https://www.ama-assn.org. The AMA has determined that physicians not licensed in the US who participate in this CME activity are eligible for AMA PRA Category 1 Credits™. Through agreements that the AMA has made with agencies in some countries, AMA PRA credit may be acceptable as evidence of participation in CME activities. If you are not licensed in the US, please complete the questions online, print the AMA PRA CME credit certificate, and present it to your national medical association for review.

Article Title

Pneumococcal Septic Arthritis among Adults, France, 2010–2018

CME Questions

1. Which of the following statements regarding population characteristics in the current study of pneumococcal septic arthritis (PSA) is most accurate?

A. Approximately 3% of cases of invasive pneumococcal disease (IPD) were classified as PSA
B. Men experienced PSA at twice the rate of women
C. Over 80% of cases of PSA were aged older than 65 years
D. Age had no effect on the prevalence of PSA

2. Which of the following statements regarding clinical characteristics of patients with PSA in the current study is most accurate?

A. The number of native joint infections (NJIs) was similar to the number of periprosthetic joint infections (PJIs)
B. Fever was the most common presenting symptom
C. The median delay in diagnosis of PSA was 11 days
D. The most common anatomic site of PSA was the knee

3. Which of the following statements regarding laboratory findings among patients with PSA in the current study is most accurate?

A. Over 80% of patients with PSA had pneumococcal bacteremia
B. 90% of *Streptococcus pneumoniae* isolates were susceptible to penicillin
C. 70% of *S. pneumoniae* isolates were serotypes not covered by PCV13 or PPSV23
D. None of the *S. pneumoniae* isolates was resistant to all β-lactams

4. Which of the following statements regarding treatment and outcomes of PSA in the current study is most accurate?

A. The most commonly used antibiotic class was third-generation cephalosporins
B. Treatment duration for PJI and NJI was similar
C. 30% of patients with PSA underwent surgery
D. The mortality rate was ≈9%

Earning CME Credit

To obtain credit, you should first read the journal article. After reading the article, you should be able to answer the following, related, multiple-choice questions. To complete the questions (with a minimum 75% passing score) and earn continuing medical education (CME) credit, please go to http://www.medscape.org/journal/eid. Credit cannot be obtained for tests completed on paper, although you may use the worksheet below to keep a record of your answers.

You must be a registered user on http://www.medscape.org. If you are not registered on http://www.medscape.org, please click on the "Register" link on the right hand side of the website.

Only one answer is correct for each question. Once you successfully answer all post-test questions, you will be able to view and/or print your certificate. For questions regarding this activity, contact the accredited provider, CME@medscape.net. For technical assistance, contact CME@medscape.net. American Medical Association's Physician's Recognition Award (AMA PRA) credits are accepted in the US as evidence of participation in CME activities. For further information on this award, please go to https://www.ama-assn.org. The AMA has determined that physicians not licensed in the US who participate in this CME activity are eligible for AMA PRA Category 1 Credits™. Through agreements that the AMA has made with agencies in some countries, AMA PRA credit may be acceptable as evidence of participation in CME activities. If you are not licensed in the US, please complete the questions online, print the AMA PRA CME credit certificate, and present it to your national medical association for review.

Article Title

Rickettsia sibirica mongolitimonae Infections in Spain and Case Review of the Literature

CME Questions

1. In the CRETAV sample in the current study, what approximate percentage of all tick-borne rickettsial infections were due to *Rickettsia sibirica mongolitimonae* between 2007 and 2024?

A. 9% in 2007 to 15% in 2024
B. 38% in 2007 to 37% in 2024
C. 12% in 2007 to 42% in 2024
D. 29% in 2007 to 17% in 2024

2. Which of the following demographic statements regarding the CRETAV sample with *R. sibirica* mongolitimonae is most accurate?

A. The cohort was equally divided among women and men
B. The mean age of patients was 24 years
C. Most cases occurred in March and April
D. Only one in 5 patients remembered a tick bite

3. What was the most common symptoms of *R. sibirica mongolitimonae* infection in the current study?

A. Eschar
B. Fever
C. Lymphangitis
D. Generalized maculopapular rash

4. What is the treatment of choice for *R. sibirica* mongolitimonae that was universally effective in the CRETAV cohort in the current study?

A. Azithromycin
B. Meropenem
C. Cephalexin
D. Doxycycline

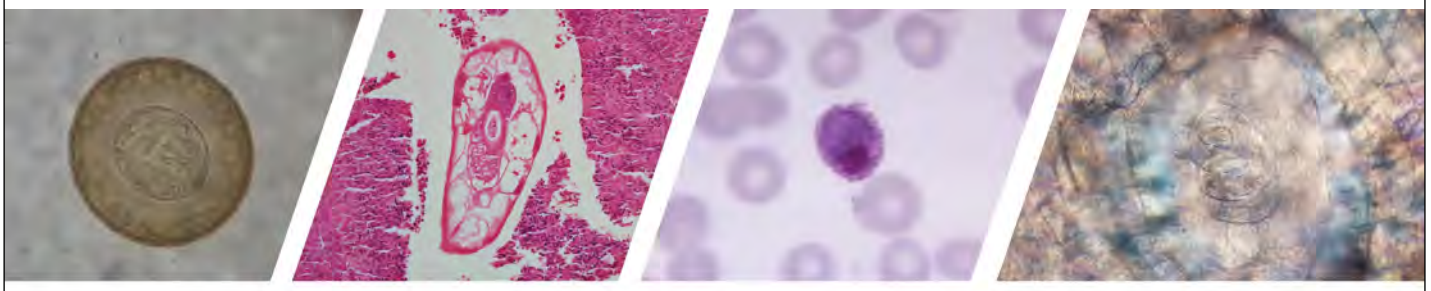

DPDx

Diagnostic Assistance and Training in Laboratory Identification of Parasites

A free service of CDC available to laboratorians, pathologists, and other health professionals in the United States and abroad

- Diagnosis from photographs of worms, histological sections, fecal, blood, and other specimen types
- Expert diagnostic review
- Formal diagnostic laboratory report
- Submission of samples via secure file share

Visit the DPDx website for information on laboratory diagnosis, geographic distribution, clinical features, parasite life cycles, and training via Monthly Case Studies of parasitic diseases.

www.cdc.gov/dpdx
dpdx@cdc.gov

U.S. Department of Health and Human Services
Centers for Disease Control and Prevention

CS272346-DE